Prolonging the Longevity of Budding Yeast: New Aging-Delaying Plant Extracts and the Identification of their Cellular Signaling Pathways

Pamela Dakik

A Thesis
in
The Department
of
Biology

Presented in Partial Fulfillment of the Requirements
For the Degree of
Doctor of Philosophy (Biology) at
Concordia University
Montreal, Quebec, Canada

July 2020

CONCORDIA UNIVERSITY

SCHOOL OF GRADUATE STUDIES

This is to certify that the thesis prepared

By: Pamela Dakik

Entitled: Prolonging the Longevity of Budding Yeast: New Aging-Delaying Plant Extracts and the Identification of their Cellular Signaling Pathways

and submitted in partial fulfillment of the requirements for the degree of

Doctor Of Philosophy (Biology)

complies with the regulations of the University and meets the accepted standards with respect to originality and quality.

Signed by the final examining committee:

_____Chair
Dr. Cameron Skinner

_____ External Examiner
Dr. Nancy Braverman

_____ External to Program
Dr. Paul Joyce

_____ Examiner
Dr. Madoka Gray-Mitsumune

_____ Examiner
Dr. Alisa Piekny

_____Thesis Co-Supervisor
Dr. Vladimir Titorenko

Approved by _____
Dr. Robert Weladji, Graduate Program Director

August 28, 2020

_____
Dr. André Roy, Dean
Faculty of Arts and Science

ABSTRACT

Prolonging the Longevity of Budding Yeast: New Aging-Delaying Plant Extracts and the Identification of their Cellular Signaling Pathways

Pamela Dakik, Ph.D.

Concordia University, 2020

In studies presented in this thesis, we used a robust cell viability assay to conduct two screens of commercially available plant extract libraries in search of plant extracts that can delay chronological aging and prolong the longevity of the budding yeast *S. cerevisiae*. Many of the plant extracts in the library have been used for centuries in traditional Chinese and other herbal medicines or the Mediterranean and other customary diets. None of these plant extracts, however, were previously tested for their ability to slow aging and extend the longevity of any organism. Our screens have allowed us to discover twenty-one plant extracts that significantly prolong the longevity of chronologically aging yeast cells that are not limited in calorie supply. We provided evidence that each of these longevity-extending plant extracts is a geroprotector that lowers the rate of yeast chronological aging and elicits a hormetic stress response. Our findings demonstrated that the efficiencies of aging delay and longevity extension by many of these geroprotective plant extracts significantly exceed those for any of the chemical compounds previously known for their abilities to slow aging and prolong lifespan in yeasts, filamentous fungi, nematodes, fruit flies, daphnias, mosquitoes, honey bees, fish, mammals and cultured human cells. Our findings also revealed that each of the twenty-one geroprotective plant extracts mimics in limited in calorie supply yeast cells

that are not the aging-delaying, longevity-extending, stress-protecting, metabolic and physiological effects of a caloric restriction diet. We also demonstrated that the discovered geroprotective plant extracts elicit partially overlapping effects on a distinct set of longevity-defining cellular processes. Such processes include the coupled mitochondrial respiration, maintenance of the electrochemical potential across the inner mitochondrial membrane, preservation of the cellular homeostasis of reactive oxygen species, protection of cellular macromolecules from reactive oxygen species-inflicted oxidative damage, maintenance of cell resistance to oxidative and thermal stresses, the efficiency of the lipolytic cleavage of neutral lipids deposited and stored in lipid droplets. We provided evidence that some of the discovered geroprotective plant extracts slow yeast chronological aging because they target different hubs, nodes and/or links of the longevity-defining network integrating specific evolutionarily conserved signaling pathways and protein kinases.

Acknowledgments

I would like to start by thanking my supervisor, Dr. Vladimir Titorenko, for inspiring my interest in cellular biology. His guidance, support and patience during the years have been instrumental in my research. Secondly, I would like to recognize my committee members, Dr. Alisa Piekny and Dr. Madoka Gray-Mitsumune, for their expert suggestions and valuable guidance throughout my degree. I am eternally grateful to Concordia University and all its members for the wonderful facilities, encouraging environment and supportive awards that enabled me to pursue my dream. Through the years, fellow graduate students became friends. To Monica Enith Lozano Rodriguez, Vicky Lutchman, Mélissa McAuley, Darya Mitrofanova, Jennifer Anne Baratang Junio, Anna Leonov, Anthony Arlia-Ciommo, Younes Medkour and Karamat Mohammad, thank you for your support and brilliance. I would like to acknowledge the numerous volunteers, undergraduate students and international exchange students for their valuable help with the experiments and for transforming the laboratory into a vibrant inspiration-filled workplace. Finally, I extend my warmest and sincere gratitude to my family and friends for supporting me every step of the way.

Table of Contents

LIST OF FIGURES AND TABLES xii

ABBREVIATIONS xxi

1 INTRODUCTION 1

1.1 Two different modes of cellular aging in *S. cerevisiae* 2

1.2 Several nutrient-responsive and energy-sensing signaling pathways and protein kinases converge into a network that controls the rate of yeast chronological aging 3

1.3 Spatiotemporal organization and regulation of cellular processes controlled by the longevity signaling network define yeast chronological lifespan 5

1.3.1 Age-related changes in the concentrations of certain intermediates in glycolytic and non-glycolytic pathways of carbohydrate metabolism define the CLS of *S. cerevisiae* 5

1.3.2 The intracellular concentration of trehalose is an essential contributor to longevity regulation in *S. cerevisiae* because trehalose controls cellular protein homeostasis 10

1.3.3 Mitochondrial functionality and reactive oxygen species (ROS) production in mitochondria contribute to longevity regulation in *S. cerevisiae* because they orchestrate many cellular processes outside of these organelles 11

1.3.4 The peroxisomal protein import in chronologically aging yeast affects the longevity-defining processes outside of peroxisomes, thus contributing to longevity regulation in *S. cerevisiae* 16

1.4 Spatiotemporal dynamics of intercompartmental communications define the chronology of cellular aging in yeast 19

1.5 Some phytochemicals delay aging and prolong the longevity of budding yeast 26

1.6 Certain combinations of the geroprotective chemicals that target different longevity-defining processes exhibit a synergistic effect on the extent of aging delay and longevity extension 28

1.7 Thesis outline and contributions of colleagues 31

2 DISCOVERY OF PLANT EXTRACTS THAT DELAY YEAST

CHRONOLOGICAL AGING AND HAVE DIFFERENT EFFECTS ON LONGEVITY-DEFINING CELLULAR PROCESSES 36

2.1 Introduction 36

2.2 Materials and methods 36

2.2.1 Yeast strains, media and culture conditions 36

2.2.2 CLS assay 36

2.2.3 A screen for PEs that can extend yeast CLS 37

2.2.4 Oxygen consumption assay (cellular respiration measurement) 37

2.2.5 Live-cell fluorescence microscopy for measuring the mitochondrial membrane potential 37

2.2.6 Live-cell fluorescence microscopy for measuring the formation of reactive oxygen species (ROS)…. 38

2.2.7 Live-cell fluorescence microscopy for examining neutral lipids deposited in lipid droplets (LDs)….. 38

2.2.8 Measurement of oxidative damage to cellular proteins 39

2.2.9 Measurement of oxidative damage to cellular membrane lipids 39

2.2.10 Measurement of the frequency of spontaneous mutations in nuclear DNA 40

2.2.11 Measurement of the frequency of spontaneous mutations in mitochondrial DNA 40

2.2.12 Plating assays for the analysis of resistance to oxidative and thermal stresses 40

2.2.13 Miscellaneous procedures 41

2.2.14 Statistical analysis 41

2.3 Results 41

2.3.1 A screen for PEs that can extend the longevity of chronologically aging yeast 41

2.3.2 For each of the six lifespan-prolonging PEs, the longevity-extending efficacy under CR conditions is significantly lower than that under non-CR conditions 55

2.3.3Each of the six longevity-extending PEs is a geroprotector which postpones the onset and slows the advancement of yeast chronological aging because it causes a hormetic stress

response 55

2.3.4 Each of the six lifespan-extending PEs alters the age-related chronology of longevity-defining traits of mitochondrial functionality 58

2.3.5 The six lifespan-extending PEs differently influence the extent of age-related oxidative damage to cellular proteins, membrane lipids, mitochondrial and nuclear genomes 65

2.3.6 The six lifespan-extending PEs differently influence the resistance of chronologically aging yeast to chronic oxidative and thermal stresses 68

2.3.7 Each of the six lifespan-extending PEs causes rapid degradation of neutral lipids deposited in lipid droplets…. 70

2.4 Discussion 71

2.4.1 Each of the six longevity-extending PEs increases lifespan more efficiently than any lifespan-prolonging chemical compound presently known 76

2.4.2 Future perspectives 81

3 SIX PLANT EXTRACTS SLOW THE CHRONOLOGICAL AGING OF *S. CEREVISIAE* THROUGH DIFFERENT SIGNALING PATHWAYS 84

3.1 Introduction 84

3.2 Materials and methods 84

3.2.1 Yeast strains, media and culture conditions 84

3.2.2 Aging-delaying plant extracts (PEs) 84

3.2.3 CLS assay 85

3.2.4 Miscellaneous procedures 85

3.2.5 Statistical analysis 85

3.3 Results 86

3.3.1 The rationale of our experimental approach 86

3.3.2 PE4 slows yeast chronological aging by attenuating the inhibitory effect of TORC1 on SNF1….. 87

3.3.3 PE5 slows chronological aging by weakening two branches of the PKA pathway 93

3.3.4 PE6 slows chronological aging by coordinating processes that are not integrated into the signaling network of longevity regulation 96

3.3.5 PE8 slows chronological aging by weakening the inhibitory effect of PKA on SNF1 100

3.3.6 PE12 slows chronological aging by stimulating Rim15 103

3.3.7 PE21 slows chronological aging by inhibiting a PKH1/2-sensitive form of Sch9 107

3.4 Discussion 110

4 PAIRWISE COMBINATIONS OF PLANT EXTRACTS THAT SLOW YEAST CHRONOLOGICAL AGING THROUGH DIFFERENT SIGNALING PATHWAYS DISPLAY SYNERGISTIC EFFECTS ON THE EXTENT OF THE AGING DELAY 115

4.1 Introduction 115

4.2 Materials and methods 115

4.2.1 Yeast strains, media and culture conditions 115

4.2.2 Aging-delaying plant extracts (PEs) 116

4.2.3 Chronological lifespan (CLS) assay 116

4.2.4 Statistical analysis 116

4.3 Results 117

4.3.1 Our hypothesis on possible synergistic longevity-extending effects of certain pairwise combinations of the six aging-delaying PEs and/or spermidine and resveratrol .. 117

4.3.2 An effect-based model that we used to assess if a pairwise combination of aging-delaying chemical compounds has a synergistic effect on the extent of the aging delay 119

4.3.3 Mixtures of PE4 and PE5, PE4 and PE6, PE4 and PE12, and PE4 and PE21 have synergistic effects on the extent of the aging delay 120

4.3.4 A mixture of PE4 and PE8 does not slow down yeast chronological aging in a synergistic manner 127

4.3.5 Pairwise combinations of PE5 and PE6, PE5 and PE8, PE5 and PE12, and PE5 and PE21 delay yeast chronological aging in a synergistic fashion 129

4.3.6 Mixtures of PE6 and PE8, PE6 and PE12, and PE6 and PE21 synergistically extend the longevity of chronologically aging yeast 135

4.3.7 Pairwise combinations of PE8 with PE12 or PE21 synergistically slow down yeast chronological aging 140

4.3.8 A mixture of PE12 and PE21 slows yeast chronological aging in a synergistic manner 143

4.3.9 Pairwise combinations of spermidine with PE4, PE5, PE6, PE8, PE12 or PE21 have synergistic effects on the extent of the aging delay 145

4.3.10 Mixtures of resveratrol with PE4, PE5, PE6, PE8, PE12 or PE21 synergistically slow down yeast chronological aging 155

4.4 Discussion 164

5 DISCOVERY OF FIFTEEN NEW GEROPROTECTIVE PLANT EXTRACTS AND IDENTIFICATION OF CELLULAR PROCESSES THEY AFFECT TO PROLONG THE CHRONOLOGICAL LIFESPAN OF BUDDING YEAST 166

5.1 Introduction 167

5.2 Materials and methods 167

5.2.1 Yeast strains, media and growth conditions 167

5.2.2 Chronological lifespan (CLS) assay 168

5.2.3 Miscellaneous procedures 168

5.2.4 Statistical analysis 169

5.3 Results 169

5.3.1 Identification of new PEs that prolong the longevity of chronologically aging budding yeast…… 169

5.3.2 Each of the fifteen longevity-prolonging PEs mimics longevity extension by CR 186

5.3.3 Each of the fifteen longevity-prolonging PEs is a geroprotector that extends the longevity of chronologically aging yeast because it decreases the rate of aging and stimulates a hormetic stress response 190

5.3.4 Each of the fifteen geroprotective PEs intensifies mitochondrial respiration and alters the pattern of age-related changes in intracellular ROS 193

5.3.5 Each of the fifteen geroprotective PEs decreases the extent of age-related oxidative damage to cellular proteins, and many of them slow the aging-associated buildup of oxidatively impaired membrane lipids as well as mitochondrial and nuclear DNA 196

5.3.6 Each of the fifteen geroprotective PEs increases cell resistance to long-term oxidative and thermal stresses…. 202

5.4 Discussion 205

5.4.1 Future perspectives 206

6 GENERAL DISCUSSION 209

7 REFERENCES 212

List of Figures and Tables

Figure 1.1. The replicative and chronological modes of aging in the budding yeast *Saccharomyces cerevisiae* ……..…….. 3
Figure 1.2. Several nutrient-responsive and energy-sensing signaling pathways and protein kinases converge into a network that controls the rate of chronological aging in *S. cerevisiae* ……. 4
Figure 1.3. The longevity of chronologically aging *S. cerevisiae* depends on the intensity of metabolic flow through glycolytic and non-glycolytic pathways of carbohydrate metabolism …….. 8
Figure 1.4. Trehalose contributes to the chronological aging of S. cerevisiae because trehalose controls cellular proteostasis ……. 11
Figure 1.5. A model for how the coupled mitochondrial respiration, mitochondrial membrane potential maintenance and mitochondrial ROS production in chronologically "young" yeast cells that advance through D and PD phases of culturing define their CLS …….. 14
Figure 1.6. A model for how the age-related efficiency of peroxisomal protein import in chronologically aging yeast cells define their CLS by influencing a distinct set of processes inside and outside of peroxisomes ……. 19
Figure 1.7. A model for how various organelle-organelle and organelle-cytosol communications influence yeast chronological aging …….. 25
Table 1.1. The main classes of phytochemicals with respect to their chemical nature …….. 27
Table 1.2. The survival and reproduction advantages that phytochemicals provide to plants …….. 27
Table 2.1. A list of plant extracts used in this study …….. 42
Table 2.2. Properties of plant extracts used in this study …….. 43
Figure 2.1. PE4, PE5, PE6 and PE8, but not PE1, PE2, PE3 or PE7, extend the CLS of WT yeast grown under non-CR conditions …… 46
Figure 2.2. PE12, but not PE9, PE10, PE11, PE13, PE14, PE15 or PE16, extends the CLS of WT yeast grown under non-CR conditions …….. 47
Figure 2.3. PE21, but not PE17, PE18, PE19, PE20, PE22, PE24 or PE25, extends the CLS of WT yeast grown under non-CR conditions …….. 48
Figure 2.4. PE27, PE28, PE29, PE30, PE31, PE32, PE33 and PE34 do not extend the CLS of WT yeast grown under non-CR conditions …….. 49
Figure 2.5. PE35, PE36 and PE37 do not extend the CLS of WT yeast grown under

non-CR conditions …… 50
Figure 2.6. PE4, PE5, PE6, PE8, PE12 and PE21 extend the chronological lifespan (CLS) of yeast grown under non-caloric restriction (non-CR) conditions …… 51
Figure 2.7. PE5 and PE21, but not PE4, PE6, PE8 or PE12, extend the CLS of yeast grown under CR conditions …….. 52
Figure 2.8. The longevity-extending efficacy under non-CR conditions significantly exceeds that under CR conditions for each of the six lifespan-prolonging Pes ……. 53
Figure 2.9. PE4, PE5, PE6, PE8, PE12 and PE21 do not cause significant effects on the growth of WT yeast under non-CR conditions …… .54
Figure 2.10. PE4, PE5, PE6, PE8, PE12 and PE21 do not cause significant effects on the growth of WT yeast under CR conditions …… 57
Figure 2.11. Analysis of the Gompertz mortality function indicates that PE4, PE5, PE6, PE8, PE12 and PE21 significantly decrease the rate of chronological aging in yeast …….. 58
Figure 2.12. PE4, PE5, PE6, PE8, PE12 and PE21 alter the age-related chronology of mitochondrial oxygen consumption by yeast grown under non-CR conditions …… 60
Figure 2.13. PE4, PE5, PE6, PE8, PE12 and PE21 sustain healthy populations of functional mitochondria that exhibit high mitochondrial membrane potential ($\Delta\Psi m$) in chronologically aging yeast grown under non-CR conditions ……. 61
Figure 2.14. PE4, PE5, PE6, PE8, PE12 and PE21 significantly delay an age-dependent decline in the number of WT cells that exhibit high mitochondrial membrane potential under non-CR conditions …… 62
Figure 2.15. PE4, PE5, PE6, PE8, PE12 and PE21 significantly delay an age-dependent decline in the number of WT cells that exhibit high mitochondrial membrane potential under non-CR conditions …… 63
Figure 2.16. In yeast grown under non-CR conditions, PE4, PE5, PE6, PE8, PE12 and PE21 alter the patterns of age-related changes in intracellular reactive oxygen species (ROS) known to be generated mainly as by-products of mitochondrial respiration …… 64
Figure 2.17. PE4, PE5, PE6, PE8, PE12 and PE21 delay an age-dependent rise in the extent of oxidative damage to cellular proteins in chronologically aging yeast grown under non-CR conditions …… 66
Figure 2.18. PE4, PE5, PE6, PE8, PE12 and PE21 slow down an age-dependent rise in the frequency of spontaneous point mutations in the RIB2 and RIB3 loci of mitochondrial

DNA (mtDNA) in chronologically aging yeast cultured under non-CR conditions. PE12 and PE21, but not PE4, PE5, PE6 or PE8, have similar effects on the frequency of spontaneous point mutations in the CAN1 gene of nuclear DNA (nDNA) …… 67
Figure 2.19. PE4, PE5, PE6, PE8, PE12 and PE21 enhance the ability of chronologically aging yeast grown under non-CR conditions to resist chronic oxidative stress …… 69
Figure 2.20. PE4, PE5, PE6, PE8, PE12 and PE21 exhibit different effects on the ability of chronologically aging yeast grown under non-CR conditions to resist chronic thermal stress …… 70
Figure 2.21. PE4, PE5, PE6, PE8, PE12 and PE21 induce rapid consumption of neutral lipids deposited in lipid droplets (LDs) of chronologically aging yeast grown under non-CR conditions …… 72
Figure 2.22. PE4, PE5, PE6, PE8, PE12 and PE21 significantly accelerate an age-dependent decline in the number of WT cells that exhibit LDs under non-CR conditions …… 73
Figure 2.23. PE4, PE5, PE6, PE8, PE12 and PE21 significantly accelerate an age-dependent decline in the number of WT cells that exhibit LDs under non-CR conditions …… 74
Figure 2.24. Figure 13. PE4, PE5, PE6, PE8, PE12 and PE21 delay yeast chronological aging and have different effects on several longevity-defining cellular processes …… 75
Table 2.3. Percent increase of lifespan by geroprotective PEs discovered in this study and by longevity-extending chemical compounds that have been previously identified …….. 76
Table 3.1. Single-gene-deletion mutations used in this study and their known effects on longevity-defining signaling pathways and longevity of chronologically aging *S. cerevisiae* …….. 86
Figure 3.1. A logical framework for identifying signaling pathways and/or protein kinases controlled by the longevity-extending PE(x) and PE(y) …… 88
Figure 3.2. PE4 extends yeast CLS by weakening the restraining action of TORC1 on SNF1 …… 89
Table 3.2. p Values for pairs of survival curves of a yeast strain cultured with or without the indicated plant extract (PE) …… 90
Table 3.3. p Values for pairs of survival curves of the wild-type (WT) and mutant strain, both cultured in the presence of the indicated PE …… 90
Figure 3.3. PE4 is unable to prolong the chronological lifespans (CLS) of the *tor1Δ* and *snf1Δ* mutant strains and has additive CLS-extending effects with the *ras2Δ*, *sch9Δ* and *pkh2Δ* mutations…….. 91
Figure 3.4. Analysis of the Gompertz mortality function indicates that PE4 slows yeast

chronological aging by weakening the inhibitory effect of TORC1 on SNF1 …….. 92
Figure 3.5. PE5 extends yeast CLS by weakening two branches of the PKA signaling pathway …. 94
Figure 3.6. PE5 is unable to prolong the chronological lifespan (CLS) of the *ras2Δ* mutant strain, has an additive CLS-extending effect with the *sch9Δ* mutation, and increases yeast CLS in synergy with the *tor1Δ* and *pkh2Δ* mutations …… 95
Figure 3.7. Analysis of the Gompertz mortality function indicates that PE5 slows yeast chronological aging by weakening two branches of the PKA signaling pathway …… 96
Figure 3.8. PE6 extends yeast CLS independently of presently known longevity-defining signaling pathways/protein kinases …….. 97
Figure 3.9. PE6 has additive CLS-extending effects with the *rim15Δ*, *sch9Δ* and *atg1Δ* mutations; PE6 also increases yeast CLS in synergy with the *tor1Δ*, *ras2Δ*, *pkh2Δ* and *snf1Δ* mutations ……. 98
Figure 3.10. Analysis of the Gompertz mortality function indicates that PE6 slows yeast chronological aging independently of presently known longevity-defining signaling pathways/protein kinases …….. 99
Figure 3.11. PE8 extends yeast CLS by weakening the inhibitory effect of PKA on SNF1 …… 101
Figure 3.12. PE8 is unable to extend the chronological lifespans (CLS) of the *ras2Δ* and *snf1Δ* mutant strains, shows an additive CLS-extending effect with the *sch9Δ* mutation, and increases yeast CLS in synergy with the *tor1Δ* and *pkh2Δ* mutations …….. 102
Figure 3.13. Analysis of the Gompertz mortality function indicates that PE8 slows yeast chronological aging by weakening the inhibitory effect of PKA on SNF1 …… 103
Figure 3.14. PE12 prolongs yeast CLS by stimulating Rim15 ……. 104
Figure 3.15. PE12 is unable to extend the chronological lifespan (CLS) of the rim15Δ mutant strain, has additive CLS-extending effects with the *tor1Δ*, *ras2Δ* and *sch9Δ* mutations, and increases yeast CLS in synergy with the *pkh2Δ* mutation …… 105
Figure 3.16. Analysis of the Gompertz mortality function indicates that PE12 slows yeast chronological aging by stimulating Rim15 ……. 106
Figure 3.17. PE21 extends yeast CLS by weakening a PKH1/2-sensitive form of Sch9 …… 108
Figure 3.18. PE21 extends the chronological lifespan (CLS) of the *sch9Δ* mutant strain significantly less efficient than that of the wild-type (WT) strain, has additive CLS-extending effects with the *tor1Δ* and *ras2Δ* mutations, and increases yeast CLS in synergy with the *pkh2Δ* mutation ……. 109

Figure 3.19. Analysis of the Gompertz mortality function indicates that PE21 slows yeast chronological aging by inhibiting a PKH1/2-sensitive form of Sch9 …… 110
Figure 3.20. A model for how PE4, PE5, PE6, PE8, PE12 and PE21 slow yeast chronological aging via the longevity-defining network of signaling pathways/protein kinases …… 111
Figure 4.1. PE4, PE5, PE8, PE12, PE21 and spermidine (S) delay yeast chronological aging because they regulate various pro-aging or anti-aging nodes, edges and modules of an evolutionarily conserved signaling network known to control the rate of aging ……. 118
Table 4.1. This study assessed how each possible pairwise combination of PE4, PE5, PE6, PE8, PE12 and PE21 or of one of these PEs and spermidine (S) or resveratrol (R) influences yeast chronological aging …….. 119
Figure 4.2. The longevity-extending efficiency of a mixture of 0.3% PE4 and 0.3% PE5 statistically significantly exceeds those of PE4 and PE5, each being used at the optimal concentration of 0.5%. Thus, PE4 and PE5 enhance the longevity-extending efficiency of each other …… 122
Figure 4.3. The longevity-extending efficiency of a mixture of 0.5% PE4 and 0.5% PE6 statistically significantly exceeds those of PE4 and PE6, which were used at the optimal concentration of 0.5% or 1.0% (respectively) ……. 124
Figure 4.4. The longevity-extending efficiency of a mixture of 0.3% PE4 and 0.1% PE12 statistically significantly exceeds those of PE4 and PE12, which were used at the optimal concentration of 0.5% or 0.1% (respectively) ……. 125
Figure 4.5. The longevity-extending efficiency of a mixture of 0.5% PE4 and 0.1% PE21 statistically significantly exceeds those of PE4 and PE21, which were used at the optimal concentration of 0.5% or 0.1% (respectively) …… 126
Figure 4.6. The longevity-extending efficiency of a mixture of 0.5% PE4 and 0.5% PE8 is not statistically different from those of PE4 and PE8, which were used at the optimal concentration of 0.5% or 0.3% (respectively) ……. 128
Figure 4.7. The longevity-extending efficiency of a mixture of 0.3% PE5 and 0.3% PE6 statistically significantly exceeds those of PE5 and PE6, which were used at the optimal concentration of 0.5% or 1.0% (respectively) ……. 130
Figure 4.8. The longevity-extending efficiency of a mixture of 0.1% PE5 and 0.1% PE8 statistically significantly exceeds those of PE5 and PE8, which were used at the optimal concentration of 0.5% or 0.3% (respectively) ……. 131

Figure 4.9. The longevity-extending efficiency of a mixture of 0.1% PE5 and 0.1% PE12 statistically significantly exceeds those of PE5 and PE12, which were used at the optimal concentration of 0.5% or 0.1% (respectively) …….. 133
Figure 4.10. The longevity-extending efficiency of a mixture of 0.1% PE5 and 0.1% PE21 statistically significantly exceeds those of PE5 and PE21, which were used at the optimal concentration of 0.5% or 0.1% (respectively) ……. 134
Figure 4.11. The longevity-extending efficiency of a mixture of 0.3% PE6 and 0.3% PE8 statistically significantly exceeds those of PE6 and PE8, which were used at the optimal concentration of 1.0% or 0.3% (respectively) ……. 136
Figure 4.12. The longevity-extending efficiency of a mixture of 0.3% PE6 and 0.1% PE12 statistically significantly exceeds those of PE6 and PE12, which were used at the optimal concentration of 1.0% or 0.1% (respectively) ……. 138
Figure 4.13. The longevity-extending efficiency of a mixture of 0.1% PE6 and 0.1% PE21 statistically significantly exceeds those of PE6 and PE21, which were used at the optimal concentration of 1.0% or 0.1% (respectively) ……. 139
Figure 4.14. The longevity-extending efficiency of a mixture of 0.1% PE8 and 0.1% PE12 statistically significantly exceeds those of PE8 and PE12, which were used at the optimal concentration of 0.3% or 0.1% (respectively) ……. 141
Figure 4.15. The longevity-extending efficiency of a mixture of 0.1% PE8 and 0.1% PE21 statistically significantly exceeds those of PE8 and PE21, which were used at the optimal concentration of 0.3% or 0.1% (respectively) ……. 142
Figure 4.16. The longevity-extending efficiency of a mixture of 0.1% PE12 and 0.1% PE21 statistically significantly exceeds those of PE12 and PE21, each being used at the optimal concentration of 0.1% ……... 144
Figure 4.17. The longevity-extending efficiency of a mixture of 0.1% PE4 and 100 μM spermidine (S) statistically significantly exceeds those of PE4 and S, which were used at the optimal concentration of 0.5% or 100 μM (respectively) …….. 146
Figure 4.18. The longevity-extending efficiency of a mixture of 0.3% PE5 and 100 μM spermidine (S) statistically significantly exceeds those of PE5 and S, which were used at the optimal concentration of 0.5% or 100 μM (respectively) ……... 148
Figure 4.19. The longevity-extending efficiency of a mixture of 0.5% PE6 and 100 μM spermidine (S) statistically significantly exceeds those of PE6 and S, which were used at

the optimal concentration of 1.0% or 100 μM (respectively) …….. 149
Figure 4.20. The longevity-extending efficiency of a mixture of 0.1% PE8 and 100 μM spermidine (S) statistically significantly exceeds those of PE8 and S, which were used at the optimal concentration of 0.3% or 100 μM (respectively) …….. 150
Figure 4.21. The longevity-extending efficiency of a mixture of 0.1% PE12 and 100 μM spermidine (S) statistically significantly exceeds those of PE12 and S, which were used at the optimal concentration of 0.1% or 100 μM (respectively) …….. 152
Figure 4.22. The longevity-extending efficiency of a mixture of 0.1% PE21 and 100 μM spermidine (S) statistically significantly exceeds those of PE21 and S, which were used at the optimal concentration of 0.1% or 100 μM (respectively) …….. 154
Figure 4.23. The longevity-extending efficiency of a mixture of 0.5% PE4 and 50 μM resveratrol (R) statistically significantly exceeds those of PE4 and R, which were used at the optimal concentration of 0.5% or 50 μM (respectively) …… 156
Figure 4.24. The longevity-extending efficiency of a mixture of 0.3% PE5 and 50 μM resveratrol (R) statistically significantly exceeds those of PE5 and R, which were used at the optimal concentration of 0.5% or 50 μM (respectively) ……. 158
Figure 4.25. The longevity-extending efficiency of a mixture of 0.5% PE6 and 50 μM resveratrol (R) statistically significantly exceeds those of PE6 and R, which were used at the optimal concentration of 1.0% or 50 μM (respectively) ……. 159
Figure 4.26. The longevity-extending efficiency of a mixture of 0.3% PE8 and 50 μM resveratrol (R) statistically significantly exceeds those of PE8 and R, which were used at the optimal concentration of 0.3% or 50 μM (respectively) ……. 160
Figure 4.27. The longevity-extending efficiency of a mixture of 0.1% PE12 and 50 μM resveratrol (R) statistically significantly exceeds those of PE12 and R, which were used at the optimal concentration of 0.1% or 50 μM (respectively) …… 162
Figure 4.28. The longevity-extending efficiency of a mixture of 0.1% PE21 and 50 μM resveratrol (R) statistically significantly exceeds those of PE21 and R, which were used at the optimal concentration of 0.1% or 50 μM (respectively) …… 153
Table 5.1. Properties of plant extracts (PEs) used to conduct a new screen for PEs that can prolong the longevity of chronologically aging budding yeast …….. 169
Figure 5.1. PE26, PE39 and PE42, but not PE38, PE40, PE41, PE43 or PE44, increase the mean and maximum CLS of WT yeast cultured under non-CR conditions on 2% (w/v) glucose … 176

Figure 5.2. PE47, but not PE45, PE46, PE48, PE49, PE50, PE51 or PE52, increases the mean and maximum CLS of WT yeast cultured under non-CR conditions on 2% (w/v) glucose … 177
Figure 5.3. PE59, but not PE53, PE54, PE55, PE56, PE57, PE58 or PE60, increases the mean and maximum CLS of WT yeast cultured under non-CR conditions on 2% (w/v) glucose … 178
Figure 5.4. PE64 and PE68, but not PE61, PE62, PE63, PE65, PE66 or PE67, increase the mean and maximum CLS of WT yeast cultured under non-CR conditions on 2% (w/v) glucose … 179
Figure 5.5. PE69, PE72 and PE75, but not PE70, PE71, PE73, PE74 or PE76, increase the mean and maximum CLS of WT yeast cultured under non-CR conditions on 2% (w/v) glucose … 180
Figure 5.6. PE77, PE78, PE79, PE81 and PE83, but not PE80, PE82 or PE84, increase the mean and maximum CLS of WT yeast cultured under non-CR conditions on 2% (w/v) glucose … 181
Figure 5.7. Neither PE85, PE86, PE87, PE88 nor PE89 can increase the mean or maximum CLS of WT yeast cultured under non-CR conditions on 2% (w/v) glucose …… 182
Figure 5.8. 0.5% (w/v) PE26, 0.5% (w/v) PE39, 0.5% (w/v) PE42, 0.3% (w/v) PE47, 0.3% (w/v) PE59, 0.1% (w/v) PE64, 0.5% (w/v) PE68 and 1.0% (w/v) PE69 exhibit the highest extending effects on the chronological lifespan (CLS) of wild-type (WT) yeast cultured under non-CR conditions on 2% (w/v) glucose …….. 183
Figure 5.9. 0.1% (w/v) PE72, 0.3% (w/v) PE75, 0.5% (w/v) PE77, 0.3% (w/v) PE78, 0.5% (w/v) PE79, 0.3% (w/v) PE81 and 0.5% (w/v) PE83 exhibit the highest extending effects on the CLS of WT yeast cultured under non-CR conditions on 2% (w/v) glucose …….. 184
Figure 5.10. None of the fifteen longevity-extending PEs statistically significantly affects glucose consumption by WT yeast cultured under non-CR conditions on 2% (w/v) glucose ……. 185
Figure 5.11. None of the fifteen longevity-extending PEs statistically significantly alters the growth rate and maximum cell yield of WT yeast cultures under non-CR conditions on 2% (w/v) glucose …… 186
Figure 5.12. 0.5% (w/v) PE26, 0.5% (w/v) PE39, 0.5% (w/v) PE42, 0.3% (w/v) PE59 and 0.5% (w/v) PE68 (but not 0.3% (w/v) PE47, 0.1% (w/v) PE64 or 1.0% (w/v) PE69) extend the CLS of WT yeast cultured under CR conditions on 0.5% (w/v) glucose …… 188
Figure 5.13. 0.3% (w/v) PE78 and 0.5% (w/v) PE83 (but not 0.1% (w/v) PE72, 0.3% (w/v) PE75, 0.5% (w/v) PE77, 0.5% (w/v) PE79 or 0.3% (w/v) PE81) extend the CLS of WT yeast cultured under CR conditions on 0.5% (w/v) glucose …….. 189
Figure 5.14. Each of the fifteen PEs extends the longevity of chronologically aging yeast under non-CR conditions on 2% (w/v) glucose significantly more efficiently than it does

under CR conditions on 0.5% (w/v) glucose …… 190
Figure 5.15. Each of the fifteen PEs extends the longevity of chronologically aging yeast because it decreases the rate of aging but not because it lowers the baseline mortality rate …… 192
Figure 5.16. Each of the fifteen geroprotective PEs stimulates mitochondrial respiration in yeast cultured under non-CR conditions …… 194
Figure 5.17. Each of the fifteen geroprotective PEs alters the age-related chronology of changes in intracellular ROS in yeast cultured under non-CR conditions …… 196
Figure 5.18. Each of the fifteen geroprotective PEs decreases the extent of age-related oxidative damage to cellular proteins in yeast cultured under non-CR conditions ……... 198
Figure 5.19. Many of the fifteen geroprotective PEs slow the aging-associated buildup of oxidatively impaired membrane lipids in yeast cultured under non-CR conditions ……. 199
Figure 5.20. Each of the fifteen geroprotective PEs decreases the frequencies of *rib2* and *rib3* mutations in mitochondrial DNA (mtDNA) of yeast cultured under non-CR conditions …….. 201
Figure 5.21. PE26, PE39, PE42, PE59, PE64, PE69, PE75, PE78, PE79 and PE81 (but not PE47, PE68, PE72, PE77 or PE83) cause a statistically significant decline in the frequencies of can1 mutations in nuclear DNA (nDNA) of yeast cultured under non-CR conditions …….. 202
Figure 5.22. Each of the fifteen geroprotective PEs makes yeast more resistant to chronic (long-term) oxidative and thermal stresses ……. 204

Abbreviations

CFU, colony-forming units

CLS, chronological lifespan

CR, caloric restriction

DHR, Dihydrorhodamine 123

DIC, differential interference contrast

ETC, electron transport chain

IMM, inner mitochondrial membrane

IMS, the intermembrane space

mtDNA, mitochondrial DNA

nDNA, nuclear DNA

OMM, outer mitochondrial membrane

PKA, protein kinase A

RLS, replicative lifespan

ROS, reactive oxygen species

R123, Rhodamine 123

Snf1, sucrose non-fermenting, protein 1

TORC1, a target of rapamycin complex 1

CHAPTER 1

1 Introduction

The budding yeast *Saccharomyces cerevisiae* is a unicellular eukaryote with a sequenced genome [1, 2]. Advanced methods for biochemical, genetic, cell biological, chemical biological, system biological and microfluidic dissection analyses have been developed to elucidate mechanisms underlying many cellular processes in this yeast [1-10]. After these mechanisms have been characterized by studies with yeast, they appeared to operate in the same way in many multicellular eukaryotes [1-4, 10-13]. Due to the availability of comprehensive molecular analyses and because both the chronological and replicative lifespans of *S. cerevisiae* are short and easy to measure, this yeast has been successfully used as a model organism in aging research [5-8, 11-20]. This research provided evidence that the basic principles and molecular mechanisms of cellular aging and its delay by specific genetic, dietary and chemical interventions are evolutionarily conserved [5-8, 11-31].

1.1 Two different modes of cellular aging in *S. cerevisiae*

Two different modes of aging exist in budding yeast. They are known as the replicative and chronological modes (Figure 1.1). These two modes of yeast aging are usually examined separately from each other, using robust laboratory assays [32-35].

Because budding yeast reproduction occurs by asymmetric cell divisions, the replicative mode of yeast aging in the laboratory is measured by using a micromanipulator to remove every new daughter cell formed by budding [33, 35]. The total number of daughter buds that each mother cell can make is then calculated (Figure 1.1) [33, 35]. The replicative mode of yeast aging is believed to imitate the aging of mitotic human cell types capable of dividing [14, 15, 18, 36, 37]. However, recent findings suggest that replicative aging in yeast may also serve as a suitable model for the aging of post-mitotic tissues and the aging of the whole organism in the nematode *Caenorhabditis elegans* and in humans [37-39].

The chronological mode of yeast aging is measured as the length of time during which a yeast cell remains viable after an arrest of its growth and division [32, 40, 41]. A simple clonogenic assay is used to measure yeast chronological aging in the laboratory. This assay assesses the percentage of yeast cells that remain viable in liquid cultures at different time points after a cell population enters the stationary (ST), non-proliferative phase (Figure 1.1) [15, 34, 40]. To assess cell viability in the clonogenic assay, the ability of a yeast cell to form a colony after being

transferred from liquid culture to the surface of a solid nutrient-rich medium is measured [15, 34, 40]. The chronological mode of yeast aging is likely to mimic the aging of post-mitotic human cell types incapable of dividing [14, 15, 17, 42, 43]. However, there is evidence that yeast chronological aging may converge with yeast replicative aging into a single aging process (44-49).

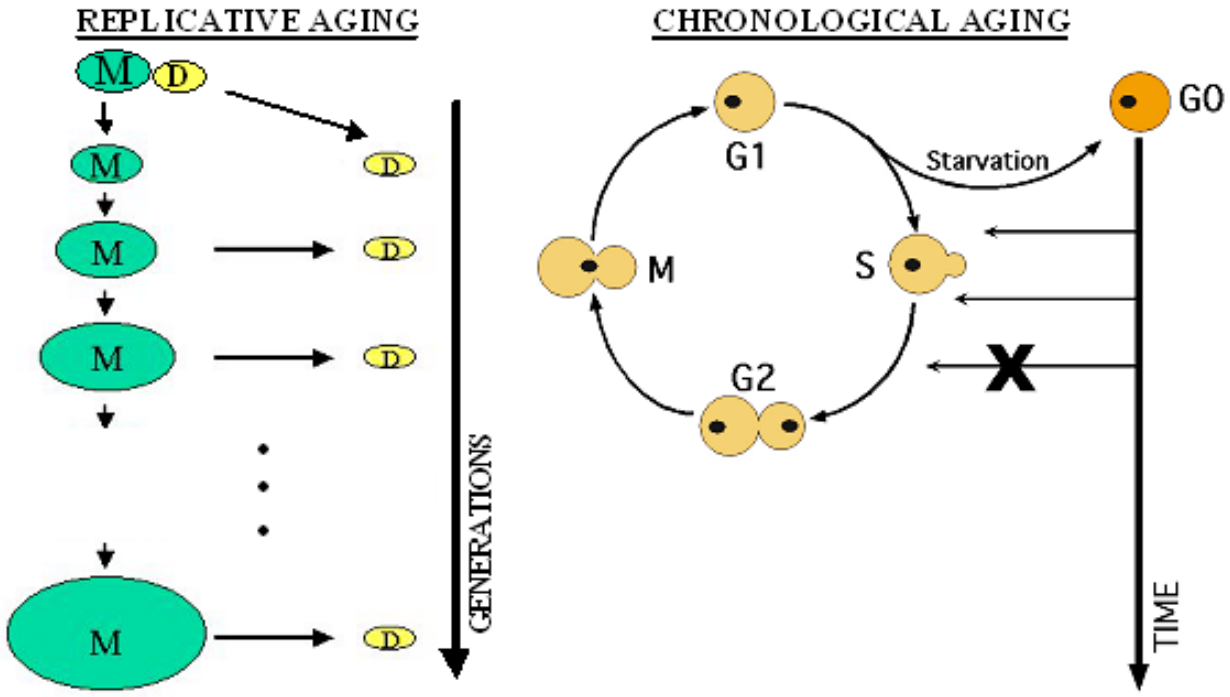

Figure 1.1. The replicative and chronological modes of aging in the budding yeast *Saccharomyces cerevisiae*. Replicative aging is studied by measuring the maximum number of daughter cells (buds) that a mother cell can produce before becoming senescent (i.e., being unable to reproduce by budding on the surface of a fresh solid medium. Chronological aging is studied by measuring the length of time during which a cell remains viable (i.e., can form a colony if placed on the surface of a fresh solid medium) after an arrest of its growth and division. From: Consortium for the Determination of Public Pathways Regulating Longevity (http://www.uwaging.org/ellison/).

1.2 Several nutrient-responsive and energy-sensing signaling pathways and protein kinases converge into a network that controls the rate of yeast chronological aging

One of the major aspects of cellular aging that been conserved in evolution is the integration of specific signaling pathways and protein kinases into a network; this network controls the rate of cellular aging and regulates the longevity of the entire organism [11, 17, 23, 28, 30, 50-

59]. In chronologically aging yeast, this longevity regulation network integrates the following signaling pathways and protein kinases (Figure 1.2): 1) the pro-aging TORC1 (target of rapamycin complex 1) pathway [60-63], 2) the pro-aging PKA (protein kinase A) pathway [64-68], 3) the pro-aging PKH1/2 (Pkb-activating kinase homolog) pathway [69-73], 4) the anti-aging SNF1 (sucrose non-fermenting) pathway [74-79], 5) the anti-aging ATG (autophagy) pathway [80-88], and 6) the pro-aging protein kinase Sch9, which is stimulated by the TORC1 and PKH1/2 pathways [15, 89-94], and 7) the anti-aging protein kinase Rim15, which is inhibited by the TORC1, PKA and PKH1/2 pathways [15, 66, 68, 94-96]. This network of signaling pathways and protein kinases coordinates specific longevity-defining cellular processes. Among these processes are stress responses, protein synthesis in the cytosol and mitochondria, maintenance of nuclear and mitochondrial genomes, autophagy, mitochondrial respiration, peroxisome biogenesis, gluconeogenesis, lipid metabolism, glyoxylate cycle, glycogen synthesis and degradation, and the synthesis of amino acids and fatty acids (Figure 1.2) [11, 15, 17, 51, 55, 59, 62, 73, 94-107]. Information flow along this network in yeast is controlled by such aging-delaying chemical compounds as resveratrol, rapamycin, caffeine, spermidine, myriocin, methionine sulfoxide, lithocholic acid and cryptotanshinone [11, 14, 32, 72, 84, 108-116].

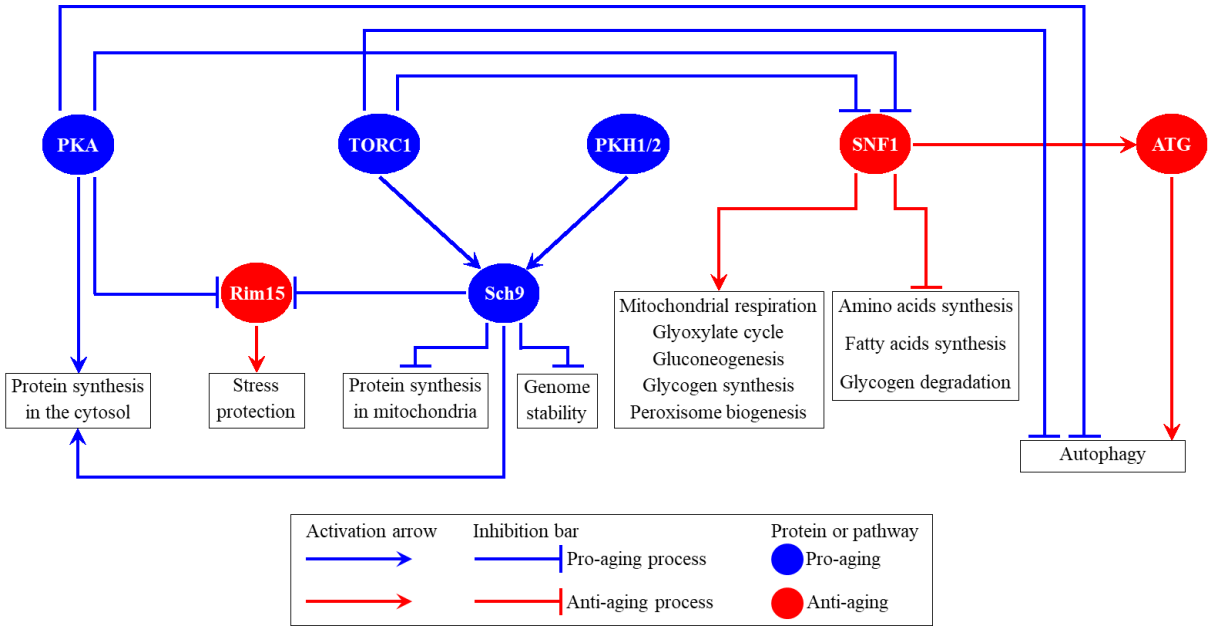

Figure 1.2. Several nutrient-responsive and energy-sensing signaling pathways and protein kinases converge into a network that controls the rate of chronological aging in *S. cerevisiae*. This network coordinates longevity-defining cellular processes named in the boxes. Activation arrows and inhibition bars denote pro-aging processes (displayed in blue color) or anti-aging

processes (shown in red color). Pro-aging or anti-aging signaling pathways and protein kinases are displayed in blue or red color, respectively. Please see text for additional details. Abbreviations: ATG, autophagy; PKA, protein kinase A; PKH1/2, Pkb-activating kinase homologs 1 and 2; Rim15, an anti-aging protein kinase; Sch9, a pro-aging protein kinase; SNF1, sucrose non-fermenting protein 1; TORC1, the target of rapamycin complex 1.

1.3 Spatiotemporal organization and regulation of cellular processes controlled by the longevity signaling network define yeast chronological lifespan

Recent findings provided evidence that specific cellular processes occurring early in the life of a yeast cell, before its proliferation in a liquid medium is arrested, define the chronological lifespan (CLS) of this cell [15, 17, 32, 55, 59, 62, 87, 98, 100-102, 117-134]. These cellular processes are under the control of the longevity regulation signaling network schematically depicted above (Figure 1.2). These cellular processes are known for their essential roles in metabolism, growth and division, stress protection, cellular homeostasis maintenance, survival and regulated death of chronologically aging yeast [15, 17, 32, 55, 59, 62, 87, 98, 100-102, 117-134].

1.3.1 Age-related changes in the concentrations of certain intermediates in glycolytic and non-glycolytic pathways of carbohydrate metabolism define the CLS of *S. cerevisiae*

Longevity of a chronologically aging yeast cell depends on the relative rates of coordinated metabolite flows through glycolytic and non-glycolytic pathways of carbohydrate metabolism early in life (i.e., when it still actively grows and divides) [6, 15, 32, 42, 43, 45, 59, 98, 123, 126-129, 131, 135, 140-142]. It has been shown that specific mutations, diets or chemicals can prolong yeast CLS because they alter such coordinated metabolite flows in yeast that still actively proliferates [32, 42, 43, 45, 128, 129, 131, 135, 139, 140-142]. Based on these findings, our laboratory proposed a model to explain the mechanistic links that may exist between glycolytic and non-glycolytic pathways of carbohydrate metabolism, longevity-defining cellular processes, and the CLS of yeast. This model is shown in Figure 1.3.

The available data indicate that glucose (the only exogenous carbon source used in most laboratory studies of yeast chronological aging) enters both glycolysis and the pentose phosphate pathway (PPP) in yeast cells that actively proliferate during logarithmic (L) growth phase (Figure 1.3) [32, 34, 40, 59, 128]. During the L phase, the glycolytic pathway yields pyruvate, whereas the

PPP produces ribose-5-phosphate and NADPH (Figure 1.3). Ribose-5-phosphate is consumed for nucleic acid synthesis while NADPH provides reducing equivalents needed to synthesize fatty acids, sterols and amino acids (Figure 1.3) [124, 126, 128, 143]. NADPH produced in the PPP also donates electrons to the thioredoxin and glutathione reductase systems, both of which are indispensable for the maintenance of cellular redox homeostasis (Figure 1.3) [126, 128, 143]. The thioredoxin and glutathione reductase systems are essential for the ability of a caloric restriction (CR) diet to prolong yeast CLS [126, 128]. This is because these two NADPH-supported systems protect many thiol-containing proteins in the cytosol, nucleus and mitochondria from oxidative damage, especially in yeast cells that advance through the L phase of cell culturing (Figure 1.3) [126, 128].

A culture of chronologically aging yeast exits the L phase of rapid growth and enters the diauxic (D) and then post-diauxic (PD) phases of slow growth when it consumes glucose exogenously added to the medium at the beginning of cell culturing [30, 32, 34, 138]. Pyruvate, the final product of the glycolytic glucose metabolism, can enter several carbon metabolism pathways during D and PD phases of culturing. As described below, all these pathways yield metabolites playing essential roles in regulating cellular processes that define the longevity of chronologically aging yeast [6, 15, 32, 42, 43, 45, 59, 98, 119, 123, 127-129, 131, 135, 136, 138, 139, 140].

One of these pathways of carbon metabolism is fermentation, which generates ethanol and/or acetic acid (depending on the type of growth medium and aeration conditions used for cell culturing) in the cytosol of yeast cells that advance through D and PD phases of culturing (Figure 1.3) [6, 15, 42, 43, 45, 32, 119, 135, 138, 140]. The steady-state concentration of ethanol is defined by the relative enzymatic activities of Adh1p (an enzyme involved in ethanol synthesis) and Adh2p (an enzyme involved in the oxidative degradation of ethanol) (Figure 1.3) [15, 119, 135, 138, 140]. The steady-state concentration of ethanol is an essential contributor to longevity regulation of chronologically aging yeast because this product of glucose fermentation inhibits the β-oxidation of fatty acids in peroxisomes, which is an anti-aging process that extends yeast CLS (Figure 1.3) [32, 110].

Another product of glucose fermentation in the cytosol of yeast cells that advance through D and PD phases of culturing is acetic acid, a product of the Ald6p-dependent acetaldehyde dehydrogenase reaction. The steady-state concentration of acetic acid contributes to longevity

regulation of chronologically aging yeast because acetic acid promotes an age-related mode of apoptotic programmed cell death (PCD), a process that shortens yeast CLS (Figure 1.3) [15, 42, 43, 45, 141]. Acetic acid is not the only product of the Ald6p-dependent acetaldehyde dehydrogenase reaction. NADPH is another product of this enzymatic reaction (Figure 1.3) [124, 128, 143]. Like the NADPH generated in the PPP, NADPH produced in the Ald6p-dependent reaction allows the thioredoxin and glutathione reductase systems to protect many thiol-containing proteins from oxidative damage. Because such NADPH-driven protection enables the maintenance of cellular redox homeostasis, it is an essential longevity assurance process (Figure 1.3) [126, 128, 143].

Acetic acid formed in the cytosol as a product of glucose fermentation can be further converted to acetyl-CoA in an enzymatic reaction catalyzed by Acs2p, a protein that resides in the cytosol and nucleus (Figure 1.3) [139, 143]. A nuclear pool of acetyl-CoA generated in the Acs2p-dependent reaction can be used for the hyperacetylation of histone H3 [139]. Because such hyperacetylation selectively inhibits transcription of the ATG5, ATG7, ATG11 and ATG14 genes (all of which encode proteins involved in the anti-aging process of autophagy), it shortens yeast CLS (Figure 1.3) [139].

In addition to being fermented to ethanol and/or acetic acid, glucose fermentation can also yield glycerol in yeast cells that advance through D and PD phases of culturing [119]. It has been proposed that glucose fermentation to glycerol in these cells and glycerol itself may extend yeast CLS through three different mechanisms. First, glucose fermentation to glycerol slows the flow of metabolites into glucose fermentation to ethanol and/or acetic acid, thus lowering the concentrations of these two glucose fermentation products exhibiting strong pro-aging potential (Figure 1.3) [42, 119]. Because glucose fermentation to glycerol decelerates the formation of ethanol and acetic acid, it is called a “phantom carbon source” [119]. Second, glycerol is known as a potent inducer of yeast cell resistance to chronic oxidative, thermal and osmotic stresses [119]. Such stress-protecting ability of glycerol may also contribute to the extension of yeast CLS (Figure 1.3) [119]. Third, it has been proposed that glucose fermentation to glycerol may help to maintain an NAD+/NADH ratio at a level that allows the extension of yeast CLS (Figure 1.3) [119].

Pyruvate, the final product of the glycolytic glucose metabolism, can also enter the gluconeogenesis pathway that yields glucose (Figure 1.3) [32, 101, 125, 140]. The pool of glucose formed gluconeogenetically can be used for the synthesis of trehalose (Figure 1.3) [32, 101, 125,

140]. In yeast cells that advance through the D and PD phases of culturing, trehalose prolongs yeast CLS because it enhances the maintenance of cellular proteostasis (see next section of the Thesis) [32, 101]. In contrast, in yeast cells that enter the ST phase of culturing, trehalose shortens yeast CLS because it interferes with the refolding of misfolded, partially folded and unfolded cellular proteins (see next section of the Thesis) [32, 101].

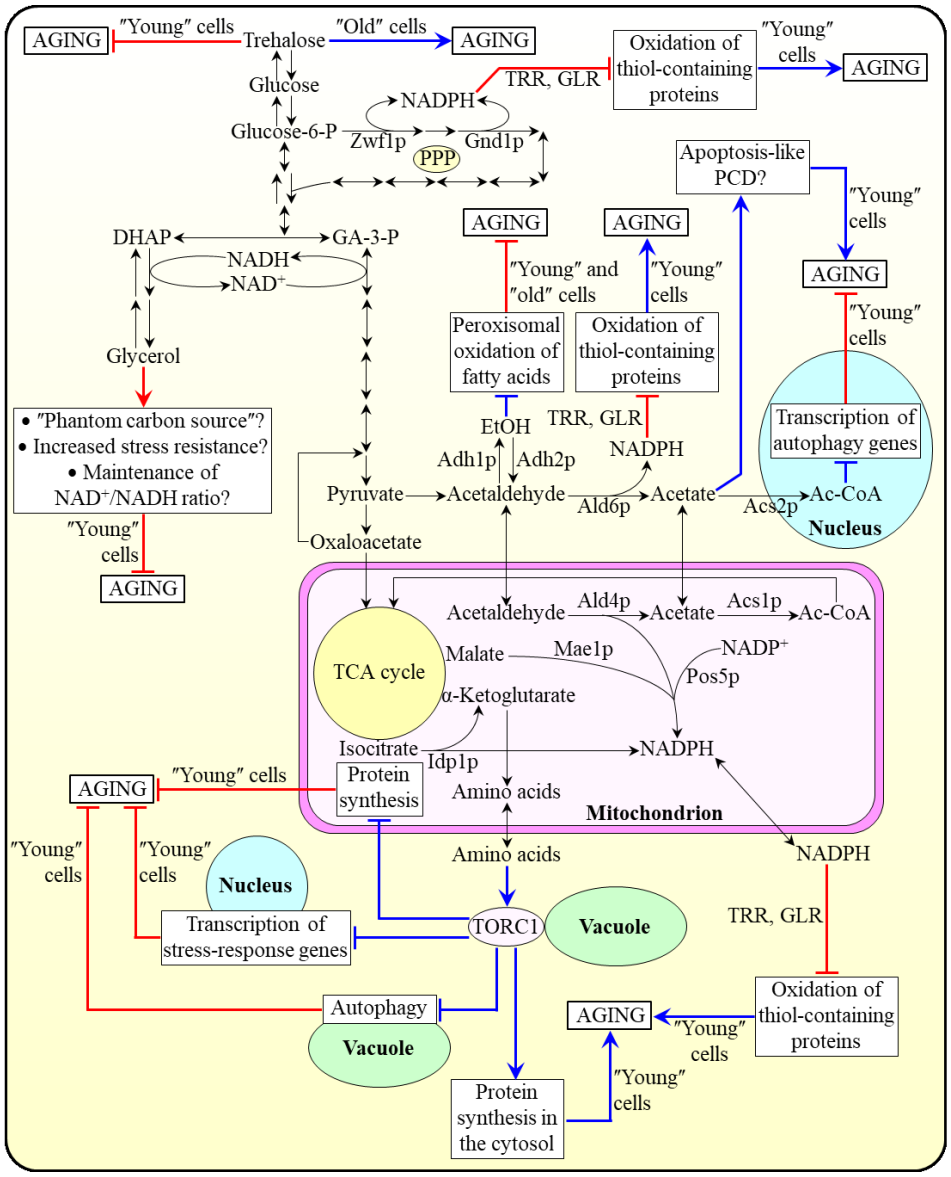

Figure 1.3. The longevity of chronologically aging *S. cerevisiae* depends on the intensity of metabolic flow through glycolytic and non-glycolytic pathways of carbohydrate metabolism. A model shown here explains how glycolytic and non-glycolytic pathways of glucose metabolism influence specific cellular processes essential for longevity assurance in chronologically "young" (proliferating) and chronologically "old" (non-proliferating) yeast. Activation arrows and inhibition bars signify pro-aging processes (shown in blue color) or anti-aging processes (presented in red color). Please see text for additional details. Ac-CoA, acetyl-CoA; DHAP,

dihydroxyacetone phosphate; EtOH, ethanol; GA-3-P, glyceraldehyde-3-phosphate; GLR, glutathione reductase; PCD, programmed cell death; TCA, tricarboxylic acid; TORC1, the target of rapamycin complex 1; TRR, thioredoxin reductase.

In addition to the essential roles that pyruvate, acetaldehyde and acetic acid play in regulating yeast longevity by affecting some cellular processes in the cytosol, they also define yeast CLS because they influence several longevity-defining processes confined to or coordinated by mitochondria (Figure 1.3).

As described below, the mitochondrial tricarboxylic acid (TCA) cycle is the central hub coordinating these processes.

The malate and isocitrate intermediates of the TCA cycle are the substrates for the Mae1p- and Idp1p-dependent (respectively) synthesis of NADPH in mitochondria (Figure 1.3) [124, 128, 143]. The acetaldehyde and $NADP^+$ pools in mitochondria also serve as the substrates for NADPH synthesis in these organelles via Ald4p-dependent and Pos5p-dependent (respectively) reactions (Figure 1.3) [124, 128, 143]. After being formed in mitochondria, NADPH is exported into the cytosol where it can be used (akin to the cytosolic pool of NADPH generated in the PPP and the Ald6p-dependent reaction) to help the thioredoxin and glutathione reductase systems in sustaining cellular redox homeostasis and extending yeast CLS (see above in my Thesis).

Oxaloacetate and α-ketoglutarate (two other intermediates of the mitochondrial TCA cycle) are the substrates for the synthesis of amino acids in mitochondria (Figure 1.3) [124, 143, 144]. Following their synthesis in mitochondria and exit into the cytosol, some of these amino acids (i.e., aspartate, asparagine, glutamate and glutamine) stimulate the protein kinase activity of TORC1 on the surface of vacuoles (Figure 1.3) [55, 61, 94, 96, 144-146]. After being stimulated by the amino acids, TORC1 shortens yeast CLS because it phosphorylates and alters the activities of many proteins implicated in longevity-defining cellular processes (Figure 1.3). The following four longevity-shortening effects of such TORC1-dependent protein phosphorylation are known: 1) the pro-aging process of protein synthesis in the cytosol is activated, 2) the anti-aging process of autophagy in vacuoles is inhibited, 3) the anti-aging process of transcription of many nuclear genes involved in stress protection is also inhibited, and 4) the anti-aging process of mitochondrial protein synthesis is inhibited as well (Figure 1.3) [53, 61, 62, 94, 96, 118, 144-146].

In sum, the intensity of metabolic flow through glycolytic and non-glycolytic pathways of carbohydrate metabolism defines the longevity of chronologically aging *S. cerevisiae* because it

orchestrates many pro-aging and anti-aging cellular processes in various cellular locations. The relative impacts of the critical intermediates of these metabolic pathways in regulating longevity of chronologically aging budding yeast remain to be determined.

1.3.2 The intracellular concentration of trehalose is an essential contributor to longevity regulation in *S. cerevisiae* because trehalose controls cellular protein homeostasis

A body of evidence indicates that trehalose is indispensable for sustaining cellular protein homeostasis (proteostasis) because this non-reducing disaccharide regulates protein folding, misfolding, unfolding, refolding, oxidative damage, solubility and aggregation *in vivo* and *in vitro* [101, 147-151].

The involvement of trehalose in cellular proteostasis maintenance underlies its essential roles in regulating the longevity of chronologically aging budding yeast. It needs to be emphasized that trehalose regulates yeast CLS differently in chronologically "young" and chronologically "old" yeast (Figure 1.4).

Trehalose has an anti-aging role in chronologically "young" yeast cells that advance through the D and PD phases of culturing because it is present at the concentrations that elicit the following three effects on cellular proteostasis. First, trehalose binding to newly formed cellular proteins increases the stability of their native folding conformations and slows their conversion into abnormally folded and/or unfolded protein forms (Figure 1.4) [32, 101]. Second, trehalose suppresses the formation of insoluble protein aggregates because it protects the extensive regions of hydrophobic side chain amino acids from the aqueous environment; such regions can be found in misfolded, partially folded and unfolded proteins (Figure 1.4) [32, 101]. Third, trehalose indirectly inhibits the aggregation of oxidatively damaged proteins because it prevents the oxidative damage of abnormally folded proteins (Figure 1.4) [32, 101].

Trehalose has a pro-aging role in chronologically "old" yeast cells that enter the ST (non-proliferative) phase of culturing because it suppresses the chaperone-assisted refolding of misfolded, partially folded and unfolded proteins (Figure 1.4) [101, 152-155]. Such a pro-aging role of trehalose in chronologically "old" yeast is due to its high affinity to exposed stretches of hydrophobic amino acid residues that are abundant in aberrantly folded proteins. Because trehalose binds to these stretches of hydrophobic amino acid residues, it prevents their interaction with molecular chaperones needed for protein folding (Figure 1.4) [101, 152-155].

In sum, these findings provide evidence that, depending on the trehalose concentration in chronologically aging yeast cells, it can play a dual role in regulating longevity.

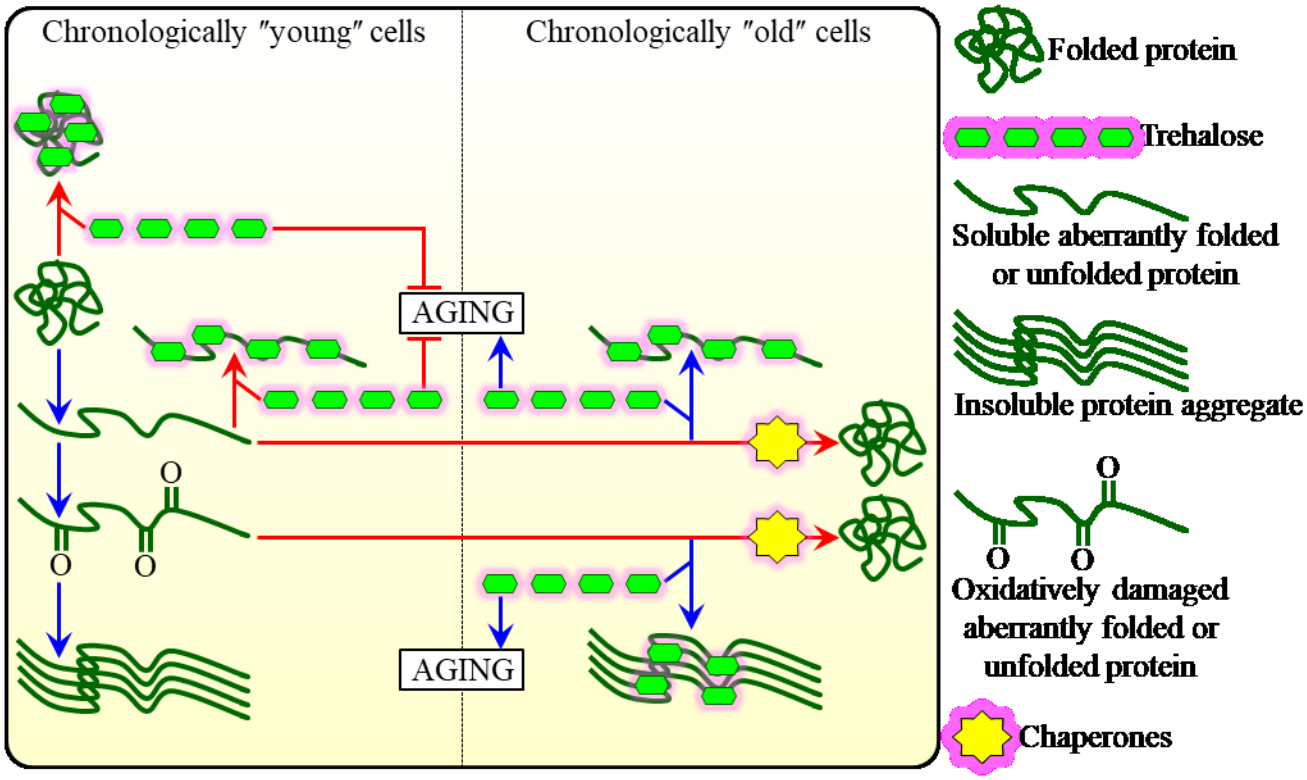

Figure 1.4. Trehalose contributes to the chronological aging of *S. cerevisiae* because trehalose controls cellular proteostasis. A model for molecular mechanisms through which trehalose controls the process of cellular aging in yeast because it regulates protein folding, misfolding, unfolding, refolding, oxidative damage, solubility and aggregation. Trehalose controls cellular aging differently in chronologically "young" and chronologically "old" yeast. Activation arrows and inhibition bars signify pro-aging processes (shown in blue color) or anti-aging processes (presented in red color). Please see text for additional details.

1.3.3 Mitochondrial functionality and reactive oxygen species (ROS) production in mitochondria contribute to longevity regulation in *S. cerevisiae* because they orchestrate many cellular processes outside of these organelles

Growing evidence supports the notion that the functional state of mitochondria and their ROS producing capacity in chronologically "young" yeast cells advancing through D and PD phases of culturing define yeast CLS [15, 32, 41, 62, 87, 102, 103, 110, 117, 118, 120-122, 129-132, 134, 156-158]. Two major aspects of mitochondrial functionality contribute to longevity regulation in budding yeast. They include the capability of electron transport chain (ETC) coupled

to ATP synthesis [15, 32, 62, 87, 102, 103, 110, 117, 118, 125, 133, 134, 157] and the value of mitochondrial membrane potential across the inner mitochondrial membrane (IMM), which depends on the efficiency of the ETC-dependent proton exchange between the matrix to the intermembrane space (IMS) [15, 32, 62, 87, 102, 110, 118, 122]. Mitochondrial ROS producing capacity, which also contributes to longevity regulation in budding yeast, is defined by the extent of coupling between the ETC and oxidative phosphorylation (OXPHOS) system in mitochondria [62, 118].

Based on the effects on the mitochondrial ETC, OXPHOS system and ROS production of certain longevity-extending mutations, dietary regimens and chemicals in chronologically "young" yeast cells [15, 32, 41, 62, 87, 102, 103, 110, 117, 118, 120-122, 125, 130-134, 156-158], a model can be proposed to explain how coupled mitochondrial respiration, mitochondrial membrane potential maintenance and mitochondrial ROS production in these cells define yeast CLS. The model is shown in Figure 1.5.

According to the model, the capacities of the above mitochondrial processes in chronologically "young" yeast cells cultured under non-CR conditions on 2% glucose are below a critical threshold; as a result, these cells acquire and sustain a pro-aging pattern of longevity-defining processes (Figure 1.5; these capacities are shown in green) [32, 120, 125, 133, 134]. The model also posits that the capacities of these mitochondrial processes in chronologically "young" yeast cells cultured under so-called "mild" CR conditions on 0.5% glucose are above the critical threshold; because of that, these cells develop and maintain an anti-aging pattern of longevity-defining processes taking place not only inside of mitochondria but also outside of these organelles (Figure 1.5; these capacities are shown in red color) [32, 62, 87, 102, 103, 110, 118, 122, 125, 134]. The model further suggests that the capacities of coupled mitochondrial respiration, mitochondrial membrane potential maintenance and mitochondrial ROS production significantly exceed the critical threshold in chronologically "young" yeast cells cultured under so-called "strong" CR conditions on 0.2% glucose; consequently, the longevity of these cells is lower than that of cells cultured under mild CR conditions (Figure 1.5; these capacities are shown in blue color) [32, 102, 103, 110].

Five major longevity regulation pathways control the capacities of coupled mitochondrial respiration, mitochondrial membrane potential maintenance and mitochondrial ROS production in chronologically "young" yeast cells (Figure 1.5). Each of these pathways is described below. The

nutrient-responsive and energy-sensing TOR signaling pathway uses the rapamycin-sensitive protein kinase Tor1p to suppress the mitochondrial synthesis of the OXPHOS enzymes encoded by mitochondrial DNA (mtDNA) (Figure 1.5) [62, 110, 118, 122, 125]. A CR pathway inhibits Tor1p and also operates in a Tor1p-independent manner to sustain the coupled mitochondrial respiration, mitochondrial membrane potential and mitochondrial ROS at an optimal for longevity extension level in chronologically "young" yeast cells (Figure 1.5) [15, 32, 62, 110, 118, 119, 122, 125, 138]. The mitochondrial base-excision repair enzyme Ntg1p orchestrates a pathway for the maintenance of mitochondrial genome integrity (Figure 1.5) [158]. The receptor protein Atg32p on the mitochondrial surface for selective autophagic degradation of aged, dysfunctional or damaged mitochondria is a crucial player in the mitophagy pathway of mitochondrial quality control (Figure 1.5) [87]. Exogenously added lithocholic acid (LCA) enters yeast cells [102, 103], amasses mainly in the IMM and initiates a pathway for specific, longevity-extending remodeling of the mitochondrial membrane lipidome (Figure 1.5) [102, 103]. The TOR and CR pathways [15, 32, 62, 110, 118, 119, 122, 125, 138], as well as the TOR and Ntg1p pathways [158], partially overlap and act together to orchestrate coordinated control of the coupled mitochondrial respiration, mitochondrial membrane potential maintenance and mitochondrial ROS production in chronologically "young" yeast cells (Figure 1.5). This is in contrast to a CR pathway and an LCA-dependent pathway for mitochondrial membrane lipidome remodeling [102, 103], as well as with a CR pathway and the Ntg1p-dependent pathway [158]; these pathways do not overlap and act independently to elicit a synergistic stimulation of the above mitochondrial processes.

The efficiency of the coupled mitochondrial respiration, the value of mitochondrial membrane potential and the concentration of mitochondrially produced ROS in chronologically "young" yeast cells control many "downstream" longevity-defining processes in several cellular locations (Figure 1.5). These processes are essential contributors to longevity regulation in chronologically aging yeast and are described below. One of the downstream processes is the maintenance of the homeostasis of trehalose, which (as described above in my Thesis) sustains cellular proteostasis in both chronologically "young" and chronologically "old" yeast cells (Figure 1.5) [32, 101]. The maintenance of the high concentrations of glycogen, a reserve carbohydrate, in chronologically "young" and "old" yeast cells under CR conditions [32] is another downstream process (Figure 1.5). The maintenance of neutral lipid homeostasis within the endoplasmic reticulum (ER) and lipid droplets (LD) [32, 110, 159, 160] is also a downstream process (Figure

1.5). Downstream processes include fatty acid oxidation in peroxisomes (Figure 1.5) [32, 110, 159, 160]

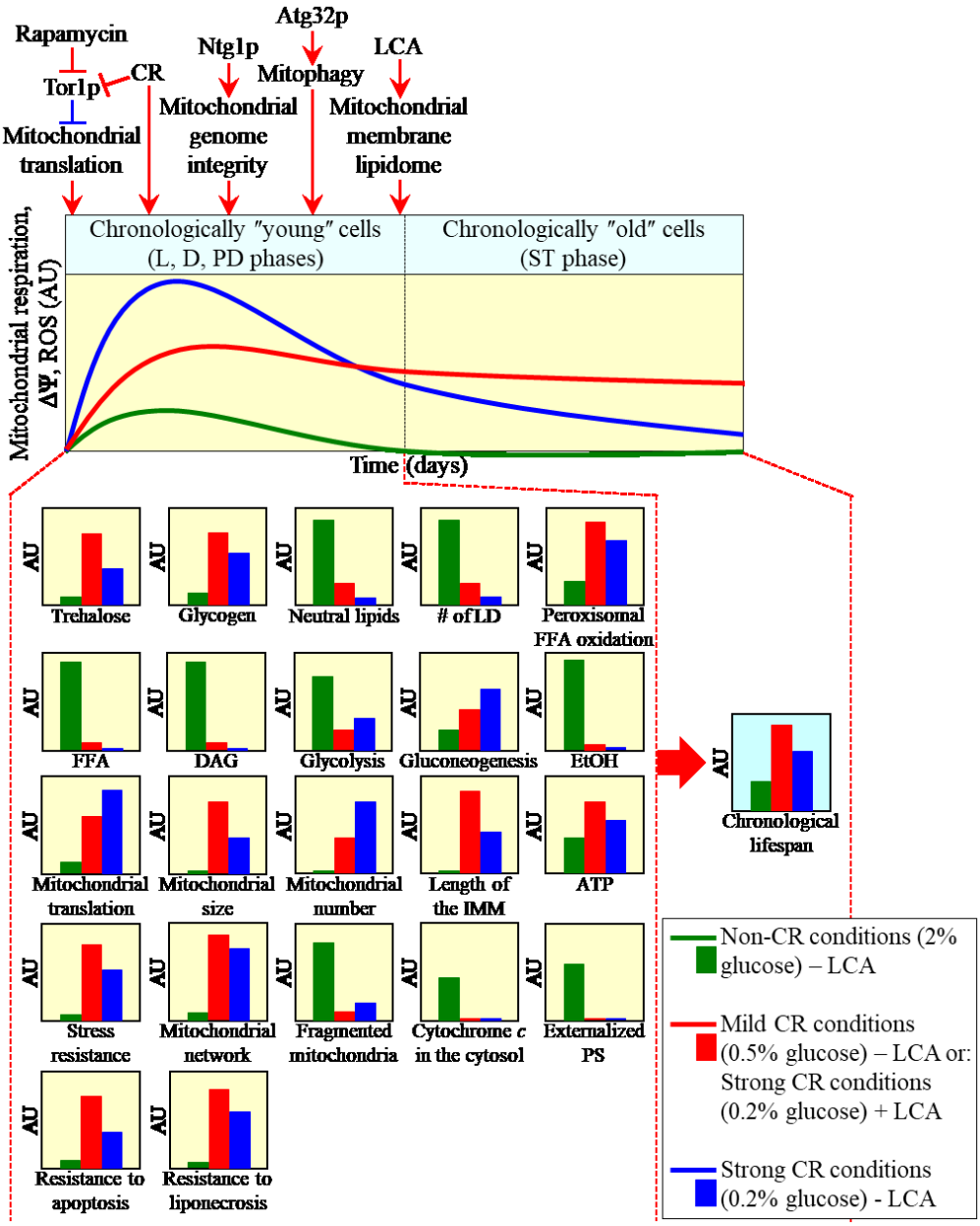

Figure 1.5. A model for how the coupled mitochondrial respiration, mitochondrial membrane potential maintenance and mitochondrial ROS production in chronologically "young" yeast cells that advance through D and PD phases of culturing define their CLS. Activation arrows and inhibition bars denote pro-aging processes (shown in blue color) or anti-aging processes (shown in red color). Please see text for additional details. CR, caloric restriction; D, diauxic growth phase; DAG, diacylglycerol; EtOH, ethanol; FFA, non-esterified ("free") fatty acids; IMM, inner mitochondrial membrane; L, logarithmic growth phase; LCA, lithocholic acid; LD, lipid droplet; PD, post-diauxic growth phase; PS, phosphatidylserine; ROS, reactive oxygen species; ST, stationary growth phase; ΔΨm, the electrochemical potential across the IMM.

Another downstream process is the maintenance of the homeostasis of non-esterified ("free") fatty acids (FFA) and diacylglycerol (DAG), both of which cause an age-related form of the liponecrotic PCD in chronologically aging yeast (Figure 1.5) [32, 110, 161]. Downstream processes include the regulation of intracellular ethanol concentration by coordinating the relative rates of glycolysis and gluconeogenesis (see above in my Thesis) (Figure 1.5) [32, 110]. The mitochondrial translation is a downstream process that contributes to longevity assurance in chronologically aging yeast (Figure 1.5) [32, 62, 118, 122]. Another downstream process is the maintenance of a proper balance between the fusion of mitochondria and their fission; this process is an essential contributor to preserving mitochondrial size and number, sustaining the extended length of mitochondrial cristae, and synthesizing elevated levels of ATP (Figure 1.5) [32, 87, 102, 110]. Downstream processes include the establishment and maintenance of cell resistance to chronic oxidative, thermal and osmotic stresses (Figure 1.5) [15, 32, 62, 100, 110, 122, 125, 138]. Another downstream process is an age-related commitment to apoptotic PCD through the fragmentation of a tubular mitochondrial network, the exit of cytochrome c from fragmented mitochondria into the cytosol and phosphatidylserine (PS) externalization within the plasma membrane (Figure 1.5) [32, 110]. Among downstream processes are also the development and maintenance of cell resistance to age-related modes of apoptotic and liponecrotic PCD in response to a rise in the concentrations of hydrogen peroxide (a form of ROS) or palmitoleic acid, respectively (Figure 1.5) [32, 100, 110, 161].

Mitochondrially generated ROS in chronologically "young" yeast cells contribute to longevity regulation via two mitochondria-to-nucleus retrograde signaling pathways [95, 99, 130, 132, 158, 162]. One of these pathways of retrograde signaling consists in the ability of mitochondrially generated ROS, if present in hormetic concentrations, to activate transcriptional factors Gis1p, Msn2p and Msn4p in the nucleus; once activated by ROS, Gis1p, Msn2p and Msn4p stimulate transcription of many genes essential for stress resistance, stationary phase survival, carbohydrate metabolism, nutrient sensing and longevity assurance [95, 99, 162]. In another pathway of retrograde signaling, hormetic concentrations of mitochondrially produced ROS promote the ability of the DNA damage response (DDR) kinase Tel1p to phosphorylate and activate the DDR kinase Rad53p [158]. After being activated by the Tel1p-dependent phosphorylation, Rad53p phosphorylates and inactivates the histone demethylase Rph1p bound to

sub-telomeric chromatin regions [158]. The resulting inactivation of Rph1p suppresses the transcription of sub-telomeric chromatin regions, lowers telomeric DNA damage and eventually prolongs the longevity of chronologically aging yeast [158].

In sum, these findings imply that the coupled mitochondrial respiration, mitochondrial membrane potential maintenance and mitochondrial ROS production in chronologically "young" cells that advance through D and PD phases of culturing play essential roles in regulating longevity of chronologically aging yeast.

1.3.4 Peroxisomal protein import in chronologically aging yeast affects the longevity-defining processes outside of peroxisomes, thus contributing to longevity regulation in *S. cerevisiae*

The import of proteins into the peroxisome of a eukaryotic cell is known to depend on the cytosolic shuttling receptor Pex5p for proteins containing the peroxisomal targeting signal type 1 (PTS1) and on the cytosolic shuttling receptor Pex7p for proteins containing PTS2 [163-165]. It has been shown that the efficiency with which proteins are imported into the peroxisome in yeast and other eukaryotes declines with the chronological age of their cells [59, 123, 166, 167]. It has also been shown that the efficiency of peroxisomal protein import influences two types of cellular processes, namely: 1) fatty acid oxidation, hydrogen peroxide formation and decomposition, and anaplerotic metabolism in the peroxisome and 2) the unidirectional and bidirectional types of flow of soluble metabolites and lipids between the peroxisome and other cellular compartments [55, 59, 123, 127, 168-172]. The available data also indicate that the unidirectional and bidirectional communications between the peroxisome and several other cellular compartments contribute to longevity regulation because they affect some longevity-defining processes taking place in these other compartments [55, 59, 98, 123, 127, 168-173].

Based on these findings, our laboratory proposed a model to explain the mechanistic links that may exist between the age-related efficiency of peroxisomal protein import, peroxisomal functionality, communications between peroxisomes and other cellular compartments, and longevity of chronologically aging *S. cerevisiae*. This model is shown in Figure 1.6.

According to the model, three groups of proteins are efficiently imported into peroxisomes within chronologically "young" yeast cells that advance through D and PD phases of culturing. These three groups of proteins are described below. First, enzymes that catalyze the decomposition

of hydrogen peroxide and other ROS within the peroxisome; these enzymes include the catalase Cta1p and peroxiredoxin Pmp20p [55, 59, 110, 123, 159, 160, 174]. Second, enzymes involved in the β-oxidation of fatty acids to acetyl-CoA within the peroxisome; these enzymes include the fatty-acyl coenzyme A oxidase Fox1p, the 3-hydroxyacyl-CoA dehydrogenase and enoyl-CoA hydratase Fox2p, and the 3-ketoacyl-CoA thiolase Fox3p [55, 59, 110, 123, 159, 160, 174]. Third, enzymes catalyzing the anaplerotic conversion of acetyl-CoA to citrate and acetyl-carnitine to facilitate the replenishment of TCA cycle intermediates destined for mitochondria; these enzymes include the citrate synthase Cit2p and acetyl-carnitine synthase Cat2p (respectively) [55, 59, 110, 123, 159, 160, 174].

The model further posits that the efficient peroxisomal import of all these enzymes within chronologically "young" yeast cells promotes three groups of longevity-extending processes confined to peroxisomes and other cellular compartments. These three groups of longevity-extending processes are described below. First, the extent of oxidative damage to peroxisomal proteins and membrane lipids declines (Figure 1.6) [32, 55, 59, 123, 127, 160]. Second, so-called stress-response hormesis is established because chronologically "young" yeast cells can sustain peroxisomally produced hydrogen peroxide at a threshold concentration that is insufficient to elicit oxidative damage to cellular molecules but sufficient to activate transcription of nuclear genes essential for cell survival (Figure 1.6) [32, 55, 59, 123, 127, 160]. Third, the TCA cycle and ETC in mitochondria are stimulated to help chronologically "young" cells in sustaining mitochondrially produced ROS at a non-toxic level that can promote transcription of nuclear genes coding for many stress-protecting proteins (Figure 1.6) [32, 55, 59, 123, 127, 160].

The model also envisions that the peroxisomal import of the polyamine oxidase Fms1p, an enzyme involved in the synthesis of the natural polyamine called spermidine [111, 175], may contribute to the ability of the peroxisome to stimulate pro-longevity processes outside of this organelle (Figure 1.6). Spermidine prolongs the longevity of chronologically aging yeast because it activates autophagy, a pro-longevity cytoprotective process of degrading damaged and dysfunctional macromolecules and organelles within the vacuole [83, 84, 176]. It has been shown that the intracellular concentration of spermidine in chronologically "young" yeast is substantially higher than that in chronologically "old" yeast [83]. Therefore, the model suggests that Fms1p import into peroxisomes of chronologically "young" yeast is more efficient than that into peroxisomes of chronologically "old" yeast (Figure 1.6). As a result, the chronologically "young"

yeast cells can develop and maintain a cellular pattern that allows them to age slower and survive longer because they more proficiently eliminate damaged and dysfunctional macromolecules and organelles (Figure 1.6).

According to the model, the Pex5p- and Pex7p-dependent peroxisomal import of Cta1p, Pmp20p, Fox1p, Fox2p, Fox3p, Cit2p, Cat2p and Fms1p deteriorates within chronologically "old" yeast cells (Figure 1.6). Because of that, four groups of longevity-shortening processes are accelerated in these cells. These four groups of longevity-shortening processes are described below. First, the intracellular concentration of peroxisomally produced hydrogen peroxide is increased above a cytotoxic level, thereby promoting the oxidative damage to cellular macromolecules (Figure 1.6) [32, 55, 59, 98, 110, 123, 127, 136, 159-161, 177-183]. Second, the efficiency of peroxisomal oxidation of fatty acids originated from the neutral lipids triacylglycerols (TAG) that are synthesized in the ER and deposited within LD is decreased; as a result, the concentrations of FFA and DAG rise above a critical threshold to cause an age-related form of liponecrotic PCD (Figure 1.6) [32, 55, 59, 98, 110, 123, 127, 136, 159-161, 177-183]. Third, the replenishment of TCA cycle intermediates in peroxisomes intended for the TCA cycle in mitochondria deteriorates; because of that, the mitochondrial ETC and electrochemical potential across the IMM decline, mitochondrial network undergoes fragmentation, cytochrome *c* and other pro-apoptotic proteins exit fragmented mitochondria, and an age-related form of apoptotic PCD is stimulated (Figure 1.6) [32, 55, 59, 98, 110, 123, 127, 136, 159-161, 177-183]. Fourth, the peroxisome-dependent synthesis of spermidine is decreased, thus attenuating the pro-longevity process of autophagy (Figure 1.6) [83, 84, 111,175, 176].

The model also reflects that chronologically "young" and "old" yeast cells cultured in a nutrient-rich medium under longevity-shortening non-CR conditions amass ethanol, a product of glucose fermentation [32, 136]. Ethanol has been shown to slow down Fox1p-, Fox2p- and Fox3p-dependent peroxisomal oxidation of FFA because it represses the synthesis of Fox1p, Fox2p and Fox3p (Figure 1.6) [174, 184]. The ethanol-dependent decline in peroxisomal oxidation of FFA under non-CR conditions elicits the following two responses. First, it suppresses the pro-longevity process of the replenishment of TCA cycle intermediates intended for mitochondria because it decelerates peroxisomal oxidation of FFA to acetyl-CoA, thus weakening the anaplerotic conversion of acetyl-CoA to citrate and acetyl-carnitine (Figure 1.6) [59, 123, 174, 184]. Second, it promotes an age-related form of liponecrotic PCD because it causes a buildup of the non-

oxidized FFA and DAG inducers of such PCD (Figure 1.6) [32, 59, 98, 110, 123, 136, 161]. None of these effects of ethanol has been observed in chronologically "young" or chronologically "old" yeast cells cultured under longevity-extending CR conditions because these cells do not amass ethanol (Figure 1.6) [32, 59, 98, 110, 123, 136, 161]. Thus, the inability of these cells to accumulate ethanol is an essential contributing factor to yeast CLS extension by CR.

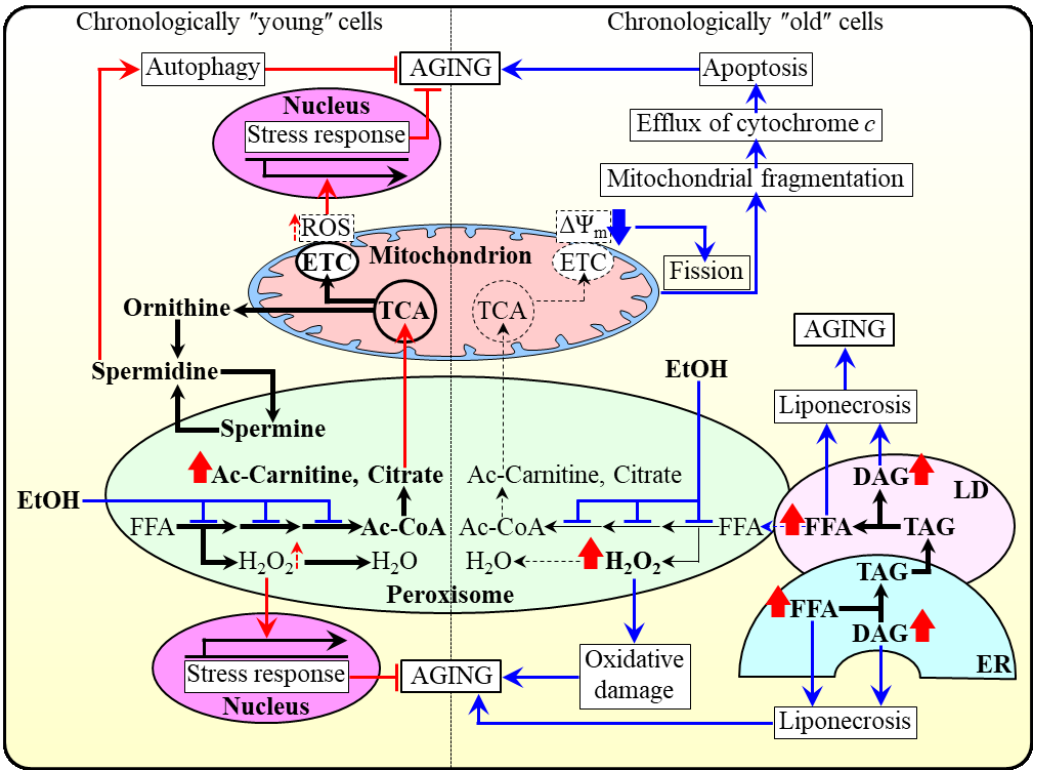

Figure 1.6. A model for how the age-related efficiency of peroxisomal protein import in chronologically aging yeast cells define their CLS by influencing a distinct set of processes inside and outside of peroxisomes. Activation arrows and inhibition bars signify pro-aging processes (shown in blue color) or anti-aging processes (shown in red color). Please see text for additional details. Ac-Carnitine, acetyl-carnitine; Ac-CoA, acetyl-CoA; DAG, diacylglycerol; ER, endoplasmic reticulum; ETC, electron transport chain; EtOH, ethanol; FFA, non-esterified ("free") fatty acids; LD, lipid droplet; ROS, reactive oxygen species; TAG, triacylglycerols; TCA, tricarboxylic acid cycle; ΔΨm, the electrochemical potential across the inner mitochondrial membrane.

Collectively, these findings provide evidence that the upregulated peroxisomal protein import in chronologically "young" cells that advance through D and PD phases of culturing play essential roles in prolonging the longevity of chronologically aging yeast.

1.4 Spatiotemporal dynamics of intercompartmental communications define the

chronology of cellular aging in yeast

New evidence implies that various organelle-organelle and organelle-cytosol communications play essential roles in chronological aging of *S. cerevisiae*. The molecular mechanisms underlying the vital roles of intercompartmental communications in yeast chronological aging have begun to emerge. The scope of this section of my Thesis is to analyze recent progress in understanding such mechanisms critically. My analysis suggests a model for how temporally and spatially coordinated movements of specific metabolites between various cellular compartments impact yeast chronological aging. In my model, diverse changes in these key metabolites are restricted to critical longevity-defining periods of chronological lifespan (CLS). In each of these periods, a limited set of proteins responds to such changes of the metabolites by altering the rate and efficiency of a particular cellular process essential for longevity regulation. Spatiotemporal dynamics of alterations in these longevity-defining cellular processes orchestrate the development and maintenance of a pro- or anti-aging cellular pattern.

Recent studies have revealed that various intercompartmental communications (i.e., organelle-organelle and organelle-cytosol) play essential roles in chronological aging of yeast cultured in media with glucose as the only carbon source [55, 98, 107, 123]. A model for how such communications impact yeast chronological aging is depicted schematically in Figure 1.7. The model includes the notion that the longevity-defining intercompartmental communications involve unidirectional and bidirectional movements of a distinct set of metabolites between mitochondria and the cytosol, mitochondria and peroxisomes, mitochondria and the nucleus, peroxisomes and the nucleus, mitochondria and vacuoles, the ER and the plasma membrane (PM), the ER and the cytosol, the PM and the cytosol, the PM and vacuoles, the ER and LD, and LD and peroxisomes (Figure 1.7). The intracellular concentrations of such metabolites and/or the rates of their movement between cellular compartments undergo age-related changes. In the proposed model, different changes of the key metabolites are temporally restricted to several longevity-defining periods; the term “checkpoints” has been coined to describe these critical periods in yeast CLS (Figure 1.7). [17, 100, 101, 106]. Most of these checkpoints occur early in the life of chronologically aging yeast cells, during D and PD growth phases. Some of the checkpoints are late-life checkpoints that exist in the non-proliferative ST phase of culturing. At each of these checkpoints, the changes of the key metabolites are detected by a distinct set of checkpoint-specific proteins called “master regulators” [17, 185]. The model further posits that each of these master

regulators can respond to a change of the detected key metabolite by altering the rate and efficiency of a certain cellular process essential for longevity regulation (Figure 1.7). By establishing the rates and efficiencies of different longevity-defining cellular processes throughout the CLS, the checkpoint-specific master regulators set up a pro- or anti-aging cellular pattern [17, 185].

At checkpoint 1, which exists early in the D growth phase, two oxidative reactions of the pentose phosphate pathway (PPP) in the cytosol and four enzymatic reactions in mitochondria create NADPH (Figure 1.7) [17, 124, 126, 128]. NADPH provides reducing equivalents for the synthesis of amino acids, fatty acids, and sterols [124, 143]. NADPH is also a donor of electrons for thioredoxin and glutathione reductase systems. As mentioned above, both these reductase systems contribute to the establishment and maintenance of an anti-aging cellular pattern because they protect many thiol-containing proteins from oxidative damage; such thiol-containing proteins reside in the nucleus, mitochondria and cytosol (Figure 1.7) [126, 128].

Glycerol is produced by glucose fermentation in the cytosol [143]. At checkpoint 2, glycerol plays an essential role in the establishment and maintenance of an anti-aging cellular pattern by affecting the following three cellular processes: 1) glucose fermentation to glycerol weakens its fermentation to ethanol and acetic acid, both known to be pro-aging metabolites in yeast, 2) glucose fermentation to glycerol enables to sustain the NAD+/NADH ratio that slows yeast chronological aging, and 3) glycerol increases resistance to acute oxidative, thermal, and osmotic stresses that accelerate yeast chronological aging (Figure 1.7) [17, 42, 119].

As mentioned above, the non-reducing disaccharide trehalose is synthesized from glucose in the cytosol of chronologically "young" yeast cells that advance through D and PD phases of culturing [32, 101]. The rate of such synthesis sustains cellular trehalose homeostasis and is modulated by the efficiency of coupled mitochondrial respiration [125]. The effectiveness of such respiration is, in turn, modulated by the rate of peroxisome-to-mitochondria transfer of citrate and acetyl-carnitine [17, 59, 174, 186, 187]. At checkpoint 3, trehalose is essential for maintaining an anti-aging pattern of cellular proteostasis because it attenuates the misfolding, aggregation and oxidative damage of newly synthesized polypeptides (Figure 1.7) [17, 32, 101].

During D and PD growth phases, the intracellular concentration of hydrogen peroxide (H_2O_2) in chronologically aging yeast depends on the efficiencies with which this major ROS is produced by and released from mitochondria and peroxisomes [110, 130, 132, 158]. If the concentration of H_2O_2 at checkpoint 4 is sustained at a sub-lethal ("hormetic") level, it elicits the

establishment of an anti-aging cellular pattern by stimulating the master regulators Gis1, Msn2, and Msn4. In the nucleus, these three transcriptional factors activate expression of genes that encode proteins involved in heat-shock and DNA-damage responses, ROS decomposition, cell cycle progression and transition to quiescence, autophagy, maintenance of cell wall integrity, trehalose synthesis and degradation, glycogen synthesis and degradation, glycolysis and gluconeogenesis, the pentose phosphate pathway, glycerol and amino acid synthesis, ergosterol synthesis, maintenance of glutathione and thioredoxin homeostasis, methylglyoxal detoxification, maintenance of heavy metal ion homeostasis, potassium transport, and mitochondrial electron transport; these proteins are needed for resistance to thermal, oxidative, osmotic, low pH, carbon source starvation, sorbic acid, high ethanol concentration, and DNA-damage stresses (Figure 1.7) [66, 188-191].

At checkpoint 5, H_2O_2 produced by and released from mitochondria and peroxisomes modulates a signaling pathway, which includes the DNA damage response kinases Tel1 and Rad53 (both of which are anti-aging master regulators) and the histone demethylase Rph1 (a pro-aging master regulator) (Figure 1.7) [130]. If the concentration of H_2O_2 at this checkpoint is sustained at a hormetic level, it stimulates the Tel1-dependent phosphorylation/activation of Rad53, which in response phosphorylates and inactivates Rph1 (Figure 1.7) [132, 158]. The resulting inactivation of Rph1 establishes an anti-aging cellular pattern because it allows to attenuate the Rph1-dependent transcription of sub-telomeric chromatin regions in the nucleus, thereby lessening the extent of telomeric DNA damage (Figure 1.7) [130, 132, 158].

During D and PD growth phases, the amino acids aspartate, asparagine, glutamate, and glutamine are synthesized from intermediates of the TCA cycle in mitochondria [124, 143]. After being released into the cytosol, these amino acids stimulate protein kinase (PK) activity of the TOR complex 1 (TORC1) at the surface of vacuoles (Figure 1.7) [61, 94, 96, 144, 145, 146]. Following its activation, TORC1 acts as a pro-aging master regulator at checkpoint 6 by phosphorylating the nutrient-sensory PK Sch9 and the Tap42 protein. Once phosphorylated, Sch9 and Tap42 accelerate the pro-aging process of protein synthesis in the cytosol by stimulating ribosome biogenesis and augmenting translation initiation (Figure 1.7) [94, 96, 192-194]. The TOR complex 2 (TORC2) at the PM also functions as a pro-aging master regulator at checkpoint 6. If activated, TORC2 phosphorylates the PK Ypk1. After being phosphorylated, Ypk1 stimulates the synthesis of complex sphingolipids in the ER. These sphingolipids then stimulate the PKs Pkh1

and Pkh2, both of which in response phosphorylate Sch9 to intensify the pro-aging process of protein synthesis in the cytosol (Figure 1.7) [72, 73, 89, 194-196].

At checkpoint 7, the amino acids aspartate, asparagine, glutamate, and glutamine are released from mitochondria and activate TORC1 at the surface of vacuoles. Active TORC1 sets off a pro-aging cellular pattern by phosphorylating Sch9, which then attenuates the anti-aging process of protein synthesis in mitochondria (Figure 1.7) [62, 94, 96, 118, 146].

At checkpoint 8, the efflux of the amino acids aspartate, asparagine, glutamate and glutamine from mitochondria, the resulting activation of TORC1 at the vacuolar surface and subsequent phosphorylation of Sch9 cause retention of the nutrient-sensory PK Rim15 in the cytosol (Figure 1.7) [97, 197]. Because under such conditions Rim15 cannot enter the nucleus, it is unable to stimulate Msn2, Msn4 and Gis1; these three transcriptional activators can orchestrate an anti-aging transcriptional program in the nucleus only if Rim15 stimulates them (Figure 1.7) [96, 97, 146, 197, 198]. Furthermore, protein kinase A (PKA) activity at the cytosolic leaflet of the PM also contributes to the establishment of a pro-aging cellular pattern at checkpoint 8. This PK activity inhibits nuclear import of Msn2 and Msn4, thus turning off an anti-aging transcriptional program driven - in a Rim15-dependent manner - by these two transcriptional activators (Figure 1.7) [63, 96, 97, 199]. Moreover, a study on a methionine restriction-induced delay of yeast chronological aging implies that excess of methionine can elicit a pro-aging cellular pattern at checkpoint 8 by activating the tRNA methyltransferase Ncl1 in the cytosol (Figure 1.7) [200]. This decreases the concentration of non-methylated tRNAs, attenuates the efflux of cytochrome *c* (Cyc1) from mitochondria and mitigates the nuclear import of the cytosolic Rtg1/Rtg2/Rtg3 heterotrimeric transcriptional factor, which is required for the stimulation of an anti-aging transcriptional program in the nucleus (Figure 1.7) [200].

If TORC1 at the surface of vacuoles is activated by the release of the amino acids aspartate, asparagine, glutamate, and glutamine from mitochondria at checkpoint 9, active TORC1 phosphorylates the autophagy-initiating protein Atg13 (Figure 1.7) [94, 96, 146, 201]. At this checkpoint, Atg13 can also be phosphorylated by PKA kinase activity confined to the cytosolic face of the PM (Figure 1.7) [146, 202-204]. The TORC1- and PKA-driven phosphorylation of Atg13 at checkpoint 9 inhibits autophagosome formation in the cytosol, thus suppressing the anti-aging process of autophagy (Figure 1.7) [146, 202-204]. Furthermore, a study on the methionine restriction-induced delay of yeast chronological aging revealed that the excess of methionine in

the cytosol could trigger a pro-aging cellular pattern at checkpoint 9 because it weakens autophagy, either by stimulating TORC1 at the vacuolar surface or by attenuating autophagosome formation in the cytosol (Figure 1.7) [205]. Such methionine-driven weakening of autophagy accelerates aging by decreasing the extent of vacuolar acidification and by increasing acetic acid accumulation in cultural medium (Figure 1.7) [200, 206]. Moreover, mitochondria, peroxisomes and the cytosol house individual reactions for the synthesis of the polyamine spermidine (Figure 1.7) [111, 127, 175]. At checkpoint 9, spermidine inhibits the histone acetyltransferases Iki3 and Sas3 (Figure 1.7) [83]. Although such spermidine-driven inhibition of Iki3 and Sas3 causes a global decline in the acetylation of histone H3 and silencing of numerous genes in the nucleus, histones in the promoter regions of several ATG (autophagy) genes get acetylated under these conditions [83, 84, 176, 207]. The resulting selective activation of transcription of these genes at checkpoint 9 promotes the anti-aging process of autophagy (Figure 1.7). Also, a fraction of acetic acid in the cytosol can be imported into the nucleus and then converted into acetyl-CoA in the Acs2-dependent reaction [139]. At checkpoint 9, this acetyl-CoA selectively represses the transcription of nuclear ATG genes, thus suppressing the anti-aging process of autophagy (Figure 1.7) [139, 208].

Chronologically aging yeast cells produce acetic acid as follows: 1) it is generated as the alternative product of glucose fermentation in the cytosol and 2) it is formed in the Ald4-dependent reaction in mitochondria, from which acetic acid can be released into the cytosol (Figure 1.7) [15, 17, 42, 143]. At the late-life checkpoint 10 in the ST phase, a pool of acetic acid in the cytosol accelerates yeast chronological aging because it elicits an age-related form of apoptotic PD (Figure 1.7) [15, 17, 42, 43, 45].

While at the early-life checkpoint 3, trehalose is essential for maintaining an anti-aging pattern of cellular proteostasis (see above in my Thesis), this non-reducing disaccharide sets off a pro-aging cellular pattern at the late-life checkpoint 11 in ST phase. This is because in chronologically “old” yeast cells, which do not grow or divide, trehalose covers hydrophobic amino acid side chains of misfolded and unfolded proteins (Figure 1.7) [17, 32, 101]. Such side chains are needed to be recognized by a group of molecular chaperones that help to refold these misfolded and unfolded proteins [152-155]. By competing with molecular chaperones for binding to such clusters of hydrophobic amino acids, trehalose attenuates the anti-aging process of maintaining cellular proteostasis (Figure 1.7) [17, 32, 101].

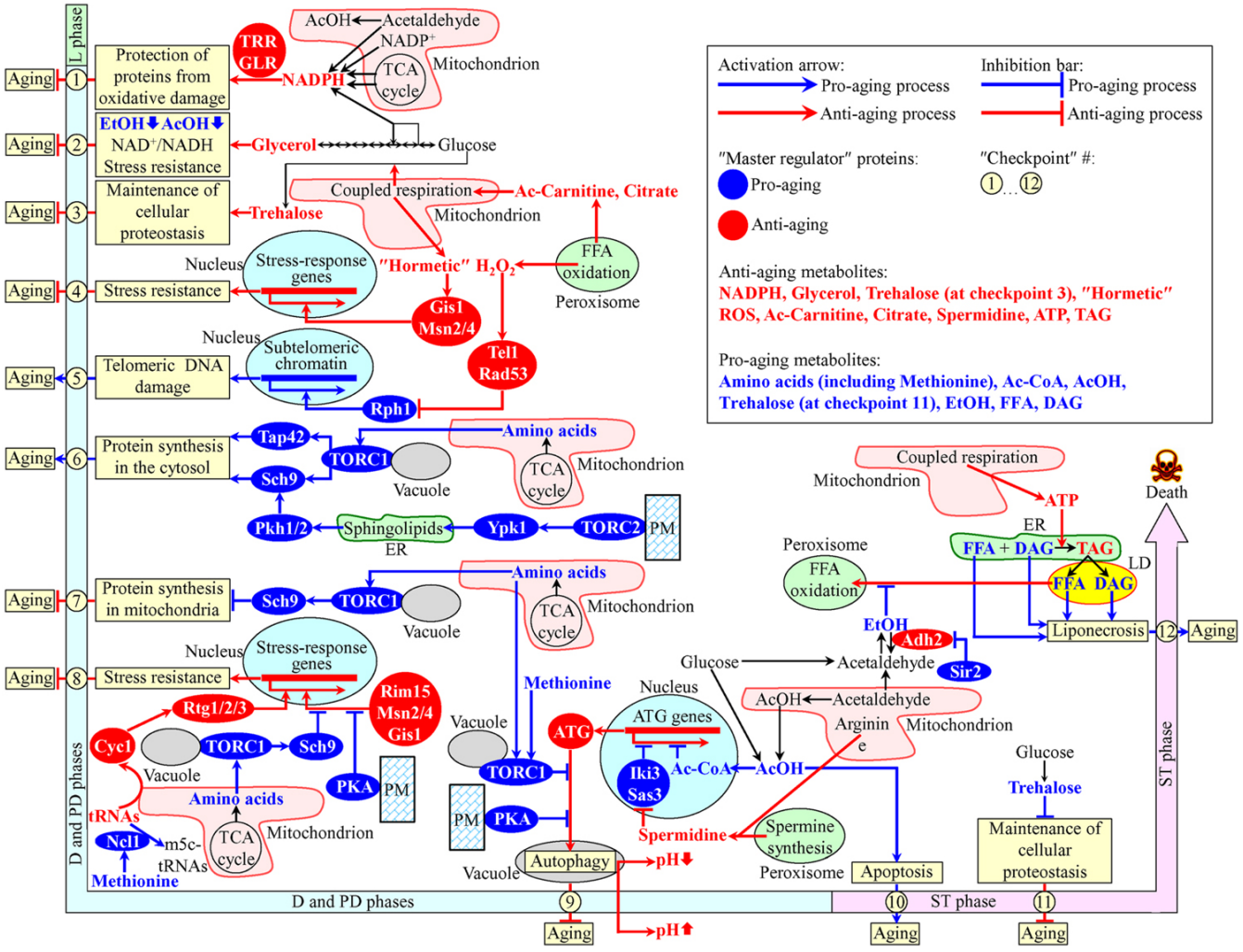

Figure 1.7. A model for how various organelle-organelle and organelle-cytosol communications influence yeast chronological aging. These communications involve movements of specific metabolites between multiple cellular compartments. Different changes in these metabolites are temporally restricted to longevity-defining periods called checkpoints. At each checkpoint, the changes of these metabolites are detected by specific master regulator proteins. Because each of the master regulator proteins modulates specific longevity-defining cellular processes, a coordinated in space and time action of these proteins orchestrates the development and maintenance of a pro- or anti-aging cellular pattern. See the text for details. Ac-Carnitine, acetyl-carnitine; Ac-CoA, acetyl-CoA; AcOH, acetic acid; DAG, diacylglycerol; EtOH, ethanol; FFA, free (non-esterified) fatty acids; m5c-tRNAs, 5-methylcytosine tRNAs; PKA, protein kinase A; PM, the plasma membrane; ROS, reactive oxygen species; TAG, triacylglycerols; TCA, tricarboxylic; TORC, the target of rapamycin complex; tRNAs, transfer RNAs.

At the late-life checkpoint 12 in ST phase, the excessive accumulation of free (non-esterified) fatty acids (FFA) and diacylglycerol (DAG) in cellular membranes accelerates yeast chronological aging because it triggers an age-related form of liponecrotic PD (Figure 1.7) [17,

32, 136, 209, 210]. ATP, which is produced mainly in mitochondria, slows age-related liponecrosis by providing the energy needed for the detoxification of FFA in the ER through the incorporation of FFA into TAG and other neutral lipids (Figure 1.7) [17, 161, 210]. Ethanol, a product of glucose fermentation, accelerates age-related liponecrosis by suppressing peroxisomal oxidation of FFA that are generated in LD due to lipolysis of TAG and other neutral lipids (Figure 1.7) [17, 32, 136, 185]. The sirtuin deacetylase Sir2 promotes ethanol accumulation by inactivating the Adh2 isoform of alcohol dehydrogenase, which is required for ethanol catabolism (Figure 1.7) [135].

In sum, my analysis indicates that intercompartmental communications in yeast cells are integrated into a convoluted network involving unidirectional and bidirectional movements of specific metabolites between cellular compartments. Different changes in the intracellular concentrations and the rates of flow of these metabolites are restricted to critical longevity-defining periods of yeast CLS called checkpoints. Specific proteins known as master regulators can detect the changes of the key metabolites at each of these checkpoints. The checkpoint-specific master regulator proteins contribute to setting up a pro- or anti-aging cellular pattern because each of these proteins controls specific longevity-defining cellular processes.

1.5 Some phytochemicals delay aging and prolong the longevity of budding yeast

Plants, and some non-pathogenic endophytic bacteria and fungi living within the plants, use an evolutionarily conserved set of primary biochemical pathways to satisfy their fundamental metabolic needs in energy and biosynthetic products [211-221]. They also use their secondary biochemical pathways to synthesize many secondary metabolites called phytochemicals [211-221]. Based on chemical nature, phytochemicals belong to several main classes [215, 222-228]. All these main classes are listed in Table 1.1. A commonly accepted view is that the biosynthetic pathways for phytochemicals have evolved for increasing the chances of plants and non-pathogenic endophytic microorganisms inhabiting plants to survive and reproduce within their natural ecological niches [211-213, 215-223, 229-251]. The survival and reproduction advantages that various phytochemicals acting as interspecies chemical signals can provide to the host plant autotrophic organisms and their non-pathogenic endophytic microorganismal residents are shown in Table 1.2.

Table 1.1. The main classes of phytochemicals with respect to their chemical nature.

Chemical class of phytochemicals	Names of chemical compounds
Phenolic compounds	Flavonoids, phenolic acids, hydroxycinnamic acids, lignans, tyrosol esters, stilbenoids and alkylresorcinols
Terpenes	Carotenoids, monoterpenes, saponins, some modified lipid species and triterpenoids
Betalains	Betacyanins and betaxanthins
Polysulfides	Allyl methyl trisulfides
Organosulfides	Diallyl disulfides
Indoles	Indole-3-carbinol and 3,3'-diindolylmethane
Protease inhibitors	Protease inhibitors from soybeans, seeds, legumes, potatoes and cereals
Organic acids	Oxalic and anacardic acids
Modified purines	Caffeine and related purine alkaloids
Quinones	Catechin quinones (epigallocatechin gallate and gallocatechin gallate)
Polyamines	Putrescine, spermidine and spermine

Table 1.2. The survival and reproduction advantages that phytochemicals provide to plants.

The survival and reproduction advantage
Help plants to survive many environmental stresses
Protect plants from viral, bacterial, yeast and fungal infections
Defend plants from invading insects, herbivorous animals and competitor plant species
Protect plants from environmental pollutants
Attract pollinators and other symbiotes to plants
Attract the natural predators of herbivorous insects and animals to plants

Phytochemicals provide survival and reproduction advantages not only to plants. Phytochemicals can also decelerate cellular and organismal aging, prolong longevity and improve the health of evolutionarily distant heterotrophic organisms [215, 223-228, 231, 232, 237, 249, 252-270]. The scope of this section of my Thesis is to analyze recent progress in understanding mechanisms underlying the aging-delaying (geroprotective), longevity-prolonging and health-improving effects of phytochemicals on budding yeast. These effects are outlined below in this section.

The polyamine spermidine extends the longevity of chronologically aging yeast because it inhibits histone acetyltransferases, thus eliciting the deacetylation of histone H3 [83]. The resulting rise in the abundance of non-acetylated histone H3 stimulates transcription of many autophagy-related genes, promotes autophagic clearance of dysfunctional macromolecules and organelles, and postpones the onset of an age-related form of necrotic PCD [83].

The quinone compound called cryptotanshinone increases yeast CLS because it suppresses the pro-aging protein kinases Tor1, Sch9 and Gcn2 [227]. Cryptotanshinone also stimulates mitochondrial superoxide dismutase Sod2, thereby decreasing the concentration of intracellular ROS below a toxic threshold [227].

The polyphenolic compound called resveratrol is a geroprotector in replicatively aging budding yeast because it activates Sir2, a member of the conserved sirtuin family of NAD^+-dependent protein deacetylases, thus lowering the frequency of rDNA recombination and increasing DNA stability [271].

The modified purine called caffeine prolongs the longevity of chronologically aging yeast because it inhibits specifically the pro-aging PK activity of TORC1, thereby suppressing the TORC1-dependent phosphorylation of the anti-aging PK called Rim15 [197]. The ensuing dephosphorylation of Rim15 activates it and initiates a Rim15-driven cascade of events that ultimately promote transcription of genes encoding heat-shock proteins and molecular chaperones [197]. The resulting rise in the abundance of these facilitators of protein folding enhances the anti-aging process of cellular proteostasis [197].

The polyphenolic compound called phloridzin prolongs the replicative lifespan of budding yeast because it activates transcription of the genes encoding Sod1 (a cytosolic form of superoxide dismutase), Sod2 and Sir2 proteins [272]. The ensuing rise in the enzymatic activities of these three proteins lowers intracellular concentrations of ROS, thus increasing cell resistance to oxidative stress [272].

The flavonoid compound called quercetin extends yeast CLS because it lowers the intracellular concentrations of ROS, reduces the efficacies of glutathione oxidation and lipid peroxidation, lessens the extent of protein carbonylation, and decreases cell susceptibility to oxidative stress [273].

1.6 Certain combinations of the geroprotective chemicals that target different longevity-defining processes exhibit a synergistic effect on the extent of aging delay and longevity extension

Different patient-customized combinations of Chinese plants have been for centuries used in traditional Chinese herbal medicine to prevent and treat a wide range of human diseases [274-277]. The recent use of high-throughput "omics," system biological and bioinformatic approaches

in animal models of many human diseases and cultured human cells has revealed that these combinations of Chinese plants affect multiple cellular and organismal processes [277-281]. The term "network pharmacology" (also known as "Traditional Chinese Medicine [TCM] network pharmacology") has been introduced to describe such systemic effects of various combinations of Chinese herbs on the cellular and organismal networks integrating multiple disease-related processes [282-292]. The key tenet of the TCM network pharmacology concept is that the high therapeutic effectiveness, a multitude of targeted pathologies and limited side effects of Chinese herbal medicine are due to the ability of cocktails of plant chemical compounds to affect multiple molecular targets through numerous low-affinity interactions [277, 282-295]. A body of evidence supports the notion that, by modulating different nodes, edges and modules of these disease-specific networks, the combined action of Chinese herb mixtures allows to restore cellular and organismal homeostasis differently altered in diverse human diseases [277, 281, 288, 292-295].

The two critical conceptual advances in our understanding of the biology of human diseases are the following: 1) many (in not all) human diseases are due to various perturbations in complex networks that assimilate specific signaling, metabolic and other molecular pathways, and 2) rational design of particular combinations of pure drugs and/or natural chemical compounds, each targeting different nodes, edges or modules of such networks, may yield potent multicomponent therapies with limited side effects and lowered potential of drug resistance development [296-309]. An expansion of such multi-component therapies with the help of high-throughput screening methods for identifying effective combinations of therapeutic compounds represents an essential strategy of modern medicine [296-310]. This strategy has been successfully used for the development of multicomponent and multitargeted therapeutics for the treatment of complex human diseases, including cancer, infectious diseases, central nervous system disorders, Alzheimer's disease, hypertension, chronic obstructive pulmonary disease, asthma and acquired immunodeficiency syndrome [296, 305, 307, 308, 310-322]. The significant progress in developing multicomponent and multitargeted therapeutics has been facilitated by the advances in mathematical, computational and pharmacological approaches to study compound combination effects [310, 322-331].

Incidence rates of many human chronic diseases increase with age [332-336]. Because an age-related dysregulation of specific cellular and organismal processes is the primary cause of these chronic diseases, they are considered as diseases associated with aging [333, 334, 337-339].

Among these aging-associated human diseases are cardiovascular diseases, chronic obstructive pulmonary disease, chronic kidney disease, diabetes, osteoarthritis, osteoporosis, sarcopenia, stroke, neurodegenerative diseases (including Parkinson's, Alzheimer's and Huntington's diseases), and many forms of cancer [334-343]. The major aspects and underlying mechanisms of aging and aging-associated pathology have been conserved throughout evolution; they include the following: 1) the hallmark events of aging, such as the age-related accumulation of genomic damage, deterioration of telomeres, epigenetic perturbations, impairment of cellular proteostasis, deregulation of nutrient-sensing systems, a decline in mitochondrial functionality, accumulation of senescent cells, decrease of the abundance and functionality of stem cells, and deterioration of intercellular communications [344], and 2) the nutrient- and energy-sensing signaling network of longevity regulation, which integrates the insulin/insulin-like growth factor 1 (IGF-1) pathway, AMP-activated protein kinase/target of rapamycin (AMPK/TOR) pathway, cAMP/protein kinase A (cAMP/PKA) pathway and sirtuin-governed protein deacetylation module [339–341, 344-346].

Some of the known hallmarks of aging and signaling pathways of longevity regulation are specifically targeted by certain individually added chemical compounds (either synthetic drugs or natural chemicals) that delay the onset and decelerate the progression of the aging process in eukaryotes across species [333, 337-343, 347-349]. It needs to be emphasized that none of these individually added aging-delaying chemical compounds could affect all hallmarks of aging or modulate all signaling pathways of longevity regulation [337-340, 348, 349]. It has been therefore proposed that, if two or more aging-delaying chemical compounds each targeting a different hallmark and/or signaling pathway of aging are added together, their combination may have an additive or a synergistic effect on the extent of aging delay and longevity extension [347-350]. The following multicomponent combinations of chemical compounds have been proposed for such therapeutic multiplexing of aging delay and longevity extension: 1) a three-component mixture of epigallocatechin gallate (an activator of cAMP synthesis), N-acetyl-L-cysteine (an inhibitor of cell proliferation pathways) and myricetin (an activator of integrin signaling, DNA repair, cAMP synthesis and hypoxia signaling) [347], 2) a seven-component mixture of rapalogs (including rapamycin and its synthetic drug analogs, all of which are inhibitors of the pro-aging TOR pathway), metformin (an activator of AMPK, which is a primary cellular regulator of glucose and lipid metabolism), losartan or lisinopril (both of which are inhibitors of angiotensin II signaling), a statin (such as atorvastatin, simvastatin or lovastatin, all of which decrease blood cholesterol

levels), propranolol (a non-cardioselective beta-adrenergic antagonist), aspirin (an inhibitor of cyclooxygenase) and a phosphodiesterase 5 inhibitor, in combination with physical exercise and caloric restriction (CR) diet or intermittent fasting [349, 351], and 3) a three-component mixture of rapamycin, acarbose (an a-glucosidase inhibitor) and a cardiolipin-binding peptide [350].

Recent studies in mice have supported the notion that a combination of the aging-delaying chemical compounds that target different aging-associated processes may exhibit a synergistic effect on the extent of aging delay; this combination included rapamycin and metformin [352, 353]. This notion has also been supported by the following studies in model eukaryotic organisms: 1) pairwise combinations of rapamycin and wortmannin (an inhibitor of phosphoinositide 3-kinase), rapamycin and pyrrolidine dithiocarbamates (PDTC; inhibitors of the NF-κB pathway), and wortmannin and PDTC have been shown to exhibit synergistic effects on the extent of *Drosophila melanogaster* lifespan extension [354], 2) a pairwise combination of rapamycin and an inhibitor of the stress-activated c-Jun N-terminal kinase have been demonstrated to act in synergy to prolong the longevity of the coastal marine and salt-lake rotifer *Brachionus manjavacas* [355], 3) some double and triple combinations of synthetic drugs and natural chemicals that target the IGF-1, transforming growth factor β and sterol regulatory element-binding protein signaling pathways of longevity regulation have been shown to extend the lifespan of the nematode *Caenorhabditis elegans* in a synergistic manner [356], and 4) rapamycin and myriocin (an inhibitor of sphingolipid synthesis) act in synergy to extend chronological lifespan in the budding yeast Saccharomyces cerevisiae and the fission yeast *Schizosaccharomyces pombe* [357, 358].

1.7 Thesis outline and contributions of colleagues

All the research presented in this thesis was performed under the supervision of Dr. Vladimir Titorenko at Concordia University. Dr. Titorenko developed the research project concepts and outlines, analyzed experimental results and prepared the manuscripts that make-up this thesis. I contributed to the execution of experiments, data analysis and preparation of manuscripts.

Chapter 1 serves as an introduction to the topic of aging in yeast addressed in this thesis. In Chapter 2 of my thesis, the objective was to perform a screen for previously unknown aging-delaying (geroprotective) chemical compounds extracted from various plants. In the described screen for geroprotectors, a mixture of chemicals present in a plant extract (PE) was added

exogenously to a culture of the budding yeast *S. cerevisiae*. The ability of each of the tested PEs to prolong yeast CLS was assessed with the help of a robust plating assay for monitoring changes in an age-related survival (clonogenicity) of yeast cells. The screen revealed six PEs that prolong yeast CLS much more efficiently than any of the longevity-extending geroprotectors yet described. We provided evidence that each of these PEs is a geroprotector that postpones the onset and decelerates the advancement of yeast chronological aging by promoting a hormetic stress response. We demonstrated that each of these geroprotective PEs affects several cellular processes known to regulate longevity in evolutionarily distant organisms. I performed experiments presented in figures 2.9, 2.10, 2.12, 2.18, 2.19 and 2.20, and prepared these figures. I also prepared figure 2.24. The experiments shown in figures 2.1-2.8, 2.11, 2.13-2.17 were carried out by Vicky Lutchman, Mélissa McAuley, Younes Medkour and me. The experiments shown in figures 2.21-2.23 were carried out by Mélissa McAuley and Younes Medkour. All data presented in Chapter 2 were published in Oncotarget. 2016; 7:16542-16566. Dr. Titorenko provided the intellectual leadership of this project. He also edited the first draft of Chapter 2 of my thesis and the entire manuscript of the above article.

Because studies presented in Chapter 2 led to the discovery of six geroprotective PEs and revealed a distinct set of longevity-defining cellular processes controlled by each of them, the objective of studies presented in Chapter 3 was to examine how each of the six PEs influences the information flow through a signaling network that regulates longevity in yeast and other eukaryotes; this evolutionarily conserved network integrates several signaling pathways and protein kinases. To attain the above objective, in Chapter 3 we investigated how single-gene-deletion mutations eliminating each of these signaling pathways and kinases influence the aging-delaying efficiency of each of the six geroprotective PEs. We provided evidence that each of the six geroprotective PEs targets a different hub, node and/or link of the signaling network governing longevity regulation in chronologically aging *S. cerevisiae*. I performed experiments presented in figures 3.2-3.4, 3.8-3.10 and 3.14-3.16, and prepared these figures. I also prepared figures 3.1 and 3.20. The experiments shown in tables 3.2 and 3.3, figures 3.5-3.7, 3.11-3.13 and 3.17-3.19 were carried out by Vicky Lutchman, Mélissa McAuley, Berly Cortes and me. All data presented in Chapter 3 were published in Oncotarget. 2016; 7:50845-50863. Dr. Titorenko intellectually directed this project. He also corrected the first draft of Chapter 3 of my thesis and the entire manuscript of the above article.

Because studies described in Chapter 3 of my Thesis revealed that the six geroprotective plant extracts target different signaling pathways and protein kinases integrated into a signaling network of longevity regulation, we hypothesized that a combination of two of them or a combination of one of them and spermidine or resveratrol (two other geroprotectors) might have a synergistic effect on the extent of aging delay only if each component of this combination targets a different element of the network. The objective of the studies presented in Chapter 4 was to test the hypothesis. To attain this objective, we investigated longevity-extending efficiencies of all possible pairwise combinations of the six geroprotective plant extracts or one of them and spermidine or resveratrol in chronologically aging yeast. Our investigation supported the above hypothesis and provided evidence that only pairwise combinations of geroprotective chemicals that delay aging because they target different elements of the network slow aging synergistically. I carried out experiments presented in figures 4.2-4.6, 4.11-4.13 and 4.23-4.28, and prepared these figures. I also prepared figure 4.1 and table 4.1. The experiments shown in figures 4.7-4.10 and 4.14-4.22 were performed by Monica Lozano Rodriguez, Mélissa McAuley, Vicky Lutchman and Berly Cortes. All data presented in Chapter 4 were published in Oncotarget. 2019; 10:313-338. Dr. Titorenko provided the intellectual leadership of this project. He also corrected the first draft of Chapter 4 of my thesis and the entire manuscript of the above article.

The objective of studies described in Chapter 5 of my thesis was to search for commercially available plant extracts that can substantially prolong the chronological lifespan of budding yeast. We aimed at discovering previously unknown geroprotective natural chemicals. Our search for new geroprotective compounds led to a discovery of fifteen plant extracts that prolong the longevity of chronologically aging yeast not limited in calorie supply. We provided evidence that each of these plant extracts is a geroprotector that decreases the rate of yeast chronological aging and promotes a hormetic stress response. We also demonstrated that each of the fifteen geroprotective plant extracts mimics the longevity-extending, stress-protecting, metabolic and physiological effects of a caloric restriction diet in yeast not limited in calorie supply. We revealed that the fifteen geroprotective plant extracts elicit partially overlapping effects on specific longevity-defining cellular processes. I carried out experiments presented in figures 5.1-5.3, 5.7, 5.8, 5.11, 5.13, 5.14, 5.16, 5.20 and 5.21, and prepared these figures. I also made table 5.1. The experiments shown in figures 5.4-5.6, 5.9, 5.10, 5.12, 5.15, 5.17-5.19 and 5.22 were conducted by Monica Lozano Rodriguez, Jennifer Anne Baratang Junio, Darya Mitrofanova, Tala Tafakori,

Tarek Taifour, Vicky Lutchman and Eugenie Samson. All findings described in Chapter 5 have been submitted for publication as a manuscript of a research paper. Dr. Titorenko intellectually directed this project. He also corrected the first draft of Chapter 5 of my thesis and the entire manuscript of the above article.

CHAPTER 2

2 Discovery of plant extracts that delay yeast chronological aging and have different effects on longevity-defining cellular processes

2.1 Introduction

The main goal of our research was to use the budding yeast *S. cerevisiae* as a model organism to uncover novel chemical compounds that can slow aging and postpone the onset of aging-associated diseases in evolutionarily distant eukaryotic organisms. Some age-delaying (geroprotective) compounds have already been discovered from extractions of certain plants [116, 225, 258]. Thus, the first step our lab took in order to discover new geroprotectors of plant origin, was to conduct a screen of various plant extracts (PEs). We aimed to screen for compounds that successfully extended yeast chronological lifespan (CLS). This chapter illustrates the finding of six PEs that increase CLS much more efficiently than other known longevity-extending chemicals. In addition, it highlights the effects these PEs have on several longevity-defining cellular processes.

2.2 Materials and methods

2.2.1 Yeast strains, media and culture conditions

The wild-type strain *Saccharomyces cerevisiae* BY4742 (*MATa his3Δ1 leu2Δ lys2Δ ura3Δ*) from Thermo Scientific/Open Biosystems was grown in a synthetic minimal YNB medium (0.67% Yeast Nitrogen Base without amino acids) initially containing 2% or 0.5% glucose and supplemented with 20 mg/l histidine, 30 mg/l leucine, 30 mg/l lysine and 20 mg/l uracil. Cells were cultured at 30°C with rotational shaking at 200 rpm in Erlenmeyer flasks at a "flask volume/medium volume" ratio of 5:1.

2.2.2 CLS assay

A sample of cells was taken from a culture at a certain day after cell inoculation and PE addition into the medium. A fraction of the sample was diluted to determine the total number of cells using a hemacytometer. Another fraction of the cell sample was diluted, and serial dilutions of cells were plated in duplicate onto YEP (1% yeast extract, 2% peptone) plates containing 2% glucose as carbon source. After 2 d of incubation at 30°C, the number of colony-forming units

(CFU) per plate was counted. The number of CFU was considered as the number of viable cells in a sample. For each culture, the percentage of viable cells was calculated as follows: (number of viable cells per ml/total number of cells per ml) × 100. The percentage of viable cells in the mid-logarithmic growth phase was set at 100%.

2.2.3 A screen for PEs that can extend yeast CLS

CLS analysis in the presence of diverse PEs was conducted as described above. A 20% stock solution of each PE in ethanol was made on the day of adding this PE to cell cultures. For each PE, the stock solution was added to the growth medium with 2% glucose immediately following cell inoculation into the medium. The final concentration of each PE in the medium was 0.02%, 0.04%, 0.06%, 0.08%, 0.1%, 0.3%, 0.5% or 1.0%.

2.2.4 Oxygen consumption assay (cellular respiration measurement)

A sample of cells was taken from a culture at a certain time-point. Cells were pelleted by centrifugation and resuspended in 1 ml of fresh YP (1% yeast extract, 2% bactopeptone) medium containing 0.05% glucose. Oxygen uptake by cells was measured continuously in a 2-ml stirred chamber using a custom-designed biological oxygen monitor (Science Technical Center of Concordia University) equipped with a Clark-type oxygen electrode.

2.2.5 Live-cell fluorescence microscopy for measuring the mitochondrial membrane potential

The mitochondrial membrane potential ($\Delta\Psi_m$) was measured in live yeast by fluorescence microscopy of Rhodamine 123 (R123) staining. For R123 staining, 5×10^6 cells were harvested by centrifugation for 1 min at 21,000 × g at room temperature and then resuspended in 100 µl of 50 mM sodium citrate buffer (pH 5.0) containing 2% glucose. R123 was added to a final concentration of 10 µM. Following incubation in the dark for 30 min at room temperature, the cells were washed twice in 50 mM sodium citrate buffer (pH 5.0) containing 2% glucose and then analyzed by fluorescence microscopy. Images were collected with a Zeiss Axioplan fluorescence microscope (Zeiss) mounted with a SPOT Insight 2-megapixel color mosaic digital camera (Spot Diagnostic Instruments). For evaluating the percentage of R123-positive cells, the UTHSCSA

Image Tool (Version 3.0) software was used to calculate both the total number of cells and the number of stained cells. Fluorescence of individual R123-positive cells in arbitrary units was determined by using the UTHSCSA Image Tool software (Version 3.0). In each of 3 independent experiments, the value of the median fluorescence was calculated by analyzing at least 800-1000 cells that were collected at each time-point. The median fluorescence values were plotted as a function of the number of days cells were cultured.

2.2.6 Live-cell fluorescence microscopy for measuring the formation of reactive oxygen species (ROS)

ROS production was measured microscopically by incubating cells with dihydrorhodamine 123 (DHR). In the cell, this non-fluorescent compound can be oxidized by ROS to form the fluorescent chromophore rhodamine 123. DHR was stored in the dark at -20^{o}C as 50 µl aliquots of a 1 mg/ml solution in ethanol. The staining of cells with DHR was performed as follows. The required amount of the 50 µ DHR aliquot (1 mg/ml) was recovered from the freezer and warmed to room temperature. The solution of DHR was then centrifuged at 21,000 × g for 5 min to clear it of any aggregates of fluorophores. For cell cultures with a titer of 10^7 cells/ml, 100 µl was recovered from the cell culture for the treatment. If the cell titer was lower, proportionally larger volumes were used. Then, 6 µl of the 1 mg/ml DHR was added to each 100 µl aliquot of the culture. After a 2-h incubation in the dark at room temperature, the samples were centrifuged at 21,000 × g for 5 min. Pellets were resuspended in 10 ml of PBS buffer (20 mM KH_2PO_4/KOH, pH 7.5, and 150 mM NaCl). Then, 5 µl of mounting medium was added to a microscope slide with each sample, and the slide was overlaid with a coverslip, and sealed using nail polish. Once the slides were prepared, they were visualized under the Zeiss Axioplan fluorescence microscope mounted with a SPOT Insight 2-megapixel color mosaic digital camera. Fluorescence of individual DHR-positive cells in arbitrary units was determined by using the UTHSCSA Image Tool software (Version 3.0). In each of 3-5 independent experiments, the value of the median fluorescence was calculated by analyzing at least 800-1000 cells that were collected at each time point. The median fluorescence values were plotted as a function of the number of days cells were cultured.

2.2.7 Live-cell fluorescence microscopy for examining neutral lipids deposited in lipid droplets (LDs)

BODIPY 493/503 staining for visualizing neutral lipids deposited in LDs was performed as follows. Formaldehyde-fixed cells were permeabilized by treatment with 0.2% Triton X-100 for 6 min and incubated with 10 μM BODIPY 493/503 in 20 mM Tris-HCl (pH 7.5), 150 mM NaCl for 15 min to label LDs. Live imaging was performed on a Leica DM6000B epifluorescence microscope equipped with a high-resolution Hamamatsu Orca ER CCD camera using immersion oil and a 100X objective. Images were acquired with 20-ms exposures using PerkinElmer Volocity software. Image files were exported as TIFFs then opened in ImageJ, where the percentage of cells with LDs was counted.

2.2.8 Measurement of oxidative damage to cellular proteins

Yeast cells were harvested by centrifugation for 1 min at 21,000 × g at room temperature. The cell pellet was resuspended in 1 ml of ice-cold 50 mM KH_2PO_4/KOH buffer (pH 7.5) + 1 mM EDTA. The cells were sonicated on ice, harvested by centrifugation for 5 min at 21,000 × g at 4ºC and then resuspended in 200 μl of ice-cold 50 mM KH_2PO_4/KOH buffer (pH 7.5) + 1 mM EDTA. The Protein Carbonyl Assay Kit (#10005020; Cayman Chemical) was used to measure protein carbonylation (i.e., oxidative protein damage) as the amount of protein-hydrazone produced in the DNPH (2,4-dinitrophenylhydrazine) reaction at an absorbance of 360 nm.

2.2.9 Measurement of oxidative damage to cellular membrane lipids

Yeast cells were harvested by centrifugation for 3 min at 16,000 × g at room temperature. The cell pellet was washed with ice-cold ABC buffer (155 mM ammonium bicarbonate, pH 8.0) by centrifugation for 3 min at 16,000 × g at 4ºC, and then resuspended in 1 ml of ice-cold ABC buffer. Then, 200 μl of glass beads were added, and the sample was vortexed for 5 min. After that, 1 ml of ice-cold nanopore water was added, and the sample was transferred to a 15-ml glass centrifuge tube. Then, 3 ml of chloroform/methanol (17:1) mixture was added, and the sample was vortexed at 4°C for 2 h. The sample was subjected to centrifugation at 3000 × g for 5 min at room temperature to form two phases. The lower organic phase was transferred to a new 15-ml glass tube. The solvent was evaporated off under nitrogen flow or in a vacuum evaporator. The lipid film was dissolved in 100 μl of methanol/chloroform (2:1) mixture. The PeroXOquant Quantitative Peroxide Assay Kit assay kit (#23285; Thermo Scientific Pierce) was used to measure lipid hydroperoxides as the Fe^{3+} complexes with the xylenol orange dye at an absorbance of 595

nm.

2.2.10 Measurement of the frequency of spontaneous mutations in nuclear DNA

The frequency of spontaneous point mutations in the *CAN1* gene of nuclear DNA was evaluated by measuring the frequency of mutations that caused resistance to the antibiotic canavanine. A sample of cells was removed from each culture at various time-points. Cells were plated in triplicate onto YNB (0.67% Yeast Nitrogen Base without amino acids [#DF0919153; Fisher Scientific]) plates containing 2% glucose and supplemented with *L*-canavanine (50 mg/l), histidine, leucine, lysine and uracil (#C1625, #H8125, #L8912, #L5751 and #U0750, respectively; all from Sigma). Serial dilutions of each sample were then plated in triplicate onto YP plates containing 2% glucose for measuring the number of viable cells. The number of CFU was counted after 4 d of incubation at 30^{o}C. For each culture, the frequency of mutations that caused resistance to canavanine was calculated as follows: number of CFU per ml on YNB plates containing 2% glucose, *L*-canavanine (50 mg/l), histidine, leucine, lysine and uracil/number of CFU per ml on YP plates containing 2% glucose.

2.2.11 Measurement of the frequency of spontaneous mutations in mitochondrial DNA

The frequency of spontaneous point mutations in the *rib2* and *rib3* loci of mitochondrial DNA (mtDNA) was evaluated by measuring the frequency of mtDNA mutations that caused resistance to the antibiotic erythromycin. These mutations impair only the mtDNA. A sample of cells was removed from each culture at various time-points. Cells were plated in triplicate onto YP plates containing 3% glycerol and erythromycin (1 mg/ml) [#227330050; Acros Organics]. Also, serial dilutions of each sample were plated in triplicate onto YP plates containing 3% glycerol as a carbon source for measuring the number of respiratory-competent (rho^{+}) cells. The number of CFU was counted after 6 d of incubation at 30^{o}C. For each culture, the frequency of mutations that caused resistance to erythromycin was calculated as follows: the number of CFU per ml on YP plates containing 3% glycerol and erythromycin/number of CFU per ml on YP plates containing 3% glycerol.

2.2.12 Plating assays for the analysis of resistance to oxidative and thermal stresses

For the analysis of hydrogen peroxide (oxidative stress) resistance, serial dilutions (1:10^{0}

to $1:10^5$) of cells removed from each culture at various time-points were spotted onto two sets of plates. One set of plates contained YP medium with 2% glucose alone, whereas the other set contained YP medium with 2% glucose supplemented with 5 mM hydrogen peroxide. Pictures were taken after a 3-day incubation at 30ºC.

For the analysis of thermal stress resistance, serial dilutions ($1:10^0$ to $1:10^5$) of cells removed from each culture at various time-points were spotted onto two sets of plates containing YP medium with 2% glucose. One set of plates was incubated at 30ºC. The other set of plates was initially incubated at 60ºC for 60 min and was then transferred to 30ºC. Pictures were taken after a 3-day incubation at 30ºC.

2.2.13 Miscellaneous procedures

The age-specific mortality rate (qx) [359-361], Gompertz slope or mortality rate coefficient (α) [360, 361], and mortality rate doubling time (MRDT) [360, 361] were calculated as previously described.

2.2.14 Statistical analysis

Statistical analysis was performed using Microsoft Excel's (2010) Analysis ToolPack-VBA. All data are presented as mean ± SEM. The *p* values for comparing the means of two groups (using an unpaired two-tailed *t* test) and survival curves (using a two-tailed *t* test) were calculated with the help of the GraphPad Prism statistics software.

2.3 Results

2.3.1 A screen for PEs that can extend the longevity of chronologically aging yeast

We began with 35 known plant extracts that we screened for an increase in yeast chronological lifespan. The origin and properties of the PEs can be found summarized in tables 2.1 and 2.2, respectively. We used the wild-type strain BY4742 cultured in a synthetic minimal YNB medium with an initial 2% glucose. This is because yeast cells cultured under these conditions have been shown to age chronologically under non-caloric restrictions (non-CR) that accelerate aging in different yeast genetic backgrounds including BY4742 [14, 15, 17]. The chronological life-span assay we used, preformed in a controlled environment, described above

and in many of our published papers [32], relies mostly on the number of colony-forming units (CFU).

Table 2.1. A list of plant extracts used in this study.

Abbreviated name	Botanical name	Plant part used	Commercial source
PE1	*Echinacea purpurea*	Whole plant	Idunn Technologies
PE2	*Astragalus membranaceous*	Root	Idunn Technologies
PE3	*Rhodiola rosea L.*	Root	Idunn Technologies
PE4	*Cimicifuga racemosa*	Root and rhizome	Idunn Technologies
PE5	*Valeriana officinalis L.*	Root	Idunn Technologies
PE6	*Passiflora incarnate L.*	Whole plant	Idunn Technologies
PE7	*Polygonum cuspidatum*	Root and rhizome	Idunn Technologies
PE8	*Ginkgo biloba*	Leaf	Idunn Technologies
PE9	*Zingiber officinale Roscoe*	Rhizome	Idunn Technologies
PE10	*Theobroma cacao L.*	Cacao nibs	Idunn Technologies
PE11	*Camellia sinensis L. Kuntze*	Leaf	Idunn Technologies
PE12	*Apium graveolens L.*	Seed	Idunn Technologies
PE13	*Scutellaria baicalensis*	Root	Idunn Technologies
PE14	*Euterpe oleracea*	Fruit	Idunn Technologies
PE15	*Withania somnifera*	Root and leaf	Idunn Technologies
PE16	*Phyllanthus emblica*	Fruit	Idunn Technologies
PE17	*Camellia sinensis*	Leaf	Idunn Technologies
PE18	*Pueraria lobata*	Root	Idunn Technologies
PE19	*Silybum marianum*	Seed	Idunn Technologies
PE20	*Eleutherococcus senticosus*	Root and stem	Idunn Technologies
PE21	*Salix alba*	Bark	Idunn Technologies
PE22	*Glycine max L.*	Bean	Idunn Technologies
PE24	*Calendula officinalis*	Flower	Idunn Technologies
PE25	*Salvia miltiorrhiza*	Root	Idunn Technologies
PE27	*Panax quinquefolium*	Root	Idunn Technologies
PE28	*Harpagophytum procumbens*	Root	Idunn Technologies
PE29	*Olea europaea L.*	Leaf	Idunn Technologies
PE30	*Gentiana lutea*	Root	Idunn Technologies
PE31	*Piper nigrum*	Fruit	Idunn Technologies
PE32	*Aesculus hippocastanum*	Seed	Idunn Technologies
PE33	*Mallus pumila Mill.*	Fruit	Idunn Technologies
PE34	*Fragaria spp.*	Fruit	Idunn Technologies
PE35	*Ribes nigrum*	Leaf	Idunn Technologies
PE36	*Dioscorea opposita*	Root	Idunn Technologies
PE37	*Cinnamomum verum*	Bark	Idunn Technologies

Table 2.2. Properties of plant extracts used in this study.

Abbreviated name	Properties
PE1	Extraction solvent: ethanol (75%)/water (25%). Extract ratio: 4/1. Composition: natural extract, maltodextrin.
PE2	Extraction solvent: denatured ethanol (70%)/water (30%). Extract ratio: 10/1. Composition: natural extract (40-50%), gum arabic (50-60%).
PE3	Extraction solvent: ethanol (60-80%)/water (40-20%). Extract ratio: 15-20/1. Composition: natural extract (80-100%), maltodextrin (0-20%).
PE4	Extract ratio: 6-8/1. Composition: natural extract (28-38%), maltodextrin (60-70%), tricalcium phosphate (0-5%).
PE5	Extraction solvent: denatured ethanol/water. Extract ratio: ~ 6/1. Composition: natural extract, maltodextrin, silica (0-1%).
PE6	Extraction solvent: water (100%). Extract ratio: 4/1. Composition: natural extract, maltodextrin.
PE7	Extraction solvent: ethanol (80%)/water (20%). Extract ratio: 40/1. Composition: natural extract (90-100%), maltodextrin (0-10%).
PE8	Extraction solvent: ethanol/water. Extract ratio: 50/1. Composition: natural extract.
PE9	Extraction solvent: ethanol/water. Composition: natural extract (96%), gingerols (4%).
PE10	Natural powder/final product ratio: 2-3/1. Composition: natural powder.
PE11	Extraction solvent: ethyl acetate (90%)/water (10%). Extract ratio: 6/1. Composition: natural extract (100%).
PE12	Extraction solvent: ethanol (90%)/water (10%). Extract ratio: 8/1. Composition: natural extract, maltodextrin, modified starch, silica.
PE13	Extraction solvent: ethanol/water. Extract ratio: 4/1. Composition: natural extract.
PE14	Extraction solvent: ethanol/water. Extract ratio: 4/1. Composition: natural extract.
PE15	Extraction solvent: water. Extract ratio: 9/1. Composition: withanolide glycoside conjugates (10%), oligosaccharides (32%), free withanolides (0.5%).
PE16	Extraction solvent: water. Composition: hydrolyzable tannins (>60%), including Emblicanin-A, Emblicanin-B, Punigluconin, Pedunculagin.
PE17	Composition: tea polyphenols (>90%), including epigallocatechin gallate (>40%).
PE18	Composition: flavonoids (>40%), including puerarin.
PE19	Extraction solvent: ethanol/water. Composition: silymarin (>80%).
PE20	Extraction solvent: water. Composition: eleutheroside B+E (>0.8%).
PE21	Extraction solvent: ethanol/water. Composition: salicin (>25%).
PE22	Composition: isoflavones (40%).
PE24	Composition: lutein (>5%).
PE25	Composition: tanshinones, isotanshinones, cryptotanshinone, isocryptotanshinone, dihydrotanshinone, hydroxytanshinones.

PE27	Composition: ginsenosides (10%, by HPLC-UV), quintozene-free.
PE28	Extraction solvent: ethanol/water. Extract ratio: 40/1. Composition: harpagosides (20%, by HPLC-UV).
PE29	Extraction solvent: ethanol (70%)/water (30%). Extract ratio: 5-10/1. Composition: natural extract, maltodextrin, silica (0.2%).
PE30	Composition: isogentisin (0.04%).
PE31	Extraction solvent: ethanol. Extract ratio: 10/1. Composition: piperine (>90%).
PE32	Composition: aescin (20%).
PE33	Extraction solvent: ethanol (70%)/water (30%). Extract ratio: 120-130/1. Composition: natural extract (60-70%), maltodextrin (30-40%).
PE34	Extract ratio: 5/1. Composition: natural extract, including polyphenols (>2%).
PE35	Extraction solvent: water. Composition: polyphenols (15%, by HPLC-UV).
PE36	Composition: diosgenine (>16%, by HPLC-UV).
PE37	Extraction solvent: water. Composition: polyphenols (25%, by HPLC-UV).

Initially, we did not know the optimal concentration we would need for each of the PEs in order to see potential results. Thus, we decided to test the PEs at multiple plausible final concentrations ranging from 0.02% to 1.0% at the time of cell inoculation. Three different outcomes were possible, either the plant-extracts had no effect on the lifespan of chronologically aging yeast or they in fact managed to either increase or decrease CLS. Indeed, all three outcomes were observed. Some of the plant extracts we tested did not change the mean and the maximum chronological lifespan of yeast under the specific conditions we set. Such plant extracts included PE9, PE13, PE16, PE22, PE28 and PE36 (Figure 2.2-Figure 2.5). We also observed, with other plant extracts, the opposite of the desired effect. In said cases, the PEs, at final concentrations ranging from 0.08% to 1.0%, reduced the mean and/or maximum CLS of the yeast under non-caloric restrictions. Among them are PE1-PE3, PE7, PE10, PE11, PE14, PE15, PE17-PE20, PE24, PE25, PE27, PE29-PE35 and PE37 (Figure 2.1-Figure 2.5). Lastly, 6 out of the 35 PEs we had in our library managed to increase both the mean and maximum CLS of yeast cells grown under non-CR conditions. It was also made apparent that though, in some cases, multiple final concentrations, did increase CLS, one concentration showed better results with a higher effect on CLS increase than the others. The names of the PEs and the optimal final concentration are as follows: 1) 0.5% PE4 from *Cimicifuga racemosa* (Figure 2.1, Figure 2.6A, Figure 2.8A and 2.8B); 2) 0.5% PE5 from *Valeriana officinalis* L. (Figure 2.1, Figure 2.6B, Figure 2.8A and 2.8B); 3) 1.0% PE6 from *Passiflora incarnata L*. (Figure 2.1, Figure 2.6C, Figure 2.8A and 2.8B); 4) 0.3% PE8 from *Ginkgo biloba* (Figure 2.1, Figure 2.6D, Figure 2.8A and 2.8B); 5) 0.1% PE12 from *Apium graveolens L*. (Figure 2.2, Figure 2.6E, Figure 2.8A and 2.8B); and 6) 0.1% PE21 from *Salix alba* (Figure 2.3,

Figure 2.6F, Figure 2.8A and 2.8B).

None of the six lifespan-extending plant extracts affected the growth rates of the yeast cells in the logarithmic (L) and post-diauxic (PD) phases or impacted the maximum cell density in the stationary (ST) phase of yeast cultures under non-CR conditions on 2% glucose (Figure 2.9). In this case, it is unlikely that the results observed from the addition of the 6 PEs, are due to a decrease in growth rate or an added resistance to toxic substances that accumulate during culturing in synthetic minimal YNB medium.

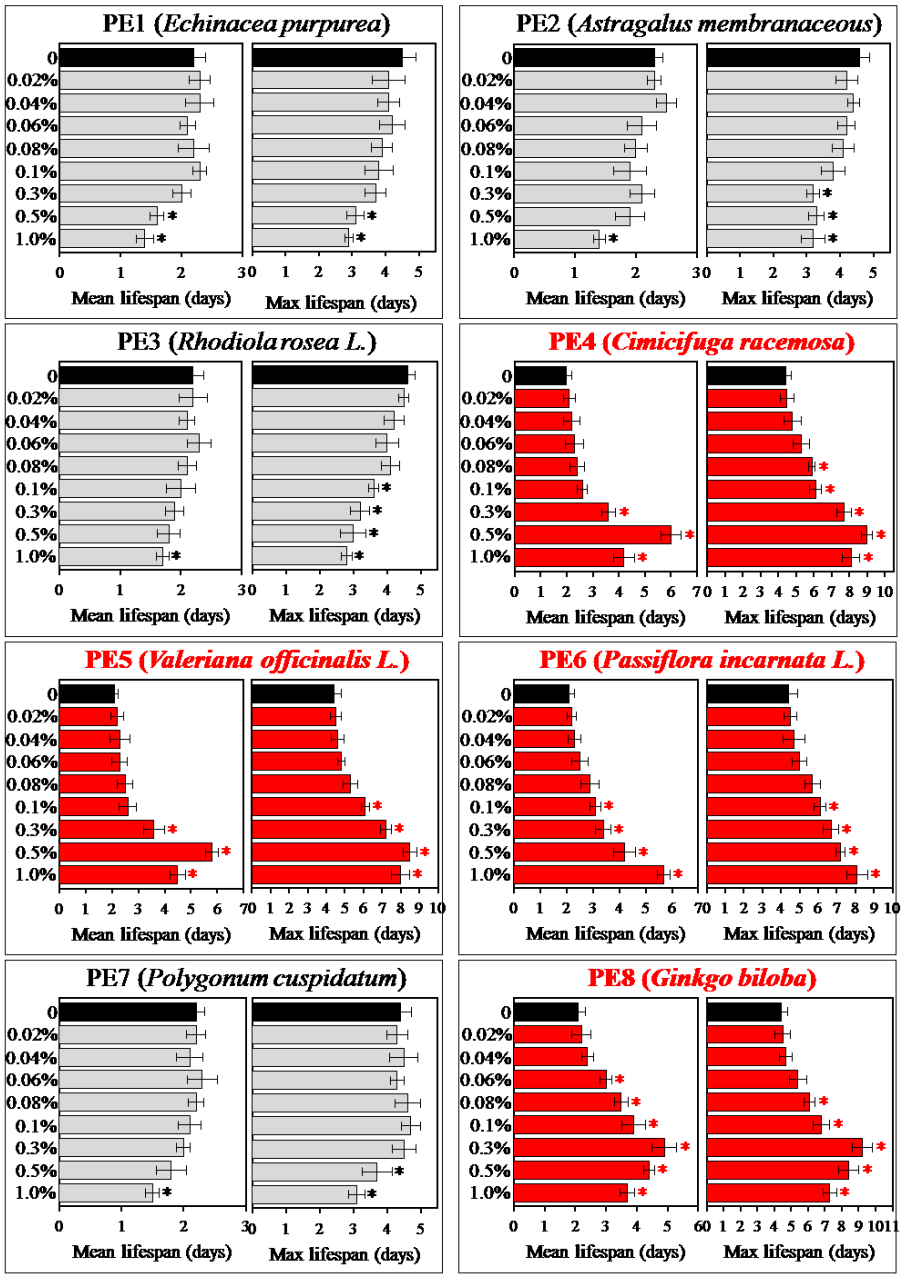

Figure 2.1. PE4, PE5, PE6 and PE8, but not PE1, PE2, PE3 or PE7, extend the CLS of WT yeast grown under non-CR conditions. WT cells were grown in the synthetic minimal YNB medium initially containing 2% glucose (non-CR conditions), in the presence of a PE or its absence. The mean and maximum lifespans of chronologically aging WT strain cultured under non-CR conditions without a PE or with a PE added at various concentrations are shown; data are presented as means ± SEM (n = 6-21; * $p < 0.05$; the p values for comparing the means of two groups were calculated with the help of the GraphPad Prism statistics software using an unpaired two-tailed t test). Note that PE1, PE2, PE3 and PE7 can shorten the CLS of WT yeast under non-CR conditions if added at high concentrations (n = 6; * $p < 0.05$; the p values for comparing the means of two groups were calculated with the help of the GraphPad Prism statistics software using an unpaired two-tailed t test).

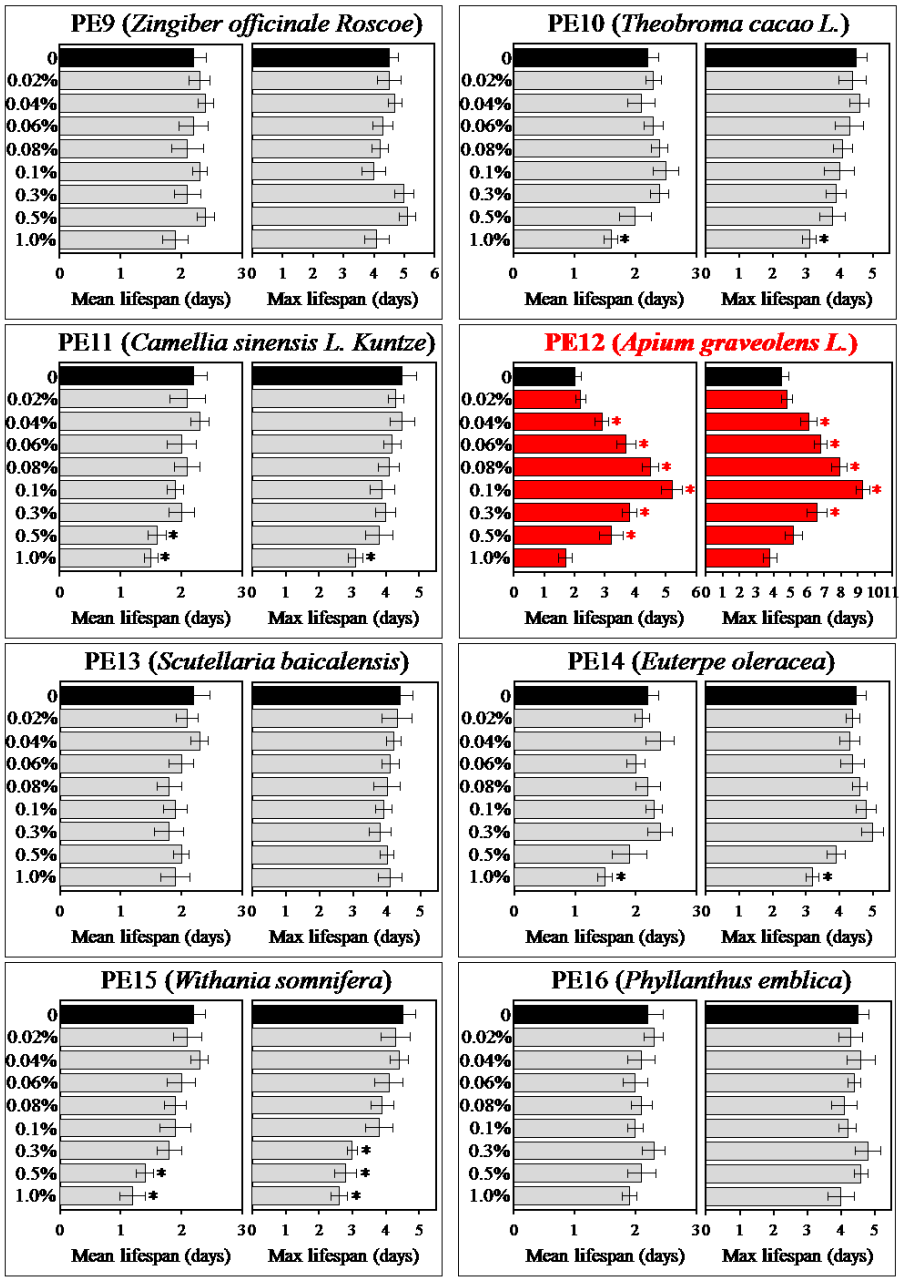

Figure 2.2. PE12, but not PE9, PE10, PE11, PE13, PE14, PE15 or PE16, extends the CLS of WT yeast grown under non-CR conditions. WT cells were grown in the synthetic minimal YNB medium initially containing 2% glucose (non-CR conditions), in the presence of a PE or its absence. The mean and maximum lifespans of chronologically aging WT strain cultured under non-CR conditions without a PE or with a PE added at various concentrations are shown; data are presented as means ± SEM (n = 6-29; * $p < 0.05$; the p values for comparing the means of two groups were calculated with the help of the GraphPad Prism statistics software using an unpaired two-tailed t test). Note that PE10, PE11, PE14 and PE15 can shorten the CLS of WT yeast under non-CR conditions if added at high concentrations (n = 6; * $p < 0.05$; the p values for comparing the means of two groups were calculated with the help of the GraphPad Prism statistics software using an unpaired two-tailed t test).

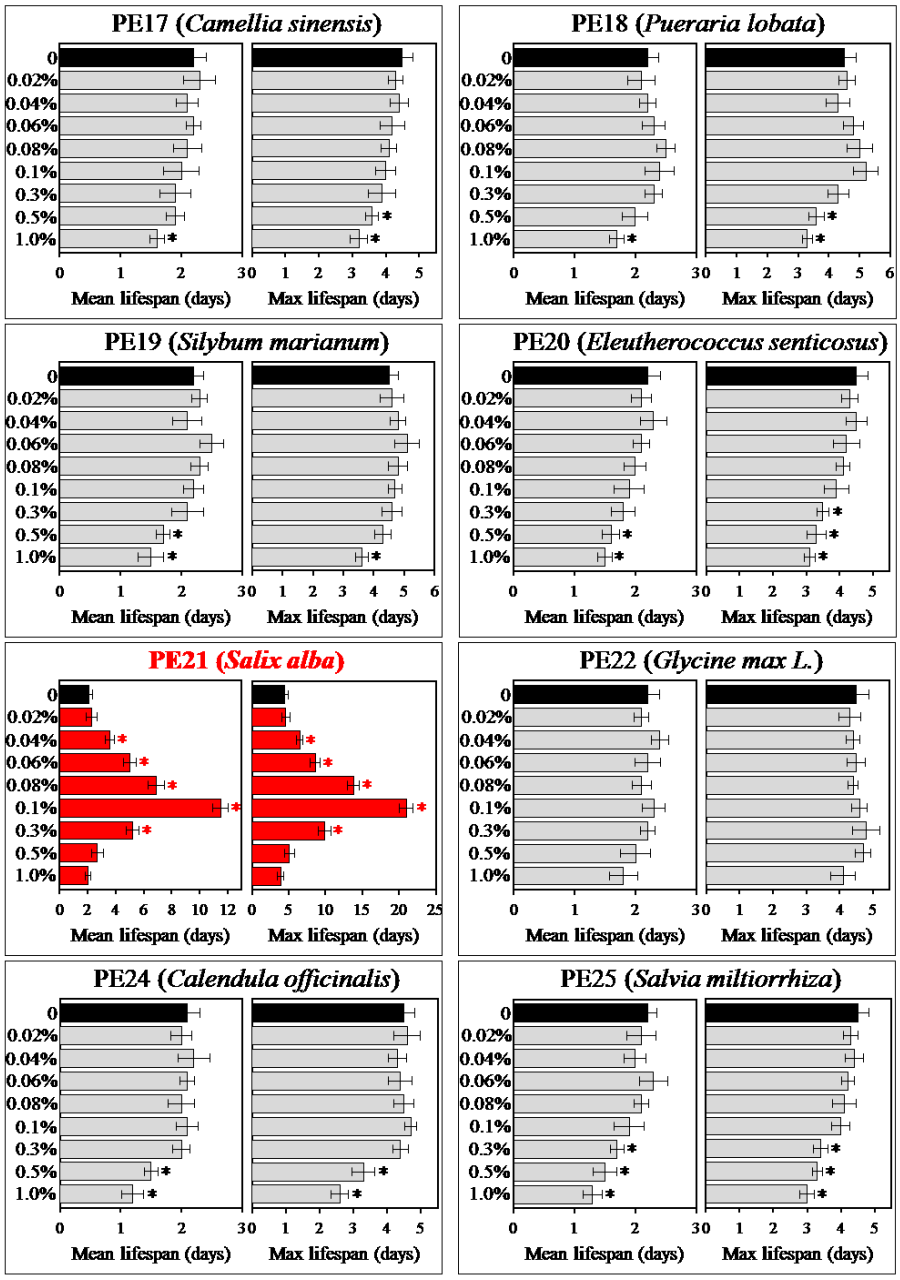

Figure 2.3. PE21, but not PE17, PE18, PE19, PE20, PE22, PE24 or PE25, extends the CLS of WT yeast grown under non-CR conditions. WT cells were grown in the synthetic minimal YNB medium initially containing 2% glucose (non-CR conditions), in the presence of a PE or its absence. The mean and maximum lifespans of chronologically aging WT strain cultured under non-CR conditions without a PE or with a PE added at various concentrations are shown; data are presented as means ± SEM (n = 6-35; * $p < 0.05$; the p values for comparing the means of two groups were calculated with the help of the GraphPad Prism statistics software using an unpaired two-tailed t test). Note that PE17, PE18, PE19, PE20, PE24 and PE25 can shorten the CLS of WT yeast under non-CR conditions if added at high concentrations (n = 6; * $p < 0.05$; the p values for comparing the means of two groups were calculated with the help of the GraphPad Prism statistics software using an unpaired two-tailed t test).

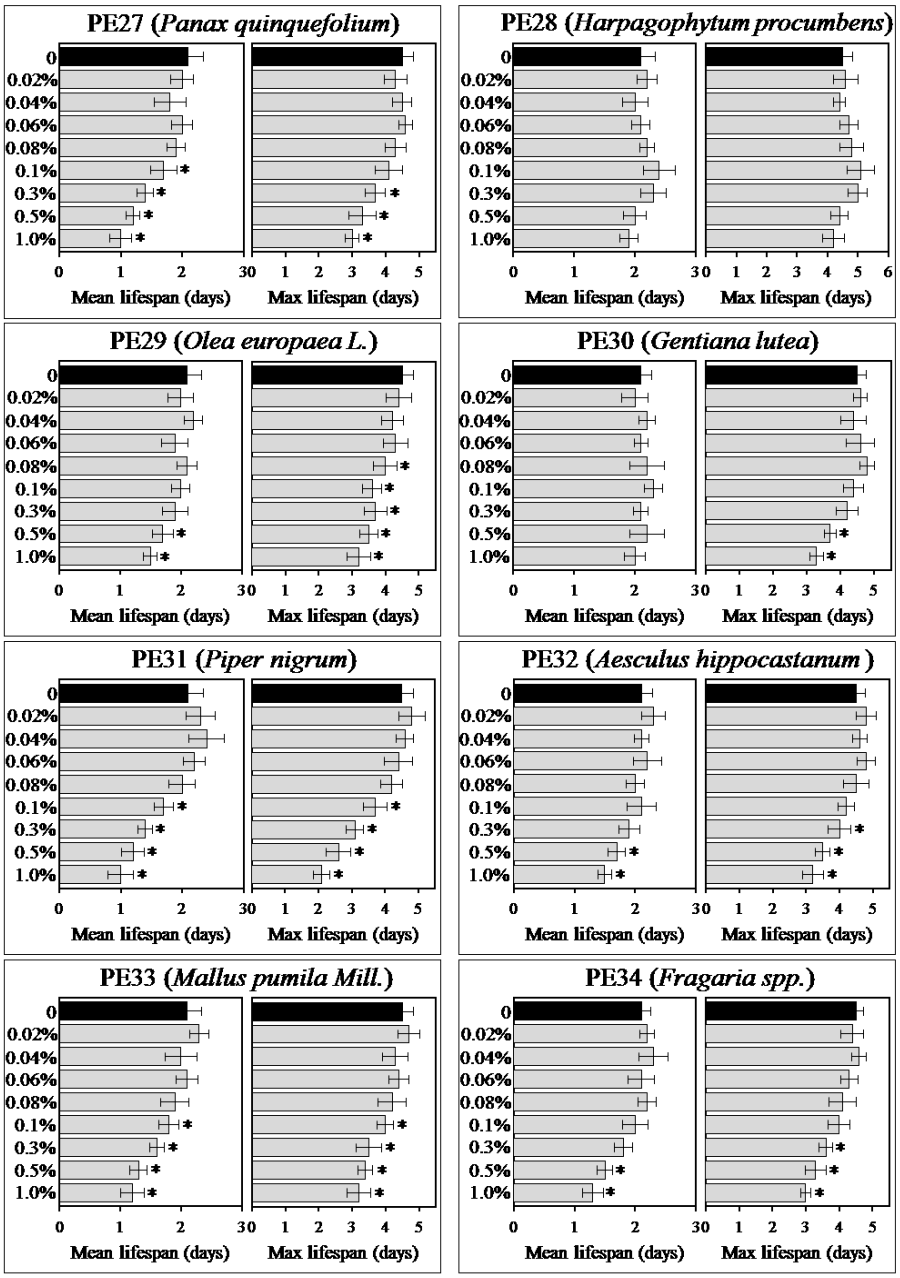

Figure 2.4. PE27, PE28, PE29, PE30, PE31, PE32, PE33 and PE34 do not extend the CLS of WT yeast grown under non-CR conditions. WT cells were grown in the synthetic minimal YNB medium initially containing 2% glucose (non-CR conditions), in the presence of a PE or its absence. The mean and maximum lifespans of chronologically aging WT strain cultured under non-CR conditions without a PE or with a PE added at various concentrations are shown; data are presented as means ± SEM (n = 5-6; * $p < 0.05$; the p values for comparing the means of two groups were calculated with the help of the GraphPad Prism statistics software using an unpaired two-tailed t test). Note that PE 27, PE29, PE30, PE31, PE32, PE33 and PE34 can shorten the CLS of WT yeast under non-CR conditions if added at high concentrations (n = 6; * $p < 0.05$; the p values for comparing the means of two groups were calculated with the help of the GraphPad Prism statistics software using an unpaired two-tailed t test).

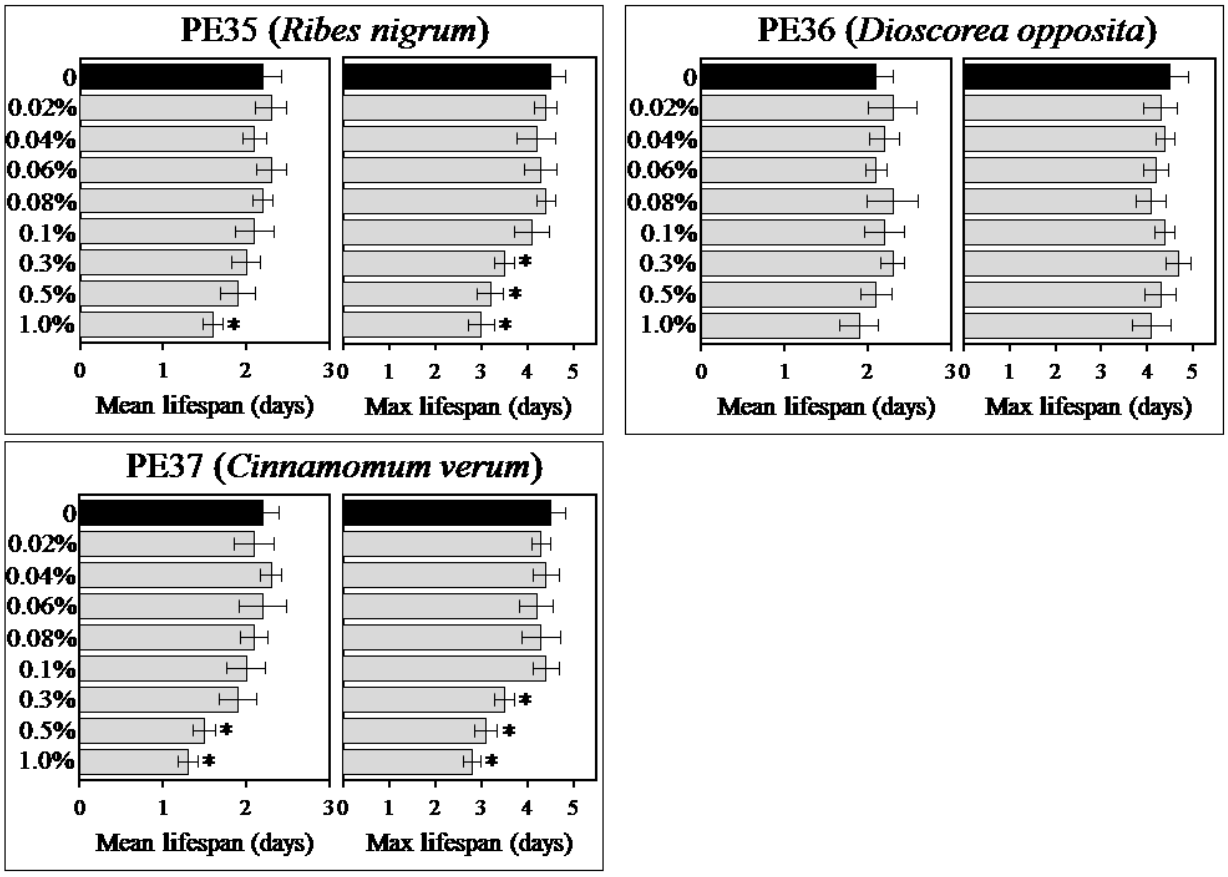

Figure 2.5. PE35, PE36 and PE37 do not extend the CLS of WT yeast grown under non-CR conditions. WT cells were grown in the synthetic minimal YNB medium initially containing 2% glucose (non-CR conditions), in the presence of a PE or its absence. The mean and maximum lifespans of chronologically aging WT strain cultured under non-CR conditions without a PE or with a PE added at various concentrations are shown; data are presented as means ± SEM (n = 5-6; * $p < 0.05$; the p values for comparing the means of two groups were calculated with the help of the GraphPad Prism statistics software using an unpaired two-tailed t test). Note that PE 35 and PE37 can shorten the CLS of WT yeast under non-CR conditions if added at high concentrations (n = 6; * $p < 0.05$; the p values for comparing the means of two groups were calculated with the help of the GraphPad Prism statistics software using an unpaired two-tailed t test).

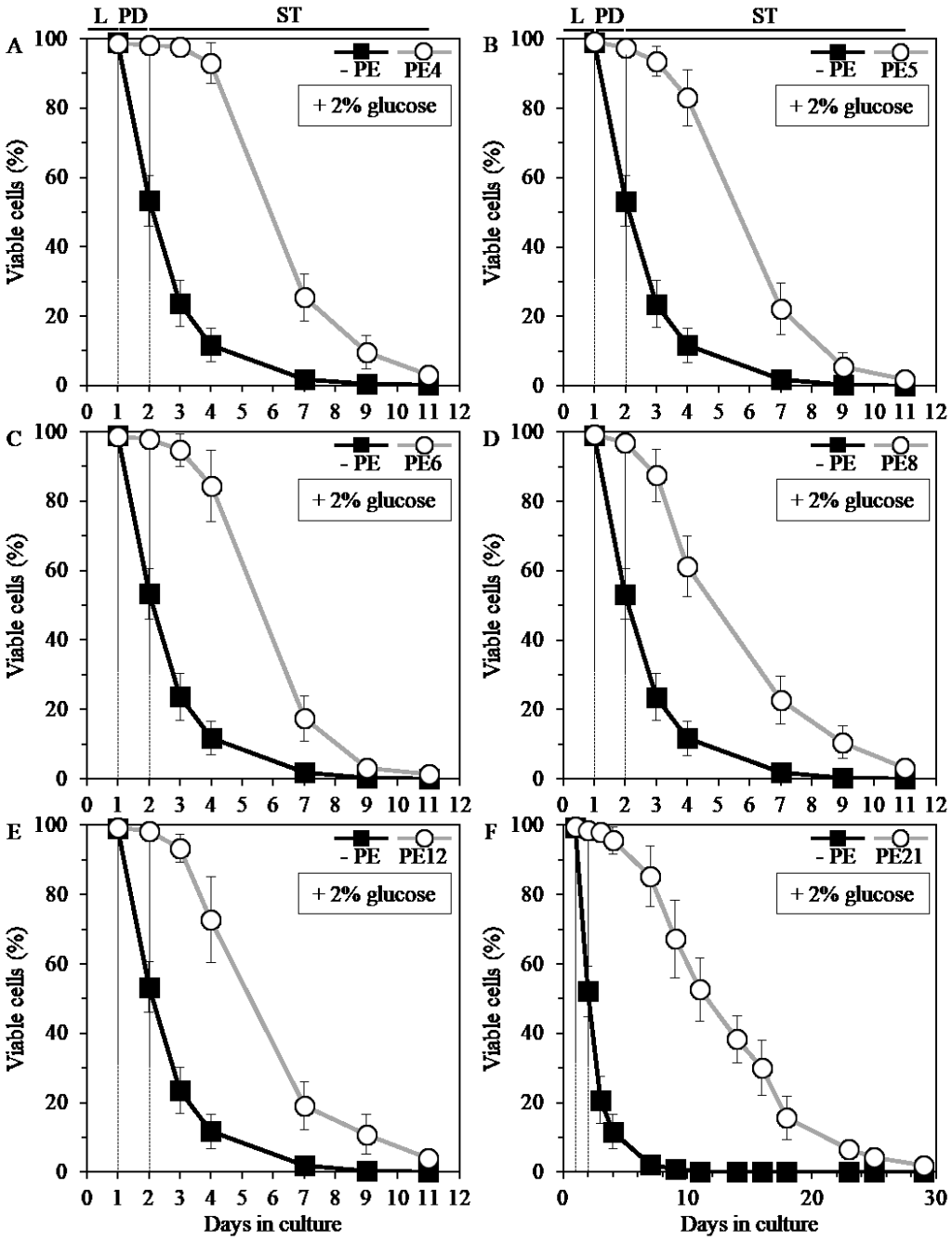

Figure 2.6. PE4, PE5, PE6, PE8, PE12 and PE21 extend the chronological lifespan (CLS) of yeast grown under non-caloric restriction (non-CR) conditions. Wild-type (WT) cells were grown in the synthetic minimal YNB medium (0.67% Yeast Nitrogen Base without amino acids) initially containing 2% glucose in the presence of a PE or its absence. Survival curves of chronologically aging WT strain cultured with or without 0.5% PE4 (A), 0.5% PE5 (B), 1% PE6 (C), 0.3% PE8 (D), 0.1% PE12 (E) or 0.1% PE21 (F) are shown. Data are presented as means ± SEM (n = 21-35). CLS extension was significant for each of the PEs tested ($p < 0.05$; the p values for comparing survival curves were calculated with the help of the GraphPad Prism statistics software). Abbreviations: Logarithmic (L), post-diauxic (PD) or stationary (ST) growth phase.

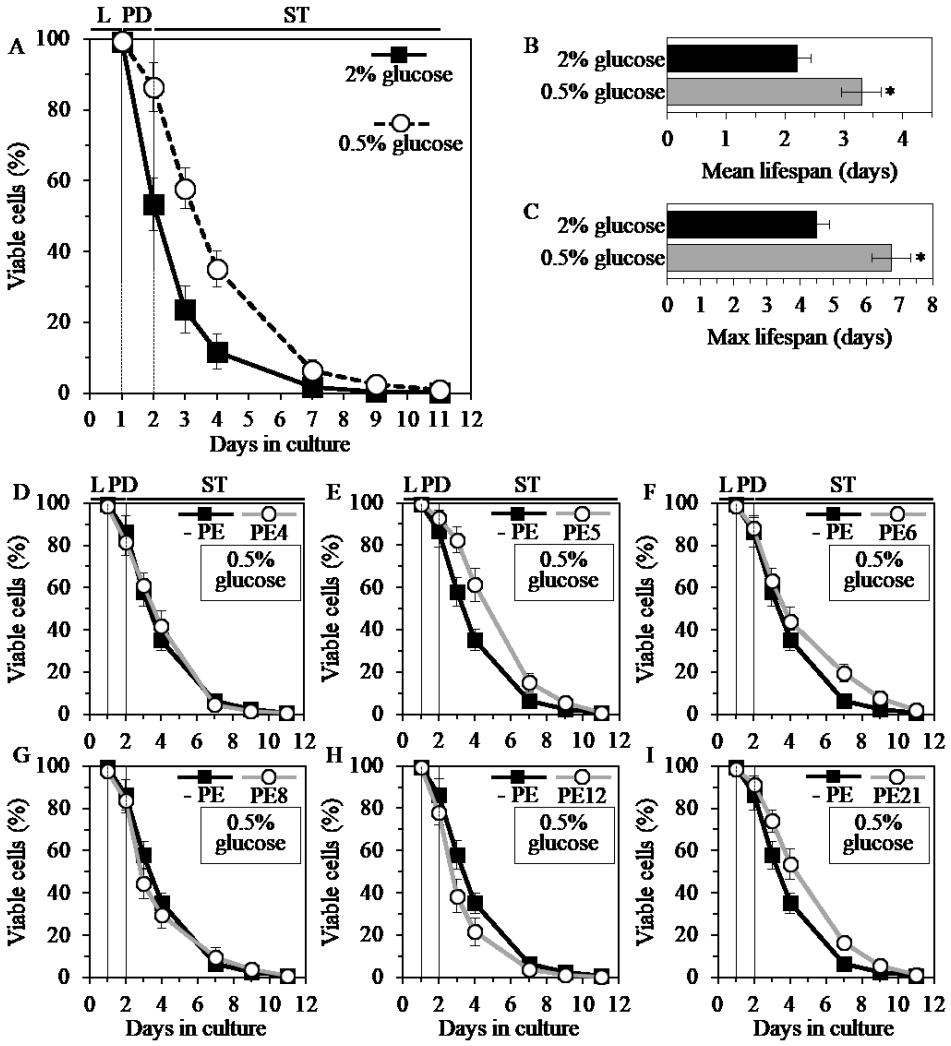

Figure 2.7. PE5 and PE21, but not PE4, PE6, PE8 or PE12, extend the CLS of yeast grown under CR conditions. WT cells were grown in the synthetic minimal YNB medium initially containing 0.5% glucose (CR conditions) or 2% glucose (non-CR conditions), in the presence of a PE or its absence. Survival curves (A), the mean (B) and maximum (C) lifespans of chronologically aging WT strain cultured under CR or non-CR conditions in the absence of a PE are shown; data are presented as means ± SEM (n = 5-7). CR caused significant extension of CLS (A) ($p < 0.05$; the p values for comparing survival curves were calculated with the help of the GraphPad Prism statistics software). CR extended both the mean (B) and maximum (C) lifespans (* $p < 0.05$; the p values for comparing the means of two groups were calculated with the help of the GraphPad Prism statistics software using an unpaired two-tailed t test). Survival curves of chronologically aging WT strain cultured under CR on 0.5% glucose with or without 0.5% PE4 (D), 0.5% PE5 (E), 1% PE6 (F), 0.3% PE8 (G), 0.1% PE12 (H) or 0.1% PE21 (I) are shown; data are presented as means ± SEM (n = 5-7). CLS extension under CR on 0.5% glucose was significant for PE5 and PE21 ($p < 0.05$; the p values for comparing survival curves were calculated with the help of the GraphPad Prism statistics software). CLS extension under CR on 0.5% glucose was not significant for PE4, PE6, PE8 and PE12. Abbreviations: Logarithmic (L), post-diauxic (PD) or stationary (ST) growth phase.

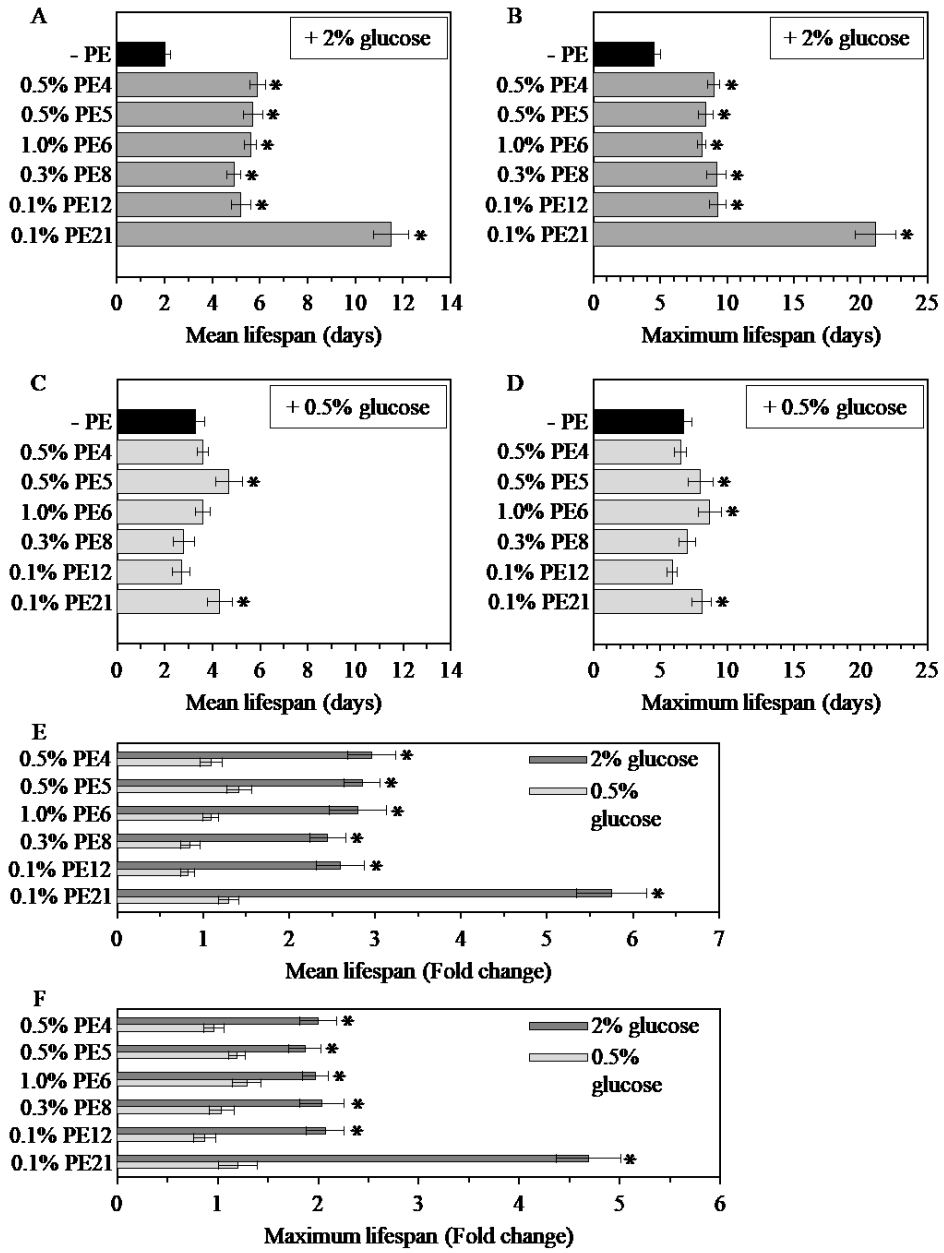

Figure 2.8. The longevity-extending efficacy under non-CR conditions significantly exceeds that under CR conditions for each of the six lifespan-prolonging PEs. WT cells were grown in the synthetic minimal YNB medium initially containing 0.5% glucose (CR conditions) or 2% glucose (non-CR conditions), in the presence of a PE or its absence. The mean (A, C and E) and maximum (B, D and F) lifespans of chronologically aging WT strain cultured under CR (C, D, E and F) or non-CR (A, B, E and F) conditions in the absence of a PE or in the presence of 0.5% PE4, 0.5% PE5, 1% PE6, 0.3% PE8, 0.1% PE12 or 0.1% PE21 are shown; data are presented as means ± SEM (n = 5-7; * $p < 0.05$). The extent to which each of the PE tested increases the mean and maximum lifespans under non-CR conditions exceeds that under CR conditions (* $p < 0.05$; the p values for comparing the means of two groups were calculated with the help of the GraphPad Prism statistics software using an unpaired two-tailed t test).

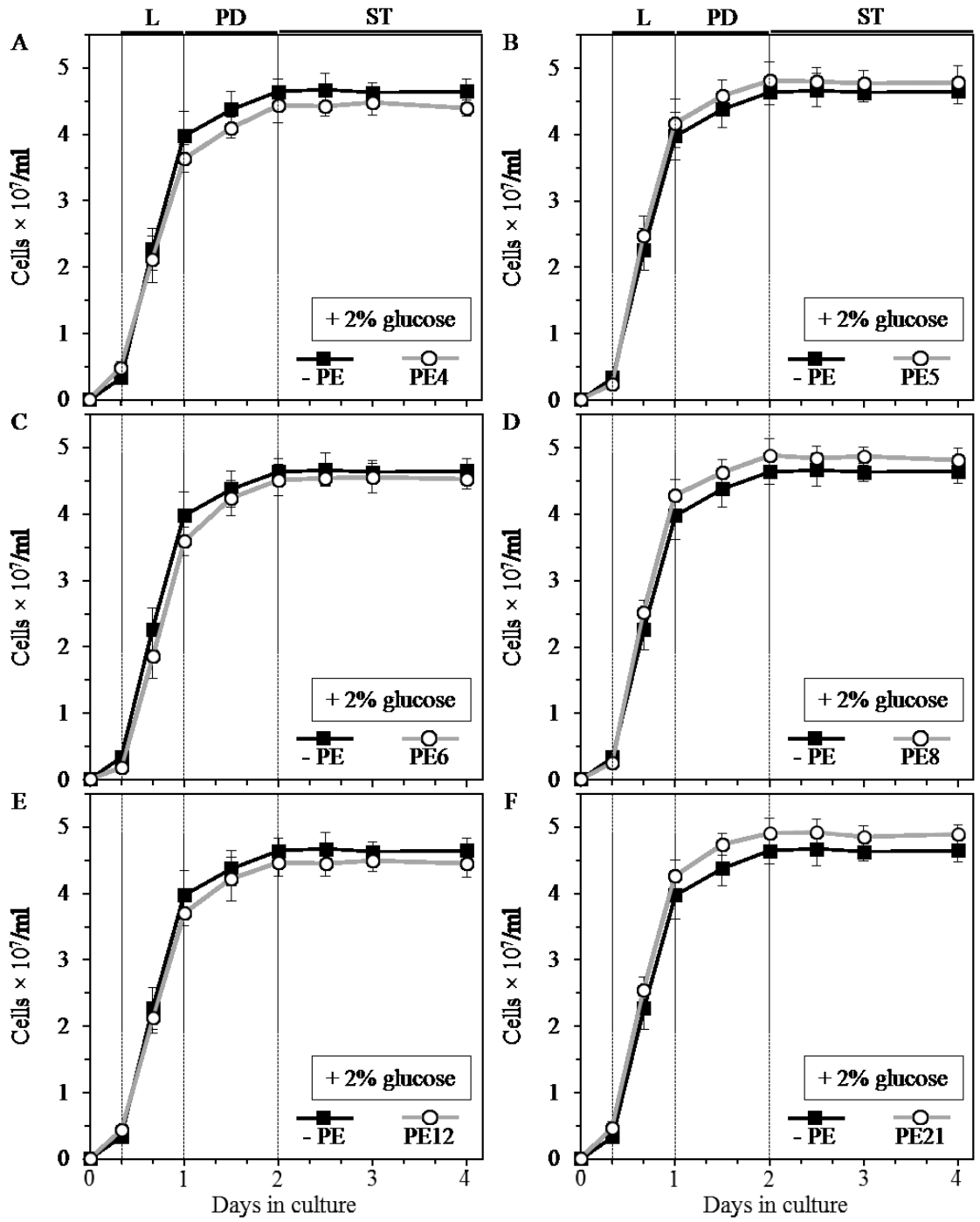

Figure 2.9. PE4, PE5, PE6, PE8, PE12 and PE21 do not cause significant effects on the growth of WT yeast under non-CR conditions. WT cells were grown in the synthetic minimal YNB medium initially containing 2% glucose (non-CR conditions), in the absence of a PE or in the presence of 0.5% PE4 (A), 0.5% PE5 (B), 1% PE6 (C), 0.3% PE8 (D), 0.1% PE12 (E) or 0.1% PE21 (F). Kinetics of cell growth is shown (n = 8-14). Abbreviations: Logarithmic (L), post-diauxic (PD) or stationary (ST) growth phase.

2.3.2 For each of the six lifespan-prolonging PEs, the longevity-extending efficacy under CR conditions is significantly lower than that under non-CR conditions

It has been previously shown that chronologically aging yeast grown under caloric restriction conditions (with 0.5% glucose) are able to live longer than yeast cultured under non-CR conditions (with 2% glucose). In addition, the capacity of the CR diet has been observed for yeast cultured in media of different nutrient compositions [14, 15, 17]. With that in mind, we decided to test the efficiency of the CR diet on lifespan extension on yeast cultured in the YNB medium with and without six plant extracts. Firstly, our test results (Figure 2.7A-2.7C) showed that if we cultured yeast in YNB medium with 0.5% glucose, the CR diet significantly increased both the mean and maximum CLS of *S. cerevisiae.* Secondly, our findings suggested that the addition of PEs to yeast grown under CR conditions had various effects. In fact, both 0.5% of PE5 and 0.1% of PE21 extended the mean CLS of yeast grown under the previously mentioned conditions (Figure 2.7D-2.7I, Figure 2.8C). On the other hand, 0.5% PE5, 1.0% PE6 and 0.1% PE21 were revealed to extend the maximum CLS of yeast grown under CR conditions (Figure 2.7D-2.7I, Figure 2.8D). Notably, the growth rates of yeast cultures in the L and PD phases, as well as the maximum cell density in the ST phase, remained unaltered under CR conditions similar to non-CR conditions (Figure 2.10). After comparing the capacity of PEs to extend mean and maximum CLS of yeast, our results (figures 2.8A-2.8F) show that the six PEs were able to extend the mean and maximum CLS of yeast cultured under non-CR conditions (2% glucose) to an even larger extent than that of yeast under CR (0.5% glucose). This observation indicates that each of these PEs could potentially mimic the longevity-extending effect of CR.

2.3.3 Each of the six longevity-extending PEs is a geroprotector which postpones the onset and slows the advancement of yeast chronological aging because it causes a hormetic stress response

Our previous results indicated that PE4, PE5, PE6, PE8, PE12 and PE21 greatly prolong the mean CLS of yeast cultured under non-CR conditions (Figures 2.1-2.3, Figure 2.6A, Figure 2.8A and 2.8B). When contemplating the aging of an organism, the mean lifespan is said to be directly proportional to the survival rates of organisms in the population during the development and maturity stages. In addition, the mean lifespan is believed to be influenced by certain

environmental factors referred to as extrinsic factors [359, 362-364]. Hence, it is reasonable that the six PEs can decrease the extrinsic rate of yeast chronological aging before cell entry into quiescence or senescence.

Furthermore, we revealed that the same six plant extracts also increase the maximum CLS of yeast cultured under non-CR conditions (Figures 2.1-2.3, Figure 2.6A, Figure 2.8A and 2.8B). Maximum lifespan is believed to reflect the duration of "healthy" life period (i.e., healthspan) during the quiescence/senescence stage of organismal aging; maximum lifespan is likely to be controlled by certain intrinsic (cellular and organismal) longevity modifiers [48, 359, 362, 363, 365, 366]. One could, therefore, conclude that PE4, PE5, PE6, PE8, PE12 and PE21 also decrease the intrinsic rate of yeast chronological aging after cell entry into quiescence or senescence.

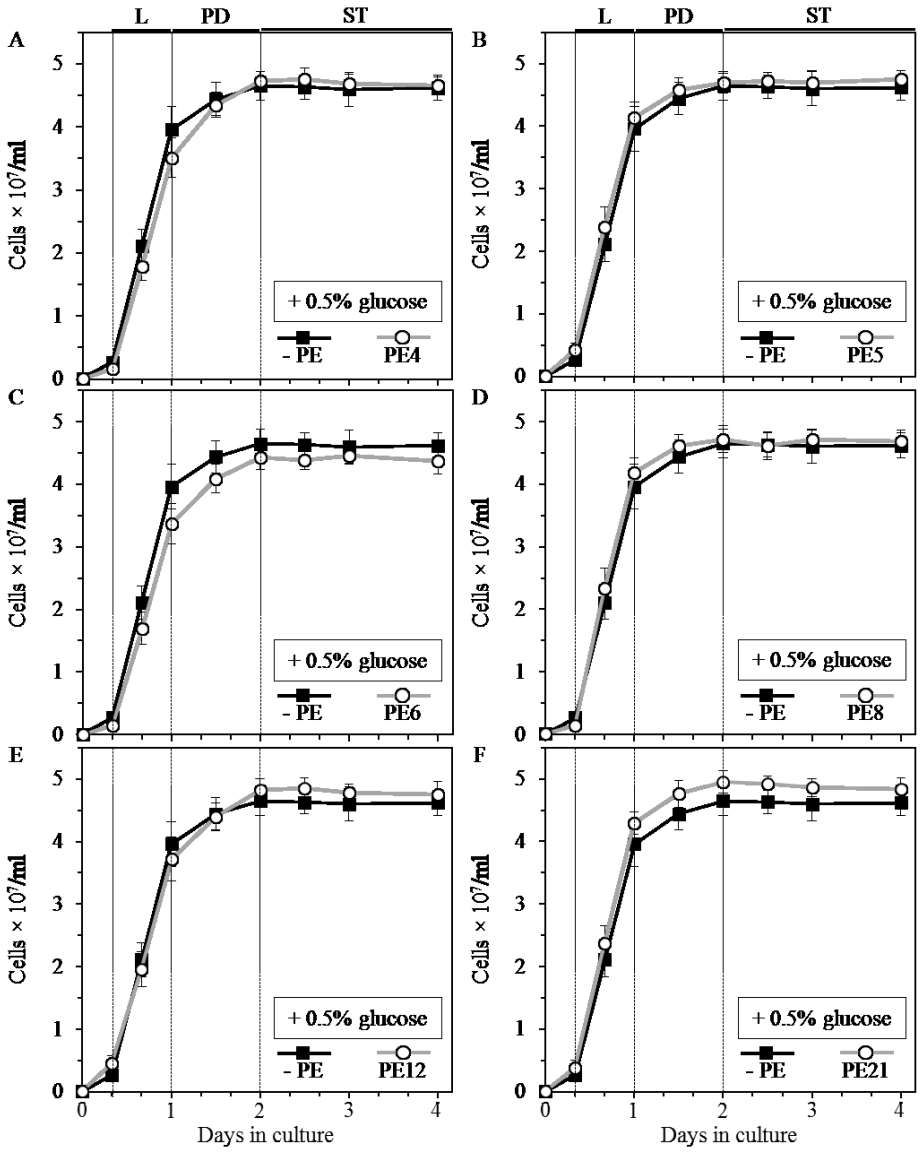

Figure 2.10. PE4, PE5, PE6, PE8, PE12 and PE21 do not cause significant effects on the growth of WT yeast under CR conditions. WT cells were grown in the synthetic minimal YNB medium initially containing 0.5% glucose (CR conditions), in the absence of a PE or in the presence of 0.5% PE4 (**A**), 0.5% PE5 (**B**), 1% PE6 (**C**), 0.3% PE8 (**D**), 0.1% PE12 (**E**) or 0.1% PE21 (**F**). Kinetics of cell growth is shown (n = 6-9). Abbreviations: Logarithmic (L), post-diauxic (PD) or stationary (ST) growth phase.

Our analysis of the Gompertz mortality function further validated the conclusion that PE4, PE5, PE6, PE8, PE12 and PE21 considerably decrease the rate of yeast chronological aging. Indeed, we found that each of these longevity-extending PEs causes a substantial decline in the slope of the Gompertz mortality rate (also known as mortality rate coefficient α) and a considerable rise in the mortality rate doubling time (MRDT) (Figure 2.11A-2.11G). Such changes in the values of α and MRDT are characteristic of interventions that decrease the rate of progression through the process of biological aging [359, 367, 368].

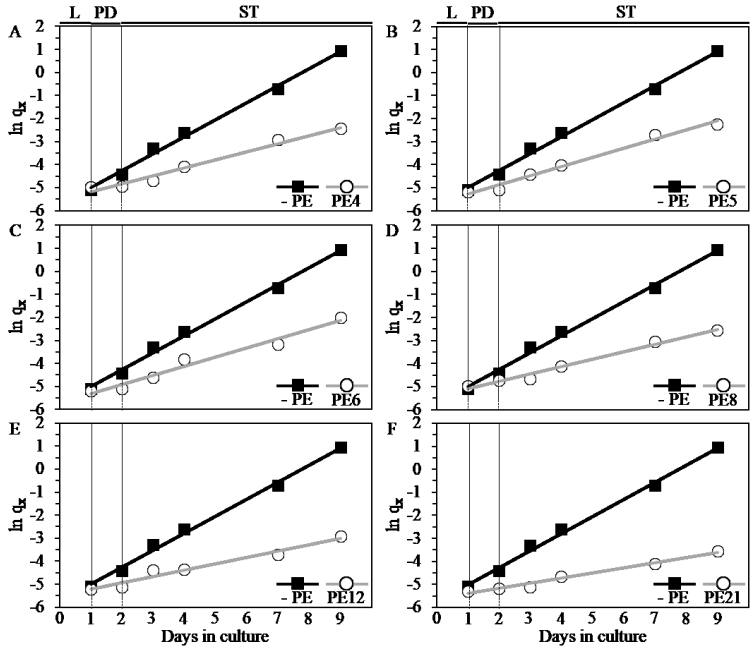

G

PE	α (Gompertz slope or mortality rate coefficient)	MRDT (mortality rate doubling time)	Rate of aging
- PE	0.74	0.94	
0.5% PE4	0.35	1.98	⬇ decreased
0.5% PE5	0.38	1.82	⬇ decreased
1.0% PE6	0.40	1.73	⬇ decreased
0.3% PE8	0.32	2.17	⬇ decreased
0.1% PE12	0.28	2.48	⬇ decreased
0.1% PE21	0.22	3.15	⬇ decreased

Figure 2.11. Analysis of the Gompertz mortality function indicates that PE4, PE5, PE6, PE8, PE12 and PE21 significantly decrease the rate of chronological aging in yeast. WT cells were

grown in synthetic minimal YNB medium initially containing 2% glucose in the presence of a PE or its absence. Survival curves shown in Figs. 2.6A-2.6F were used to calculate the age-specific mortality rates (q_x) of chronologically aging WT yeast populations cultured with or without 0.5% PE4 (A), 0.5% PE5 (B), 1% PE6 (C), 0.3% PE8 (D), 0.1% PE12 (E) or 0.1% PE21 (F). Each of these longevity-extending PEs caused a substantial decrease in the slope of the Gompertz mortality rate (also known as mortality rate coefficient α) and a considerable increase in the mortality rate doubling time (MRDT) (G). The values of q_x, α and MRDT were calculated as described in Materials and methods. Abbreviations: Logarithmic (L), post-diauxic (PD) or stationary (ST) growth phase.

Of note, our analyses of how different concentrations of PE4, PE5, PE6, PE8, PE12 and PE21 influence yeast longevity under non-CR conditions revealed that each of them causes a so-called "hormetic" stress response in chronologically aging yeast concerning longevity. Indeed, the dose-response curves (i.e., the curves that reflect relationships between PE concentrations and mean or maximum CLS) for PE4, PE5, PE8, PE12 and PE21 were inverted U-shaped. Besides, the dose-response curve for PE6 was J-shaped (Figure 2.1-2.3). Such nonlinear and biphasic dose-response curves signify a hormetic type of stress response, in which 1) lower (hormetic) concentrations of a chemical compound increase the survival of a cell or an organism by stimulating biological processes that allow cellular or organismal stress at a level below a threshold of toxicity, whereas 2) higher concentrations of this chemical compound decrease the survival of a cell or an organism by creating stress that exceeds such threshold [116, 254, 369-371].

2.3.4 Each of the six lifespan-extending PEs alters the age-related chronology of longevity-defining traits of mitochondrial functionality

We hypothesized that PE4, PE5, PE6, PE8, PE12 and PE21 slow yeast chronological aging by influencing specific cellular processes. We sought to identify these longevity-defining processes. Certain aspects of mitochondrial functionality (such as mitochondrial respiration, mitochondrial membrane potential and mitochondrial reactive oxygen species [ROS] homeostasis) are known to define the rate of chronological aging in yeast [15, 17, 24, 32, 55, 59, 62, 87, 102, 103, 106, 110, 118, 122, 125, 132, 134, 158]. We, therefore, assessed how PE4, PE5, PE6, PE8, PE12 and PE21 impact these longevity-defining processes in chronologically aging yeast cultures under non-CR conditions on 2% glucose.

We found that each of the six lifespan-extending PEs stimulates coupled mitochondrial respiration, which was assessed by measuring the rate of oxygen consumption by yeast cells. PE4,

PE8 and PE12 significantly decreased the extent to which such respiration declined in ST-phase cultures (Figure 2.12A, 2.12D and 2.12E), whereas PE5, PE6 and PE21 considerably increased the rate of mitochondrial respiration in yeast during the PD and ST phases of culturing (Figure 2.12B, 2.12C and 2.12F).

We also found that each of the six lifespan-extending PEs sustains healthy populations of functional mitochondria that have high mitochondrial membrane potential (ΔΨm). PE4, PE8 and PE12 substantially decreased the extent to which ΔΨm declined during the PD and ST phases of culturing (Figure 2.13A, 2.13D and 2.13E; Figures 2.14 and 2.15), whereas PE5, PE6 and PE21 prevented such decline (Figure 2.13A, 2.13D and 2.13E; Figures 2.14 and 2.15).

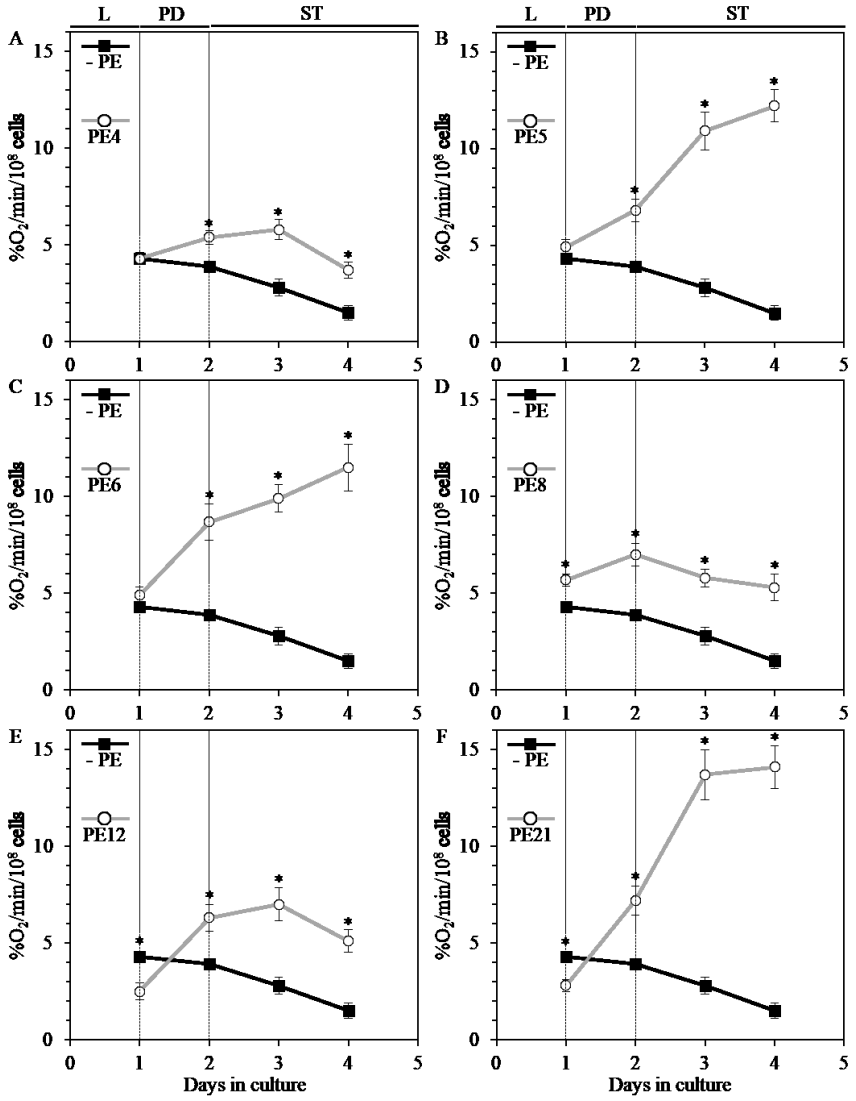

Figure 2.12. PE4, PE5, PE6, PE8, PE12 and PE21 alter the age-related chronology of mitochondrial oxygen consumption by yeast grown under non-CR conditions. WT cells were

grown in the synthetic minimal YNB medium initially containing 2% glucose in the presence of a PE or its absence. A polarographic assay was used to measure oxygen uptake by live yeast cells, as described in Materials and methods. Age-dependent changes in the rate of mitochondrial oxygen consumption by chronologically aging WT strain cultured under non-CR conditions on 2% glucose with or without 0.5% PE4 (A), 0.5% PE5 (B), 1% PE6 (C), 0.3% PE8 (D), 0.1% PE12 (E) or 0.1% PE21 (F) are shown; data are presented as means ± SEM (n = 7-9; * $p < 0.05$; the p values for comparing the means of two groups were calculated with the help of the GraphPad Prism statistics software using an unpaired two-tailed t test). Abbreviations: Logarithmic (L), post-diauxic (PD) or stationary (ST) growth phase.

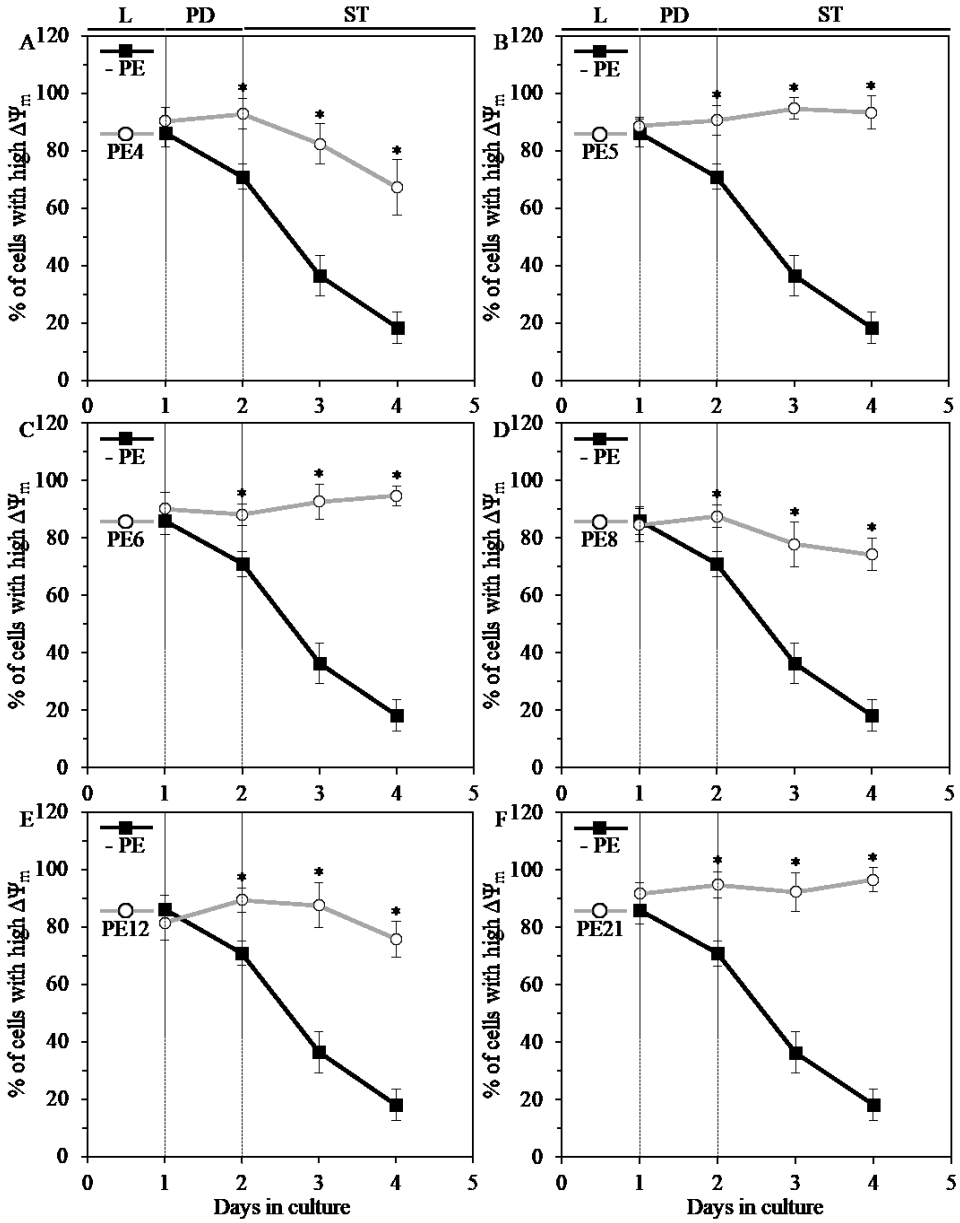

Figure 2.13. PE4, PE5, PE6, PE8, PE12 and PE21 sustain healthy populations of functional mitochondria that exhibit high mitochondrial membrane potential (ΔΨm) in chronologically aging yeast grown under non-CR conditions. WT cells were grown in the synthetic minimal

YNB medium initially containing 2% glucose in the presence of a PE or its absence. ΔΨm was measured in live yeast by fluorescence microscopy of Rhodamine 123 staining, as described in Materials and methods. Age-dependent changes in the percentage of WT cells displaying high ΔΨm in chronologically aging yeast cultures under non-CR conditions on 2% glucose with or without 0.5% PE4 (A), 0.5% PE5 (B), 1% PE6 (C), 0.3% PE8 (D), 0.1% PE12 (E) or 0.1% PE21 (F) are shown; data are presented as means ± SEM (n = 3-4; * $p < 0.05$; the p values for comparing the means of two groups were calculated with the help of the GraphPad Prism statistics software using an unpaired two-tailed t test). Abbreviations: Logarithmic (L), post-diauxic (PD) or stationary (ST) growth phase.

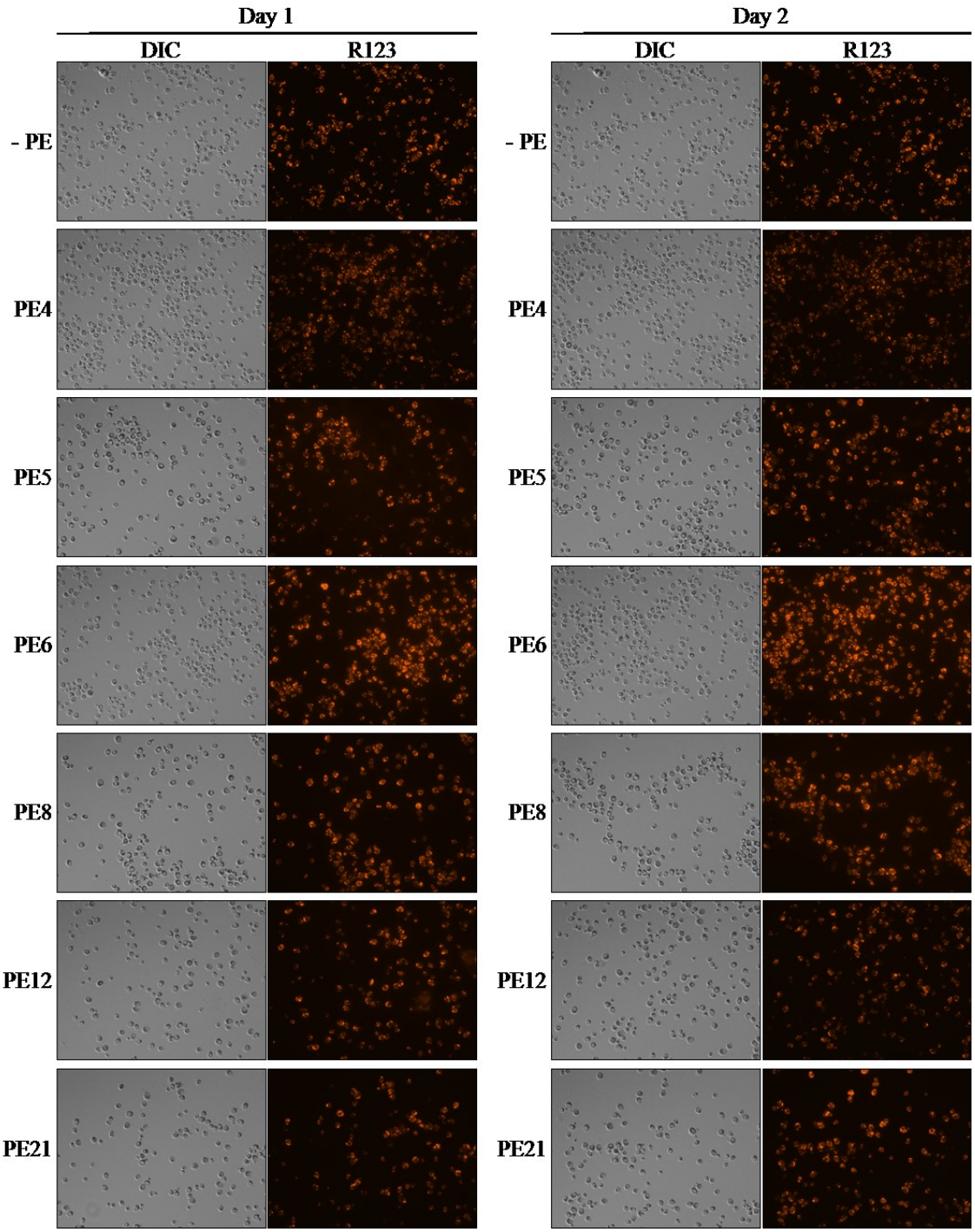

Figure 2.14. PE4, PE5, PE6, PE8, PE12 and PE21 significantly delay an age-dependent decline in the number of WT cells that exhibit high mitochondrial membrane potential under non-CR conditions. WT cells were grown in the synthetic minimal YNB medium initially containing 2% glucose in the presence of a PE or its absence. Yeast cells were recovered at days 1 and 2 of culturing, stained with Rhodamine 123 (R123) for visualizing cells displaying high mitochondrial membrane potential, and subjected to live-cell fluorescence microscopy and differential interference contrast (DIC) microscopy as described in Materials and methods.

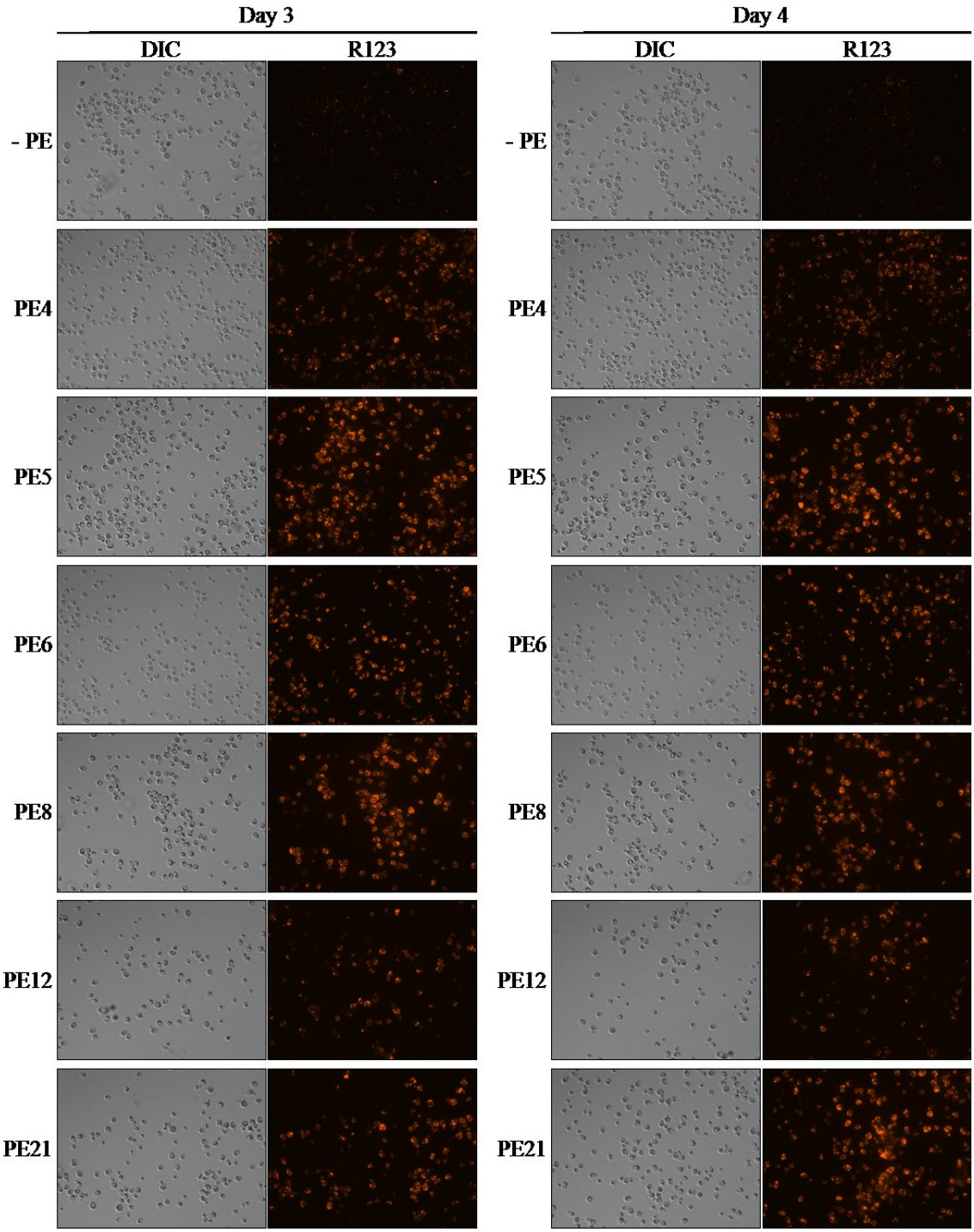

Figure 2.15. PE4, PE5, PE6, PE8, PE12 and PE21 significantly delay an age-dependent decline in the number of WT cells that exhibit high mitochondrial membrane potential under non-CR conditions. WT cells were grown in the synthetic minimal YNB medium initially containing 2% glucose in the presence of a PE or its absence. Yeast cells were recovered at days 3 and 4 of culturing, stained with R123 for visualizing cells displaying high mitochondrial membrane potential, and subjected to live-cell fluorescence microscopy and DIC microscopy as described in Materials and methods.

PE4, PE5, PE6, PE8, PE12 and PE21 also caused significant changes in the age-related chronology of intracellular ROS, which in yeast and other organisms are known to be formed mainly as by-products of mitochondrial respiration [66, 179]. Each of these PEs decreased the extent to which the intracellular concentration of mitochondrially generated ROS declined during the PD and ST phases of culturing (Figure 2.16A-2.16F). On days 3 and 4 of culturing, ROS concentrations in yeast exposed to PE4, PE5, PE6, PE8, PE12 or PE21 exceeded those in yeast cultured without it (Figure 2.16A-2.16F).

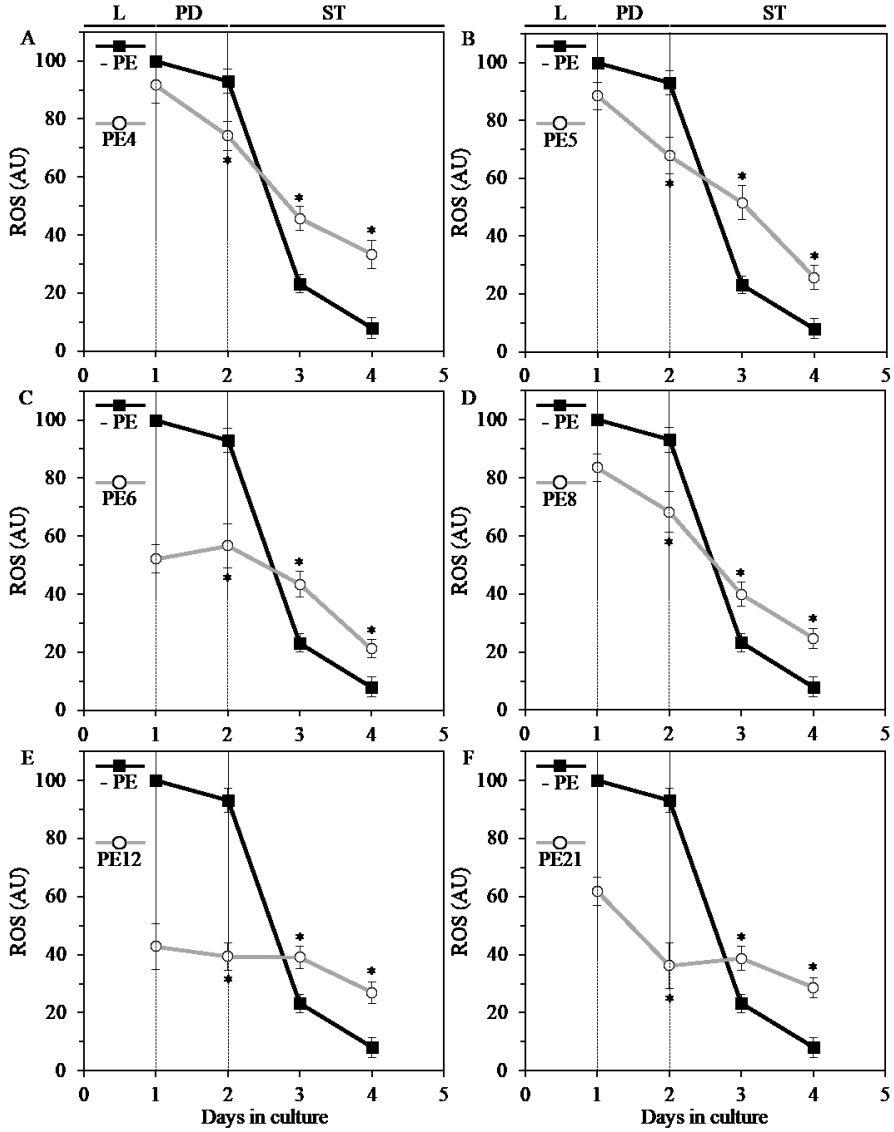

Figure 2.16. In yeast grown under non-CR conditions, PE4, PE5, PE6, PE8, PE12 and PE21 alter the patterns of age-related changes in intracellular reactive oxygen species (ROS) known to be generated mainly as by-products of mitochondrial respiration. WT cells were grown in the synthetic minimal YNB medium initially containing 2% glucose in the presence of a

PE or its absence. The intracellular concentrations of ROS were measured in live yeast by fluorescence microscopy of dihydrorhodamine 123 staining, as described in Materials and methods. Age-dependent changes in ROS concentrations within chronologically aging WT cells cultured under non-CR conditions on 2% glucose with or without 0.5% PE4 (A), 0.5% PE5 (B), 1% PE6 (C), 0.3% PE8 (D), 0.1% PE12 (E) or 0.1% PE21 (F) are shown. Data are presented as means ± SEM (n = 3-4; * $p < 0.05$; the p values for comparing the means of two groups were calculated with the help of the GraphPad Prism statistics software using an unpaired two-tailed t test). Abbreviations: Logarithmic (L), post-diauxic (PD) or stationary (ST) growth phase.

2.3.5 The six lifespan-extending PEs differently influence the extent of age-related oxidative damage to cellular proteins, membrane lipids, mitochondrial and nuclear genomes

A body of evidence supports the following view on the relationships between cellular ROS, oxidative molecular damage and aging in organisms across species: 1) if cellular concentrations of ROS exceed a threshold of toxicity, ROS cause oxidative damage to proteins, lipids and DNA, 2) oxidative damage to these macromolecules accumulates with age, and 3) cumulative oxidative damage to the different types of macromolecules is one of the major causes of aging [123, 372-379]. We, therefore, examined how PE4, PE5, PE6, PE8, PE12 and PE21 influence the extent of oxidative damage to proteins, lipids and DNA in chronologically aging yeast cultured under non-CR conditions on 2% glucose.

We found that each of the six lifespan-extending PEs postpones the onset of an age-related rise in the extent of oxidative damage to cellular proteins. PE6, PE12 and PE21 decreased oxidative carbonylation of proteins in yeast cells advancing through the ST phase of culturing (Figure 2.17C, 2.17E and 2.17F). PE4, PE5 and PE8 elicited such inhibitory effect on oxidative protein damage only later in the ST phase, on day 4 of culturing (Figure 2.17A, 2.17B and 2.17D).

Furthermore, PE5, PE6, PE8, PE12 and PE21 (but not PE4) caused a significant decline in the levels of oxidatively damaged membrane lipids; such decline was observed late in the ST phase, on days 3 and/or 4 of culturing (Figure 2.17H-2.17L).

Moreover, PE4, PE5, PE6, PE8, PE12 and PE21 decreased the frequencies of spontaneous point mutations in the *RIB2* and *RIB3* genes of mitochondrial DNA (mtDNA) (Figure 2.18A-2.18F) - likely due to a reduced extent of oxidative damage to mtDNA in yeast cells exposed to any of these PEs. Such inhibitory effects of the six lifespan-extending PEs on oxidative damage to mtDNA were observed late in the ST phase, on day 4 of culturing.

We also found that PE12 and PE21 (but not PE4, PE5, PE6 or PE8) caused a significant decline in the frequencies of spontaneous point mutations in the *CAN1* gene of nuclear DNA (nDNA) (Figure 2.18K and 2.18L) - possibly due to a decreased degree of oxidative damage to nDNA in yeast cells cultured in the presence of PE12 or PE21. Such inhibitory effects of PE12 or PE21 on oxidative damage to nDNA were also observed late in the ST phase, on day 4 of culturing.

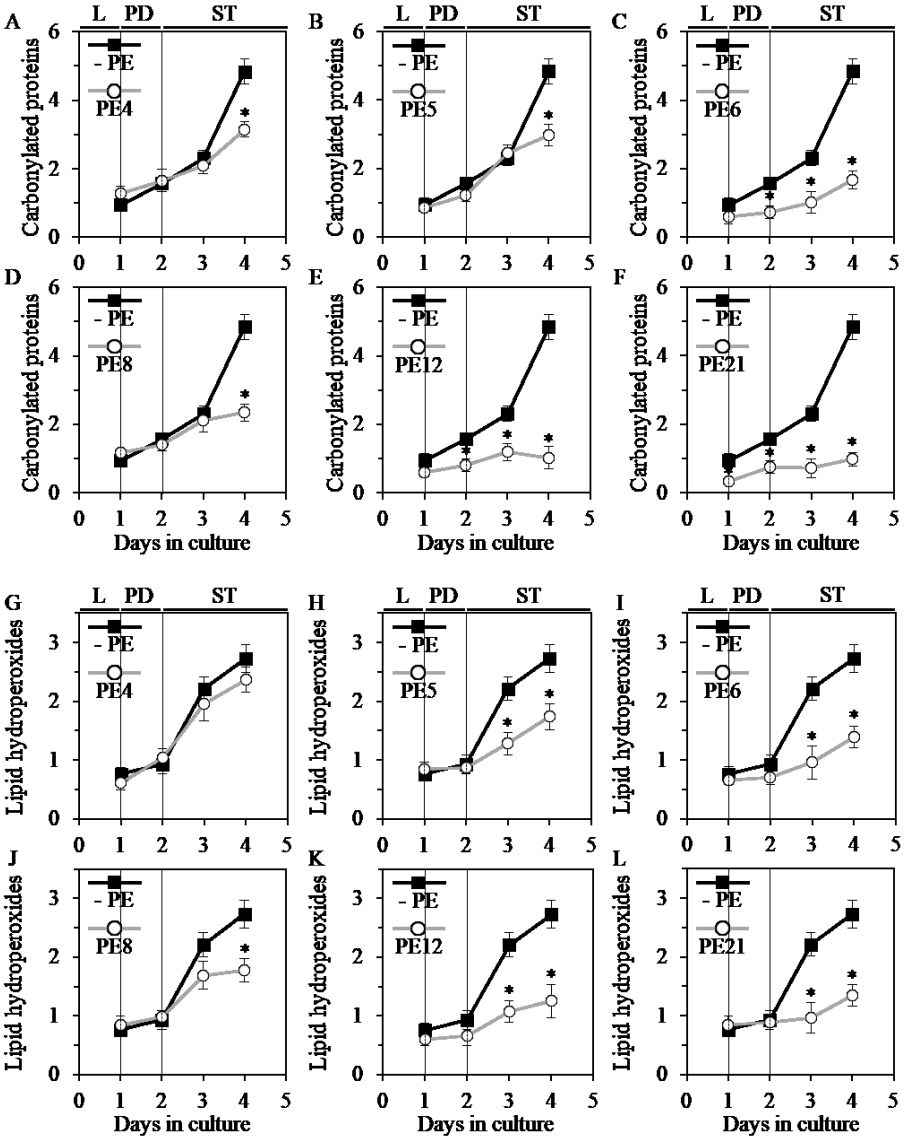

Figure 2.17. PE4, PE5, PE6, PE8, PE12 and PE21 delay an age-dependent rise in the extent of oxidative damage to cellular proteins in chronologically aging yeast grown under non-CR conditions. PE5, PE6, PE8, PE12 and PE21, but not PE4, have similar effects on the extent of oxidative damage to membrane lipids. WT cells were grown in the synthetic minimal YNB medium initially containing 2% glucose in the presence of a PE or its absence. Carbonylated cellular proteins (A – F) and oxidatively damaged membrane lipids (G – L) were determined as described in Materials and methods. Age-dependent changes in the concentrations of these

oxidatively damaged macromolecules within chronologically aging WT cells cultured under non-CR conditions on 2% glucose with or without 0.5% PE4 (A and G), 0.5% PE5 (B and H), 1% PE6 (C and I), 0.3% PE8 (D and J), 0.1% PE12 (E and K) or 0.1% PE21 (F and L) are shown; data are presented as means ± SEM (n = 2-4; * $p < 0.05$; the p values for comparing the means of two groups were calculated with the help of the GraphPad Prism statistics software using an unpaired two-tailed t test). Abbreviations: Logarithmic (L), post-diauxic (PD) or stationary (ST) growth phase.

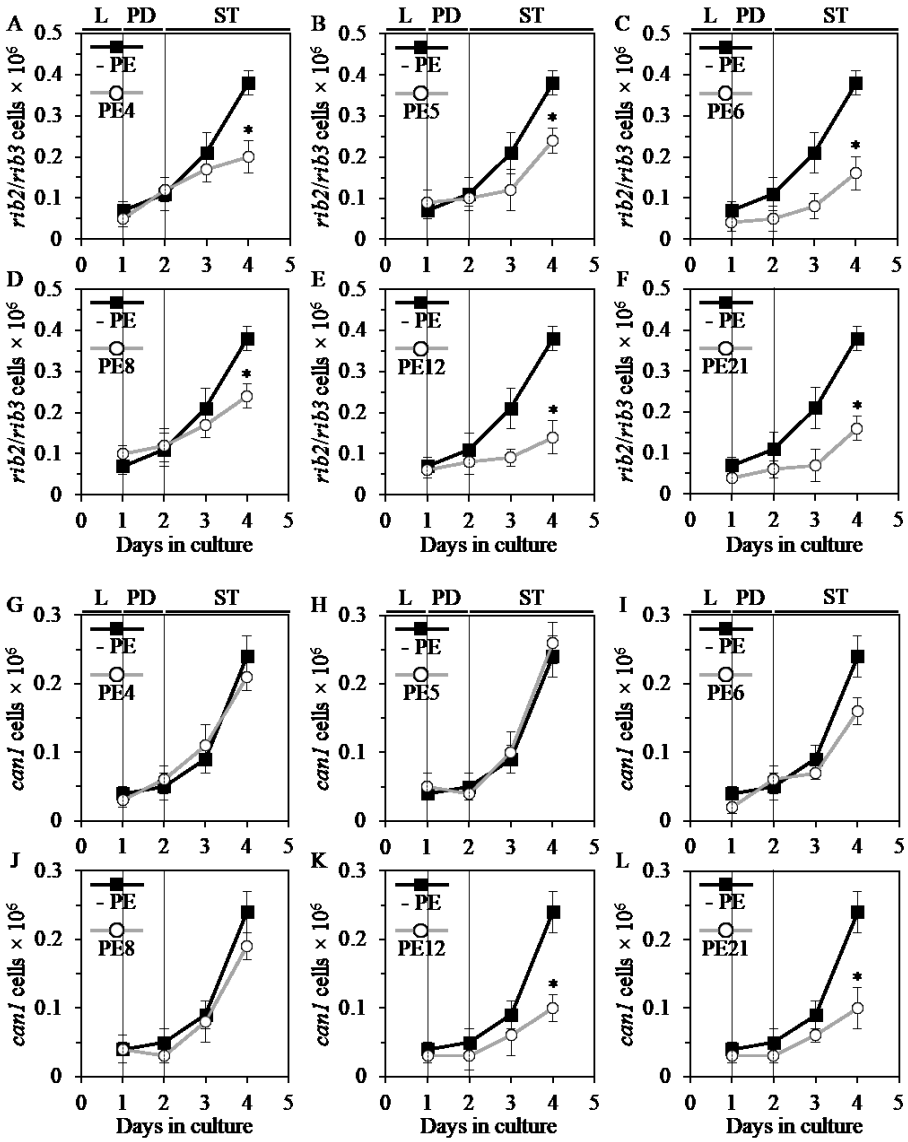

Figure 2.18. PE4, PE5, PE6, PE8, PE12 and PE21 slow down an age-dependent rise in the frequency of spontaneous point mutations in the *RIB2* and *RIB3* loci of mitochondrial DNA (mtDNA) in chronologically aging yeast cultured under non-CR conditions. PE12 and PE21, but not PE4, PE5, PE6 or PE8, have similar effects on the frequency of spontaneous point mutations in the *CAN1* gene of nuclear DNA (nDNA). WT cells were grown in the synthetic minimal YNB medium initially containing 2% glucose in the presence of a PE or its absence. The frequency of spontaneous point mutations in the *RIB2* and *RIB3* loci of mtDNA (A - F), as well as

the frequency of spontaneous point mutations in the *CAN1* gene of nDNA (G - L), were measured as described in Materials and methods. Age-dependent changes in the frequencies of these mtDNA and nDNA mutations in chronologically aging WT cells cultured under non-CR conditions on 2% glucose with or without 0.5% PE4 (A and G), 0.5% PE5 (B and H), 1% PE6 (C and I), 0.3% PE8 (D and J), 0.1% PE12 (E and K) or 0.1% PE21 (F and L) are shown; data are presented as means ± SEM (n = 3-5; * $p < 0.05$; the p values for comparing the means of two groups were calculated with the help of the GraphPad Prism statistics software using an unpaired two-tailed t test). Abbreviations: Logarithmic (L), post-diauxic (PD) or stationary (ST) growth phase.

2.3.6 The six lifespan-extending PEs differently influence the resistance of chronologically aging yeast to chronic oxidative and thermal stresses

A wealth of research has shown that the development of resistance to chronic (long-term) oxidative and/or thermal stresses can extend longevity in organisms across species, including yeast [11, 14, 15, 17, 32, 68, 178, 179, 254, 370, 371, 380-382]. We, therefore, assessed how PE4, PE5, PE6, PE8, PE12 and PE21 influence the abilities of chronologically aging yeast cultured under non-CR conditions to resist chronic oxidative and thermal stresses.

Chronic oxidative stress was administered by recovering yeast cells advancing through the L, PD or ST phases of culturing in liquid YNB medium initially containing 2% glucose, spotting these cells on solid YEP medium with 2% glucose and 5 mM hydrogen peroxide, and incubating them for 3 days. We found that PE6, PE12 and PE21 significantly increase cell resistance to chronic oxidative stress in yeast cultures advancing through the L, PD and ST phases of culturing (Figure 2.19A and 2.19B). PE4, PE5 and PE8 enhanced the ability of cells to resist chronic oxidative stress only in yeast cultures advancing through the ST phase but did not alter such ability during the L and PD phases of culturing (Figure 2.19A and 2.19B).

Chronic thermal stress was administered by recovering yeast cells advancing through the L, PD or ST phases of culturing in liquid YNB medium initially containing 2% glucose, spotting these cells on solid YEP medium with 2% glucose and incubating at 60°C for 60 min, and then transferring plates with these cells to 30°C and incubating at this temperature for 3 days. We found that PE6, PE8, PE12 and PE21 increase cell resistance to chronic thermal stress only in yeast cultures advancing through the ST phase of culturing (Figure 2.20A and 2.20B). In contrast, each of these four lifespan-extending PEs weakened the ability of cells to resist chronic thermal stress during the L and PD phases of culturing (Figure 2.20A and 2.20B). Furthermore, neither PE4 nor PE5 altered cell resistance to chronic thermal stress in yeast cultures advancing through the ST

phase of culturing (Figure 2.20A and 2.20B). PE4 did not affect the ability of cells to resist chronic thermal stress also during the L and PD phases of culturing, whereas PE5 weakened such ability in yeast cultures advancing through these two phases of culturing (Figure 2.20A and 2.20B).

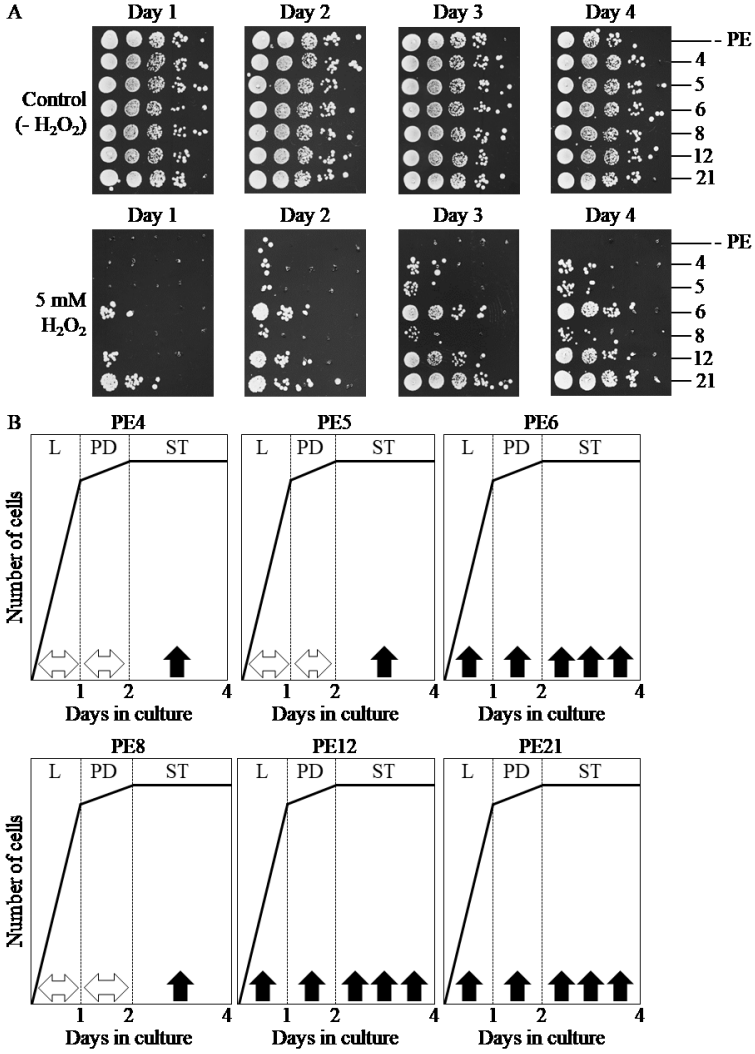

Figure 2.19. PE4, PE5, PE6, PE8, PE12 and PE21 enhance the ability of chronologically aging yeast grown under non-CR conditions to resist chronic oxidative stress. WT cells were grown in the synthetic minimal YNB medium initially containing 2% glucose in the presence of a PE or its absence. (A) Spot assays for monitoring oxidative stress resistance were performed as described in Materials and methods. Serial 10-fold dilutions of cells recovered at different days of culturing were spotted on plates with solid YEP medium containing 2% glucose as carbon source, with or without 5 mM hydrogen peroxide. All pictures were taken after a 3-d incubation at 30ºC. (B) A model for how 0.5% PE4, 0.5% PE5, 1% PE6, 0.3% PE8, 0.1% PE12 and 0.1% PE21 influence the resistance of yeast to chronic oxidative stress during the logarithmic (L), post-diauxic (PD) or stationary (ST) phases of growth. ⇔ or ⬆ Denote unaltered or enhanced, respectively, cell resistance to chronic oxidative stress during a particular phase of growth. Abbreviations: Logarithmic (L), post-diauxic (PD) or stationary (ST) growth phase.

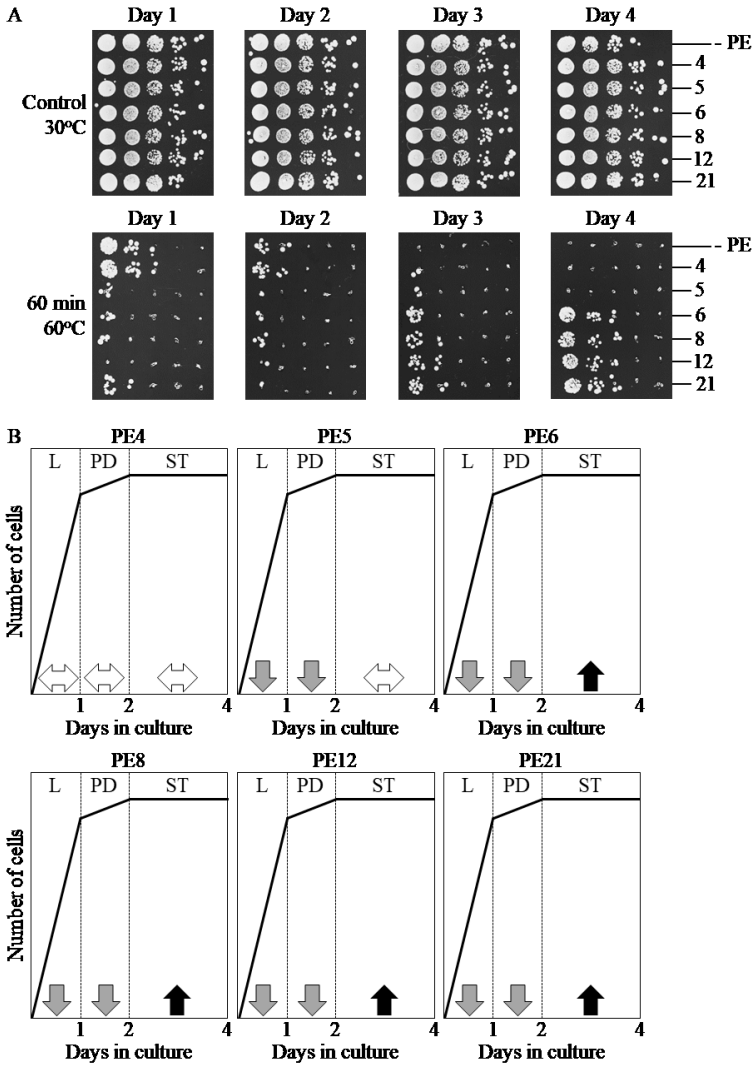

Figure 2.20. PE4, PE5, PE6, PE8, PE12 and PE21 exhibit different effects on the ability of chronologically aging yeast grown under non-CR conditions to resist chronic thermal stress. WT cells were grown in the synthetic minimal YNB medium initially containing 2% glucose in the presence of a PE or its absence. (A) Spot assays for monitoring thermal stress resistance were performed as described in Materials and methods. Serial 10-fold dilutions of cells recovered at different days of culturing were spotted on plates with solid YEP medium containing 2% glucose as carbon source. Plates were initially incubated at 30ºC (control) or 60ºC for 60 min and were then transferred to 30ºC. All pictures were taken after a 3-d incubation at 30ºC. (B) A model for how 0.5% PE4, 0.5% PE5, 1% PE6, 0.3% PE8, 0.1% PE12 and 0.1% PE21 influence the resistance of yeast to chronic thermal stress during the logarithmic (L), post-diauxic (PD) or stationary (ST) phases of growth. ⇔⇩ or ⬆ Denote unaltered, reduced or enhanced, respectively, cell resistance to chronic thermal stress during a particular phase of growth. Abbreviations: Logarithmic (L), post-diauxic (PD) or stationary (ST) growth phase.

2.3.7 Each of the six lifespan-extending PEs causes rapid degradation of neutral lipids deposited in lipid droplets

Triacylglycerols and steryl esters are uncharged (and therefore are called "neutral" or "nonpolar") classes of lipids that can be found in cells of all eukaryotic organisms [183, 383, 384]. After being initially synthesized in the endoplasmic reticulum and then deposited in lipid droplets (LDs), these two highly hydrophobic lipids can undergo lipolytic degradation to provide substrates for the synthesis of phospholipids and sphingolipids [183, 385-388]. New evidence supports the view that the biosynthesis, storage and lipolysis of neutral lipids are longevity assurance processes; importantly, it has been shown that these processes can be controlled by specific dietary and pharmacological interventions known to slow aging in various eukaryotes, including yeast [9, 17, 32, 98, 110, 113, 127, 136, 161, 210, 388-402]. We, therefore, used live-cell fluorescence microscopy to examine how PE4, PE5, PE6, PE8, PE12 and PE21 influence the age-related dynamics of changes in the intracellular concentration of neutral lipids confined to LDs in chronologically aging yeast grown under non-CR conditions.

We found that each of the six lifespan-extending PEs causes a rapid age-related decline in the number of yeast cells having LDs (Figures 2.21A–2.21F; Figures 2.22 and 2.23). In contrast, no significant changes in the number of cells with LDs were seen in yeast advancing through the L, PD and ST phases of culturing in medium without a PE (Figures 2.21A-2.21F; Figures 2.22 and 2.23). These findings show that in chronologically aging yeast grown under non-CR conditions, each of the six lifespan-extending PEs causes rapid lipolytic degradation of neutral lipids stored in LDs.

2.4 Discussion

In this study, we performed a screen for PEs capable of extending the longevity of the chronologically aging yeast. Our screen uncovered six PEs (which we call PE4, PE5, PE6, PE8, PE12 and PE21) that can significantly increase yeast CLS. We demonstrated that each of these PEs is a geroprotector postponing the onset and slowing the advancement of yeast chronological aging because it causes a hormetic stress response. We provided evidence that each of these geroprotective PEs has different effects on cellular processes known to assure longevity in organisms across species. Such effects include the following: 1) amplified mitochondrial respiration and membrane potential, 2) increased or decreased concentrations of ROS, 3) decreased oxidative damage to cellular proteins, membrane lipids, and mitochondrial and nuclear genomes, 4) enhanced cell resistance to oxidative and thermal stresses, and 5) accelerated degradation of

neutral lipids deposited in LDs (Figure 2.24). These findings provide critical new insights into mechanisms through which some chemical compounds of plant origin can slow biological aging.

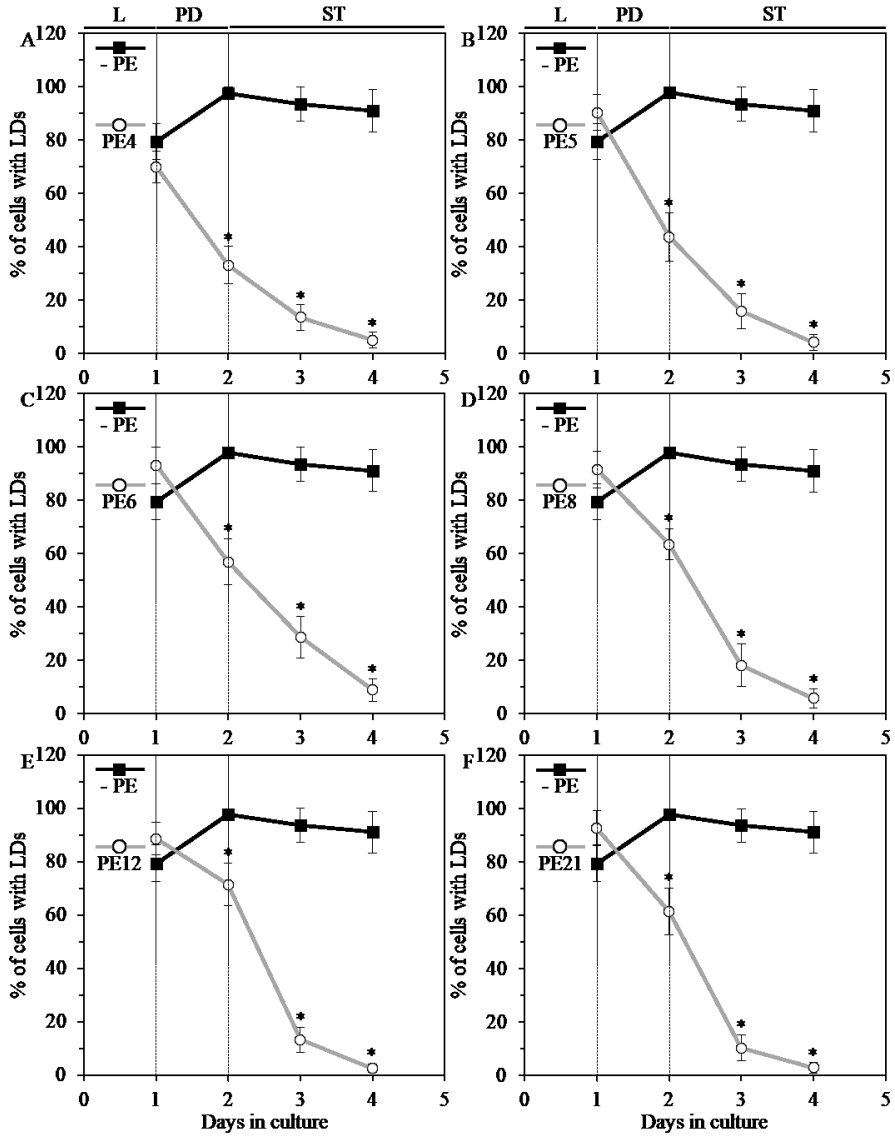

Figure 2.21. PE4, PE5, PE6, PE8, PE12 and PE21 induce rapid consumption of neutral lipids deposited in lipid droplets (LDs) of chronologically aging yeast grown under non-CR conditions. WT cells were grown in the synthetic minimal YNB medium initially containing 2% glucose in the presence of a PE or its absence. Neutral lipids deposited in LDs were measured in live yeast by fluorescence microscopy of BODIPY 493/503 staining, as described in Materials and methods. Age-dependent changes in the percentage of WT cells exhibiting LDs in chronologically aging yeast cultures under non-CR conditions on 2% glucose with or without 0.5% PE4 (A), 0.5% PE5 (B), 1% PE6 (C), 0.3% PE8 (D), 0.1% PE12 (E) or 0.1% PE21 (F) are shown; data are presented as means ± SEM (n = 3-4; * $p < 0.05$; the p values for comparing the means of two groups were calculated with the help of the GraphPad Prism statistics software using an unpaired

two-tailed *t* test). Abbreviations: Logarithmic (L), post-diauxic (PD) or stationary (ST) growth phase.

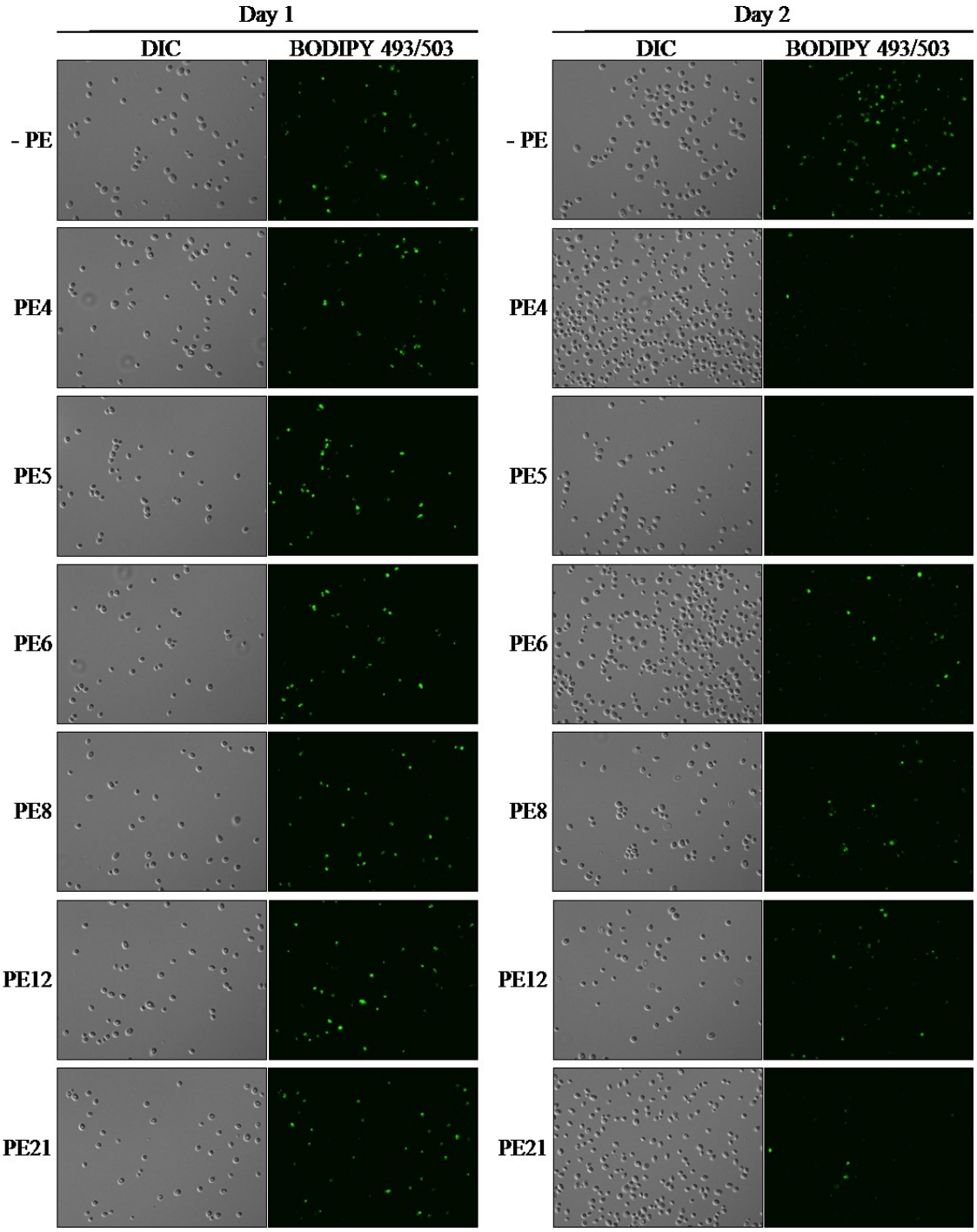

Figure 2.22. PE4, PE5, PE6, PE8, PE12 and PE21 significantly accelerate an age-dependent decline in the number of WT cells that exhibit LDs under non-CR conditions. WT cells were grown in the synthetic minimal YNB medium initially containing 2% glucose in the presence of a PE or its absence. Yeast cells were recovered at days 1 and 2 of culturing, stained with BODIPY 493/503 for visualizing cells displaying neutral lipids deposited in LDs, and subjected to live-cell

fluorescence microscopy and differential interference contrast (DIC) microscopy as described in Materials and methods.

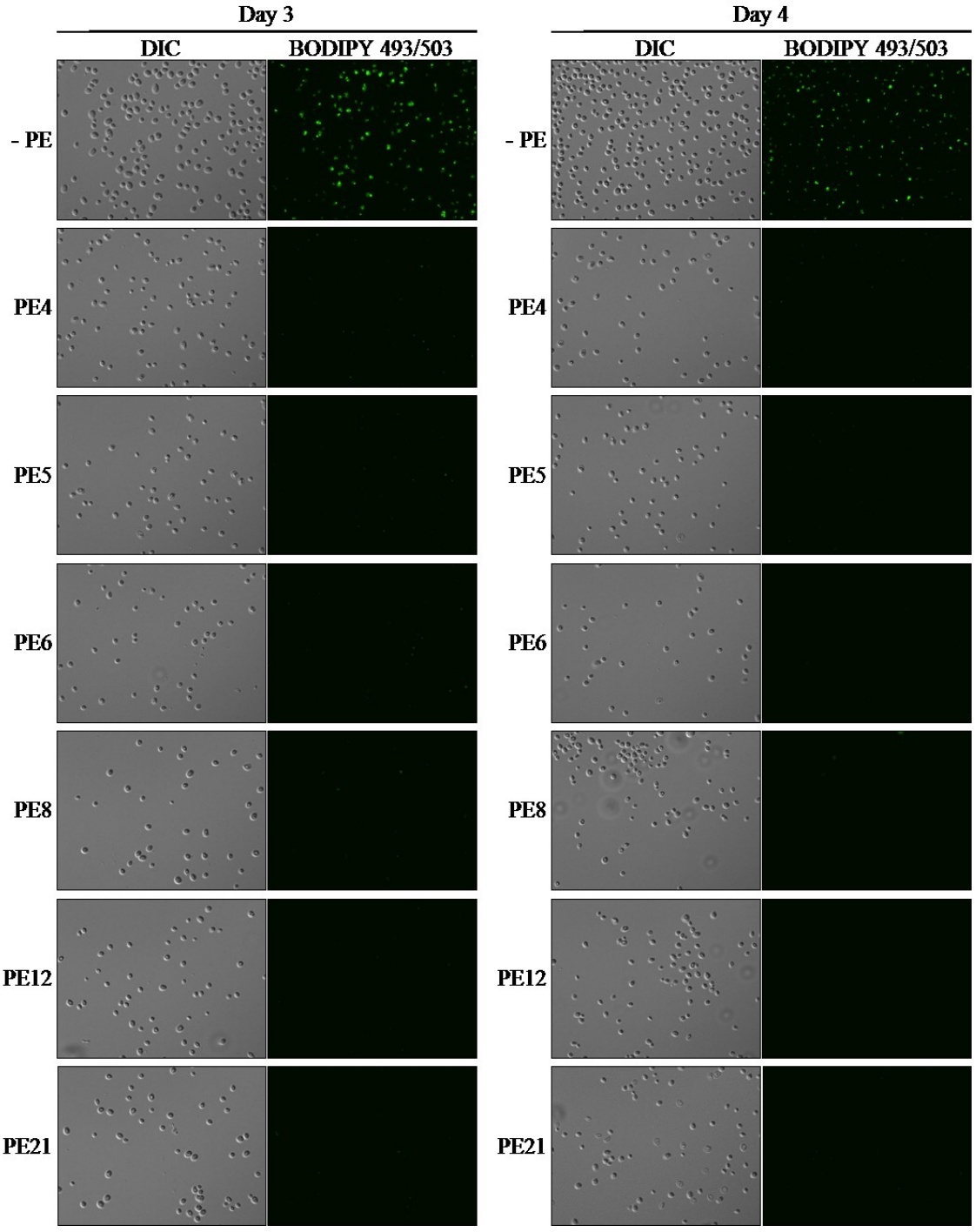

Figure 2.23. PE4, PE5, PE6, PE8, PE12 and PE21 significantly accelerate an age-dependent decline in the number of WT cells that exhibit LDs under non-CR conditions. WT cells were grown in the synthetic minimal YNB medium initially containing 2% glucose in the presence of a PE or its absence. Yeast cells were recovered at days 3 and 4 of culturing, stained with BODIPY 493/503 for visualizing cells displaying neutral lipids deposited in LDs, and subjected to live-cell

fluorescence microscopy and differential interference contrast (DIC) microscopy as described in Materials and methods.

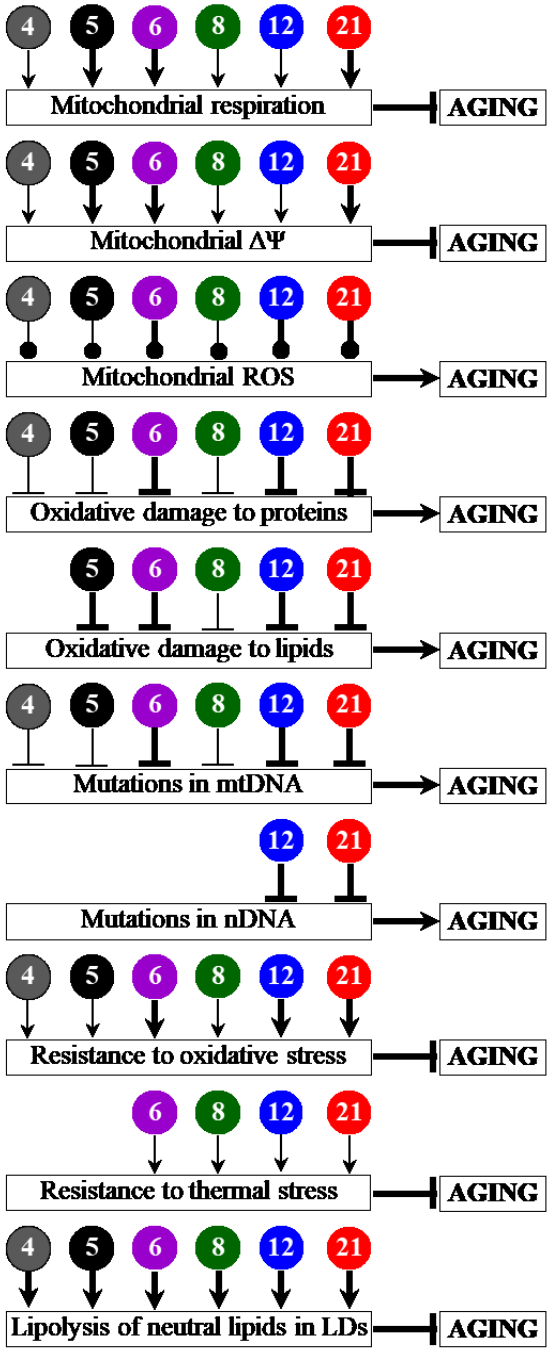

Figure 2.24. PE4, PE5, PE6, PE8, PE12 and PE21 delay yeast chronological aging and have different effects on several longevity-defining cellular processes. Arrows pointing at boxes with the terms of longevity-defining cellular processes denote activation of these processes, T bars denote inhibition of these processes, whereas lines with filled circles denote a change in the age-related chronology of intracellular ROS. The thickness of such arrows, T bars and lines with filled circles correlates with the extent to which a PE activates, inhibits or alters the age-related chronology (respectively) of a particular longevity-defining cellular process. Arrows and T bars

pointing at boxes with the term "AGING" denote acceleration or deceleration (respectively) of yeast chronological aging.

2.4.1 Each of the six longevity-extending PEs increases lifespan more efficiently than any lifespan-prolonging chemical compound presently known

Our findings indicate that the efficiency of longevity extension by PE4, PE5, PE6, PE8, PE12 or PE21 significantly exceeds that for any of the 42 chemical compounds known to increase lifespan in yeasts, filamentous fungi, nematodes, fruit flies, daphnias, mosquitoes, honey bees, fishes, mammals and cultured human cells (Table 2.3). Indeed, under non-CR conditions, these longevity-extending PEs increase the mean and maximum CLS of yeast by 145%–475% and 80%–369%, respectively (Figure 2.8A and 2.8B; Table 2.3); the corresponding rows in Table 2.3 are highlighted in yellow. In contrast, any of the 42 currently known lifespan-extending chemical compounds has been shown to extend cellular and/or organismal lifespan in evolutionarily distant eukaryotes much less efficiently, within the 5% to 75% range (Table 2.3) [61-63, 83, 197, 227, 271, 273, 368, 403-451]. Only two chemical compounds, spermidine under non-CR conditions and lithocholic acid under CR-conditions, have been reported to have the lifespan-extending efficiencies that are comparable to those for PE4, PE5, PE6, PE8 and PE12 (Table 2.3) [83, 102, 110]. Specifically, both these pharmacological interventions were demonstrated to increase the RLS and/or CLS of yeast and human peripheral blood mononuclear cells by 83%-200%; the corresponding rows in Table 2.3 are highlighted in green. Of note, PE21 appears to be the most potent longevity-extending pharmacological intervention presently known. It increases the mean and maximum CLS of yeast by 475% and 369%, respectively (Figure 2.8A and 2.8B; Table 2.3).

Table 2.3. Percent increase of lifespan by geroprotective PEs in this study and by longevity-extending chemical compounds that have been previously identified.

PE or chemical compound	% increase of lifespan* [reference]	Organism exhibiting lifespan increase
0.5% PE4	195% (mean CLS) [this study] 100% (max** CLS) [this study]	*S. cerevisiae*
0.5% PE5	185% (mean CLS) [this study] 87% (max CLS) [this study]	*S. cerevisiae*

1.0 % PE6	180% (mean CLS) [this study] 80% (max CLS) [this study]	*S. cerevisiae*
0.3% PE8	145% (mean CLS) [this study] 104% (max) [this study]	*S. cerevisiae*
0.1% PE12	160% (mean CLS) [this study] 107% (max CLS) [this study]	*S. cerevisiae*
0.1% PE21	475% (mean CLS) [this study] 369% (max CLS) [this study]	*S. cerevisiae*
Acteoside	24 - 25% (female); 16 - 18% (male) (mean OLS) [419] 9 - 13% (female); 9 - 15% (male) (max OLS) [419]	The fruit fly *Drosophila melanogaster*
Butein	55% (mean RLS) [271]	*S. cerevisiae*
Caffeic acid	11% (mean OLS) [440]	The nematode *Caenorhabditis elegans*
Caffeine	8% (median CLS) [197] 46% (mean CLS) [449] 17% (max CLS) [449] 52% (mean OLS) [438]; 37% (mean OLS) [448] 29% (median OLS) [438]	*S. cerevisiae* The yeast *Schizosaccharomyces pombe* *C. elegans*
Catechin	15% (mean OLS) [427] 14% (median OLS) [427]	*C. elegans*
Celastrol	13% (mean OLS) [409]	Mouse model of amyotrophic lateral sclerosis
Curcumin, tetrahydrocurcumin	13% - 39% (mean OLS) [437] 26% (females; mean OLS); 16% (males; mean OLS) [433, 451] 75% (median OLS) [444]	*C. elegans* *D. melanogaster*, including 5 different models of the Alzheimer's disease
Crocin	37% - 58% (max OLS) [425]	Dalton's lymphoma ascites bearing mice

Cryptotanshinone	34% (mean CLS) [227]	*S. cerevisiae*
Cyanidin	2% - 6% (max RLS; untreated cells); 14 - 21% (max RLS; prematurely aging cells pre-treated with H_2O_2) [431]	WI-38 human diploid fibroblasts
Diallyl trisulfide	13% (mean OLS) [439]	*C. elegans*
Ellagic acid	9% (mean OLS); 11% - 13% (median OLS) [442]	*C. elegans*
Epigallocatechin gallate	10% - 14% (mean OLS) [423]	*C. elegans*
Epicatechin	42% (mean OLS) [450] 3% (max OLS) [450] 8% (mean OLS) [450]	*D. melanogaster* Obese diabetic mice
Ferulsinaic acid	18% (mean CLS) [441] 42% (max OLS) [441]	*C. elegans*
Fisetin	31% (mean RLS) [271] 6% (mean OLS) [411] 6% (median OLS) [411]	*S. cerevisiae* *C. elegans*
Fucoxanthin	14% (mean OLS) [368] 24% (max OLS) [368] 33% - 49% (females; median OLS); 33% (males; median OLS) [368] 22% - 27% (females; max OLS); 12% - 17% (males; max OLS) [368]	*C. elegans* *D. melanogaster*
Gallic acid	12% (mean OLS) [442] 14% (median OLS) [442]	*C. elegans*
HDTIC-1, HDTIC-2	14% - 38% (max RLS) [405]	Human fetal lung diploid fibroblasts
Icariin, icariside II	31% (mean OLS) [436]	*C. elegans*
Kaempferol	10% (mean OLS) [411] 6% (median OLS) [411]	*C. elegans*
Lipoic acid	21% (median OLS) [415] 12% (females; average OLS); 15% (females; median OLS) [406]	*C. elegans* *D. melanogaster*

	4% (males; average OLS); 4% (males; median OLS) [406]	
Lithocholic acid	146% (mean CLS) [102, 110] 100% (max CLS) [102, 110]	*S. cerevisiae*
Metformin	40% (median OLS) [434] 38% (mean OLS) [414] 10% (max OLS) [414]	*C. elegans* Mice
Methionine sulfoximine	78% (mean CLS) [61] 63% (max CLS) [61]	*S. cerevisiae*
Mianserin	25% (mean OLS) [413]	*C. elegans*
Myricetin	15% (mean OLS) [446] 17% (median OLS) [446] 24% (max OLS) [446]	*C. elegans*
Nordihydroguaiaretic acid	10% (median OLS) [407] 32% (max OLS) [407] 12% (median OLS) [422] 12% (mean OLS) [403] 42% - 64% (mean OLS) [404]	Mouse model of Alzheimer's disease Male mice *D. melanogaster* Mosquitoes
Oleuropein	15% (max RLS) [412]	Human embryonic fibroblasts
Phloridzin	35% (mean RLS) [272] 41% (max RLS) [272]	*S. cerevisiae*
Propyl gallate	41% (median OLS) [415]	*C. elegans*
Quercetin	60% (mean CLS) [273] 15% (mean OLS) [418] 18% (mean OLS) [426] 14% (median OLS) [443] 5% (max RLS) [432]	*S. cerevisiae* *C. elegans* Human embryonic fibroblasts
Rapamycin	16% (mean RLS) [63] 36% (mean CLS) [62] 17% (mean OLS) [430]	*S. cerevisiae* *D. melanogaster*

	23% (max OLS) [430] 13% (females; mean OLS); 9% (males; mean OLS) [428] 14% (females; max OLS); 9% (males; max OLS) [428]	Mice
Reserpine	64% (mean OLS); 50% (max OLS) [421] 52% (mean OLS) [424]	*C. elegans* *C. elegans* model of Alzheimer's disease
Resveratrol	61% (mean RLS) [271] 10% (mean OLS) [408] 20% (females; mean OLS); 16% (males; mean OLS) [408] 56% (median OLS) [410] 59% (max OLS) [410] 38% (mean OLS) [447] 4% (max OLS) [420]	*S. cerevisiae* *C. elegans* *D. melanogaster* The short-lived fish *Nothobranchius furzeri* The honey bee *Apis mellifera* Mice on a high-calorie diet
Rosmarinic acid	10% (mean OLS) [440]	*C. elegans*
SkQ1	38% (mean CLS) [429] 16% (max CLS) [429] 69% (mean CLS) [429] 64% (max CLS) [429] 13% (females; mean OLS) [429] 7% (females; max OLS) [429] 43% (mean OLS) [429] 58% (max OLS) [429] 52% (mean OLS) [429] 34% (max OLS) [429]	The fungus *Podospora anserina* The crustacean *Ceriodaphnia affinis* *D. melanogaster* p53-Deficient mice Tumor-bearing immunodeficient mice
Sodium nitroprusside	60% (max RLS) [416]	Human peripheral blood mononuclear cells
Spermidine	200% (mean CLS) [83] 183% (mean RLS) [83]	*S. cerevisiae*

	17% (max RLS) [83]	
	15% (mean OLS) [83] 14% (max) OLS) [83] 30% (mean OLS) [83] 8% (max OLS) [83]	*C. elegans* *D. melanogaster*
	178% (max RLS) [83]	Human peripheral blood mononuclear cells
Tannic acid	18% - 25% (mean OLS) [435, 438, 442]; 18% (median OLS) [435, 442] 59% (max OLS) [438]	*C. elegans*
Taxifolin	26% (median OLS) [415]	*C. elegans*
Trolox	15% (median OLS) [415]	*C. elegans*
Tyrosol	21% (mean OLS); 21% (median OLS) [445] 11% (maximum OLS) [445]	*C. elegans*
Valproic acid	35% (mean OLS) [417] 42% (max OLS) [417]	*C. elegans*

2.4.2 Future perspectives

In the future, it would be necessary to explore the following critical aspects of the mechanisms through which each of the six longevity-extending PEs slows biological aging.

First, it is intriguing to identify the individual chemical compounds responsible for the ability of each of these PEs to postpone the onset and decrease the rate of yeast chronological aging. Such identification is already underway in our laboratory; of note, it is conceivable that only some combinations of certain chemicals composing these PEs (but not individual chemical compounds per se) can be responsible for their extremely high efficiencies as aging-delaying interventions.

Second, it is interesting to elucidate how genetic interventions that impair any of the few nutrient-responding and energy-sensing signaling pathways known to define the longevity of chronologically aging yeast [14, 15, 17, 110] influence the extent to which each of the six longevity-extending PEs can slow aging. These studies may allow us to identify protein

components of the longevity-defining signaling pathways that are targeted by each of the PEs. These studies may also reveal that certain combinations of these PEs and genetically impaired components of pro-aging signaling pathways have additive or synergistic effects on the efficiencies of lifespan and healthspan extensions.

Third, it is important to investigate how various combinations of the six longevity-extending PEs with each other and with presently known aging-delaying chemical compounds alter the extent of CLS extension in yeast. These studies may identify combinations of various pharmacological interventions that impose substantial additive or synergistic effects on the efficiencies with which organismal lifespan and healthspan can be prolonged.

Fourth, our ongoing studies indicate that the six longevity-extending PEs also extend longevities of other eukaryotic model organisms, delay the onset of age-related diseases and/or exhibit anti-tumor effects. In this regard, it needs to be mentioned that genetic, dietary and pharmacological interventions known to delay aging in yeast and other eukaryotes have been shown to selectively kill cultured human cancer cells and/or decrease the incidence of cancer [56, 113, 209, 334, 335, 452-460]. The challenge for the future is to uncover mechanisms through which the six geroprotective PEs prolong healthy lifespan and decelerate tumorigenesis.

CHAPTER 3

3 Six plant extracts slow the chronological aging of *S. cerevisiae* through different signaling pathways

3.1 Introduction

As described in Chapter 2 of my Thesis, we discovered six plant extracts that delay yeast chronological aging more efficiently than any chemical compound presently known. The rate of aging in yeast is controlled by an evolutionarily conserved network of integrated signaling pathways and protein kinases. Here, we investigated how single-gene-deletion mutations that eliminate each of these pathways and kinases influence the aging-delaying efficiencies of the six geroprotective plant extracts. Our findings indicate that these extracts slow aging in the following ways: 1) plant extract 4 lowers the efficiency with which the pro-aging TORC1 pathway suppresses the anti-aging SNF1 pathway, 2) plant extract 5 alleviates two different branches of the pro-aging PKA pathway, 3) plant extract 6 organizes processes that are not integrated into the network of presently known signaling pathways and protein kinases, 4) plant extract 8 weakens the inhibitory action of PKA on SNF1, 5) plant extract 12 stimulates the anti-aging protein kinase Rim15, and 6) plant extract 21 suppresses a form of the pro-aging protein kinase Sch9 that is activated by the pro-aging PKH1/2 pathway. Chapter 3 describes these findings.

3.2 Materials and methods

3.2.1 Yeast strains, media and culture conditions

The wild-type strain *Saccharomyces cerevisiae* BY4742 (*MATα his3*Δ *leu2*Δ *lys2*Δ *ura3*Δ) and single-gene-deletion mutant strains in the BY4742 genetic background (all from Thermo Scientific/Open Biosystems) were cultured in a synthetic minimal YNB medium (0.67% (w/v) Yeast Nitrogen Base without amino acids) initially containing 2% (w/v) glucose and supplemented with 20 mg/l histidine, 30 mg/l leucine, 30 mg/l lysine and 20 mg/l uracil. Cells were cultured at 30^{o}C with rotational shaking at 200 rpm in Erlenmeyer flasks at a "flask volume/medium volume" ratio of 5:1.

3.2.2 Aging-delaying plant extracts (PEs)

0.5% (w/v) PE4 from *Cimicifuga racemosa*, 0.5% (w/v) PE5 from *Valeriana officinalis L.*,

1.0% (w/v) PE6 from *Passiflora incarnata L*., 0.3% (w/v) PE8 from *Ginkgo biloba*, 0.1% (w/v) PE12 from *Apium graveolens L*. and 0.1% (w/v) PE21 from *Salix alba* were used [461]. A 20% (w/v) stock solution of each PE in ethanol was made on the day of adding this PE to cell cultures. For each PE, the stock solution was added to growth medium with 2% (w/v) glucose immediately following cell inoculation into the medium.

3.2.3 CLS assay

A sample of cells was taken from a culture at a certain day following cell inoculation and PE addition into the medium. A fraction of the sample was diluted to determine the total number of cells using a hemacytometer. Another fraction of the cell sample was diluted, and serial dilutions of cells were plated in duplicate onto YEP (1% (w/v) yeast extract, 2% (w/v) peptone) plates containing 2% (w/v) glucose as carbon source. After 2 d of incubation at 30°C, the number of colony-forming units (CFU) per plate was counted. The number of CFU was defined as the number of viable cells in a sample. For each culture, the percentage of viable cells was calculated as follows: (number of viable cells per ml/total number of cells per ml) × 100. The percentage of viable cells in the mid-logarithmic growth phase was set at 100%.

3.2.4 Miscellaneous procedures

The age-specific mortality rate (q_x) [359, 360], Gompertz slope or mortality rate coefficient (α) [360, 361], and mortality rate doubling time (MRDT) [360, 361] were calculated as previously described. The value of q_x was calculated as the number of cells that lost viability (i.e., are unable to form a colony on the surface of a solid nutrient-rich medium) during each time interval divided by the number of viable (i.e., clonogenic) cells at the end of the interval. The natural logarithms of the values of q_x for each time interval were plotted against time. The value of α was calculated as the slope of the Gompertz mortality line, whereas the value of MRDT was calculated as $\ln 2/\alpha$.

3.2.5 Statistical analysis

Statistical analysis was performed using Microsoft Excel's (2010) Analysis ToolPack-VBA. All data on cell survival are presented as mean ± SEM. The *p* values for comparing the means of two groups (using an unpaired two-tailed *t* test) and survival curves (using a two-tailed *t* test) were calculated with the help of the GraphPad Prism statistics software.

3.3 Results

3.3.1 The rationale of our experimental approach

PE4, PE5, PE6, PE8, PE12 and PE21 may have different effects on signaling pathways and/or protein kinases integrated into the signaling network of longevity regulation. To identify the signaling pathways and protein kinases through which each of these PEs slows yeast chronological aging, we examined such effects. Specifically, we elucidated how mutations that eliminate these signaling pathways and protein kinases affect the efficiency with which each of the six geroprotective PEs extends yeast CLS. Table 3.1 shows the single-gene-deletion mutations used in this study. This table also demonstrates how each of the mutations affects different longevity-defining signaling pathways and protein kinases, and how it alters yeast CLS. We investigated the effects of the following single-gene-deletion mutations shown in Table 3.1: 1) *tor1Δ*, which impairs the pro-aging TORC1 pathway and increases CLS [61, 62], 2) *ras2Δ*, which weakens the pro-aging PKA pathway and extends CLS [64], 3) *rim15Δ*, which eliminates the anti-aging protein kinase Rim15 and shortens CLS [66], 4) *sch9Δ*, which removes the pro-aging protein kinase Sch9 and prolongs CLS [66], 5) *pkh2Δ*, which weakens the pro-aging PKH1/2 pathway and extends CLS [43, 70], 6) *snf1Δ*, which impairs the anti-aging SNF1 pathway and shortens CLS [74, 95], and 7) *atg1Δ*, which weakens the anti-aging ATG pathway and decreases CLS [81, 82].

Table 3.1. Single-gene-deletion mutations used in this study and their known effects on longevity-defining signaling pathways and longevity of chronologically aging *S. cerevisiae*.

Single-gene-deletion mutation	Protein eliminated	Longevity-defining signaling pathway(s) affected	Effect on longevity
tor1Δ	Tor1	TORC1	⬆Extended [61, 62]
ras2Δ	Ras2	PKA	⬆Extended [64]
rim15Δ	Rim15	TORC1, PKA, PKH1/2	⇩Shortened [66]
sch9Δ	Sch9	TORC1, PKA	⬆Extended [66]
pkh2Δ	Pkh2	PKH1/2	⬆Extended [43, 70]
snf1Δ	Snf1	SNF1	⇩Shortened [74, 95]
atg1Δ	Atg1	ATG	⇩Shortened [81, 82]

A logical framework for identifying signaling pathways and/or protein kinases controlled by each of the six geroprotective PEs is schematically shown in Figure 3.1. Pro-aging signaling pathways or protein kinases A and B in this Figure are displayed in black color, whereas their anti-aging counterparts C and D are shown in grey color. One could envision that if a PE(x) extends yeast CLS by inhibiting a pro-aging pathway/protein kinase A, this PE: 1) is unable to prolong the longevity of the *ΔA* mutant strain lacking this signaling pathway/protein kinase (Figure 3.1B), 2) exhibits an additive or synergistic longevity-extending effect with the *ΔB* mutation, which eliminates the pro-aging signaling pathway/protein kinase B (Figure 3.1B), and 3) can extend the longevity of the *ΔC* or *ΔD* mutant strain, which lacks the anti-aging signaling pathway/protein kinase C or D (respectively), but to a lesser extent than that of wild-type (WT) strain (Figure 3.1B). It is also conceivable that if a PE(y) prolongs yeast CLS by activating an anti-aging pathway/protein kinase C, this PE: 1) displays an additive or synergistic longevity-extending effect with the *ΔA* or *ΔB* mutation, which eliminates the pro-aging signaling pathway/protein kinase A or B (respectively) (Figure 3.1C), 2) is incapable of extending the longevity of the *ΔC* mutant strain deficient in the anti-aging signaling pathway/protein kinase C (Figure 3.1C), and 3) can prolong the longevity of the *ΔD* mutant strain, which lacks the anti-aging signaling pathway/protein kinase D, although not as considerably as that of WT strain (Figure 3.1C).

3.3.2 PE4 slows yeast chronological aging by attenuating the inhibitory effect of TORC1 on SNF1

PE4 exhibited additive longevity-extending effects with the *ras2Δ*, *sch9Δ* and *pkh2Δ* mutations, which eliminate different signaling pathways/protein kinases comprising the longevity-defining network (Figure 3.2A, Tables 3.2 and 3.3, Figure 3.3; note that data for the mock-treated WT strain and the WT strain cultured with PE4 are replicated in all graphs of Figure 3.2A and Figure 3.3). PE4 elicited a decline in the slope of the Gompertz mortality rate (also known as mortality rate coefficient α) and a rise in the mortality rate doubling time (MRDT) for *ras2Δ*, *sch9Δ* and *pkh2Δ* (Figure 3.4; note that data for the mock-treated WT strain and the WT strain cultured with PE4 are replicated in all graphs of this figure). Such changes in the values of α and MRDT are characteristic of interventions that lower the rate of biological aging [355, 360, 361, 367, 368]. Thus, PE4 slows yeast chronological aging independently of the pro-aging PKA pathway, the pro-aging PKH1/2 pathway or the pro-aging protein kinase Sch9.

PE4 extended longevities of the *rim15Δ* and *atg1Δ* mutant strains, although to a lesser extent than that of WT strain (Figure 3.2A, Tables 3.2 and 3.3, Figure 3.3). PE4 decreased the value of α and increased the value of MRDT for *rim15Δ* and *atg1Δ*, though not as significantly as for WT (Figure 3.4). Hence, PE4 slows yeast chronological aging not through the anti-aging protein kinase Rim15 or the anti-aging ATG pathway.

PE4 was unable to increase the CLS of *tor1Δ* and *snf1Δ* (Figure 3.2A, Tables 3.2 and 3.3, Figure 3.3) and did not alter the values of α or MRDT for these mutant strains (Figure 3.4). We concluded that PE4 slows yeast chronological aging via the pro-aging TORC1 pathway and the anti-aging SNF1 pathway, by deteriorating the known [96, 99] inhibitory effect of TORC1 on SNF1 (Figure 3.2B).

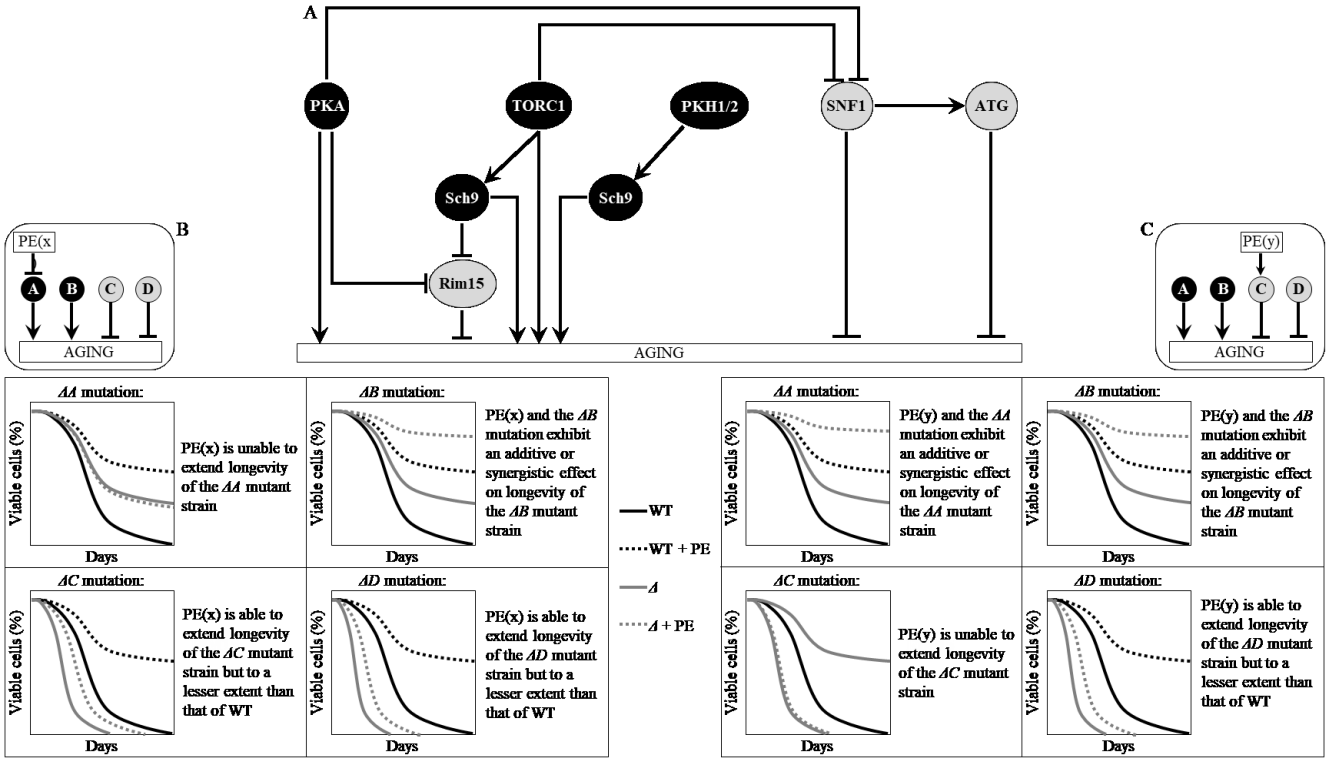

Figure 3.1. A logical framework for identifying signaling pathways and/or protein kinases controlled by the longevity-extending PE(x) and PE(y). (A) A schematic depiction of a network that integrates several signaling pathways and protein kinases to define the rate of yeast chronological aging. Pro-aging signaling pathways or protein kinases A and B are shown in black color. Anti-aging signaling pathways or protein kinases C and D are displayed in grey color. Abbreviations are as in Figure 1.2. (B) Predicted effect of PE(x), which extends yeast CLS by inhibiting a pro-aging pathway/protein kinase A, on the longevity of the *ΔA*, *ΔB*, *ΔC* or *ΔD* mutant strain lacking a signaling pathway/protein kinase A, B, C or D. (C) Predicted effect of PE(y), which extends yeast CLS by activating an anti-aging pathway/protein kinase C, on the longevity of the *ΔA*, *ΔB*, *ΔC* or *ΔD* mutant strain lacking the corresponding signaling pathway/protein kinase.

Abbreviation: WT, wild-type strain.

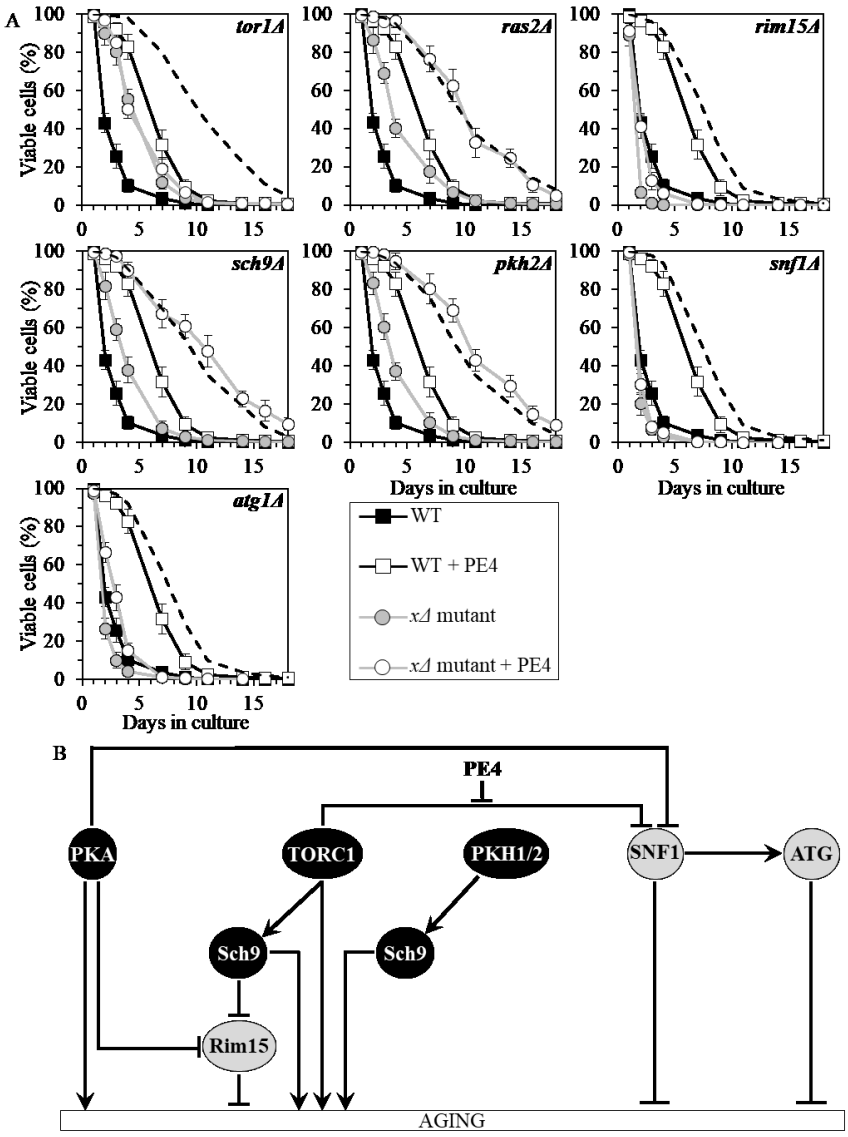

Figure 3.2. PE4 extends yeast CLS by weakening the restraining action of TORC1 on SNF1. (A) Cells of the wild-type (WT) and indicated mutant strains were grown in the synthetic minimal YNB medium (0.67% Yeast Nitrogen Base without amino acids) initially containing 2% glucose, in the presence of 0.5% PE4 (ethanol was used as a vehicle at the final concentration of 2.5%) or in its absence (cells were subjected to ethanol-mock treatment). Survival curves of chronologically aging WT and mutant strains cultured with or without 0.5% PE4 are shown. Data are presented as means ± SEM (n = 7). The dotted line indicates the predicted survival curve of a particular mutant strain cultured with PE4 if this PE exhibits an additive longevity-extending effect with the mutation. Data for the mock-treated WT strain are replicated in all graphs of this Figure and all graphs of Figure 3.5. Data for each of the mock-treated mutant strains presented in this Figure are reproduced in the corresponding graphs of Figure 3.5. Data for the WT strain cultured with PE4 are replicated in all graphs of this Figure. (B) The effect of PE4 on the signaling pathways and protein kinases comprising the longevity-defining signaling network. This effect is inferred from the data presented in (A), Tables 3.2 and 3.3, and Figures 3.3 and 3.4. Abbreviations: as in the

legend to Figure 1.2.

Table 3.2. *p* Values for pairs of survival curves of a yeast strain cultured with or without the indicated plant extract (PE). Survival curves shown in Figs. 3.2A, 3.5, 3.8, 3.11, 3.14 and 3.17 were compared. The survival curve of a strain cultured with the indicated PE was considered statistically different from the survival curve of the same strain cultured without it if the *p* value was lower than 0.05; such *p* values are shown in red color. For each pair of survival curves with the *p* value less than 0.05, the survival rate of the strain cultured with the indicated PE was higher than the survival rate of the same strain cultured without it. The *p* values for comparing pairs of survival curves were calculated as described in Materials and methods.

Strain without PE	**Same strain with the indicated PE**					
	PE4	**PE5**	**PE6**	**PE8**	**PE12**	**PE21**
WT	**< 0.0001**	**< 0.0001**	**< 0.0001**	**< 0.0001**	**< 0.0001**	**< 0.0001**
tor1Δ	0.8899	**< 0.0001**	**< 0.0001**	**< 0.0001**	**< 0.0001**	**< 0.0001**
ras2Δ	**< 0.0001**	0.3664	**< 0.0001**	0.41888	**< 0.0001**	**< 0.0001**
rim15Δ	**0.0042**	**0.0168**	**< 0.0001**	**0.0184**	0.6453	**< 0.0001**
sch9Δ	**< 0.0001**	**< 0.0001**	**< 0.0001**	**0.0006**	**< 0.0001**	**0.0306**
pkh2Δ	**< 0.0001**	**< 0.0001**	**< 0.0001**	**< 0.0001**	**< 0.0001**	**< 0.0001**
snf1Δ	0.5873	**0.0075**	**< 0.0001**	0.7124	**0.0132**	**< 0.0001**
atg1Δ	**0.0027**	**0.0061**	**< 0.0001**	**0.0086**	**0.0208**	**< 0.0001**

Table 3.3. *p* Values for pairs of survival curves of the wild-type (WT) and mutant strain, both cultured in the presence of the indicated PE. Survival curves shown in Figures 3.2A, 3.5, 3.8, 3.11, 3.14 and 3.17 were compared. The survival curve for the WT strain cultured with the indicated PE was considered statistically different from the survival curve for the mutant strain cultured with this PE if the *p* value was lower than 0.05. The *p* values less than 0.05 are shown in red color if the survival rate of the mutant strain cultured with the indicated PE was higher than the survival rate of the WT strain cultured with this PE. The *p* values less than 0.05 are displayed in blue color if the survival rate of the mutant strain cultured with the indicated PE was lower than the survival rate of the WT strain cultured with this PE. The *p* values for comparing pairs of survival curves were calculated as described in Materials and methods.

PE4	*tor1Δ* + PE4	*ras2Δ* + PE4	*rim15Δ* + PE4	*sch9Δ* + PE4	*pkh2Δ* + PE4	*snf1Δ* + PE4	*atg1Δ* + PE4
WT + PE4	0.0827	**0.0002**	**< 0.0001**	**0.0004**	**0.0007**	**< 0.0001**	**< 0.0001**

PE5	*tor1Δ* + PE5	*ras2Δ* + PE5	*rim15Δ* + PE5	*sch9Δ* + PE5	*pkh2Δ* + PE5	*snf1Δ* + PE5	*atg1Δ* + PE5
WT + PE5	**< 0.0001**	0.0724	**< 0.0001**	**0.0008**	**< 0.0001**	**< 0.0001**	**0.0004**

PE6	*tor1Δ* + PE6	*ras2Δ* + PE6	*rim15Δ* + PE6	*sch9Δ* + PE6	*pkh2Δ* + PE6	*snf1Δ* + PE6	*atg1Δ* + PE6
WT + PE6	**< 0.0001**	**< 0.0001**	**0.0364**	**0.0008**	**< 0.0001**	**< 0.0001**	**< 0.0001**

PE8	*tor1Δ* + PE8	*ras2Δ* + PE8	*rim15Δ* + PE8	*sch9Δ* + PE8	*pkh2Δ* + PE8	*snf1Δ* + PE8	*atg1Δ* + PE8
WT + PE8	**< 0.0001**	**0.0124**	**< 0.0001**	**0.0032**	**< 0.0001**	**< 0.0001**	**0.0008**

PE12	*tor1Δ* + PE12	*ras2Δ* + PE12	*rim15Δ* + PE12	*sch9Δ* + PE12	*pkh2Δ* + PE12	*snf1Δ* + PE12	*atg1Δ* + PE12
WT + PE12	**0.0003**	**0.0011**	**< 0.0001**	**0.0018**	**< 0.0001**	**0.0004**	**0.0012**

PE21	*tor1Δ* + PE21	*ras2Δ* + PE21	*rim15Δ* + PE21	*sch9Δ* + PE21	*pkh2Δ* + PE21	*snf1Δ* + PE21	*atg1Δ* + PE21
WT + PE21	**0.0036**	**0.0062**	**0.0109**	**< 0.0001**	**0.0044**	**0.0009**	**0.0086**

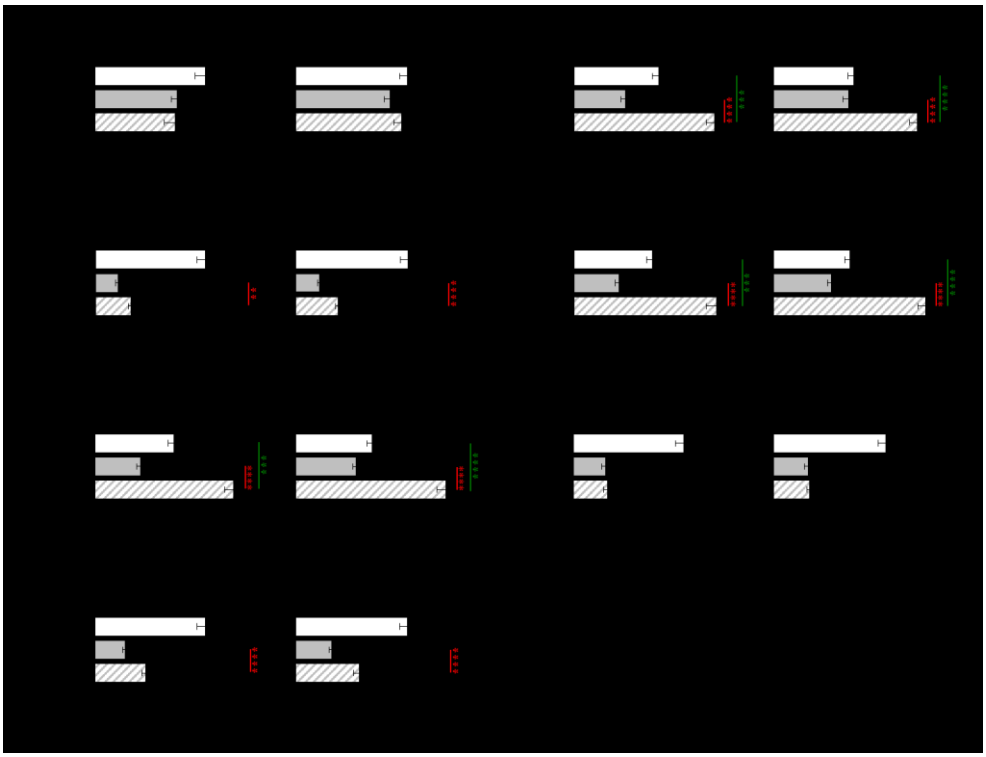

Figure 3.3. PE4 is unable to prolong the chronological lifespans (CLS) of the *tor1Δ* and *snf1Δ* mutant strains and has additive CLS-extending effects with the *ras2Δ*, *sch9Δ* and *pkh2Δ* mutations. Cells of the wild-type (WT) and indicated mutant strains were grown in the synthetic minimal YNB medium (0.67% Yeast Nitrogen Base without amino acids) initially containing 2% glucose, in the presence of 0.5% PE4 (ethanol was used as a vehicle at the final concentration of 2.5%) or in its absence (cells were subjected to ethanol-mock treatment). Survival curves shown in Figure 3.2A were used to calculate the mean and maximum CLS for WT and mutant strains cultured with or without 0.5% PE4. Data are presented as means ± SEM (n = 7; ns, not significant; *$p < 0.05$; **$p < 0.01$; ***$p < 0.001$; ****$p < 0.0001$). The ability of PE4 to cause a significant

(*$p < 0.05$; **$p < 0.01$; ***$p < 0.001$; ****$p < 0.0001$) increase in the CLS of a particular mutant strain is displayed in red color. The ability of a combination between PE4 and a particular mutation to cause a significant (*$p < 0.05$; **$p < 0.01$; ***$p < 0.001$; ****$p < 0.0001$) increase in CLS-extending efficiencies of each other (i.e. the ability of such combination to exhibit an additive extending effect on yeast CLS) is displayed in green color. Data for the mock-treated WT strain are replicated in all graphs of this Figure. Data for the WT strain cultured with PE4 are replicated in all graphs of this Figure.

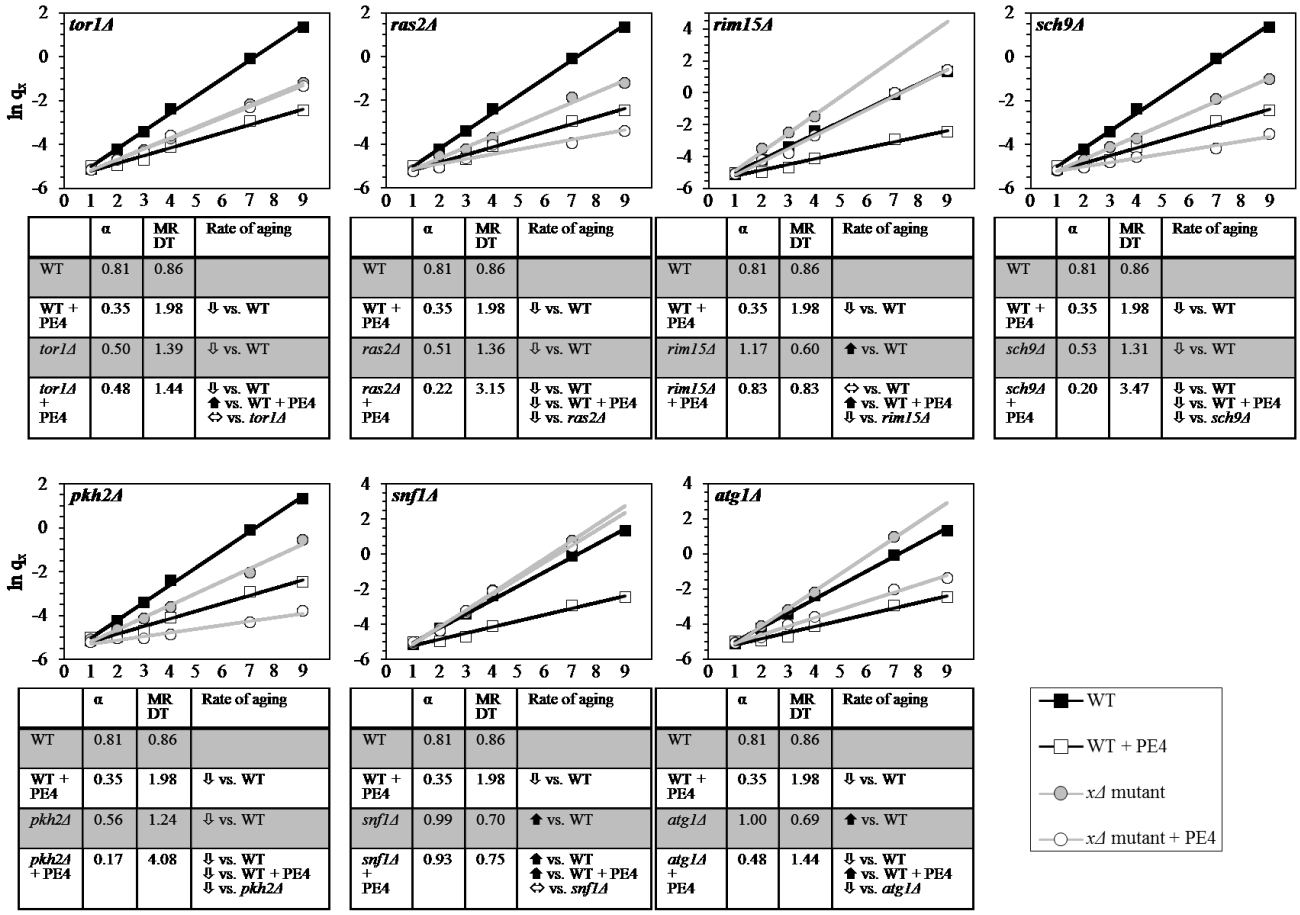

	α	MR DT	Rate of aging
WT	0.81	0.86	
WT + PE4	0.35	1.98	⇩ vs. WT
tor1Δ	0.50	1.39	⇩ vs. WT
tor1Δ + PE4	0.48	1.44	⇩ vs. WT ⇧ vs. WT + PE4 ⇔ vs. *tor1Δ*

	α	MR DT	Rate of aging
WT	0.81	0.86	
WT + PE4	0.35	1.98	⇩ vs. WT
ras2Δ	0.51	1.36	⇩ vs. WT
ras2Δ + PE4	0.22	3.15	⇩ vs. WT ⇩ vs. WT + PE4 ⇩ vs. *ras2Δ*

	α	MR DT	Rate of aging
WT	0.81	0.86	
WT + PE4	0.35	1.98	⇩ vs. WT
rim15Δ	1.17	0.60	⇧ vs. WT
rim15Δ + PE4	0.83	0.83	⇔ vs. WT ⇧ vs. WT + PE4 ⇩ vs. *rim15Δ*

	α	MR DT	Rate of aging
WT	0.81	0.86	
WT + PE4	0.35	1.98	⇩ vs. WT
sch9Δ	0.53	1.31	⇩ vs. WT
sch9Δ + PE4	0.20	3.47	⇩ vs. WT ⇩ vs. WT + PE4 ⇩ vs. *sch9Δ*

	α	MR DT	Rate of aging
WT	0.81	0.86	
WT + PE4	0.35	1.98	⇩ vs. WT
pkh2Δ	0.56	1.24	⇩ vs. WT
pkh2Δ + PE4	0.17	4.08	⇩ vs. WT ⇩ vs. WT + PE4 ⇩ vs. *pkh2Δ*

	α	MR DT	Rate of aging
WT	0.81	0.86	
WT + PE4	0.35	1.98	⇩ vs. WT
snf1Δ	0.99	0.70	⇧ vs. WT
snf1Δ + PE4	0.93	0.75	⇧ vs. WT ⇧ vs. WT + PE4 ⇔ vs. *snf1Δ*

	α	MR DT	Rate of aging
WT	0.81	0.86	
WT + PE4	0.35	1.98	⇩ vs. WT
atg1Δ	1.00	0.69	⇧ vs. WT
atg1Δ + PE4	0.48	1.44	⇩ vs. WT ⇧ vs. WT + PE4 ⇩ vs. *atg1Δ*

Figure 3.4. Analysis of the Gompertz mortality function indicates that PE4 slows yeast chronological aging by weakening the inhibitory effect of TORC1 on SNF1. Cells of the wild-type (WT) and indicated mutant strains were grown in the synthetic minimal YNB medium (0.67% Yeast Nitrogen Base without amino acids) initially containing 2% glucose, in the presence of 0.5% PE4 (ethanol was used as a vehicle at the final concentration of 2.5%) or in its absence (cells were subjected to ethanol-mock treatment). Survival curves shown in Fig. 3.2A were used to calculate the age-specific mortality rates (q_x), the Gompertz mortality rates (also known as mortality rate coefficient α) and the mortality rate doubling times (MRDT) for WT and mutant yeast populations cultured with or without 0.5% PE4. The values of q_x, α and MRDT were calculated as described in Materials and methods. Data for the mock-treated WT strain are replicated in all graphs of this Figure. Data for the WT strain cultured with PE4 are reproduced in all graphs of this Figure.

3.3.3 PE5 slows chronological aging by weakening two branches of the PKA pathway

PE5 displayed an additive longevity-extending effect with the *sch9Δ* mutation, and increased yeast CLS in synergy with the *tor1Δ* and *pkh2Δ* mutations (Figure 3.5A, Tables 3.2 and 3.3, Figure 3.6; note that data for the mock-treated WT strain and for the WT strain cultured with PE5 are replicated in all graphs of Figure 3.5A and Figure 3.6). PE5 decreased the values of α and increased the values of MRDT for chronologically aging cultures of strains carrying each of these three mutations (Figure 3.7; note that data for the mock-treated WT strain and the WT strain cultured with PE5 are replicated in all graphs of this figure). Therefore, PE5 slows aging not through TORC1, PKH1/2 or Sch9.

PE5 increased CLS of the *rim15Δ*, *snf1Δ* and *atg1Δ* mutant strains, however, to a lesser extent than that of WT strain (Figure 3.5A, Tables 3.2 and 3.3, Figure 3.6). PE5 decreased the value of α and increased the value of MRDT strains carrying each of these mutations, although not as considerably as for WT (Figure 3.7). Thus, PE5 slows aging independently of Rim15, SNF1 and ATG.

PE5 was unable to extend the CLS of *ras2Δ* (Figure 3.5A, Tables 3.2 and 3.3, Figure 3.6) and did not alter the values of α or MRDT for this mutant strain (Figure 3.7). Hence, PE5 slows aging by weakening two branches of the PKA signaling pathway (Figure 3.5B). One of these branches involves the Rim15-independent processes of autophagy inhibition and protein translation activation in the cytosol, whereas the other branch attenuates the Rim15-driven establishment of an anti-aging transcriptional program of many nuclear genes [15, 63, 68, 95-97, 99, 104, 105, 110, 199, 202, 203].

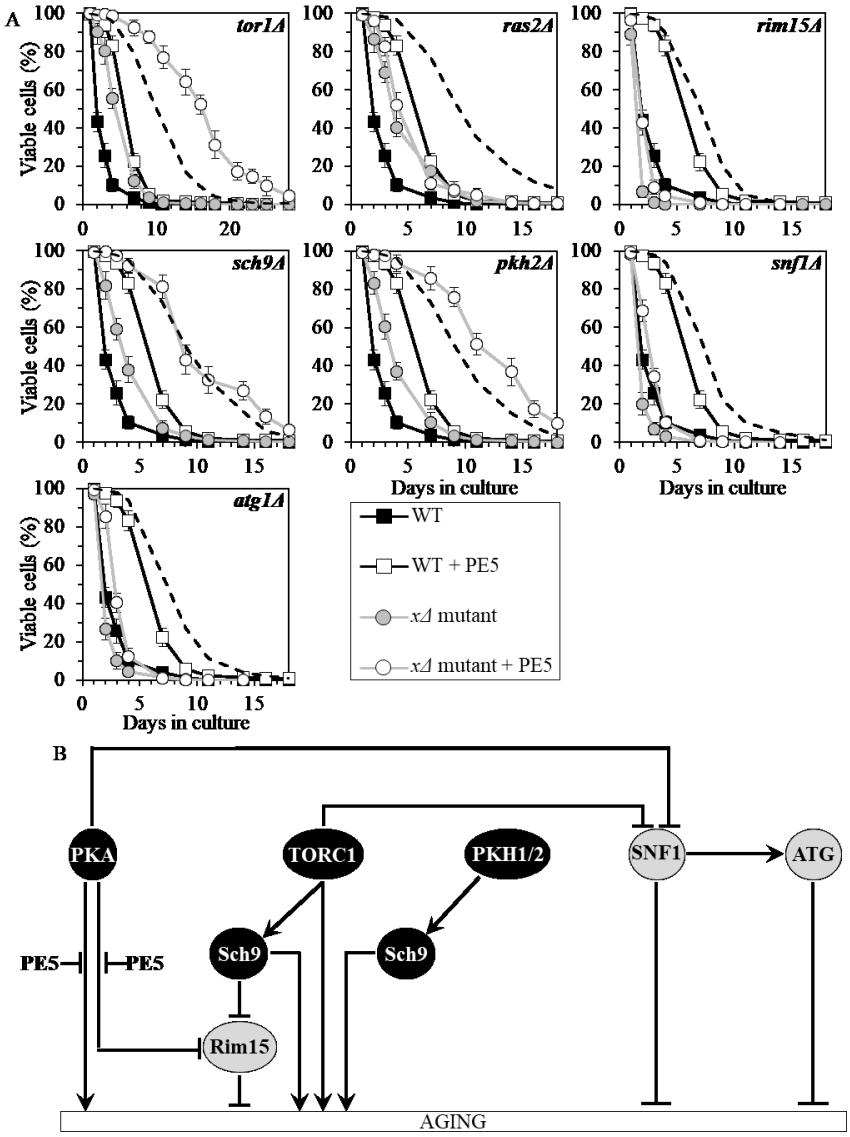

Figure 3.5. PE5 extends yeast CLS by weakening two branches of the PKA signaling pathway. (A) Cells of the wild-type (WT) and indicated mutant strains were grown in the synthetic minimal YNB medium (0.67% Yeast Nitrogen Base without amino acids) initially containing 2% glucose, in the presence of 0.5% PE5 (ethanol was used as a vehicle at the final concentration of 2.5%) or in its absence (cells were subjected to ethanol-mock treatment). Survival curves of chronologically aging WT and mutant strains cultured with or without 0.5% PE5 are shown. Data are presented as means ± SEM (n = 7). The dotted line indicates the predicted survival curve of a particular mutant strain cultured with PE5 if this PE exhibits an additive longevity-extending effect with the mutation. Data for the mock-treated WT strain are replicated in all graphs of this Figure and in all graphs of Figure 3.2. Data for each of the mock-treated mutant strains presented in this Figure are replicated in the corresponding graphs of Figure 3.2. Data for the WT strain cultured with PE5 are replicated in all graphs of this Figure. (B) The effect of PE5 on the signaling pathways and protein kinases comprising the longevity-defining network. This effect is inferred from the data presented in (A), Tables 3.2 and 3.3, and Figures 3.6 and 3.7. Abbreviations: as in the legend to Figure 1.2.

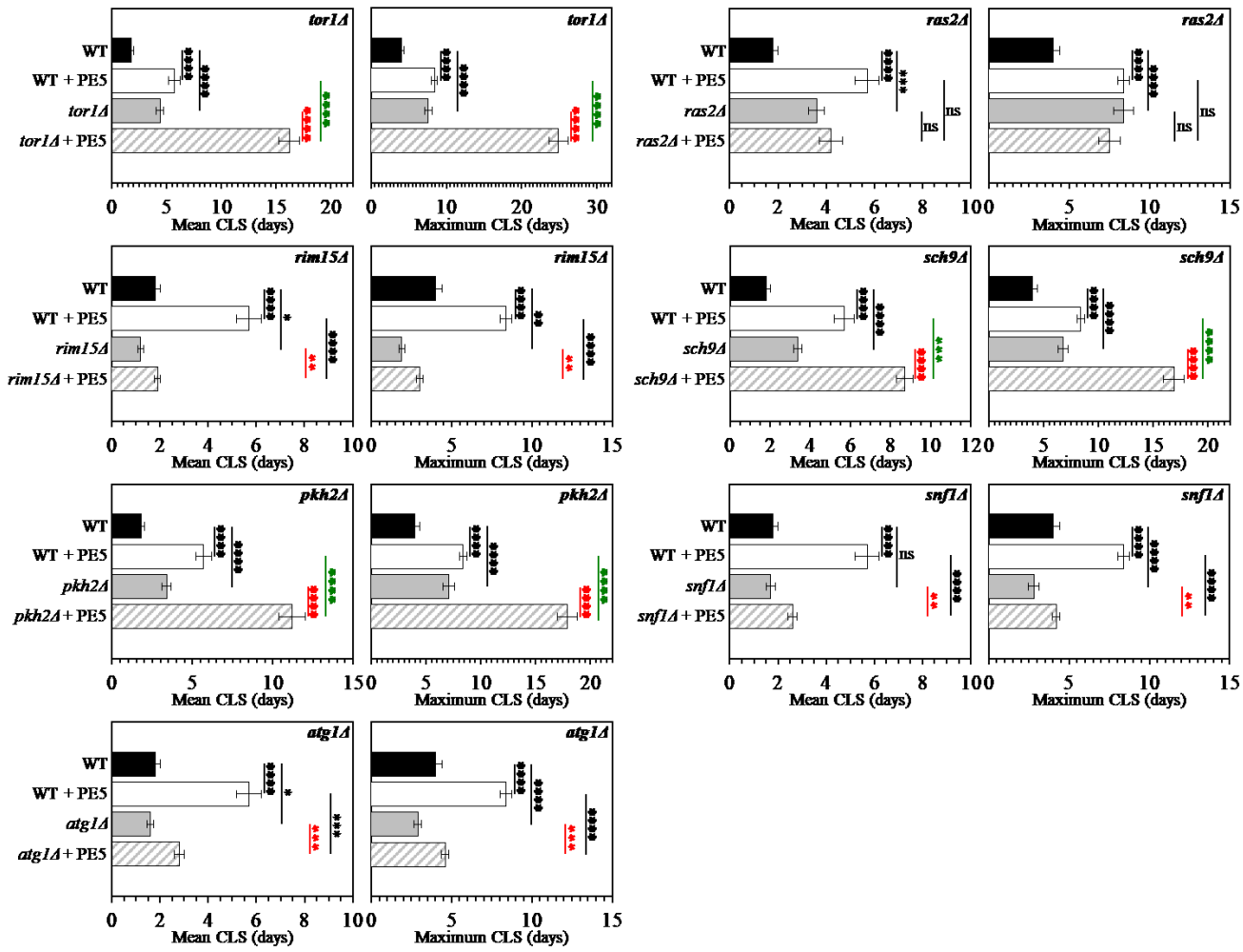

Figure 3.6. PE5 is unable to prolong the chronological lifespan (CLS) of the *ras2Δ* mutant strain, has an additive CLS-extending effect with the *sch9Δ* mutation, and increases yeast CLS in synergy with the *tor1Δ* and *pkh2Δ* mutations. Cells of the wild-type (WT) and indicated mutant strains were grown in the synthetic minimal YNB medium (0.67% Yeast Nitrogen Base without amino acids) initially containing 2% glucose, in the presence of 0.5% PE5 (ethanol was used as a vehicle at the final concentration of 2.5%) or in its absence (cells were subjected to ethanol-mock treatment). Survival curves shown in Fig. 3.5A were used to calculate the mean and maximum CLS for WT and mutant strains cultured with or without 0.5% PE5. Data are presented as means ± SEM (n = 7; ns, not significant; *$p < 0.05$; **$p < 0.01$; ***$p < 0.001$; ****$p < 0.0001$). The ability of PE5 to cause a significant (*$p < 0.05$; **$p < 0.01$; ***$p < 0.001$; ****$p < 0.0001$) increase in the CLS of a particular mutant strain is shown in red color. The ability of a combination between PE5 and a particular mutation to cause a significant (*$p < 0.05$; **$p < 0.01$; ***$p < 0.001$; ****$p < 0.0001$) increase in CLS-extending efficiencies of each other (i.e. the ability of such combination to exhibit an additive or synergistic CLS-extending effect) is displayed in green color. Data for the mock-treated WT strain are replicated in all graphs of this Figure and in all graphs of Figure 3.3. Data for each of the mock-treated mutant strains presented in this Figure are replicated in the corresponding graphs of Figure 3.3. Data for the WT strain cultured with PE5 are replicated in all graphs of this Figure.

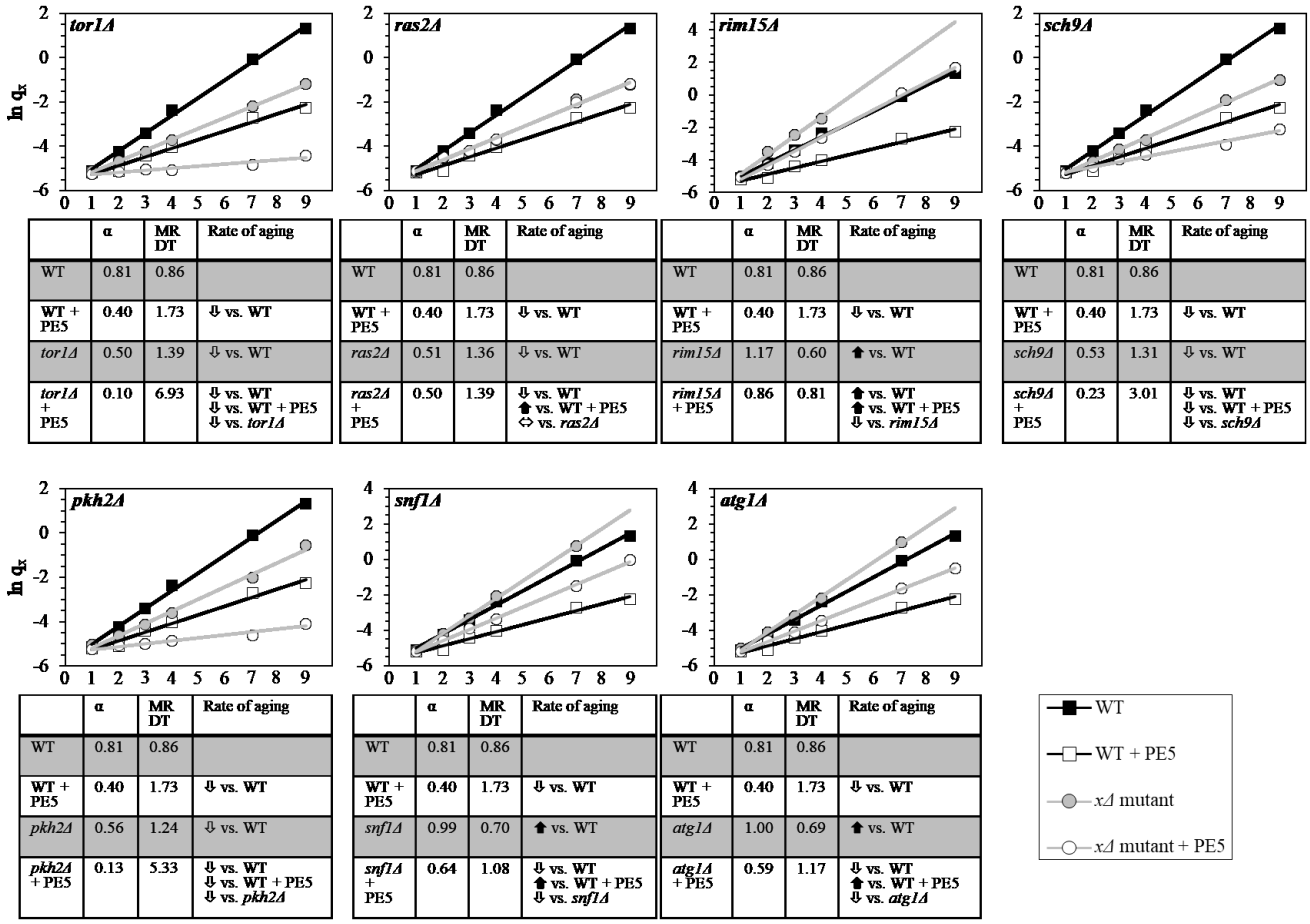

	α	MR DT	Rate of aging
WT	0.81	0.86	
WT + PE5	0.40	1.73	⇩ vs. WT
tor1Δ	0.50	1.39	⇩ vs. WT
tor1Δ + PE5	0.10	6.93	⇩ vs. WT ⇩ vs. WT + PE5 ⇩ vs. *tor1Δ*

	α	MR DT	Rate of aging
WT	0.81	0.86	
WT + PE5	0.40	1.73	⇩ vs. WT
ras2Δ	0.51	1.36	⇩ vs. WT
ras2Δ + PE5	0.50	1.39	⇩ vs. WT ⇧ vs. WT + PE5 ⇔ vs. *ras2Δ*

	α	MR DT	Rate of aging
WT	0.81	0.86	
WT + PE5	0.40	1.73	⇩ vs. WT
rim15Δ	1.17	0.60	⇧ vs. WT
rim15Δ + PE5	0.86	0.81	⇧ vs. WT ⇧ vs. WT + PE5 ⇩ vs. *rim15Δ*

	α	MR DT	Rate of aging
WT	0.81	0.86	
WT + PE5	0.40	1.73	⇩ vs. WT
sch9Δ	0.53	1.31	⇩ vs. WT
sch9Δ + PE5	0.23	3.01	⇩ vs. WT ⇩ vs. WT + PE5 ⇩ vs. *sch9Δ*

	α	MR DT	Rate of aging
WT	0.81	0.86	
WT + PE5	0.40	1.73	⇩ vs. WT
pkh2Δ	0.56	1.24	⇩ vs. WT
pkh2Δ + PE5	0.13	5.33	⇩ vs. WT ⇩ vs. WT + PE5 ⇩ vs. *pkh2Δ*

	α	MR DT	Rate of aging
WT	0.81	0.86	
WT + PE5	0.40	1.73	⇩ vs. WT
snf1Δ	0.99	0.70	⇧ vs. WT
snf1Δ + PE5	0.64	1.08	⇩ vs. WT ⇧ vs. WT + PE5 ⇩ vs. *snf1Δ*

	α	MR DT	Rate of aging
WT	0.81	0.86	
WT + PE5	0.40	1.73	⇩ vs. WT
atg1Δ	1.00	0.69	⇧ vs. WT
atg1Δ + PE5	0.59	1.17	⇩ vs. WT ⇧ vs. WT + PE5 ⇩ vs. *atg1Δ*

Figure 3.7. Analysis of the Gompertz mortality function indicates that PE5 slows yeast chronological aging by weakening two branches of the PKA signaling pathway. Cells of the wild-type (WT) and indicated mutant strains were grown in the synthetic minimal YNB medium (0.67% Yeast Nitrogen Base without amino acids) initially containing 2% glucose, in the presence of 0.5% PE5 (ethanol was used as a vehicle at the final concentration of 2.5%) or in its absence (cells were subjected to ethanol-mock treatment). Survival curves shown in Fig. 3.5A were used to calculate the age-specific mortality rates (q_x), the Gompertz mortality rates (also known as mortality rate coefficient α) and the mortality rate doubling times (MRDT) for WT and mutant yeast populations cultured with or without 0.5% PE5. The values of q_x, α and MRDT were calculated as described in Materials and methods. Data for the mock-treated WT strain are replicated in all graphs of this Figure and in all graphs of Figure 3.4. Data for each of the mock-treated mutant strains presented in this Figure are reproduced in the corresponding graphs of Figure 3.4. Data for the WT strain cultured with PE5 are replicated in all graphs of this Figure.

3.3.4 PE6 slows chronological aging by coordinating processes that are not integrated into the signaling network of longevity regulation

PE6 had additive longevity-extending effects with the *rim15Δ*, *sch9Δ* and *atg1Δ* mutations, and extended longevity synergistically with the *tor1Δ*, *ras2Δ*, *pkh2Δ* and *snf1Δ* mutations (Figure

3.8A, Tables 3.2 and 3.3, Figure 3.9; note that data for the mock-treated WT strain and for the WT strain cultured with PE6 are replicated in all graphs of Figure 3.8A and Figure 3.9). PE6 lowered the values of α and raised the values of MRDT for chronologically aging cultures of strains carrying each of these seven mutations (Figure 3.10; note that data for the mock-treated WT strain and the WT strain cultured with PE6 are replicated in all graphs of this Figure). Thus, PE6 delays aging by activating anti-aging processes and/or inhibiting pro-aging processes that are not integrated into the network of presently known signaling pathways/protein kinases (Figure 3.8B).

Although *rim15Δ*, *snf1Δ* and *atg1Δ* exhibited decreased CLS in the absence of PE6, this PE extended the CLS of each of these mutant strains to a greater extent than that of WT strain (Figure 3.8A, Tables 3.2 and 3.3, Figures 3.9 and 3.10). It is possible that the efficiency with which PE6 activates anti-aging processes and/or inhibits pro-aging processes outside of the network in the absence of Rim15, Snf1 or Atg1 may exceed such efficiency in the presence of any of these anti-aging proteins.

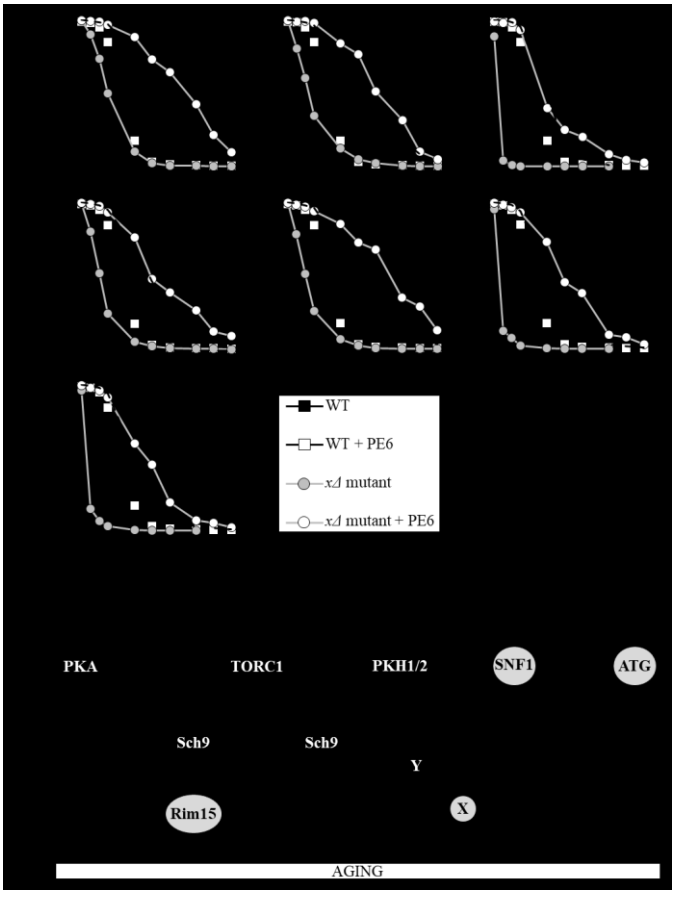

Figure 3.8. PE6 extends yeast CLS independently of presently known longevity-defining signaling pathways/protein kinases. (A) Cells of the wild-type (WT) and indicated mutant strains

were grown in the synthetic minimal YNB medium (0.67% Yeast Nitrogen Base without amino acids) initially containing 2% glucose, in the presence of 1.0% PE6 (ethanol was used as a vehicle at the final concentration of 5.0%) or in its absence (cells were subjected to ethanol-mock treatment). Survival curves of chronologically aging WT and mutant strains cultured with or without 1.0% PE6 are shown. Data are presented as means ± SEM (n = 8). The dotted line indicates the predicted survival curve of a particular mutant strain cultured with PE6 if this PE exhibits an additive longevity-extending effect with the mutation. Data for the mock-treated WT strain and the WT strain cultured with PE6 are replicated in all graphs of this Figure. (B) The effects of PE6 on anti-aging and/or pro-aging processes that are not controlled by the network of presently known signaling pathways/protein kinases. These effects are inferred from the data presented in (A), Tables 3.2 and 3.3, and Figures 3.9 and 3.10. Abbreviations: as in the legend to Figure 1.2.

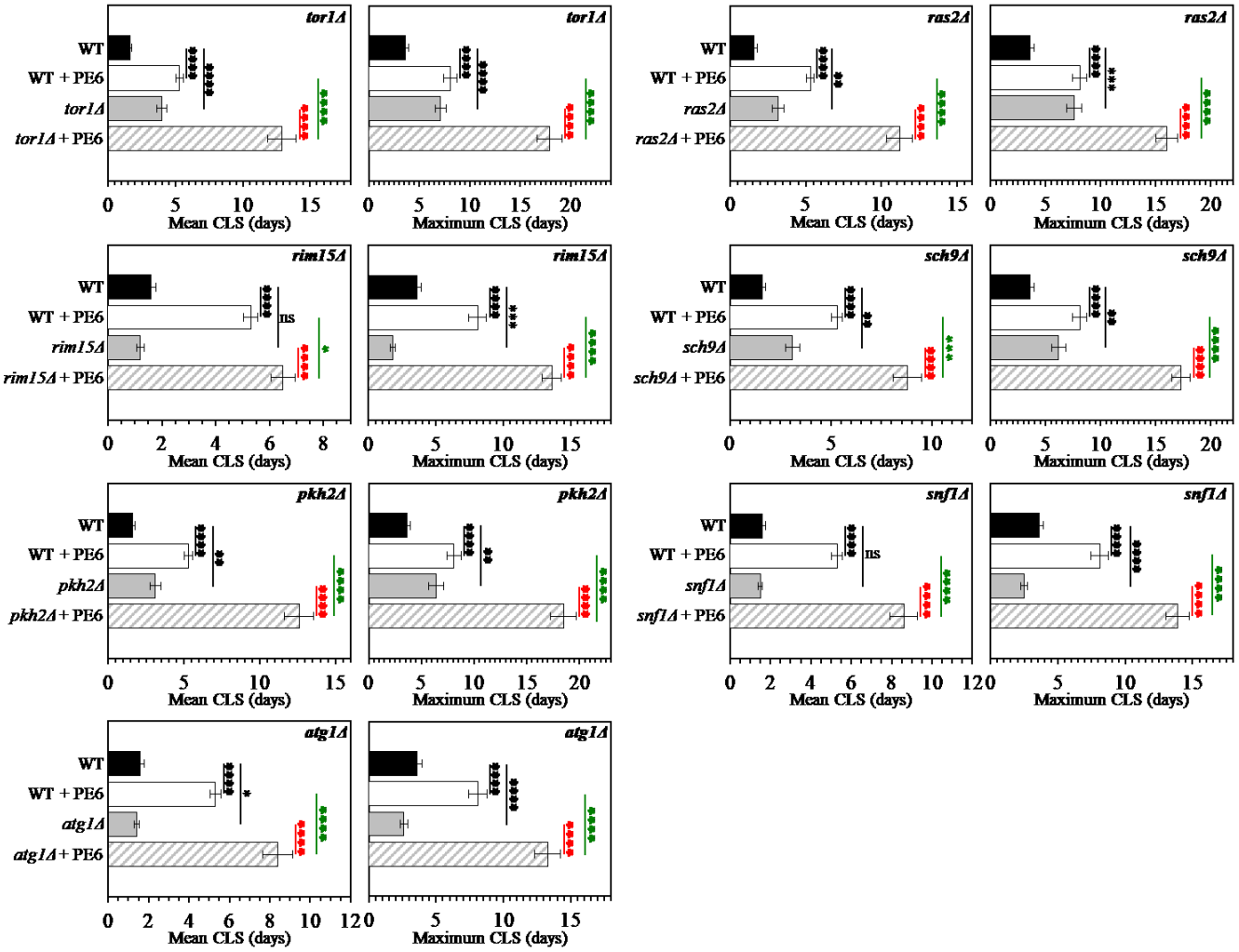

Figure 3.9. PE6 has additive CLS-extending effects with the *rim15Δ*, *sch9Δ* and *atg1Δ* mutations; PE6 also increases yeast CLS in synergy with the *tor1Δ*, *ras2Δ*, *pkh2Δ* and *snf1Δ* mutations. Cells of the wild-type (WT) and indicated mutant strains were grown in the synthetic minimal YNB medium (0.67% Yeast Nitrogen Base without amino acids) initially containing 2%

glucose, in the presence of 1.0% PE6 (ethanol was used as a vehicle at the final concentration of 5.0%) or in its absence (cells were subjected to ethanol-mock treatment). Survival curves shown in Fig. 3.8A were used to calculate the mean and maximum CLS for WT and mutant strains cultured with or without 1.0% PE6. Data are presented as means ± SEM (n = 8; ns, not significant; *$p < 0.05$; **$p < 0.01$; ***$p < 0.001$; ****$p < 0.0001$). The ability of PE6 to cause a significant (*$p < 0.05$; **$p < 0.01$; ***$p < 0.001$; ****$p < 0.0001$) increase in the CLS of a particular mutant strain is shown in red color. The ability of a combination between PE6 and a particular mutation to cause a significant (*$p < 0.05$; **$p < 0.01$; ***$p < 0.001$; ****$p < 0.0001$) increase in CLS-extending efficiencies of each other (i.e. the ability of such combination to exhibit an additive or synergistic CLS-extending effect) is displayed in green color. Data for the mock-treated WT strain and the WT strain cultured with PE6 are replicated in all graphs of this Figure.

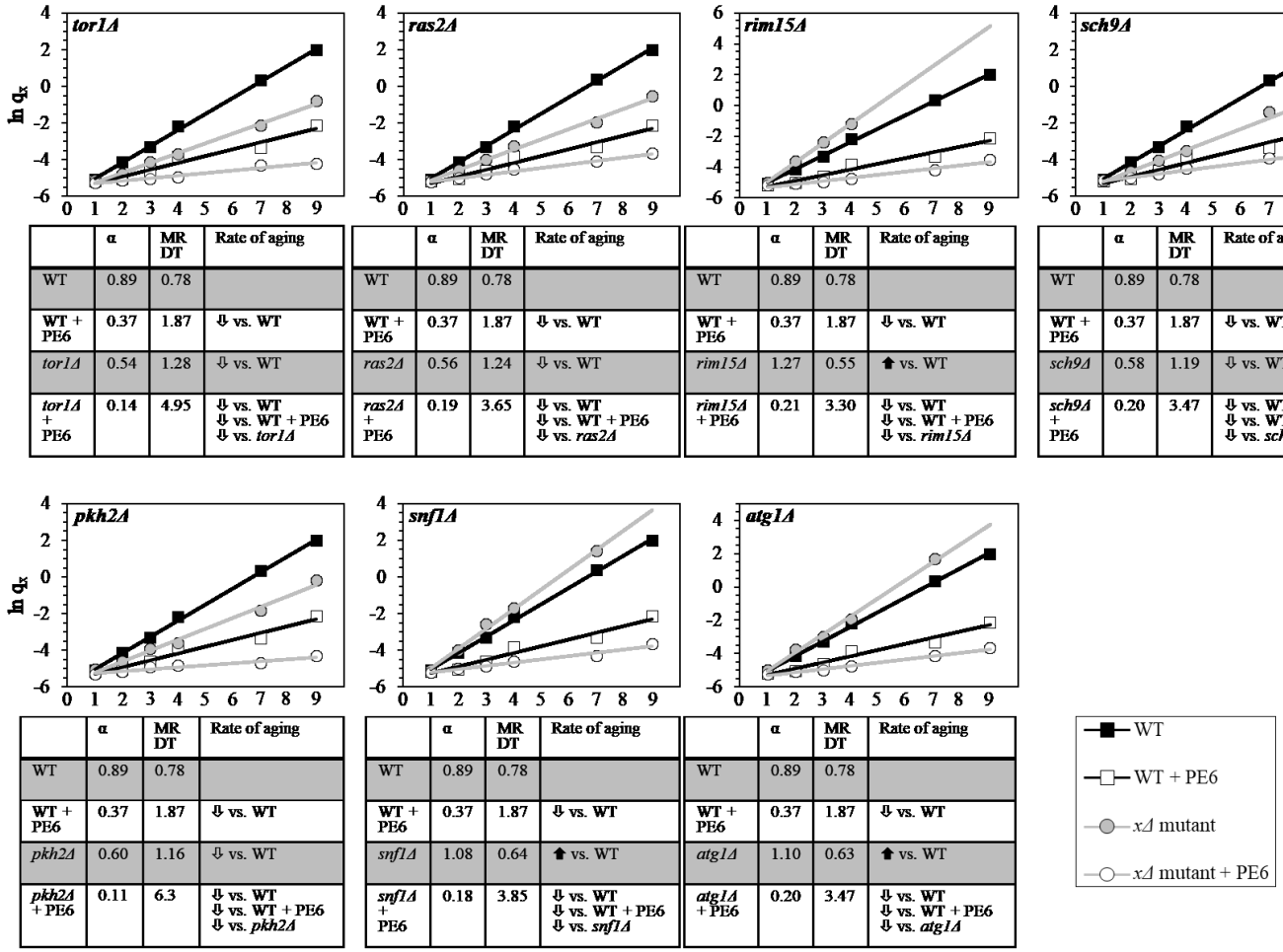

	α	MR DT	Rate of aging
WT	0.89	0.78	
WT + PE6	0.37	1.87	⇩ vs. WT
tor1Δ	0.54	1.28	⇩ vs. WT
tor1Δ + PE6	0.14	4.95	⇩ vs. WT ⇩ vs. WT + PE6 ⇩ vs. *tor1Δ*

	α	MR DT	Rate of aging
WT	0.89	0.78	
WT + PE6	0.37	1.87	⇩ vs. WT
ras2Δ	0.56	1.24	⇩ vs. WT
ras2Δ + PE6	0.19	3.65	⇩ vs. WT ⇩ vs. WT + PE6 ⇩ vs. *ras2Δ*

	α	MR DT	Rate of aging
WT	0.89	0.78	
WT + PE6	0.37	1.87	⇩ vs. WT
rim15Δ	1.27	0.55	⇧ vs. WT
rim15Δ + PE6	0.21	3.30	⇩ vs. WT ⇩ vs. WT + PE6 ⇩ vs. *rim15Δ*

	α	MR DT	Rate of aging
WT	0.89	0.78	
WT + PE6	0.37	1.87	⇩ vs. WT
sch9Δ	0.58	1.19	⇩ vs. WT
sch9Δ + PE6	0.20	3.47	⇩ vs. WT ⇩ vs. WT + PE6 ⇩ vs. *sch9Δ*

	α	MR DT	Rate of aging
WT	0.89	0.78	
WT + PE6	0.37	1.87	⇩ vs. WT
pkh2Δ	0.60	1.16	⇩ vs. WT
pkh2Δ + PE6	0.11	6.3	⇩ vs. WT ⇩ vs. WT + PE6 ⇩ vs. *pkh2Δ*

	α	MR DT	Rate of aging
WT	0.89	0.78	
WT + PE6	0.37	1.87	⇩ vs. WT
snf1Δ	1.08	0.64	⇧ vs. WT
snf1Δ + PE6	0.18	3.85	⇩ vs. WT ⇩ vs. WT + PE6 ⇩ vs. *snf1Δ*

	α	MR DT	Rate of aging
WT	0.89	0.78	
WT + PE6	0.37	1.87	⇩ vs. WT
atg1Δ	1.10	0.63	⇧ vs. WT
atg1Δ + PE6	0.20	3.47	⇩ vs. WT ⇩ vs. WT + PE6 ⇩ vs. *atg1Δ*

Figure 3.10. Analysis of the Gompertz mortality function indicates that PE6 slows yeast chronological aging independently of presently known longevity-defining signaling pathways/protein kinases. Cells of the wild-type (WT) and indicated mutant strains were grown in the synthetic minimal YNB medium (0.67% Yeast Nitrogen Base without amino acids) initially containing 2% glucose, in the presence of 1.0% PE6 (ethanol was used as a vehicle at the final

concentration of 5.0%) or in its absence (cells were subjected to ethanol-mock treatment). Survival curves shown in Fig. 3.8A were used to calculate the age-specific mortality rates (q_x), the Gompertz mortality rates (also known as mortality rate coefficient α) and the mortality rate doubling times (MRDT) for WT and mutant yeast populations cultured with or without 1.0% PE6. The values of q_x, α and MRDT were calculated as described in Materials and methods. Data for the mock-treated WT strain and the WT strain cultured with PE6 are replicated in all graphs of this Figure.

3.3.5 PE8 slows chronological aging by weakening the inhibitory effect of PKA on SNF1

PE8 displayed an additive longevity-extending effect with the *sch9Δ* mutation, and extended yeast CLS in synergy with the *tor1Δ* and *pkh2Δ* mutations (Figure 3.11A, Tables 3.2 and 3.3, Figure 3.12; note that data for the mock-treated WT strain and for the WT strain cultured with PE8 are replicated in all graphs of Figure 3.11A and Figure 3.12). PE8 decreased the values of α and increased the values of MRDT for chronologically aging cultures of strains carrying each of these three mutations (Figure 3.13; note that data for the mock-treated WT strain and the WT strain cultured with PE8 are replicated in all graphs of this Figure). Therefore, PE8 slows aging independently of Sch9, TORC1 and PKH1/2.

PE8 increased CLS of the *rim15Δ* and *atg1Δ* mutant strains, though not as considerably as for WT (Figure 3.11A, Tables 3.2 and 3.3, Figure 3.12). PE8 lowered the values of α and raised the values of MRDT for chronologically aging cultures of strains carrying each of these mutations (Figure 3.13). Hence, PE8 delays aging not through Rim15 or ATG.

PE8 was unable to extend the CLS of *ras2Δ* and *snf1Δ* (Figure 3.11A, Tables 3.2 and 3.3, Figure 3.12) and did not alter the values of α or MRDT for these mutant strains (Figure 3.13). Thus, PE8 slows aging via PKA and SNF1 by weakening the known inhibitory action of PKA on SNF1 (Figure 3.11B).

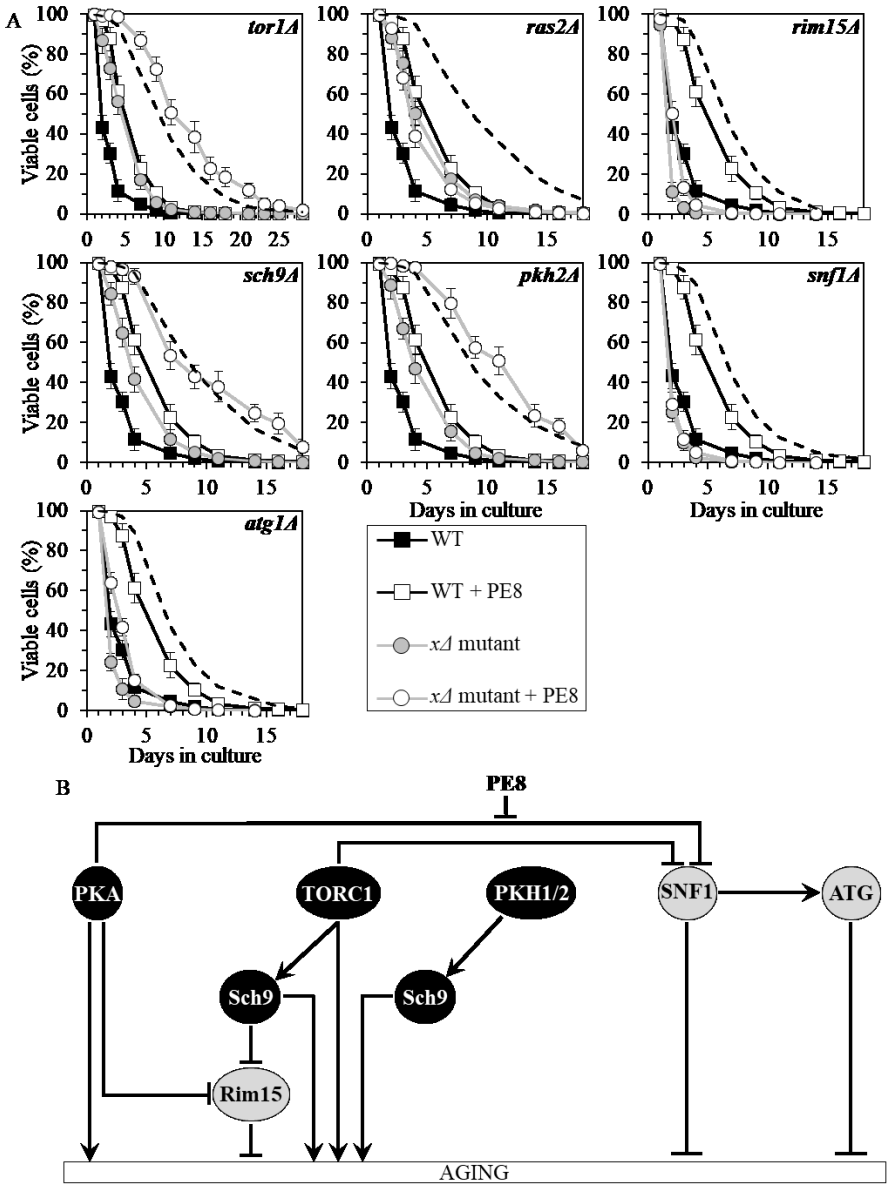

Figure 3.11. PE8 extends yeast CLS by weakening the inhibitory effect of PKA on SNF1. (A) Cells of the wild-type (WT) and indicated mutant strains were grown in the synthetic minimal YNB medium (0.67% Yeast Nitrogen Base without amino acids) initially containing 2% glucose, in the presence of 0.3% PE8 (ethanol was used as a vehicle at the final concentration of 1.5%) or in its absence (cells were subjected to ethanol-mock treatment). Survival curves of chronologically aging WT and mutant strains cultured with or without 0.3% PE8 are shown. Data are presented as means ± SEM (n = 6). The dotted line indicates the predicted survival curve of a particular mutant strain cultured with PE8 if this PE exhibits an additive longevity-extending effect with the mutation. Data for the mock-treated WT strain and the WT strain cultured with PE8 are replicated in all graphs of this Figure. (B) The effect of PE8 on the signaling pathways and protein kinases integrated into the longevity-defining network. This effect is inferred from the data presented in (A), Tables 3.2 and 3.3, and Figures 3.12 and 3.13. Abbreviations: as in the legend to Figure 1.2.

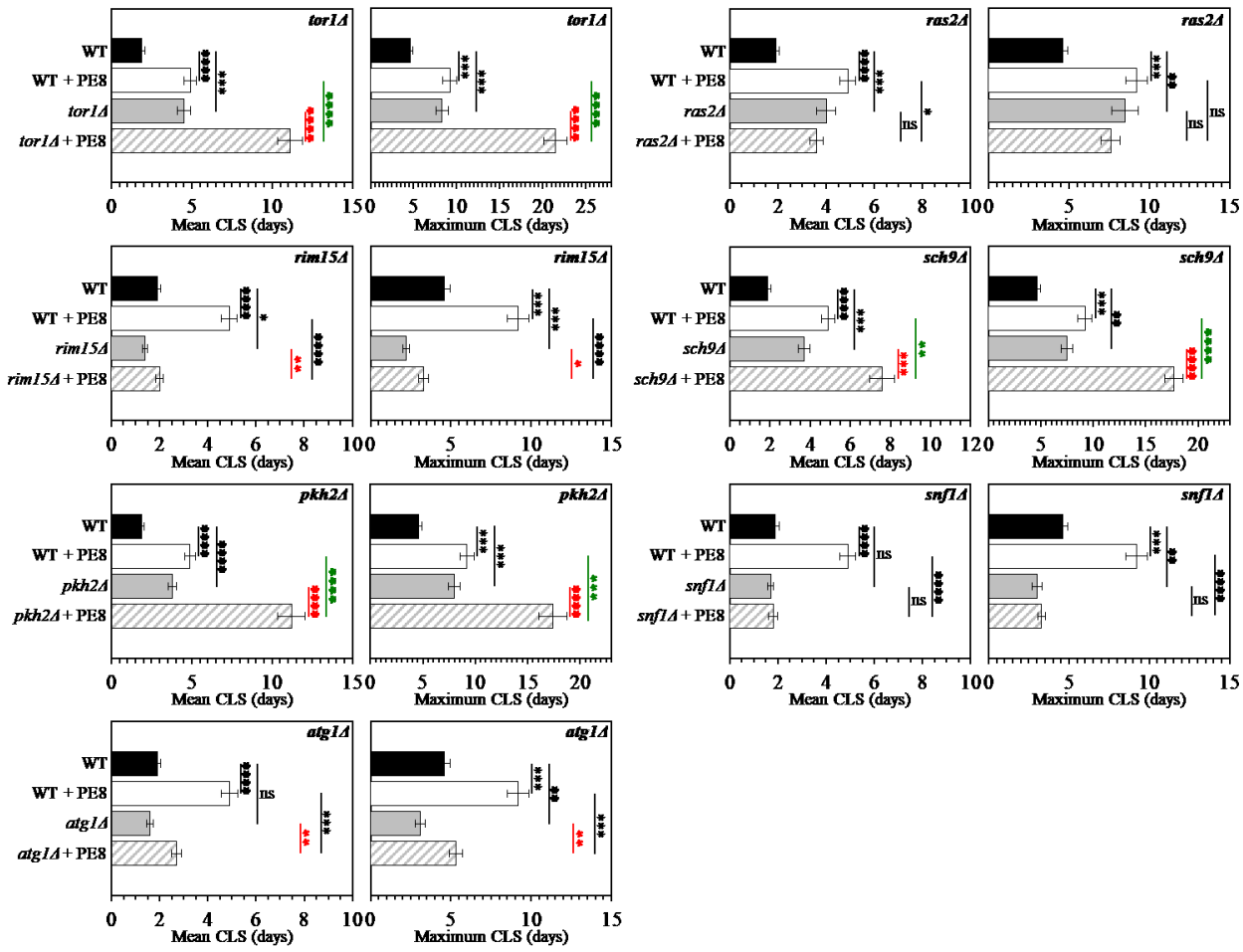

Figure 3.12. PE8 is unable to extend the chronological lifespans (CLS) of the *ras2Δ* and *snf1Δ* mutant strains, shows an additive CLS-extending effect with the *sch9Δ* mutation, and increases yeast CLS in synergy with the *tor1Δ* and *pkh2Δ* mutations. Cells of the wild-type (WT) and indicated mutant strains were grown in the synthetic minimal YNB medium (0.67% Yeast Nitrogen Base without amino acids) initially containing 2% glucose, in the presence of 0.3% PE8 (ethanol was used as a vehicle at the final concentration of 1.5%) or in its absence (cells were subjected to ethanol-mock treatment). Survival curves shown in Fig. 3.11A were used to calculate the mean and maximum CLS for WT and mutant strains cultured with or without 0.3% PE8. Data are presented as means ± SEM (n = 6; ns, not significant; *$p < 0.05$; **$p < 0.01$; ***$p < 0.001$; ****$p < 0.0001$). The ability of PE8 to cause a significant (*$p < 0.05$; **$p < 0.01$; ***$p < 0.001$; ****$p < 0.0001$) increase in the CLS of a particular mutant strain is shown in red color. The ability of a combination between PE8 and a particular mutation to elicit a significant (*$p < 0.05$; **$p < 0.01$; ***$p < 0.001$; ****$p < 0.0001$) increase in CLS-extending efficiencies of each other (i.e. the ability of such combination to exhibit an additive or synergistic CLS-extending effect) is displayed in green color. Data for the mock-treated WT strain and the WT strain cultured with PE8 are replicated in all graphs of this Figure.

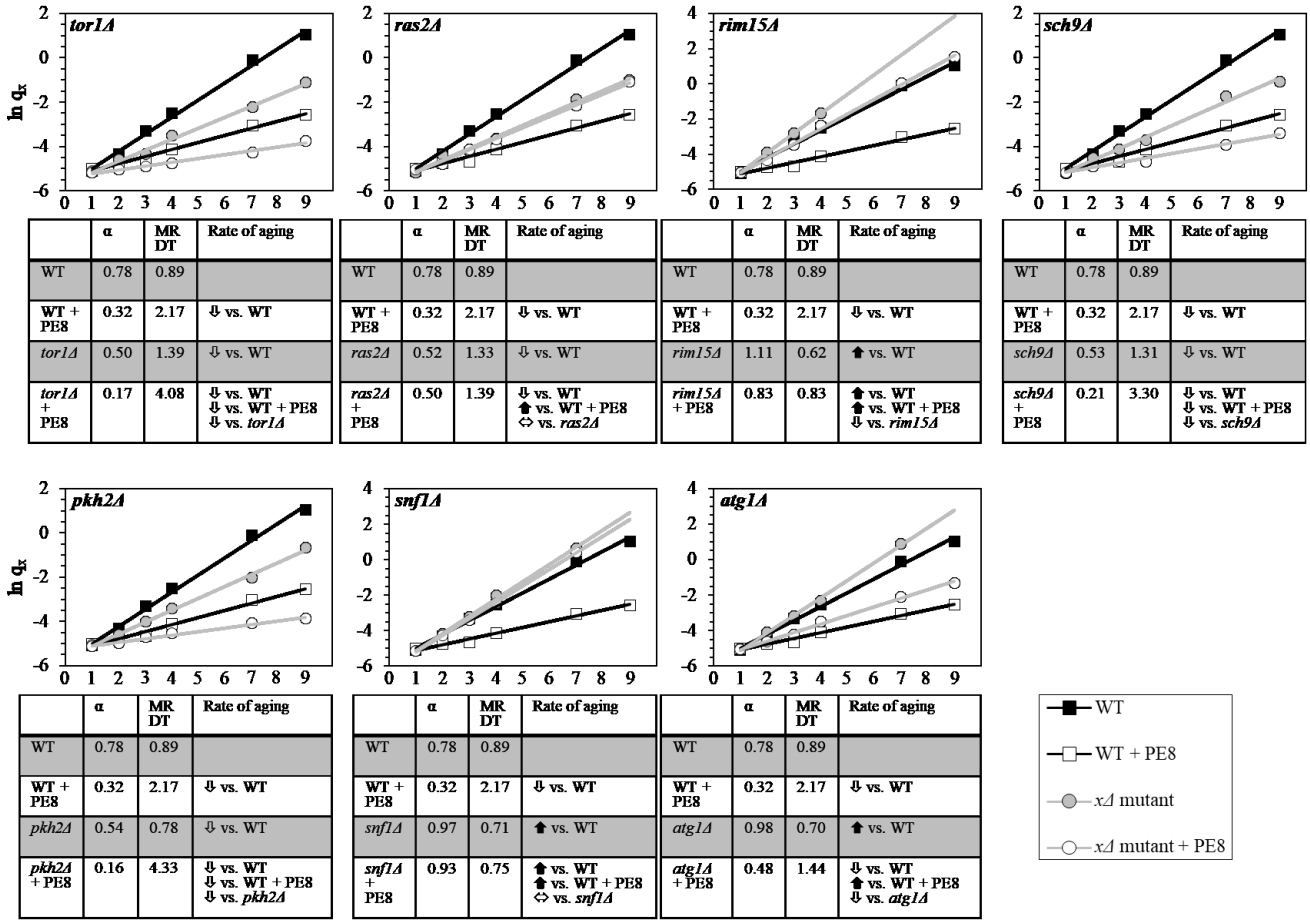

	α	MR DT	Rate of aging
WT	0.78	0.89	
WT + PE8	0.32	2.17	⇩ vs. WT
tor1Δ	0.50	1.39	⇩ vs. WT
tor1Δ + PE8	0.17	4.08	⇩ vs. WT ⇩ vs. WT + PE8 ⇩ vs. *tor1Δ*

	α	MR DT	Rate of aging
WT	0.78	0.89	
WT + PE8	0.32	2.17	⇩ vs. WT
ras2Δ	0.52	1.33	⇩ vs. WT
ras2Δ + PE8	0.50	1.39	⇩ vs. WT ⇧ vs. WT + PE8 ⇔ vs. *ras2Δ*

	α	MR DT	Rate of aging
WT	0.78	0.89	
WT + PE8	0.32	2.17	⇩ vs. WT
rim15Δ	1.11	0.62	⇧ vs. WT
rim15Δ + PE8	0.83	0.83	⇧ vs. WT ⇧ vs. WT + PE8 ⇩ vs. *rim15Δ*

	α	MR DT	Rate of aging
WT	0.78	0.89	
WT + PE8	0.32	2.17	⇩ vs. WT
sch9Δ	0.53	1.31	⇩ vs. WT
sch9Δ + PE8	0.21	3.30	⇩ vs. WT ⇩ vs. WT + PE8 ⇩ vs. *sch9Δ*

	α	MR DT	Rate of aging
WT	0.78	0.89	
WT + PE8	0.32	2.17	⇩ vs. WT
pkh2Δ	0.54	0.78	⇩ vs. WT
pkh2Δ + PE8	0.16	4.33	⇩ vs. WT ⇩ vs. WT + PE8 ⇩ vs. *pkh2Δ*

	α	MR DT	Rate of aging
WT	0.78	0.89	
WT + PE8	0.32	2.17	⇩ vs. WT
snf1Δ	0.97	0.71	⇧ vs. WT
snf1Δ + PE8	0.93	0.75	⇧ vs. WT ⇧ vs. WT + PE8 ⇔ vs. *snf1Δ*

	α	MR DT	Rate of aging
WT	0.78	0.89	
WT + PE8	0.32	2.17	⇩ vs. WT
atg1Δ	0.98	0.70	⇧ vs. WT
atg1Δ + PE8	0.48	1.44	⇩ vs. WT ⇧ vs. WT + PE8 ⇩ vs. *atg1Δ*

Figure 3.13. Analysis of the Gompertz mortality function indicates that PE8 slows yeast chronological aging by weakening the inhibitory effect of PKA on SNF1. Cells of the wild-type (WT) and indicated mutant strains were grown in the synthetic minimal YNB medium (0.67% Yeast Nitrogen Base without amino acids) initially containing 2% glucose, in the presence of 0.3% PE8 (ethanol was used as a vehicle at the final concentration of 1.5%) or in its absence (cells were subjected to ethanol-mock treatment). Survival curves shown in Fig. 3.11A were used to calculate the age-specific mortality rates (q_x), the Gompertz mortality rates (also known as mortality rate coefficient α) and the mortality rate doubling times (MRDT) for WT and mutant yeast populations cultured with or without 0.3% PE8. The values of q_x, α and MRDT were calculated as described in Materials and methods. Data for the mock-treated WT strain and the WT strain cultured with PE8 are replicated in all graphs of this Figure.

3.3.6 PE12 slows chronological aging by stimulating Rim15

PE12 increased yeast CLS synergistically with the *pkh2Δ* mutation and displayed additive longevity-extending effects with the *tor1Δ*, *ras2Δ* and *sch9Δ* mutations (Figure 3.14A, Tables 3.2 and 3.3, Figure 3.15; note that data for the mock-treated WT strain and for the WT strain cultured with PE12 are replicated in all graphs of Figure 3.14A and Figure 3.15). PE12 reduced the values

of α and augmented the values of MRDT for chronologically aging cultures of strains carrying each of these four mutations (Figure 3.16; note that data for the mock-treated WT strain and the WT strain cultured with PE12 are replicated in all graphs of this Figure). Hence, PE12 slows aging not through PKH1/2, TORC1, PKA or Sch9.

PE12 extended longevities of the *snf1Δ* and *atg1Δ* mutant strains, although to a lesser extent than that of WT strain (Figure 3.14A, Tables 3.2 and 3.3, Figure 3.15). PE12 decreased the value of α and increased the value of MRDT strains carrying each of these mutations, however not as considerably as for WT (Figure 3.16). Therefore, PE12 slows aging independently of SNF1 and ATG.

PE12 was unable to extend the CLS of *rim15Δ* (Figure 3.14A, Tables 3.2 and 3.3, Figure 3.15) and did not alter the values of α or MRDT for this mutant strain (Figure 3.16). Hence, PE12 slows aging by activating Rim15 (Figure 3.14B).

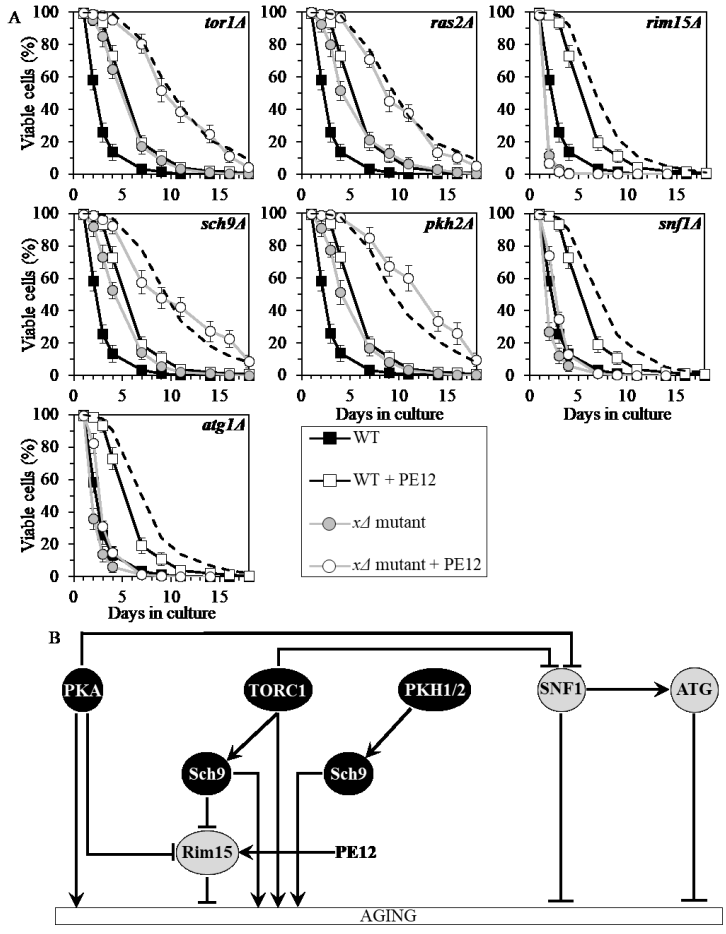

Figure 3.14. PE12 prolongs yeast CLS by stimulating Rim15. (A) Cells of the wild-type (WT)

and indicated mutant strains were grown in the synthetic minimal YNB medium (0.67% Yeast Nitrogen Base without amino acids) initially containing 2% glucose, in the presence of 0.1% PE12 (ethanol was used as a vehicle at the final concentration of 0.5%) or in its absence (cells were subjected to ethanol-mock treatment). Survival curves of chronologically aging WT and mutant strains cultured with or without 0.1% PE12 are shown. Data are presented as means ± SEM (n = 8). The dotted line indicates the predicted survival curve of a particular mutant strain cultured with PE12 if this PE exhibits an additive longevity-extending effect with the mutation. Data for the mock-treated WT strain are replicated in all graphs of this Figure. Data for the WT strain cultured with PE12 are reproduced in all graphs of this Figure. (B) The effect of PE12 on the signaling pathways and protein kinases integrated into the longevity-defining network. This effect is inferred from the data presented in (A), Tables 3.2 and 3.3, and Figures 3.15 and 3.16. Abbreviations: as in the legend to Figure 1.2.

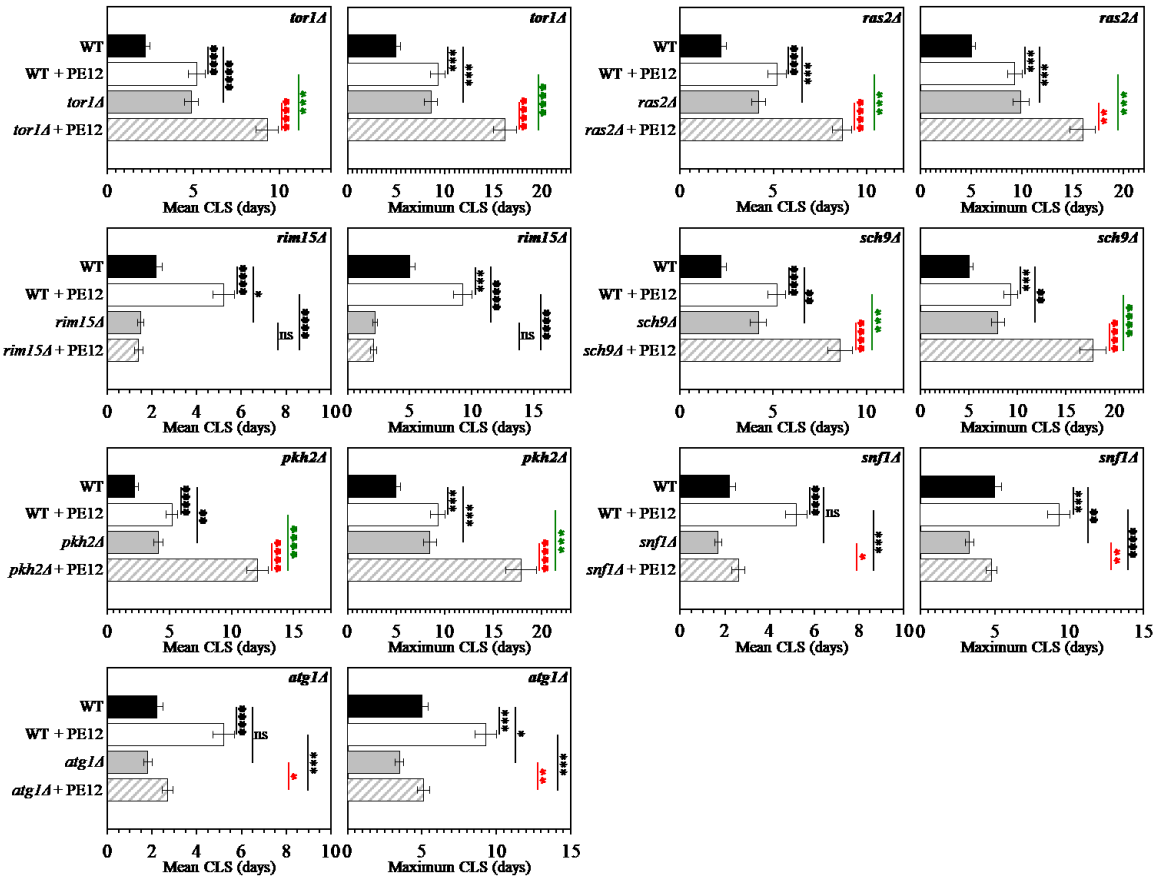

Figure 3.15. PE12 is unable to extend the chronological lifespan (CLS) of the *rim15Δ* mutant strain, has additive CLS-extending effects with the *tor1Δ*, *ras2Δ* and *sch9Δ* mutations, and increases yeast CLS in synergy with the *pkh2Δ* mutation. Cells of the wild-type (WT) and indicated mutant strains were grown in the synthetic minimal YNB medium (0.67% Yeast Nitrogen Base without amino acids) initially containing 2% glucose, in the presence of 0.1% PE12 (ethanol was used as a vehicle at the final concentration of 0.5%) or in its absence (cells were subjected to ethanol-mock treatment). Survival curves shown in Fig. 3.14A were used to calculate

the mean and maximum CLS for WT and mutant strains cultured with or without 0.1% PE12. Data are presented as means ± SEM (n = 8; ns, not significant; *$p < 0.05$; **$p < 0.01$; ***$p < 0.001$; ****$p < 0.0001$). The ability of PE12 to cause a significant (*$p < 0.05$; **$p < 0.01$; ***$p < 0.001$; ****$p < 0.0001$) increase in the CLS of a particular mutant strain is shown in red color. The ability of a combination between PE12 and a particular mutation to cause a significant (*$p < 0.05$; **$p < 0.01$; ***$p < 0.001$; ****$p < 0.0001$) increase in CLS-extending efficiencies of each other (i.e. the ability of such combination to exhibit an additive or synergistic CLS-extending effect) is displayed in green color. Data for the mock-treated WT strain are replicated in all graphs of this Figure. Data for the WT strain cultured with PE12 are replicated in all graphs of this Figure.

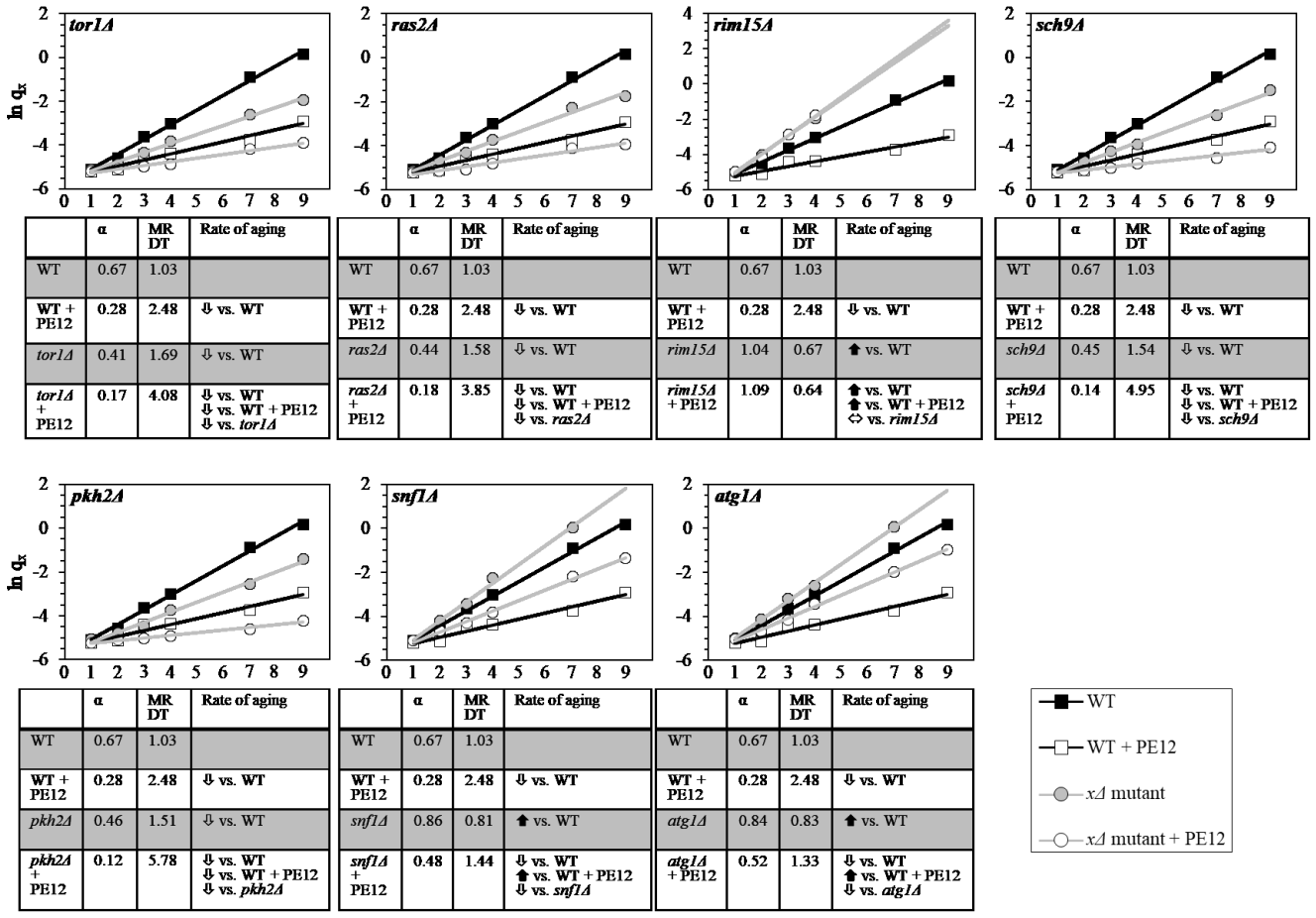

	α	MR DT	Rate of aging
WT	0.67	1.03	
WT + PE12	0.28	2.48	⇩ vs. WT
tor1Δ	0.41	1.69	⇩ vs. WT
tor1Δ + PE12	0.17	4.08	⇩ vs. WT ⇩ vs. WT + PE12 ⇩ vs. *tor1Δ*

	α	MR DT	Rate of aging
WT	0.67	1.03	
WT + PE12	0.28	2.48	⇩ vs. WT
ras2Δ	0.44	1.58	⇩ vs. WT
ras2Δ + PE12	0.18	3.85	⇩ vs. WT ⇩ vs. WT + PE12 ⇩ vs. *ras2Δ*

	α	MR DT	Rate of aging
WT	0.67	1.03	
WT + PE12	0.28	2.48	⇩ vs. WT
rim15Δ	1.04	0.67	⇧ vs. WT
rim15Δ + PE12	1.09	0.64	⇧ vs. WT ⇧ vs. WT + PE12 ⇔ vs. *rim15Δ*

	α	MR DT	Rate of aging
WT	0.67	1.03	
WT + PE12	0.28	2.48	⇩ vs. WT
sch9Δ	0.45	1.54	⇩ vs. WT
sch9Δ + PE12	0.14	4.95	⇩ vs. WT ⇩ vs. WT + PE12 ⇩ vs. *sch9Δ*

	α	MR DT	Rate of aging
WT	0.67	1.03	
WT + PE12	0.28	2.48	⇩ vs. WT
pkh2Δ	0.46	1.51	⇩ vs. WT
pkh2Δ + PE12	0.12	5.78	⇩ vs. WT ⇩ vs. WT + PE12 ⇩ vs. *pkh2Δ*

	α	MR DT	Rate of aging
WT	0.67	1.03	
WT + PE12	0.28	2.48	⇩ vs. WT
snf1Δ	0.86	0.81	⇧ vs. WT
snf1Δ + PE12	0.48	1.44	⇩ vs. WT ⇧ vs. WT + PE12 ⇩ vs. *snf1Δ*

	α	MR DT	Rate of aging
WT	0.67	1.03	
WT + PE12	0.28	2.48	⇩ vs. WT
atg1Δ	0.84	0.83	⇧ vs. WT
atg1Δ + PE12	0.52	1.33	⇩ vs. WT ⇧ vs. WT + PE12 ⇩ vs. *atg1Δ*

Figure 3.16. Analysis of the Gompertz mortality function indicates that PE12 slows yeast chronological aging by stimulating Rim15. Cells of the wild-type (WT) and indicated mutant strains were grown in the synthetic minimal YNB medium (0.67% Yeast Nitrogen Base without amino acids) initially containing 2% glucose, in the presence of 0.1% PE12 (ethanol was used as a vehicle at the final concentration of 0.5%) or in its absence (cells were subjected to ethanol-mock treatment). Survival curves shown in Fig. 3.14A were used to calculate the age-specific mortality rates (q_x), the Gompertz mortality rates (also known as mortality rate coefficient α) and the mortality rate doubling times (MRDT) for WT and mutant yeast populations cultured with or without 0.1% PE12. The values of q_x, α and MRDT were calculated as described in Materials and

methods. Data for the mock-treated WT strain are replicated in all graphs of this Figure. Data for the WT strain cultured with PE12 are replicated in all graphs of this Figure.

3.3.7 PE21 slows chronological aging by inhibiting a PKH1/2-sensitive form of Sch9

PE21 increased yeast CLS in synergy with the *pkh2Δ* mutation and displayed additive longevity-extending effects with the *tor1Δ* and *ras2Δ* mutations (Figure 3.17A, Tables 3.2 and 3.3, Figure 3.18; note that data for the mock-treated WT strain and for the WT strain cultured with PE21 are replicated in all graphs of Figure 3.17A and Figure 3.18). PE21 decreased the values of α and increased the values of MRDT for chronologically aging cultures of strains carrying each of these three mutations (Figure 3.19; note that data for the mock-treated WT strain and the WT strain cultured with PE21 are replicated in all graphs of this Figure). Thus, PE21 slows aging independently of PKH1/2, TORC1 and PKA.

PE21 increased CLS of the *rim15Δ*, *snf1Δ* and *atg1Δ* mutant strains, although to a slightly lesser extent than that of WT (Figure 3.17A, Tables 3.2 and 3.3, Figure 3.18). PE12 lowered the values of α and raised the values of MRDT for chronologically aging cultures of strains carrying each of these mutations, however somewhat less considerably than those for WT (Figure 3.19). Hence, PE12 delays aging not through Rim15, SNF1 or ATG.

PE21 extended the CLS (Figure 3.17A, Tables 3.2 and 3.3, Figure 3.18), decreased the value of α (Figure 3.19) and increased the value of MRDT (Figure 3.19) significantly less efficiently for *sch9Δ* than it did for WT. We therefore concluded that PE21 slows aging by attenuating a PKH1/2-sensitive form of Sch9 (Figure 3.17B).

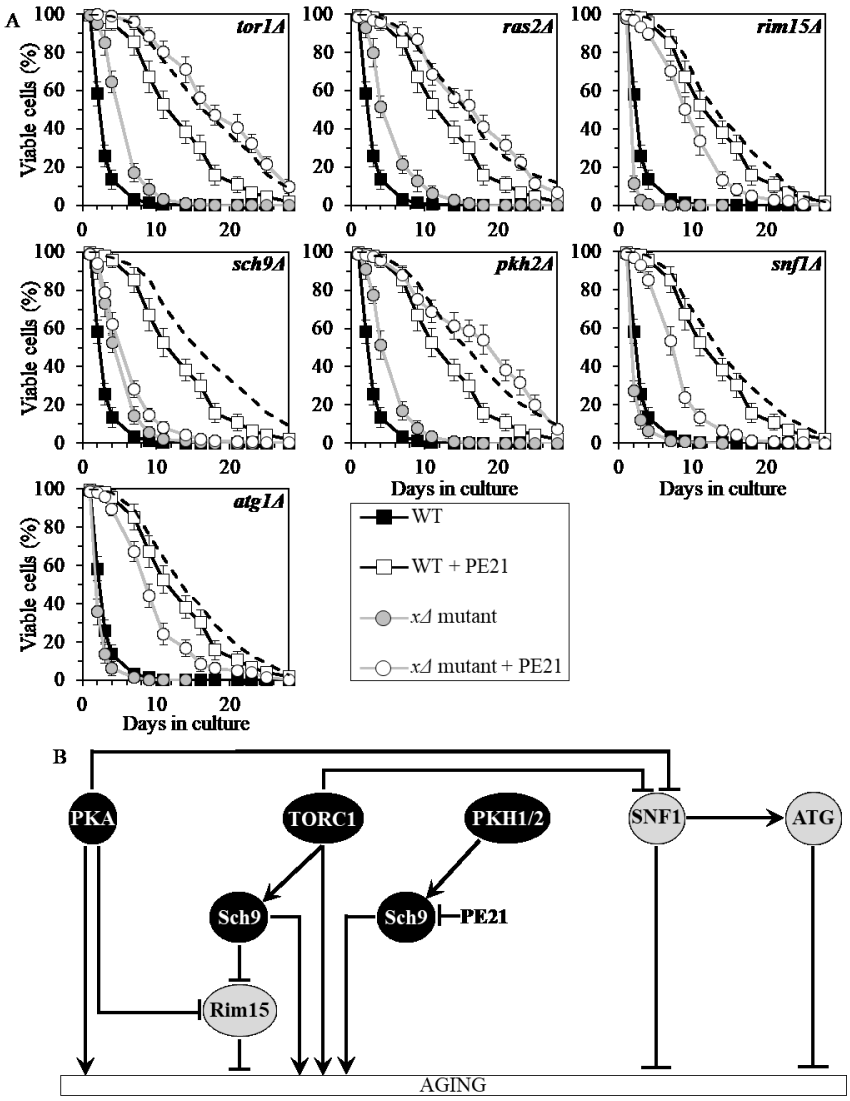

Figure 3.17. PE21 extends yeast CLS by weakening a PKH1/2-sensitive form of Sch9. (A) Cells of the wild-type (WT) and indicated mutant strains were grown in the synthetic minimal YNB medium (0.67% Yeast Nitrogen Base without amino acids) initially containing 2% glucose, in the presence of 0.1% PE21 (ethanol was used as a vehicle at the final concentration of 0.5%) or in its absence (cells were subjected to ethanol-mock treatment). Survival curves of chronologically aging WT and mutant strains cultured with or without 0.1% PE21 are shown. Data are presented as means ± SEM (n = 8). The dotted line indicates the predicted survival curve of a particular mutant strain cultured with PE21 if this PE shows an additive longevity-extending effect with the mutation. Data for the mock-treated WT strain are replicated in all graphs of this Figure and in all graphs of Figure 3.14. Data for each of the mock-treated mutant strains presented in this Figure are reproduced in the corresponding graphs of Figure 3.14. Data for the WT strain cultured with PE21 are replicated in all graphs of this Figure. (B) The effect of PE21 on the signaling pathways and protein kinases integrated into the longevity-defining network. This effect is inferred from the data presented in (A), Tables 3.2 and 3.3, and Figures 3.18 and 3.19. Abbreviations: as in the

legend to Figure 1.2.

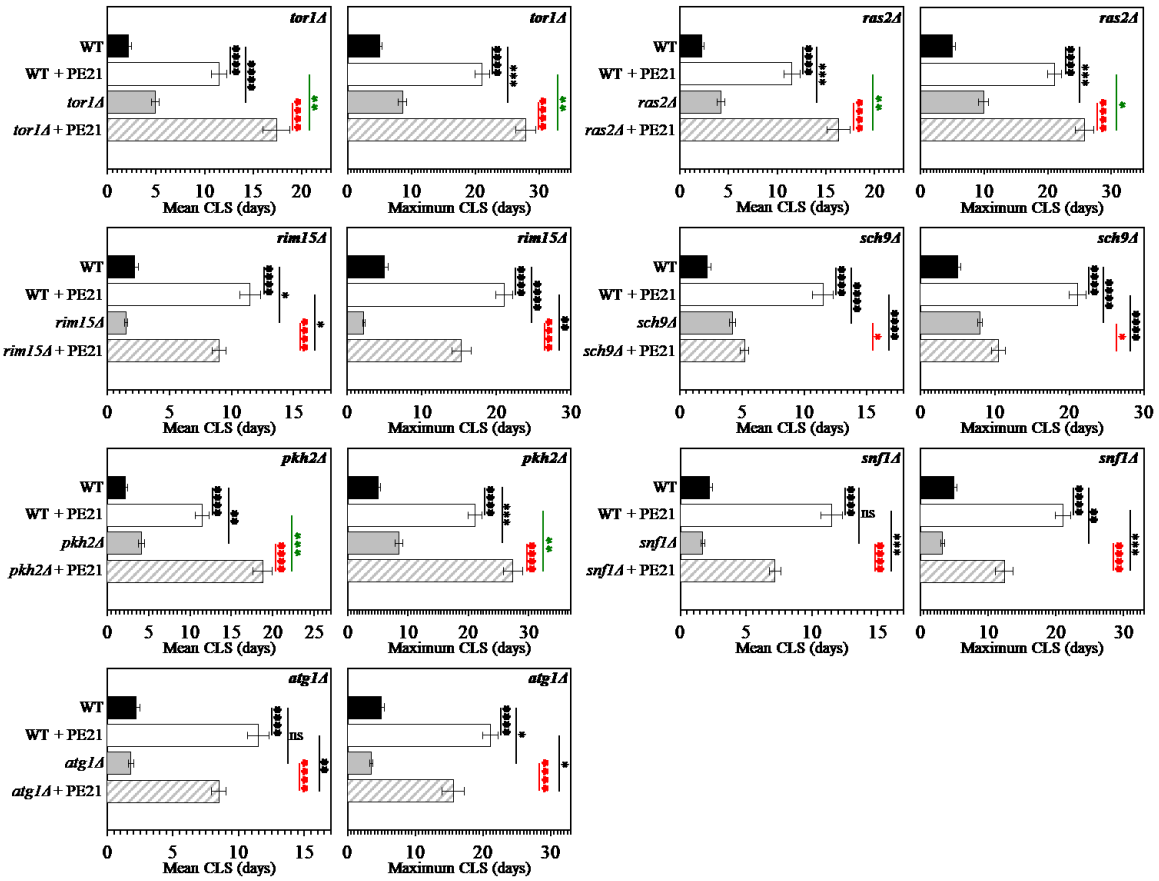

Figure 3.18. PE21 extends the chronological lifespan (CLS) of the *sch9Δ* mutant strain significantly less efficient than that of the wild-type (WT) strain, has additive CLS-extending effects with the *tor1Δ* and *ras2Δ* mutations, and increases yeast CLS in synergy with the *pkh2Δ* mutation. Cells of the WT and indicated mutant strains were grown in the synthetic minimal YNB medium (0.67% Yeast Nitrogen Base without amino acids) initially containing 2% glucose, in the presence of 0.1% PE21 (ethanol was used as a vehicle at the final concentration of 0.5%) or in its absence (cells were subjected to ethanol-mock treatment). Survival curves shown in Fig. 3.17A were used to calculate the mean and maximum CLS for WT and mutant strains cultured with or without 0.1% PE21. Data are presented as means ± SEM (n = 42 for WT; n = 5-7 for WT with PE21 and mutants strains with or without PE; ns, not significant; *$p < 0.05$; **$p < 0.01$; ***$p < 0.001$; ****$p < 0.0001$). The ability of PE21 to cause a significant (*$p < 0.05$; **$p < 0.01$; ***$p < 0.001$; ****$p < 0.0001$) increase in the CLS of a particular mutant strain is shown in red color. The ability of a combination between PE21 and a particular mutation to cause a significant (*$p < 0.05$; **$p < 0.01$; ***$p < 0.001$; ****$p < 0.0001$) increase in CLS-extending efficiencies of each other (i.e. the ability of such combination to exhibit an additive or synergistic CLS-extending effect) is displayed in green color. Data for the mock-treated WT strain are replicated in all graphs of this Figure and in all graphs of Figure 3.15. Data for each of the mock-treated mutant strains presented in this Figure are duplicated in the corresponding graphs of Figure 3.15. Data for the WT strain cultured with PE21 are replicated in all graphs of this Figure.

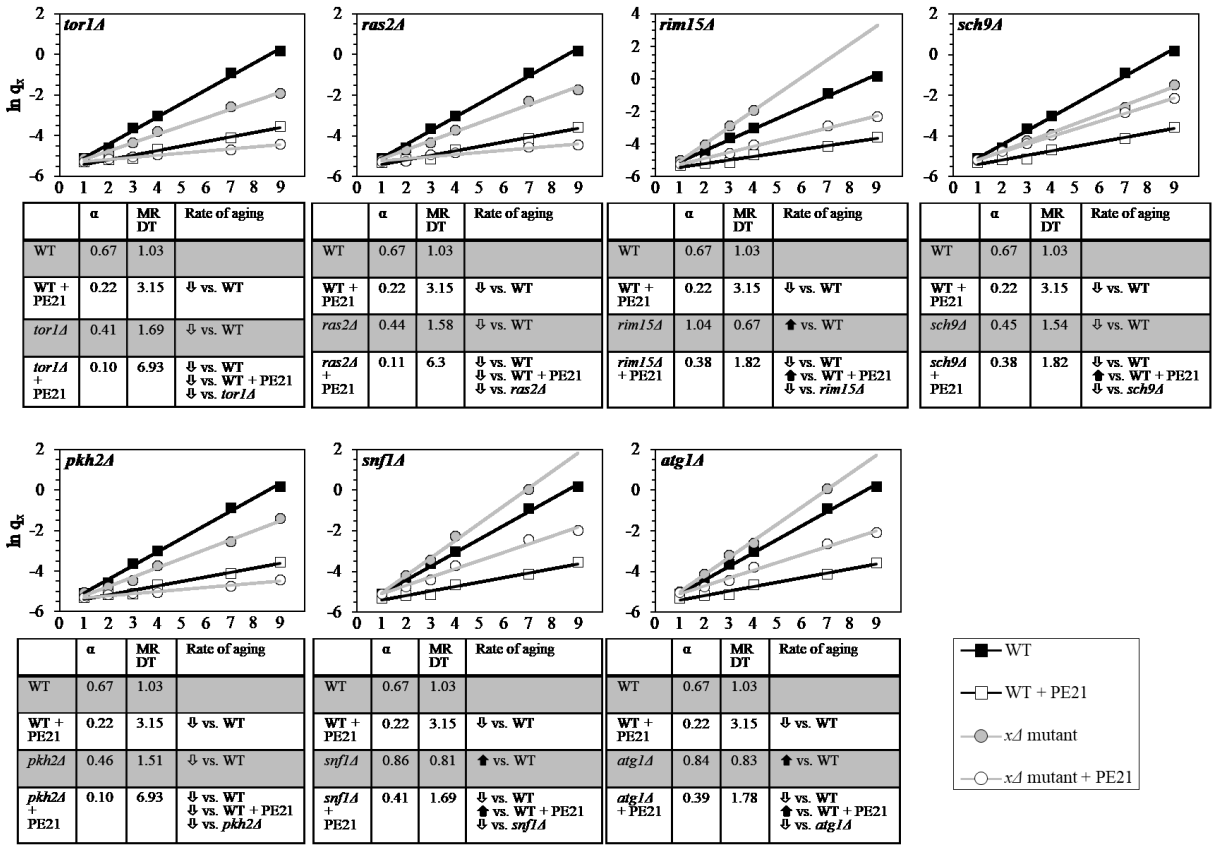

	α	MR DT	Rate of aging
WT	0.67	1.03	
WT + PE21	0.22	3.15	⇩ vs. WT
tor1Δ	0.41	1.69	⇩ vs. WT
tor1Δ + PE21	**0.10**	**6.93**	⇩ vs. WT ⇩ vs. WT + PE21 ⇩ vs. *tor1Δ*

	α	MR DT	Rate of aging
WT	0.67	1.03	
WT + PE21	0.22	3.15	⇩ vs. WT
ras2Δ	0.44	1.58	⇩ vs. WT
ras2Δ + PE21	**0.11**	**6.3**	⇩ vs. WT ⇩ vs. WT + PE21 ⇩ vs. *ras2Δ*

	α	MR DT	Rate of aging
WT	0.67	1.03	
WT + PE21	0.22	3.15	⇩ vs. WT
rim15Δ	1.04	0.67	⇧ vs. WT
rim15Δ + PE21	**0.38**	**1.82**	⇩ vs. WT ⇧ vs. WT + PE21 ⇩ vs. *rim15Δ*

	α	MR DT	Rate of aging
WT	0.67	1.03	
WT + PE21	0.22	3.15	⇩ vs. WT
sch9Δ	0.45	1.54	⇩ vs. WT
sch9Δ + PE21	**0.38**	**1.82**	⇩ vs. WT ⇧ vs. WT + PE21 ⇩ vs. *sch9Δ*

	α	MR DT	Rate of aging
WT	0.67	1.03	
WT + PE21	0.22	3.15	⇩ vs. WT
pkh2Δ	0.46	1.51	⇩ vs. WT
pkh2Δ + PE21	**0.10**	**6.93**	⇩ vs. WT ⇩ vs. WT + PE21 ⇩ vs. *pkh2Δ*

	α	MR DT	Rate of aging
WT	0.67	1.03	
WT + PE21	0.22	3.15	⇩ vs. WT
snf1Δ	0.86	0.81	⇧ vs. WT
snf1Δ + PE21	**0.41**	**1.69**	⇩ vs. WT ⇧ vs. WT + PE21 ⇩ vs. *snf1Δ*

	α	MR DT	Rate of aging
WT	0.67	1.03	
WT + PE21	0.22	3.15	⇩ vs. WT
atg1Δ	0.84	0.83	⇧ vs. WT
atg1Δ + PE21	**0.39**	**1.78**	⇩ vs. WT ⇧ vs. WT + PE21 ⇩ vs. *atg1Δ*

Figure 3.19. Analysis of the Gompertz mortality function indicates that PE21 slows yeast chronological aging by inhibiting a PKH1/2-sensitive form of Sch9. Cells of the wild-type (WT) and indicated mutant strains were grown in the synthetic minimal YNB medium (0.67% Yeast Nitrogen Base without amino acids) initially containing 2% glucose, in the presence of 0.1% PE21 (ethanol was used as a vehicle at the final concentration of 0.5%) or in its absence (cells were subjected to ethanol-mock treatment). Survival curves shown in Fig. 3.17A were used to calculate the age-specific mortality rates (q_x), the Gompertz mortality rates (also known as mortality rate coefficient α) and the mortality rate doubling times (MRDT) for WT and mutant yeast populations cultured with or without 0.1% PE21. The values of q_x, α and MRDT were calculated as described in Materials and methods. Data for the mock-treated WT strain are replicated in all graphs of this Figure and in all graphs of Figure 3.16. Data for each of the mock-treated mutant strains presented in this Figure are duplicated in the corresponding graphs of Figure 3.16. Data for the WT strain cultured with PE21 are replicated in all graphs of this Figure.

3.4 Discussion

A hypothetical model for how the six geroprotective PEs slow yeast chronological aging via the longevity-defining network of signaling pathways/protein kinases emerges from our analysis. This model is shown schematically in Figure 3.20. The model suggests that these PEs

slow aging as follows: 1) PE4 attenuates the inhibitory effect of TORC1 on SNF1, 2) PE5 weakens both the Rim15-dependent and Rim15-independent branches of the PKA signaling pathway, 3) PE6 activates anti-aging processes and/or inhibits pro-aging processes that are not integrated into the network of signaling pathways/protein kinases, 4) PE8 attenuates the inhibitory effect of PKA on SNF1, 5) PE12 activates Rim15, and 6) PE21 inhibits a PKH1/2-sensitive form of Sch9.

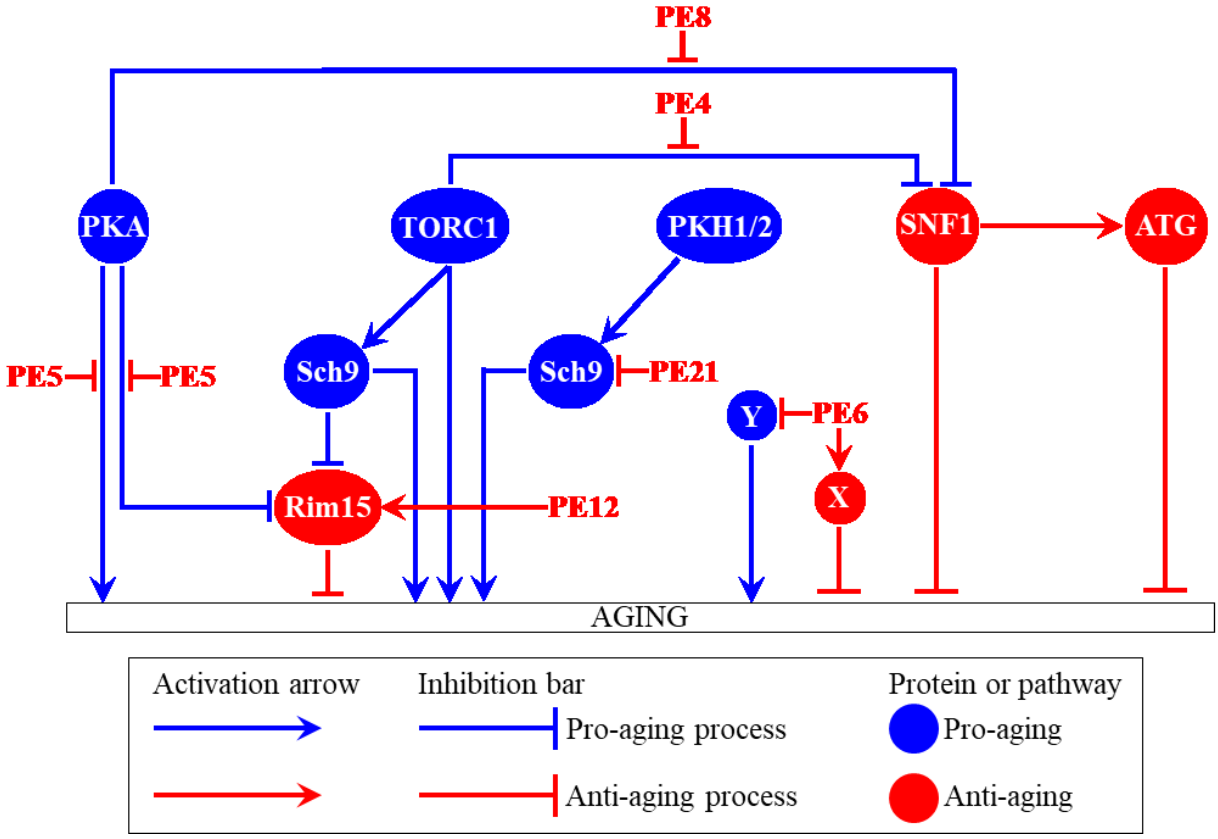

Figure 3.20. A model for how PE4, PE5, PE6, PE8, PE12 and PE21 slow yeast chronological aging via the longevity-defining network of signaling pathways/protein kinases. Activation arrows and inhibition bars denote pro-aging processes (displayed in blue color) or anti-aging processes (shown in red color). Pro-aging or anti-aging signaling pathways and protein kinases are displayed in blue or red color, respectively. Please see text for additional details. Abbreviations: as in the legend to Figure 1.2.

Thus, geroprotective chemical compounds from some plants can slow yeast chronological aging by targeting different hubs, nodes and/or links of the longevity-defining network that integrates specific evolutionarily conserved signaling pathways and protein kinases. In the future, it would be important to test the above hypothesis by investigating how each of the six aging-delaying PEs influences the physical links that connect individual hubs and nodes of the chronological aging network shown in Figure 3.20. These links are known to be mainly activating or inhibiting

phosphorylations and dephosphorylations of specific target proteins that are transiently or permanently reside in various cellular locations, including the plasma membrane, vacuole, nucleus, mitochondria or cytosol [14, 15, 17, 43, 48, 61-64, 66, 68, 70, 74, 81-83, 95-97, 99, 104, 105, 111, 116, 199, 202, 203, 340].

Of note, we found that each of the six geroprotective PEs slows aging through different signaling pathways and/or protein kinases (Figure 3.20). It is possible, therefore, that if these PEs are mixed in various combinations, some of the combinations may display additive or synergistic effects on the aging-delaying efficiencies of each other. Our ongoing studies explore this possibility.

This study also revealed that certain combinations of PE4, PE5, PE8, PE12 or PE21 and the *tor1Δ*, *ras2Δ*, *pkh2Δ* or *sch9Δ* mutation (each of which impairs a pro-aging signaling pathway or protein kinase) markedly increase aging-delaying proficiencies of each other. Furthermore, all combinations of PE6 and mutations impairing either anti-aging or pro-aging signaling pathways/protein kinases display additive or synergistic effects on the extent of the aging delay. It is known that the network of longevity-defining signaling pathways/protein kinases is controlled by such aging-delaying chemical compounds like resveratrol, rapamycin, caffeine, spermidine, myriocin, methionine sulfoxide, lithocholic acid and cryptotanshinone [14, 32, 72, 83, 84, 109-116, 340, 461]. One could envision, therefore, that certain combinations of these chemical compounds and the six PEs may have additive or synergistic effects on the aging-delaying proficiencies of each other. Our ongoing studies address the validity of this assumption.

The evolutionarily conserved nutrient-sensing signaling pathways that accelerate chronological aging in yeast (Figure 3.20) are known to stimulate chronological senescence and geroconversion of post-mitotic human cells; these pathways are likely to expedite organismal aging and cancer development in humans [462-468]. Moreover, genetic and pharmacological manipulations that weaken these signaling pathways and slow chronological aging in yeast are known to decelerate chronological senescence and geroconversion of post-mitotic human cells; it is believed that these manipulations may also slow organismal aging and tumorigenesis in humans [462-468]. Thus, some of the six geroprotective PEs that slow down yeast chronological aging through these signaling pathways (Figure 3.20) may prolong healthy lifespan and decelerate tumorigenesis.

The challenge for the future is to examine whether any of the six geroprotective PEs can

postpone the onset and/or slow the advancement of chronic diseases associated with human aging. Such diseases include arthritis, diabetes, heart disease, kidney disease, liver dysfunction, sarcopenia, stroke, neurodegenerative diseases (including Parkinson's, Alzheimer's and Huntington's diseases), and many forms of cancer [23, 26, 50, 56, 114-116, 334, 335, 338-340, 342, 359, 460, 469-475]. Because the major aspects of aging and age-related pathology are conserved across species [14, 17, 18, 26, 56, 83, 116, 340, 364, 475], it is noteworthy that this study, recent findings [461] and our ongoing research have revealed several features of the six PEs as potential interventions for decelerating chronic diseases of old age. These features are the following: 1) the six PEs are caloric restriction (CR) mimetics that imitate the aging-delaying effects of the CR diet in yeast under non-CR conditions, 2) they are geroprotectors that slow yeast aging by eliciting a hormetic stress response, 3) they extend yeast longevity more efficiently than any lifespan-prolonging chemical compound yet discovered, 4) they slow aging through signaling pathways and protein kinases implicated in such age-related pathologies as type 2 diabetes, neurodegenerative diseases, cardiac hypertrophy, cardiovascular disease, sarcopenia and cancers, and 5) they extend longevity and postpone the onset of age-related diseases in other eukaryotic model organisms. The potential of using the six geroprotective PEs for delaying the onset of age-related diseases in humans is further underscored by the fact that the Health Canada government agency classifies these PEs as safe for human consumption and recommends to use five of them as health-improving supplements with clinically proven benefits to human health [476].

CHAPTER 4

4 Pairwise combinations of plant extracts that slow yeast chronological aging through different signaling pathways display synergistic effects on the extent of the aging delay

4.1 Introduction

We have discovered, as described in Chapter 2 of my Thesis, six plant extracts that slow yeast chronological aging. Chapter 3 of my Thesis provided evidence that most of these plant extracts affect different nodes, edges and modules of an evolutionarily conserved network of longevity regulation that integrates specific signaling pathways and protein kinases. This network is also controlled by some other aging-delaying (geroprotective) chemical compounds, including spermidine and resveratrol. Studies presented in Chapter 3 of my Thesis also revealed that, if a strain carrying an aging-delaying single-gene mutation affecting a specific node, edge or module of the network is exposed to some of the six plant extracts, the mutation and the plant extract enhance geroprotective efficiencies of each other so that their combination has a synergistic effect on the extent of the aging delay. We, therefore, hypothesized that a pairwise combination of two geroprotective plant extracts or a combination of one of these plant extracts and spermidine or resveratrol might have a synergistic effect on the extent of aging delay only if each component of this combination targets a different element of the network. To test our hypothesis, we assessed longevity-extending efficiencies of all possible pairwise combinations of the six plant extracts or of one of them and spermidine or resveratrol in chronologically aging yeast. In support of our hypothesis, we show that only pairwise combinations of naturally occurring chemical compounds that slow aging through different nodes, edges and modules of the network delay aging synergistically. Chapter 4 describes these findings.

4.2 Materials and methods

4.2.1 Yeast strains, media and culture conditions

The wild-type strain *Saccharomyces cerevisiae* BY4742 (*MATα his3*Δ *leu2*Δ *lys2*Δ *ura3*Δ) and single-gene-deletion mutant strains in the BY4742 genetic background (all from Thermo Scientific/Open Biosystems) were cultured in a synthetic minimal YNB medium (0.67% (w/v) Yeast Nitrogen Base without amino acids) initially containing 2% (w/v) glucose and supplemented with 20 mg/l histidine, 30 mg/l leucine, 30 mg/l lysine and 20 mg/l uracil. Cells were cultured at

30ºC with rotational shaking at 200 rpm in Erlenmeyer flasks at a "flask volume/medium volume" ratio of 5:1.

4.2.2 Aging-delaying plant extracts (PEs)

PE4 (an extract from the root and rhizome of *Cimicifuga racemosa*), PE5 (an extract from the root of *Valeriana officinalis L.*), PE6 (an extract from the whole plant of *Passiflora incarnate L.*), PE8 (an extract from the leaf of *Ginkgo biloba*), PE12 (an extract from the seed of *Apium graveolens L.*) and PE21 (an extract from the bark of *Salix alba*) were used at the final concentration of 0.1% (w/v), 0.3% (w/v), 0.5% (w/v) or 1.0% (w/v) [461]. A stock solution of each PE in ethanol was made on the day of adding this PE to cell cultures. For each PE, the stock solution was added to growth medium with 2% (w/v) glucose immediately following cell inoculation into the medium. In a culture supplemented with a PE, ethanol was used as a vehicle at the final concentration of 2.5% (v/v). In the same experiment, yeast cells were also subjected to ethanol-mock treatment by being cultured in the growth medium, initially containing 2% glucose and 2.5% (v/v) ethanol.

4.2.3 Chronological lifespan (CLS) assay

A sample of cells was taken from a culture at a certain day following cell inoculation and PE addition into the medium. A fraction of the sample was diluted to determine the total number of cells using a hemacytometer. Another fraction of the cell sample was diluted, and serial dilutions of cells were plated in duplicate onto YEP (1% (w/v) yeast extract, 2% (w/v) peptone) plates containing 2% (w/v) glucose as carbon source. After 2 d of incubation at 30°C, the number of colony-forming units (CFU) per plate was counted. The number of CFU was defined as the number of viable cells in a sample. For each culture, the percentage of viable cells was calculated as follows: (number of viable cells per ml/total number of cells per ml) × 100. The percentage of viable cells in the mid-logarithmic growth phase was set at 100%.

4.2.4 Statistical analysis

Statistical analysis was performed using Microsoft Excel's (2010) Analysis ToolPack-VBA. All data on cell survival are presented as mean ± SEM. The p values for comparing the means of two groups using an unpaired two-tailed *t* test were calculated with the help of the

GraphPad Prism 7 statistics software. The logrank test for comparing each pair of survival curves was performed with GraphPad Prism 7. Two survival curves were considered statistically different if the *p* value was less than 0.05.

4.3 Results

4.3.1 Our hypothesis on possible synergistic longevity-extending effects of certain pairwise combinations of the six aging-delaying PEs and/or spermidine and resveratrol

A signaling network that controls the rate of yeast chronological aging is schematically depicted in Figure 4.1. This network integrates the following signaling pathways and protein kinases: 1) the pro-aging TORC1 (target of rapamycin complex 1) pathway, 2) the pro-aging PKA (protein kinase A) pathway, 3) the pro-aging PKH1/2 (Pkb-activating kinase homolog) pathway, 4) the anti-aging SNF1 (sucrose non-fermenting) pathway, 5) the anti-aging ATG (autophagy) pathway, 6) the pro-aging protein kinase Sch9, which is activated by the TORC1 and PKH1/2 pathways, and 7) the anti-aging protein kinase Rim15, which is suppressed by the TORC1, PKA and PKH1/2 pathways (Figure 4.1) [15, 17, 66, 68, 95, 96, 198, 340, 477]. The network modulates such longevity-defining cellular processes as gluconeogenesis, glyoxylate cycle, glycogen synthesis and degradation, amino acids synthesis, fatty acids synthesis, mitochondrial respiration, protein synthesis in the cytosol and mitochondria, maintenance of nuclear and mitochondrial genomes, peroxisome biogenesis, autophagy, and stress responses (Figure 4.1) [15, 17, 51, 55, 59, 73, 95-97, 99, 101, 104, 105, 198, 340, 478]. PE4, PE5, PE6, PE8, PE12 and PE21 delay yeast chronological aging because they elicit the following effects on different nodes, edges and modules of the network: 1) PE4 lessens the inhibitory action of the pro-aging TORC1 pathway on the anti-aging SNF1 pathway, 2) PE5 suppresses two different branches of the pro-aging PKA pathway, 3) PE6 regulates cellular processes that are not integrated into the network, 4) PE8 inhibits the suppressive effect of PKA on SNF1, 5) PE12 stimulates the anti-aging protein kinase Rim15, and 6) PE21 downregulates a form of the pro-aging protein kinase Sch9 that is stimulated by the pro-aging PKH1/2 pathway (Figure 4.1) [477].

It has previously demonstrated that spermidine, a polyamine of plant origin, delays the chronological mode of aging in yeast and other organisms by activating the anti-aging ATG1 (autophagy) pathway (Figure 4.1) [17, 83, 84, 111, 479]. Moreover, although resveratrol has been

shown to extend mammalian healthspan by suppressing cAMP-dependent phosphodiesterases to elicit AMPK activation [480] and by stimulating the tyrosyl transfer-RNA synthetase to promote poly(ADP-ribose) polymerase 1 auto-poly-ADP-ribosylation [481], the molecular targets of this plant phenolic compound in chronologically aging yeast remain unknown (Figure 4.1).

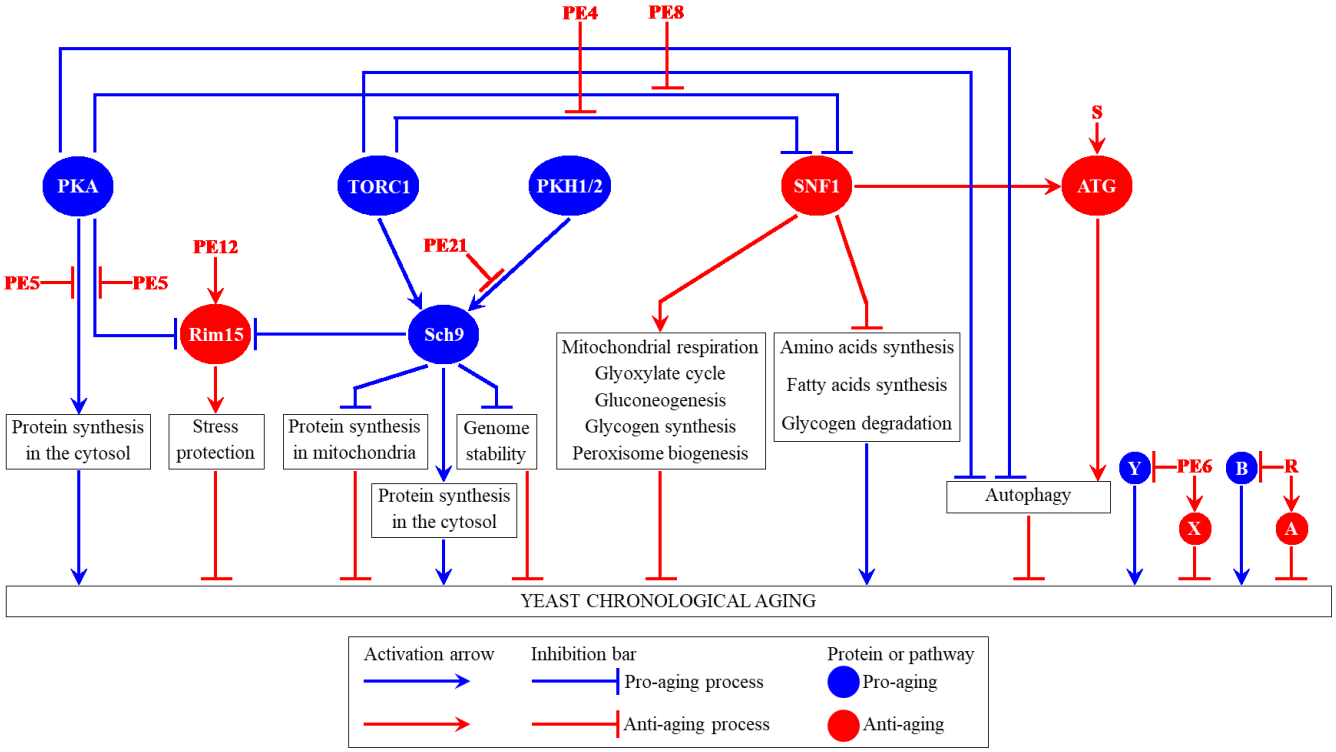

Figure 4.1. PE4, PE5, PE8, PE12, PE21 and spermidine (S) delay yeast chronological aging because they regulate various pro-aging or anti-aging nodes, edges and modules of an evolutionarily conserved signaling network known to control the rate of aging. PE6 and resveratrol (R) delay yeast chronological aging by regulating a presently unknown pro-aging or anti-aging node that may be integrated into this signaling network. The signaling network that controls the rate of yeast chronological aging coordinates various longevity-defining cellular processes; these processes are named in the boxes. Activation arrows and inhibition bars denote pro-aging processes (displayed in blue color) or anti-aging processes (shown in red color). Pro-aging or anti-aging nodes (i.e., the key protein components of pro-aging or anti-aging signaling pathways) integrated into this signaling network are displayed in blue or red color, respectively. Please see text for additional details. Abbreviations: ATG, autophagy; PKA, protein kinase A; PKH1/2, Pkb-activating kinase homologs 1 and 2; Rim15, an anti-aging protein kinase; Sch9, a pro-aging protein kinase; SNF1, sucrose non-fermenting protein 1; TORC1, target of rapamycin complex 1; A and X, presently unknown anti-aging nodes of this signaling network; B and Y, currently unknown pro-aging nodes of this signaling network.

As we have already mentioned, the following two observations provide the basis for our hypothesis: 1) most of the six aging-delaying PEs, as well as spermidine and resveratrol, modulate

different nodes, edges and modules of the signaling network that controls the rate of yeast chronological aging (Figure 4.1) [477]; the only possible exception is the demonstrated abilities of PE4 and PE8 to weaken the restraining action of two different network's edges (i.e., the pro-aging TORC1 pathway and PKA pathway, respectively) on the same node (i.e., the anti-aging SNF1 pathway) of the network (Figure 4.1) [477], and 2) certain combinations of one of the six PEs and aging-delaying single-gene mutations that affect these nodes, edges and modules display synergistic effects on the extent of yeast chronological aging delay [477]. We therefore put forward the hypothesis that most of 27 possible pairwise combinations of two aging-delaying PEs or one of these PEs and spermidine or resveratrol (Table 4.1) may slow down yeast chronological aging in a synergistic manner. We also hypothesized that a combination of PE4 and PE8 might not display a synergistic effect on the extent of yeast chronological aging delay. To test these hypotheses, we assessed longevity-extending efficiencies of all possible pairwise combinations of PE4, PE5, PE6, PE8, PE12 and PE21 or of one of these PEs and spermidine or resveratrol in chronologically aging yeast.

Table 4.1. This study assessed how each possible pairwise combination of PE4, PE5, PE6, PE8, PE12 and PE21 or of one of these PEs and spermidine (S) or resveratrol (R) influences yeast chronological aging. These pairwise combinations are displayed on a yellow color background.

	PE5	PE6	PE8	PE12	PE21	S	R
PE4	**PE4 + PE5**	**PE4 + PE6**	**PE4 + PE8**	**PE4 + PE12**	**PE4 + PE21**	**PE4 + S**	**PE4 + R**
PE5		**PE5 + PE6**	**PE5 + PE8**	**PE5 + PE12**	**PE5 + PE21**	**PE5 + S**	**PE5 + R**
PE6			**PE6 + PE8**	**PE6 + PE12**	**PE6 + PE21**	**PE6 + S**	**PE6 + R**
PE8				**PE8 + PE12**	**PE8 + PE21**	**PE8 + S**	**PE8 + R**
PE12					**PE12 + PE21**	**PE12 + S**	**PE12 + R**
PE21						**PE21 + S**	**PE21 + R**

4.3.2 An effect-based model that we used to assess if a pairwise combination of aging-delaying chemical compounds has a synergistic effect on the extent of the aging delay

Several effect-based models have been developed to assess if a pairwise combination of chemical compounds exhibits a synergistic effect on the monitored process, i.e., if the positive

effect of this combination on the process exceeds the positive effects of individual compounds comprising the combination [296, 301, 302, 323, 329, 482-485]. In this study, we have used the highest single agent (HSA) model for evaluating if two PEs or a PE and spermidine or resveratrol extend yeast longevity synergistically if used in a pairwise combination; this model has been recently used to demonstrate that certain drug combinations have synergistic effects on aging delay and healthspan extension in the nematode *C. elegans* [356]. According to the HSA model, two chemical compounds are considered to act in synergy if the effect of their combination exceeds the effect of a component of this combination that exhibits the highest effect if it is used alone [323, 329, 482, 485]. Using the HSA model, we have calculated the Combination Index (CI) value (which is considered as the standard measure of combination effect [323, 329, 482, 485]) as follows: $CI = CLS_X/CLS_{X+Y}$ (if chemical compound X is the HSA) or $CI = CLS_Y/CLS_{X+Y}$ (if chemical compound Y is the HSA) for both the mean and maximum CLS of yeast exposed to compound X alone, to compound Y alone or a mixture of compounds X and Y. We have calculated the significance of a synergistic effect (i.e., $CI < 1$) as the p value of the two-tailed t test for comparing the effect of a combination of chemical compounds (i.e., CLS_{X+Y}) to that of the HSA (i.e., CLS_X or CLS_Y for the mean and maximum CLS).

4.3.3 Mixtures of PE4 and PE5, PE4 and PE6, PE4 and PE12, and PE4 and PE21 have synergistic effects on the extent of the aging delay

PE4, PE5, PE6, PE12 or PE21 have been shown to modulate different nodes, edges and modules of the signaling network that controls the rate of yeast chronological aging [477]. Specifically, these PEs delay aging as follows: 1) PE4 weakens the restraining action of the pro-aging TORC1 pathway on the anti-aging SNF1 pathway, 2) PE5 mitigates two different branches of the pro-aging PKA pathway, 3) PE6 modulates a presently unknown pro-aging or anti-aging node that may be integrated into this network, 4) PE12 stimulates the anti-aging protein kinase Rim15, and 5) PE21 inhibits a form of the pro-aging protein kinase Sch9 that is activated by the pro-aging PKH1/2 pathway (Figure 4.1) [477]. We, therefore, hypothesized that mixtures of PE4 with PE5, PE6, PE12 or PE21 might exhibit synergistic effects on the extent of yeast chronological aging delay. To test this hypothesis, we cultured wild-type (WT) cells in the synthetic minimal medium initially containing 2% glucose, either without a PE (i.e. cells were subjected to ethanol-mock treatment) or with the following additions: 1) PE4, PE5, PE6, PE12 or PE21 alone (each

being used at the final concentration of 0.1%, 0.5% or 1.0%, see below), or 2) a mixture of 0.1%, 0.3%, 0.5% or 1.0% PE4 with PE5, PE6, PE12 or PE21 (each being used at the final concentration of 0.1%, 0.3%, 0.5% or 1.0%).

We found that the longevity-extending efficiencies of the following pairwise combinations of aging-delaying PEs statistically significantly exceed that of a PE within the pair which was considered as the HSA if this PE was used alone at the optimal aging-delaying concentration: 1) a mixture of 0.3% PE4 and 0.3% PE5 (if PE4 and PE5 were used at these final concentrations, their mixture exhibited the highest longevity-extending effect) as compared to 0.5% PE4 (which was used as the HSA for both the mean and maximum CLS), with CI = 0.63 for the mean CLS and CI = 0.56 for the maximum CLS (Figure 4.2), 2) a mixture of 0.5% PE4 and 1.0% PE6 as compared to 0.5% PE4 (which was used as the HSA for both the mean and maximum CLS) (Figure 4.3), 3) a mixture of 0.5% PE4 and 0.1% PE12 as compared to 0.5% PE4 (which was used as the HSA for the mean CLS) or 0.1% PE12 (which was used as the HSA for the maximum CLS) (Figure 4.4), and 4) a mixture of 0.5% PE4 and 0.1% PE21 as compared to 0.1% PE21 (which was used as the HSA for both the mean and maximum CLS), with CI = 0.61 for the mean CLS and CI = 0.73 for the maximum CLS (Figure 4.5).

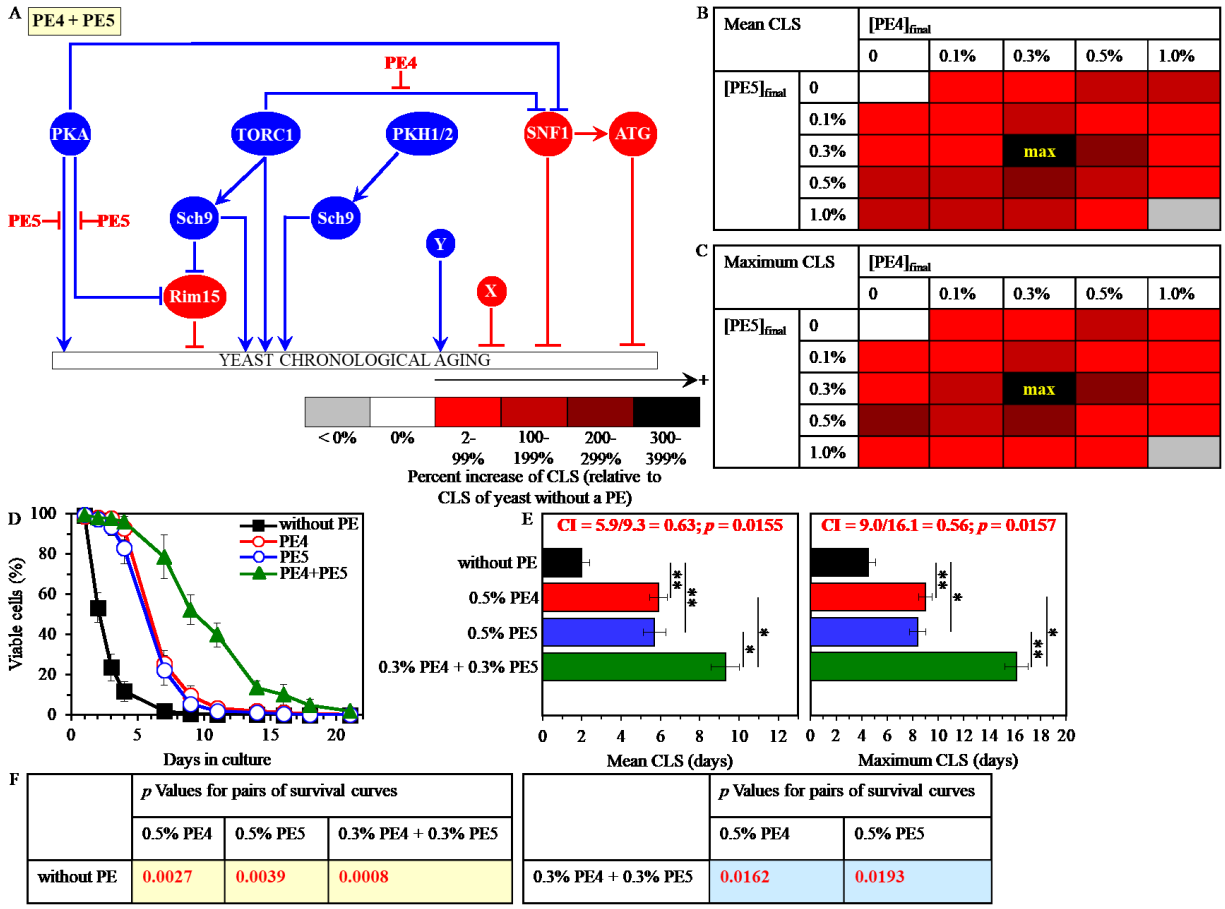

Figure 4.2. The longevity-extending efficiency of a mixture of 0.3% PE4 and 0.3% PE5 statistically significantly exceeds those of PE4 and PE5, each being used at the optimal concentration of 0.5%. Thus, PE4 and PE5 enhance the longevity-extending efficiency of each other. Hence, according to the highest single agent (HSA) model, PE4 and PE5 act in synergy to extend the longevity of chronologically aging yeast. (A) PE4 and PE5 are known to inhibit different pro-aging nodes of the signaling network that controls the rate of yeast chronological aging. PE4 weakens the restraining action of the pro-aging TORC1 pathway on the anti-aging SNF1 pathway, whereas PE5 mitigates two different branches of the pro-aging PKA pathway. (B, C) Wild-type (WT) cells were grown in the synthetic minimal YNB medium initially containing 2% glucose, with PE4 and/or PE5 (at the final concentration of 0.1%, 0.3%, 0.5% or 1.0%) or without a PE. Effects of different concentrations of PE4 and PE5 (added alone or in pairwise combinations) on the mean (B) or maximum (C) chronological lifespan (CLS) of WT cells are shown. The table cell at the intersection of the column for 0.3% PE4 and the row for 0.3% PE5 is marked "max" because the mixture of 0.3% PE4 and 0.3% PE5 exhibits the highest extending effect on the mean and maximum lifespans of chronologically aging WT cells. (D, E) WT cells were cultured in the synthetic minimal YNB medium initially containing 2% glucose and one of the following supplements: 0.5% PE4, 0.5% PE5, or a mixture of 0.3% PE4 and 0.3% PE5. In the cultures supplemented with PE4 and/or PE5, ethanol was used as a vehicle at the final concentration of 2.5%. In the same experiment, WT cells were also subjected to ethanol-mock treatment by being cultured in the synthetic minimal YNB medium, initially containing 2% glucose and 2.5% ethanol. Survival curves (D) and the mean and maximum lifespans (E) of

chronologically aging WT cells cultured without a PE (cells were subjected to ethanol-mock treatment), with 0.5% PE4, with 0.5% PE5, or with the mixture of 0.3% PE4 and 0.3% PE5 are shown. Data in D and E are presented as means ± SEM (n = 3; *$p < 0.05$; **$p < 0.01$). The Combination Index (CI) values in E were calculated as follows: $CI = CLS_{PE4}/CLS_{PE4+PE5}$ for both the mean and maximum CLS; the significance of a synergistic effect (i.e., CI < 1) is provided as the *p* value of the two-tailed *t* test for comparing the effect of a PE combination (i.e., $CLS_{PE4+PE5}$) to that of the HSA (i.e., CLS_{PE4} for both the mean and maximum CLS). (F) *p* Values for different pairs of survival curves of WT cells cultured in the presence of 0.5% PE4, 0.5% PE5, a mixture of 0.3% PE4 and 0.3% PE5, or in the absence of a PE (cells were subjected to ethanol-mock treatment) are shown. Survival curves shown in (D) were compared. Two survival curves were considered statistically different if the *p* value was less than 0.05. The *p* values for comparing pairs of survival curves using the logrank test were calculated as described in Materials and Methods. The *p* values displayed on a yellow color background indicate that 0.5% PE4, 0.5% PE5, and the mixture of 0.3% PE4 and 0.3% PE5 significantly extend the CLS of WT cells. The *p* values displayed on a blue color background indicate that the CLS-extending efficiency of the mixture of 0.3% PE4 and 0.3% PE5 significantly exceeds that of 0.5% PE4 or 0.5% PE5. Abbreviations: ATG, autophagy; PKA, protein kinase A; PKH1/2, Pkb-activating kinase homologs 1 and 2; Rim15, an anti-aging protein kinase; Sch9, a pro-aging protein kinase; SNF1, sucrose non-fermenting protein 1; TORC1, a target of rapamycin complex 1; X, a presently unknown anti-aging node of this signaling network; Y, a presently unknown pro-aging node of this signaling network.

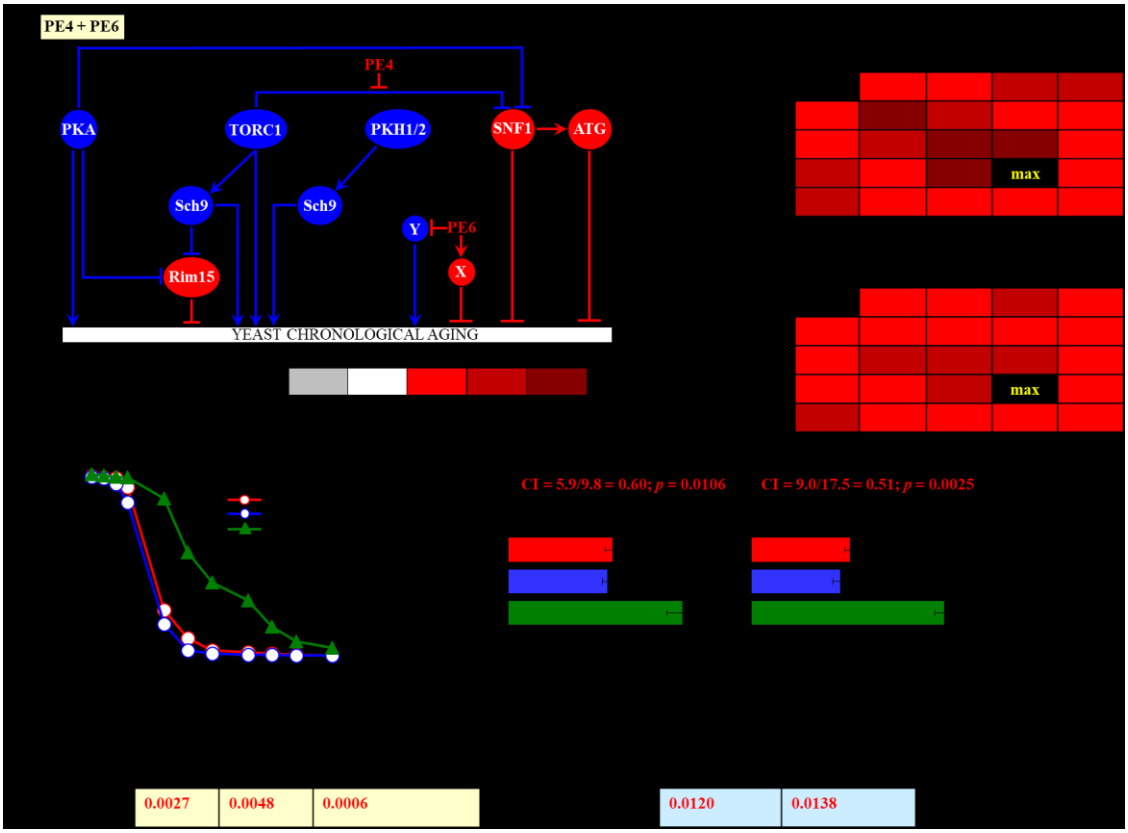

Figure 4.3. The longevity-extending efficiency of a mixture of 0.5% PE4 and 0.5% PE6 statistically significantly exceeds those of PE4 and PE6, which were used at the optimal concentration of 0.5% or 1.0% (respectively). Thus, PE4 and PE6 enhance the longevity-extending efficiency of each other. Hence, according to the highest single agent (HSA) model, PE4 and PE6 act in synergy to extend the longevity of chronologically aging yeast. (A) PE4 and PE6 are known to regulate different nodes of the signaling network that controls the rate of yeast chronological aging. PE4 weakens the restraining action of the pro-aging TORC1 pathway on the anti-aging SNF1 pathway, whereas PE6 modulates a presently unknown pro-aging or anti-aging node that may be integrated into this signaling network. (B, C) WT cells were grown in the synthetic minimal YNB medium initially containing 2% glucose, with PE4 and/or PE6 (at the final concentration of 0.1%, 0.3%, 0.5% or 1.0%) or without a PE. Effects of different concentrations of PE4 and PE6 (added alone or in pairwise combinations) on the mean (B) or maximum (C) CLS of WT cells are shown. The table cell at the intersection of the column for 0.5% PE4 and the row for 0.5% PE6 is marked "max" because the mixture of 0.5% PE4 and 0.5% PE6 exhibits the highest extending effect on the mean and maximum lifespans of chronologically aging WT cells. (D, E) WT cells were cultured in the synthetic minimal YNB medium initially containing 2% glucose and one of the following supplements: 0.5% PE4, 1.0% PE6, or a mixture of 0.5% PE4 and 0.5% PE6. In the cultures supplemented with PE4 and/or PE6, ethanol was used as a vehicle at the final concentration of 2.5%. In the same experiment, WT cells were also subjected to ethanol-mock treatment by being cultured in the synthetic minimal YNB medium, initially containing 2% glucose and 2.5% ethanol. Survival curves (D) and the mean and maximum lifespans (E) of chronologically aging WT cells cultured without a PE (cells were subjected to ethanol-mock treatment), with 0.5% PE4, with 1.0% PE6, or with the mixture of 0.5% PE4 and 0.5% PE6 are shown. Data in D and E are presented as means ± SEM (n = 3; *$p < 0.05$; **$p < 0.01$). The CI

values in E were calculated as follows: CI = $CLS_{PE4}/CLSP_{E4+PE6}$ for both the mean and maximum CLS; the significance of a synergistic effect (i.e., CI < 1) is provided as the *p* value of the two-tailed *t* test for comparing the effect of a PE combination (i.e., $CLS_{PE4+PE6}$) to that of the HSA (i.e., CLS_{PE4} for both the mean and maximum CLS). (F) *p* Values for different pairs of survival curves of WT cells cultured in the presence of 0.5% PE4, 1.0% PE6, a mixture of 0.5% PE4 and 0.5% PE6, or in the absence of a PE (cells were subjected to ethanol-mock treatment) are shown. Survival curves shown in (D) were compared. Two survival curves were considered statistically different if the *p* value was less than 0.05. The *p* values for comparing pairs of survival curves using the logrank test were calculated as described in Materials and Methods. The *p* values displayed on a yellow color background indicate that 0.5% PE4, 1.0% PE6, and the mixture of 0.5% PE4 and 0.5% PE6 significantly extend the CLS of WT cells. The *p* values displayed on a blue color background indicate that the CLS-extending efficiency of the mixture of 0.5% PE4 and 0.5% PE6 significantly exceeds that of 0.5% PE4 or 1.0% PE6. Abbreviations: as in the legend to Figure 4.2.

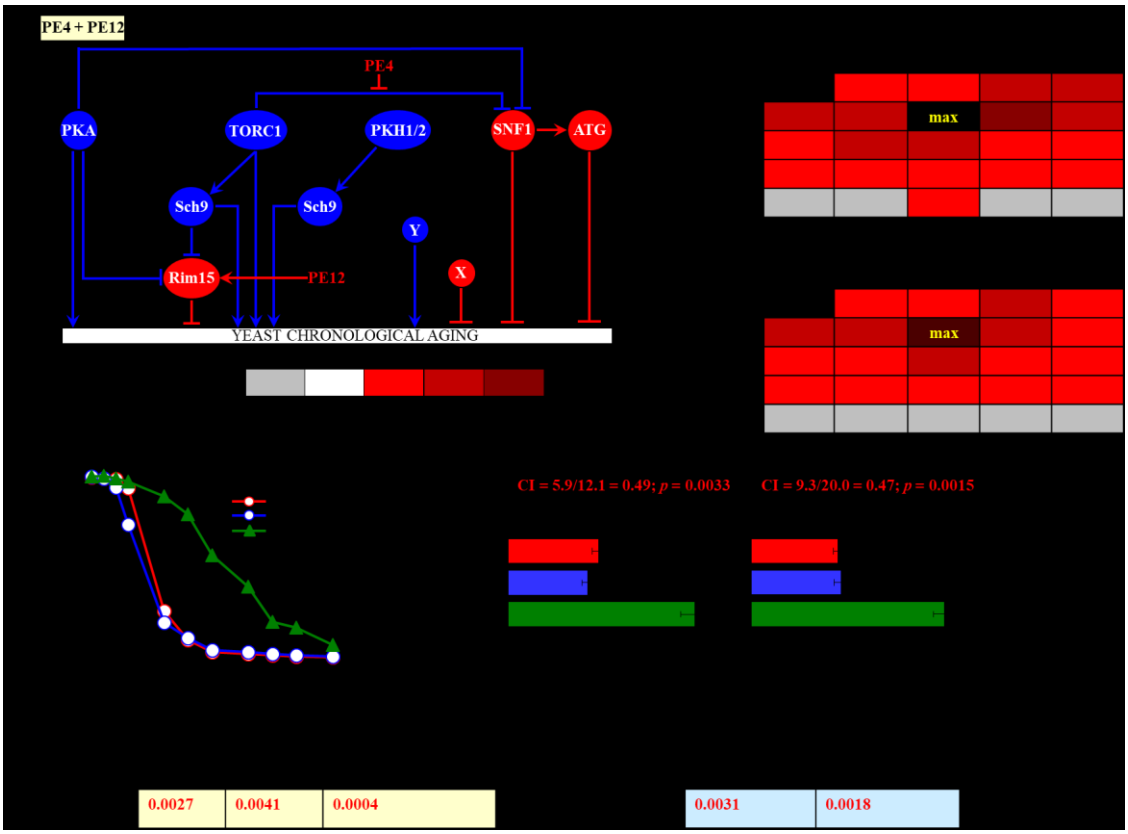

Figure 4.4. The longevity-extending efficiency of a mixture of 0.3% PE4 and 0.1% PE12 statistically significantly exceeds those of PE4 and PE12, which were used at the optimal concentration of 0.5% or 0.1% (respectively). Thus, PE4 and PE12 enhance the longevity-extending efficiency of each other. Hence, according to the HSA model, PE4 and PE12 act in synergy to extend the longevity of chronologically aging yeast. (A) PE4 and PE12 are known to inhibit different pro-aging nodes of the signaling network that controls the rate of yeast chronological aging. PE4 weakens the restraining action of the pro-aging TORC1 pathway on the anti-aging SNF1 pathway, whereas PE12 stimulates the anti-aging protein kinase Rim15. (B, C)

WT cells were grown as described in the legend to Figure 4.2, with PE4 and/or PE12 (at the final concentration of 0.1%, 0.3%, 0.5% or 1.0%) or without a PE. Effects of different concentrations of PE4 and PE12 (added alone or in pairwise combinations) on the mean (B) or maximum (C) CLS of WT cells are shown. The table cell at the intersection of the column for 0.3% PE4 and the row for 0.1% PE12 is marked "max" for a reason described in the legend to Figure 4.2. (D, E) WT cells were cultured as described in the legend to Figure 4.2, with one of the following supplements: 0.5% PE4, 0.1% PE12, or a mixture of 0.3% PE4 and 0.1% PE12. Ethanol was used as a vehicle or for mock treatment, as described in the legend to Figure 4.2. Survival curves (D) and the mean and maximum lifespans (E) of chronologically aging WT cells cultured without a PE (cells were subjected to ethanol-mock treatment), with 0.5% PE4, with 0.1% PE12, or with the mixture of 0.3% PE4 and 0.1% PE12 are shown. Data in D and E are presented as means ± SEM (n = 3; *p < 0.05; **p < 0.01). The CI and p values in E were calculated as described in the legend to Figure 4.2. (F) p Values for different pairs of survival curves of WT cells cultured in the presence of 0.5% PE4, 0.1% PE12, a mixture of 0.3% PE4 and 0.1% PE12, or in the absence of a PE (cells were subjected to ethanol-mock treatment) are shown. Survival curves shown in (D) were compared. The p values are displayed on a yellow or blue color background for the reasons described in the legend to Figure 4.2. Abbreviations: as in the legend to Figure 4.2.

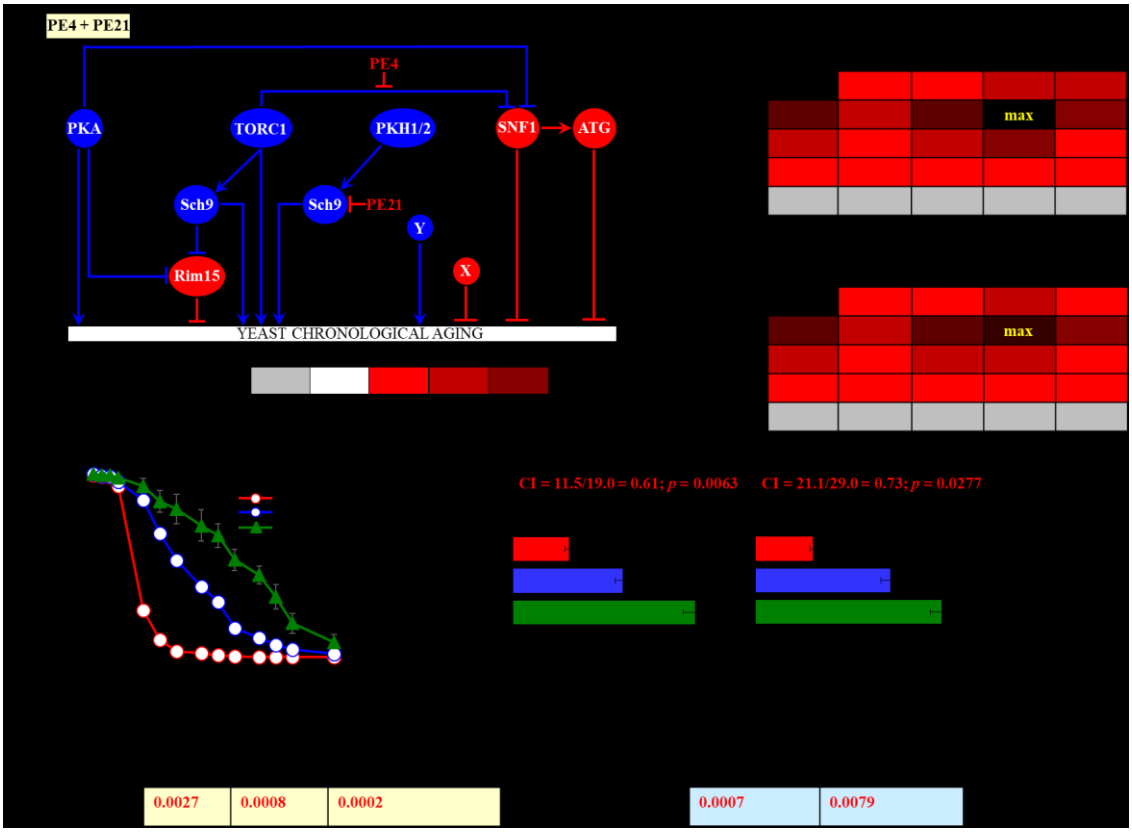

Figure 4.5. The longevity-extending efficiency of a mixture of 0.5% PE4 and 0.1% PE21 statistically significantly exceeds those of PE4 and PE21, which were used at the optimal concentration of 0.5% or 0.1% (respectively). Thus, PE4 and PE21 enhance the longevity-

extending efficiency of each other. Hence, according to the HSA model, PE4 and PE21 act in synergy to extend the longevity of chronologically aging yeast. (A) PE4 and PE21 are known to inhibit different pro-aging nodes of the signaling network that controls the rate of yeast chronological aging. PE4 weakens the restraining action of the pro-aging TORC1 pathway on the anti-aging SNF1 pathway, whereas PE21 mitigates a form of the pro-aging protein kinase Sch9 that is activated by the pro-aging PKH1/2 pathway. (B, C) WT cells were grown as described in the legend to Figure 4.2, with PE4 and/or PE21 (at the final concentration of 0.1%, 0.3%, 0.5% or 1.0%) or without a PE. Effects of different concentrations of PE4 and PE21 (added alone or in pairwise combinations) on the mean (B) or maximum (C) CLS of WT cells are shown. The table cell at the intersection of the column for 0.5% PE4 and the row for 0.1% PE21 is marked "max" for a reason described in the legend to Figure 4.2. (D, E) WT cells were cultured as described in the legend to Figure 4.2, with one of the following supplements: 0.5% PE4, 0.1% PE21, or a mixture of 0.5% PE4 and 0.1% PE21. Ethanol was used as a vehicle or for mock treatment, as described in the legend to Figure 4.2. Survival curves (D) and the mean and maximum lifespans (E) of chronologically aging WT cells cultured without a PE (cells were subjected to ethanol-mock treatment), with 0.5% PE4, with 0.1% PE21, or with the mixture of 0.5% PE4 and 0.1% PE21 are shown. Data in D and E are presented as means ± SEM (n = 3; *$p < 0.05$; **$p < 0.01$; ***$p < 0.001$). The CI and p values in E were calculated as described in the legend to Figure 4.2. (F) p Values for different pairs of survival curves of WT cells cultured in the presence of 0.5% PE4, 0.1% PE21, a mixture of 0.5% PE4 and 0.1% PE21, or in the absence of a PE (cells were subjected to ethanol-mock treatment) are shown. Survival curves shown in (D) were compared. The p values are displayed on a yellow or blue color background for the reasons described in the legend to Figure 4.2. Abbreviations: as in the legend to Figure 4.2.

In sum, these findings confirm our hypothesis that mixtures of PE4 with PE5, PE6, PE12 or PE21 slow down yeast chronological aging in a synergistic manner.

4.3.4 A mixture of PE4 and PE8 does not slow down yeast chronological aging in a synergistic manner

PE4 and PE8 have been shown to weaken the restraining action of the pro-aging TORC1 or PKA pathway on the same node (i.e., the anti-aging SNF1 pathway) of the signaling network that controls the rate of yeast chronological aging (Figure 4.1) [477]. We therefore hypothesized that PE4 and PE8 might not act in synergy to delay yeast chronological aging. To test this hypothesis, we cultured WT cells in the synthetic minimal medium initially containing 2% glucose, either without a PE (i.e. cells were subjected to ethanol-mock treatment) or with the following additions: 1) 0.5% PE4 or 0.3% PE8 alone (if PE4 or PE8 was used at this final concentration, it exhibited the highest longevity-extending effect), or 2) a mixture of 0.1%, 0.3%, 0.5% or 1.0% PE4 with 0.1%, 0.3%, 0.5% or 1.0% PE8.

In support of our hypothesis, we found that the longevity-extending efficiency of a mixture of 0.5% PE4 and 0.5% PE8 is not statistically different from those of PE4 and PE8, which were used at the optimal concentration of 0.5% or 0.3% (respectively) (Figure 4.6). The CI values were 1.16 and 1.07 for the mean CLS and the maximum CLS (respectively) when 0.5% PE4 was used as the HSA for the mean CLS and 0.3% PE8 was used as the HSA for the maximum CLS (Figure 4.6).

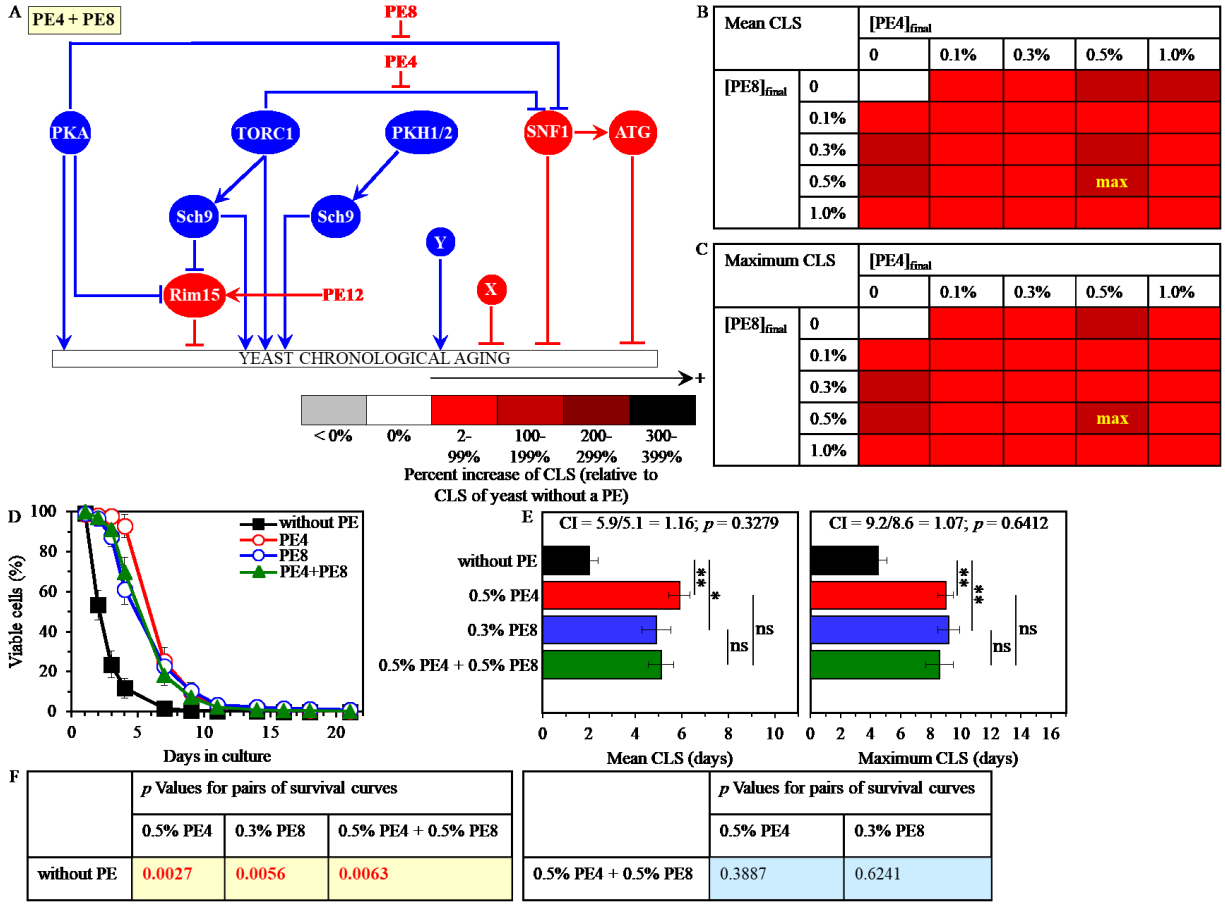

Figure 4.6. The longevity-extending efficiency of a mixture of 0.5% PE4 and 0.5% PE8 is not statistically different from those of PE4 and PE8, which were used at the optimal concentration of 0.5% or 0.3% (respectively). Thus, PE4 and PE8 do not enhance the longevity-extending efficiency of each other. Hence, according to the HSA model, PE4 and PE8 do not act in synergy to extend the longevity of chronologically aging yeast. (A) PE4 and PE8 are known to weaken the restraining action of the pro-aging TORC1 or PKA pathway on the same node (i.e., the anti-aging SNF1 pathway) of the signaling network that controls the rate of yeast chronological aging. (B, C) WT cells were grown as described in the legend to Figure 4.2, with PE4 and/or PE8 (at the final concentration of 0.1%, 0.3%, 0.5% or 1.0%) or without a PE. Effects of different concentrations of PE4 and PE8 (added alone or in pairwise combinations) on the mean (B) or maximum (C) CLS of WT cells are shown. The table cell at the intersection of the column for 0.5% PE4 and the row for 0.5% PE8 is marked "max" for a reason described in the

legend to Figure 4.2. (D, E) WT cells were cultured as described in the legend to Figure 4.2, with one of the following supplements: 0.5% PE4, 0.3% PE8, or a mixture of 0.5% PE4 and 0.5% PE8. Ethanol was used as a vehicle or for mock treatment, as described in the legend to Figure 4.2. Survival curves (D) and the mean and maximum lifespans (E) of chronologically aging WT cells cultured without a PE (cells were subjected to ethanol-mock treatment), with 0.5% PE4, with 0.3% PE8, or with the mixture of 0.5% PE4 and 0.5% PE8 are shown. Data in D and E are presented as means ± SEM (n = 3; *$p < 0.05$; **$p < 0.01$). The CI and p values in E were calculated as described in the legend to Figure 4.2. (F) p Values for different pairs of survival curves of WT cells cultured in the presence of 0.5% PE4, 0.3% PE8, a mixture of 0.5% PE4 and 0.5% PE8, or in the absence of a PE (cells were subjected to ethanol-mock treatment) are shown. Survival curves shown in (D) were compared. Abbreviations: as in the legend to Figure 4.2.

4.3.5 Pairwise combinations of PE5 and PE6, PE5 and PE8, PE5 and PE12, and PE5 and PE21 delay yeast chronological aging in a synergistic fashion

As we have already mentioned, PE5, PE6, PE8, PE12 and PE21 are known to affect different nodes, edges and modules of the signaling network that controls the rate of yeast chronological aging (Figure 4.1) [477]. We, therefore, put forward the hypothesis that pairwise combinations of PE5 and PE6, PE5 and PE8, PE5 and PE12, and PE5 and PE21 may synergistically extend the longevity of chronologically aging yeast. To test this hypothesis, WT cells were cultured in the synthetic minimal medium initially containing 2% glucose, either without a PE (i.e. cells were subjected to ethanol-mock treatment) or with the following additions: 1) PE5, PE6, PE8, PE12 or PE21 alone (each being used at the final concentration of 0.1%, 0.3%, 0.5% or 1.0%, see below), or 2) a pairwise combination of 0.1%, 0.3%, 0.5% or 1.0% PE5 and PE6, PE8, PE12 or PE21 (each being used at the final concentration of 0.1%, 0.3%, 0.5% or 1.0%).

We found that the longevity-extending efficiencies of the following pairwise combinations of aging-delaying PEs are statistically significantly higher than that of a PE component of the pair which was used as the HSA if added alone at the concentration exhibiting the highest aging-delaying effect: 1) a pairwise combination of 0.3% PE5 and 0.3% PE6 as compared to 0.5% PE5 (which was used as the HSA for both the mean and maximum CLS) (Figure 4.7), 2) a pairwise combination of 0.1% PE5 and 0.1% PE8 as compared to 0.5% PE5 (which was considered as the HSA for the mean CLS) or 0.3% PE8 (which was considered as the HSA for the maximum CLS) (Figure 4.8), 3) a pairwise combination of 0.1% PE5 and 0.1% PE12 as compared to 0.5% PE5 (which was used as the HSA for the mean CLS) or 0.1% PE12 (which was used as the HSA for the maximum CLS) (Figure 4.9), and 4) a pairwise combination of 0.1% PE5 and 0.1% PE21 as

compared to 0.1% PE21 (which was used as the HSA for both the mean and maximum CLS) (Figure 4.10).

These findings confirm our hypothesis that pairwise combinations of PE5 and PE6, PE5 and PE8, PE5 and PE12, and PE5 and PE21 synergistically extend the longevity of chronologically aging yeast.

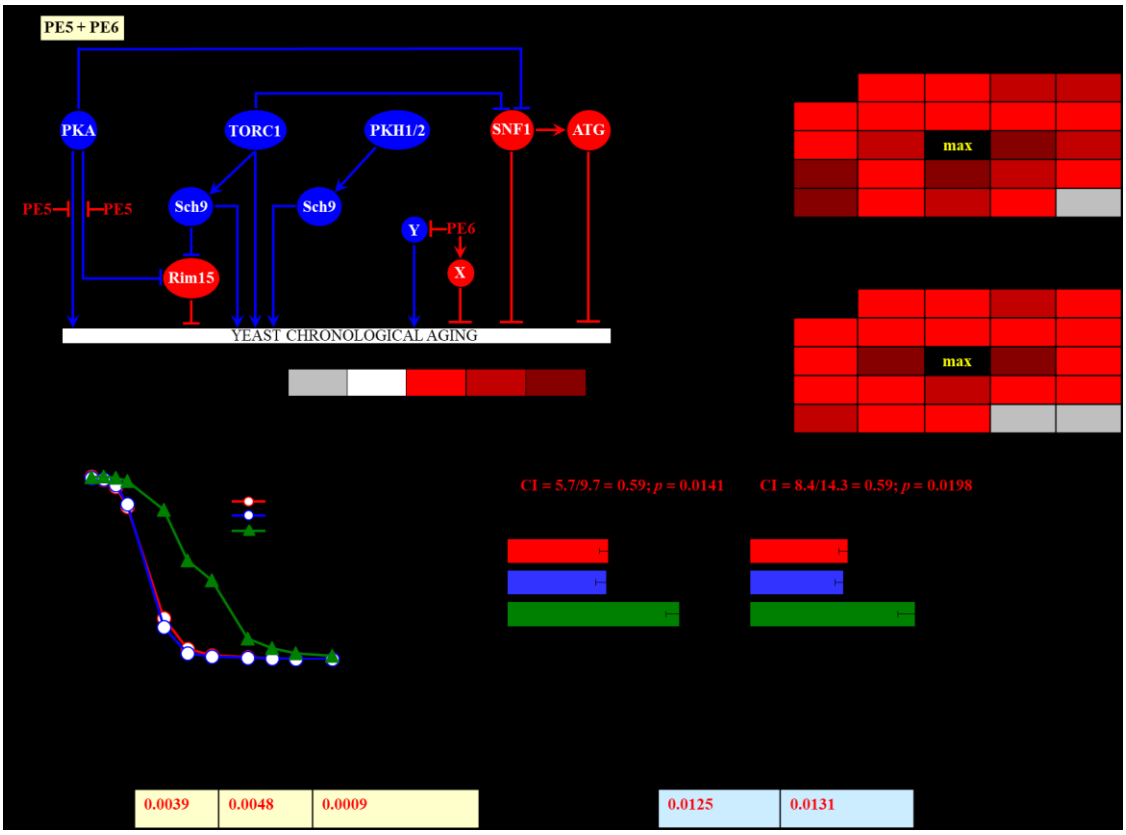

Figure 4.7. The longevity-extending efficiency of a mixture of 0.3% PE5 and 0.3% PE6 statistically significantly exceeds those of PE5 and PE6, which were used at the optimal concentration of 0.5% or 1.0% (respectively). Thus, PE5 and PE6 enhance the longevity-extending efficiency of each other. Hence, according to the highest single agent (HSA) model, PE5 and PE6 act in synergy to extend the longevity of chronologically aging yeast. (A) PE5 and PE6 are known to regulate different nodes of the signaling network that controls the rate of yeast chronological aging. PE5 mitigates two different branches of the pro-aging PKA pathway, whereas PE6 modulates a presently unknown pro-aging or anti-aging node that may be integrated into this signaling network. (B, C) WT cells were grown in the synthetic minimal YNB medium initially containing 2% glucose, with PE5 and/or PE6 (at the final concentration of 0.1%, 0.3%, 0.5% or 1.0%) or without a PE. Effects of different concentrations of PE5 and PE6 (added alone or in pairwise combinations) on the mean (B) or maximum (C) CLS of WT cells are shown. The table cell at the intersection of the column for 0.3% PE5 and the row for 0.3% PE6 is marked "max" because the mixture of 0.3% PE5 and 0.3% PE6 exhibits the highest extending effect on the mean and maximum lifespans of chronologically aging WT cells. (D, E) WT cells were cultured in the synthetic minimal YNB medium initially containing 2% glucose and one of the

following supplements: 0.5% PE5, 1.0% PE6, or a mixture of 0.3% PE5 and 0.3% PE6. In the cultures supplemented with PE5 and/or PE6, ethanol was used as a vehicle at the final concentration of 2.5%. In the same experiment, WT cells were also subjected to ethanol-mock treatment by being cultured in the synthetic minimal YNB medium, initially containing 2% glucose and 2.5% ethanol. Survival curves (D) and the mean and maximum lifespans (E) of chronologically aging WT cells cultured without a PE (cells were subjected to ethanol-mock treatment), with 0.5% PE5, with 1.0% PE6, or with the mixture of 0.3% PE5 and 0.3% PE6 are shown. Data in D and E are presented as means ± SEM (n = 3; *$p < 0.05$; **$p < 0.01$). The CI values in E were calculated as follows: CI = $CLS_{PE5}/CLS_{PE5+PE6}$ for both the mean and maximum CLS; the significance of a synergistic effect (i.e., CI < 1) is provided as the p value of the two-tailed t test for comparing the effect of a PE combination (i.e., $CLS_{PE5+PE6}$) to that of the HSA (i.e., CLS_{PE5} for both the mean and maximum CLS). (F) *p* Values for different pairs of survival curves of WT cells cultured in the presence of 0.5% PE5, 1.0% PE6, a mixture of 0.3% PE5 and 0.3% PE6, or in the absence of a PE (cells were subjected to ethanol-mock treatment) are shown. Survival curves shown in (D) were compared. Two survival curves were considered statistically different if the *p* value was less than 0.05. The *p* values for comparing pairs of survival curves using the logrank test were calculated as described in Materials and Methods. The *p* values displayed on a yellow color background indicate that 0.5% PE5, 1.0% PE6, and the mixture of 0.3% PE5 and 0.3% PE6 significantly extend the CLS of WT cells. The *p* values displayed on a blue color background indicate that the CLS-extending efficiency of the mixture of 0.3% PE5 and 0.3% PE6 significantly exceeds that of 0.5% PE5 or 1.0% PE6. Abbreviations: as in the legend to Figure 4.2.

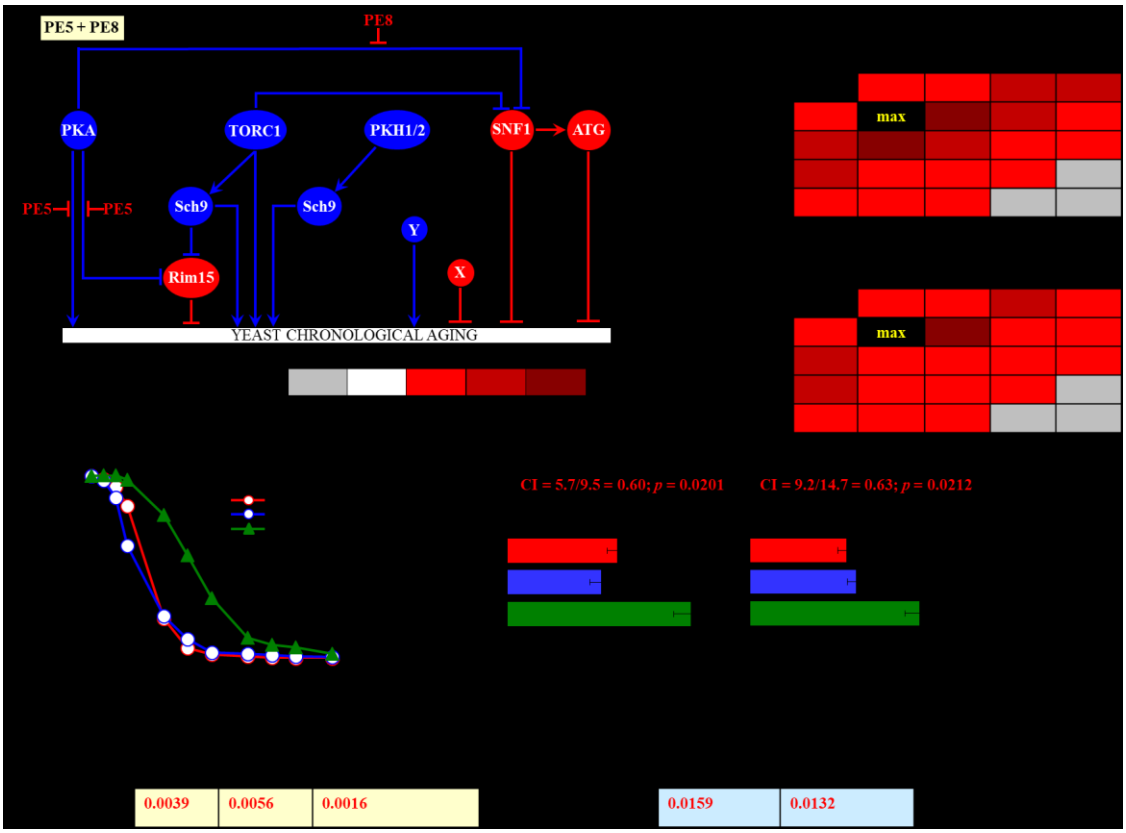

Figure 4.8. The longevity-extending efficiency of a mixture of 0.1% PE5 and 0.1% PE8 statistically significantly exceeds those of PE5 and PE8, which were used at the optimal concentration of 0.5% or 0.3% (respectively). Thus, PE5 and PE8 enhance the longevity-extending efficiency of each other. Hence, according to the HSA model, PE5 and PE8 act in synergy to extend the longevity of chronologically aging yeast. (A) PE5 and PE8 are known to inhibit different pro-aging nodes of the signaling network that controls the rate of yeast chronological aging. PE5 mitigates two different branches of the pro-aging PKA pathway, whereas PE8 weakens the restraining action of this pathway on the anti-aging SNF1 pathway. (B, C) WT cells were grown as described in the legend to Figure 4.2, with PE5 and/or PE8 (at the final concentration of 0.1%, 0.3%, 0.5% or 1.0%) or without a PE. Effects of different concentrations of PE5 and PE8 (added alone or in pairwise combinations) on the mean (B) or maximum (C) CLS of WT cells are shown. The table cell at the intersection of the column for 0.1% PE5 and the row for 0.1% PE8 is marked "max" for a reason described in the legend to Figure 4.2. (D, E) WT cells were cultured as described in the legend to Figure 4.2, with one of the following supplements: 0.5% PE5, 0.3% PE8, or a mixture of 0.1% PE5 and 0.1% PE8. Ethanol was used as a vehicle or for mock treatment, as described in the legend to Figure 4.2. Survival curves (D) and the mean and maximum lifespans (E) of chronologically aging WT cells cultured without a PE (cells were subjected to ethanol-mock treatment), with 0.5% PE5, with 0.3% PE8, or with the mixture of 0.1% PE5 and 0.1% PE8 are shown. Data in D and E are presented as means ± SEM (n = 3; $*p < 0.05$; $**p < 0.01$). The CI and *p* values in E were calculated as described in the legend to Figure 4.2. (F) *p* Values for different pairs of survival curves of WT cells cultured in the presence of 0.5% PE5, 0.3% PE8, a mixture of 0.1% PE5 and 0.1% PE8, or in the absence of a PE (cells were subjected to ethanol-mock treatment) are shown. Survival curves shown in (D) were compared. The *p* values are displayed on a yellow or blue color background for the reasons described in the legend to Figure 4.2. Abbreviations: as in the legend to Figure 4.2.

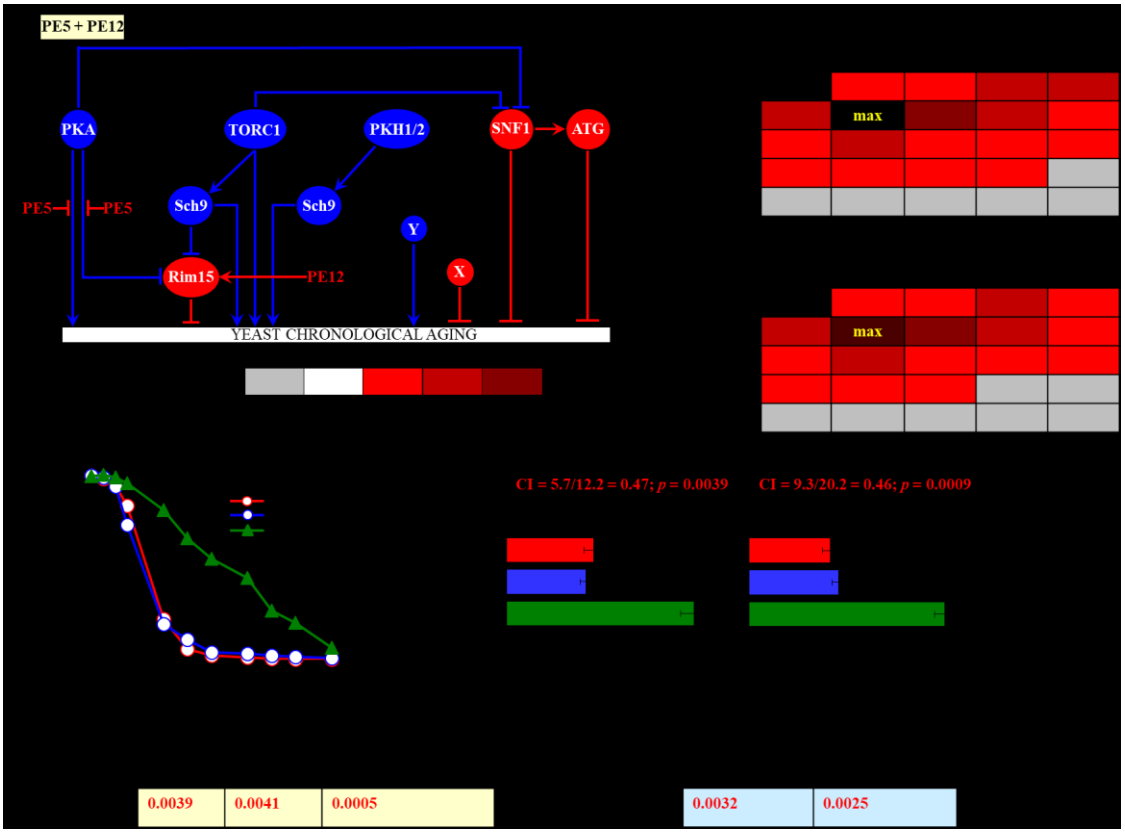

Figure 4.9. The longevity-extending efficiency of a mixture of 0.1% PE5 and 0.1% PE12 statistically significantly exceeds those of PE5 and PE12, which were used at the optimal concentration of 0.5% or 0.1% (respectively). Thus, PE5 and PE12 enhance the longevity-extending efficiency of each other. Hence, according to the highest single agent (HSA) model, PE5 and PE12 act in synergy to extend the longevity of chronologically aging yeast. (A) PE5 and PE12 are known to regulate different nodes of the signaling network that controls the rate of yeast chronological aging. PE5 mitigates two different branches of the pro-aging PKA pathway, whereas PE12 stimulates the anti-aging protein kinase Rim15. (B, C) WT cells were grown in the synthetic minimal YNB medium initially containing 2% glucose, with PE5 and/or PE12 (at the final concentration of 0.1%, 0.3%, 0.5% or 1.0%) or without a PE. Effects of different concentrations of PE5 and PE12 (added alone or in pairwise combinations) on the mean (B) or maximum (C) CLS of WT cells are shown. The table cell at the intersection of the column for 0.1% PE5 and the row for 0.1% PE12 is marked "max" because the mixture of 0.1% PE5 and 0.1% PE12 exhibits the highest extending effect on the mean and maximum lifespans of chronologically aging WT cells. (D, E) WT cells were cultured in the synthetic minimal YNB medium initially containing 2% glucose and one of the following supplements: 0.5% PE5, 0.1% PE12, or a mixture of 0.1% PE5 and 0.1% PE12. In the cultures supplemented with PE5 and/or PE12, ethanol was used as a vehicle at the final concentration of 2.5%. In the same experiment, WT cells were also subjected to ethanol-mock treatment by being cultured in the synthetic minimal YNB medium, initially containing 2% glucose and 2.5% ethanol. Survival curves (D) and the mean and maximum lifespans (E) of chronologically aging WT cells cultured without a PE (cells were subjected to ethanol-mock treatment), with 0.5% PE5, with 0.1% PE12, or with the mixture of 0.1% PE5 and 0.1% PE12 are shown. Data in D and E are presented as means ± SEM (n = 3; $*p < 0.05$; $**p < 0.01$; $***p < 0.001$). The CI values in E were calculated as follows: $CI = CLS_{PE5}/CLS_{PE5+PE12}$ for

the mean CLS and CI = $CL_{SPE12}/CLS_{PE5+PE12}$ for the maximum CLS; the significance of a synergistic effect (i.e., CI < 1) is provided as the *p* value of the two-tailed *t* test for comparing the effect of a PE combination (i.e., $CLS_{PE5+PE12}$) to that of the HSA (i.e., CLS_{PE5} for the mean CLS and CLS_{PE12} for the maximum CLS). (F) *p* Values for different pairs of survival curves of WT cells cultured in the presence of 0.5% PE5, 0.1% PE12, a mixture of 0.1% PE5 and 0.1% PE12, or in the absence of a PE (cells were subjected to ethanol-mock treatment) are shown. Survival curves shown in (D) were compared. Two survival curves were considered statistically different if the *p* value was less than 0.05. The *p* values for comparing pairs of survival curves using the logrank test were calculated as described in Materials and Methods. The *p* values displayed on a yellow color background indicate that 0.5% PE5, 0.1% PE12, and the mixture of 0.1% PE5 and 0.1% PE12 significantly extend the CLS of WT cells. The *p* values displayed on a blue color background indicate that the CLS-extending efficiency of the mixture of 0.1% PE5 and 0.1% PE12 significantly exceeds that of 0.5% PE5 or 0.1% PE12. Abbreviations: as in the legend to Figure 4.2.

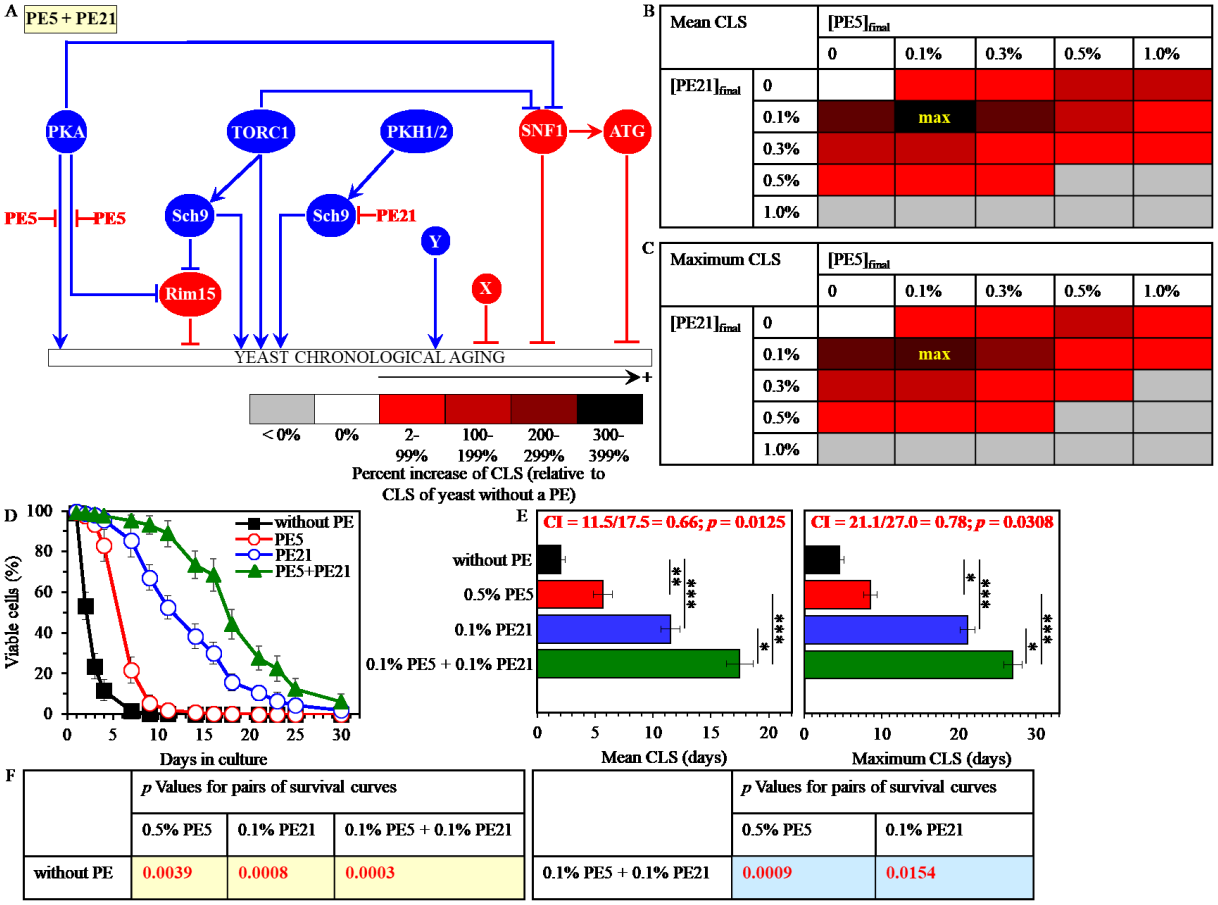

Figure 4.10. The longevity-extending efficiency of a mixture of 0.1% PE5 and 0.1% PE21 statistically significantly exceeds those of PE5 and PE21, which were used at the optimal concentration of 0.5% or 0.1% (respectively). Thus, PE5 and PE21 enhance the longevity-extending efficiency of each other. Hence, according to the HSA model, PE5 and PE21 act in synergy to extend the longevity of chronologically aging yeast. (A) PE5 and PE21 are known

to inhibit different pro-aging nodes of the signaling network that controls the rate of yeast chronological aging. PE5 mitigates two different branches of the pro-aging PKA pathway, whereas PE21 mitigates a form of the pro-aging protein kinase Sch9 that is activated by the pro-aging PKH1/2 pathway. (B, C) WT cells were grown as described in the legend to Figure 4.2, with PE5 and/or PE21 (at the final concentration of 0.1%, 0.3%, 0.5% or 1.0%) or without a PE. Effects of different concentrations of PE5 and PE21 (added alone or in pairwise combinations) on the mean (B) or maximum (C) CLS of WT cells are shown. The table cell at the intersection of the column for 0.1% PE5 and the row for 0.1% PE21 is marked "max" for a reason described in the legend to Figure 4.2. (D, E) WT cells were cultured as described in the legend to Figure 4.2, with one of the following supplements: 0.5% PE5, 0.1% PE21, or a mixture of 0.1% PE5 and 0.1% PE21. Ethanol was used as a vehicle or for mock treatment, as described in the legend to Figure 4.2. Survival curves (D) and the mean and maximum lifespans (E) of chronologically aging WT cells cultured without a PE (cells were subjected to ethanol-mock treatment), with 0.5% PE5, with 0.1% PE21, or with the mixture of 0.1% PE5 and 0.1% PE21 are shown. Data in D and E are presented as means ± SEM (n = 3; $*p < 0.05$; $**p < 0.01$; $***p < 0.001$). The CI and p values in E were calculated as described in the legend to Figure 4.2. (F) p Values for different pairs of survival curves of WT cells cultured in the presence of 0.5% PE5, 0.1% PE21, a mixture of 0.1% PE5 and 0.1% PE21, or in the absence of a PE (cells were subjected to ethanol-mock treatment) are shown. Survival curves shown in (D) were compared. The p values are displayed on a yellow or blue color background for the reasons described in the legend to Figure 1. Abbreviations: as in the legend to Figure 4.2.

4.3.6 Mixtures of PE6 and PE8, PE6 and PE12, and PE6 and PE21 synergistically extend the longevity of chronologically aging yeast

Because PE6, PE8, PE12 and PE21 are known to affect different nodes, edges and modules of the signaling network that controls the rate of yeast chronological aging (Figure 4.1) [477], we hypothesized that mixtures of PE6 with PE8, PE12 or PE21 may have synergistic effects on the efficiency of aging delay. To test this hypothesis, we cultured WT cells in the synthetic minimal medium initially containing 2% glucose, either without a PE (i.e. cells were subjected to ethanol-mock treatment) or with the following additions: 1) PE6, PE8, PE12 or PE21 alone (each being used at the final concentration of 0.1%, 0.3% or 1.0%, see below), or 2) a mixture of 0.1%, 0.3%, 0.5% or 1.0% PE6 with PE8, PE12 or PE21 (each being used at the final concentration of 0.1%, 0.3%, 0.5% or 1.0%).

We found that the longevity-extending efficiencies of the following mixtures of aging-delaying PEs are statistically significantly greater than that of a PE component of the mixture which was considered as the HSA if used alone at the concentration having the maximum aging-delaying effect: 1) a mixture of 0.3% PE6 and 0.3% PE8 as compared to 1.0% PE6 (which was considered as the HSA for the mean CLS) or 0.3% PE8 (which was considered as the HSA for the

maximum CLS) (Figure 4.11), 2) a mixture of 0.3% PE6 and 0.1% PE12 as compared to 1.0% PE6 (which was used as the HSA for the mean CLS) or 0.1% PE12 (which was used as the HSA for the maximum CLS) (Figure 4.12), and 3) a mixture of 0.1% PE6 and 0.1% PE21 as compared to 0.1% PE21 (which was considered as the HSA for both the mean and maximum CLS) (Figure 4.13).

Thus, in support of our hypothesis, mixtures of PE6 with PE8, PE12 or PE21 delay yeast chronological aging in a synergistic fashion.

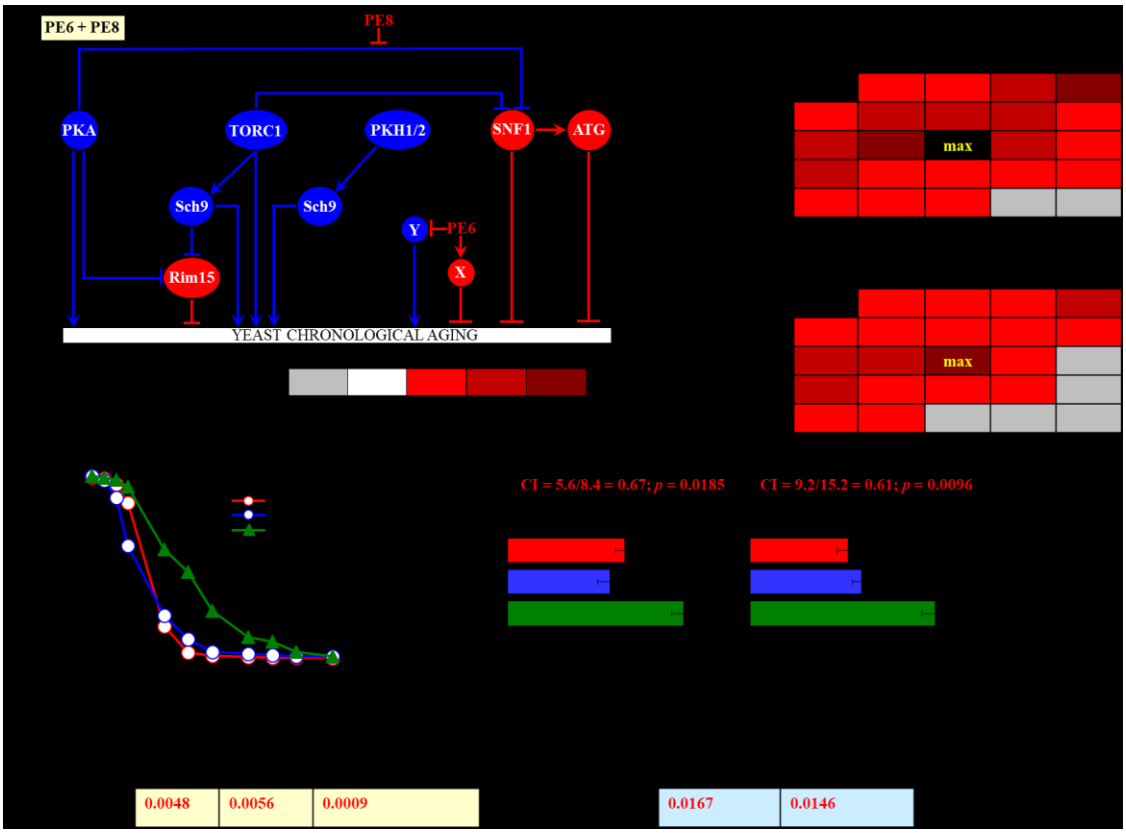

Figure 4.11. The longevity-extending efficiency of a mixture of 0.3% PE6 and 0.3% PE8 statistically significantly exceeds those of PE6 and PE8, which were used at the optimal concentration of 1.0% or 0.3% (respectively). Thus, PE6 and PE8 enhance the longevity-extending efficiency of each other. Hence, according to the highest single agent (HSA) model, PE6 and PE8 act in synergy to extend the longevity of chronologically aging yeast. (A) PE6 and PE8 are known to regulate different nodes of the signaling network that controls the rate of yeast chronological aging. PE8 weakens the restraining action of the pro-aging PKA pathway on

the anti-aging SNF1 pathway, whereas PE6 modulates a presently unknown pro-aging or anti-aging node that may be integrated into this signaling network. (B, C) WT cells were grown in the synthetic minimal YNB medium initially containing 2% glucose, with PE6 and/or PE8 (at the final concentration of 0.1%, 0.3%, 0.5% or 1.0%) or without a PE. Effects of different concentrations of PE6 and PE8 (added alone or in pairwise combinations) on the mean (B) or maximum (C) CLS of WT cells are shown. The table cell at the intersection of the column for 0.3% PE6 and the row for 0.3% PE8 is marked "max" because the mixture of 0.3% PE6 and 0.3% PE8 exhibits the highest extending effect on the mean and maximum lifespans of chronologically aging WT cells. (D, E) WT cells were cultured in the synthetic minimal YNB medium initially containing 2% glucose and one of the following supplements: 1.0% PE6, 0.3% PE8, or a mixture of 0.3% PE6 and 0.3% PE8. In the cultures supplemented with PE6 and/or PE8, ethanol was used as a vehicle at the final concentration of 2.5%. In the same experiment, WT cells were also subjected to ethanol-mock treatment by being cultured in the synthetic minimal YNB medium, initially containing 2% glucose and 2.5% ethanol. Survival curves (D) and the mean and maximum lifespans (E) of chronologically aging WT cells cultured without a PE (cells were subjected to ethanol-mock treatment), with 1.0% PE6, with 0.3% PE8, or with the mixture of 0.3% PE6 and 0.3% PE8 are shown. Data in D and E are presented as means ± SEM (n = 3; $*p < 0.05$; $**p < 0.01$). The CI values in E were calculated as follows: $CI = CLS_{PE6}/CLS_{PE6+PE8}$ for the mean CLS and $CI = CLS_{PE8}/CLS_{PE6+PE8}$ for the maximum CLS; the significance of a synergistic effect (i.e., $CI < 1$) is provided as the p value of the two-tailed t test for comparing the effect of a PE combination (i.e., $CLS_{PE6+PE8}$) to that of the HSA (i.e., CLS_{PE6} for the mean CLS and CLS_{PE8} for the maximum CLS). (F) *p* Values for different pairs of survival curves of WT cells cultured in the presence of 1.0% PE6, 0.3% PE8, a mixture of 0.3% PE6 and 0.3% PE8, or in the absence of a PE (cells were subjected to ethanol-mock treatment) are shown. Survival curves shown in (D) were compared. Two survival curves were considered statistically different if the *p* value was less than 0.05. The *p* values for comparing pairs of survival curves using the logrank test were calculated as described in Materials and Methods. The *p* values displayed on a yellow color background indicate that 1.0% PE6, 0.3% PE8, and the mixture of 0.3% PE6 and 0.3% PE8 significantly extend the CLS of WT cells. The *p* values displayed on a blue color background indicate that the CLS-extending efficiency of the mixture of 0.3% PE6 and 0.3% PE8 significantly exceeds that of 1.0% PE6 or 0.3% PE8. Abbreviations: as in the legend to Figure 4.2.

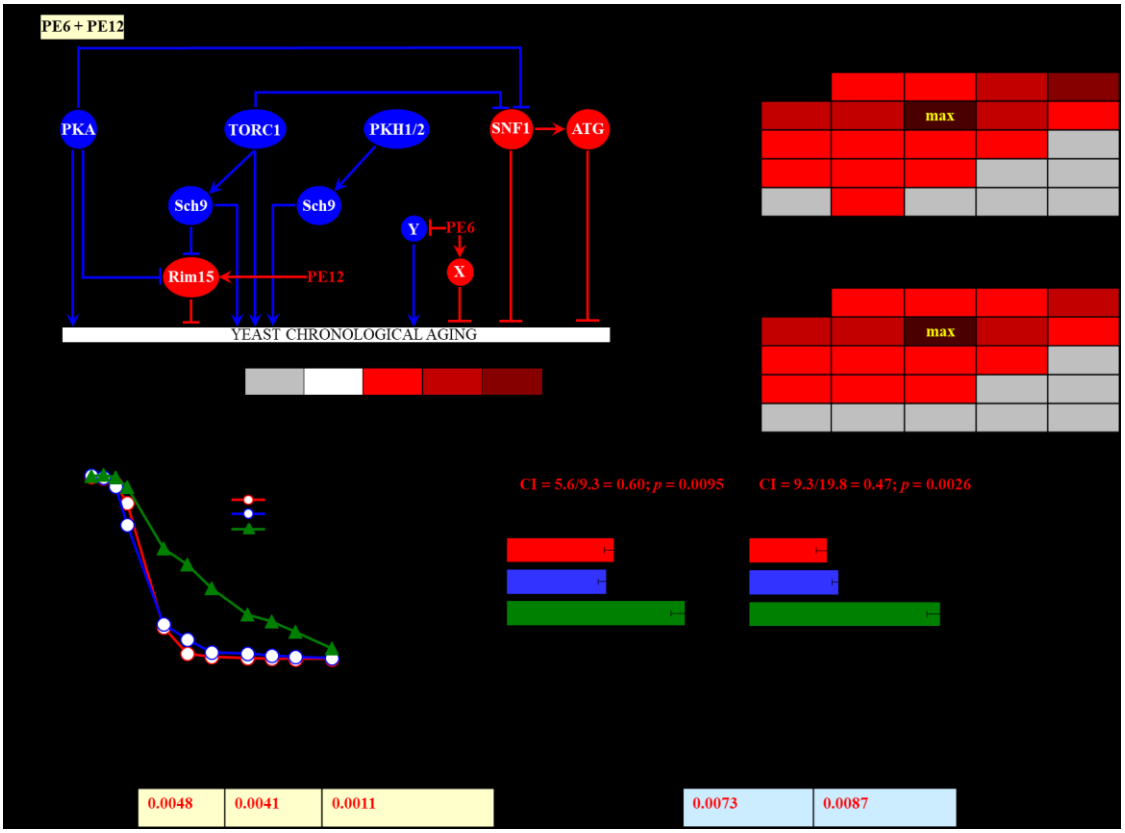

Figure 4.12. The longevity-extending efficiency of a mixture of 0.3% PE6 and 0.1% PE12 statistically significantly exceeds those of PE6 and PE12, which were used at the optimal concentration of 1.0% or 0.1% (respectively). Thus, PE6 and PE12 enhance the longevity-extending efficiency of each other. Hence, according to the HSA model, PE6 and PE12 act in synergy to extend the longevity of chronologically aging yeast. (A) PE6 and PE12 are known to regulate different nodes of the signaling network that controls the rate of yeast chronological aging. PE12 stimulates the anti-aging protein kinase Rim15 assimilated into this signaling network, whereas PE6 modulates a presently unknown pro-aging or anti-aging node that may be integrated into this network. (B, C) WT cells were grown as described in the legend to Figure 4.2, with PE6 and/or PE12 (at the final concentration of 0.1%, 0.3%, 0.5% or 1.0%) or without a PE. Effects of different concentrations of PE6 and PE12 (added alone or in pairwise combinations) on the mean (B) or maximum (C) CLS of WT cells are shown. The table cell at the intersection of the column for 0.3% PE6 and the row for 0.1% PE12 is marked "max" for a reason described in the legend to Figure 4.2. (D, E) WT cells were cultured as described in the legend to Figure 4.2, with one of the following supplements: 1.0% PE6, 0.1% PE12, or a mixture of 0.3% PE6 and 0.1% PE12. Ethanol was used as a vehicle or for mock treatment, as described in the legend to Figure 4.2. Survival curves (D) and the mean and maximum lifespans (E) of chronologically aging WT cells cultured without a PE (cells were subjected to ethanol-mock treatment), with 1.0% PE6, with 0.1% PE12, or with the mixture of 0.3% PE6 and 0.1% PE12 are shown. Data in D and E are presented as means ± SEM (n = 3; *$p < 0.05$; **$p < 0.01$). The CI and p values in E were calculated as described in the legend to Figure 4.2. (F) p Values for different pairs of survival curves of WT cells cultured in the presence of 1.0% PE6, 0.1% PE12, a mixture of 0.3% PE6 and 0.1% PE12, or in the absence of a PE (cells were subjected to ethanol-mock treatment) are shown. Survival curves shown in (D) were compared. The p values displayed on a yellow color background indicate that

1.0% PE6, 0.1% PE12, and the mixture of 0.3% PE6 and 0.1% PE12 significantly extend the CLS of WT cells. The *p* values are displayed on a yellow or blue color background for the reasons described in the legend to Figure 1. Abbreviations: as in the legend to Figure 4.2.

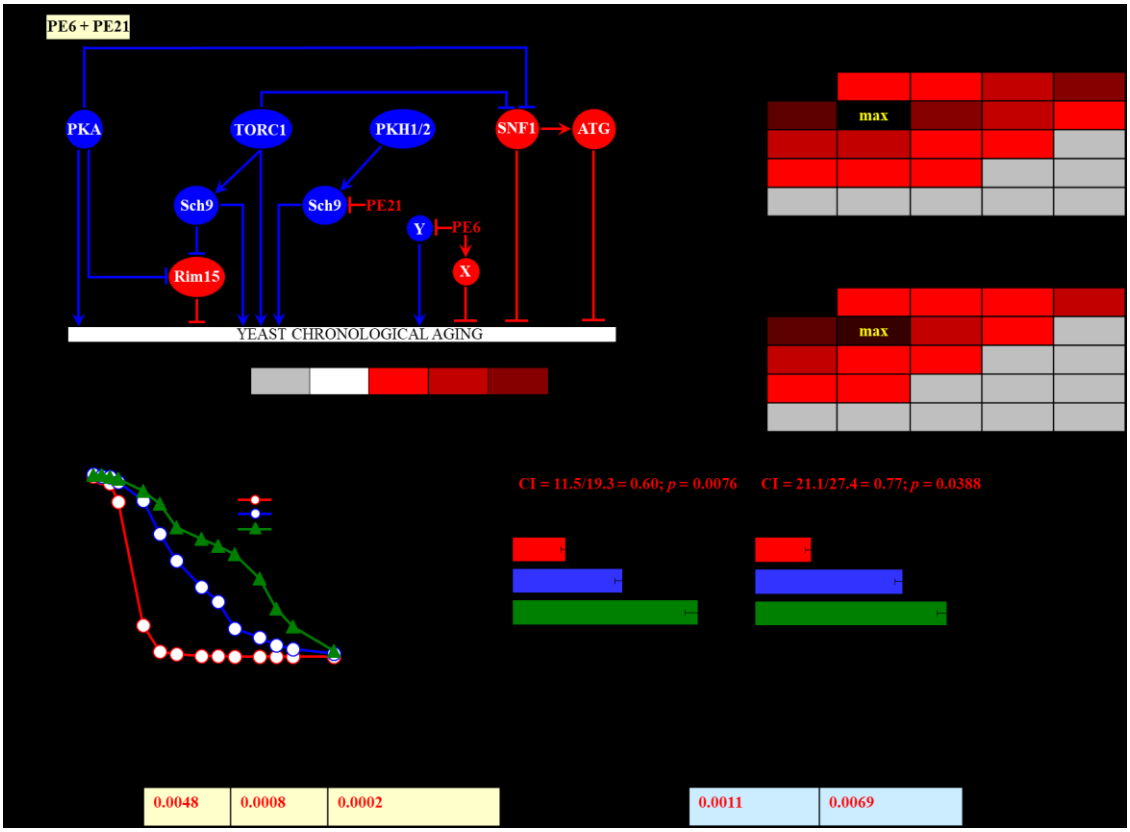

Figure 4.13. The longevity-extending efficiency of a mixture of 0.1% PE6 and 0.1% PE21 statistically significantly exceeds those of PE6 and PE21, which were used at the optimal concentration of 1.0% or 0.1% (respectively). Thus, PE6 and PE21 enhance the longevity-extending efficiency of each other. Hence, according to the highest single agent (HSA) model, PE6 and PE21 act in synergy to extend the longevity of chronologically aging yeast. (A) PE6 and PE21 are known to regulate different nodes of the signaling network that controls the rate of yeast chronological aging. PE21 mitigates a form of the pro-aging protein kinase Sch9 that is activated by the pro-aging PKH1/2 pathway, whereas PE6 modulates a presently unknown pro-aging or anti-aging node that may be integrated into this signaling network. (B, C) WT cells were grown in the synthetic minimal YNB medium initially containing 2% glucose, with PE6 and/or PE21 (at the final concentration of 0.1%, 0.3%, 0.5% or 1.0%) or without a PE. Effects of different concentrations of PE6 and PE21 (added alone or in pairwise combinations) on the mean (B) or maximum (C) CLS of WT cells are shown. The table cell at the intersection of the column for 0.1% PE6 and the row for 0.1% PE21 is marked "max" because the mixture of 0.1% PE6 and 0.1% PE21 exhibits the highest extending effect on the mean and maximum lifespans of chronologically aging WT cells. (D, E) WT cells were cultured in the synthetic minimal YNB medium initially containing 2% glucose and one of the following supplements: 1.0% PE6, 0.1% PE21, or a mixture of 0.1% PE6 and 0.1% PE21. In the cultures supplemented with PE6 and/or PE21, ethanol was used as a vehicle at the final concentration of 2.5%. In the same experiment, WT cells were also subjected to ethanol-mock treatment by being cultured in the synthetic minimal YNB medium,

initially containing 2% glucose and 2.5% ethanol. Survival curves (D) and the mean and maximum lifespans (E) of chronologically aging WT cells cultured without a PE (cells were subjected to ethanol-mock treatment), with 1.0% PE6, with 0.1% PE21, or with the mixture of 0.1% PE6 and 0.1% PE21 are shown. Data in D and E are presented as means ± SEM (n = 3; *$p < 0.05$; **$p < 0.01$; ***$p < 0.001$). The CI values in E were calculated as follows: $CI = CLS_{PE21}/CLS_{PE6+PE21}$ for both the mean and maximum CLS; the significance of a synergistic effect (i.e., CI < 1) is provided as the *p* value of the two-tailed *t* test for comparing the effect of a PE combination (i.e., $CLS_{PE6+PE21}$) to that of the HSA (i.e., CLS_{PE21} for both the mean and maximum CLS). (F) *p* Values for different pairs of survival curves of WT cells cultured in the presence of 1.0% PE6, 0.1% PE21, a mixture of 0.1% PE6 and 0.1% PE21, or in the absence of a PE (cells were subjected to ethanol-mock treatment) are shown. Survival curves shown in (D) were compared. Two survival curves were considered statistically different if the *p* value was less than 0.05. The *p* values for comparing pairs of survival curves using the logrank test were calculated as described in Materials and Methods. The *p* values displayed on a yellow color background indicate that 1.0% PE6, 0.1% PE21, and the mixture of 0.1% PE6 and 0.1% PE21 significantly extend the CLS of WT cells. The *p* values displayed on a blue color background indicate that the CLS-extending efficiency of the mixture of 0.1% PE6 and 0.1% PE21 significantly exceeds that of 1.0% PE6 or 0.1% PE21. Abbreviations: as in the legend to Figure 4.2.

4.3.7 Pairwise combinations of PE8 with PE12 or PE21 synergistically slow down yeast chronological aging

As has been noted above, PE8, PE12 and PE21 modulate different nodes, edges and modules of the signaling network that defines the rate of yeast chronological aging (Figure 4.1) [477]. We therefore put forward the hypothesis that pairwise combinations of PE8 and PE12, and PE8 and PE21 may synergistically prolong the longevity of chronologically aging yeast. To test this hypothesis, WT cells were cultured in the synthetic minimal medium initially containing 2% glucose, either without a PE (i.e. cells were subjected to ethanol-mock treatment) or with the following additions: 1) PE8, PE12 or PE21 alone (each being used at the final concentration of 0.1% or 0.3%, see below), or 2) a pairwise combination of 0.1%, 0.3%, 0.5% or 1.0% PE8 and PE12 or PE21 (each being used at the final concentration of 0.1%, 0.3%, 0.5% or 1.0%).

We found that the longevity-extending efficiencies of the following pairwise combinations of aging-delaying PEs statistically significantly exceed that of a PE component of the pair which was considered as the HSA if added alone at the concentration displaying the highest aging-delaying effect: 1) a pairwise combination of 0.1% PE8 and 0.1% PE12 as compared to 0.1% PE12 (which was considered as the HSA for both the mean and maximum CLS) (Figure 4.14), and 2) a pairwise combination of 0.1% PE8 and 0.1% PE21 as compared to 0.1% PE21 (which was used as the HSA for both the mean and maximum CLS) (Figure 4.15).

In sum, these findings confirm our hypothesis that pairwise combinations of PE8 with PE12 or PE21 synergistically prolong the longevity of chronologically aging yeast.

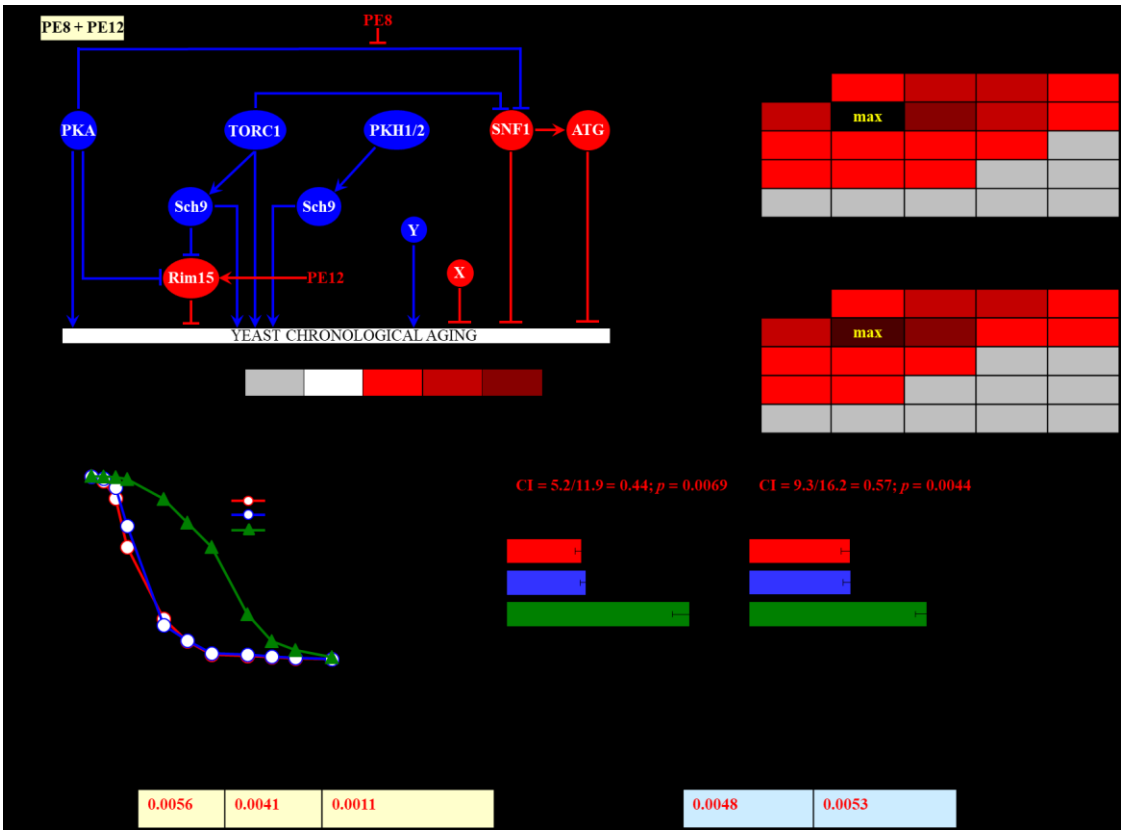

Figure 4.14. The longevity-extending efficiency of a mixture of 0.1% PE8 and 0.1% PE12 statistically significantly exceeds those of PE8 and PE12, which were used at the optimal concentration of 0.3% or 0.1% (respectively). Thus, PE8 and PE12 enhance the longevity-extending efficiency of each other. Hence, according to the HSA model, PE8 and PE12 act in synergy to extend the longevity of chronologically aging yeast. (A) PE8 and PE12 are known to regulate different nodes of the signaling network that controls the rate of yeast chronological aging. PE8 weakens the restraining action of the pro-aging PKA pathway on the anti-aging SNF1 pathway, whereas PE12 stimulates the anti-aging protein kinase Rim15 integrated into this signaling network. (B, C) WT cells were grown as described in the legend to Figure 4.2, with PE8 and/or PE12 (at the final concentration of 0.1%, 0.3%, 0.5% or 1.0%) or without a PE. Effects of different concentrations of PE8 and PE12 (added alone or in pairwise combinations) on the mean (B) or maximum (C) CLS of WT cells are shown. The table cell at the intersection of the column for 0.1% PE8 and the row for 0.1% PE12 is marked "max" for a reason described in the legend to Figure 4.2. (D, E) WT cells were cultured as described in the legend to Figure 4.2, with one of the following supplements: 0.3% PE8, 0.1% PE12, or a mixture of 0.1% PE8 and 0.1% PE12. Ethanol was used as a vehicle or for mock treatment, as described in the legend to Figure 4.2. Survival curves (D) and the mean and maximum lifespans (E) of chronologically aging WT cells cultured without a PE (cells were subjected to ethanol-mock treatment), with 0.3% PE8, with 0.1% PE12, or with the mixture of 0.1% PE8 and 0.1% PE12 are shown. Data in D and E are presented as

means ± SEM (n = 3; $**p < 0.01$). The CI and p values in E were calculated as described in the legend to Figure 4.2. (F) p Values for different pairs of survival curves of WT cells cultured in the presence of 0.3% PE8, 0.1% PE12, a mixture of 0.1% PE8 and 0.1% PE12, or in the absence of a PE (cells were subjected to ethanol-mock treatment) are shown. Survival curves shown in (D) were compared. The p values are displayed on a yellow or blue color background for the reasons described in the legend to Figure 4.2. Abbreviations: as in the legend to Figure 4.2.

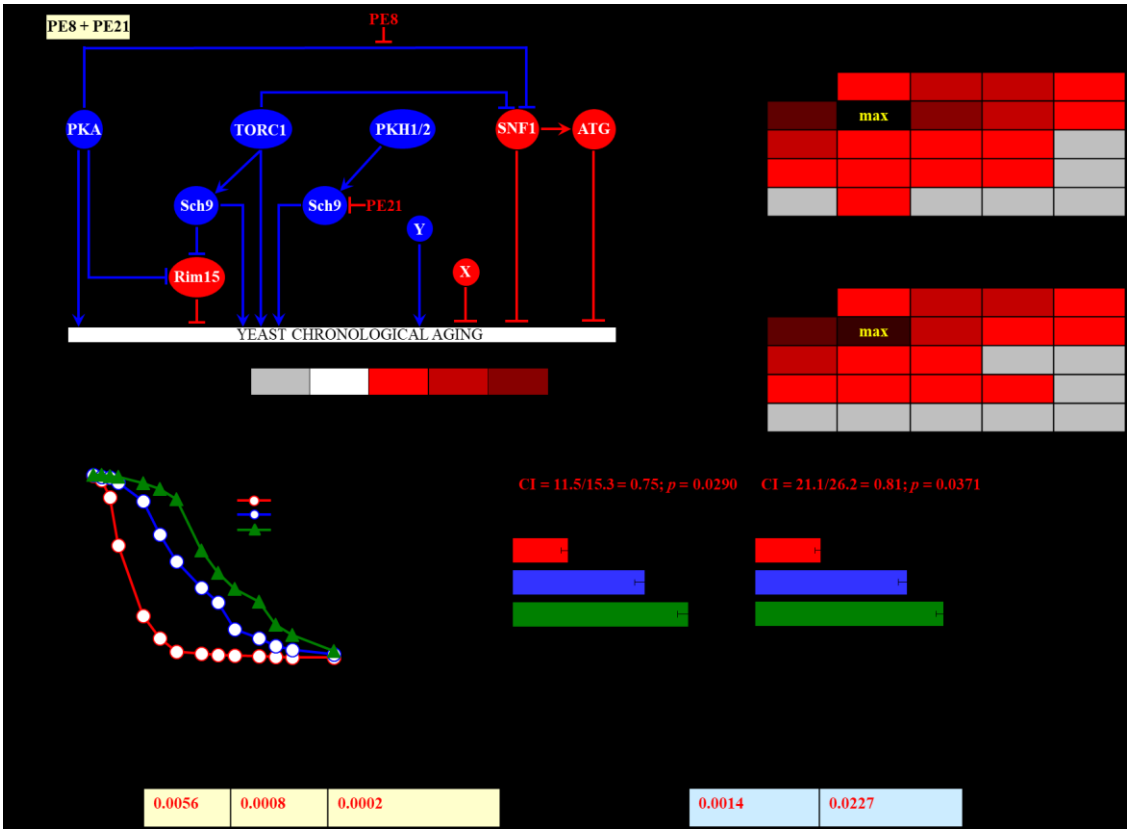

Figure 4.15. The longevity-extending efficiency of a mixture of 0.1% PE8 and 0.1% PE21 statistically significantly exceeds those of PE8 and PE21, which were used at the optimal concentration of 0.3% or 0.1% (respectively). Thus, PE8 and PE21 enhance the longevity-extending efficiency of each other. Hence, according to the highest single agent (HSA) model, PE8 and PE21 act in synergy to extend the longevity of chronologically aging yeast. (A) PE8 and PE21 are known to regulate different nodes of the signaling network that controls the rate of yeast chronological aging. PE8 weakens the restraining action of the pro-aging PKA pathway on the anti-aging SNF1 pathway, whereas PE21 mitigates a form of the pro-aging protein kinase Sch9 that is activated by the pro-aging PKH1/2 pathway. (B, C) WT cells were grown in the synthetic minimal YNB medium initially containing 2% glucose, with PE8 and/or PE21 (at the final concentration of 0.1%, 0.3%, 0.5% or 1.0%) or without a PE. Effects of different concentrations of PE6 and PE21 (added alone or in pairwise combinations) on the mean (B) or maximum (C) CLS of WT cells are shown. The table cell at the intersection of the column for 0.1% PE8 and the row for 0.1% PE21 is marked "max" because the mixture of 0.1% PE8 and 0.1% PE21 exhibits the highest extending effect on the mean and maximum lifespans of chronologically aging WT cells. (D, E) WT cells were cultured in the synthetic minimal YNB medium initially containing 2% glucose and one of the following supplements: 0.3% PE8, 0.1% PE21, or a mixture of 0.1%

PE8 and 0.1% PE21. In the cultures supplemented with PE8 and/or PE21, ethanol was used as a vehicle at the final concentration of 2.5%. In the same experiment, WT cells were also subjected to ethanol-mock treatment by being cultured in the synthetic minimal YNB medium, initially containing 2% glucose and 2.5% ethanol. Survival curves (D) and the mean and maximum lifespans (E) of chronologically aging WT cells cultured without a PE (cells were subjected to ethanol-mock treatment), with 0.3% PE8, with 0.1% PE21, or with the mixture of 0.1% PE8 and 0.1% PE21 are shown. Data in D and E are presented as means ± SEM (n = 3; *$p < 0.05$; **$p < 0.01$; ***$p < 0.001$). The CI values in E were calculated as follows: $CI = CLS_{PE21}/CLS_{PE8+PE21}$ for both the mean and maximum CLS; the significance of a synergistic effect (i.e., CI < 1) is provided as the *p* value of the two-tailed *t* test for comparing the effect of a PE combination (i.e., $CLS_{PE8+PE21}$) to that of the HSA (i.e., CLS_{PE21} for both the mean and maximum CLS). (F) *p* Values for different pairs of survival curves of WT cells cultured in the presence of 0.3% PE8, 0.1% PE21, a mixture of 0.1% PE8 and 0.1% PE21, or in the absence of a PE (cells were subjected to ethanol-mock treatment) are shown. Survival curves shown in (D) were compared. Two survival curves were considered statistically different if the *p* value was less than 0.05. The *p* values for comparing pairs of survival curves using the logrank test were calculated as described in Materials and Methods. The *p* values displayed on a yellow color background indicate that 0.3% PE8, 0.1% PE21, and the mixture of 0.1% PE8 and 0.1% PE21 significantly extend the CLS of WT cells. The *p* values displayed on a blue color background indicate that the CLS-extending efficiency of the mixture of 0.1% PE8 and 0.1% PE21 significantly exceeds that of 0.3% PE8 or 0.1% PE21. Abbreviations: as in the legend to Figure 4.2.

4.3.8 A mixture of PE12 and PE21 slows yeast chronological aging in a synergistic manner

Because PE12 and PE21 are known to affect two different nodes of the signaling network that controls the rate of yeast chronological aging (Figure 4.1) [477], we hypothesized that PE12 and PE21 might not act in synergy to delay yeast chronological aging. To test this hypothesis, we cultured WT cells in the synthetic minimal medium initially containing 2% glucose, either without a PE (i.e. cells were subjected to ethanol-mock treatment) or with the following additions: 1) 0.1% PE12 or 0.1% PE21 alone (if PE12 or PE21 was used at this final concentration, it had the greatest longevity-extending effect), or 2) a mixture of 0.1%, 0.3%, 0.5% or 1.0% PE12 with 0.1%, 0.3%, 0.5% or 1.0% PE21.

In support of our hypothesis, we found that the longevity-extending efficiency of a mixture of 0.1% PE12 and 0.1% PE21 is statistically significantly greater than that of 0.1% PE21 (which was considered as the HSA if used alone at this concentration to attain the maximum aging-delaying effect) (Figure 4.16).

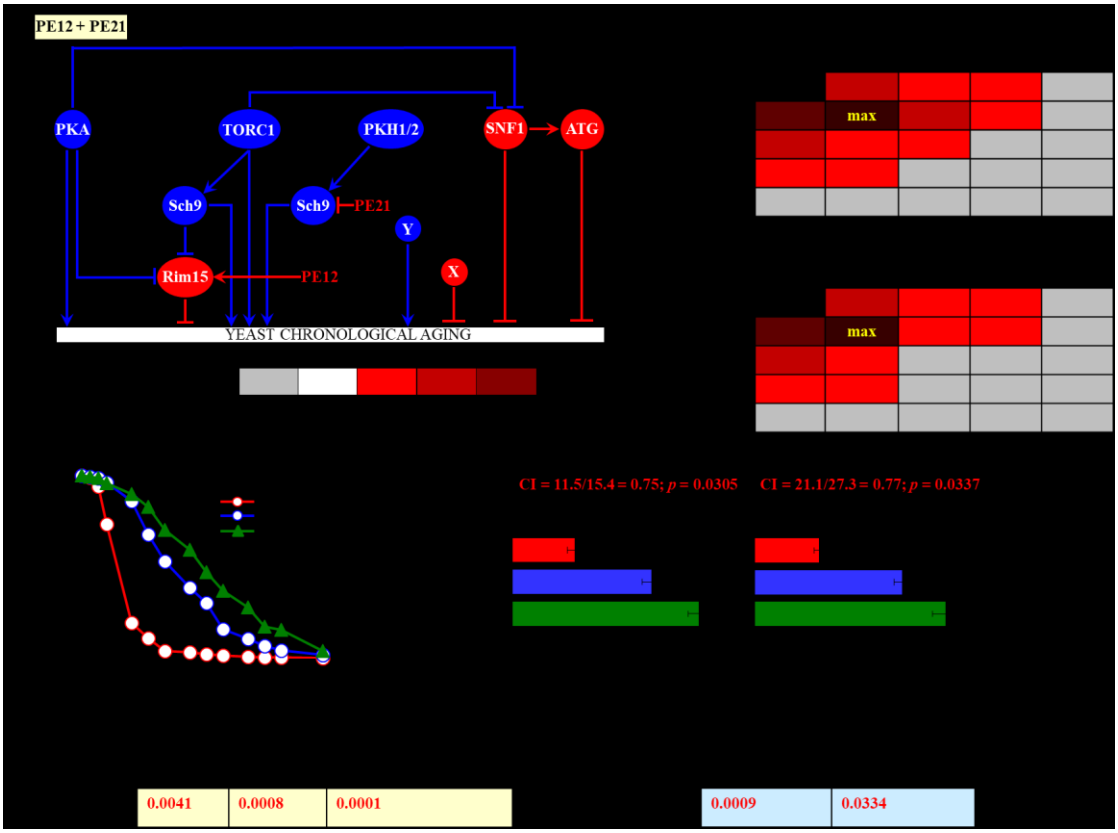

Figure 4.16. The longevity-extending efficiency of a mixture of 0.1% PE12 and 0.1% PE21 statistically significantly exceeds those of PE12 and PE21, each being used at the optimal concentration of 0.1%. Thus, PE12 and PE21 enhance the longevity-extending efficiency of each other. Hence, according to the highest single agent (HSA) model, PE12 and PE21 act in synergy to extend the longevity of chronologically aging yeast. (A) PE12 and PE21 are known to regulate different nodes of the signaling network that controls the rate of yeast chronological aging. PE12 stimulates the anti-aging protein kinase Rim15, whereas PE21 mitigates a form of the pro-aging protein kinase Sch9 that is activated by the pro-aging PKH1/2 pathway. (B, C) WT cells were grown in the synthetic minimal YNB medium initially containing 2% glucose, with PE12 and/or PE21 (at the final concentration of 0.1%, 0.3%, 0.5% or 1.0%) or without a PE. Effects of different concentrations of PE12 and PE21 (added alone or in pairwise combinations) on the mean (B) or maximum (C) CLS of WT cells are shown. The table cell at the intersection of the column for 0.1% PE12 and the row for 0.1% PE21 is marked "max" because the mixture of 0.1% PE12 and 0.1% PE21 exhibits the highest extending effect on the mean and maximum lifespans of chronologically aging WT cells. (D, E) WT cells were cultured in the synthetic minimal YNB medium initially containing 2% glucose and one of the following supplements: 0.1% PE12, 0.1% PE21, or a mixture of 0.1% PE12 and 0.1% PE21. In the cultures supplemented with PE12 and/or PE21, ethanol was used as a vehicle at the final concentration of 2.5%. In the same experiment, WT cells were also subjected to ethanol-mock treatment by being cultured in the synthetic minimal YNB medium, initially containing 2% glucose and 2.5% ethanol. Survival curves (D) and the mean and maximum lifespans (E) of chronologically aging WT cells cultured without a PE (cells were subjected to ethanol-mock treatment), with 0.1% PE12, with 0.1% PE21, or with the mixture of 0.1% PE12 and 0.1% PE21 are shown. Data in D and E are presented as means ± SEM (n = 3; *p < 0.05; **p < 0.01; ***p < 0.001). The CI values in E were calculated as follows: CI =

$CLS_{PE21}/CLS_{PE12+PE21}$ for both the mean and maximum CLS; the significance of a synergistic effect (i.e. CI < 1) is provided as the *p* value of the two-tailed *t* test for comparing the effect of a PE combination (i.e., $CLS_{PE12+PE21}$) to that of the HSA (i.e., CLS_{PE21} for both the mean and maximum CLS). (F) *p* Values for different pairs of survival curves of WT cells cultured in the presence of 0.1% PE12, 0.1% PE21, a mixture of 0.1% PE12 and 0.1% PE21, or in the absence of a PE (cells were subjected to ethanol-mock treatment) are shown. Survival curves shown in (D) were compared. Two survival curves were considered statistically different if the *p* value was less than 0.05. The *p* values for comparing pairs of survival curves using the logrank test were calculated as described in Materials and Methods. The *p* values displayed on a yellow color background indicate that 0.1% PE12, 0.1% PE21, and the mixture of 0.1% PE12 and 0.1% PE21 significantly extend the CLS of WT cells. The *p* values displayed on a blue color background indicate that the CLS-extending efficiency of the mixture of 0.1% PE12 and 0.1% PE21 significantly exceeds that of 0.1% PE12 or 0.1% PE21. Abbreviations: as in the legend to Figure 4.2.

4.3.9 Pairwise combinations of spermidine with PE4, PE5, PE6, PE8, PE12 or PE21 have synergistic effects on the extent of the aging delay

Spermidine has been shown to delay yeast chronological aging by activating the anti-aging ATG1 pathway (Figure 4.1) [17, 83, 84, 111, 479]. Neither PE4, PE5, PE6, PE8, PE12 nor PE21 affects the ATG1 node of the signaling network that defines the rate of yeast chronological aging (Figure 4.1) [477]. We, therefore, hypothesized that pairwise combinations of spermidine with PE4, PE5, PE6, PE8, PE12 or PE21 might exhibit synergistic effects on the extent of yeast chronological aging delay. To test this hypothesis, WT cells were cultured in the synthetic minimal medium initially containing 2% glucose, either without a PE (i.e. cells were subjected to ethanol-mock treatment) or with the following additions: 1) PE4, PE5, PE6, PE8, PE12 or PE21 alone (each being used at the final concentration of 0.1%, 0.3%, 0.5% or 1.0%, see below), or 2) a mixture of 50 μM, 100 μM, 200 μM or 500 μM spermidine with PE4, PE5, PE6, PE8, PE12 or PE21 (each being used at the final concentration of 0.1%, 0.3%, 0.5% or 1.0%).

We found that the longevity-extending efficiencies of the following pairwise combinations of spermidine and an aging-delaying PE statistically significantly exceed that of a PE within the pair which was considered as the HSA (i.e. if this PE was used alone at the optimal aging-delaying concentration): 1) a mixture of 0.1% PE4 and 100 μM spermidine as compared to 0.5% PE4 (which was considered as the HSA for both the mean and maximum CLS) (Figure 4.17), 2) a mixture of 0.3% PE5 and 100 μM spermidine as compared to 0.5% PE5 (which was used as the HSA for both the mean and maximum CLS) (Figure 4.18), 3) a mixture of 0.5% PE6 and 100 μM spermidine as compared to 1.0% PE6 (which was considered as the HSA for both the mean and maximum CLS)

(Figure 4.19), 4) a mixture of 0.1% PE8 and 100 μM spermidine as compared to 0.3% PE8 (which was used as the HSA for both the mean and maximum CLS) (Figure 4.20), 5) a mixture of 0.1% PE12 and 100 μM spermidine as compared to 0.1% PE12 (which was considered as the HSA for both the mean and maximum CLS) (Figure 4.21), and 6) a mixture of 0.1% PE21 and 100 μM spermidine as compared to 0.1% PE21 (which was used as the HSA for both the mean and maximum CLS) (Figure 4.22). These findings confirm our hypothesis that pairwise combinations of spermidine with PE4, PE5, PE6, PE8, PE12 or PE21 have synergistic effects on the extent of yeast chronological aging delay.

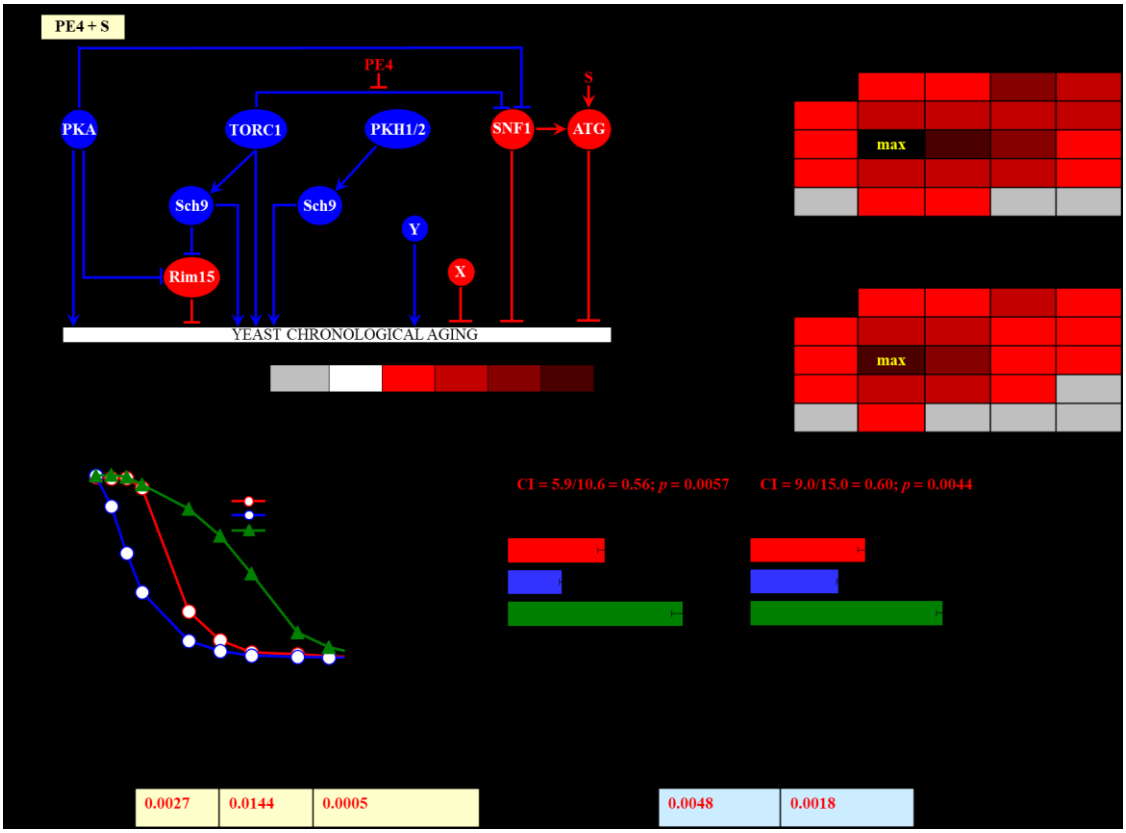

Figure 4.17. The longevity-extending efficiency of a mixture of 0.1% PE4 and 100 μM spermidine (S) statistically significantly exceeds those of PE4 and S, which were used at the optimal concentration of 0.5% or 100 μM (respectively). Thus, PE4 and S enhance the longevity-extending efficiency of each other. Hence, according to the highest single agent (HSA) model, PE4 and S act in synergy to extend the longevity of chronologically aging yeast. (A) PE4 and S are known to regulate different nodes of the signaling network that controls the rate of yeast chronological aging. PE4 weakens the restraining action of the pro-aging TORC1 pathway on the anti-aging SNF1 pathway, whereas S stimulates the anti-aging ATG pathway. (B, C) WT cells were grown in the synthetic minimal YNB medium initially containing 2% glucose, with PE4 (at the final concentration of 0.1%, 0.3%, 0.5% or 1.0%) and/or S (at the final concentration of 50

μM, 100 μM, 200 μM or 500 μM), or without a PE and S. Effects of different concentrations of PE4 and S (added alone or in pairwise combinations) on the mean (B) or maximum (C) CLS of WT cells are shown. The table cell at the intersection of the column for 0.1% PE4 and the row for 100 μM S is marked "max" because the mixture of 0.1% PE4 and 100 μM S exhibits the highest extending effect on the mean and maximum lifespans of chronologically aging WT cells. (D, E) WT cells were cultured in the synthetic minimal YNB medium initially containing 2% glucose and one of the following supplements: 0.5% PE4, 100 μM S, or a mixture of 0.1% PE4 and 100 μM S. In the cultures supplemented with PE4 and/or S, ethanol was used as a vehicle at the final concentration of 2.5%. In the same experiment, WT cells were also subjected to ethanol-mock treatment by being cultured in the synthetic minimal YNB medium, initially containing 2% glucose and 2.5% ethanol. Survival curves (D) and the mean and maximum lifespans (E) of chronologically aging WT cells cultured without a PE and S (cells were subjected to ethanol-mock treatment), with 0.5% PE4, with 100 μM S, or with the mixture of 0.1% PE4 and 100 μM S are shown. Data in D and E are presented as means ± SEM (n = 3; $*p < 0.05$; $**p < 0.01$; $***p < 0.001$). The CI values in E were calculated as follows: $CI = CLS_{PE4}/CLS_{PE4+S}$ for both the mean and maximum CLS; the significance of a synergistic effect (i.e. CI < 1) is provided as the *p* value of the two-tailed *t* test for comparing the effect of a PE combination (i.e., CLS_{PE3+S}) to that of the HSA (i.e., CLS_{PE4} for both the mean and maximum CLS). (F) *p* Values for different pairs of survival curves of WT cells cultured in the presence of 0.5% PE4, 100 μM S, a mixture of 0.1% PE4 and 100 μM S, or in the absence of a PE and S (cells were subjected to ethanol-mock treatment) are shown. Survival curves shown in (D) were compared. Two survival curves were considered statistically different if the *p* value was less than 0.05. The *p* values for comparing pairs of survival curves using the logrank test were calculated as described in Materials and Methods. The *p* values displayed on a yellow color background indicate that 0.5% PE4, 100 μM S, and the mixture of 0.1% PE4 and 100 μM S significantly extend the CLS of WT cells. The *p* values displayed on a blue color background indicate that the CLS-extending efficiency of the mixture of 0.1% PE4 and 100 μM S significantly exceeds that of 0.5% PE4 or 100 μM S. Abbreviations: as in the legend to Figure 4.2.

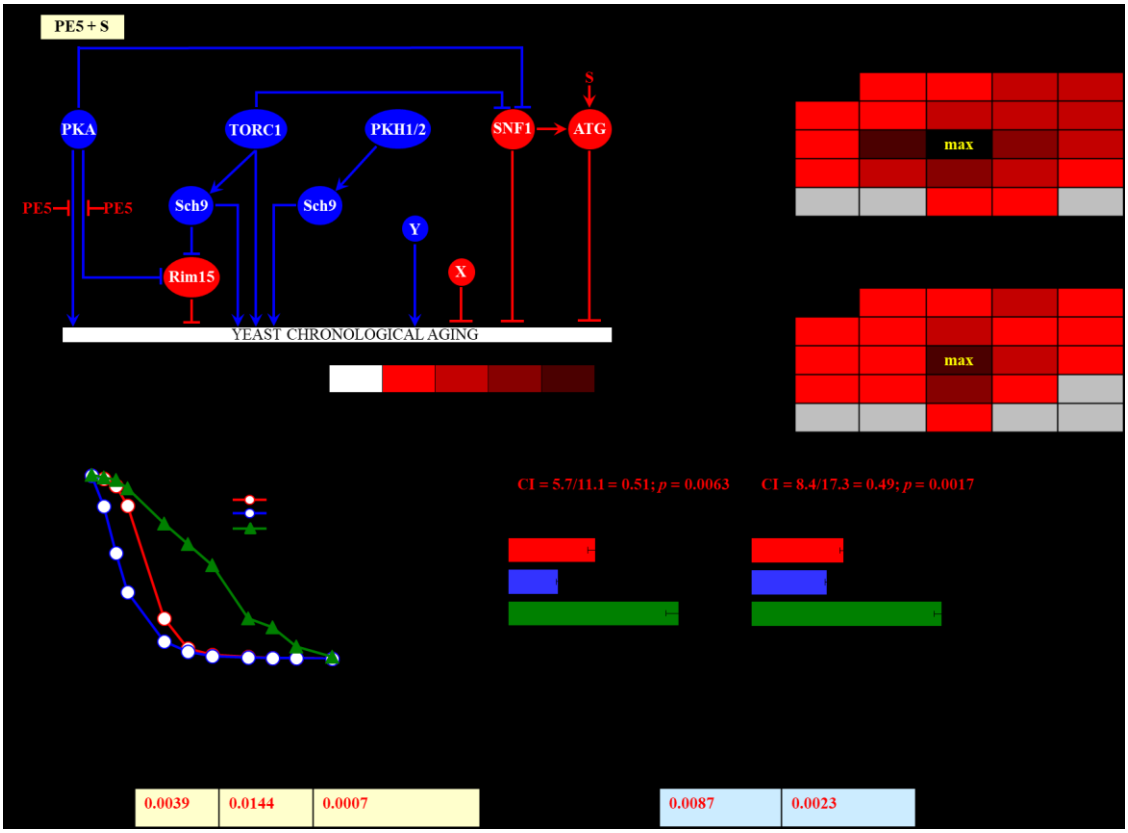

Figure 4.18. The longevity-extending efficiency of a mixture of 0.3% PE5 and 100 μM spermidine (S) statistically significantly exceeds those of PE5 and S, which were used at the optimal concentration of 0.5% or 100 μM (respectively). Thus, PE5 and S enhance the longevity-extending efficiency of each other. Hence, according to the HSA model, PE5 and S act in synergy to extend the longevity of chronologically aging yeast. (A) PE5 and S are known to regulate different nodes of the signaling network that controls the rate of yeast chronological aging. PE5 mitigates two different branches of the pro-aging PKA pathway, whereas S stimulates the anti-aging ATG pathway. (B, C) WT cells were grown as described in the legend to Figure 4.2, with PE5 (at the final concentration of 0.1%, 0.3%, 0.5% or 1.0%) and/or S (at the final concentration of 50 μM, 100 μM, 200 μM or 500 μM), or without a PE and S. Effects of different concentrations of PE5 and S (added alone or in pairwise combinations) on the mean (B) or maximum (C) CLS of WT cells are shown. The table cell at the intersection of the column for 0.3% PE5 and the row for 100 μM S is marked "max" for a reason described in the legend to Figure 4.2. (D, E) WT cells were cultured as described in the legend to Figure 4.2, with one of the following supplements: 0.5% PE5, 100 μM S, or a mixture of 0.3% PE5 and 100 μM S. Ethanol was used as a vehicle or for mock treatment as described in the legend to Figure 4.2. Survival curves (D) and the mean and maximum lifespans (E) of chronologically aging WT cells cultured without a PE and S (cells were subjected to ethanol-mock treatment), with 0.5% PE5, with 100 μM S, or with the mixture of 0.3% PE5 and 100 μM S are shown. Data in D and E are presented as means ± SEM (n = 3; *$p < 0.05$; **$p < 0.01$; ***$p < 0.001$). The CI and p values in E were calculated as described in the legend to Figure 4.2. (F) p Values for different pairs of survival curves of WT cells cultured in the presence of 0.5% PE5, 100 μM S, a mixture of 0.3% PE5 and 100 μM S, or in the absence of a PE and S (cells were subjected to ethanol-mock treatment) are shown. Survival curves shown in (D) were compared. The p values are displayed on a yellow or

blue color background for the reasons described in the legend to Figure 4.2. Abbreviations: as in the legend to Figure 4.2.

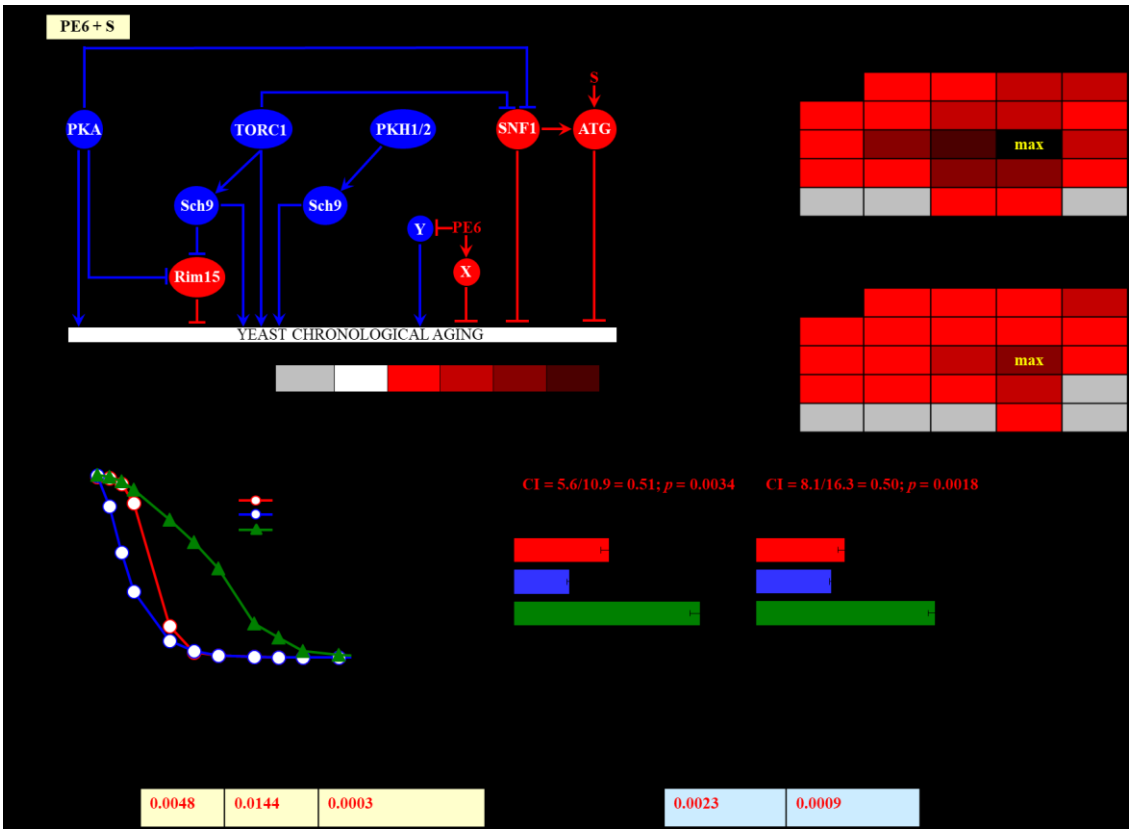

Figure 4.19. The longevity-extending efficiency of a mixture of 0.5% PE6 and 100 μM spermidine (S) statistically significantly exceeds those of PE6 and S, which were used at the optimal concentration of 1.0% or 100 μM (respectively). Thus, PE6 and S enhance the longevity-extending efficiency of each other. Hence, according to the highest single agent (HSA) model, PE6 and S act in synergy to extend the longevity of chronologically aging yeast. (A) PE6 and S are known to regulate different nodes of the signaling network that controls the rate of yeast chronological aging. S stimulates the anti-aging ATG pathway, whereas PE6 modulates a presently unknown pro-aging or anti-aging node that may be integrated into this network. (B, C) WT cells were grown in the synthetic minimal YNB medium initially containing 2% glucose, with PE6 (at the final concentration of 0.1%, 0.3%, 0.5% or 1.0%) and/or S (at the final concentration of 50 μM, 100 μM, 200 μM or 500 μM), or without a PE and S. Effects of different concentrations of PE6 and S (added alone or in pairwise combinations) on the mean (B) or maximum (C) CLS of WT cells are shown. The table cell at the intersection of the column for 0.5% PE6 and the row for 100 μM S is marked "max" because the mixture of 0.5% PE6 and 100 μM S exhibits the highest extending effect on the mean and maximum lifespans of chronologically aging WT cells. (D, E) WT cells were cultured in the synthetic minimal YNB medium initially containing 2% glucose and one of the following supplements: 1.0% PE6, 100 μM S, or a mixture of 0.5% PE6 and 100 μM S. In the cultures supplemented with PE6 and/or S, ethanol was used as a vehicle at the final concentration of 2.5%. In the same experiment, WT cells were also subjected to ethanol-mock

treatment by being cultured in the synthetic minimal YNB medium, initially containing 2% glucose and 2.5% ethanol. Survival curves (D) and the mean and maximum lifespans (E) of chronologically aging WT cells cultured without a PE and S (cells were subjected to ethanol-mock treatment), with 1.0% PE6, with 100 µM S, or with the mixture of 0.5% PE6 and 100 µM S are shown. Data in D and E are presented as means ± SEM (n = 3; *$p < 0.05$; **$p < 0.01$; ***$p < 0.001$). The CI values in E were calculated as follows: $CI = CLS_{PE6}/CLS_{PE6+S}$ for both the mean and maximum CLS; the significance of a synergistic effect (i.e. CI < 1) is provided as the *p* value of the two-tailed *t* test for comparing the effect of a PE combination (i.e., CLS_{PE6+S}) to that of the HSA (i.e., CLS_{PE6} for both the mean and maximum CLS). (F) *p* Values for different pairs of survival curves of WT cells cultured in the presence of 1.0% PE6, 100 µM S, a mixture of 0.5% PE6 and 100 µM S, or in the absence of a PE and S (cells were subjected to ethanol-mock treatment) are shown. Survival curves shown in (D) were compared. Two survival curves were considered statistically different if the *p* value was less than 0.05. The *p* values for comparing pairs of survival curves using the logrank test were calculated as described in Materials and Methods. The *p* values displayed on a yellow color background indicate that 1.0% PE6, 100 µM S, and the mixture of 0.5% PE6 and 100 µM S significantly extend the CLS of WT cells. The *p* values displayed on a blue color background indicate that the CLS-extending efficiency of the mixture of 0.5% PE6 and 100 µM S significantly exceeds that of 1.0% PE6 or 100 µM S. Abbreviations: as in the legend to Figure 4.2.

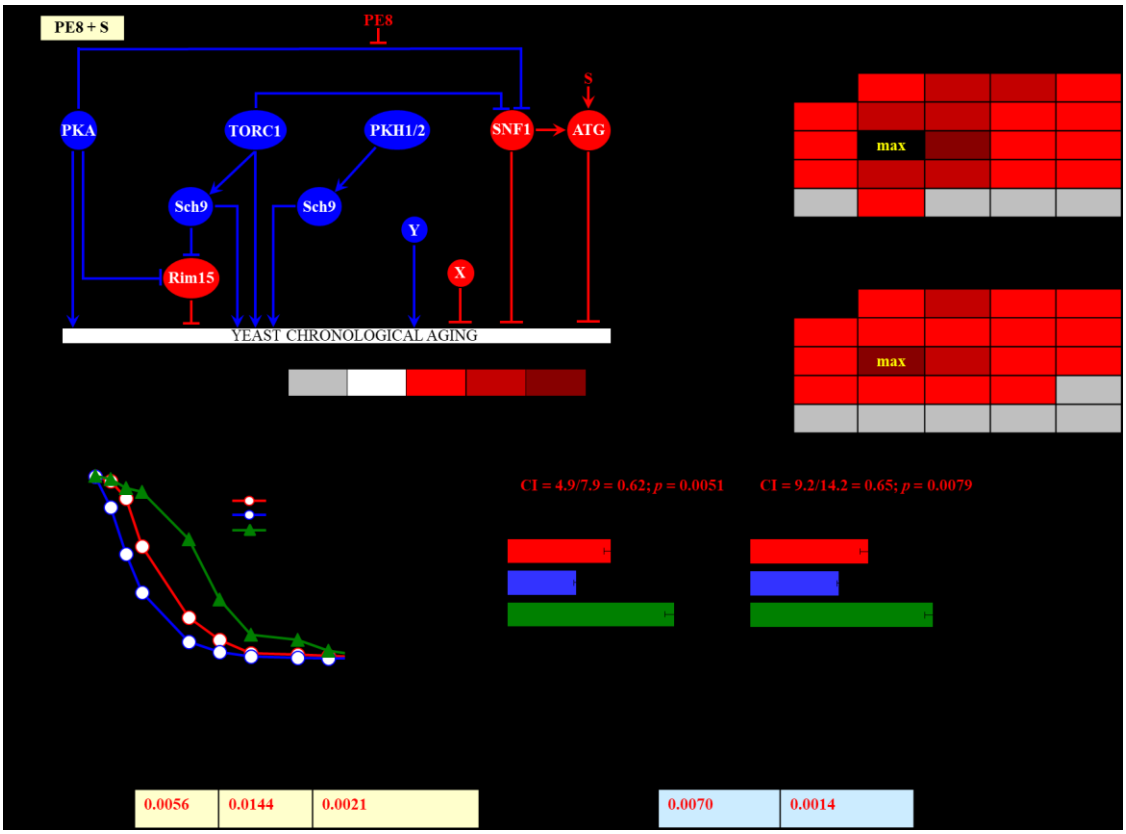

Figure 4.20. The longevity-extending efficiency of a mixture of 0.1% PE8 and 100 µM spermidine (S) statistically significantly exceeds those of PE8 and S, which were used at the

optimal concentration of 0.3% or 100 μM (respectively). Thus, PE8 and S enhance the longevity-extending efficiency of each other. Hence, according to the HSA model, PE8 and S act in synergy to extend the longevity of chronologically aging yeast. (A) PE8 and S are known to regulate different nodes of the signaling network that controls the rate of yeast chronological aging. PE8 weakens the restraining action of the pro-aging PKA pathway on the anti-aging SNF1 pathway, whereas S stimulates the anti-aging ATG pathway. (B, C) WT cells were grown as described in the legend to Figure 4.2, with PE8 (at the final concentration of 0.1%, 0.3%, 0.5% or 1.0%) and/or S (at the final concentration of 50 μM, 100 μM, 200 μM or 500 μM), or without a PE and S. Effects of different concentrations of PE8 and S (added alone or in pairwise combinations) on the mean (B) or maximum (C) CLS of WT cells are shown. The table cell at the intersection of the column for 0.1% PE8 and the row for 100 μM S is marked "max" for a reason described in the legend to Figure 4.2. (D, E) WT cells were cultured as described in the legend to Figure 4.2, with one of the following supplements: 0.3% PE8, 100 μM S, or a mixture of 0.1% PE8 and 100 μM S. Ethanol was used as a vehicle or for mock treatment as described in the legend to Figure 4.2. Survival curves (D) and the mean and maximum lifespans (E) of chronologically aging WT cells cultured without a PE and S (cells were subjected to ethanol-mock treatment), with 0.3% PE8, with 100 μM S, or with the mixture of 0.1% PE8 and 100 μM S are shown. Data in D and E are presented as means ± SEM (n = 3; *$p < 0.05$; **$p < 0.01$). The CI and p values in E were calculated as described in the legend to Figure 4.2. (F) p Values for different pairs of survival curves of WT cells cultured in the presence of 0.3% PE8, 100 μM S, a mixture of 0.1% PE8 and 100 μM S, or in the absence of a PE and S (cells were subjected to ethanol-mock treatment) are shown. Survival curves shown in (D) were compared. The p values are displayed on a yellow or blue color background for the reasons described in the legend to Figure 4.2. Abbreviations: as in the legend to Figure 4.2.

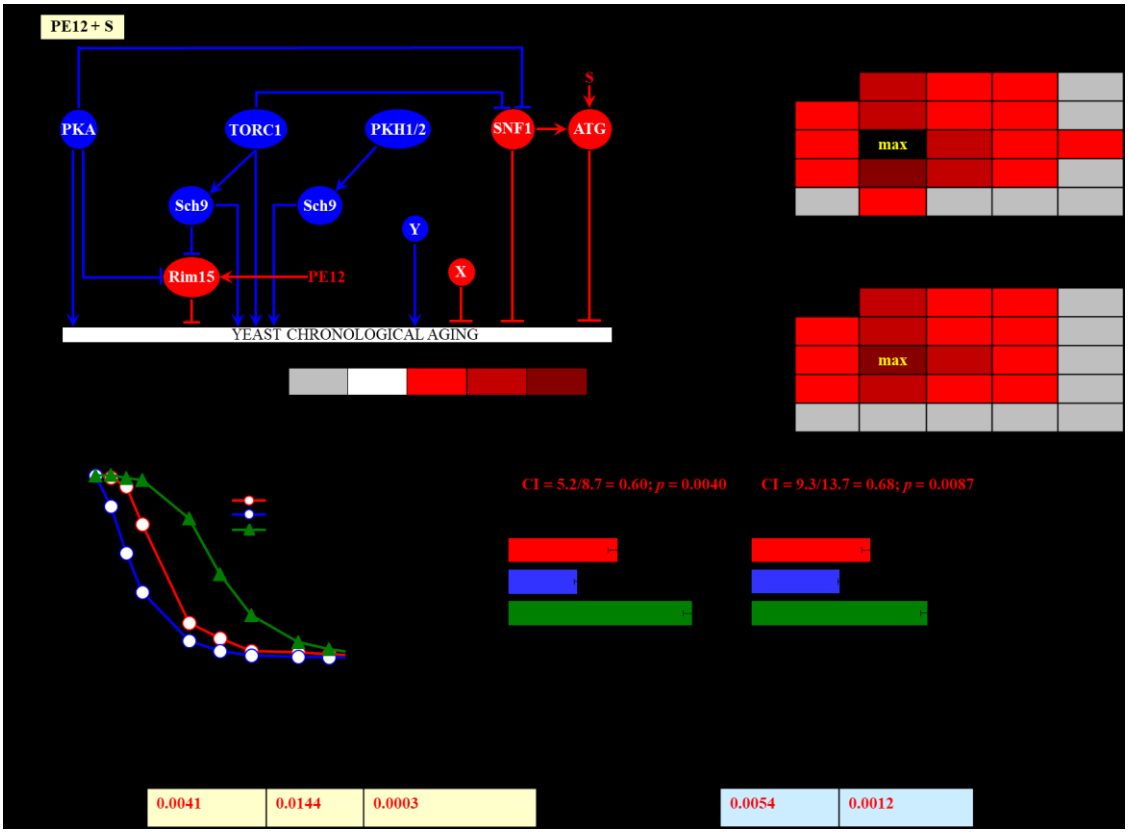

Figure 4.21. The longevity-extending efficiency of a mixture of 0.1% PE12 and 100 μM spermidine (S) statistically significantly exceeds those of PE12 and S, which were used at the optimal concentration of 0.1% or 100 μM (respectively). Thus, PE12 and S enhance the longevity-extending efficiency of each other. Hence, according to the highest single agent (HSA) model, PE12 and S act in synergy to extend the longevity of chronologically aging yeast. (A) PE12 and S are known to regulate different nodes of the signaling network that controls the rate of yeast chronological aging. PE12 activates the anti-aging protein kinase Rim15, whereas S stimulates the anti-aging ATG pathway. (B, C) WT cells were grown in the synthetic minimal YNB medium initially containing 2% glucose, with PE12 (at the final concentration of 0.1%, 0.3%, 0.5% or 1.0%) and/or S (at the final concentration of 50 μM, 100 μM, 200 μM or 500 μM), or without a PE and S. Effects of different concentrations of PE12 and S (added alone or in pairwise combinations) on the mean (B) or maximum (C) CLS of WT cells are shown. The table cell at the intersection of the column for 0.1% PE12 and the row for 100 μM S is marked "max" because the mixture of 0.1% PE12 and 100 μM S exhibits the highest extending effect on the mean and maximum lifespans of chronologically aging WT cells. (D, E) WT cells were cultured in the synthetic minimal YNB medium initially containing 2% glucose and one of the following supplements: 0.1% PE12, 100 μM S, or a mixture of 0.1% PE12 and 100 μM S. In the cultures supplemented with PE12 and/or S, ethanol was used as a vehicle at the final concentration of 2.5%. In the same experiment, WT cells were also subjected to ethanol-mock treatment by being cultured in the synthetic minimal YNB medium, initially containing 2% glucose and 2.5% ethanol. Survival curves (D) and the mean and maximum lifespans (E) of chronologically aging WT cells cultured without a PE and S (cells were subjected to ethanol-mock treatment), with 0.1% PE12, with 100 μM S, or with the mixture of 0.1% PE12 and 100 μM S are shown. Data in D and E are presented as means ± SEM (n = 3; $*p < 0.05$; $**p < 0.01$). The CI values in E were calculated as follows: CI

= CLS_{PE12}/CLS_{PE12+S} for both the mean and maximum CLS; the significance of a synergistic effect (i.e. CI < 1) is provided as the *p* value of the two-tailed *t* test for comparing the effect of a PE combination (i.e., CLS_{PE12+S}) to that of the HSA (i.e., CLS_{PE12} for both the mean and maximum CLS). (F) *p* Values for different pairs of survival curves of WT cells cultured in the presence of 0.1% PE12, 100 μM S, a mixture of 0.1% PE12 and 100 μM S, or in the absence of a PE and S (cells were subjected to ethanol-mock treatment) are shown. Survival curves shown in (D) were compared. Two survival curves were considered statistically different if the *p* value was less than 0.05. The *p* values for comparing pairs of survival curves using the logrank test were calculated as described in Materials and Methods. The *p* values displayed on a yellow color background indicate that 0.1% PE12, 100 μM S, and the mixture of 0.1% PE12 and 100 μM S significantly extend the CLS of WT cells. The *p* values displayed on a blue color background indicate that the CLS-extending efficiency of the mixture of 0.1% PE12 and 100 μM S significantly exceeds that of 0.1% PE12 or 100 μM S. Abbreviations: as in the legend to Figure 4.2.

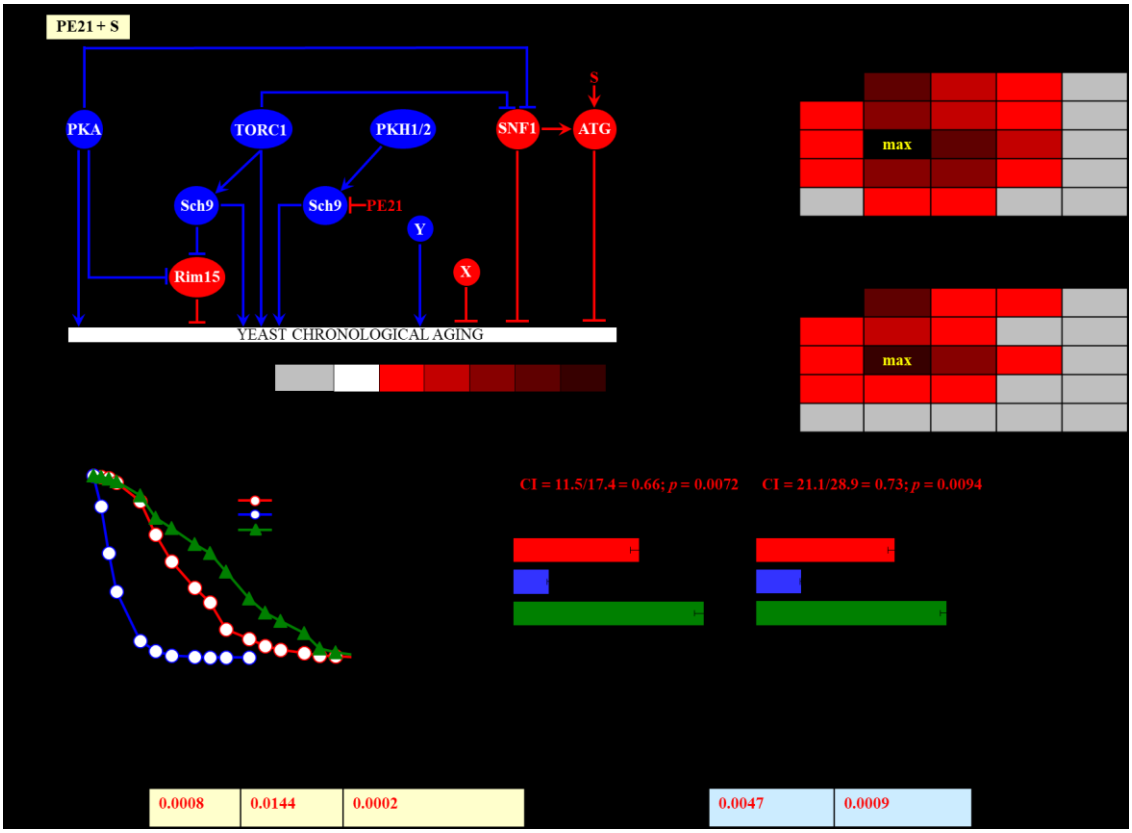

Figure 4.22. The longevity-extending efficiency of a mixture of 0.1% PE21 and 100 μM spermidine (S) statistically significantly exceeds those of PE21 and S, which were used at the optimal concentration of 0.1% or 100 μM (respectively). Thus, PE21 and S enhance the longevity-extending efficiency of each other. Hence, according to the highest single agent (HSA) model, PE21 and S act in synergy to extend the longevity of chronologically aging yeast. (A) PE21 and S are known to regulate different nodes of the signaling network that controls the rate of yeast chronological aging. PE21 mitigates a form of the pro-aging protein kinase Sch9 that is activated by the pro-aging PKH1/2 pathway, whereas S stimulates the anti-aging ATG pathway. (B, C) WT cells were grown in the synthetic minimal YNB medium initially containing 2% glucose, with PE21 (at the final concentration of 0.1%, 0.3%, 0.5% or 1.0%) and/or S (at the final concentration of 50 μM, 100 μM, 200 μM or 500 μM), or without a PE and S. Effects of different concentrations of PE21 and S (added alone or in pairwise combinations) on the mean (B) or maximum (C) CLS of WT cells are shown. The table cell at the intersection of the column for 0.1% PE21 and the row for 100 μM S is marked "max" because the mixture of 0.1% PE21 and 100 μM S exhibits the highest extending effect on the mean and maximum lifespans of chronologically aging WT cells. (D, E) WT cells were cultured in the synthetic minimal YNB medium initially containing 2% glucose and one of the following supplements: 0.1% PE21, 100 μM S, or a mixture of 0.1% PE21 and 100 μM S. In the cultures supplemented with PE21 and/or S, ethanol was used as a vehicle at the final concentration of 2.5%. In the same experiment, WT cells were also subjected to ethanol-mock treatment by being cultured in the synthetic minimal YNB medium, initially containing 2% glucose and 2.5% ethanol. Survival curves (D) and the mean and maximum lifespans (E) of chronologically aging WT cells cultured without a PE and S (cells were subjected to ethanol-mock treatment), with 0.1% PE21, with 100 μM S, or with the mixture of 0.1% PE21 and 100 μM S are shown. Data in D and E are presented as means ± SEM (n = 3;

*p < 0.05; **p < 0.01; ***p < 0.001). The CI values in E were calculated as follows: CI = CLS_{PE21}/CLS_{PE21+S} for both the mean and maximum CLS; the significance of a synergistic effect (i.e. CI < 1) is provided as the p value of the two-tailed t test for comparing the effect of a PE combination (i.e., CLS_{PE21+S}) to that of the HSA (i.e., $CLSP_{E21}$ for both the mean and maximum CLS). (F) p Values for different pairs of survival curves of WT cells cultured in the presence of 0.1% PE21, 100 μM S, a mixture of 0.1% PE21 and 100 μM S, or in the absence of a PE and S (cells were subjected to ethanol-mock treatment) are shown. Survival curves shown in (D) were compared. Two survival curves were considered statistically different if the p value was less than 0.05. The p values for comparing pairs of survival curves using the logrank test were calculated as described in Materials and Methods. The p values displayed on a yellow color background indicate that 0.1% PE21, 100 μM S, and the mixture of 0.1% PE21 and 100 μM S significantly extend the CLS of WT cells. The p values displayed on a blue color background indicate that the CLS-extending efficiency of the mixture of 0.1% PE21 and 100 μM S significantly exceeds that of 0.1% PE21 or 100 μM S. Abbreviations: as in the legend to Figure 4.2.

4.3.10 Mixtures of resveratrol with PE4, PE5, PE6, PE8, PE12 or PE21 synergistically slow down yeast chronological aging

Resveratrol modulates a presently unknown pro-aging or anti-aging node that may be integrated into the signaling network that controls the rate of yeast chronological aging (Figure 4.1). PE4, PE5, PE8, PE12 and PE21 affect known nodes, edges and modules of this network, whereas PE6 (akin to resveratrol) regulates a currently unidentified node of the network (Figure 4.1) [477]. Based on these observations, we put forward the following hypotheses: 1) mixtures of resveratrol with PE4, PE5, PE8, PE12 or PE21 may have synergistic effects on the efficiency of yeast chronological aging delay, 2) if resveratrol and PE6 target different nodes of the network, their mixture may delay yeast chronological aging in a synergistic manner, and 3) if resveratrol and PE6 target the same node of the network, resveratrol and PE6 may not act in synergy to slow down yeast chronological aging. To test these hypotheses, we cultured WT cells in the synthetic minimal medium initially containing 2% glucose, either without a PE (i.e. cells were subjected to ethanol-mock treatment) or with the following additions: 1) PE4, PE5, PE6, PE8, PE12 or PE21 alone (each being used at the final concentration of 0.1%, 0.3%, 0.5% or 1.0%, see below), or 2) a mixture of 10 μM, 20 μM, 50 μM or 100 μM resveratrol with PE4, PE5, PE6, PE8, PE12 or PE21 (each being used at the final concentration of 0.1%, 0.3%, 0.5% or 1.0%).

We found that the longevity-extending efficiencies of the following mixtures of resveratrol and an aging-delaying PE are statistically significantly greater than that of a PE within the mixture which was used as the HSA (i.e. if this PE was added alone at the optimal aging-delaying

concentration): 1) a mixture of 0.5% PE4 and 50 μM resveratrol as compared to 0.5% PE4 (which was used as the HSA for both the mean and maximum CLS) (Figure 4.23), 2) a mixture of 0.3% PE5 and 50 μM resveratrol as compared to 0.5% PE5 (which was considered as the HSA for both the mean and maximum CLS) (Figure 4.24), 3) a mixture of 0.5% PE6 and 50 μM resveratrol as compared to 1.0% PE6 (which was used as the HSA for both the mean and maximum CLS) (Figure 4.25), 4) a mixture of 0.3% PE8 and 50 μM resveratrol as compared to 0.3% PE8 (which was considered as the HSA for both the mean and maximum CLS) (Figure 4.26), 5) a mixture of 0.1% PE12 and 50 μM resveratrol as compared to 0.1% PE12 (which was used as the HSA for both the mean and maximum CLS) (Figure 4.27), and 6) a mixture of 0.1% PE21 and 50 μM resveratrol as compared to 0.1% PE21 (which was considered as the HSA for both the mean and maximum CLS) (Figure 4.28).

In sum, these findings confirm the following hypotheses: 1) mixtures of resveratrol with PE4, PE5, PE8, PE12 or PE21 exhibit synergistic effects on the efficiency of yeast chronological aging delay, and 2) if resveratrol and PE6 target different nodes of the network, a mixture of resveratrol and PE6 delays yeast chronological aging in a synergistic manner.

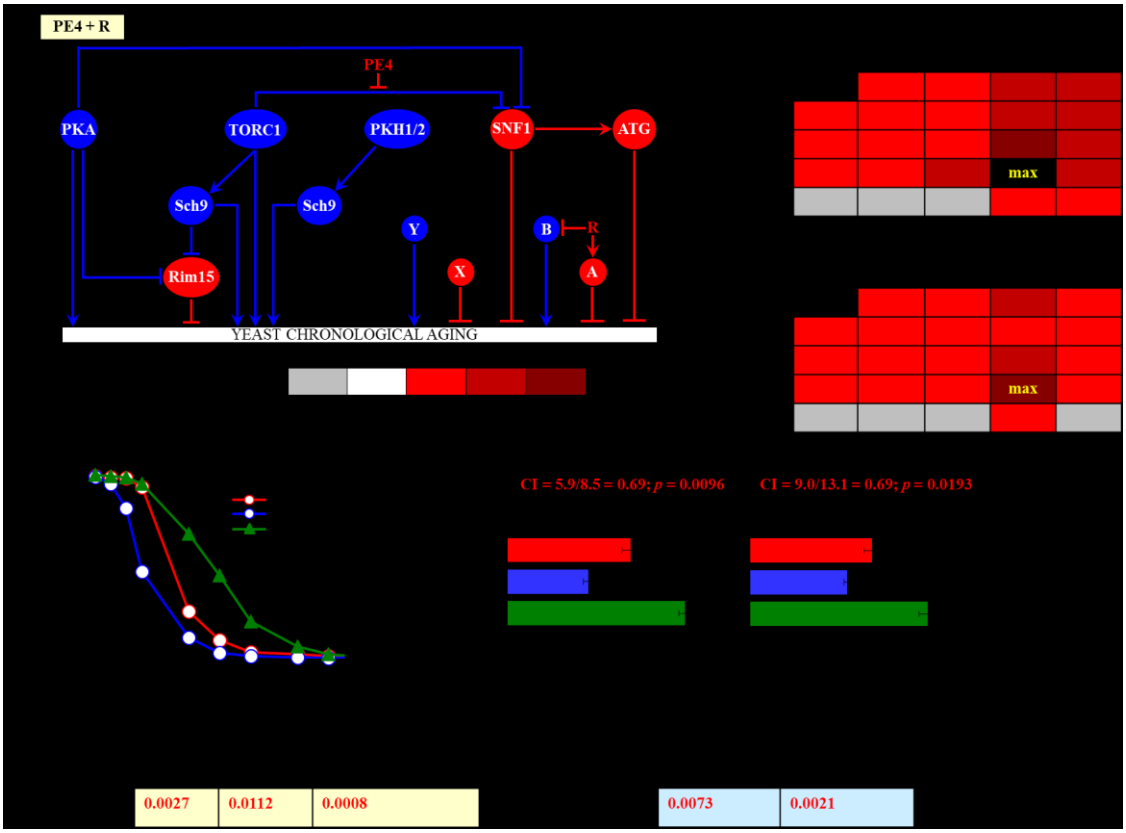

Figure 4.23. The longevity-extending efficiency of a mixture of 0.5% PE4 and 50 μM

resveratrol (R) statistically significantly exceeds those of PE4 and R, which were used at the optimal concentration of 0.5% or 50 μM (respectively). Thus, PE4 and R enhance the longevity-extending efficiency of each other. Hence, according to the HSA model, PE4 and R act in synergy to extend the longevity of chronologically aging yeast. (A) PE4 and R are known to regulate different nodes of the signaling network that controls the rate of yeast chronological aging. PE4 weakens the restraining action of the pro-aging TORC1 pathway on the anti-aging SNF1 pathway, whereas R modulates a presently unknown pro-aging or anti-aging node that may be integrated into this signaling network. (B, C) WT cells were grown as described in the legend to Figure 4.2, with PE4 (at the final concentration of 0.1%, 0.3%, 0.5% or 1.0%) and/or R (at the final concentration of 10 μM, 20 μM, 50 μM or 100 μM), or without a PE and R. Effects of different concentrations of PE4 and R (added alone or in pairwise combinations) on the mean (B) or maximum (C) CLS of WT cells are shown. The table cell at the intersection of the column for 0.5% PE4 and the row for 50 μM R is marked "max" for a reason described in the legend to Figure 4.2. (D, E) WT cells were cultured as described in the legend to Figure 4.2, with one of the following supplements: 0.5% PE4, 50 μM R, or a mixture of 0.5% PE4 and 50 μM R. Ethanol was used as a vehicle or for mock treatment as described in the legend to Figure 4.2. Survival curves (D) and the mean and maximum lifespans (E) of chronologically aging WT cells cultured without a PE and R (cells were subjected to ethanol-mock treatment), with 0.5% PE4, with 50 μM R, or with the mixture of 0.5% PE4 and 50 μM R are shown. Data in D and E are presented as means ± SEM (n = 3; *$p < 0.05$; **$p < 0.01$). The CI and p values in E were calculated as described in the legend to Figure 4.2. (F) p Values for different pairs of survival curves of WT cells cultured in the presence of 0.5% PE4, 50 μM R, a mixture of 0.5% PE4 and 50 μM R, or in the absence of a PE and R (cells were subjected to ethanol-mock treatment) are shown. Survival curves shown in (D) were compared. The p values are displayed on a yellow or blue color background for the reasons described in the legend to Figure 4.2. Abbreviations: A, a presently unknown anti-aging node of the signaling network; B, a presently unknown pro-aging node of the signaling network; other abbreviations are as in the legend to Figure 4.2.

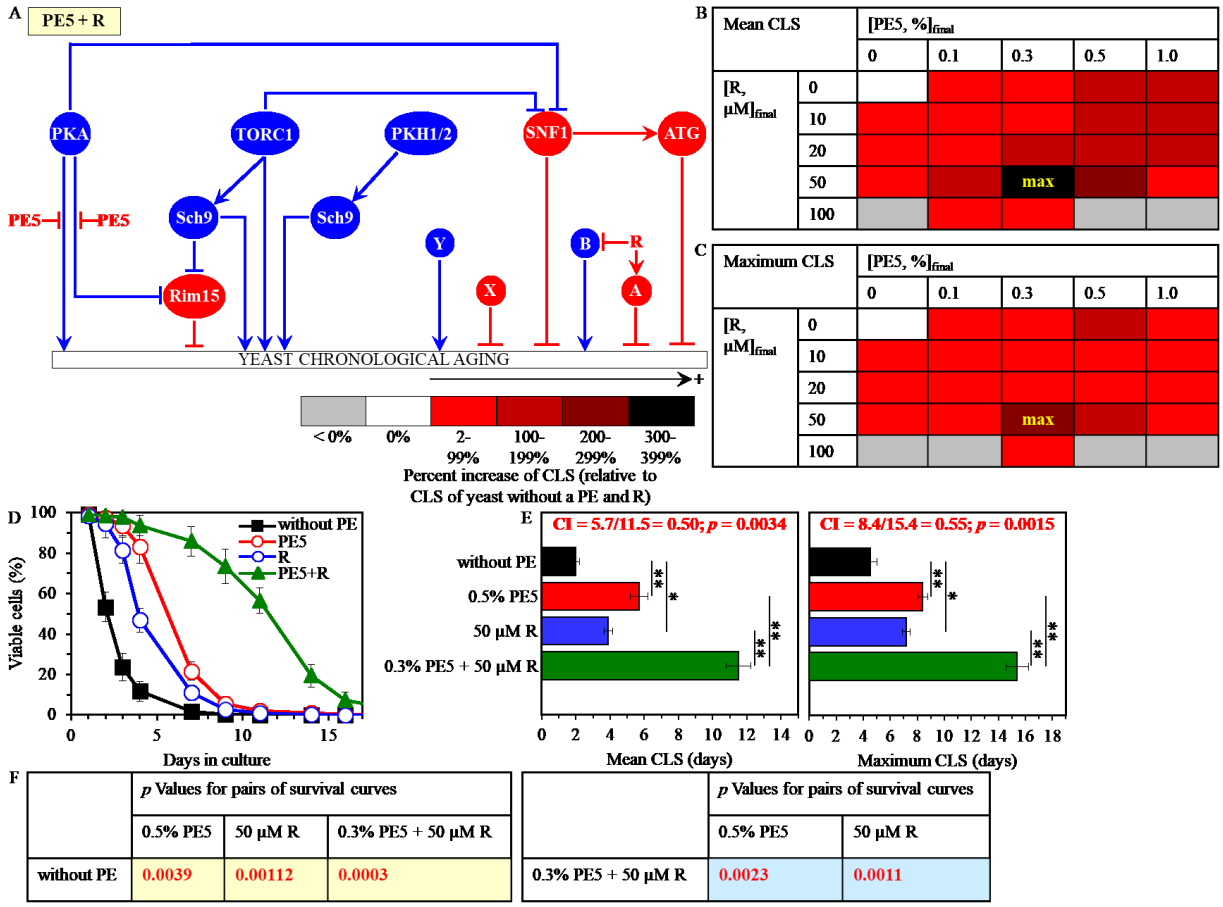

Figure 4.24. The longevity-extending efficiency of a mixture of 0.3% PE5 and 50 μM resveratrol (R) statistically significantly exceeds those of PE5 and R, which were used at the optimal concentration of 0.5% or 50 μM (respectively). Thus, PE5 and R enhance the longevity-extending efficiency of each other. Hence, according to the highest single agent (HSA) model, PE5 and R act in synergy to extend the longevity of chronologically aging yeast. (A) PE5 and R are known to regulate different nodes of the signaling network that controls the rate of yeast chronological aging. PE5 mitigates two different branches of the pro-aging PKA pathway, whereas R modulates a presently unknown pro-aging or anti-aging node that may be integrated into this signaling network. (B, C) WT cells were grown in the synthetic minimal YNB medium initially containing 2% glucose, with PE5 (at the final concentration of 0.1%, 0.3%, 0.5% or 1.0%) and/or R (at the final concentration of 10 μM, 20 μM, 50 μM or 100 μM), or without a PE and R. Effects of different concentrations of PE5 and R (added alone or in pairwise combinations) on the mean (B) or maximum (C) CLS of WT cells are shown. The table cell at the intersection of the column for 0.3% PE5 and the row for 50 μM R is marked "max" because the mixture of 0.3% PE5 and 50 μM R exhibits the highest extending effect on the mean and maximum lifespans of chronologically aging WT cells. (D, E) WT cells were cultured in the synthetic minimal YNB medium initially containing 2% glucose and one of the following supplements: 0.5% PE5, 50 μM R, or a mixture of 0.3% PE5 and 50 μM R. In the cultures supplemented with PE5 and/or R, ethanol was used as a vehicle at the final concentration of 2.5%. In the same experiment, WT cells were also subjected to ethanol-mock treatment by being cultured in the synthetic minimal YNB medium, initially containing 2% glucose and 2.5% ethanol. Survival curves (D) and the mean and maximum lifespans (E) of chronologically aging WT cells cultured without a PE and R (cells were subjected

to ethanol-mock treatment), with 0.5% PE5, with 50 μM R, or with the mixture of 0.3% PE5 and 50 μM R are shown. Data in D and E are presented as means ± SEM (n = 3; *$p < 0.05$; **$p < 0.01$). The CI values in E were calculated as follows: CI = CLS_{PE5}/CLS_{PE5+R} for both the mean and maximum CLS; the significance of a synergistic effect (i.e. CI < 1) is provided as the p value of the two-tailed t test for comparing the effect of a PE combination (i.e. CLS_{PE5+R}) to that of the HSA (i.e. CLS_{PE5} for both the mean and maximum CLS). (F) p Values for different pairs of survival curves of WT cells cultured in the presence of 0.5% PE5, 50 μM R, a mixture of 0.3% PE5 and 50 μM R, or in the absence of a PE and R (cells were subjected to ethanol-mock treatment) are shown. Survival curves shown in (D) were compared. Two survival curves were considered statistically different if the p value was less than 0.05. The p values for comparing pairs of survival curves using the logrank test were calculated as described in Materials and Methods. The p values displayed on a yellow color background indicate that 0.5% PE5, 50 μM R, and the mixture of 0.3% PE5 and 50 μM R significantly extend the CLS of WT cells. The p values displayed on a blue color background indicate that the CLS-extending efficiency of the mixture of 0.3% PE5 and 50 μM R significantly exceeds that of 0.5% PE5 or 50 μM R. Abbreviations: as in the legend to Figure 4.2.

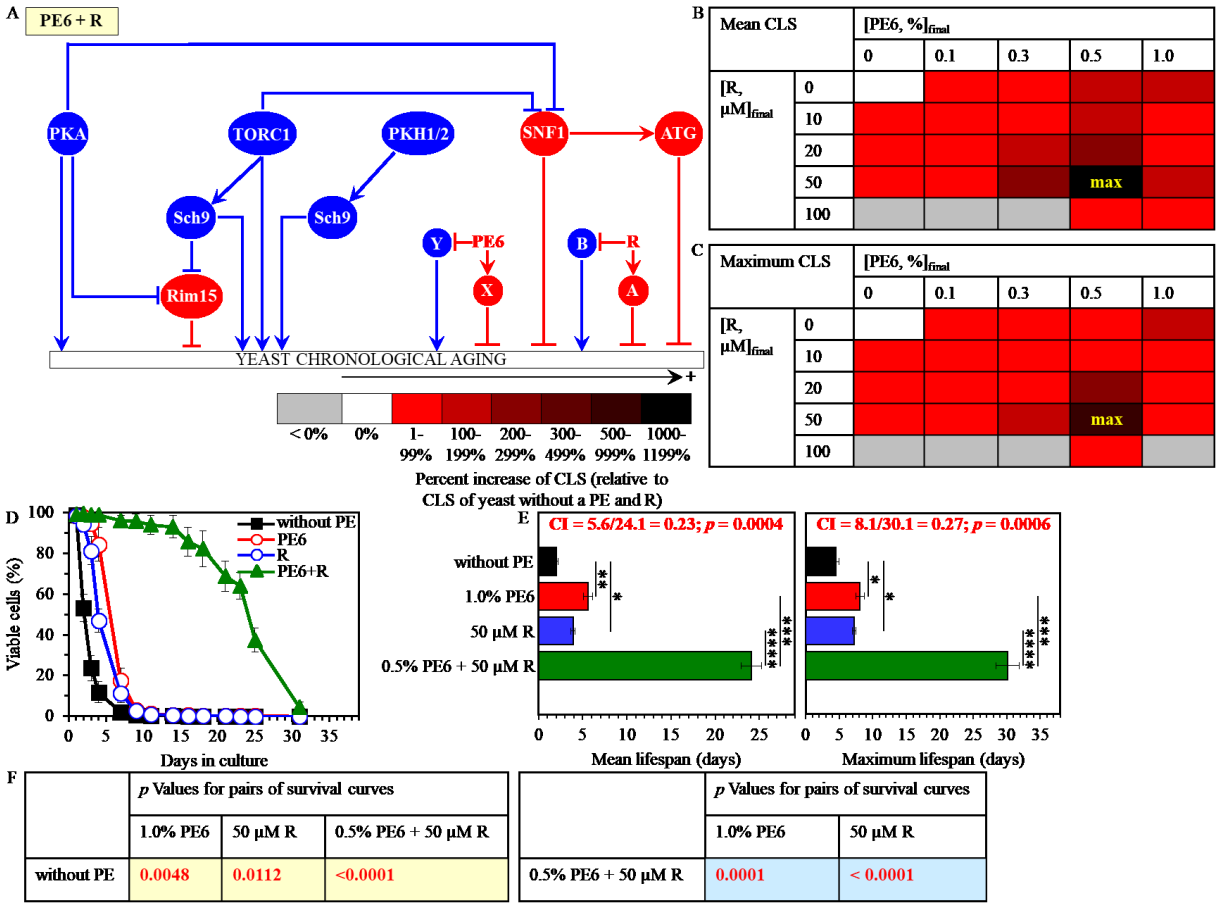

F

	p Values for pairs of survival curves		
	1.0% PE6	50 μM R	0.5% PE6 + 50 μM R
without PE	0.0048	0.0112	<0.0001

	p Values for pairs of survival curves	
	1.0% PE6	50 μM R
0.5% PE6 + 50 μM R	0.0001	< 0.0001

Figure 4.25. The longevity-extending efficiency of a mixture of 0.5% PE6 and 50 μM resveratrol (R) statistically significantly exceeds those of PE6 and R, which were used at the optimal concentration of 1.0% or 50 μM (respectively). Thus, PE6 and R enhance the longevity-extending efficiency of each other. Hence, according to the HSA model, PE6 and R act in synergy to extend the longevity of chronologically aging yeast. (A) PE6 and R regulate

different pro-aging or anti-aging nodes that may be integrated into the signaling network controlling the rate of yeast chronological aging; the identities of proteins that form these nodes are presently unknown. (B, C) WT cells were grown as described in the legend to Figure 4.2, with PE6 (at the final concentration of 0.1%, 0.3%, 0.5% or 1.0%) and/or R (at the final concentration of 10 μM, 20 μM, 50 μM or 100 μM), or without a PE and R. Effects of different concentrations of PE6 and R (added alone or in pairwise combinations) on the mean (B) or maximum (C) CLS of WT cells are shown. The table cell at the intersection of the column for 0.5% PE6 and the row for 50 μM R is marked "max" for a reason described in the legend to Figure 4.2. (D, E) WT cells were cultured as described in the legend to Figure 4.2, with one of the following supplements: 0.5% PE6, 50 μM R, or a mixture of 0.5% PE6 and 50 μM R. Ethanol was used as a vehicle or for mock treatment as described in the legend to Figure 4.2. Survival curves (D) and the mean and maximum lifespans (E) of chronologically aging WT cells cultured without a PE and R (cells were subjected to ethanol-mock treatment), with 1.0% PE6, with 50 μM R, or with the mixture of 0.5% PE6 and 50 μM R are shown. Data in D and E are presented as means ± SEM (n = 3; *$p < 0.05$; **$p < 0.01$; ***$p < 0.001$; ****$p < 0.0001$). The CI and p values in E were calculated as described in the legend to Figure 4.2. (F) p Values for different pairs of survival curves of WT cells cultured in the presence of 1.0% PE6, 50 μM R, a mixture of 0.5% PE6 and 50 μM R, or in the absence of a PE and R (cells were subjected to ethanol-mock treatment) are shown. Survival curves shown in (D) were compared. The p values are displayed on a yellow or blue color background for the reasons described in the legend to Figure 4.2. Abbreviations: as in the legend to Figure 4.2.

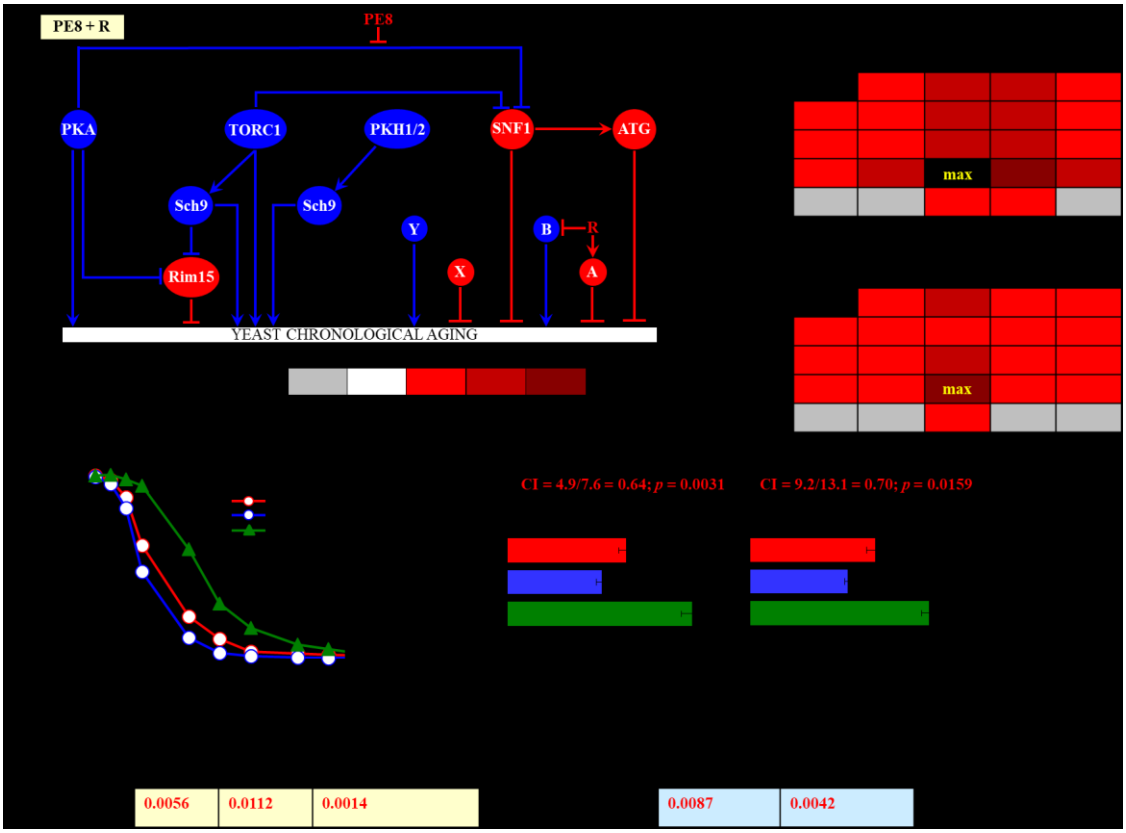

Figure 4.26. The longevity-extending efficiency of a mixture of 0.3% PE8 and 50 μM resveratrol (R) statistically significantly exceeds those of PE8 and R, which were used at the optimal concentration of 0.3% or 50 μM (respectively). Thus, PE8 and R enhance the

longevity-extending efficiency of each other. Hence, according to the highest single agent (HSA) model, PE8 and R act in synergy to extend the longevity of chronologically aging yeast. (A) PE8 and R are known to regulate different nodes of the signaling network that controls the rate of yeast chronological aging. PE8 weakens the restraining action of the pro-aging PKA pathway on the anti-aging SNF1 pathway, whereas R modulates a presently unknown pro-aging or anti-aging node that may be integrated into this signaling network. (B, C) WT cells were grown in the synthetic minimal YNB medium initially containing 2% glucose, with PE8 (at the final concentration of 0.1%, 0.3%, 0.5% or 1.0%) and/or R (at the final concentration of 10 μM, 20 μM, 50 μM or 100 μM), or without a PE and R. Effects of different concentrations of PE8 and R (added alone or in pairwise combinations) on the mean (B) or maximum (C) CLS of WT cells are shown. The table cell at the intersection of the column for 0.3% PE8 and the row for 50 μM R is marked "max" because the mixture of 0.3% PE8 and 50 μM R exhibits the highest extending effect on the mean and maximum lifespans of chronologically aging WT cells. (D, E) WT cells were cultured in the synthetic minimal YNB medium initially containing 2% glucose and one of the following supplements: 0.3% PE8, 50 μM R, or a mixture of 0.3% PE8 and 50 μM R. In the cultures supplemented with PE8 and/or R, ethanol was used as a vehicle at the final concentration of 2.5%. In the same experiment, WT cells were also subjected to ethanol-mock treatment by being cultured in the synthetic minimal YNB medium, initially containing 2% glucose and 2.5% ethanol. Survival curves (D) and the mean and maximum lifespans (E) of chronologically aging WT cells cultured without a PE and R (cells were subjected to ethanol-mock treatment), with 0.3% PE8, with 50 μM R, or with the mixture of 0.3% PE8 and 50 μM R are shown. Data in D and E are presented as means ± SEM (n = 3; **p* < 0.05; ***p* < 0.01). The CI values in E were calculated as follows: CI = CLS_{PE8}/CLS_{PE8+R} for both the mean and maximum CLS; the significance of a synergistic effect (i.e. CI < 1) is provided as the *p* value of the two-tailed *t* test for comparing the effect of a PE combination (i.e. CLS_{PE8+R}) to that of the HSA (i.e. CLS_{PE8} for both the mean and maximum CLS). (F) *p* Values for different pairs of survival curves of WT cells cultured in the presence of 0.3% PE8, 50 μM R, a mixture of 0.3% PE8 and 50 μM R, or in the absence of a PE and R (cells were subjected to ethanol-mock treatment) are shown. Survival curves shown in (D) were compared. Two survival curves were considered statistically different if the *p* value was less than 0.05. The *p* values for comparing pairs of survival curves using the logrank test were calculated as described in Materials and Methods. The *p* values displayed on a yellow color background indicate that 0.3% PE8, 50 μM R, and the mixture of 0.3% PE8 and 50 μM R significantly extend the CLS of WT cells. The *p* values displayed on a blue color background indicate that the CLS-extending efficiency of the mixture of 0.3% PE8 and 50 μM R significantly exceeds that of 0.3% PE8 or 50 μM R. Abbreviations: as in the legend to Figure 4.2.

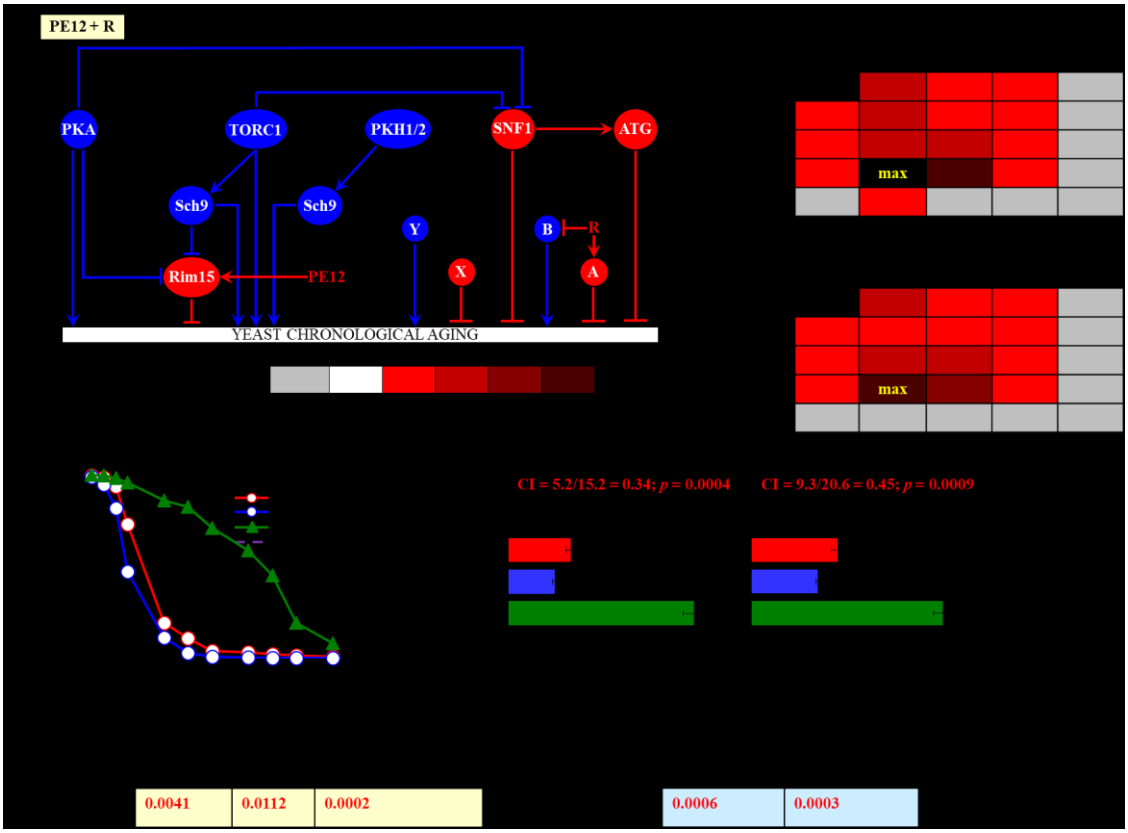

Figure 4.27. The longevity-extending efficiency of a mixture of 0.1% PE12 and 50 μM resveratrol (R) statistically significantly exceeds those of PE12 and R, which were used at the optimal concentration of 0.1% or 50 μM (respectively). Thus, PE12 and R enhance the longevity-extending efficiency of each other. Hence, according to the HSA model, PE12 and R act in synergy to extend the longevity of chronologically aging yeast. (A) PE12 and R regulate different nodes of the signaling network that controls the rate of yeast chronological aging. PE12 stimulates the anti-aging protein kinase Rim15, whereas R modulates a presently unknown pro-aging or anti-aging node that may be integrated into this signaling network. (B, C) WT cells were grown as described in the legend to Figure 4.2, with PE12 (at the final concentration of 0.1%, 0.3%, 0.5% or 1.0%) and/or R (at the final concentration of 10 μM, 20 μM, 50 μM or 100 μM), or without a PE and R. Effects of different concentrations of PE12 and R (added alone or in pairwise combinations) on the mean (B) or maximum (C) CLS of WT cells are shown. The table cell at the intersection of the column for 0.1% PE12 and the row for 50 μM R is marked "max" for a reason described in the legend to Figure 4.2. (D, E) WT cells were cultured as described in the legend to Figure 4.2, with one of the following supplements: 0.1% PE12, 50 μM R, or a mixture of 0.1% PE12 and 50 μM R. Ethanol was used as a vehicle or for mock treatment as described in the legend to Figure 4.2. Survival curves (D) and the mean and maximum lifespans (E) of chronologically aging WT cells cultured without a PE and R (cells were subjected to ethanol-mock treatment), with 0.1% PE12, with 50 μM R, or with the mixture of 0.1% PE12 and 50 μM R are shown. Data in D and E are presented as means ± SEM (n = 3; *$p < 0.05$; **$p < 0.01$; ***$p < 0.001$). The CI and p values in E were calculated as described in the legend to Figure 4.2. (F) p Values for different pairs of survival curves of WT cells cultured in the presence of 0.1% PE12, 50 μM R, a mixture of 0.1% PE12 and 50 μM R, or in the absence of a PE and R (cells were subjected to ethanol-mock treatment) are shown. Survival curves shown in (D) were compared.

The *p* values are displayed on a yellow or blue color background for the reasons described in the legend to Figure 4.2. Abbreviations: as in the legend to Figure 4.2.

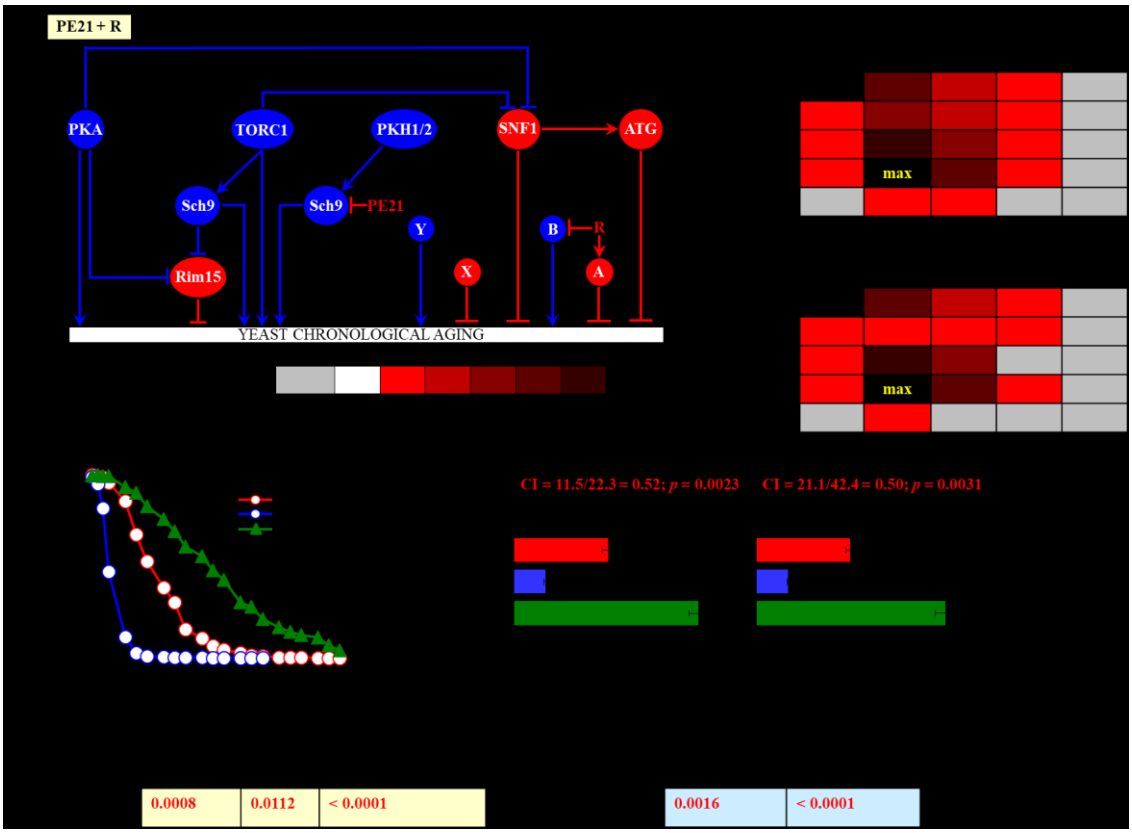

Figure 4.28. The longevity-extending efficiency of a mixture of 0.1% PE21 and 50 µM resveratrol (R) statistically significantly exceeds those of PE21 and R, which were used at the optimal concentration of 0.1% or 50 µM (respectively). Thus, PE21 and R enhance the longevity-extending efficiency of each other. Hence, according to the HSA model, PE21 and R act in synergy to extend the longevity of chronologically aging yeast. (A) PE21 and R regulate different nodes of the signaling network that controls the rate of yeast chronological aging. PE21 mitigates a form of the pro-aging protein kinase Sch9 that is activated by the pro-aging PKH1/2 pathway, whereas R modulates a presently unknown pro-aging or anti-aging node that may be integrated into this signaling network. (B, C) WT cells were grown as described in the legend to Figure 4.2, with PE21 (at the final concentration of 0.1%, 0.3%, 0.5% or 1.0%) and/or R (at the final concentration of 10 µM, 20 µM, 50 µM or 100 µM), or without a PE and R. Effects of different concentrations of PE21 and R (added alone or in pairwise combinations) on the mean (B) or maximum (C) CLS of WT cells are shown. The table cell at the intersection of the column for 0.1% PE21 and the row for 50 µM R is marked "max" for a reason described in the legend to Figure 4.2. (D, E) WT cells were cultured in the synthetic minimal YNB medium initially containing 2% glucose and one of the following supplements: 0.1% PE21, 50 µM R or a mixture of 0.1% PE21 and 50 µM R. Ethanol was used as a vehicle or for mock treatment as described in the legend to Figure 4.2. Survival curves (D) and the mean and maximum lifespans (E) of chronologically aging WT cells cultured without a PE and R (cells were subjected to ethanol-mock

treatment), with 0.1% PE21, with 50 μM R, or with the mixture of 0.1% PE21 and 50 μM R are shown. Data in D and E are presented as means ± SEM (n = 3; *$p < 0.05$; **$p < 0.01$; ***$p < 0.001$; ****$p < 0.0001$). The CI and p values in E were calculated as described in the legend to Figure 4.2. (F) p Values for different pairs of survival curves of WT cells cultured in the presence of 0.1% PE21, 50 μM R, a mixture of 0.1% PE21 and 50 μM R, or in the absence of a PE and R (cells were subjected to ethanol-mock treatment) are shown. Survival curves shown in (D) were compared. The p values are displayed on a yellow or blue color background for the reasons described in the legend to Figure 4.2. Abbreviations: as in the legend to Figure 4.2.

4.4 Discussion

The objective of this proof-of-concept study was to test our hypothesis that a mixture of two aging-delaying PEs or a combination of one of these PEs and spermidine or resveratrol may delay yeast chronological aging and synergistically extend yeast longevity only if each of the two components of this mixture affects a different node, edge or module of the signaling network of longevity regulation. To attain this objective, we performed a systematic assessment of longevity-extending proficiencies of all possible pairwise combinations of PE4, PE5, PE6, PE8, PE12 and PE21 or of one of these PEs and spermidine or resveratrol in chronologically aging *S. cerevisiae*. In support of our hypothesis, we provided evidence that pairwise combinations of naturally occurring chemical compounds that slow yeast chronological aging through different nodes, edges and modules of this evolutionarily conserved network exhibit synergistic effects on the magnitude of aging delay. It needs to be emphasized that studies in mice, fruit flies, aquatic invertebrates, nematodes, and budding and fission yeast have recently demonstrated that a two- or three-component combination of the aging-delaying chemical compounds that target different aging-associated processes or signaling pathways synergistically delay aging and prolong healthy lifespan [352-358]. Given that the major aspects and underlying mechanisms of aging and aging-associated pathology have been conserved throughout evolution [13-15, 17, 19, 83, 114-116, 340, 479, 486, 487], findings in budding yeast presented here and the above findings in other model eukaryotic organisms [352-358] support the proposed idea [347-351] that multi-component combinations of chemical compounds that target different aging-associated processes or signaling pathways can be used for therapeutic multiplexing of aging delay and healthspan improvement in humans.

Of note, our recent study has revealed that PE4, PE5, PE6, PE8, PE12 and PE21 are geroprotectors that delay the onset and decrease the rate of yeast chronological aging by triggering a hormetic stress response and differently altering the following longevity-defining cellular

processes: 1) the maintenance of mitochondrial respiration and membrane potential, 2) the preservation of reactive oxygen species homeostasis, 3) the protection of cellular proteins, membrane lipids, and mitochondrial and nuclear genomes from oxidative damage, 4) cell defense from acute oxidative and thermal stresses, and 5) the lipolytic degradation of neutral lipids deposited in lipid droplets [461]. In the future, it would be interesting to investigate how the two-component mixes of the six aging-delaying PEs that synergistically delay yeast chronological aging influence each of these cellular processes. This will allow us to gain insight into the mechanisms through which each of these pairwise combinations of PEs can delay the onset and decelerate the progression of the cellular aging process.

CHAPTER 5

5 Discovery of fifteen new geroprotective plant extracts and identification of cellular processes they affect to prolong the chronological lifespan of budding yeast

5.1 Introduction

In a quest for previously unknown geroprotective natural chemicals, we used a robust cell viability assay to search for commercially available plant extracts that can substantially prolong the chronological lifespan of budding yeast. Many of these plant extracts have been used in traditional Chinese and other herbal medicines or the Mediterranean and other customary diets. Our search led to a discovery of fifteen plant extracts that significantly extend the longevity of chronologically aging yeast not limited in calorie supply. We show that each of these longevity-extending plant extracts is a geroprotector that decreases the rate of yeast chronological aging and promotes a hormetic stress response. We also show that each of the fifteen geroprotective plant extracts mimics the longevity-extending, stress-protecting, metabolic and physiological effects of a caloric restriction diet in yeast cells that are not limited in calorie supply. We provide evidence that the fifteen geroprotective plant extracts exhibit partially overlapping effects on a distinct set of longevity-defining cellular processes. These effects include a rise in coupled mitochondrial respiration, an altered age-related chronology of changes in reactive oxygen species abundance, protection of cellular macromolecules from oxidative damage, and an age-related increase in the resistance to long-term oxidative and thermal stresses. Chapter 5 describes all these findings.

5.2 Materials and methods

5.2.1 Yeast strains, media and growth conditions

The wild-type (WT) strain *Saccharomyces cerevisiae* BY4742 (*MATα his3Δ1 leu2Δ0 lys2Δ0 ura3Δ0*) and single-gene-deletion mutant strains in the BY4742 genetic background (all from Thermo Scientific/Open Biosystems) were grown in a synthetic minimal YNB medium (0.67% (w/v) Yeast Nitrogen Base without amino acids from Fisher Scientific; #DF0919-15-3) initially containing 2% (w/v) or 0.5% (w/v) glucose (#D16-10; Fisher Scientific), 20 mg/l *L*-histidine (# H8125; Sigma), 30 mg/l *L*-leucine (#L8912; Sigma), 30 mg/l *L*-lysine (#L5501; Sigma) and 20 mg/l uracil (#U0750; Sigma), with a PE or without it. A stock solution of each PE in ethanol was made on the day of adding this PE to cell cultures. For each PE, the stock solution

was added to growth medium with 2% (w/v) or 0.5% (w/v) glucose immediately following cell inoculation into the medium. In a culture supplemented with a PE, ethanol was used as a vehicle at the final concentration of 2.5% (v/v). In the same experiment, yeast cells were also subjected to ethanol-mock treatment by being cultured in growth medium initially containing 2% (w/v) or 0.5% (w/v) glucose and 2.5% (v/v) ethanol. Cells were cultured at 30^{o}C with rotational shaking at 200 rpm in Erlenmeyer flasks at a "flask volume/medium volume" ratio of 5:1.

5.2.2 Chronological lifespan (CLS) assay

A sample of cells was taken from a culture at a certain day following cell inoculation and PE addition into the medium. A fraction of the sample was diluted to determine the total number of cells using a hemacytometer. Another fraction of the cell sample was diluted, and serial dilutions of cells were plated in duplicate onto YEP medium (1% (w/v) yeast extract, 2% (w/v) peptone; both from Fisher Scientific; #BP1422-2 and #BP1420-2, respectively) containing 2% (w/v) glucose (#D16-10; Fisher Scientific) as carbon source. After 2 d of incubation at 30oC, the number of colony-forming units (CFU) per plate was counted. The number of CFU was defined as the number of viable cells in a sample. For each culture, the percentage of viable cells was calculated as follows: (number of viable cells per ml/total number of cells per ml) × 100. The percentage of viable cells in the mid-logarithmic growth phase was set at 100%.

5.2.3 Miscellaneous procedures

The age-specific mortality rate [359, 361], Gompertz slope or mortality rate coefficient (G) [360, 361], and mortality rate doubling time (MRDT) [360, 361] were calculated as previously described. The value of the mortality rate was calculated as the number of cells that lost viability (i.e., are unable to form a colony on the surface of a solid nutrient-rich medium) during each time interval divided by the number of viable (i.e., clonogenic) cells at the end of the interval. The natural logarithms of the mortality rate values for each time point were plotted against days of cell culturing. The coefficient G of the age-specific mortality rate was calculated as the slope of the Gompertz mortality line, whereas the value of MRDT was calculated as 0.693/G. Oxygen consumption assay for monitoring mitochondrial respiration [32], ROS measurement in live yeast [101], fluorescence microscopy [32], quantitative assays for oxidatively damaged proteins and membrane lipids [87], measurements of the frequencies of spontaneous mutations in mitochondrial

and nuclear DNA [100], plating assays for the analysis of resistance to oxidative and thermal stresses [100], and glucose concentration measurement assay [101] have been described elsewhere. All these procedures and methods are detailed in Chapter 2 of my Thesis.

5.2.4 Statistical analysis

Statistical analysis was performed using Microsoft Excel's Analysis ToolPack-VBA. All data on cell survival are presented as mean ± SEM. The p values for comparing the means of two groups using an unpaired two-tailed t-test were calculated with the help of the GraphPad Prism 7 statistics software. The logrank test for comparing each pair of survival curves was performed with GraphPad Prism 7. Two survival curves were considered statistically different if the p value was less than 0.05.

5.3 Results

5.3.1 Identification of new PEs that prolong the longevity of chronologically aging budding yeast

In search of new geroprotective PEs, we performed a screen of fifty-three commercially available PEs. The origin and properties of these PEs are shown in Table 5.1. These PEs are believed to have positive effects on human health, and many of them have been used in traditional Chinese and other herbal medicines or the Mediterranean and other long-established diets.

Table 5.1. Properties of plant extracts (PEs) used to conduct a new screen for PEs that can prolong the longevity of chronologically aging budding yeast.

Abbreviated name of a PE	The botanical name of a plant	Plant part used to make a PE	Properties of a PE	A commercial source of a PE
PE26	*Serenoa repens*	Berry	Extraction solvent: carbon dioxide. Extract ratio: 15:1. Composition: natural extract (oil) (45-55%), silica (45-55%).	Idunn Technologies
PE38	*Centella asiatica*	Herb	Extraction solvent: alcohol (50-70%), water (30-50%). Extract ratio: (8-12):1. Composition: 10% asiaticoside, 30% total triterpenes.	Idunn Technologies

PE39	*Hypericum perforatum*	Aerial parts	Extraction solvent: ethanol (60-80%), water (20-40%). Extract ratio: (5-10):1. Composition: 0.3% hypericin.	Idunn Technologies
PE40	*Boswellia serrata*	Resin	Extraction solvent: methanol (80%), water (20%). Extract ratio: 20:1. Composition: 65% boswellic acids.	Idunn Technologies
PE41	*Ruscus aculeatus*	Root	Extraction solvent: ethanol (70-80%), water (20-30%). Extract Ratio: 8:1. Composition: 10% ruscogenins.	Idunn Technologies
PE42	*Ilex paraguariensis*	Leaf	Extraction solvent: water. Extract ratio: (3-10):1. Composition: 2% caffeine.	Idunn Technologies
PE43	*Schisandra chinensis*	Berry	Extraction solvent: ethanol (30%), water (70%). Extract ratio: 4/1, 1% schizandrins.	Idunn Technologies
PE44	*Cynara scolymus L.*	Leaf	Extraction solvent: water. Extract ratio: 4:1. Composition: > 5% cynarin.	Idunn Technologies
PE45	*Allium cepa L.*	Bulb skin	Extraction solvent: ethanol (70%), water (30 %). Extract ratio: (20-25):1. Composition: > 5% quercetin glycoside derivates.	Idunn Technologies
PE46	*Matricaria recutita L.*	Flower	Extraction solvent: ethanol (80%), water (20%). Extract ratio: 5:1. Composition: 3% apigenins.	Idunn Technologies
PE47	*Ocimum tenuiflorum*	Leaf	Extraction solvent: ethanol (90%), water (10%). Extract ratio: 10:1. Composition: > 5% ursolic acid.	Idunn Technologies
PE48	*Rhaphanus sativus L. var. niger*	Root	Extraction solvent alcohol (60-80%), water (40-20%). Extract ratio: 4:1. Composition: unknown.	Idunn Technologies
PE49	*Rosmarinus officinalis L.*	Leaf	Extraction solvent: acetone. Extract ratio: (35-50):1. Composition: > 50% carnosic acid.	Idunn Technologies
PE50	*Angelica archangelica L.*	Root	Extraction solvent: ethanol (50%), water (50%). Extract ratio: 4:1. Composition: > 3% organic acids.	Idunn Technologies

PE51	*Epimedium grandiflorum*	Herb	Extraction solvent: ethanol (60%), water (40%). Extract ratio: 20:1. Composition: 20% icariin.	Idunn Technologies
PE52	*Bacopa monnieri*	Leaf	Extraction solvent: aqueous alcohol. Extract ratio: 10:1. Composition: 20% bacosides.	Idunn Technologies
PE53	*Phaseolus vulgaris*	Bean	Extraction solvent: aqueous alcohol. Extract ratio: 10:1. Composition: unknown.	Idunn Technologies
PE54	*Allium sativum L.*	Bulb	Extraction solvent: water. Extract ratio: 120:1. Composition: 4.5% alliin.	Idunn Technologies
PE55	*Morus alba*	Leaf	Extraction solvent: ethanol (70%), water (30%). Extract ratio: 4:1. Composition: 1% 1-deoxynojirimycin.	Idunn Technologies
PE56	*Saphora Japonica*	Flower	Extraction solvent: ethanol, water. Extract ratio: unknown. Composition: rutin (40%), quercetin (60%).	Idunn Technologies
PE57	*Morus nigra*	Fruit	Extraction solvent: ethanol, water. Extract ratio: 4:1. Composition: unknown.	Idunn Technologies
PE58	*Magnolia officinalis*	Bark	Extraction solvent: unknown. Extract ratio: (35-40):1. Composition: 40% honokiol.	Idunn Technologies
PE59	*Solidago virgaurea*	Herb	Extraction solvent: ethanol (30%), water (70%). Extract ratio: 4:1. Composition: > 2% flavonoid hyperosides.	Idunn Technologies
PE60	*Astragalus membranaceus*	Root	Extraction solvent: ethanol, water. Extract ratio: 8:1. Composition: 16% polysaccharides.	Idunn Technologies
PE61	*Lepidium meyenii*	Root	Extraction solvent: water, then ethanol (96%) and water (4%). Extract ratio: (22-27):1. Composition: 0.6% macamides and macaenes.	Idunn Technologies
PE62	*Taraxacum officinale*	Leaf	Extraction solvent: ethanol (70-80%), water (20-30%). Extract ratio: (4-7):1. Composition: 3% vitexin.	Idunn Technologies
PE63	*Taraxacum officinale*	Root	Extraction solvent: ethanol (60%), water (40%). Extract	Idunn Technologies

			ratio: 15:1. Composition: 0.3-0.4% phenolic acids (chicoric, chlorogenic and caftaric acids).	
PE64	*Citrus sinensis*	Fruit	Extraction solvent: unknown. Extract ratio: unknown. Composition: ≥ 20% limonene.	Idunn Technologies
PE65	*Piper methysticum*	Root	Extraction solvent: ethanol (65%), water (35%,). Extract ratio: 8:1. Composition: > 30% kavalactones.	Idunn Technologies
PE66	*Handroanthus chrysotrichus*	Bark	Extraction solvent: ethanol (70%), water (30%). Extract ratio: (9-15):1. Composition: unknown.	Idunn Technologies
PE67	*Euterpe oleracea*	Fruit	Extraction solvent: water. Extract ratio: 20:1. Composition: > 10% polyphenols.	Idunn Technologies
PE68	*Humulus lupulus*	Whole plant	Extraction solvent: unknown. Extract ratio: (5.5-6.5):1. Composition: unknown.	Idunn Technologies
PE69	*Vitis vinifera*	Grape skin	Extraction solvent: ethanol (30%), water (70%). Extract ratio: 450:1. Composition: ≥ 5% trans-resveratrol.	Idunn Technologies
PE70	*Vitis vinifera*	Grape	Extraction solvent: water (4%), ethanol (96%). Extract ratio: 200:1. Composition: ≥ 20% oligostilbenes.	Idunn Technologies
PE71	*Malus domestica* + *Vitis vinifera*	Grape + Fruit	Extraction solvent: water (5%), ethanol (95%). Extract ratio: (500-600):1. Composition: ≥ 95% polyphenols.	Idunn Technologies
PE72	*Andrographis paniculata*	Whole plant	Extraction solvent: unknown. Extract ratio: unknown. Composition: ≥ 20% andrographolids.	Idunn Technologies
PE73	*Oryza sativa* fermented with *Monascus purpureus* yeast	Fermented rice	Extraction solvent: unknown. Extract ratio: unknown. Composition: ≥ 20% monacolin K.	Idunn Technologies
PE74	*Melissa officinalis*	Leaf	Extraction solvent: unknown. Extract ratio: 4:1. Composition: ≥ 1% rosmarinic acid.	Idunn Technologies
PE75	*Hydrastis*	Root	Extraction solvent: ethanol	Idunn

	canadensis		(75%), water (25%). Extract ratio: (5-7):1. Composition: ≥ 5% berberine and other alkaloids.	Technologies
PE76	*Polygonum cuspidatum*	Root	Extraction solvent: unknown. Extract ratio: unknown. Composition: ≥ 20% resveratrol.	Idunn Technologies
PE77	*Trigonella foenum-graecum*	Seed	Extraction solvent: ethanol (60%), water (40%). Extract ratio: (5-8):1. Composition: 50% saponins.	Idunn Technologies
PE78	*Berberis vulgaris*	Root bark	Extraction solvent: ethanol (50%), water (50%). Extract ratio: (10-12):1. Composition: 6% berberine.	Idunn Technologies
PE79	*Crataegus monogyna*	Leaf, flower and stem	Extraction solvent: ethanol (80%), water (20%). Extract ratio: (3-6):1. Composition: 1.5% flavonoids.	Idunn Technologies
PE80	*Sophora japonica L.*	Flower bud	Extraction solvent: water. Extract ratio: (16-20):1. Composition: 95% quercetin.	Idunn Technologies
PE81	*Taraxacum erythrospermum*	Leaf	Extraction solvent: ethanol (70-80%), water (20-30%). Extract ratio: (4-7):1. Composition: 3% vitexin.	Idunn Technologies
PE82	*NA*	NA	Na-RALA Powder, Sodium R-lipoate (> 80 % Total R-lipoic Acid) from synthesis.	Idunn Technologies
PE83	*Ilex paraguariensis*	Whole plant	Extraction solvent: unknown. Extract ratio: unknown. Composition: unknown.	Idunn Technologies
PE84	*Vitis vinifera L.*	Seed	Extraction solvent: ethanol, water. Extract ratio: unknown. Composition: 95% polyphenols.	Idunn Technologies
PE85	*Ganoderma lucidum*	Mushroom body	Extraction solvent: unknown. Extract ratio: unknown. Composition: unknown.	Idunn Technologies
PE86	*Panax ginseng*	Root	Extraction solvent: unknown. Extract ratio: unknown. Composition: unknown.	Idunn Technologies
PE87	*Lycium barbarum*	Whole plant	Extraction solvent: unknown. Extract ratio: unknown. Composition: unknown.	Idunn Technologies
PE88	*Hemerocallis*	Flower	Extraction solvent: unknown.	Idunn

	fulva		Extract ratio: unknown. Composition: unknown.	Technologies
PE89	*Curcuma L.*	Root	Extraction solvent: unknown. Extract ratio: unknown. Composition: curcumin solid lipid microparticles to improve absorption.	Idunn Technologies

To conduct the screen, we exploited a robust clonogenic cell viability assay for measuring yeast CLS [461]. In this assay, the wild-type (WT) strain BY4742 was cultured in the synthetic minimal YNB medium initially containing 2% (w/v) glucose, as described in Materials and Methods. Cells of budding yeast cultured under such non-caloric restriction (non-CR) conditions are known to age chronologically faster than the ones cultured under CR conditions on 0.2% (w/v) or 0.5% (w/v) glucose [14, 15, 17, 461].

At the time of cell inoculation into the culturing medium, we added each of the assessed PEs at a final concentration ranging from 0.02% (w/v) to 1.0% (w/v). We found that PE40, PE41, PE44, PE50, PE53, PE66, PE73, PE84, PE86 and PE87 do not affect the mean and maximum CLS of WT yeast if exogenously supplemented within this wide range of initial concentrations (Figures 5.1-5.7). In contrast, PE38, PE43, PE45, PE46, PE48, PE49, PE51, PE52, PE54-PE58, PE60-PE63, PE65, PE67, PE70, PE71, PE74, PE76, PE80, PE82, PE85, PE88 and PE89 were cytotoxic at certain concentrations; they decreased the mean and/or maximum CLS of WT yeast if used at the final concentrations in the 0.1 (w/v) to 1.0% (w/v) range (Figures 5.1-5.7).

Our screen revealed that fifteen of fifty-three tested PEs statistically significantly increase the mean and maximum CLS of WT yeast cultured under non-CR conditions on 2% (w/v) glucose (Figures 5.1-5.6; Figures 5.8-5.9). Each of these fifteen PEs extended the longevity of chronologically aging WT yeast if used within a specific concentration range and exhibited the highest longevity-extending effect at a certain concentration within this range (Figures 5.1-5.6). The following PEs exhibited the highest longevity-extending effect under non-CR conditions of cell culturing: 0.5% (w/v) PE26 from berries of *Serenoa repens* (Figures 5.1 and 5.8A), 0.5% (w/v) PE39 from aerial parts of *Hypericum perforatum* (Figures 5.1 and 5.8B), 0.5% (w/v) PE42 from leaves of *Ilex paraguariensis* (Figures 5.1 and 5.8C), 0.3% (w/v) PE47 from leaves of *Ocimum tenuiflorum* (Figures 5.1 and 5.8D), 0.3% (w/v) PE59 from the whole plant of *Solidago virgaurea* (Figures 5.1 and 5.8E), 0.1% (w/v) PE64 from fruits of *Citrus sinensis* (Figures 5.4 and 5.8F), 0.5% (w/v) PE68 from the whole plant of *Humulus lupulus* (Figures 5.4 and 5.8G), 1.0% (w/v)

PE69 from grape skins of *Vitis vinifera* (Figures 5.5 and 5.8H), 0.1% (w/v) PE72 from the whole plant of *Andrographis paniculata* (Figures 5.5 and 5.9A), 0.3% (w/v) PE75 from roots of *Hydrastis canadensis* (Figures 5.5 and 5.9B), 0.5% (w/v) PE77 from seeds of *Trigonella foenum-graecum* (Figures 5.6 and 5.9C), 0.3% (w/v) PE78 from root barks of *Berberis vulgaris* (Figures 5.6 and 5.9D), 0.5% (w/v) PE79 from leaves, flowers and stems of *Crataegus monogyna* (Figures 5.6 and 5.9E), 0.3% (w/v) PE81 from leaves of *Taraxacum erythrospermum* (Figures 5.6 and 5.9F), and 0.5% (w/v) PE83 from the whole plant of *Ilex paraguariensis* (Figures 5.6 and 5.9G).

We found that none of the fifteen longevity-extending PEs displays a statistically significant effect on glucose consumption during culturing of WT cells under non-CR conditions on 2% (w/v) glucose (Figure 5.10). This finding shows that each of these PEs prolongs the longevity of chronologically aging yeast not because it alters the concentration of exogenous glucose and, thus, not because it affects the metabolic rate of this major source of carbon and energy. We also found that none of the fifteen longevity-extending PEs exhibits a statistically significant effect on the growth rate and maximum cell yield of WT yeast cultures under non-CR conditions (Figure 5.11). Based on this observation, we concluded that each of them extends the longevity of chronologically aging yeast not because it slows cell proliferation and, thus, not because it desensitizes yeast to harmful chemical compounds produced when cells proliferate.

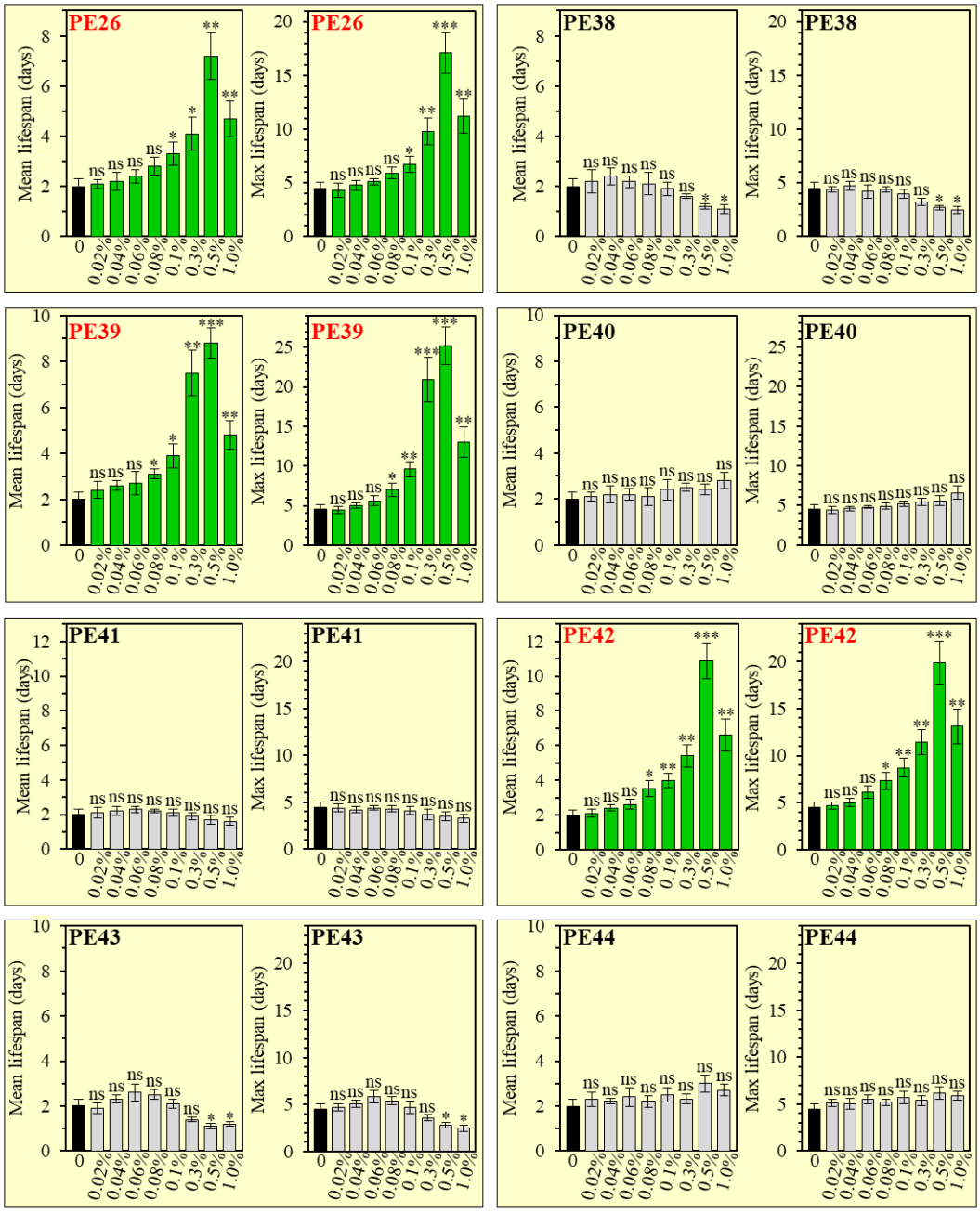

Figure 5.1. PE26, PE39 and PE42, but not PE38, PE40, PE41, PE43 or PE44, increase the mean and maximum CLS of WT yeast cultured under non-CR conditions on 2% (w/v) glucose. WT cells were cultured in the synthetic minimal YNB medium initially containing 2% (w/v) glucose, in the presence of a PE or its absence. The mean and maximum lifespans of chronologically aging WT strain cultured under non-CR conditions without a PE or with a PE added at various concentrations are shown; data are presented as means ± SEM (n = 6; * $p < 0.05$, ** $p < 0.01$, *** $p < 0.001$, *ns*, not significant; the *p* values for comparing the means of two groups were calculated using an unpaired two-tailed *t* test as described in Materials and Methods). Note that PE38 and PE43 can decrease the CLS of WT yeast under non-CR conditions if added at a final concentration of 0.5 (w/v) or 1.0% (w/v).

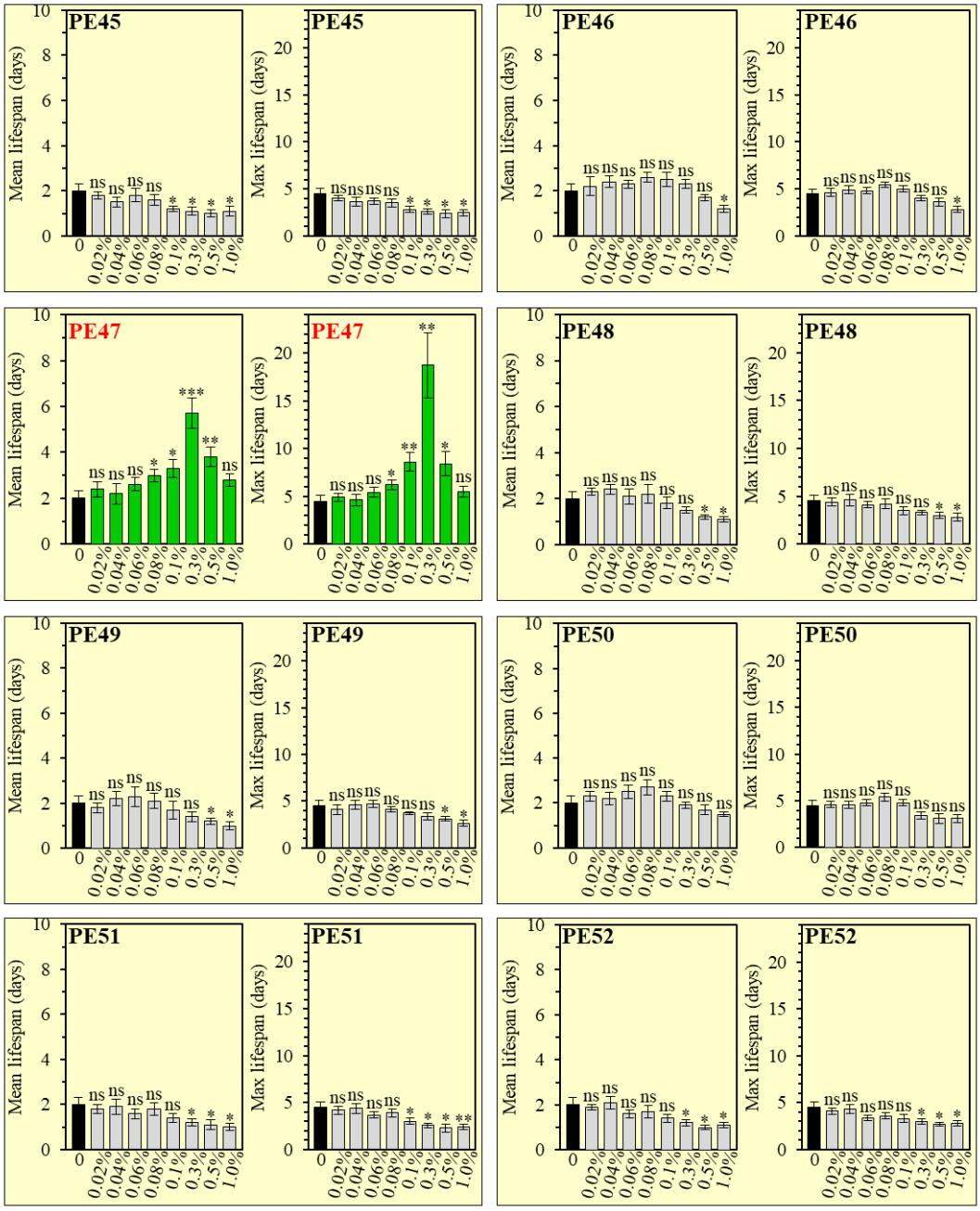

Figure 5.2. PE47, but not PE45, PE46, PE48, PE49, PE50, PE51 or PE52, increases the mean and maximum CLS of WT yeast cultured under non-CR conditions on 2% (w/v) glucose. WT cells were cultured as described in the legend to Figure 5.1. The mean and maximum lifespans of chronologically aging WT strain cultured under non-CR conditions without a PE or with a PE added at various concentrations are shown; data are presented as means ± SEM (n = 6; * $p < 0.05$, ** $p < 0.01$, *** $p < 0.001$, *ns*, not significant; the p values for comparing the means of two groups were calculated as described in the legend to Figure 5.1). Note that PE45, PE46, PE48, PE49, PE51 and PE52 can decrease the CLS of WT yeast under non-CR conditions if added at a final concentration ranging from 0.1% (w/v) to 1.0% (w/v).

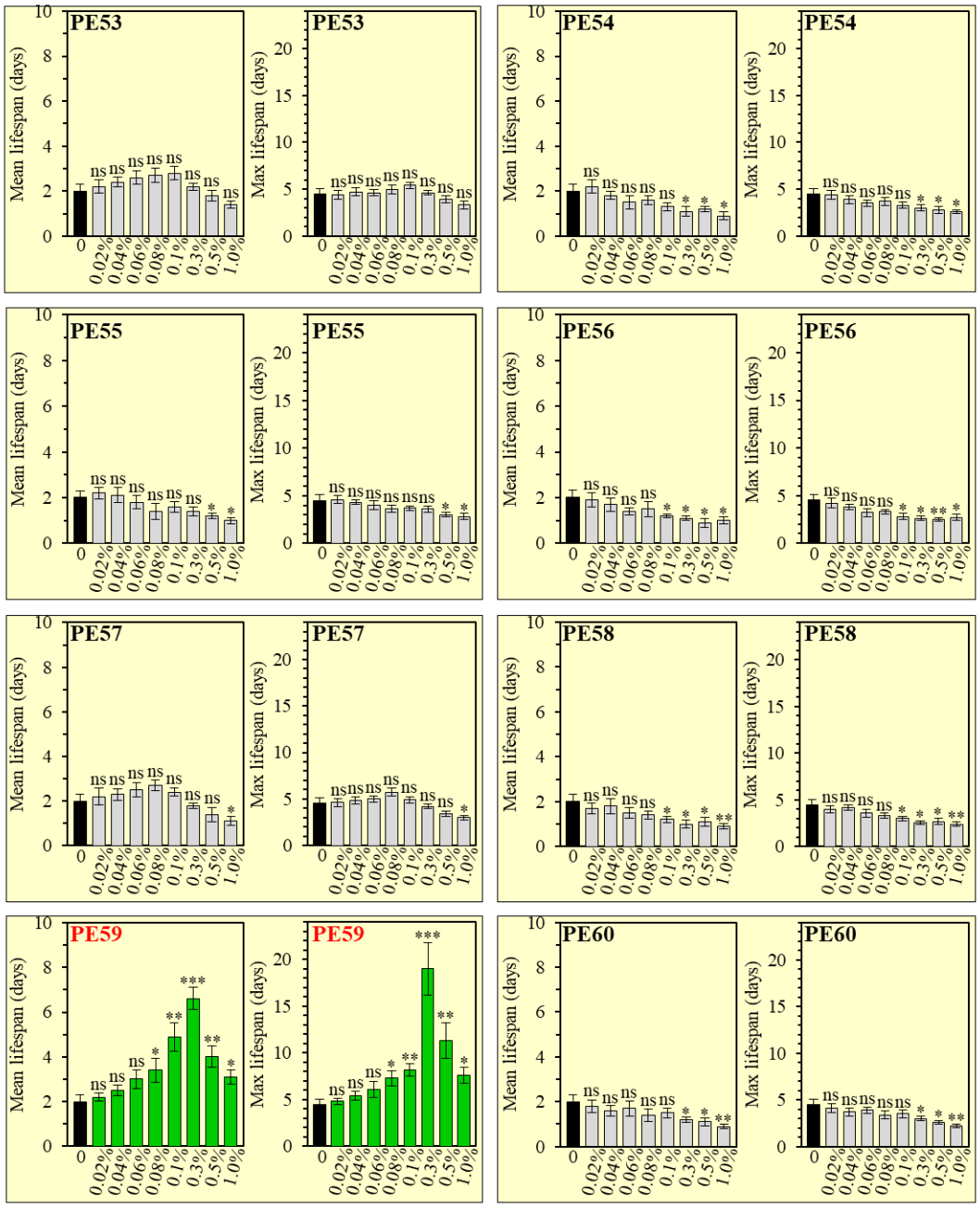

Figure 5.3. PE59, but not PE53, PE54, PE55, PE56, PE57, PE58 or PE60, increases the mean and maximum CLS of WT yeast cultured under non-CR conditions on 2% (w/v) glucose. WT cells were cultured as described in the legend to Figure 5.1. The mean and maximum lifespans of chronologically aging WT strain cultured under non-CR conditions without a PE or with a PE added at various concentrations are shown; data are presented as means ± SEM (n = 6; * $p < 0.05$, ** $p < 0.01$, *** $p < 0.001$, *ns*, not significant; the *p* values for comparing the means of two groups were calculated as described in the legend to Figure 5.1). Note that PE54, PE55, PE56, PE57, PE58 and PE60 can decrease the CLS of WT yeast under non-CR conditions if added at a final concentration ranging from 0.1% (w/v) to 1.0% (w/v).

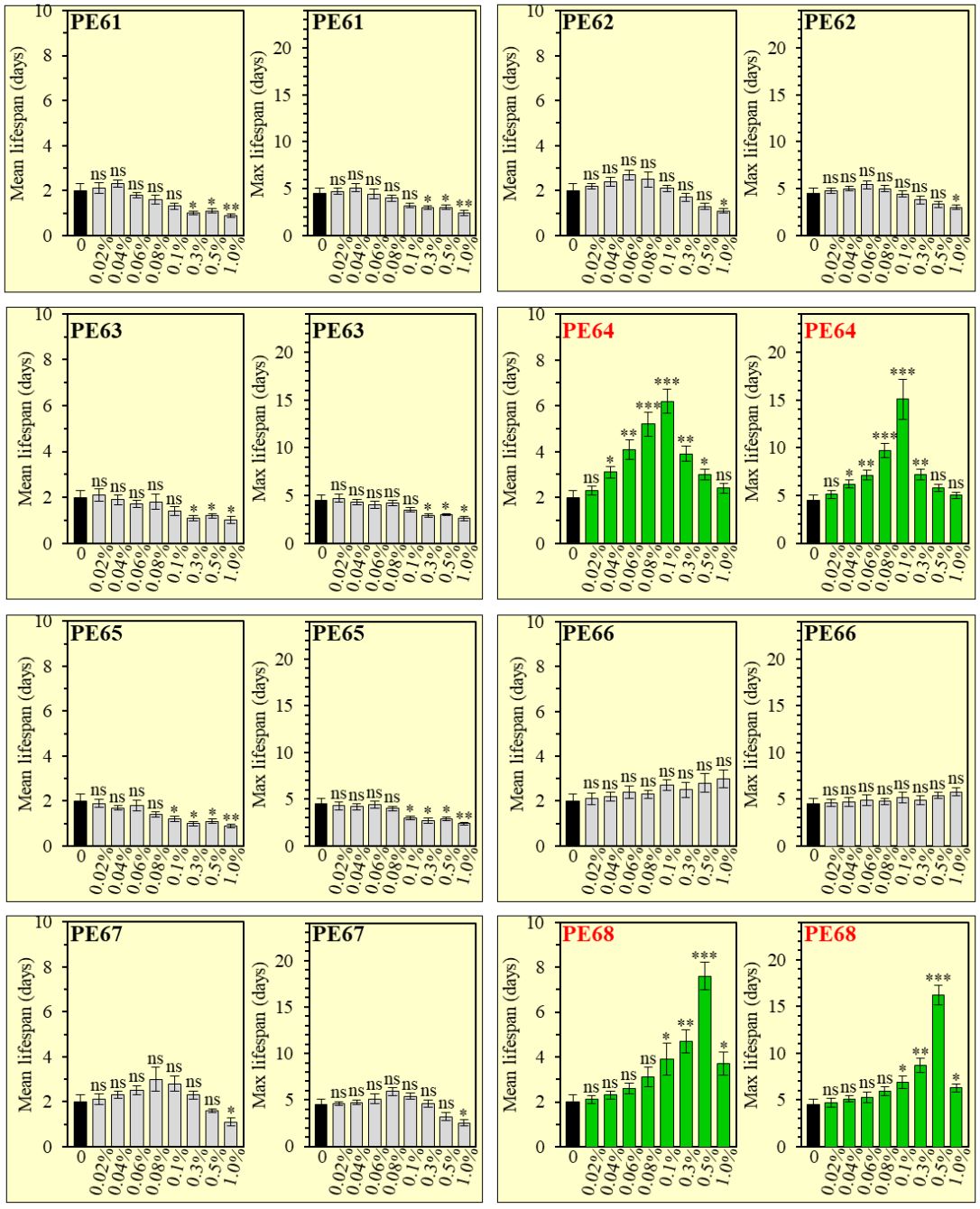

Figure 5.4. PE64 and PE68, but not PE61, PE62, PE63, PE65, PE66 or PE67, increase the mean and maximum CLS of WT yeast cultured under non-CR conditions on 2% (w/v) glucose. WT cells were cultured as described in the legend to Figure 5.1. The mean and maximum lifespans of chronologically aging WT strain cultured under non-CR conditions without a PE or with a PE added at various concentrations are shown; data are presented as means ± SEM (n = 6; * $p < 0.05$, ** $p < 0.01$, *** $p < 0.001$, *ns*, not significant; the *p* values for comparing the means of two groups were calculated as described in the legend to Figure 5.1). Note that PE61, PE62, PE63, PE65 and PE67 can decrease the CLS of WT yeast under non-CR conditions if added at a final concentration ranging from 0.1% (w/v) to 1.0% (w/v).

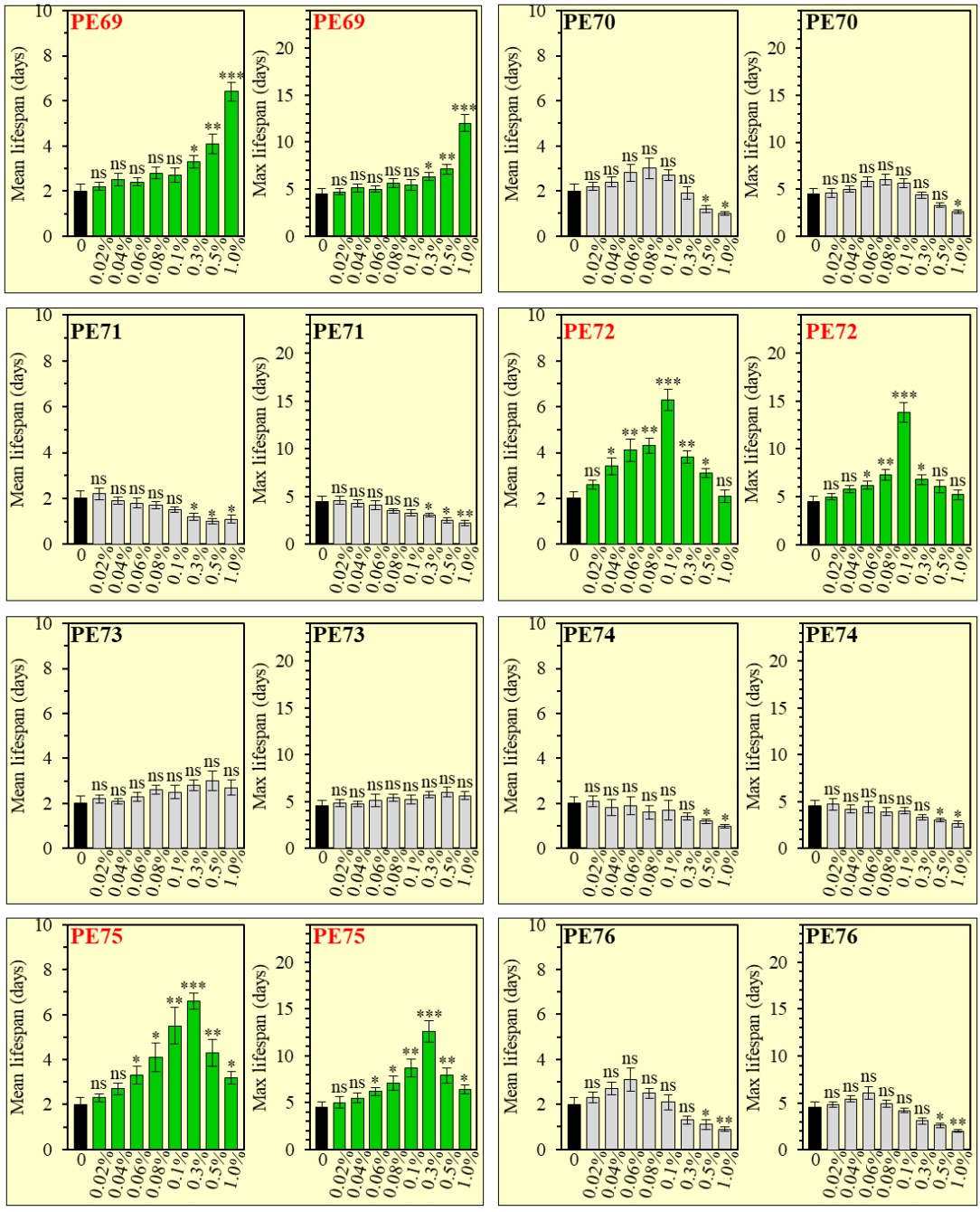

Figure 5.5. PE69, PE72 and PE75, but not PE70, PE71, PE73, PE74 or PE76, increase the mean and maximum CLS of WT yeast cultured under non-CR conditions on 2% (w/v) glucose. WT cells were cultured as described in the legend to Figure 5.1. The mean and maximum lifespans of chronologically aging WT strain cultured under non-CR conditions without a PE or with a PE added at various concentrations are shown; data are presented as means ± SEM (n = 6; * $p < 0.05$, ** $p < 0.01$, *** $p < 0.001$, *ns*, not significant; the *p* values for comparing the means of two groups were calculated as described in the legend to Figure 5.1). Note that PE70, PE71, PE74 and PE76 can decrease the CLS of WT yeast under non-CR conditions if added at a final concentration ranging from 0.3% (w/v) to 1.0% (w/v).

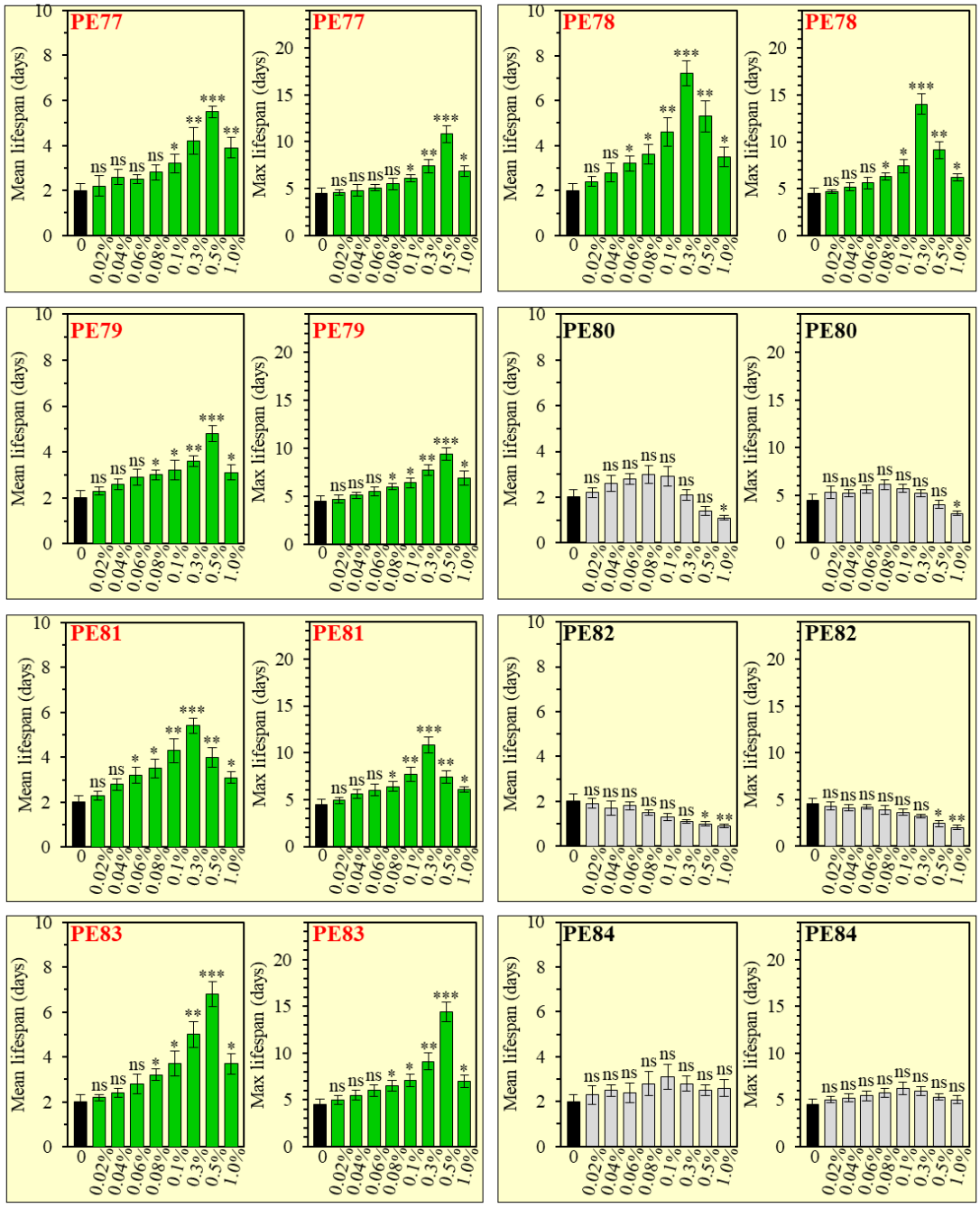

Figure 5.6. PE77, PE78, PE79, PE81 and PE83, but not PE80, PE82 or PE84, increase the mean and maximum CLS of WT yeast cultured under non-CR conditions on 2% (w/v) glucose. WT cells were cultured as described in the legend to Figure 5.1. The mean and maximum lifespans of chronologically aging WT strain cultured under non-CR conditions without a PE or with a PE added at various concentrations are shown; data are presented as means ± SEM (n = 6; * $p < 0.05$, ** $p < 0.01$, *** $p < 0.001$, *ns*, not significant; the p values for comparing the means of two groups were calculated as described in the legend to Figure 5.1). Note that PE80 and PE82 can decrease the CLS of WT yeast under non-CR conditions if added at a final concentration of 0.5% (w/v) or 1.0% (w/v).

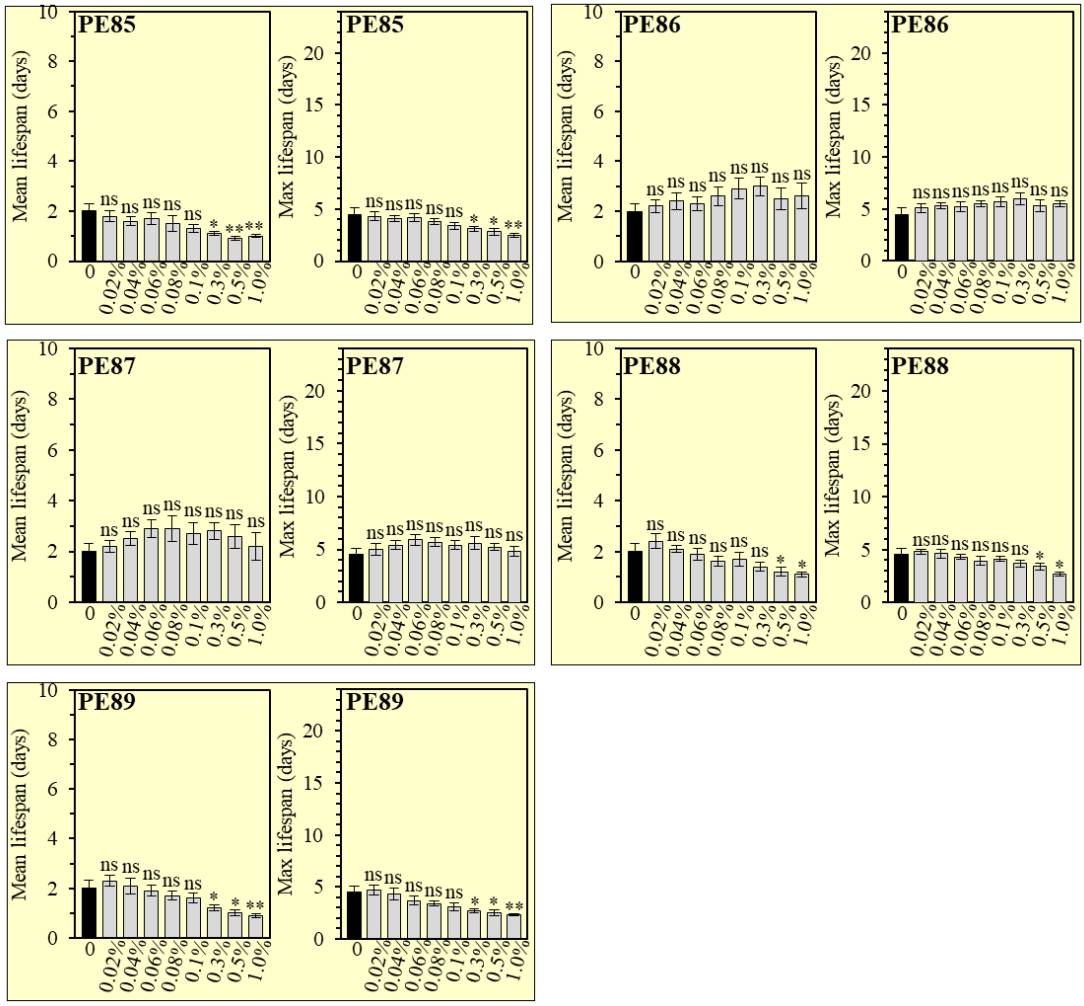

Figure 5.7. Neither PE85, PE86, PE87, PE88 nor PE89 can increase the mean or maximum CLS of WT yeast cultured under non-CR conditions on 2% (w/v) glucose. WT cells were cultured as described in the legend to Figure 5.1. The mean and maximum lifespans of chronologically aging WT strain cultured under non-CR conditions without a PE or with a PE added at various concentrations are shown; data are presented as means ± SEM (n = 6; * $p < 0.05$, ** $p < 0.01$, *ns*, not significant; the *p* values for comparing the means of two groups were calculated as described in the legend to Figure 5.1). Note that PE85, PE88 and PE89 can decrease the CLS of WT yeast under non-CR conditions if added at a final concentration ranging from 0.3% (w/v) to 1.0% (w/v).

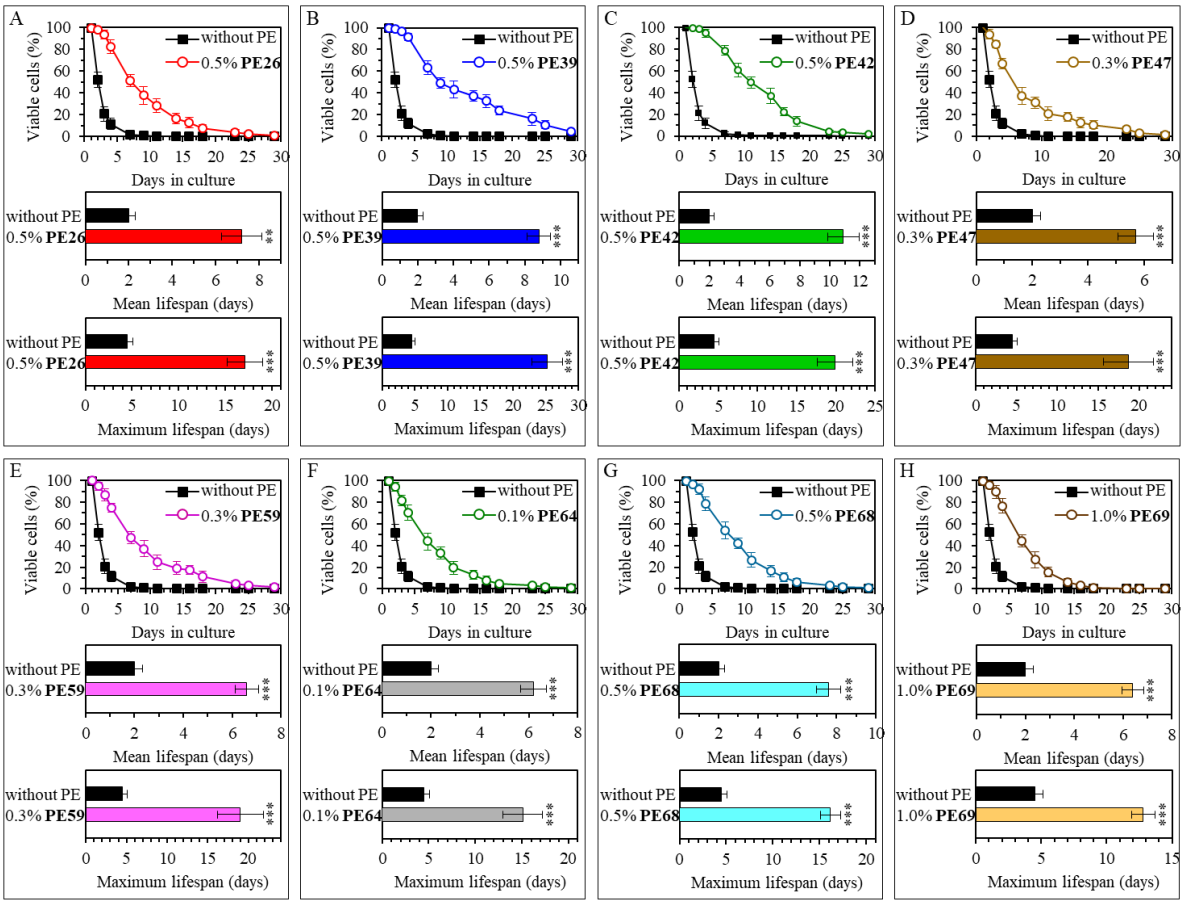

Figure 5.8. 0.5% (w/v) PE26, 0.5% (w/v) PE39, 0.5% (w/v) PE42, 0.3% (w/v) PE47, 0.3% (w/v) PE59, 0.1% (w/v) PE64, 0.5% (w/v) PE68 and 1.0% (w/v) PE69 exhibit the highest extending effects on the chronological lifespan (CLS) of wild-type (WT) yeast cultured under non-CR conditions on 2% (w/v) glucose. WT cells were cultured in the synthetic minimal YNB medium initially containing 2% (w/v) glucose, in the presence of a PE or its absence. In the cultures supplemented with a PE, ethanol was used as a vehicle at a final concentration of 2.5% (v/v). In the same experiment, WT cells were also subjected to ethanol-mock treatment by being cultured in the synthetic minimal YNB medium initially containing 2% (w/v) glucose and 2.5% (v/v) ethanol. Survival curves (the upper panels in A-H) and the mean and maximum lifespans (the lower two panels in A-H) of chronologically aging WT cells cultured without a PE (cells were subjected to ethanol-mock treatment) or with a PE (which was added at the concentration optimal for CLS extension) are shown. Data are presented as means ± SEM (n = 6). In the upper panels in A-H, CLS extension was significant for each of the PEs tested ($p < 0.05$; the p values for comparing each pair of survival curves were calculated using the logrank test as described in Materials and Methods). In the lower two panels in A-H, *$p < 0.05$, **$p < 0.01$, ***$p < 0.001$; the p values for comparing the means of two in groups were calculated using an unpaired two-tailed t test as described in Materials and Methods). Data for mock-treated WT cells are replicated in graphs A-H of this Figure. Data for WT cells cultured with a PE added at the concentration optimal for CLS extension are replicated in Figure 5.1 (for 0.5% (w/v) PE26, 0.5% (w/v) PE39 and 0.5% (w/v) PE42), Figure 5.2 (for 0.3% (w/v) PE47), Figure 5.3 (for 0.3% (w/v) PE59), Figure 5.4 (for 0.1% (w/v) PE64 and 0.5% (w/v) PE68) and Figure 5.5 (for 1.0% (w/v) PE69).

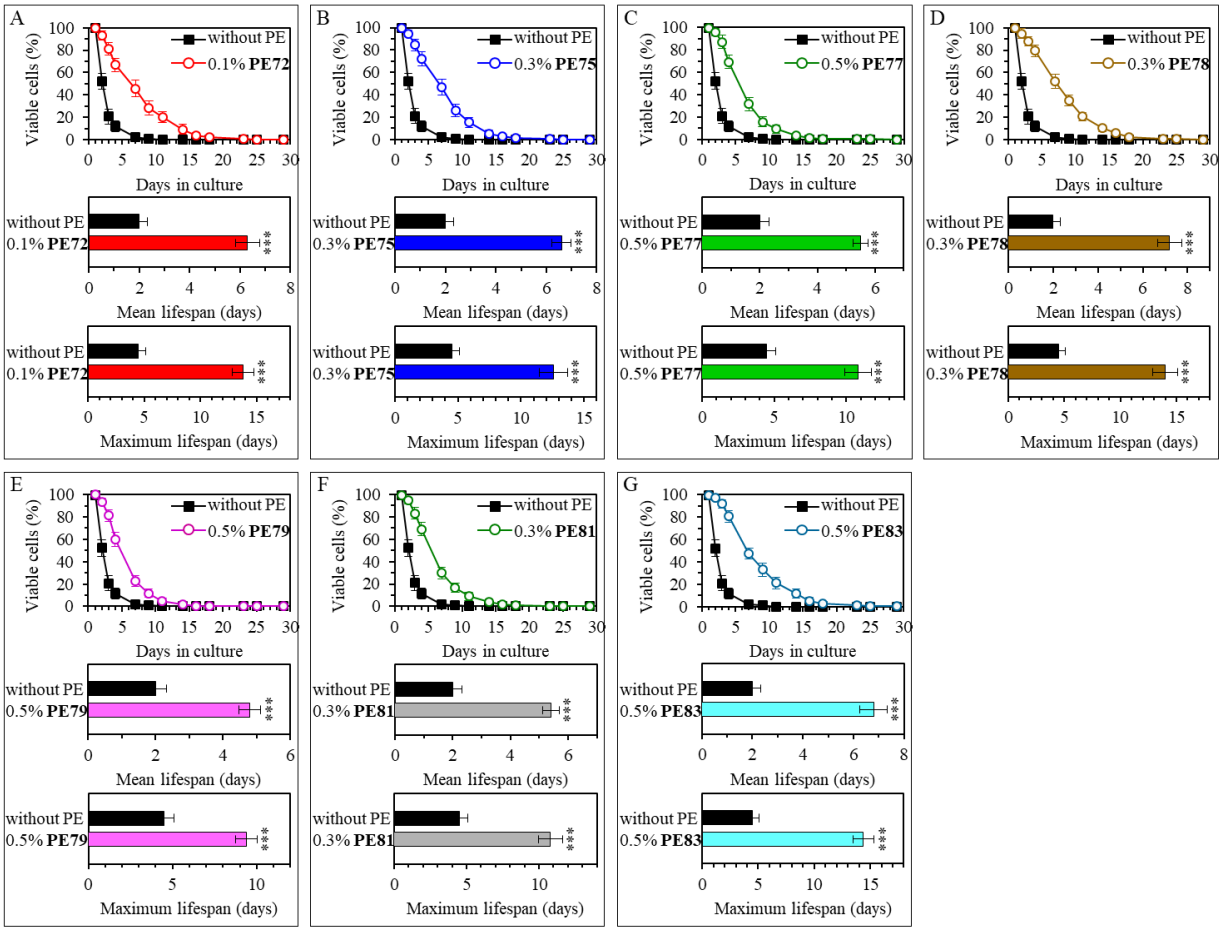

Figure 5.9. 0.1% (w/v) PE72, 0.3% (w/v) PE75, 0.5% (w/v) PE77, 0.3% (w/v) PE78, 0.5% (w/v) PE79, 0.3% (w/v) PE81 and 0.5% (w/v) PE83 exhibit the highest extending effects on the CLS of WT yeast cultured under non-CR conditions on 2% (w/v) glucose. WT cells were cultured in the synthetic minimal YNB medium initially containing 2% (w/v) glucose, in the presence of a PE or its absence. In the cultures supplemented with a PE, ethanol was used as a vehicle at a final concentration of 2.5% (v/v). In the same experiment, WT cells were also subjected to ethanol-mock treatment by being cultured in the synthetic minimal YNB medium initially containing 2% (w/v) glucose and 2.5% (v/v) ethanol. Survival curves (the upper panels in A-G) and the mean and maximum lifespans (the lower two panels in A-G) of chronologically aging WT cells cultured without a PE (cells were subjected to ethanol-mock treatment) or with a PE (which was added at the concentration optimal for CLS extension) are shown. Data are presented as means ± SEM (n = 6). In the upper panels in A-G, CLS extension was significant for each of the PEs tested ($p < 0.05$; the p values for comparing each pair of survival curves were calculated using the logrank test as described in Materials and Methods). In the lower two panels in A-G, *$p < 0.05$, **$p < 0.01$, ***$p < 0.001$; the p values for comparing the means of two in groups were calculated using an unpaired two-tailed t test as described in Materials and Methods). Data for mock-treated WT cells are replicated in graphs A-G of this Figure. Data for WT cells cultured with a PE added at the concentration optimal for CLS extension are replicated in Figure 5.4 (for 0.1% (w/v) PE72 and 0.3% (w/v) PE75) and Figure 5.6 (for 0.5% (w/v) PE77, 0.3% (w/v) PE78, 0.5% (w/v) PE79, 0.3% (w/v) PE81 and 0.5% (w/v) PE83).

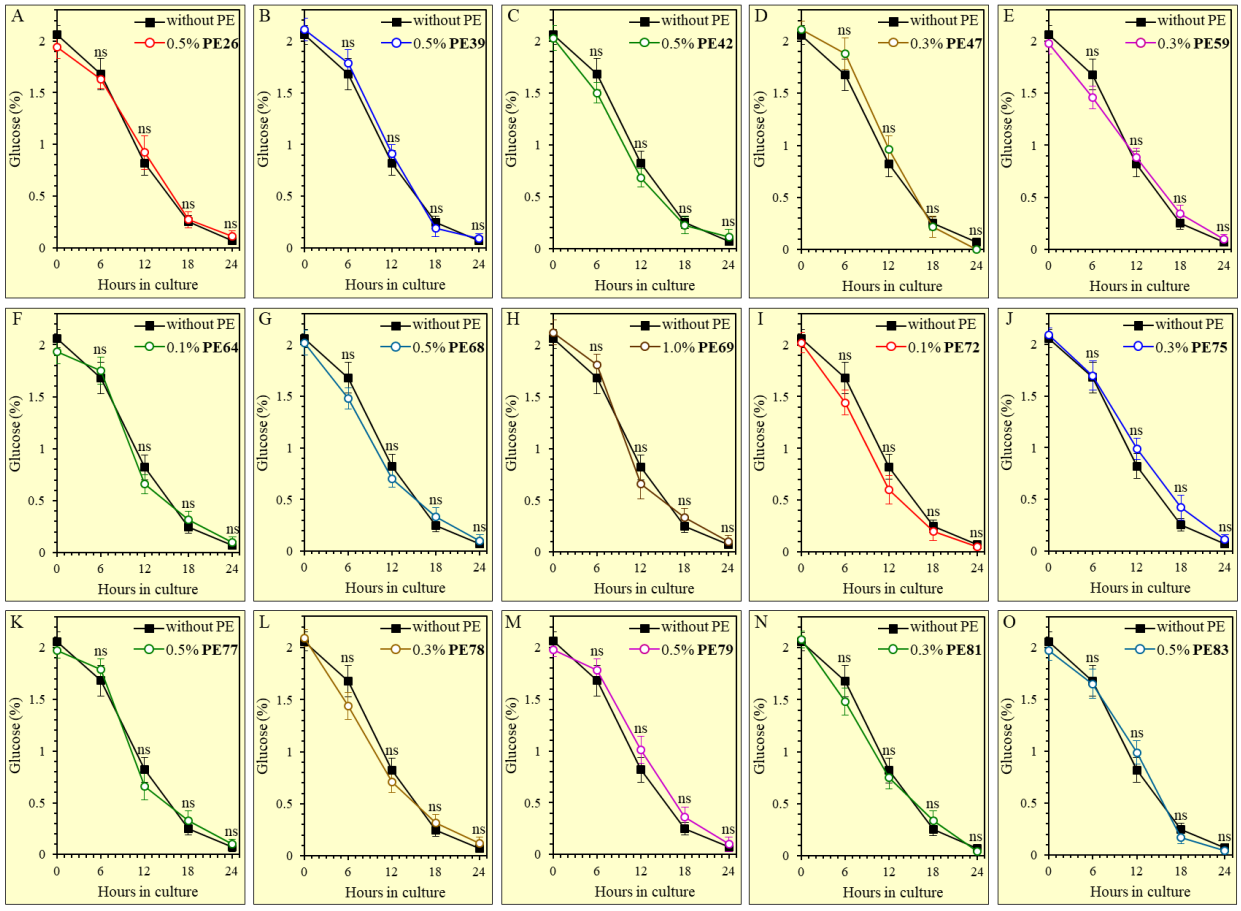

Figure 5.10. None of the fifteen longevity-extending PEs statistically significantly affects glucose consumption by WT yeast cultured under non-CR conditions on 2% (w/v) glucose. WT cells were cultured in the synthetic minimal YNB medium initially containing 2% (w/v) glucose, in the presence of a longevity-extending PE (which was added at an optimal longevity-extending concentration) or its absence. Glucose concentration in the extracellular medium was measured as described in Materials and Methods. Data are presented as means ± SEM (n = 3; *ns*, not significant).

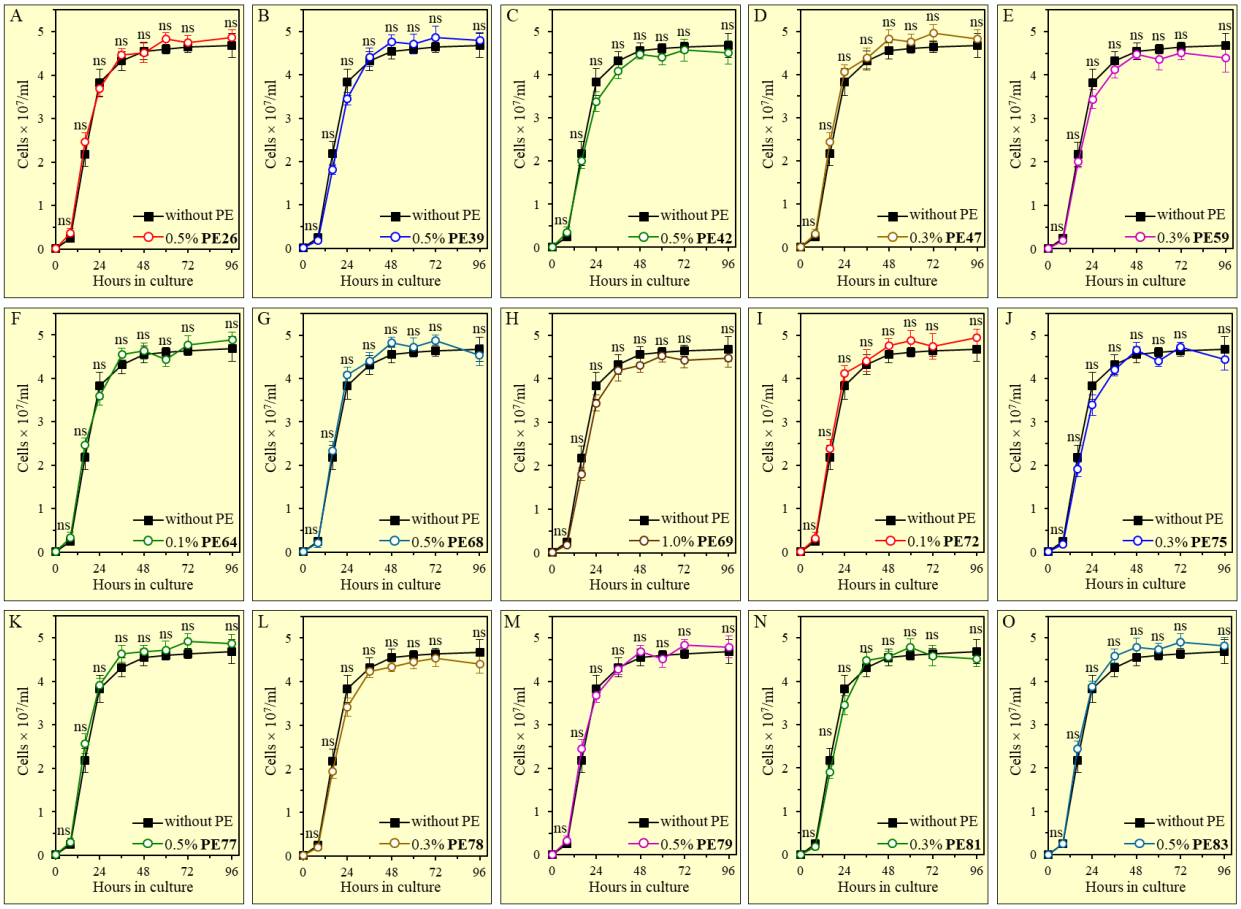

Figure 5.11. None of the fifteen longevity-extending PEs statistically significantly alters the growth rate and maximum cell yield of WT yeast cultures under non-CR conditions on 2% (w/v) glucose. WT cells were cultured in the synthetic minimal YNB medium initially containing 2% (w/v) glucose, in the presence of a longevity-extending PE (which was added at an optimal longevity-extending concentration) or its absence. Cell number was measured as described in Materials and Methods. Data are presented as means ± SEM (n = 3; *ns*, not significant).

5.3.2 Each of the fifteen longevity-prolonging PEs mimics longevity extension by CR

CR without malnutrition is a low-calorie dietary regimen that extends lifespan in many evolutionarily distant organisms and improves healthspan in laboratory rodents and rhesus monkeys [11, 15, 488-490]. Certain natural chemicals and synthetic drugs have been shown to elicit the CR-like lifespan-extending and healthspan-improving effects even under non-CR conditions (i.e., when calorie supply is not limited) [491-496]. These natural and synthetic chemical compounds are called CR mimetics (CRMs) if they not only extend longevity under non-CR conditions but also if they exhibit three other effects. First, CRMs do not impair food intake. Second, CRMs have CR-like effects on metabolism and physiology. Third, akin to CR, CRMs decrease the susceptibility to diverse stresses [492, 495]. In the present study, we found that each

of the fifteen longevity-extending PEs increases yeast CLS under non-CR conditions on 2% (w/v) glucose (Figures 5.1-5.6, Figures 5.8 and 5.9) and none of them compromises glucose intake during culturing under these conditions (Figure 5.10). Thus, it seems that all these PEs are CRMs. This conclusion is further supported by our observations that each of the fifteen longevity-extending PEs exhibits CR-like effects on several aspects of cell metabolism and stress resistance (see below).

Of note, we previously reported that if the CR diet is administered by culturing yeast in the YNB medium initially containing 0.5% (w/v) glucose, it significantly increases both the mean and maximum CLS of *S. cerevisiae* [461]. In the present study, we investigated how each of the fifteen PEs that extends longevity under non-CR conditions influences the longevity of yeast cultured under CR conditions on 0.5% (w/v) glucose. We found that eight of the fifteen PEs that prolong the longevity of chronologically aging yeast under non-CR conditions do not increase either the mean or the maximum CLS of *S. cerevisiae* under CR conditions (Figures 5.12 and 5.13). These PEs included 0.3% (w/v) PE47 (Figure 5.12D), 0.1% (w/v) PE64 (Figure 5.12F), 1.0% (w/v) PE69 (Figure 5.12H), 0.1% (w/v) PE72 (Figure 5.13A), 0.3% (w/v) PE75 (Figure 5.13B), 0.5% (w/v) PE77 (Figure 5.13C), 0.5% (w/v) PE79 (Figure 5.13E) and 0.3% (w/v) PE81 (Figure 5.13F). It seems conceivable, therefore, that each of these eight PEs increases yeast CLS because it modulates the same or highly overlapping sets of longevity-defining cellular processes under both CR and non-CR conditions.

We also revealed that seven of the fifteen PEs that extend yeast longevity under non-CR conditions also increase both the mean and maximum CLS of *S. cerevisiae* under CR conditions (Figures 5.12 and 5.13). 0.5% (w/v) PE26 (Figure 5.12A), 0.5% (w/v) PE39 (Figure 5.12B), 0.5% (w/v) PE42 (Figure 5.12C), 0.3% (w/v) PE59 (Figure 5.12E), 0.5% (w/v) PE68 (Figure 5.12G), 0.3% (w/v) PE78 (Figure 5.13D) and 0.5% (w/v) PE83 (Figure 5.13G) were among these PEs. Therefore, we hypothesize that each of these seven PEs increases yeast CLS under CR conditions because it regulates the sets of longevity-defining cellular processes that differ from (or only partially overlap with) the ones it modulates under non-CR conditions.

We then compared the efficiency with which each of the fifteen PEs increases yeast CLS under non-CR conditions to that under CR conditions. Our comparison revealed that each of these PEs extends the longevity of chronologically aging yeast under non-CR conditions significantly more efficiently than it does under CR conditions (Figure 5.14). This finding shows that each of

the fifteen PEs is a more effective longevity-prolonging intervention in chronologically aging yeast not-limited in calorie supply than it is in yeast placed on a CR diet.

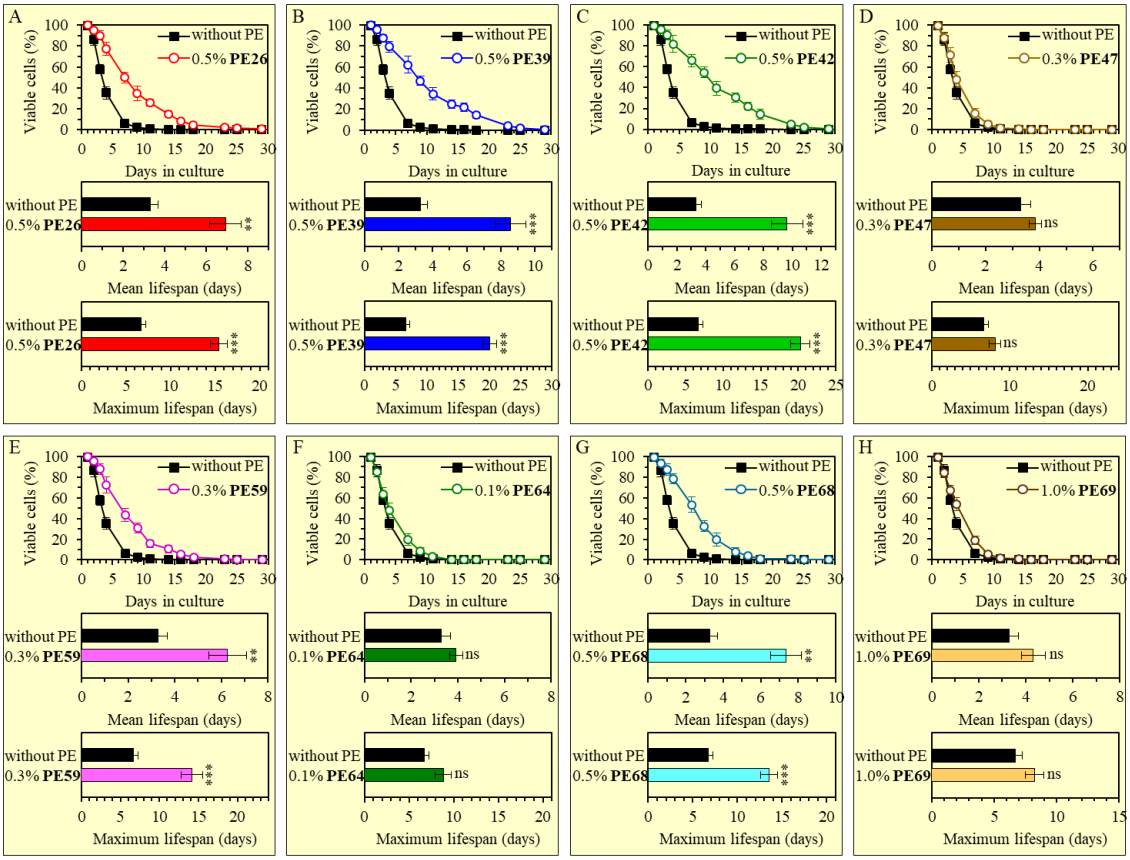

Figure 5.12. 0.5% (w/v) PE26, 0.5% (w/v) PE39, 0.5% (w/v) PE42, 0.3% (w/v) PE59 and 0.5% (w/v) PE68 (but not 0.3% (w/v) PE47, 0.1% (w/v) PE64 or 1.0% (w/v) PE69) extend the CLS of WT yeast cultured under CR conditions on 0.5% (w/v) glucose. WT cells were cultured in the synthetic minimal YNB medium initially containing 0.5% (w/v) glucose, in the presence of a PE or its absence. In the cultures supplemented with a PE, ethanol was used as a vehicle at a final concentration of 2.5% (v/v). In the same experiment, WT cells were also subjected to ethanol-mock treatment by being cultured in the synthetic minimal YNB medium initially containing 0.5% (w/v) glucose and 2.5% (v/v) ethanol. Survival curves (the upper panels in A-H) and the mean and maximum lifespans (the lower two panels in A-H) of chronologically aging WT cells cultured without a PE (cells were subjected to ethanol-mock treatment) or with a PE (which was added at the concentration optimal for CLS extension under non-CR conditions) are shown. Data are presented as means ± SEM (n = 6). In the upper panels in A-C, E and F, CLS extension was significant for each of the PEs tested ($p < 0.05$; the p values for comparing each pair of survival curves were calculated using the logrank test as described in Materials and Methods). In the lower two panels in A-C, E and F, $^{**}p < 0.01$, $^{***}p < 0.001$; the p values for comparing the means of two in groups were calculated using an unpaired two-tailed t test as described in Materials and Methods). In the upper panels in D, F and H, CLS extension was statistically not significant for each of the PEs tested (the p values for comparing each pair of survival curves were calculated

using the logrank test as described in Materials and Methods). In the lower two panels in D, F and H, *ns*, not significant; the *p* values for comparing the means of two in groups were calculated using an unpaired two-tailed *t* test as described in Materials and Methods). Data for mock-treated WT cells are replicated in graphs A-H of this Figure and graphs A-G of Figure 5.13.

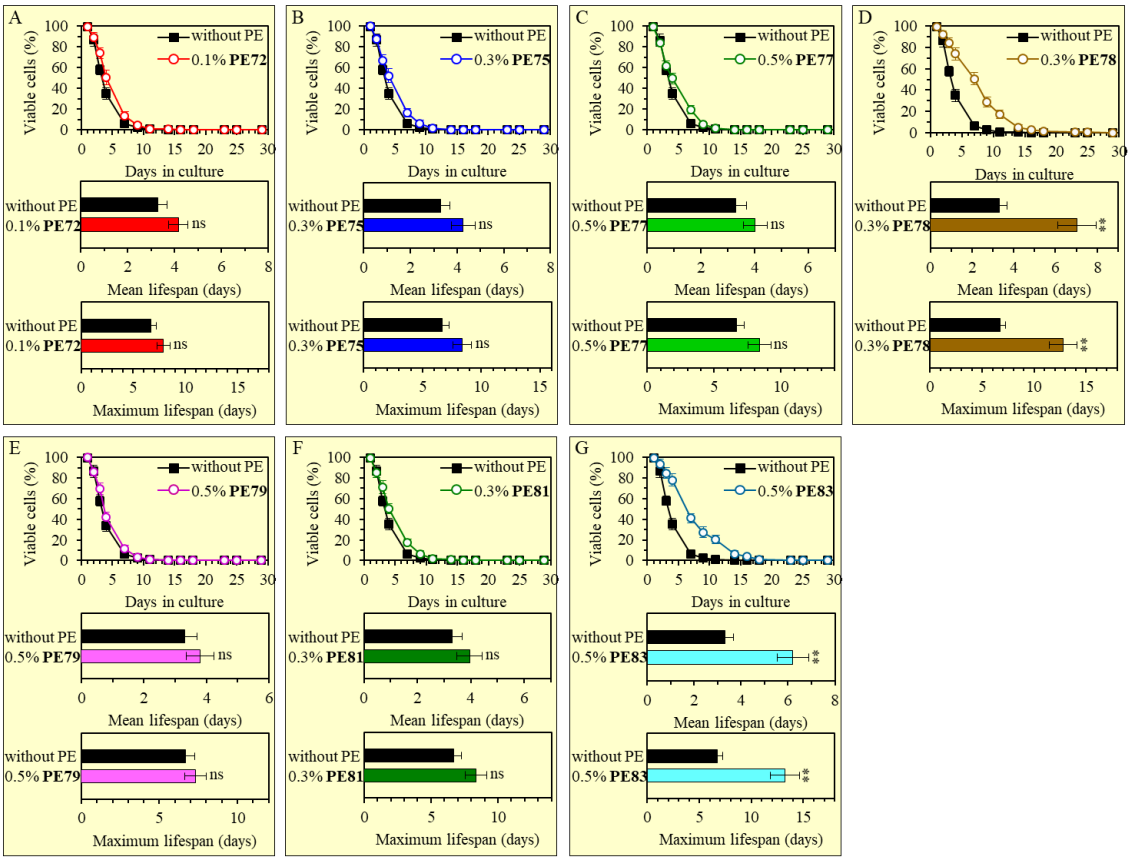

Figure 5.13. 0.3% (w/v) PE78 and 0.5% (w/v) PE83 (but not 0.1% (w/v) PE72, 0.3% (w/v) PE75, 0.5% (w/v) PE77, 0.5% (w/v) PE79 or 0.3% (w/v) PE81) extend the CLS of WT yeast cultured under CR conditions on 0.5% (w/v) glucose. WT cells were cultured in the synthetic minimal YNB medium initially containing 0.5% (w/v) glucose, in the presence of a PE or its absence. In the cultures supplemented with a PE, ethanol was used as a vehicle at a final concentration of 2.5% (v/v). In the same experiment, WT cells were also subjected to ethanol-mock treatment by being cultured in the synthetic minimal YNB medium initially containing 0.5% (w/v) glucose and 2.5% (v/v) ethanol. Survival curves (the upper panels in A-G) and the mean and maximum lifespans (the lower two panels in A-G) of chronologically aging WT cells cultured without a PE (cells were subjected to ethanol-mock treatment) or with a PE (which was added at the concentration optimal for CLS extension under non-CR conditions) are shown. Data are presented as means ± SEM (n = 6). In the upper panels in D and G, CLS extension was significant for each of the PEs tested ($p < 0.05$; the *p* values for comparing each pair of survival curves were calculated using the logrank test as described in Materials and Methods). In the lower two panels in D and G, $^{**}p < 0.01$; the *p* values for comparing the means of two in groups were calculated using an unpaired two-tailed *t* test as described in Materials and Methods). In the upper panels in A-C, E and F, CLS extension was statistically not significant for each of the PEs tested (the *p*

values for comparing each pair of survival curves were calculated using the logrank test as described in Materials and Methods). In the lower two panels in A-C, E and F, *ns*, not significant; the *p* values for comparing the means of two in groups were calculated using an unpaired two-tailed *t* test as described in Materials and Methods). Data for mock-treated WT cells are replicated in graphs A-G of this Figure and graphs A-H of Figure 5.12.

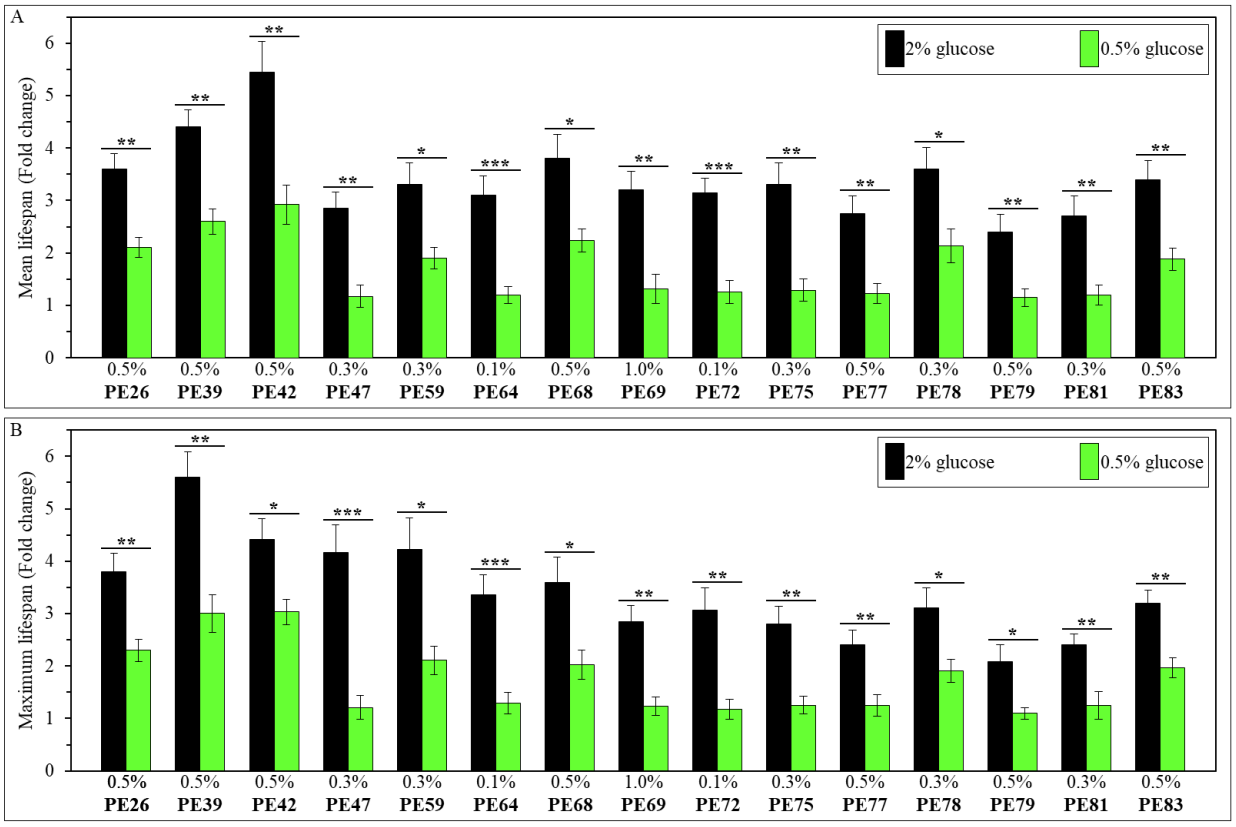

Figure 5.14. Each of the fifteen PEs extends the longevity of chronologically aging yeast under non-CR conditions on 2% (w/v) glucose significantly more efficiently than it does under CR conditions on 0.5% (w/v) glucose. WT cells were cultured in the synthetic minimal YNB medium initially containing 2% (w/v) or 0.5% (w/v) glucose, in the presence of a PE or its absence. In the cultures supplemented with a PE, ethanol was used as a vehicle at a final concentration of 2.5% (v/v). In the same experiment, WT cells were also subjected to ethanol-mock treatment by being cultured in the synthetic minimal YNB medium initially containing 0.5% (w/v) or 2% (w/v) glucose and 2.5% (v/v) ethanol. The extent to which each of the PE tested increases the mean (A) and maximum (B) CLS under non-CR and CR conditions was calculated based on the data presented in Figures 5.8, 5.9, 5.12 and 5.13. *$p < 0.05$, **$p < 0.01$, ***$p < 0.001$; the *p* values for comparing the means of two in groups were calculated using an unpaired two-tailed *t* test as described in Materials and Methods.

5.3.3 Each of the fifteen longevity-prolonging PEs is a geroprotector that extends the longevity of chronologically aging yeast because it decreases the rate of aging and stimulates a hormetic stress response

The rate of biological aging at the demographic level depends on the health of a population and can be determined by measuring an age-specific mortality rate of this population [359-361, 497, 498]. The mortality rates of evolutionarily distant organisms rise with age [359, 361, 367, 497, 498]. The Gompertz mortality function equation can describe this age-related rise in the mortality rate; this equation can be graphically presented as mortality rate data plotted on a semi-log scale against biological age [359, 361, 366, 367, 498]. Geroprotective interventions (also known as geroprotectors) can extend the longevity of organisms across phyla by causing three different effects on the Gompertz mortality function. Some geroprotectors can lower a so-called "baseline" mortality rate by eliciting an equal decline in the mortality rate at any biological age, without affecting a slope of the Gompertz mortality rate [359, 360, 498-500]. This slope is known as the coefficient G of the age-specific mortality rate; it is inversely proportional to the rate of biological aging [359, 360, 498-500]. Other geroprotectors can decrease the rate of biological aging because they lower the value of G, thus raising the value of the mortality rate doubling time (MRDT; MRDT = 0.693/G) [359, 360, 368, 498, 501]. The longevity-extending effects of some other geroprotective interventions can represent a combination of both the drop in the baseline mortality rate and the decline in the value of G (which raises the value of MRDT) [359-361, 498, 500].

We sought to investigate whether each of the fifteen PEs extends yeast longevity by lowering the baseline mortality rate, decreasing the rate of biological aging or by altering both these rates. Therefore, we conducted the Gompertz mortality rate analysis of WT cells under non-CR conditions that were either treated with one of these PEs or subjected to mock treatment. We found the following: 1) none of the fifteen longevity-prolonging PEs affects the baseline mortality rate, and 2) each of them elicits a decline in the coefficient G of the age-specific mortality rate and causes a rise in the value of MRDT (Figure 5.15). Based on these observations, we concluded that each of these PEs is a geroprotector that lengthens the longevity of chronologically aging yeast because it lowers the rate of aging but not because it decreases the baseline mortality rate.

Our data allow us to conclude that each of the fifteen longevity-prolonging PEs slows yeast chronological aging because it decreases both the extrinsic and the intrinsic rates of aging. This conclusion is based on our findings that each of these PEs extends both the mean and maximum CLS of yeast (Figures 5.8 and 5.9). The mean lifespans of evolutionarily distant organisms are thought to depend on specific environmental (extrinsic) factors to which cells are exposed before

they enter the quiescent or senescent state [359, 362-364]. In contrast, the maximum lifespans of organisms across species are considered to rely on specific cellular and organismal longevity modifiers that operate after cells enter the quiescent or senescent state [359, 362, 363, 365, 366].

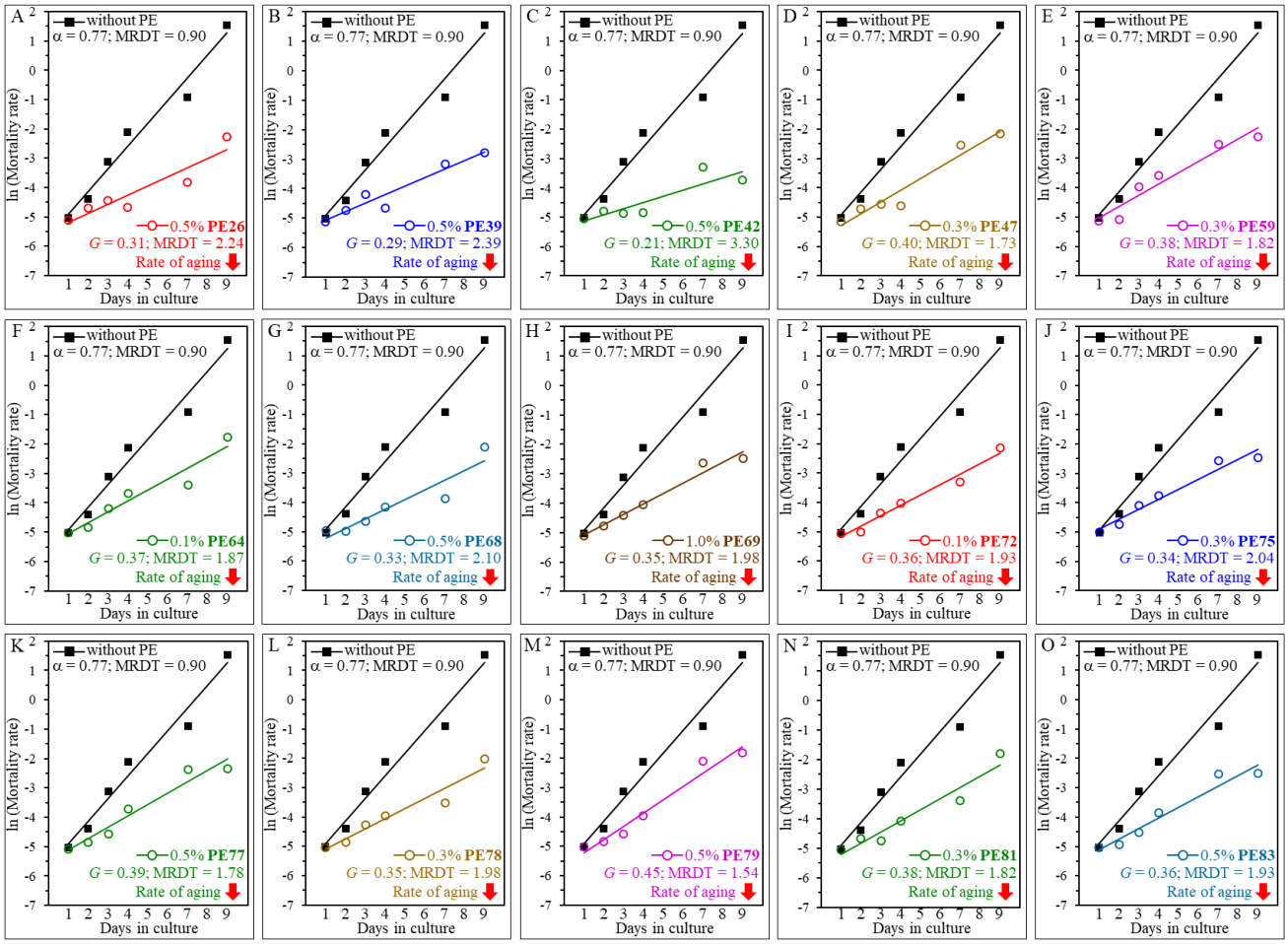

Figure 5.15. Each of the fifteen PEs extends the longevity of chronologically aging yeast because it decreases the rate of aging but not because it lowers the baseline mortality rate. WT cells were cultured in the synthetic minimal YNB medium initially containing 2% (w/v) glucose, in the presence of a PE or its absence. In the cultures supplemented with a PE, ethanol was used as a vehicle at a final concentration of 2.5% (v/v). In the same experiment, WT cells were also subjected to ethanol-mock treatment by being cultured in the synthetic minimal YNB medium initially containing 2% (w/v) glucose and 2.5% (v/v) ethanol. Survival curves shown in Figures 5.8 and 5.9 were used to calculate the age-specific mortality rates of chronologically aging WT yeast populations cultured without a PE (cells were subjected to ethanol-mock treatment) or with a PE (which was added at the concentration optimal for CLS extension). The natural logarithms of the mortality rate values for each time point were plotted against days of cell culturing. The values of the age-specific mortality rates, Gompertz slope (also known as the mortality rate coefficient G) and mortality rate doubling time (MRDT) were calculated as described in Materials and Methods. Each of the fifteen longevity-extending PEs caused a

substantial decline in the value of G and a considerable rise in the value of MRDT.

Our data also show that the ability of each of the fifteen longevity-prolonging PEs to decelerate yeast chronological aging correlates with (and is possibly caused by) its ability to elicit a "hormetic" stress response. A characteristic feature of such a response is a nonlinear and biphasic (i.e., inverted U-shaped or J-shaped) dose-response curve [112, 116, 254, 502, 503]. As we found, the curves that reflect relationships between PE concentrations and mean or maximum yeast CLS are inverted U-shaped or J-shaped for all these PEs [Figures 5.1-5.6].

5.3.4 Each of the fifteen geroprotective PEs intensifies mitochondrial respiration and alters the pattern of age-related changes in intracellular ROS

A distinct set of cellular processes is known to define the rate of yeast chronological aging [15, 17, 31, 32, 41, 59, 185, 238, 504-506]. These processes include coupled mitochondrial respiration [15, 17, 24, 32, 62, 118, 122, 125, 185]. We investigated how each of the fifteen geroprotective PEs influences an age-related chronology of changes in coupled mitochondrial respiration, which we measured as the rate of oxygen consumption by yeast cells. We found that each of these PEs causes a statistically significant increase in the rate of mitochondrial respiration on days 3 and 4 of culturing in the YNB medium initially containing 2% (w/v) glucose (Figure 5.16). On these days of culturing in the YNB medium with 2% (w/v) glucose, yeast cells are known to enter and proceed through a stationary (ST) phase of culturing [461].

We found that the fifteen geroprotective PEs belong to two different groups regarding their effects on the age-related dynamics of changes in coupled mitochondrial respiration under non-CR conditions. The first group of these PEs includes PE47, PE64, PE69, PE72, PE75, PE77, PE79 and PE81. Although all these geroprotective PEs allowed the yeast to maintain the rates of mitochondrial respiration significantly exceeding those in yeast subjected to ethanol-mock treatment, none of them prevented an age-related decline in mitochondrial respiration during the ST phase of culturing (Figures 5.16D, 5.16F, 5.16H, 5.16I, 5.16J, 5.16K, 5.16M and 5.16N). Of note, all geroprotective PEs from the first group were able to extend yeast CLS only under non-CR conditions on 2% (w/v) glucose (Figures 5.8D, 5.8F, 5.8H, 5.9A, 5.9B, 5.9C, 5.9E and 5.9F) but not under CR conditions on 0.5% (w/v) glucose (Figures 5.12D, 5.12F, 5.12H, 5.13A, 5.13B, 5.13C, 5.13E and 5.13F). The second group of geroprotective PEs includes PE26, PE39, PE42,

PE59, PE68, PE78 and PE83. These PEs increased the rate of mitochondrial respiration and sustained it high in ST-phase cultures that were recovered on day 4 (Figures 5.16A, 5.16B, 5.16C, 5.16E, 5.16G, 5.16L and 5.16O). Noteworthy, all geroprotective PEs from the second group were able to extend yeast CLS under both non-CR conditions on 2% (w/v) glucose (Figures 5.8A, 5.8B, 5.8C, 5.8E, 5.8G, 5.9D and 5.9G) and CR conditions on 0.5% (w/v) glucose (Figures 5.12A, 5.12B, 5.12C, 5.12E, 5.12G, 5.13D and 5.13G).

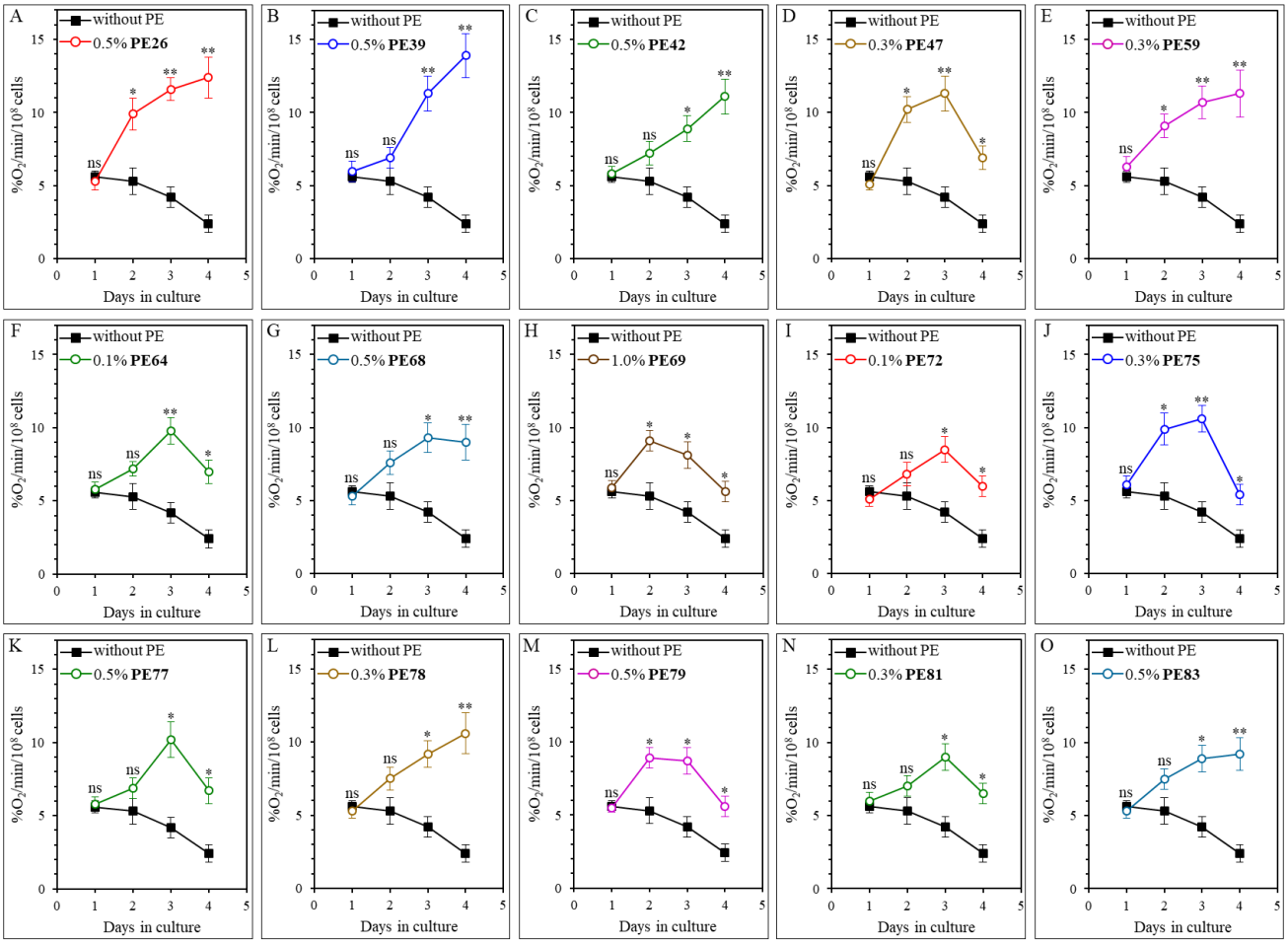

Figure 5.16. Each of the fifteen geroprotective PEs stimulates mitochondrial respiration in yeast cultured under non-CR conditions. WT cells were cultured in the synthetic minimal YNB medium initially containing 2% (w/v) glucose, in the presence of a PE or its absence. In the cultures supplemented with a PE, ethanol was used as a vehicle at a final concentration of 2.5% (v/v). In the same experiment, WT cells were also subjected to ethanol-mock treatment by being cultured in the synthetic minimal YNB medium initially containing 2% (w/v) glucose and 2.5% (v/v) ethanol. Oxygen uptake by live yeast cells was measured using polarography, as described in Materials and Methods. Age-related changes in the rate of mitochondrial oxygen consumption are shown. Data are presented as means ± SEM (n = 3; *$p < 0.05$, **$p < 0.01$, *ns*, not significant; the

p values for comparing the means of two in groups were calculated using an unpaired two-tailed *t* test as described in Materials and Methods).

The primary by-products of coupled mitochondrial respiration are several ROS [179, 376, 507]. These ROS of mitochondrial origin are known for their essential roles in defining the rate of aging in organisms across species, including *S. cerevisiae* [121, 185, 376, 507-513].

We found that all fifteen geroprotective PEs alter the age-related dynamics of changes in intracellular ROS (Figure 5.17). Each of these PEs slowed an age-related decline in intracellular ROS on days 3 and 4 of culturing, thus enabling a moderate but statistically significant rise in intracellular ROS during the ST phase (Figure 5.17). During the post-diauxic (PD) phase on day 2 of culturing, most of the fifteen geroprotective PEs (other than PE69; Figure 5.17H) elicited a modest but statistically decline in intracellular ROS (Figure 5.17).

Noteworthy, as described below, we found that there are two different groups of geroprotective PEs with respect to their effects on intracellular ROS during the logarithmic (L) phase on day 1.

PE47, PE64, PE69, PE72, PE75, PE77, PE79 and PE81 did not elicit a substantial change in intracellular ROS during the L phase of culturing on day 1 (Figures 5.17D, 5.17F, 5.17H, 5.17I, 5.17J, 5.17K, 5.17M and 5.17N). Al of them extended yeast CLS only under non-CR conditions on 2% (w/v) glucose (Figures 5.8D, 5.8F, 5.8H, 5.9A, 5.9B, 5.9C, 5.9E and 5.9F) but not under CR conditions on 0.5% (w/v) glucose (Figures 5.12D, 5.12F, 5.12H, 5.13A, 5.13B, 5.13C, 5.13E and 5.13F).

In contrast, PE26, PE39, PE42, PE59, PE68, PE78 and PE83 caused a substantial decline in intracellular ROS during the L phase of culturing on day 1 (Figures 5.17A, 5.17B, 5.17C, 5.17E, 5.17G, 5.17L and 5.17O). All these geroprotective PEs stimulated mitochondrial respiration and sustained it high in ST-phase cultures (Figures 5.16A, 5.16B, 5.16C, 5.16E, 5.16G, 5.16L and 5.16O). All of them were also capable of prolonging yeast CLS under both non-CR conditions on 2% (w/v) glucose (Figures 5.8A, 5.8B, 5.8C, 5.8E, 5.8G, 5.9D and 5.9G) and CR conditions on 0.5% (w/v) glucose (Figures 5.12A, 5.12B, 5.1210C, 5.12E, 5.12G, 5.13D and 5.13G).

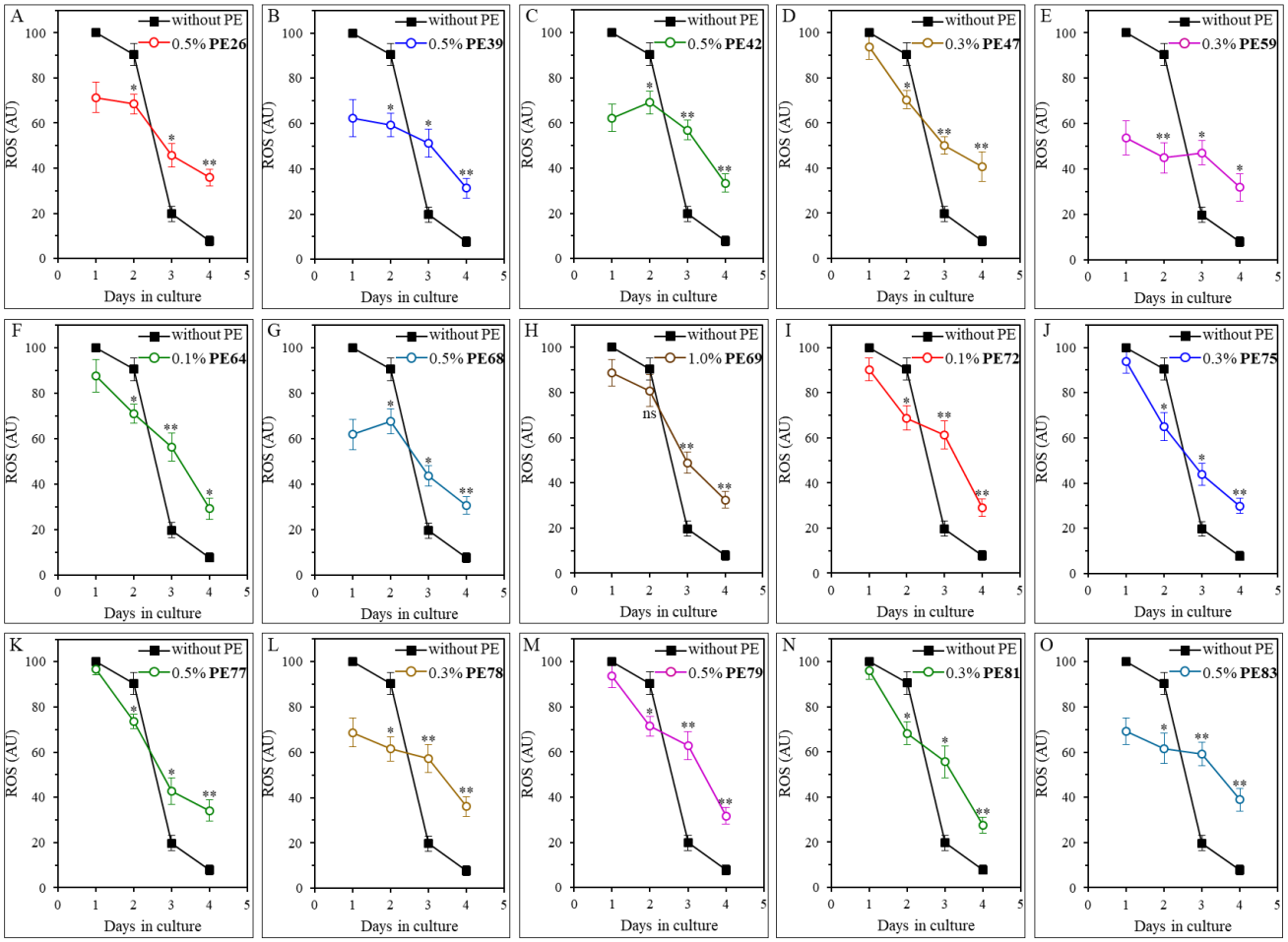

Figure 5.17. Each of the fifteen geroprotective PEs alters the age-related chronology of changes in intracellular ROS in yeast cultured under non-CR conditions. WT cells were cultured in the synthetic minimal YNB medium initially containing 2% (w/v) glucose, in the presence of a PE or its absence. In the cultures supplemented with a PE, ethanol was used as a vehicle at a final concentration of 2.5% (v/v). In the same experiment, WT cells were also subjected to ethanol-mock treatment by being cultured in the synthetic minimal YNB medium initially containing 2% (w/v) glucose and 2.5% (v/v) ethanol. The intracellular concentrations of ROS were measured in live yeast by fluorescence microscopy of dihydrorhodamine 123 staining, as described in Materials and Methods. Age-related changes in the intracellular concentration of ROS are shown. Data are presented as means ± SEM (n = 3; *$p < 0.05$, **$p < 0.01$, *ns*, not significant; the *p* values for comparing the means of two in groups were calculated using an unpaired two-tailed *t* test as described in Materials and Methods).

5.3.5 Each of the fifteen geroprotective PEs decreases the extent of age-related oxidative damage to cellular proteins, and many of them slow the aging-associated buildup of oxidatively impaired membrane lipids as well as mitochondrial and nuclear DNA

An age-related rise in the intracellular ROS above a toxic threshold has been shown to

cause oxidative damage to cellular proteins, lipids and nucleic acids [59, 123, 179, 372-379, 507, 510-513]. The aging-associated accumulation of these oxidized macromolecules is one of the essential contributors to the aging process in yeast and other organisms [59, 123, 179, 372-379, 507, 510-513].

Each of the fifteen geroprotective PEs perturbed the age-related chronology of changes in intracellular ROS (see above). Therefore, we investigated whether each of them also influences the aging-associated accumulation of oxidatively impaired proteins, lipids and DNA in yeast cells cultured under non-CR conditions on 2% (w/v) glucose.

We found that all fifteen geroprotective PEs elicit a statistically significant decline in the abundance of oxidatively damaged (carbonylated) cellular proteins in ST-phase cultures recovered on day 4 (Figure 5.18).

We noticed that these geroprotective PEs belong to two different groups regarding their effects on the extent of protein carbonylation in yeast cells taken on day 1, 2 or 3 of culturing.

The first group of these PEs includes PE47, PE64, PE69, PE72, PE75, PE77, PE79 and PE81, all of which did not cause a statistically significant decline in the abundance of oxidatively damaged proteins within yeast cells recovered on day 1, 2 or 3 of culturing (Figures 5.18D, 5.18F, 5.18H, 5.18I, 5.18J, 5.18K, 5.18M and 5.18N). All geroprotective PEs from the first group extended yeast CLS only under non-CR conditions on 2% (w/v) glucose (Figures 5.8D, 5.8F, 5.8H, 5.9A, 5.9B, 5.9C, 5.9E and 5.9F) but not under CR conditions on 0.5% (w/v) glucose (Figures 5.12D, 5.12F, 5.12H, 5.13A, 5.13B, 5.13C, 5.13E and 5.13F).

The second group of geroprotective PEs includes PE26, PE39, PE42, PE59, PE68, PE78 and PE83, all of which substantially lowered the abundance of oxidatively damaged proteins in yeast recovered on day 1, 2 or 3 of culturing (Figures 5.18A, 5.18B, 5.18C, 5.18E, 5.18G, 5.18L and 5.18O). Only for PE78 and PE83 such effects on protein carbonylation were not statistically significant in yeast taken on day 1 of culturing (Figures 5.18L and 5.18O). All geroprotective PEs from the second group increased yeast CLS under both non-CR conditions on 2% (w/v) glucose (Figures 5.8A, 5.8B, 5.8C, 5.8E, 5.8G, 5.9D and 5.9G) and CR conditions on 0.5% (w/v) glucose (Figures 5.12A, 5.12B, 5.12C, 5.12E, 5.12G, 5.13D and 5.13G).

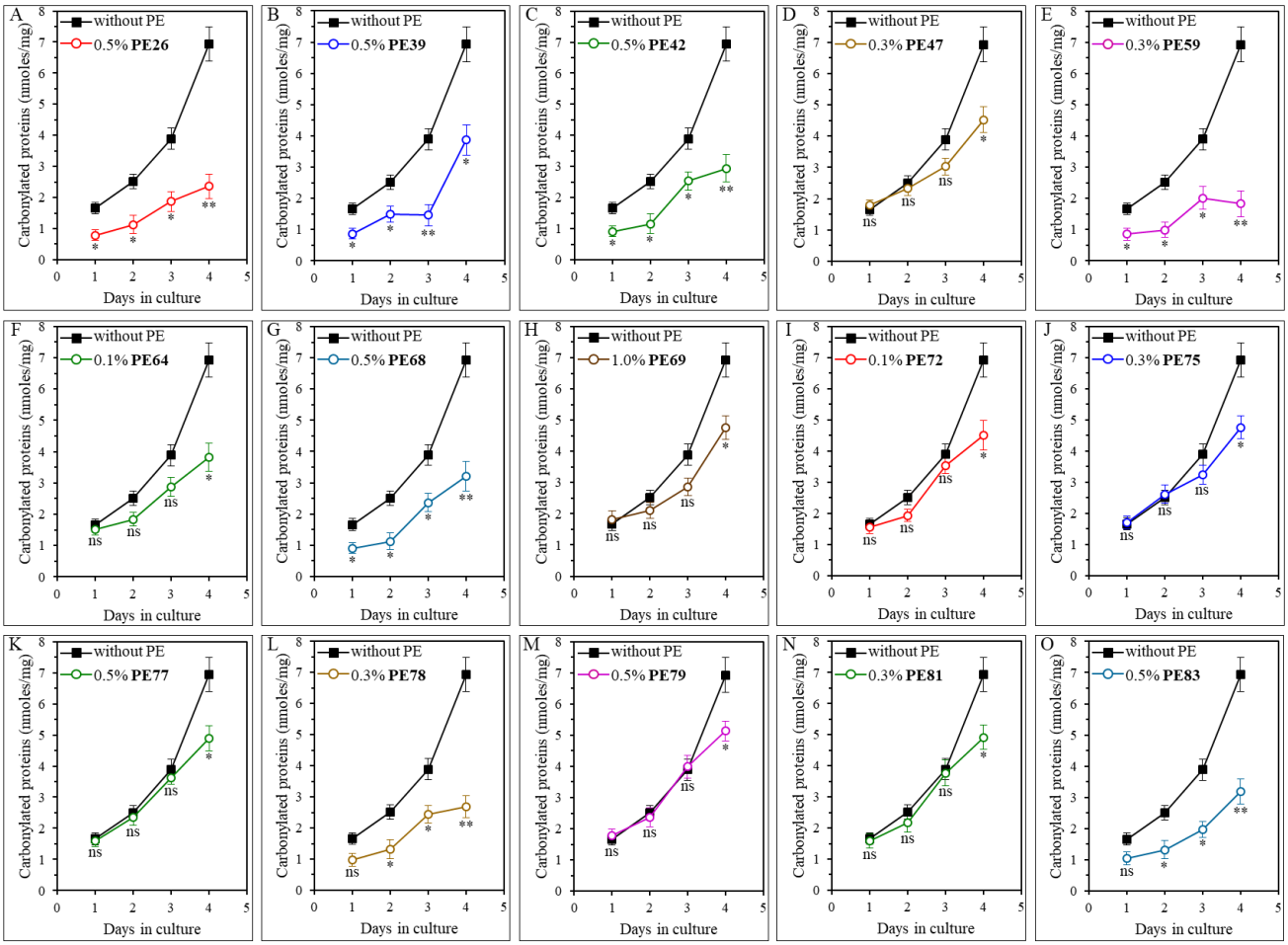

Figure 5.18. Each of the fifteen geroprotective PEs decreases the extent of age-related oxidative damage to cellular proteins in yeast cultured under non-CR conditions. WT cells were cultured in the synthetic minimal YNB medium initially containing 2% (w/v) glucose, in the presence of a PE or its absence. In the cultures supplemented with a PE, ethanol was used as a vehicle at a final concentration of 2.5% (v/v). In the same experiment, WT cells were also subjected to ethanol-mock treatment by being cultured in the synthetic minimal YNB medium initially containing 2% (w/v) glucose and 2.5% (v/v) ethanol. The concentrations of oxidatively damaged (carbonylated) proteins were measured as described in Materials and Methods. Age-related changes in the intracellular concentration (nmoles/mg protein) of carbonylated proteins are shown. Data are presented as means ± SEM (n = 3; *$p < 0.05$, **$p < 0.01$, *ns*, not significant; the *p* values for comparing the means of two in groups were calculated using an unpaired two-tailed *t* test as described in Materials and Methods).

Our analysis of how each of the fifteen geroprotective PEs influences the extent of oxidative damage to membrane lipids revealed that PE26, PE39, PE42, PE47, PE59, PE64, PE68, PE69, PE72, PE75, PE78 and PE83 statistically significantly decrease it in ST-phase cultures recovered on day 4 (Figures 5.19A-5.19J, 5.19L and 5.19O). For PE77, PE79 and PE81, a decline

in the abundance of oxidatively impaired membrane lipids in yeast cells taken on day 4 of culturing was noticeable but not statistically significant (Figures 5.19K, 5.19M and 5.19N). We also found that only those of the fifteen geroprotective PEs that extend yeast CLS under both non-CR and CR conditions significantly lower the abundance of oxidized membrane lipids even in yeast recovered on day 3 of culturing on 2% (w/v) glucose (Figures 5.19A, 5.19B, 5.19C, 5.19E, 5.19G, 5.19L and 5.19O for PE26, PE39, PE42, PE59, PE68, PE78 and PE83). In contrast, a decline in the abundance of oxidatively damaged membrane lipids on day 3 of culturing on 2% (w/v) glucose was noticeable but not statistically significant for any of the geroprotective PEs that increased yeast CLS only under non-CR conditions (Figures 5.19D, 5.19F, 5.19H, 5.19I, 5.19J, 5.19K, 5.19M and 5.19N for PE47, PE64, PE69, PE72, PE75, PE77, PE79 and PE81).

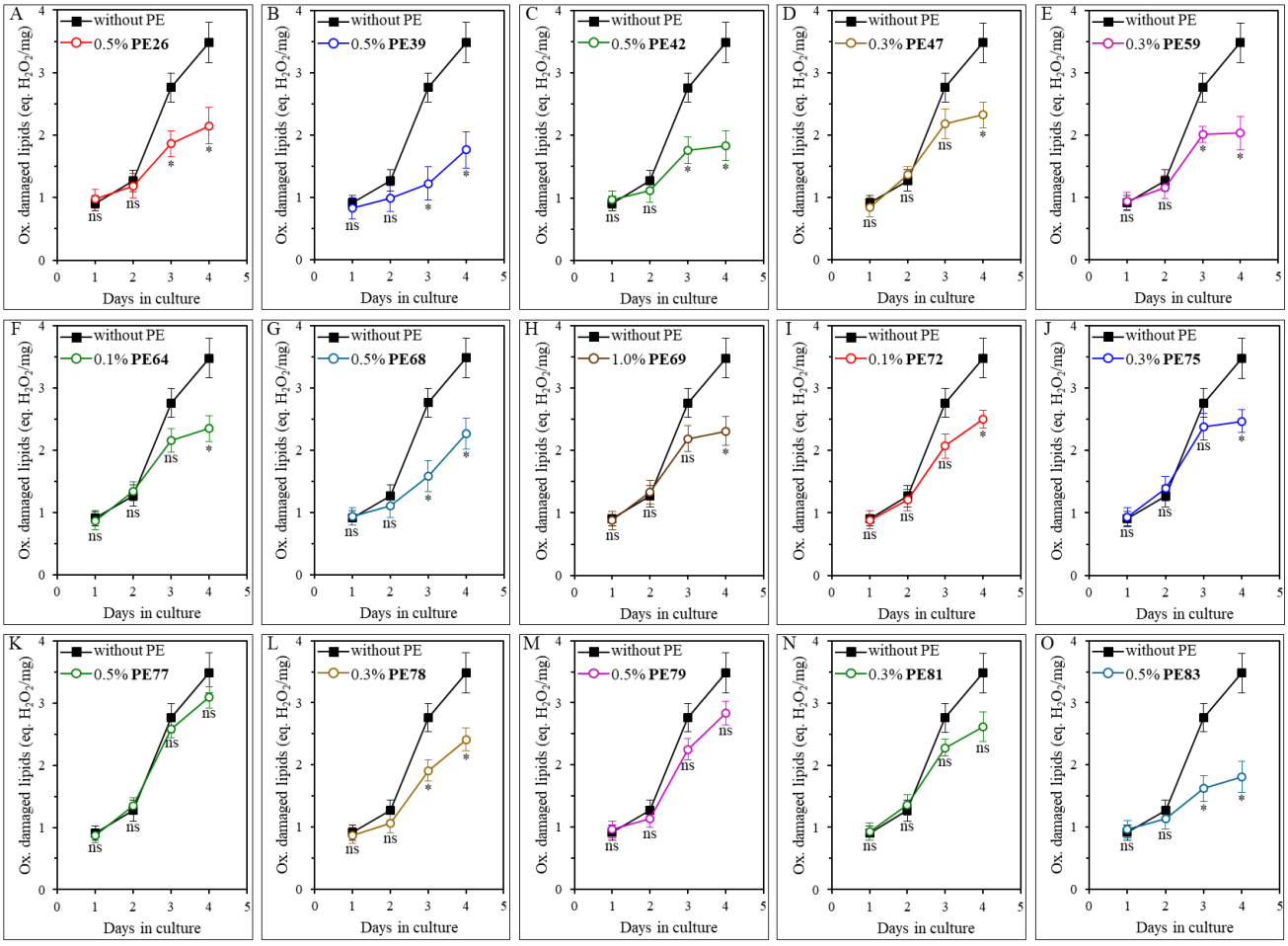

Figure 5.19. Many of the fifteen geroprotective PEs slow the aging-associated buildup of oxidatively impaired membrane lipids in yeast cultured under non-CR conditions. WT cells were cultured in the synthetic minimal YNB medium initially containing 2% (w/v) glucose, in the

presence of a PE or its absence. In the cultures supplemented with a PE, ethanol was used as a vehicle at a final concentration of 2.5% (v/v). In the same experiment, WT cells were also subjected to ethanol-mock treatment by being cultured in the synthetic minimal YNB medium initially containing 2% (w/v) glucose and 2.5% (v/v) ethanol. The concentrations of oxidatively damaged membrane lipids were measured as described in Materials and Methods. Age-related changes in the intracellular concentration (equivalents of nmoles H_2O_2/mg protein) of oxidatively damaged membrane lipids are shown. Data are presented as means ± SEM (n = 3; *$p < 0.05$, *ns*, not significant; the *p* values for comparing the means of two in groups were calculated using an unpaired two-tailed *t* test as described in Materials and Methods).

We also examined how each of the fifteen geroprotective PEs influences the extent of oxidative damage to mitochondrial DNA (mtDNA) and nuclear DNA (nDNA). The oxidative damage to each of these two types of DNA molecules is known to cause an aging-associated buildup of mutations in mtDNA and nDNA [514-518]. Therefore, we investigated the effect of each of the fifteen geroprotective PEs on the frequencies of spontaneous point mutations in the *RIB2* and *RIB3* genes of mtDNA [32, 110] as well as the frequencies of spontaneous point mutations in the *CAN1* gene of nDNA [32 110]. We found that all fifteen geroprotective PEs statistically significantly decrease the incidences of *rib2* and *rib3* mutations in mtDNA of yeast recovered from the ST phase on day 4 but not on any other day of culturing (Figure 5.20). Furthermore, PE26, PE39, PE42, PE59, PE64, PE69, PE75, PE78, PE79 and PE81 caused a statistically significant decline in the frequencies of can1 mutations in nDNA of yeast cells that were taken from the ST phase on day 4 of culturing only (Figures 5.21A-5.21C, 5.21E, 5.21F, 5.21H, 5.21J and 5.21L-5.21N). In contrast, neither PE47, PE68, PE72, PE77 nor PE83 elicited a significant change in the incidences of these mutations in nDNA of yeast recovered on any day of culturing (Figures 5.21D, 5.21G, 5.21I, 5.21K and 5.21O, respectively).

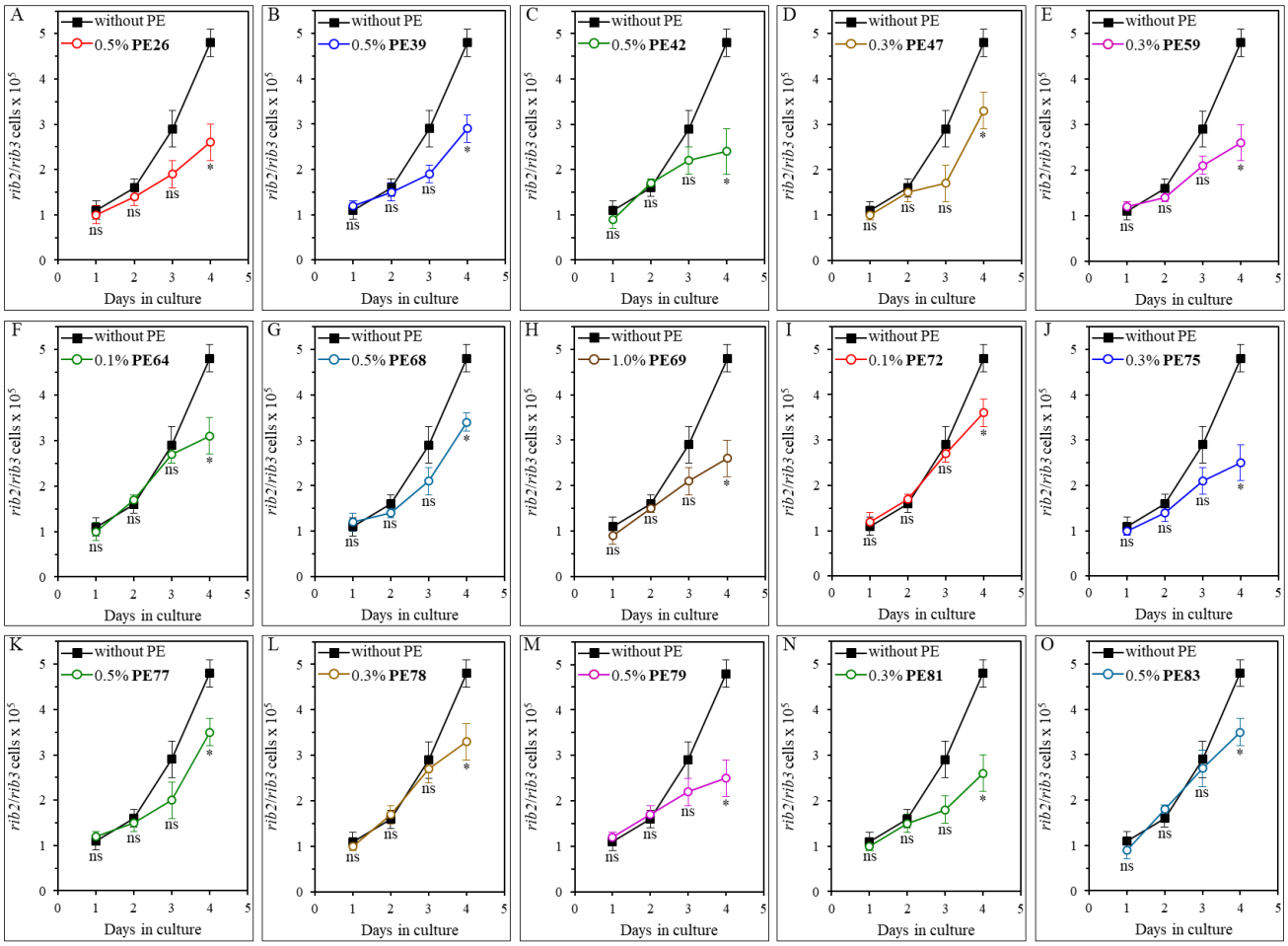

Figure 5.20. Each of the fifteen geroprotective PEs decreases the frequencies of *rib2* and *rib3* mutations in mitochondrial DNA (mtDNA) of yeast cultured under non-CR conditions. WT cells were cultured in the synthetic minimal YNB medium initially containing 2% (w/v) glucose, in the presence of a PE or its absence. In the cultures supplemented with a PE, ethanol was used as a vehicle at a final concentration of 2.5% (v/v). In the same experiment, WT cells were also subjected to ethanol-mock treatment by being cultured in the synthetic minimal YNB medium initially containing 2% (w/v) glucose and 2.5% (v/v) ethanol. The incidences of spontaneous point mutations in the *RIB2* and *RIB3* genes of mtDNA were measured as described in Materials and Methods. Age-related changes in the frequencies of these mtDNA mutations are shown. Data are presented as means ± SEM (n = 3; *$p < 0.05$, *ns*, not significant; the *p* values for comparing the means of two in groups were calculated using an unpaired two-tailed *t* test as described in Materials and Methods).

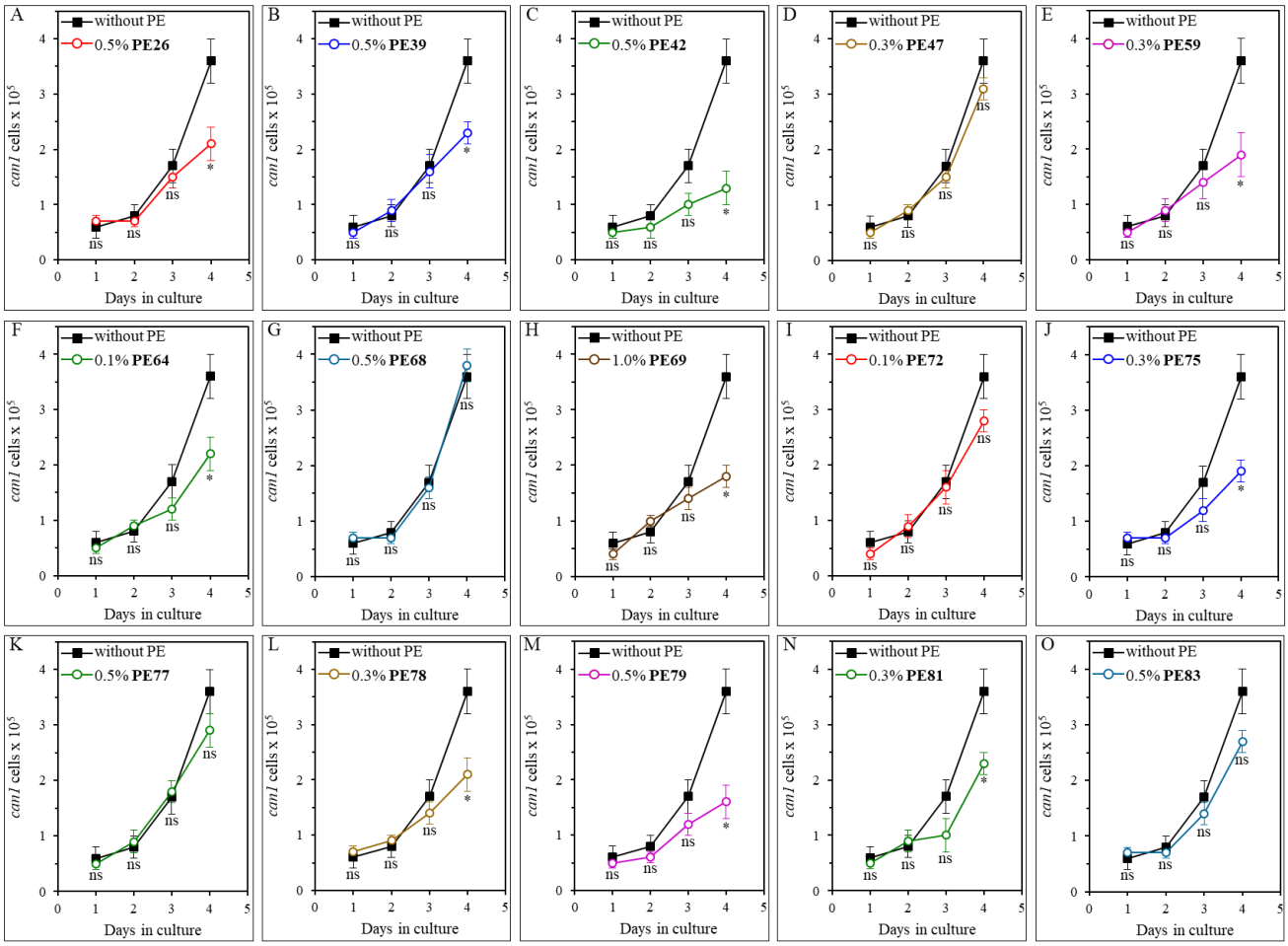

Figure 5.21. PE26, PE39, PE42, PE59, PE64, PE69, PE75, PE78, PE79 and PE81 (but not PE47, PE68, PE72, PE77 or PE83) cause a statistically significant decline in the frequencies of *can1* mutations in nuclear DNA (nDNA) of yeast cultured under non-CR conditions. WT cells were cultured in the synthetic minimal YNB medium initially containing 2% (w/v) glucose, in the presence of a PE or its absence. In the cultures supplemented with a PE, ethanol was used as a vehicle at a final concentration of 2.5% (v/v). In the same experiment, WT cells were also subjected to ethanol-mock treatment by being cultured in the synthetic minimal YNB medium initially containing 2% (w/v) glucose and 2.5% (v/v) ethanol. The incidences of spontaneous point mutations in the *CAN1* gene of nDNA were measured as described in Materials and Methods. Age-related changes in the frequencies of these nDNA mutations are shown. Data are presented as means ± SEM (n = 3; *$p < 0.05$, *ns*, not significant; the *p* values for comparing the means of two in groups were calculated using an unpaired two-tailed *t* test as described in Materials and Methods).

5.3.6 Each of the fifteen geroprotective PEs increases cell resistance to long-term oxidative and thermal stresses

Genetic, dietary and chemical interventions that decrease cell susceptibility to chronic

(long-term) oxidative and/or thermal stresses have been shown to decelerate the aging process and extend longevity in yeast and other organisms across species [15, 17, 32, 68, 112, 178, 179, 254, 380-382, 501, 503]. Therefore, we investigated the effect of each of the fifteen geroprotective PEs on the susceptibility of chronologically aging yeast cells to these two types of chronic stresses.

To examine aging-associated changes in cell susceptibility to these long-term stresses, we recovered aliquots of yeast cells on days 1, 2, 3 and 4 of culturing under non-CR conditions in liquid YNB medium with 2% (w/v) glucose. To assess cell susceptibility to chronic oxidative stress, we spotted serial dilutions of these cell aliquots on solid YEP medium with 2% (w/v) glucose and 5 mM hydrogen peroxide and incubated them for 3 days. To assess cell susceptibility to chronic thermal stress, we spotted serial dilutions of these cell aliquots on solid YEP medium with 2% (w/v) glucose, incubated at 60^{o}C for 60 min, transferred the plates to 30^{o}C and incubated at this temperature for 3 days.

We found that each of the fifteen geroprotective PEs makes yeast cells more resistant to chronic oxidative and thermal stresses, especially cells in ST-phase cultures recovered on days 3 and 4 (Figures 5.22B and 5.22C, respectively).

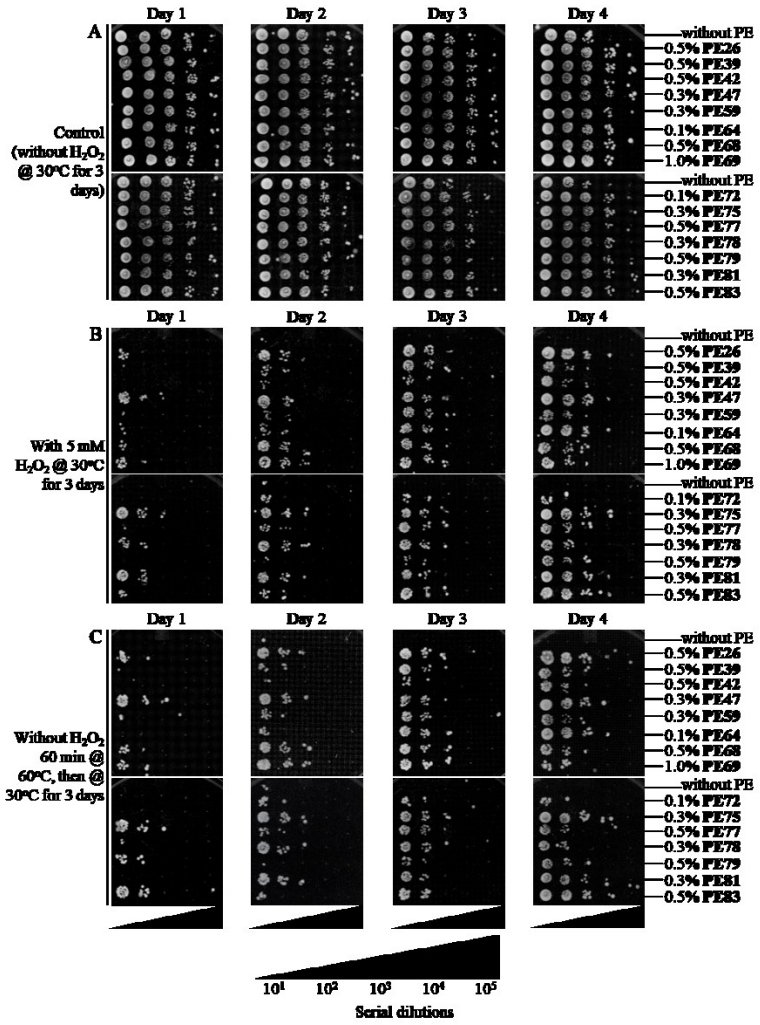

Figure 5.22. Each of the fifteen geroprotective PEs makes yeast more resistant to chronic (long-term) oxidative and thermal stresses. WT cells were cultured in the synthetic minimal YNB medium initially containing 2% (w/v) glucose, in the presence of a PE or its absence. In the cultures supplemented with a PE, ethanol was used as a vehicle at a final concentration of 2.5% (v/v). In the same experiment, WT cells were also subjected to ethanol-mock treatment by being cultured in the synthetic minimal YNB medium initially containing 2% (w/v) glucose and 2.5% (v/v) ethanol. Spot assays for examining cell resistance to chronic oxidative (B) and thermal (C) stresses were performed as described in Materials and Methods. (A) In control samples, serial 10-fold dilutions of cells recovered on different days of culturing were spotted on plates with solid YEP medium containing 2% (w/v) glucose. All pictures were taken after a 3-d incubation at 30°C. (B) In samples subjected to long-term oxidative stress, serial 10-fold dilutions of cells recovered on different days of culturing were spotted on plates with solid YEP medium containing 2% (w/v) glucose and 5 mM hydrogen peroxide. All pictures were taken after a 3-d incubation at 30°C. (C) In samples subjected to long-term thermal stress, serial 10-fold dilutions of cells recovered on different days of culturing were spotted on plates with solid YEP medium containing 2% (w/v) glucose, incubated at 60°C for 60 min and then transferred to 30°C. All pictures were taken after a 3-d incubation at 30°C.

5.4 Discussion

We discovered fifteen PEs that extend the longevity of chronologically aging budding yeast. All these PEs originate from plants used in traditional Chinese and other herbal medicines or the Mediterranean and other long-established diets. However, none of these PEs has been previously known for its ability to prolong lifespan in yeast or other organisms.

Our data indicate that each of the fifteen longevity-extending PEs prolongs yeast CLS not because it slows the metabolism of glucose, the only source of carbon and energy added to the growth medium. We also revealed that the longevity-extending ability of each of the fifteen PEs is not caused by its negative effect on the proliferation of yeast cells. Thus, it seems likely that none of these PEs can prolong yeast CLS because it slows the formation and release of harmful products of cell proliferation.

Our study provides evidence that each of the fifteen longevity-extending PEs satisfies all the criteria previously proposed for a CRM. CRMs are chemical interventions that can mimic the CR-like lifespan-increasing and healthspan-improving effects even if calorie supply is not limited [491-496]. Indeed, we uncovered the following. First, each of the fifteen PEs prolongs yeast CLS under non-CR conditions. Second, none of these PEs impairs glucose uptake and metabolism. Third, each of them exhibits CR-like effects on specific aspects of metabolism and physiology; these effects include an increased rate of coupled mitochondrial respiration, an altered chronology of changes in intracellular ROS, and a decline in the oxidative damage to cellular proteins, membrane lipids and mtDNA. Fourth, each of them makes cells more resistant to long-term oxidative and thermal stresses. Of note, PE26, PE39, PE42, PE59, PE68, PE78 and PE83 can prolong yeast CLS even under CR conditions, when all cellular processes that limit longevity under non-CR conditions are likely to be suppressed. Therefore, it seems conceivable that each of these seven PEs may stimulate the longevity-extending cellular processes and/or may suppress the longevity-shortening cellular processes that operate only under CR conditions.

Our analyses of the Gompertz mortality rates and dose-response curves have led us to the following two conclusions. First, each of the fifteen PEs prolongs yeast CLS because it is a geroprotective agent that decreases the rate of chronological aging but has no effect on the baseline mortality rate. Second, each of these PEs promotes a hormetic stress response in chronologically aging yeast.

In this study, we discovered that the fifteen geroprotective PEs differently affect three

groups of cellular processes in chronologically aging yeast, as summarized below.

First, each of the fifteen geroprotective PEs significantly increases the rate of coupled mitochondrial respiration and slows a decline in intracellular ROS (known to be the primary products of mitochondrial respiration) within yeast cells that enter and proceed through the ST phase of culturing.

Second, each of them substantially suppresses oxidative damage to cellular proteins and mtDNA in ST-phase yeast cells that enter day 4 of culturing. We noticed that twelve of these geroprotective PEs also significantly decrease oxidative damage to membrane lipids in ST-phase yeast cells on day 4, whereas PE77, PE79 and PE81 cause a statistically insignificant decline in oxidized membrane lipids within these cells. We also found that ten of these geroprotective PEs significantly reduce oxidative damage to nDNA, while neither PE47, PE68, PE72, PE77 nor PE83 exhibits such effect on nDNA.

Third, each of them significantly decreases cell susceptibility to long-term oxidative and thermal stresses, especially the susceptibility of yeast cells that enter and proceed through the ST phase of culturing.

5.4.1 Future perspectives

Our goals for the future research of the fifteen geroprotective PEs described here are outlined below.

First, we are interested in investigating and understanding the molecular and cellular mechanisms through which each of these PEs slows yeast chronological aging. We have recently described mechanisms underlying the aging-delaying action of PE21 [519], an extract from the white willow *Salix alba* we discovered in our previous screen for geroprotective PEs [461].

Second, we would like to explore how each of the fifteen geroprotective PEs may coordinate the information flow through a longevity-defining network of signaling pathways and protein kinases operating in budding yeast and other organisms. This network incorporates the pro-aging TORC1, PKA and PKH1/2 pathways as well as the pro-aging serine/threonine-protein kinase Sch9 [11, 15, 17, 477]. This network also integrates the anti-aging SNF1 and ATG pathways as well as the anti-aging serine/threonine-protein kinase Rim15 [11, 15, 17, 477]. Our recent study has revealed that each of the six geroprotective PEs we discovered in the previous screen [461] slows yeast chronological aging through different functional modules of this longevity-defining

signaling network [477]. Of note, pairwise mixes of these six geroprotective PEs slow the process of yeast chronological aging in a synergistic or additive manner only if they include the PEs that target different modules of this network [520]. Therefore, we are interested in investigating how different combinations of the fifteen geroprotective PEs described here influence the extent of yeast chronological aging delay. We will be looking for the combinations of geroprotective PEs that exhibit synergistic or additive effects on the extent of yeast chronological aging delay.

Third, the Health Canada government agency defines thirteen of the fifteen geroprotective PEs described here as the ones that are safe for human consumption [476]. The agency recommends using eight of them as health-improving supplements with clinically proven benefits to human health [476]. Among these health-improving PEs are PE26, PE47, PE59, PE64, PE69, PE75, PE77 and PE83 [476]. For each of them, Health Canada provides a detailed description of the source material, routes of administration, doses and dosage forms, uses or purposes, durations of use, risk information, cautions and warnings, contraindications, known adverse reactions, non-medicinal ingredients, specifications, references cited and reviewed, examples of appropriate dosage preparations, and frequencies of use [476]. Our ongoing collaborative research aims to investigate which of the eight geroprotective PEs recommended by Health Canada as healthspan-extending dietary additives for humans can increase the replicative lifespan of cultured human fibroblasts or for delaying the onset of aging-associated human diseases. These diseases include arthritis, diabetes, heart disease, kidney disease, liver dysfunction, sarcopenia, stroke, neurodegenerative diseases (including Parkinson's, Alzheimer's and Huntington's diseases), and many forms of cancer [11, 23, 26, 50, 56, 114-116, 335, 338, 339, 342, 359, 460, 469-472, 474, 475, 479, 521].

CHAPTER 6

6 General discussion

In studies presented in this thesis, we used a robust cell viability assay to conduct two screens of commercially available plant extract libraries in search of those plant extracts (PEs) that can delay chronological aging and prolong the longevity of the budding yeast *S. cerevisiae*. Many of the PEs in the library have been used for centuries in traditional Chinese and other herbal medicines or the Mediterranean and other customary diets. Of note, none of these PEs was previously tested for its ability to slow aging and extend the longevity of any organism. Our screens have allowed us to discover twenty-one PEs that significantly prolong the longevity of chronologically aging yeast cells that are not limited in calorie supply. We provided evidence that each of these longevity-extending PEs is a geroprotector that lowers the rate of yeast chronological aging and elicits a hormetic stress response. Our findings demonstrated that the efficiencies of aging delay and longevity extension by many of these geroprotective PEs significantly exceed those for any of the chemical compounds previously known for their abilities to slow aging and prolong lifespan in yeasts, filamentous fungi, nematodes, fruit flies, daphnias, mosquitoes, honey bees, fishes, mammals and cultured human cells. Our findings also revealed that each of the twenty-one geroprotective PEs mimics the aging-delaying, longevity-extending, stress-protecting, metabolic and physiological effects of a caloric restriction diet in yeast cells that are not limited in calorie supply. We also demonstrated that the discovered geroprotective PEs elicit partially overlapping effects on a distinct set of longevity-defining cellular processes. Such processes include the coupled mitochondrial respiration, maintenance of the electrochemical potential across the inner mitochondrial membrane, preservation of the cellular homeostasis of reactive oxygen species (ROS), protection of cellular macromolecules from ROS-inflicted oxidative damage, maintenance of cell resistance to oxidative and thermal stresses, the efficiency of the lipolytic cleavage of neutral lipids deposited and stored in lipid droplets (LDs). We provided evidence that some of the discovered geroprotective PEs slow yeast chronological aging because they target different hubs, nodes and/or links of the longevity-defining network integrating specific evolutionarily conserved signaling pathways and protein kinases.

A challenge for the future is to characterize the individual chemical compounds responsible for the ability of each of the discovered geroprotective PEs to postpone the onset and decrease the rate of yeast chronological aging. Such characterization is already underway in our laboratory. Furthermore, the other future challenge is to investigate and understand the molecular and cellular

mechanisms through which each of the discovered geroprotective PEs slows the chronological mode of aging in *S. cerevisiae*. Moreover, our ongoing collaborative research aims to investigate which of the thirteen (out of twenty-one) geroprotective PEs recommended by Health Canada as healthspan-extending dietary additives for humans can increase the replicative lifespan of cultured human fibroblasts or for delaying the onset of aging-associated diseases in mice models. These diseases include arthritis, diabetes, heart disease, kidney disease, liver dysfunction, sarcopenia, stroke, neurodegenerative diseases (including Parkinson's, Alzheimer's and Huntington's diseases), and different forms of cancer.

CHAPTER 7

7 References

1. Botstein D, Fink GR. Yeast: an experimental organism for 21st Century biology. Genetics. 2011; 189:695-704.

2. Duina AA, Miller ME, Keeney JB. Budding yeast for budding geneticists: a primer on the Saccharomyces cerevisiae model system. Genetics. 2014; 197:33-48.63.

3. Weissman J, Guthrie C, Fink GR. Guide to yeast genetics: Functional genomics, proteomics, and other systems analyses. Academic Press, Burlington, 2010.

4. Horst Feldmann H. (ed.). Yeast: Molecular and cell biology. Wiley-Blackwell, Weinheim, 2012.

5. Lee SS, Avalos Vizcarra I, Huberts DH, Lee LP, Heinemann M. Whole lifespan microscopic observation of budding yeast aging through a microfluidic dissection platform. Proc Natl Acad Sci USA. 2012; 109:4916-4920.

6. Sutphin GL, Olsen BA, Kennedy BK, Kaeberlein M. Genome-wide analysis of yeast aging. Subcell Biochem. 2012; 57:251-289.

7. Xie Z, Zhang Y, Zou K, Brandman O, Luo C, Ouyang Q, Li H. Molecular phenotyping of aging in single yeast cells using a novel microfluidic device. Aging Cell. 2012; 11:599-606.

8. Zhang Y, Luo C, Zou K, Xie Z, Brandman O, Ouyang Q, Li H. Single cell analysis of yeast replicative aging using a new generation of microfluidic device. PloS One. 2012; 7: e48275.

9. Richard VR, Bourque SD, Titorenko VI. Metabolomic and lipidomic analyses of chronologically aging yeast. Methods Mol Biol. 2014; 1205:359-373.

10. Strynatka KA, Gurrola-Gal MC, Berman JN, McMaster CR. How surrogate and chemical genetics in model organisms can suggest therapies for human genetic diseases. Genetics. 2018;

208:833-851.

11. Fontana L, Partridge L, Longo VD. Extending healthy life span - from yeast to humans. Science. 2010; 328:321-326.

12. Bilinski T, Bylak A, Zadrag-Tecza R. The budding yeast Saccharomyces cerevisiae as a model organism: possible implications for gerontological studies. Biogerontology. 2017; 18:631-640.

13. Zimmermann A, Hofer S, Pendl T, Kainz K, Madeo F, Carmona-Gutierrez D. Yeast as a tool to identify anti-aging compounds. FEMS Yeast Res. 2018; 18: foy020.

14. Kaeberlein M. Lessons on longevity from budding yeast. Nature. 2010; 464:513-519.

15. Longo VD, Shadel GS, Kaeberlein M, Kennedy B. Replicative and chronological aging in Saccharomyces cerevisiae. Cell Metab. 2012; 16:18-31.

16. Sutphin GL, Olsen BA, Kennedy BK, Kaeberlein M. Genome-wide analysis of yeast aging. Subcell Biochem. 2012; 57:251-289.

17. Arlia-Ciommo A, Leonov A, Piano A, Svistkova V, Titorenko VI. Cell-autonomous mechanisms of chronological aging in the yeast Saccharomyces cerevisiae. Microbial Cell. 2014; 1:164-178.

18. Denoth Lippuner A, Julou T, Barral Y. Budding yeast as a model organism to study the effects of age. FEMS Microbiol Rev. 2014; 38:300-325.

19. Garay E, Campos SE, Gonzalez de la Cruz J, AP Gaspar, Jinich A, Deluna A. High-resolution profiling of stationary-phase survival reveals yeast longevity factors and their genetic interactions. PLoS Genet. 2014; 10: e1004168.

20. He C, Zhou C, Kennedy BK. The yeast replicative aging model. Biochim Biophys Acta. 2018;

1864:2690-2696.

21. Alic N, Partridge L. Death and dessert: nutrient signalling pathways and ageing. Curr Opin Cell Biol. 2011; 23:738-743.

22. Johnson SC, Rabinovitch PS, Kaeberlein M. mTOR is a key modulator of ageing and age-related disease. Nature. 2013 Jan 17;493(7432):338-45.

23. Fontana L, Partridge L. Promoting health and longevity through diet: from model organisms to humans. Cell. 2015; 161:106-118.

24. Ruetenik A, Barrientos A. Dietary restriction, mitochondrial function and aging: from yeast to humans. Biochim Biophys Acta. 2015; 1847:1434-1447.

25. Janssens GE, Veenhoff LM. Evidence for the hallmarks of human aging in replicatively aging yeast. Microb Cell. 2016; 3:263-274.

26. Kaeberlein M. The biology of aging: Citizen scientists and their pets as a bridge between research on model organisms and human subjects. Vet Pathol. 2016; 53:291-298.

27. Kapahi P, Kaeberlein M, Hansen M. Dietary restriction and lifespan: Lessons from invertebrate models. Ageing Res Rev. 2017; 39:3-14.

28. Akbari M, Kirkwood TBL, Bohr VA. Mitochondria in the signaling pathways that control longevity and health span. Ageing Res Rev. 2019; 54:100940.

29. Andréasson C, Ott M, Büttner S. Mitochondria orchestrate proteostatic and metabolic stress responses. EMBO Rep. 2019; 20: e47865.

30. Sampaio-Marques B, Burhans WC, Ludovico P. Yeast at the forefront of research on ageing and age-related diseases. Prog Mol Subcell Biol. 2019; 58:217-242.

31. Banerjee R, Joshi N, Nagotu S. Cell organelles and yeast longevity: an intertwined regulation. Curr Genet. 2020; 66:15-41.

32. Goldberg AA, Bourque SD, Kyryakov P, Gregg C, Boukh-Viner T, Beach A, Burstein MT, Machkalyan G, Richard V, Rampersad S, Cyr D, Milijevic S, Titorenko VI. Effect of calorie restriction on the metabolic history of chronologically aging yeast. Exp Gerontol. 2009; 44:555-571.

33. Steffen KK, Kennedy BK, Kaeberlein M. Measuring replicative life span in the budding yeast. J Vis Exp. 2009; 28: 1209.

34. Hu J, Wei M, Mirisola MG, Longo VD. Assessing chronological aging in Saccharomyces cerevisiae. Methods Mol Biol. 2013; 965:463-472.

35. Sinclair DA. Studying the replicative life span of yeast cells. Methods Mol Biol. 2013; 1048:49-63.

36. Steinkraus KA, Kaeberlein M, Kennedy BK. Replicative aging in yeast: the means to the end. Annu Rev Cell Dev Biol. 2008; 24:29-54.

37. McCormick MA, Delaney JR, Tsuchiya M, Tsuchiyama S, Shemorry A, Sim S, Chou AC, Ahmed U, Carr D, Murakami CJ, Schleit J, Sutphin GL, Wasko BM, Bennett CF, Wang AM, Olsen B, Beyer RP, Bammler TK, Prunkard D, Johnson SC, Pennypacker JK, An E, Anies A, Castanza AS, Choi E, Dang N, Enerio S, Fletcher M, Fox L, Goswami S, Higgins SA, Holmberg MA, Hu D, Hui J, Jelic M, Jeong KS, Johnston E, Kerr EO, Kim J, Kim D, Kirkland K, Klum S, Kotireddy S, Liao E, Lim M, Lin MS, Lo WC, Lockshon D, Miller HA, Moller RM, Muller B, Oakes J, Pak DN, Peng ZJ, Pham KM, Pollard TG, Pradeep P, Pruett D, Rai D, Robison B, Rodriguez AA, Ros B, Sage M, Singh MK, Smith ED, Snead K, Solanky A, Spector BL, Steffen KK, Tchao BN, Ting MK, Vander Wende H, Wang D, Welton KL, Westman EA, Brem RB, Liu XG, Suh Y, Zhou Z, Kaeberlein M, Kennedy BK. A comprehensive analysis of replicative lifespan

in 4,698 single-gene deletion strains uncovers conserved mechanisms of aging. Cell Metab. 2015 Nov 3;22(5):895-906.

38. Ghavidel A, Baxi K, Ignatchenko V, Prusinkiewicz M, Arnason TG, Kislinger T, Carvalho CE, Harkness TA. A genome scale screen for mutants with delayed exit from mitosis: Ire1-independent induction of autophagy integrates ER homeostasis into mitotic lifespan. PLoS Genet. 2015; 11: e1005429.

39. Janssens GE, Veenhoff LM. Evidence for the hallmarks of human aging in replicatively aging yeast. Microb Cell. 2016; 3:263-274.

40. Fabrizio P, Longo VD. The chronological life span of Saccharomyces cerevisiae. Methods Mol Biol. 2007; 371: 89-95.

41. Piper PW. Maximising the yeast chronological lifespan. Subcell Biochem. 2012; 57:145-159.

42. Burtner CR, Murakami CJ, Kennedy BK, Kaeberlein M. A molecular mechanism of chronological aging in yeast. Cell Cycle. 2009; 8:1256-1270.

43. Burtner CR, Murakami CJ, Olsen B, Kennedy BK, Kaeberlein M. A genomic analysis of chronological longevity factors in budding yeast. Cell Cycle. 2011; 10:1385-1396.

44. Mirisola MG, Longo VD. Acetic acid and acidification accelerate chronological and replicative aging in yeast. Cell Cycle. 2012; 11:3532-3533.

45. Murakami C, Delaney JR, Chou A, Carr D, Schleit J, Sutphin GL, An EH, Castanza AS, Fletcher M, Goswami S, Higgins S, Holmberg M, Hui J, Jelic M, Jeong KS, Kim JR, Klum S, Liao E, Lin MS, Lo W, Miller H, Moller R, Peng ZJ, Pollard T, Pradeep P, Pruett D, Rai D, Ros V, Schuster A, Singh M, Spector BL, Vander Wende H, Wang AM, Wasko BM, Olsen B, Kaeberlein M. pH neutralization protects against reduction in replicative lifespan following chronological aging in yeast. Cell Cycle. 2012; 11:3087-3096.

46. Polymenis M, Kennedy BK. Chronological and replicative lifespan in yeast: do they meet in the middle? Cell Cycle. 2012; 11:3531-3532.

47. Delaney JR, Murakami C, Chou A, Carr D, Schleit J, Sutphin GL, An EH, Castanza AS, Fletcher M, Goswami S, Higgins S, Holmberg M, Hui J, Jelic M, Jeong KS, Kim JR, Klum S, Liao E, Lin MS, Lo W, Miller H, Moller R, Peng ZJ, Pollard T, Pradeep P, Pruett D, Rai D, Ros V, Schuster A, Singh M, Spector BL, Wende HV, Wang AM, Wasko BM, Olsen B, Kaeberlein M. Dietary restriction and mitochondrial function link replicative and chronological aging in Saccharomyces cerevisiae. Exp Gerontol. 2013; 48:1006-1013.

48. Arlia-Ciommo A, Piano A, Leonov A, Svistkova V, Titorenko VI. Quasi-programmed aging of budding yeast: a trade-off between programmed processes of cell proliferation, differentiation, stress response, survival and death defines yeast lifespan. Cell Cycle. 2014; 13:3336-3349.

49. Molon M, Zadrag-Tecza R, Bilinski T. The longevity in the yeast Saccharomyces cerevisiae: A comparison of two approaches for assessment the lifespan. Biochem Biophys Res Commun. 2015; 460:651-656.

50. Blagosklonny MV, and Hall MN. Growth and aging: a common molecular mechanism. Aging (Albany NY). 2009; 1: 357-362.

51. Kapahi P, Chen D, Rogers AN, Katewa SD, Li PW, Thomas EL and Kockel L. With TOR, less is more: a key role for the conserved nutrient-sensing TOR pathway in aging. Cell Metab. 2010; 11: 453-465.

52. Evans DS, Kapahi P, Hsueh WC, and Kockel L. TOR signaling never gets old: aging, longevity and TORC1 activity. Ageing Res Rev. 2011; 10: 225-227.

53. Jazwinski SM. The retrograde response and other pathways of interorganelle communication in yeast replicative aging. Subcell Biochem. 2012; 57: 79-100.

54. Jazwinski SM. The retrograde response: when mitochondrial quality control is not enough. Biochim Biophys Acta. 2013; 1833: 400-409.

55. Leonov A, and Titorenko VI. A network of interorganellar communications underlies cellular aging. IUBMB Life. 2013; 65: 665-674.

56. López-Otín C, Blasco MA, Partridge L, Serrano M, and Kroemer G. The hallmarks of aging. Cell. 2013; 153: 1194-1217.

57. Bitto A, Wang AM, Bennett CF, and Kaeberlein M. Biochemical genetic pathways that modulate aging in multiple species. Cold Spring Harb Perspect Med. 2015; 5: a025114.

58. Chantranupong L, Wolfson RL, and Sabatini DM. Nutrient-sensing mechanisms across evolution. Cell. 2015; 161: 67-83.

59. Titorenko VI, and Terlecky SR. Peroxisome metabolism and cellular aging. Traffic. 2011; 12: 252-259.

60. Kaeberlein M, Powers RW 3rd, Steffen KK, Westman EA, Hu D, Dang N, Kerr EO, Kirkland KT, Fields S, and Kennedy BK. Regulation of yeast replicative life span by TOR and Sch9 in response to nutrients. Science. 2005; 310: 1193-1196.

61. Powers RW 3rd, Kaeberlein M, Caldwell SD, Kennedy BK, and Fields S. Extension of chronological life span in yeast by decreased TOR pathway signaling. Genes Dev. 2006; 20: 174-184.

62. Bonawitz ND, Chatenay-Lapointe M, Pan Y, and Shadel GS. Reduced TOR signaling extends chronological life span via increased respiration and upregulation of mitochondrial gene expression. Cell Metab. 2007; 5: 265-277.

63. Medvedik O, Lamming DW, Kim KD, and Sinclair DA. MSN2 and MSN4 link calorie restriction and TOR to sirtuin-mediated lifespan extension in Saccharomyces cerevisiae. PLoS Biol. 2007; 5: e261.

64. Longo VD. Mutations in signal transduction proteins increase stress resistance and longevity in yeast, nematodes, fruit flies, and mammalian neuronal cells. Neurobiol Aging. 1999; 20: 479-486.

65. Lin SJ, Defossez PA, and Guarente L. Requirement of NAD and SIR2 for life-span extension by calorie restriction in Saccharomyces cerevisiae. Science. 2000; 289: 2126-2128.

66. Fabrizio P, Pozza F, Pletcher SD, Gendron CM, and Longo VD. Regulation of longevity and stress resistance by Sch9 in yeast. Science. 2001; 292: 288-290.

67. Fabrizio P, Liou LL, Moy VN, Diaspro A, Valentine JS, Gralla EB, and Longo VD. SOD2 functions downstream of Sch9 to extend longevity in yeast. Genetics. 2003; 163: 35-46.

68. Wei M, Fabrizio P, Hu J, Ge H, Cheng C, Li L, and Longo VD. Life span extension by calorie restriction depends on Rim15 and transcription factors downstream of Ras/PKA, Tor, and Sch9. PLoS Genet. 2008; 4: e13.

69. Burtner CR, Murakami CJ, Olsen B, Kennedy BK, and Kaeberlein M. A genomic analysis of chronological longevity factors in budding yeast. Cell Cycle. 2011; 10: 1385-1396.

70. Huang X, Liu J, and Dickson RC. Down-regulating sphingolipid synthesis increases yeast lifespan. PLoS Genet. 2012; 8: e1002493.

71. Liu J, Huang X, Withers BR, Blalock E, Liu K, and Dickson RC. Reducing sphingolipid synthesis orchestrates global changes to extend yeast lifespan. Aging Cell. 2013; 12: 833-841.

72. Huang X, Withers BR, and Dickson RC. Sphingolipids and lifespan regulation. Biochim

Biophys Acta. 2014; 1841: 657-664.

73. Teixeira V, and Costa V. Unraveling the role of the Target of Rapamycin signaling in sphingolipid metabolism. Prog Lipid Res. 2016; 61: 109-133.

74. Thompson-Jaeger S, François J, Gaughran JP, and Tatchell K. Deletion of SNF1 affects the nutrient response of yeast and resembles mutations which activate the adenylate cyclase pathway. Genetics. 1991; 129: 697-706.

75. Ashrafi K, Lin SS, Manchester JK, and Gordon JI. Sip2p and its partner snf1p kinase affect aging in S. cerevisiae. Genes Dev. 2000; 14: 1872-1885.

76. Lin SS, Manchester JK, and Gordon JI. Sip2, an N-myristoylated beta subunit of Snf1 kinase, regulates aging in Saccharomyces cerevisiae by affecting cellular histone kinase activity, recombination at rDNA loci, and silencing. J Biol Chem. 2003; 278: 13390-13397.

77. Lu JY, Lin YY, Sheu JC, Wu JT, Lee FJ, Chen Y, Lin MI, Chiang FT, Tai TY, Berger SL, Zhao Y, Tsai KS, Zhu H, Chuang LM, and Boeke JD. Acetylation of yeast AMPK controls intrinsic aging independently of caloric restriction. Cell. 2011; 146: 969-979.

78. Friis RM, Glaves JP, Huan T, Li L, Sykes BD, and Schultz MC. Rewiring AMPK and mitochondrial retrograde signaling for metabolic control of aging and histone acetylation in respiratory-defective cells. Cell Rep. 2014; 7: 565-574.

79. Jiao R, Postnikoff S, Harkness TA, and Arnason TG. The SNF1 kinase ubiquitin-associated domain restrains its activation, activity, and the yeast life span. J Biol Chem. 2015; 290: 15393-15404.

80. Tang F, Watkins JW, Bermudez M, Gray R, Gaban A, Portie K, Grace S, Kleve M, Craciun G. A lifespan extending form of autophagy employs the vacuole-vacuole fusion machinery. Autophagy. 2008; 4:874-886.

81. Alvers AL, Fishwick LK, Wood MS, Hu D, Chung HS, Dunn WA Jr, and Aris JP. Autophagy and amino acid homeostasis are required for chronological longevity in Saccharomyces cerevisiae. Aging Cell. 2009; 8:353-369.

82. Alvers AL, Wood MS, Hu D, Kaywell AC, Dunn WA Jr, and Aris JP. Autophagy is required for extension of yeast chronological life span by rapamycin. Autophagy. 2009; 5:847-849.

83. Eisenberg T, Knauer H, Schauer A, Büttner S, Ruckenstuhl C, Carmona-Gutierrez D, Ring J, Schroeder S, Magnes C, Antonacci L, Fussi H, Deszcz L, Hartl R, Schraml E, Criollo A, Megalou E, Weiskopf D, Laun P, Heeren G, Breitenbach M, Grubeck-Loebenstein B, Herker E, Fahrenkrog B, Fröhlich KU, Sinner F, Tavernarakis N, Minois N, Kroemer G, and Madeo F. Induction of autophagy by spermidine promotes longevity. Nat Cell Biol. 2009; 11:1305-1314.

84. Morselli E, Galluzzi L, Kepp O, Criollo A, Maiuri MC, Tavernarakis N, Madeo F, and Kroemer G. Autophagy mediates pharmacological lifespan extension by spermidine and resveratrol. Aging (Albany NY). 2009; 1:961-970.

85. Matecic M, Smith DL, Pan X, Maqani N, Bekiranov S, Boeke JD, and Smith JS. A microarray-based genetic screen for yeast chronological aging factors. PLoS Genet. 2010; 6: e1000921.

86. Aris JP, Alvers AL, Ferraiuolo RA, Fishwick LK, Hanvivatpong A, Hu D, Kirlew C, Leonard MT, Losin KJ, Marraffini M, Seo AY, Swanberg V, Westcott JL, Wood MS, Leeuwenburgh C, and Dunn WA Jr. Autophagy and leucine promote chronological longevity and respiration proficiency during calorie restriction in yeast. Exp Gerontol. 2013; 48:1107-1119.

87. Richard VR, Leonov A, Beach A, Burstein MT, Koupaki O, Gomez-Perez A, Levy S, Pluska L, Mattie S, Rafesh R, Iouk T, Sheibani S, Greenwood M, Vali H, Titorenko VI. Macromitophagy is a longevity assurance process that in chronologically aging yeast limited in calorie supply sustains functional mitochondria and maintains cellular lipid homeostasis. Aging (Albany NY). 2013; 5:234-269.

88. Klionsky DJ et al. (several hundred co-authors). Guidelines for the use and interpretation of assays for monitoring autophagy (3rd edition). Autophagy. 2016; 12:1-222.

89. Urban J, Soulard A, Huber A, Lippman S, Mukhopadhyay D, Deloche O, Wanke V, Anrather D, Ammerer G, Riezman H, Broach JR, De Virgilio C, Hall MN, and Loewith R. Sch9 is a major target of TORC1 in Saccharomyces cerevisiae. Mol Cell. 2007; 26: 663-674.

90. Wei M, Fabrizio P, Hu J, Ge H, Cheng C, Li L, and Longo VD. Life span extension by calorie restriction depends on Rim15 and transcription factors downstream of Ras/PKA, Tor, and Sch9. PLoS Genet. 2008; 4: e13.

91. Huang X, Liu J, and Dickson RC. Down-regulating sphingolipid synthesis increases yeast lifespan. PLoS Genet. 2012; 8: e1002493.

92. Liu J, Huang X, Withers BR, Blalock E, Liu K, and Dickson RC. Reducing sphingolipid synthesis orchestrates global changes to extend yeast lifespan. Aging Cell. 2013; 12: 833-841.

93. Huang X, Withers BR, and Dickson RC. Sphingolipids and lifespan regulation. Biochim Biophys Acta. 2014; 1841: 657-664.

94. Swinnen E, Ghillebert R, Wilms T, and Winderickx J. Molecular mechanisms linking the evolutionary conserved TORC1-Sch9 nutrient signalling branch to lifespan regulation in Saccharomyces cerevisiae. FEMS Yeast Res. 2014; 14: 17-32.

95. De Virgilio C. The essence of yeast quiescence. FEMS Microbiol Rev. 2012; 36:306-339.

96. Conrad M, Schothorst J, Kankipati HN, Van Zeebroeck G, Rubio-Texeira M, and Thevelein JM. Nutrient sensing and signaling in the yeast Saccharomyces cerevisiae. FEMS Microbiol Rev. 2014; 38:254-299.

97. Smets B, Ghillebert R, De Snijder P, Binda M, Swinnen E, De Virgilio C, and Winderickx J. Life in the midst of scarcity: adaptations to nutrient availability in Saccharomyces cerevisiae. Curr Genet. 2010; 56:1-32.

98. Beach A, and Titorenko, V.I. In search of housekeeping pathways that regulate longevity. Cell Cycle. 2011; 10:3042-3044.

99. Broach JR. Nutritional control of growth and development in yeast. Genetics. 2012; 192:73-105.

100. Burstein MT, Kyryakov P, Beach A, Richard VR, Koupaki O, Gomez-Perez A, Leonov A, Levy S, Noohi F, Titorenko VI. Lithocholic acid extends longevity of chronologically aging yeast only if added at certain critical periods of their lifespan. Cell Cycle. 2012; 11:3443-3462.

101. Kyryakov P, Beach A, Richard VR, Burstein MT, Leonov A, Levy S, and Titorenko VI. Caloric restriction extends yeast chronological lifespan by altering a pattern of age-related changes in trehalose concentration. Front Physiol. 2012; 3:256.

102. Beach A, Richard VR, Leonov A, Burstein MT, Bourque SD, Koupaki O, Juneau M, Feldman R, Iouk T, and Titorenko VI. Mitochondrial membrane lipidome defines yeast longevity. Aging (Albany NY). 2013; 5:551-574.

103. Burstein MT, and Titorenko VI. A mitochondrially targeted compound delays aging in yeast through a mechanism linking mitochondrial membrane lipid metabolism to mitochondrial redox biology. Redox Biol. 2014; 2:305-307.

104. Engelberg D, Perlman R, and Levitzki A. Transmembrane signaling in Saccharomyces cerevisiae as a model for signaling in metazoans: state of the art after 25 years. Cell Signal. 2014; 26:2865-2878.

105. Rødkaer SV, and Faergeman NJ. Glucose- and nitrogen sensing and regulatory mechanisms

in Saccharomyces cerevisiae. FEMS Yeast Res. 2014; 14:683-696.

106. Beach A, Richard VR, Bourque S, Boukh-Viner T, Kyryakov P, Gomez-Perez A, Arlia-Ciommo A, Feldman R, Leonov A, Piano A, Svistkova V, and Titorenko VI. Lithocholic bile acid accumulated in yeast mitochondria orchestrates a development of an anti-aging cellular pattern by causing age-related changes in cellular proteome. Cell Cycle. 2015; 14:1643-1656.

107. Medkour Y, Titorenko VI. Mitochondria operate as signaling platforms in yeast aging. Aging (Albany NY). 2016; 8:212-213.

108. Eisenberg T, Knauer H, Schauer A, Büttner S, Ruckenstuhl C, Carmona-Gutierrez D, Ring J, Schroeder S, Magnes C, Antonacci L, Fussi H, Deszcz L, Hartl R, Schraml E, Criollo A, Megalou E, Weiskopf D, Laun P, Heeren G, Breitenbach M, Grubeck-Loebenstein B, Herker E, Fahrenkrog B, Fröhlich KU, Sinner F, Tavernarakis N, Minois N, Kroemer G, and Madeo F. Induction of autophagy by spermidine promotes longevity. Nat Cell Biol. 2009; 11:1305-1314.

109. Goldberg AA, Kyryakov P, Bourque SD, and Titorenko VI. Xenohormetic, hormetic and cytostatic selective forces driving longevity at the ecosystemic level. Aging (Albany NY). 2010; 2:361-370.

110. Goldberg AA, Richard VR, Kyryakov P, Bourque SD, Beach A, Burstein MT, Glebov A, Koupaki O, Boukh-Viner T, Gregg C, Juneau M, English AM, Thomas DY, and Titorenko VI. Chemical genetic screen identifies lithocholic acid as an anti-aging compound that extends yeast chronological life span in a TOR-independent manner, by modulating housekeeping longevity assurance processes. Aging (Albany NY). 2010; 2:393-414.

111. Minois N, Carmona-Gutierrez D, and Madeo F. Polyamines in aging and disease. Aging (Albany NY). 2011; 3:716-732.

112. Burstein MT, Beach A, Richard VR, Koupaki O, Gomez-Perez A, Goldberg AA, Kyryakov P, Bourque SD, Glebov A, and Titorenko VI. Interspecies chemical signals released into the

environment may create xenohormetic, hormetic and cytostatic selective forces that drive the ecosystemic evolution of longevity regulation mechanisms. Dose-Response. 2012; 10:75-82.

113. Arlia-Ciommo A, Piano A, Svistkova V, Mohtashami S, and Titorenko VI. Mechanisms underlying the anti-aging and anti-tumor effects of lithocholic bile acid. Int J Mol Sci. 2014; 15:16522-16543.

114. de Cabo R, Carmona-Gutierrez D, Bernier M, Hall MN, and Madeo F. The search for antiaging interventions: from elixirs to fasting regimens. Cell. 2014; 157:1515-1526.

115. Hubbard BP, and Sinclair DA. Small molecule SIRT1 activators for the treatment of aging and age-related diseases. Trends Pharmacol Sci. 2014; 35:146-154.

116. Leonov A, Arlia-Ciommo A, Piano A, Svistkova V, Lutchman V, Medkour Y, and Titorenko VI. Longevity extension by phytochemicals. Molecules. 2015; 20:6544-6572.

117. Bonawitz ND, Shadel GS. Rethinking the mitochondrial theory of aging: the role of mitochondrial gene expression in lifespan determination. Cell Cycle. 2007; 6:1574-1578.

118. Pan Y, Shadel GS. Extension of chronological life span by reduced TOR signaling requires down-regulation of Sch9p and involves increased mitochondrial OXPHOS complex density. Aging (Albany NY). 2009; 1:131-145.

119. Wei M, Fabrizio P, Madia F, Hu J, Ge H, Li LM, Longo VD. Tor1/Sch9-regulated carbon source substitution is as effective as calorie restriction in life span extension. PLoS Genet. 2009; 5: e1000467.

120. Mesquita A, Weinberger M, Silva A, Sampaio-Marques B, Almeida B, Leão C, Costa V, Rodrigues F, Burhans WC, Ludovico P. Caloric restriction or catalase inactivation extends yeast chronological lifespan by inducing H2O2 and superoxide dismutase activity. Proc Natl Acad Sci USA. 2010; 107:15123-81512.

121. Pan Y. Mitochondria, reactive oxygen species, and chronological aging: a message from yeast. Exp Gerontol. 2011; 46:847-852.

122. Pan Y, Schroeder EA, Ocampo A, Barrientos A, Shadel GS. Regulation of yeast chronological life span by TORC1 via adaptive mitochondrial ROS signaling. Cell Metab. 2011; 13:668-678.

123. Beach A, Burstein MT, Richard VR, Leonov A, Levy S, Titorenko VI. Integration of peroxisomes into an endomembrane system that governs cellular aging. Front Physiol. 2012; 3: 4.

124. Cai L, Tu BP. Driving the cell cycle through metabolism. Annu Rev Cell Dev Biol. 2012; 28:59-87.

125. Ocampo A, Liu J, Schroeder EA, Shadel GS, Barrientos A. Mitochondrial respiratory thresholds regulate yeast chronological life span and its extension by caloric restriction. Cell Metab. 2012; 16:55-67.

126. Barral Y. A new answer to old questions. Elife. 2013; 2: e00515.

127. Beach A, Titorenko VI. Essential roles of peroxisomally produced and metabolized biomolecules in regulating yeast longevity. Subcell Biochem. 2013; 69:050--167.

128. Brandes N, Tienson H, Lindemann A, Vitvitsky V, Reichmann D, Banerjee R, Jakob U. Timeline of redox events in aging postmitotic cells. Elife. 2013; 2: e00306.

129. Hachinohe M, Yamane M, Akazawa D, Ohsawa K, Ohno M, Terashita Y, Masumoto H. A reduction in age-enhanced gluconeogenesis extends lifespan. PLoS One. 2013; 8: e54011.

130. Mirisola MG, Longo VD. A radical signal activates the epigenetic regulation of longevity. Cell Metab. 2013; 17:812-813.

131. Orlandi I, Ronzulli R, Casatta N, Vai M. Ethanol and acetate acting as carbon/energy sources negatively affect yeast chronological aging. Oxid Med Cell Longev. 2013; 2013: 802870.

132. Schroeder EA, Raimundo N, Shadel GS. Epigenetic silencing mediates mitochondria stress-induced longevity. Cell Metab. 2013; 17:954-964.

133. Tahara EB, Cunha FM, Basso TO, Della Bianca BE, Gombert AK, Kowaltowski AJ. Calorie restriction hysteretically primes aging Saccharomyces cerevisiae toward more effective oxidative metabolism. PLoS One. 2013; 8: e56388.

134. Martins D, Titorenko VI, English AM. Cells with impaired mitochondrial H2O2 sensing generate less •OH radicals and live longer. Antioxid Redox Signal. 2014; 21:1490-1503.

135. Fabrizio P, Gattazzo C, Battistella L, Wei M, Cheng C, McGrew K, Longo VD. Sir2 blocks extreme life-span extension. Cell. 2005 Nov 18;123(4):655-67.

136. Goldberg AA, Bourque SD, Kyryakov P, Boukh-Viner T, Gregg C, Beach A, Burstein MT, Machkalyan G, Richard V, Rampersad S, Titorenko VI. A novel function of lipid droplets in regulating longevity. Biochem Soc Trans. 2009; 37:1050-1055.

137. Wei M, Fabrizio P, Madia F, Hu J, Ge H, Li LM, Longo VD. Tor1/Sch9-regulated carbon source substitution is as effective as calorie restriction in life span extension. PLoS Genet. 2009; 5: e1000467.

138. Longo VD, Fabrizio P. Chronological aging in Saccharomyces cerevisiae. Subcell Biochem. 2012; 57:101-121.

139. Eisenberg T, Schroeder S, Andryushkova A, Pendl T, Küttner V, Bhukel A, Mariño G, Pietrocola F, Harger A, Zimmermann A, Moustafa T, Sprenger A, Jany E, Büttner S, Carmona-Gutierrez D, Ruckenstuhl C, Ring J, Reichelt W, Schimmel K, Leeb T, Moser C, Schatz S, Kamolz

LP, Magnes C, Sinner F, Sedej S, Fröhlich KU, Juhasz G, Pieber TR, Dengjel J, Sigrist SJ, Kroemer G, Madeo F. Nucleocytosolic depletion of the energy metabolite acetyl-coenzyme a stimulates autophagy and prolongs lifespan. Cell Metab. 2014 Mar 4;19(3):431-44.

140. Hu J, Wei M, Mirzaei H, Madia F, Mirisola M, Amparo C, Chagoury S, Kennedy B, Longo VD. Tor-Sch9 deficiency activates catabolism of the ketone body-like acetic acid to promote trehalose accumulation and longevity. Aging Cell. 2014; 13:457-467.

141. Burtner CR, Murakami CJ, Kaeberlein M. A genomic approach to yeast chronological aging. Methods Mol Biol. 2009; 548:101-114.

142. Longo VD, Fabrizio P. Chronological aging in Saccharomyces cerevisiae. Subcell Biochem. 2012; 57:101-121.

143. Fraenkel DG (2011). Yeast intermediary metabolism. Cold Spring Harbor Laboratory Press, Cold Spring Harbor.

144. Crespo JL, Powers T, Fowler B, Hall MN. The TOR-controlled transcription activators GLN3, RTG1, and RTG3 are regulated in response to intracellular levels of glutamine. Proc Natl Acad Sci USA. 2002; 99:6784-6789.

145. Jewell JL, Russell RC, Guan KL. Amino acid signalling upstream of mTOR. Nat Rev Mol Cell Biol. 2013; 14:133-139.

146. Shimobayashi M, Hall MN. Making new contacts: the mTOR network in metabolism and signalling crosstalk. Nat Rev Mol Cell Biol. 2014; 15:155-162.

147. Singer MA, Lindquist S. Multiple effects of trehalose on protein folding in vitro and in vivo. Mol Cell. 1998; 1:639-648.

148. Singer MA, Lindquist S. Thermotolerance in Saccharomyces cerevisiae: the Yin and Yang of

trehalose. Trends Biotechnol. 1998; 16:460-468.

149. Benaroudj N, Lee DH, Goldberg AL. Trehalose accumulation during cellular stress protects cells and cellular proteins from damage by oxygen radicals. J Biol Chem. 2001; 276:24261-24267.

150. Elbein AD, Pan YT, Pastuszak I, Carroll D. New insights on trehalose: a multifunctional molecule. Glycobiology. 2003; 13:17R-27R.

151. Jain NK, Roy I. Effect of trehalose on protein structure. Protein Sci. 2009; 18:24-36.

152. Chen B, Retzlaff M, Roos T, Frydman J. Cellular strategies of protein quality control. Cold Spring Harb Perspect Biol. 2011; 3: a004374.

153. Lindquist SL, Kelly JW. Chemical and biological approaches for adapting proteostasis to ameliorate protein misfolding and aggregation diseases: progress and prognosis. Cold Spring Harb Perspect Biol. 2011; 3: a004507.

154. Taylor RC, Dillin A. Aging as an event of proteostasis collapse. Cold Spring Harb Perspect Biol. 2011; 3: a004440.

155. Kim YE, Hipp MS, Bracher A, Hayer-Hartl M, Hartl FU. Molecular chaperone functions in protein folding and proteostasis. Annu Rev Biochem. 2013; 82:323-355.

156. Piper PW, Harris NL, MacLean M. Preadaptation to efficient respiratory maintenance is essential both for maximal longevity and the retention of replicative potential in chronologically ageing yeast. Mech Ageing Dev. 2006; 127:733-740.

157. Lavoie H, Whiteway M. Increased respiration in the sch9Delta mutant is required for increasing chronological life span but not replicative life span. Eukaryot Cell. 2008; 7:1127-1135.

158. Schroeder EA, Shadel GS. Crosstalk between mitochondrial stress signals regulates yeast

chronological lifespan. Mech Ageing Dev. 2014; 135:41-49.

159 Kawałek A, Lefevre SD, Veenhuis M, van der Klei IJ. Peroxisomal catalase deficiency modulates yeast lifespan depending on growth conditions. Aging (Albany NY). 2013; 5:67-83.

160. Lefevre SD, van Roermund CW, Wanders RJ, Veenhuis M, van der Klei IJ. The significance of peroxisome function in chronological aging of Saccharomyces cerevisiae. Aging Cell. 2013; 12:784-793.

161. Sheibani S, Richard VR, Beach A, Leonov A, Feldman R, Mattie S, Khelghatybana L, Piano A, Greenwood M, Vali H, Titorenko VI. Macromitophagy, neutral lipids synthesis, and peroxisomal fatty acid oxidation protect yeast from "liponecrosis", a previously unknown form of programmed cell death. Cell Cycle. 2014; 13:138-147.

162. Orzechowski Westholm J, Tronnersjö S, Nordberg N, Olsson I, Komorowski J, Ronne H. Gis1 and Rph1 regulate glycerol and acetate metabolism in glucose depleted yeast cells. PLoS One. 2012; 7: e31577.

163. Ma C, Agrawal G, Subramani S. Peroxisome assembly: matrix and membrane protein biogenesis. J Cell Biol. 2011; 193:7-16.

164. Liu X, Ma C, Subramani S. Recent advances in peroxisomal matrix protein import. Curr Opin Cell Biol. 2012; 24:484-489.

165. Hasan S, Platta HW, Erdmann R. Import of proteins into the peroxisomal matrix. Front Physiol. 2013; 4: 261.

166. Legakis JE, Koepke JI, Jedeszko C, Barlaskar F, Terlecky LJ, Edwards HJ, Walton PA, Terlecky SR. Peroxisome senescence in human fibroblasts. Mol Biol Cell. 2002; 13:4243-4255.

167. Terlecky SR, Koepke JI, Walton PA. Peroxisomes and aging. Biochim Biophys Acta. 2006;

1763:1749-1754.

168. Ivashchenko O, Van Veldhoven PP, Brees C, Ho YS, Terlecky SR, Fransen M. Intraperoxisomal redox balance in mammalian cells: oxidative stress and interorganellar cross-talk. Mol Biol Cell. 2011; 22:1440-1451.

169. Islinger M, Grille S, Fahimi HD, Schrader M. The peroxisome: an update on mysteries. Histochem Cell Biol. 2012; 137:547-574.

170. Walton PA, Pizzitelli M. Effects of peroxisomal catalase inhibition on mitochondrial function. Front Physiol. 2012; 3: 108.

171. Wang B, Van Veldhoven PP, Brees C, Rubio N, Nordgren M, Apanasets O, Kunze M, Baes M, Agostinis P, Fransen M. Mitochondria are targets for peroxisome-derived oxidative stress in cultured mammalian cells. Free Radic Biol Med. 2013; 65:882-894.

172. Nordgren M, Fransen M. Peroxisomal metabolism and oxidative stress. Biochimie. 2014; 98:56-62.

173. Titorenko VI, Rachubinski RA. The peroxisome: orchestrating important developmental decisions from inside the cell. J Cell Biol. 2004; 164:641-645.

174. Hiltunen JK, Mursula AM, Rottensteiner H, Wierenga RK, Kastaniotis AJ, Gurvitz A. The biochemistry of peroxisomal beta-oxidation in the yeast Saccharomyces cerevisiae. FEMS Microbiol Rev. 2003; 27:35-64.

175. Minois N. Molecular basis of the 'anti-aging' effect of spermidine and other natural polyamines - a mini-review. Gerontology. 2014; 60:319-326.

176. Morselli E, Mariño G, Bennetzen MV, Eisenberg T, Megalou E, Schroeder S, Cabrera S, Bénit P, Rustin P, Criollo A, Kepp O, Galluzzi L, Shen S, Malik SA, Maiuri MC, Horio Y, López-

Otín C, Andersen JS, Tavernarakis N, Madeo F, Kroemer G. Spermidine and resveratrol induce autophagy by distinct pathways converging on the acetylproteome. J Cell Biol. 2011; 192:615-629.

177. Binns D, Januszewski T, Chen Y, Hill J, Markin VS, Zhao Y, Gilpin C, Chapman KD, Anderson RG, Goodman JM. An intimate collaboration between peroxisomes and lipid bodies. J Cell Biol. 2006; 173:719-731.

178. D'Autréaux B, Toledano MB. ROS as signalling molecules: mechanisms that generate specificity in ROS homeostasis. Nat Rev Mol Cell Biol. 2007; 8:813-824.

179. Giorgio M, Trinei M, Migliaccio E, Pelicci PG. Hydrogen peroxide: a metabolic by-product or a common mediator of ageing signals? Nat Rev Mol Cell Biol. 2007; 8:722-728.

180. Veal EA, Day AM, Morgan BA. Hydrogen peroxide sensing and signaling. Mol Cell. 2007; 26:1-14.

181. Goodman JM. The gregarious lipid droplet. J Biol Chem. 2008; 283:28005-28009.

182. Adeyo O, Horn PJ, Lee S, Binns DD, Chandrahas A, Chapman KD, Goodman JM. The yeast lipin orthologue Pah1p is important for biogenesis of lipid droplets. J Cell Biol. 2011; 192:1043-1055.

183. Kohlwein SD, Veenhuis M, van der Klei IJ. Lipid droplets and peroxisomes: key players in cellular lipid homeostasis or a matter of fat - store 'em up or burn 'em down. Genetics. 2013; 193:1-50.

184. van der Klei IJ, Yurimoto H, Sakai Y, Veenhuis M. The significance of peroxisomes in methanol metabolism in methylotrophic yeast. Biochim Biophys Acta. 2006; 1763:1453-1462.

185. Beach A, Leonov A, Arlia-Ciommo A, Svistkova V, Lutchman V, Titorenko VI. Mechanisms

by which different functional states of mitochondria define yeast longevity. Int J Mol Sci. 2015; 16:5528-5554.

186. Epstein CB, Waddle JA, Hale W 4th, Davé V, Thornton J, Macatee TL, Garner HR, Butow RA. Genome-wide responses to mitochondrial dysfunction. Mol Biol Cell. 2001; 12:297-308.

187. Traven A, Wong JM, Xu D, Sopta M, Ingles CJ. Interorganellar communication. Altered nuclear gene expression profiles in a yeast mitochondrial DNA mutant. J Biol Chem. 2001; 276:4020-4027.

188. Martínez-Pastor MT, Marchler G, Schüller C, Marchler-Bauer A, Ruis H, Estruch F. The Saccharomyces cerevisiae zinc finger proteins Msn2p and Msn4p are required for transcriptional induction through the stress response element (STRE). EMBO J. 1996; 15:2227-2235.

189. Schmitt AP, McEntee K. Msn2p, a zinc finger DNA-binding protein, is the transcriptional activator of the multistress response in Saccharomyces cerevisiae. Proc Natl Acad Sci USA. 1996; 93:5777-5782.

190. Boy-Marcotte E, Perrot M, Bussereau F, Boucherie H, Jacquet M. Msn2p and Msn4p control a large number of genes induced at the diauxic transition which are repressed by cyclic AMP in Saccharomyces cerevisiae. J Bacteriol. 1998; 180:1044-1052.

191. Causton HC, Ren B, Koh SS, Harbison CT, Kanin E, Jennings EG, Lee TI, True HL, Lander ES, Young RA. Remodeling of yeast genome expression in response to environmental changes. Mol Biol Cell. 2001; 12:323-337.

192. Hinnebusch AG. Translational regulation of GCN4 and the general amino acid control of yeast. Annu Rev Microbiol. 2005; 59:407-450.

193. Huber A, Bodenmiller B, Uotila A, Stahl M, Wanka S, Gerrits B, Aebersold R, Loewith R. Characterization of the rapamycin-sensitive phosphoproteome reveals that Sch9 is a central

coordinator of protein synthesis. Genes Dev. 2009; 23:1929-1943.

194. Eltschinger S, Loewith R. TOR complexes and the maintenance of cellular homeostasis. Trends Cell Biol. 2016; 26:148-159.

195. Roelants FM, Torrance PD, Thorner J. Differential roles of PDK1- and PDK2-phosphorylation sites in the yeast AGC kinases Ypk1, Pkc1 and Sch9. Microbiology. 2004; 150: 3289-3304.

196. Liu K, Zhang X, Lester RL, Dickson RC. The sphingoid long chain base phytosphingosine activates AGC-type protein kinases in Saccharomyces cerevisiae including Ypk1, Ypk2, and Sch9. J Biol Chem. 2005; 280:22679-22687.

197. Wanke V, Cameroni E, Uotila A, Piccolis M, Urban J, Loewith R, De Virgilio C. Caffeine extends yeast lifespan by targeting TORC1. Mol Microbiol. 2008; 69:277-285.

198. Swinnen E, Ghillebert R, Wilms T, Winderickx J. Molecular mechanisms linking the evolutionary conserved TORC1-Sch9 nutrient signalling branch to lifespan regulation in Saccharomyces cerevisiae. FEMS Yeast Res. 2014; 14:17-32.

199. Lee P, Cho BR, Joo HS, Hahn JS. Yeast Yak1 kinase, a bridge between PKA and stress-responsive transcription factors, Hsf1 and Msn2/Msn4. Mol Microbiol. 2008; 70:882-895.

200. Johnson JE, Johnson FB. Methionine restriction activates the retrograde response and confers both stress tolerance and lifespan extension to yeast, mouse and human cells. PLoS One. 2014; 9: e97729.

201. Laplante M, Sabatini DM. mTOR signaling in growth control and disease. Cell. 2012; 149:274-293.

202. Yorimitsu T, Zaman S, Broach JR, Klionsky DJ. Protein kinase A and Sch9 cooperatively

regulate induction of autophagy in Saccharomyces cerevisiae. Mol Biol Cell. 2007; 18:4180-4189.

203. Stephan JS, Yeh YY, Ramachandran V, Deminoff SJ, Herman PK. The Tor and PKA signaling pathways independently target the Atg1/Atg13 protein kinase complex to control autophagy. Proc Natl Acad Sci USA. 2009; 106:17049-1054.

204. Stephan, J. S., Yeh, Y. Y., Ramachandran, V., Deminoff, S. J., and Herman, P. K. (2010). The Tor and cAMP-dependent protein kinase signaling pathways coordinately control autophagy in Saccharomyces cerevisiae. Autophagy 6, 294–295.

205. Ruckenstuhl C, Netzberger C, Entfellner I, Carmona-Gutierrez D, Kickenweiz T, Stekovic S, Gleixner C, Schmid C, Klug L, Sorgo AG, Eisenberg T, Büttner S, Mariño G, Koziel R, Jansen-Dürr P, Fröhlich KU, Kroemer G, Madeo F. Lifespan extension by methionine restriction requires autophagy-dependent vacuolar acidification. PLoS Genet. 2014; 10: e1004347.

206. Wu Z, Song L, Liu SQ, Huang D. Independent and additive effects of glutamic acid and methionine on yeast longevity. PLoS One. 2013; 8: e79319.

207. Madeo F, Tavernarakis N, Kroemer G. Can autophagy promote longevity? Nat Cell Biol. 2010; 12:842-846.

208. Schroeder S, Pendl T, Zimmermann A, Eisenberg T, Carmona-Gutierrez D, Ruckenstuhl C, Mariño G, Pietrocola F, Harger A, Magnes C, Sinner F, Pieber TR, Dengjel J, Sigrist SJ, Kroemer G, Madeo F. Acetyl-coenzyme A: a metabolic master regulator of autophagy and longevity. Autophagy. 2014; 10:1335-1337.

209. Arlia-Ciommo A, Svistkova V, Mohtashami S, Titorenko VI. A novel approach to the discovery of anti-tumor pharmaceuticals: searching for activators of liponecrosis. Oncotarget. 2016; 7:5204-5225.

210. Richard VR, Beach A, Piano A, Leonov A, Feldman R, Burstein MT, Kyryakov P, Gomez-

Perez A, Arlia-Ciommo A, Baptista S, Campbell C, Goncharov D, Pannu S, Patrinos D, Sadri B, Svistkova V, Victor A, Titorenko VI. Mechanism of liponecrosis, a distinct mode of programmed cell death. Cell Cycle. 2014; 13:3707-3726.

211. Harborne JR. Introduction to ecological biochemistry, 4th edition. Elsevier Inc., London, 1993.

212. Gershenzon J. The cost of plant chemical defense against herbivory: a biochemical perspective. In: Insect-plant interactions. Bernays EA (ed.). CRC Press, Boca Raton, 1994; pp. 105-173.

213. Reymond P, Weber H, Damond M, Farmer EE. Differential gene expression in response to mechanical wounding and insect feeding in Arabidopsis. Plant Cell. 2000; 12:707-720.

214. Hermsmeier D, Schittko U, Baldwin IT. Molecular interactions between the specialist herbivore Manduca sexta (Lepidoptera, Sphingidae) and its natural host Nicotiana attenuata. I. Large-scale changes in the accumulation of growth- and defense-related plant mRNAs. Plant Physiol. 2001; 125:683-700.

215. Strobel G, Daisy B, Castillo U, Harper J. Natural products from endophytic microorganisms. J Nat Prod. 2004; 67:257-268.

216. Verma VC, Kharwar RN, Strobel GA. Chemical and functional diversity of natural products from plant associated endophytic fungi. Nat Prod Commun. 2009; 4:1511-1532.

217. Yu H, Zhang L, Li L, Zheng C, Guo L, Li W, Sun P, Qin L. Recent developments and future prospects of antimicrobial metabolites produced by endophytes. Microbiol Res. 2010; 165:437-449.

218. Kennedy DO, Wightman EL. Herbal extracts and phytochemicals: plant secondary metabolites and the enhancement of human brain function. Adv Nutr. 2011; 2:32-50.

219. Bascom-Slack CA, Arnold AE, Strobel SA. IBI series winner. Student-directed discovery of the plant microbiome and its products. Science. 2012; 338:485-486.

220. Aly AH, Debbab A, Proksch P. Fungal endophytes - secret producers of bioactive plant metabolites. Pharmazie. 2013; 68:499-505.

221. Mousa WK, Raizada MN. The diversity of anti-microbial secondary metabolites produced by fungal endophytes: an interdisciplinary perspective. Front Microbiol. 2013; 4: 65.

222. Hansen BG, Halkier BA. New insight into the biosynthesis and regulation of indole compounds in Arabidopsis thaliana. Planta. 2005; 221:603-606.

223. Hooper PL, Hooper PL, Tytell M, Vígh L. Xenohormesis: health benefits from an eon of plant stress response evolution. Cell Stress Chaperones. 2010; 15:761-770.

224. Higdon J, Drake VJ. An evidence-based approach to phytochemicals and other dietary factors, 2nd ed. Thieme, New York, 2012.

225. Menendez JA, Joven J, Aragonès G, Barrajón-Catalán E, Beltrán-Debón R, Borrás-Linares I, Camps J, Corominas-Faja B, Cufí S, Fernández-Arroyo S, Garcia-Heredia A, Hernández-Aguilera A, Herranz-López M, Jiménez-Sánchez C, López-Bonet E, Lozano-Sánchez J, Luciano-Mateo F, Martin-Castillo B, Martin-Paredero V, Pérez-Sánchez A, Oliveras-Ferraros C, Riera-Borrull M, Rodríguez-Gallego E, Quirantes-Piné R, Rull A, Tomás-Menor L, Vazquez-Martin A, Alonso-Villaverde C, Micol V, Segura-Carretero A. Xenohormetic and anti-aging activity of secoiridoid polyphenols present in extra virgin olive oil: a new family of gerosuppressant agents. Cell Cycle. 2013; 12:555-578.

226. Si H, Liu D. Dietary antiaging phytochemicals and mechanisms associated with prolonged survival. J Nutr Biochem. 2014; 25:581-591.

227. Wu Z, Song L, Liu SQ, Huang D. Tanshinones extend chronological lifespan in budding yeast Saccharomyces cerevisiae. Appl Microbiol Biotechnol. 2014; 98:8617-8628.

228. Somani SJ, Modi KP, Majumdar AS, Sadarani BN. Phytochemicals and their potential usefulness in inflammatory bowel disease. Phytother Res. 2015; 29:339-350.

229. Wink M. Evolution of secondary metabolites from an ecological and molecular phylogenetic perspective. Phytochemistry. 2003; 64:3-19.

230. Tahara S. A journey of twenty-five years through the ecological biochemistry of flavonoids. Biosci Biotechnol Biochem. 2007; 71:1387-1404.

231. Murakami A. Modulation of protein quality control systems by food phytochemicals. J Clin Biochem Nutr. 2013; 52:215-227.

232. Adrian M, Jeandet P, Veneau J, Weston LA, Bessis R. Biological activity of resveratrol, a stilbenic compound from grapevines, against Botrytis cinerea, the causal agent for gray mold. J Chem Ecol. 1997; 23:1689-1702.

233. Heath MC. Hypersensitive response-related death. Plant Mol Biol. 2000; 44:321-334.

234. Trewavas A, Stewart D. Paradoxical effects of chemicals in the diet on health. Curr Opin Plant Biol. 2003; 6:185-190.

235. Arimura G, Kost C, Boland W. Herbivore-induced, indirect plant defences. Biochim Biophys Acta. 2005; 1734:91-111.

236. Brencic A, Winans SC. Detection of and response to signals involved in host-microbe interactions by plant-associated bacteria. Microbiol Mol Biol Rev. 2005; 69:155-194.

237. Mattson MP, Son TG, Camandola S. Viewpoint: mechanisms of action and therapeutic

potential of neurohormetic phytochemicals. Dose Response. 2007; 5:174-186.

238. Santiago R, Malvar RA. Role of dehydrodiferulates in maize resistance to pests and diseases. Int J Mol Sci. 2010; 11:691-703.

239. Tang K, Zhan JC, Yang HR, Huang WD. Changes of resveratrol and antioxidant enzymes during UV-induced plant defense response in peanut seedlings. J Plant Physiol. 2010; 167:95-102.

240. Arimura G, Ozawa R, Maffei ME. Recent advances in plant early signaling in response to herbivory. Int J Mol Sci. 2011; 12:3723-3739.

241. Barros-Rios J, Malvar RA, Jung HJ, Santiago R. Cell wall composition as a maize defense mechanism against corn borers. Phytochemistry. 2011; 72:365-371.

242. Bednarek P. Sulfur-containing secondary metabolites from Arabidopsis thaliana and other Brassicaceae with function in plant immunity. Chembiochem. 2012; 13:1846-1859.

243. Nwachukwu ID, Slusarenko AJ, Gruhlke MC. Sulfur and sulfur compounds in plant defence. Nat Prod Commun. 2012; 7:395-400.

244. Huot OB, Nachappa P, Tamborindeguy C. The evolutionary strategies of plant defenses have a dynamic impact on the adaptations and interactions of vectors and pathogens. Insect Sci. 2013; 20:297-306.

245. Kazan K, Lyons R. Intervention of Phytohormone Pathways by Pathogen Effectors. Plant Cell. 2014; 26:2285-2309.

246. Porras-Alfaro A, Bayman P. Hidden fungi, emergent properties: endophytes and microbiomes. Annu Rev Phytopathol. 2011; 49:291-315.

247. Zhao J, Shan T, Mou Y, Zhou L. Plant-derived bioactive compounds produced by endophytic

fungi. Mini Rev Med Chem. 2011; 11:159-168.

248. Kusari S, Hertweck C, Spiteller M. Chemical ecology of endophytic fungi: origins of secondary metabolites. Chem Biol. 2012; 19:792-798.

249. Nath A, Raghunatha P, Joshi SR. Diversity and Biological Activities of Endophytic Fungi of Emblica officinalis, an Ethnomedicinal Plant of India. Mycobiology. 2012; 40:8-13.

250. Zhang Y, Han T, Ming Q, Wu L, Rahman K, Qin L. Alkaloids produced by endophytic fungi: a review. Nat Prod Commun. 2012; 7:963-968.

251. Lebeis SL. The potential for give and take in plant-microbiome relationships. Front Plant Sci. 2014; 5: 287.

252. Harikumar KB, Aggarwal BB. Resveratrol: a multitargeted agent for age-associated chronic diseases. Cell Cycle. 2008; 7:1020-1035.

253. Son TG, Camandola S, Mattson MP. Hormetic dietary phytochemicals. Neuromolecular Med. 2008; 10:236-246.

254. Calabrese V, Cornelius C, Dinkova-Kostova AT, Iavicoli I, Di Paola R, Koverech A, Cuzzocrea S, Rizzarelli E, Calabrese EJ. Cellular stress responses, hormetic phytochemicals and vitagenes in aging and longevity. Biochim Biophys Acta. 2012; 1822:753-783.

255. Dong Y, Guha S, Sun X, Cao M, Wang X, Zou S. Nutraceutical interventions for promoting healthy aging in invertebrate models. Oxid Med Cell Longev. 2012; 2012: 718491.

256. Lamming DW, Sabatini DM, Baur JA. Pharmacologic Means of Extending Lifespan. J Clin Exp Pathol. 2012; Suppl 4: 7327.

257. Vauzour D. Dietary polyphenols as modulators of brain functions: biological actions and

molecular mechanisms underpinning their beneficial effects. Oxid Med Cell Longev. 2012; 2012: 914273.

258. Argyropoulou A, Aligiannis N, Trougakos IP, Skaltsounis AL. Natural compounds with anti-ageing activity. Nat Prod Rep. 2013; 30:1412-1437.

259. Lee JH, Khor TO, Shu L, Su ZY, Fuentes F, Kong AN. Dietary phytochemicals and cancer prevention: Nrf2 signaling, epigenetics, and cell death mechanisms in blocking cancer initiation and progression. Pharmacol Ther. 2013; 137:153-171.

260. Lucanic M, Lithgow GJ, Alavez S. Pharmacological lifespan extension of invertebrates. Ageing Res Rev. 2013; 12:445-458.

261. Monroy A, Lithgow GJ, Alavez S. Curcumin and neurodegenerative diseases. Biofactors. 2013; 39:122-132.

262. de Cabo R, Carmona-Gutierrez D, Bernier M, Hall MN, Madeo F. The search for antiaging interventions: from elixirs to fasting regimens. Cell. 2014; 157:1515-1526.

263. Grabacka MM, Gawin M, Pierzchalska M. Phytochemical modulators of mitochondria: the search for chemopreventive agents and supportive therapeutics. Pharmaceuticals (Basel). 2014; 7:913-942.

264. Hubbard BP, Sinclair DA. Small molecule SIRT1 activators for the treatment of aging and age-related diseases. Trends Pharmacol Sci. 2014; 35:146-154.

265. Kennedy DO. Polyphenols and the human brain: plant “secondary metabolite” ecologic roles and endogenous signaling functions drive benefits. Adv Nutr. 2014; 5:515-533.

266. Koch K, Havermann S, Büchter C, Wätjen W. Caenorhabditis elegans as model system in pharmacology and toxicology: effects of flavonoids on redox-sensitive signalling pathways and

ageing. ScientificWorldJournal. 2014; 2014: 920398.

267. Lee J, Jo DG, Park D, Chung HY, Mattson MP. Adaptive cellular stress pathways as therapeutic targets of dietary phytochemicals: focus on the nervous system. Pharmacol Rev. 2014; 66:815-868.

268. Mansuri ML, Parihar P, Solanki I, Parihar MS. Flavonoids in modulation of cell survival signalling pathways. Genes Nutr. 2014; 9: 400.

269. Rege SD, Geetha T, Griffin GD, Broderick TL, Babu JR. Neuroprotective effects of resveratrol in Alzheimer disease pathology. Front Aging Neurosci. 2014; 6: 218.

270. Hubbard BP, Sinclair DA. Small molecule SIRT1 activators for the treatment of aging and age-related diseases. Trends Pharmacol Sci. 2014; 35:146-154.

271. Howitz KT, Bitterman KJ, Cohen HY, Lamming DW, Lavu S, Wood JG, Zipkin RE, Chung P, Kisielewski A, Zhang LL, Scherer B, Sinclair DA. Small molecule activators of sirtuins extend Saccharomyces cerevisiae lifespan. Nature. 2003; 425:191-196.

272. Xiang L, Sun K, Lu J, Weng Y, Taoka A, Sakagami Y, Qi J. Anti-aging effects of phloridzin, an apple polyphenol, on yeast via the SOD and Sir2 genes. Biosci Biotechnol Biochem. 2011; 75:854-858.

273. Belinha I, Amorim MA, Rodrigues P, de Freitas V, Moradas-Ferreira P, Mateus N, Costa V. Quercetin increases oxidative stress resistance and longevity in Saccharomyces cerevisiae. J Agric Food Chem. 2007; 55:2446-2451.

274. Yuan R, Lin Y. Traditional Chinese medicine: an approach to scientific proof and clinical validation. Pharmacol Ther. 2000; 86:191-198.

275. Tang JL, Liu BY, Ma KW. Traditional Chinese medicine. Lancet. 2008; 372:1938-1940.

276. Xu Z. Modernization: one step at a time. Nature. 2011; 480: S90-S92.

277. Hao C, Xiao PG. Network pharmacology: a Rosetta Stone for traditional Chinese medicine. Drug Dev Res. 2014; 75:299-312.

278. Buriani A, Garcia-Bermejo ML, Bosisio E, Xu Q, Li H, Dong X, Simmonds MS, Carrara M, Tejedor N, Lucio-Cazana J, Hylands PJ. Omic techniques in systems biology approaches to traditional Chinese medicine research: present and future. J Ethnopharmacol. 2012; 140:535-544.

279. Uzuner H, Bauer R, Fan TP, Guo DA, Dias A, El-Nezami H, Efferth T, Williamson EM, Heinrich M, Robinson N, Hylands PJ, Hendry BM, Cheng YC, Xu Q. Traditional Chinese medicine research in the post-genomic era: good practice, priorities, challenges and opportunities. J Ethnopharmacol. 2012; 140:458-468.

280. Xue R, Fang Z, Zhang M, Yi Z, Wen C, Shi T. TCMID: traditional Chinese Medicine integrative database for herb molecular mechanism analysis. Nucleic Acids Res. 2013; 41: D1089-D1095.

281. Sánchez-Vidaña DI, Rajwani R, Wong MS. The use of omic technologies applied to traditional Chinese medicine research. Evid Based Complement Alternat Med. 2017; 2017: 6359730.

282. Hopkins AL. Network pharmacology. Nat Biotechnol. 2007; 25:1110-1111.

283. Li S, Zhang ZQ, Wu LJ, Zhang XG, Li YD, Wang YY. Understanding ZHENG in traditional Chinese medicine in the context of neuro-endocrine-immune network. IET Syst Biol. 2007; 1:51-60.

284. Li S, Zhang B. Traditional Chinese medicine network pharmacology: theory, methodology and application. Chin J Nat Med. 2013; 11:110-120.

285. Tao W, Xu X, Wang X, Li B, Wang Y, Li Y, Yang L. Network pharmacology-based prediction of the active ingredients and potential targets of Chinese herbal Radix Curcumae formula for application to cardiovascular disease. J Ethnopharmacol. 2013; 145:1-10.

286. Liang X, Li H, Li S. A novel network pharmacology approach to analyse traditional herbal formulae: the Liu-Wei-Di-Huang pill as a case study. Mol Biosyst. 2014; 10:1014-1022.

287. Tang F, Tang Q, Tian Y, Fan Q, Huang Y, Tan X. Network pharmacology-based prediction of the active ingredients and potential targets of Mahuang Fuzi Xixin decoction for application to allergic rhinitis. J Ethnopharmacol. 2015; 176:402-412.

288. Li S. Exploring traditional Chinese medicine by a novel therapeutic concept of network target. Chin J Integr Med. 2016; 22:647-552.

289. Fang J, Wang L, Wu T, Yang C, Gao L, Cai H, Liu J, Fang S, Chen Y, Tan W, Wang Q. Network pharmacology-based study on the mechanism of action for herbal medicines in Alzheimer treatment. J Ethnopharmacol. 2017; 196:281-292.

290. Zeng L, Yang K. Exploring the pharmacological mechanism of Yanghe Decoction on HER2-positive breast cancer by a network pharmacology approach. J Ethnopharmacol. 2017; 199:68-85.

291. Chen L, Cao Y, Zhang H, Lv D, Zhao Y, Liu Y, Ye G, Chai Y. Network pharmacology-based strategy for predicting active ingredients and potential targets of Yangxinshi tablet for treating heart failure. J Ethnopharmacol. 2018; 219:359-368.

292. Zuo H, Zhang Q, Su S, Chen Q, Yang F, Hu Y. A network pharmacology-based approach to analyse potential targets of traditional herbal formulas: an example of Yu Ping Feng decoction. Sci Rep. 2018; 8: 11418.

293. Ding F, Zhang Q, Ung CO, Wang Y, Han Y, Hu Y, Qi J. An analysis of chemical ingredients

network of Chinese herbal formulae for the treatment of coronary heart disease. PLoS One. 2015; 10: e0116441.

294. Liang H, Ruan H, Ouyang Q, Lai L. Herb-target interaction network analysis helps to disclose molecular mechanism of traditional Chinese medicine. Sci Rep. 2016; 6: 36767.

295. Zhang Y, Mao X, Su J, Geng Y, Guo R, Tang S, Li J, Xiao X, Xu H, Yang H. A network pharmacology-based strategy deciphers the underlying molecular mechanisms of Qixuehe Capsule in the treatment of menstrual disorders. Chin Med. 2017; 12: 23.

296. Borisy AA, Elliott PJ, Hurst NW, Lee MS, Lehar J, Price ER, Serbedzija G, Zimmermann GR, Foley MA, Stockwell BR, Keith CT. Systematic discovery of multicomponent therapeutics. Proc Natl Acad Sci U S A. 2003; 100:7977-7982.

297. Csermely P, Agoston V, Pongor S. The efficiency of multi-target drugs: the network approach might help drug design. Trends Pharmacol Sci. 2005; 26:178-182.

298. Keith CT, Borisy AA, Stockwell BR. Multicomponent therapeutics for networked systems. Nat Rev Drug Discov. 2005; 4:71-78.

299. Smalley KS, Haass NK, Brafford PA, Lioni M, Flaherty KT, Herlyn M. Multiple signaling pathways must be targeted to overcome drug resistance in cell lines derived from melanoma metastases. Mol Cancer Ther. 2006; 5:1136-1144.

300. Kitano H. A robustness-based approach to systems-oriented drug design. Nat Rev Drug Discov. 2007; 6:202-210.

301. Zimmermann GR, Lehár J, Keith CT. Multi-target therapeutics: when the whole is greater than the sum of the parts. Drug Discov Today. 2007; 12:34-42.

302. Lehár J, Stockwell BR, Giaever G, Nislow C. Combination chemical genetics. Nat Chem

Biol. 2008; 4:674-681.

303. Podolsky SH, Greene JA. Combination drugs—hype, harm, and hope. N Engl J Med. 2011; 365:488-491.

304. Csermely P, Korcsmáros T, Kiss HJ, London G, Nussinov R. Structure and dynamics of molecular networks: a novel paradigm of drug discovery: a comprehensive review. Pharmacol Ther. 2013; 138:333-408.

305. Baym M, Stone LK, Kishony R. Multidrug evolutionary strategies to reverse antibiotic resistance. Science. 2016; 351: aad3292.

306. He B, Lu C, Zheng G, He X, Wang M, Chen G, Zhang G, Lu A. Combination therapeutics in complex diseases. J Cell Mol Med. 2016; 20:2231-2240.

307. Lopez JS, Banerji U. Combine and conquer: challenges for targeted therapy combinations in early phase trials. Nat Rev Clin Oncol. 2017; 14:57-66.

308. Singh N, Yeh PJ. Suppressive drug combinations and their potential to combat antibiotic resistance. J Antibiot (Tokyo). 2017; 70:1033-1042.

309. Hao T, Wang Q, Zhao L, Wu D, Wang E, Sun J. Analyzing of molecular networks for human diseases and drug discovery. Curr Top Med Chem. 2018; 18:1007-1014.

310. Weiss A, Nowak-Sliwinska P. Current trends in multidrug optimization: an alley of future successful treatment of complex disorders. SLAS Technol. 2017; 22:254-275.

311. Nelson HS. Advair: combination treatment with fluticasone propionate/salmeterol in the treatment of asthma. J Allergy Clin Immunol. 2001; 107:398-416.

312. Glass G. Cardiovascular combinations. Nat Rev Drug Discov. 2004; 3:731-732.

313. Herrick TM, Million RP. Tapping the potential of fixed-dose combinations. Nat Rev Drug Discov. 2007; 6:513-514.

314. Pangalos MN, Schechter LE, Hurko O. Drug development for CNS disorders: strategies for balancing risk and reducing attrition. Nat Rev Drug Discov. 2007; 6:521-532.

315. Kummar S, Chen HX, Wright J, Holbeck S, Millin MD, Tomaszewski J, Zweibel J, Collins J, Doroshow JH. Utilizing targeted cancer therapeutic agents in combination: novel approaches and urgent requirements. Nat Rev Drug Discov. 2010; 9:843-856.

316. Humphrey RW, Brockway-Lunardi LM, Bonk DT, Dohoney KM, Doroshow JH, Meech SJ, Ratain MJ, Topalian SL, Pardoll DM. Opportunities and challenges in the development of experimental drug combinations for cancer. J Natl Cancer Inst. 2011; 103:1222-1226.

317. Casado JL, Bañón S. Dutrebis (lamivudine and raltegravir) for use in combination with other antiretroviral products for the treatment of HIV-1 infection. Expert Rev Clin Pharmacol. 2015; 8:709-718.

318. Horita N, Kaneko T. Role of combined indacaterol and glycopyrronium bromide (QVA149) for the treatment of COPD in Japan. Int J Chron Obstruct Pulmon Dis. 2015; 10:813-822.

319. Yang J, Tang H, Li Y, Zhong R, Wang T, Wong S, Xiao G, Xie Y. DIGRE: drug-induced genomic residual effect model for successful prediction of multidrug effects. CPT Pharmacometrics Syst Pharmacol. 2015; 4: e1.

320. Patel SJ, Kuten SA, Musick WL, Gaber AO, Monsour HP, Knight RJ. Combination drug products for HIV-A word of caution for the transplant clinician. Am J Transplant. 2016; 16:2479-2482.

321. Spitzer M, Robbins N, Wright GD. Combinatorial strategies for combating invasive fungal

infections. Virulence. 2017; 8:169-185.

322. Yin Z, Deng Z, Zhao W, Cao Z. Searching synergistic dose combinations for anticancer drugs. Front Pharmacol. 2018; 9: 535.

323. Lehár J, Zimmermann GR, Krueger AS, Molnar RA, Ledell JT, Heilbut AM, Short GF 3rd, Giusti LC, Nolan GP, Magid OA, Lee MS, Borisy AA, Stockwell BR, Keith CT. Chemical combination effects predict connectivity in biological systems. Mol Syst Biol. 2007; 3: 80.

324. Yeh P, Kishony R. Networks from drug-drug surfaces. Mol Syst Biol. 2007; 3: 85.

325. Chou TC. Drug combination studies and their synergy quantification using the Chou-Talalay method. Cancer Res. 2010; 70:440-446.

326. Tallarida RJ. Quantitative methods for assessing drug synergism. Genes Cancer. 2011; 2:1003-1008.

327. Zou J, Ji P, Zhao YL, Li LL, Wei YQ, Chen YZ, Yang SY. Neighbor communities in drug combination networks characterize synergistic effect. Mol Biosyst. 2012; 8:3185-3196.

328. Bansal M, Yang J, Karan C, Menden MP, Costello JC, Tang H, Xiao G, Li Y, Allen J, Zhong R, Chen B, Kim M, Wang T, et al, and NCI-DREAM Community. A community computational challenge to predict the activity of pairs of compounds. Nat Biotechnol. 2014; 32:1213-1222.

329. Foucquier J, Guedj M. Analysis of drug combinations: current methodological landscape. Pharmacol Res Perspect. 2015; 3: e00149.

330. Yadav B, Wennerberg K, Aittokallio T, Tang J. Searching for drug synergy in complex dose-response landscapes using an interaction potency Model. Comput Struct Biotechnol J. 2015; 13:504-513.

331. Li X, Qin G, Yang Q, Chen L, Xie L. Biomolecular network-based synergistic drug combination discovery. Biomed Res Int. 2016; 2016: 8518945.

332. Harman D. The aging process: major risk factor for disease and death. Proc Natl Acad Sci USA. 1991; 88:5360-5363.

333. Blagosklonny MV. Validation of anti-aging drugs by treating age-related diseases. Aging (Albany NY). 2009; 1:281-288.

334. Niccoli T, Partridge L. Ageing as a risk factor for disease. Curr Biol. 2012; 22: R741–R52.

335. Kaeberlein M. Longevity and aging. F1000Prime Rep. 2013; 5: 5.

336. Kaeberlein M. The biology of aging: citizen scientists and their pets as a bridge between research on model organisms and human subjects. Vet Pathol. 2016; 53:291-298.

337. de Cabo R, Carmona-Gutierrez D, Bernier M, Hall MN, Madeo F. The search for antiaging interventions: from elixirs to fasting regimens. Cell. 2014; 157:1515-1526.

338. Kennedy BK, Berger SL, Brunet A, Campisi J, Cuervo AM, Epel ES, Franceschi C, Lithgow GJ, Morimoto RI, Pessin JE, Rando TA, Richardson A, Schadt EE, et al. Geroscience: linking aging to chronic disease. Cell. 2014; 159:709-713.

339. Longo VD, Antebi A, Bartke A, Barzilai N, Brown-Borg HM, Caruso C, Curiel TJ, de Cabo R, Franceschi C, Gems D, Ingram DK, Johnson TE, Kennedy BK, et al. Interventions to slow aging in humans: are we ready? Aging Cell. 2015; 14:497-510.

340. Fontana L, Partridge L, Longo VD. Extending healthy life span—from yeast to humans. Science. 2010; 328:321-326.

341. López-Otín C, Blasco MA, Partridge L, Serrano M, Kroemer G. The hallmarks of aging. Cell.

2013; 153:1194-1217.

342. Carvalhal Marques F, Volovik Y, Cohen E. The roles of cellular and organismal aging in the development of late-onset maladies. Annu Rev Pathol. 2015; 10:1-23.

343. Fontana L, Partridge L. Promoting health and longevity through diet: from model organisms to humans. Cell. 2015; 161:106-118.

344. Mazucanti CH, Cabral-Costa JV, Vasconcelos AR, Andreotti DZ, Scavone C, Kawamoto EM. Longevity pathways (mTOR, SIRT, Insulin/IGF-1) as key modulatory targets on aging and neurodegeneration. Curr Top Med Chem. 2015; 15:2116-2138.

345. Burkewitz K, Weir HJ, Mair WB. AMPK as a Pro-longevity Target. Exp Suppl. 2016; 107:227-256.

346. Pan H, Finkel T. Key proteins and pathways that regulate lifespan. J Biol Chem. 2017; 292:6452-6460.

347. Aliper A, Belikov AV, Garazha A, Jellen L, Artemov A, Suntsova M, Ivanova A, Venkova L, Borisov N, Buzdin A, Mamoshina P, Putin E, Swick AG, et al. In search for geroprotectors: in silico screening and in vitro validation of signalome-level mimetics of young healthy state. Aging (Albany NY). 2016; 8:2127-2152.

348. Moskalev A, Chernyagina E, Tsvetkov V, Fedintsev A, Shaposhnikov M, Krut'ko V, Zhavoronkov A, Kennedy BK. Developing criteria for evaluation of geroprotectors as a key stage toward translation to the clinic. Aging Cell. 2016; 15:407-415.

349. Blagosklonny MV. From rapalogs to anti-aging formula. Oncotarget. 2017; 8:35492-35507.

350. Ladiges W, Liggitt D. Testing drug combinations to slow aging. Pathobiol Aging Age Relat Dis. 2017; 8: 1407203.

351. Blagosklonny MV. Koschei the immortal and anti-aging drugs. Cell Death Dis. 2014; 5: e1552.

352. Strong R, Miller RA, Antebi A, Astle CM, Bogue M, Denzel MS, Fernandez E, Flurkey K, Hamilton KL, Lamming DW, Javors MA, de Magalhães JP, Martinez PA, et al. Longer lifespan in male mice treated with a weakly estrogenic agonist, an antioxidant, an α-glucosidase inhibitor or a Nrf2-inducer. Aging Cell. 2016; 15:872-884.

353. Weiss R, Fernandez E, Liu Y, Strong R, Salmon AB. Metformin reduces glucose intolerance caused by rapamycin treatment in genetically heterogeneous female mice. Aging (Albany NY). 2018; 10:386-401.

354. Danilov A, Shaposhnikov M, Plyusnina E, Kogan V, Fedichev P, Moskalev A. Selective anticancer agents suppress aging in Drosophila. Oncotarget. 2013; 4:1507-1526.

355. Snell TW, Johnston RK, Rabeneck B, Zipperer C, Teat S. Joint inhibition of TOR and JNK pathways interacts to extend the lifespan of Brachionus manjavacas (Rotifera). Exp Gerontol. 2014; 52:55-69.

356. Admasu TD, Chaithanya Batchu K, Barardo D, Ng LF, Lam VY, Xiao L, Cazenave-Gassiot A, Wenk MR, Tolwinski NS, Gruber J. Drug synergy slows aging and improves healthspan through IGF and SREBP lipid signaling. Dev Cell. 2018; 47:67-79.

357. Huang X, Liu J, Withers BR, Samide AJ, Leggas M, Dickson RC. Reducing signs of aging and increasing lifespan by drug synergy. Aging Cell. 2013; 12:652-660.

358. Huang X, Leggas M, Dickson RC. Drug synergy drives conserved pathways to increase fission yeast lifespan. PLoS One. 2015; 10: e0121877.

359. McDonald RB. Biology of aging. Garland Science, Taylor & Francis Group, LLC. 2014;

Chapters 1 and 2, Pages 1-54.

360. de Magalhães JP, Cabral JA, Magalhães D. The influence of genes on the aging process of mice: a statistical assessment of the genetics of aging. Genetics. 2005; 169: 265-274.

361. Finch CE. Longevity, senescence, and the genome. University of Chicago Press, Chicago, 1990.

362. Abrams PA. Evolutionary biology: mortality and lifespan. Nature. 2004; 431:1048–1049.

363. Kirkwood TB. Understanding the odd science of aging. Cell. 2005; 120:437–447.

364. Medkour Y, Svistkova V, Titorenko VI. Cell-non-autonomous mechanisms underlying cellular and organismal aging. Int Rev Cell Mol Biol. 2016; 321:259-297.

365. Blagosklonny MV. Answering the ultimate question "what is the proximal cause of aging?" Aging (Albany NY). 2012; 4:861-877.

366. Fries JF, Bruce B, Chakravarty E. Compression of morbidity 1980–2011: a focused review of paradigms and progress. J Aging Res. 2011; 2011: 261702.

367. Gavrilov LA, Gavrilova NS. The biology of life span: a quantitative approach. New York, New York/Chur, Switzerland, Harwood Academic, 1991.

368. Lashmanova E, Proshkina E, Zhikrivetskaya S, Shevchenko O, Marusich E, Leonov S, Melerzanov A, Zhavoronkov A, Moskalev A. Fucoxanthin increases lifespan of Drosophila melanogaster and Caenorhabditis elegans. Pharmacol Res. 2015; 100:228-241.

369. Burstein MT, Beach A, Richard VR, Koupaki O, Gomez-Perez A, Goldberg AA, Kyryakov P, Bourque SD, Glebov A, Titorenko VI. Interspecies chemical signals released into the environment may create xenohormetic, hormetic and cytostatic selective forces that drive the

ecosystemic evolution of longevity regulation mechanisms. Dose Response. 2012a; 10:75–82.

370. Calabrese EJ, Mattson MP. Hormesis provides a generalized quantitative estimate of biological plasticity. J Cell Commun Signal. 2011; 5:25–38.

371. Goldberg AA, Kyryakov P, Bourque SD, Titorenko VI. Xenohormetic, hormetic and cytostatic selective forces driving longevity at the ecosystemic level. Aging (Albany NY). 2010b; 2:461–470.

372. Cui H, Kong Y, Zhang H. Oxidative stress, mitochondrial dysfunction, and aging. J Signal Transduct. 2012; 2012: 646354.

373. Ray PD, Huang BW, Tsuji Y. Reactive oxygen species (ROS) homeostasis and redox regulation in cellular signaling. Cell Signal. 2012; 24:981-990.

374. Gladyshev VN. The origin of aging: imperfectness-driven non-random damage defines the aging process and control of lifespan. Trends Genet. 2013; 29:506-512.

375. Gladyshev VN. The free radical theory of aging is dead. Long live the damage theory! Antioxid Redox Signal. 2014; 20:727-731.

376. Ristow M, Schmeisser K. Mitohormesis: Promoting health and lifespan by increased levels of reactive oxygen species (ROS). Dose Response. 2014; 12:288-341.

377. Schieber M, Chandel NS. ROS function in redox signaling and oxidative stress. Curr Biol. 2014; 24: R453-R462.

378. Shadel GS, Horvath TL. Mitochondrial ROS signaling in organismal homeostasis. Cell. 2015; 163:560-569.

379. Wang Y, Hekimi S. Mitochondrial dysfunction and longevity in animals: Untangling the knot.

2015; 350:1204-1207.

380. Gems D, Partridge L. Stress-response hormesis and aging: “that which does not kill us makes us stronger”. Cell Metab. 2008; 7:200-203.

381. Calabrese V, Cornelius C, Cuzzocrea S, Iavicoli I, Rizzarelli E, Calabrese EJ. Hormesis, cellular stress response and vitagenes as critical determinants in aging and longevity. Mol Aspects Med. 2011; 32:279-304.

382. Veal E, Day A. Hydrogen peroxide as a signaling molecule. Antioxid Redox Signal. 2011; 15:147-151.

383. Walther TC, Farese RV Jr. Lipid droplets and cellular lipid metabolism. Annu Rev Biochem. 2012; 81:687–714.

384. Koch B, Schmidt C, Daum G. Storage lipids of yeasts: a survey of nonpolar lipid metabolism in Saccharomyces cerevisiae, Pichia pastoris, and Yarrowia lipolytica. FEMS Microbiol Rev. 2014; 38:892–915.

385. Klug L, Daum G. Yeast lipid metabolism at a glance. FEMS Yeast Res. 2014; 14:369–388.

386. Ohsaki Y, Suzuki M, Fujimoto T. Open questions in lipid droplet biology. Chem Biol. 2014; 21:86–96.

387. Pol A, Gross SP, Parton RG. Review: biogenesis of the multifunctional lipid droplet: lipids, proteins, and sites. J Cell Biol. 2014; 204:635–646.

388. Wang CW. Lipid droplet dynamics in budding yeast. Cell Mol Life Sci. 2015; 72:2677–2695.

389. Blüher M, Kahn BB, Kahn CR. Extended longevity in mice lacking the insulin receptor in adipose tissue. Science. 2003; 299:572–574.

390. Chiu CH, Lin WD, Huang SY, Lee YH. Effect of a C/EBP gene replacement on mitochondrial biogenesis in fat cells. Genes Dev. 2004; 18:1970–1975.

391. Picard F, Kurtev M, Chung N, Topark-Ngarm A, Senawong T, Machado De Oliveira R, Leid M, McBurney MW, Guarente L. Sirt1 promotes fat mobilization in white adipocytes by repressing PPAR-γ. Nature. 2004; 429:771–776.

392. Grönke S, Mildner A, Fellert S, Tennagels N, Petry S, Müller G, Jäckle H, Kühnlein RP. Brummer lipase is an evolutionary conserved fat storage regulator in Drosophila. Cell Metab. 2005; 1:323–330.

393. Haemmerle G, Lass A, Zimmermann R, Gorkiewicz G, Meyer C, Rozman J, Heldmaier G, Maier R, Theussl C, Eder S, Kratky D, Wagner EF, Klingenspor M, et al. Defective lipolysis and altered energy metabolism in mice lacking adipose triglyceride lipase. Science. 2006; 312:734–737.

394. Russell SJ, Kahn CR. Endocrine regulation of ageing. Nat Rev Mol Cell Biol. 2007; 8:681–691.

395. Blüher M. Fat tissue and long life. Obes Facts. 2008; 1:176–182.

396. Wang MC, O'Rourke EJ, Ruvkun G. Fat metabolism links germline stem cells and longevity in C. elegans. Science. 2008; 322:957–960.

397. Narbonne P, Roy R. Caenorhabditis elegans dauers need LKB1/AMPK to ration lipid reserves and ensure long-term survival. Nature. 2009; 457:210–214.

398. Greenberg AS, Coleman RA, Kraemer FB, McManaman JL, Obin MS, Puri V, Yan QW, Miyoshi H, Mashek DG. The role of lipid droplets in metabolic disease in rodents and humans. J Clin Invest. 2011; 121:2102–2110.

399. Zechner R, Zimmermann R, Eichmann TO, Kohlwein SD, Haemmerle G, Lass A, Madeo F. FAT SIGNALS - lipases and lipolysis in lipid metabolism and signaling. Cell Metab. 2012; 15:279–291.

400. Krahmer N, Farese RV Jr, Walther TC. Balancing the fat: lipid droplets and human disease. EMBO Mol Med. 2013; 5:905–915.

401. Rambold AS, Cohen S, Lippincott-Schwartz J. Fatty acid trafficking in starved cells: regulation by lipid droplet lipolysis, autophagy, and mitochondrial fusion dynamics. Dev Cell. 2015; 32:678–692.

402. Welte MA. Expanding roles for lipid droplets. Curr Biol. 2015; 25: R470–R481.

403. Miquel J, Fleming J and Economos AC. Antioxidants, metabolic rate and aging in Drosophila. Arch Gerontol Geriatr. 1982; 1:159-165.

404. Richie JP Jr, Mills BJ and Lang CA. Dietary nordihydroguaiaretic acid increases the life span of the mosquito. Proc Soc Exp Biol Med. 1986; 183:81-85.

405. Wang P, Zhang Z, Ma X, Huang Y, Liu X, Tu P and Tong T. HDTIC-1 and HDTIC-2, two compounds extracted from Astragali Radix, delay replicative senescence of human diploid fibroblasts. Mech Ageing Dev. 2003; 124:1025-1034.

406. Bauer JH, Goupil S, Garber GB and Helfand SL. An accelerated assay for the identification of lifespan-extending interventions in Drosophila melanogaster. Proc Natl Acad Sci USA. 2004; 101:12980-12985.

407. West M, Mhatre M, Ceballos A, Floyd RA, Grammas P, Gabbita SP, Hamdheydari L, Mai T, Mou S, Pye QN, Stewart C, West S, Williamson KS, Zemlan F and Hensley K. The arachidonic acid 5-lipoxygenase inhibitor nordihydroguaiaretic acid inhibits tumor necrosis factor alpha

activation of microglia and extends survival of G93A-SOD1 transgenic mice. J Neurochem. 2004; 91:133-143.

408. Wood JG, Rogina B, Lavu S, Howitz K, Helfand SL, Tatar M and Sinclair D. Sirtuin activators mimic caloric restriction and delay ageing in metazoans. Nature. 2004; 430:686-689.

409. Kiaei M, Kipiani K, Petri S, Chen J, Calingasan NY and Beal MF. Celastrol blocks neuronal cell death and extends life in transgenic mouse model of amyotrophic lateral sclerosis. Neurodegener Dis. 2005; 2:246-254.

410. Valenzano DR, Terzibasi E, Genade T, Cattaneo A, Domenici L and Cellerino A. Resveratrol prolongs lifespan and retards the onset of age-related markers in a short-lived vertebrate. Curr Biol. 2006; 16:296-300.

411. Kampkötter A, Gombitang Nkwonkam C, Zurawski RF, Timpel C, Chovolou Y, Wätjen W and Kahl R. Effects of the flavonoids kaempferol and fisetin on thermotolerance, oxidative stress and FoxO transcription factor DAF-16 in the model organism Caenorhabditis elegans. Arch Toxicol. 2007; 81:849-858.

412. Katsiki M, Chondrogianni N, Chinou I, Rivett AJ and Gonos ES. The olive constituent oleuropein exhibits proteasome stimulatory properties in vitro and confers life span extension of human embryonic fibroblasts. Rejuvenation Res. 2007; 10:157-172.

413. Petrascheck M, Ye X and Buck LB. An antidepressant that extends lifespan in adult Caenorhabditis elegans. Nature. 2007; 450:553-556.

414. Anisimov VN, Berstein LM, Egormin PA, Piskunova TS, Popovich IG, Zabezhinski MA, Tyndyk ML, Yurova MV, Kovalenko IG, Poroshina TE and Semenchenko AV. Metformin slows down aging and extends life span of female SHR mice. Cell Cycle. 2008; 7:2769-2773.

415. Benedetti MG, Foster AL, Vantipalli MC, White MP, Sampayo JN, Gill MS, Olsen A and

Lithgow GJ. Compounds that confer thermal stress resistance and extended lifespan. Exp Gerontol. 2008; 43:882-891.

416. Engel N and Mahlknecht U. Aging and anti-aging: unexpected side effects of everyday medication through sirtuin1 modulation. Int J Mol Med. 2008; 21:223-232.

417. Evason K, Collins JJ, Huang C, Hughes S and Kornfeld K. Valproic acid extends Caenorhabditis elegans lifespan. Aging Cell. 2008; 7:305-317.

418. Kampkötter A, Timpel C, Zurawski RF, Ruhl S, Chovolou Y, Proksch P and Wätjen W. Increase of stress resistance and lifespan of Caenorhabditis elegans by quercetin. Comp Biochem Physiol B Biochem Mol Biol. 2008; 149:314-323.

419. Pan W, Jiang S, Luo P, Wu J and Gao P. Isolation, purification and structure identification of antioxidant compound from the roots of Incarvillea younghusbandii Sprague and its life span prolonging effect in Drosophila melanogaster. Nat Prod Res. 2008; 22:719-725.

420. Pearson KJ, Baur JA, Lewis KN, Peshkin L, Price NL, Labinskyy N, Swindell WR, Kamara D, Minor RK, Perez E, Jamieson HA, Zhang Y, Dunn SR, Sharma K, Pleshko N, Woollett LA, Csiszar A, Ikeno Y, Le Couteur D, Elliott PJ, Becker KG, Navas P, Ingram DK, Wolf NS, Ungvari Z, Sinclair DA and de Cabo R. Resveratrol delays age-related deterioration and mimics transcriptional aspects of dietary restriction without extending life span. Cell Metab. 2008; 8:157-168.

421. Srivastava D, Arya U, SoundaraRajan T, Dwivedi H, Kumar S and Subramaniam JR. Reserpine can confer stress tolerance and lifespan extension in the nematode C. elegans. Biogerontology. 2008; 9:309-316.

422. Strong R, Miller RA, Astle CM, Floyd RA, Flurkey K, Hensley KL, Javors MA, Leeuwenburgh C, Nelson JF, Ongini E, Nadon NL, Warner HR and Harrison DE. Nordihydroguaiaretic acid and aspirin increase lifespan of genetically heterogeneous male mice.

Aging Cell. 2008; 7:641-650.

423. Abbas S and Wink M. Epigallocatechin gallate from green tea (Camellia sinensis) increases lifespan and stress resistance in Caenorhabditis elegans. Planta Med. 2009; 75:216-221.

424. Arya U, Dwivedi H and Subramaniam JR. Reserpine ameliorates Abeta toxicity in the Alzheimer's disease model in Caenorhabditis elegans. Exp Gerontol. 2009; 44:462-466.

425. Bakshi HA, Sam S, Feroz A, Ravesh Z, Shah GA and Sharma M. Crocin from Kashmiri saffron (Crocus sativus) induces in vitro and in vivo xenograft growth inhibition of Dalton's lymphoma (DLA) in mice. Asian Pac J Cancer Prev. 2009; 10:887-890.

426. Pietsch K, Saul N, Menzel R, Stürzenbaum SR and Steinberg CE. Quercetin mediated lifespan extension in Caenorhabditis elegans is modulated by age-1, daf-2, sek-1 and unc-43. Biogerontology. 2009; 10:565-578.

427. Saul N, Pietsch K, Menzel R, Stürzenbaum SR and Steinberg CE. Catechin induced longevity in C. elegans: from key regulator genes to disposable soma. Mech Ageing Dev. 2009; 130:477-486.

428. Harrison DE, Strong R, Sharp ZD, Nelson JF, Astle CM, Flurkey K, Nadon NL, Wilkinson JE, Frenkel K, Carter CS, Pahor M, Javors MA, Fernandez E and Miller RA. Rapamycin fed late in life extends lifespan in genetically heterogeneous mice. Nature. 2009; 460:392-395.

429. Skulachev VP, Anisimov VN, Antonenko YN, Bakeeva LE, Chernyak BV, Erichev VP, Filenko OF, Kalinina NI, Kapelko VI, Kolosova NG, Kopnin BP, Korshunova GA, Lichinitser MR, Obukhova LA, Pasyukova EG, Pisarenko OI, Roginsky VA, Ruuge EK, Senin II, Severina II, Skulachev MV, Spivak IM, Tashlitsky VN, Tkachuk VA, Vyssokikh MY, Yaguzhinsky LS, Zorov DB. An attempt to prevent senescence: a mitochondrial approach. Biochim Biophys Acta. 2009; 1787:437-461.

430. Bjedov I, Toivonen JM, Kerr F, Slack C, Jacobson J, Foley A and Partridge L. Mechanisms of life span extension by rapamycin in the fruit fly Drosophila melanogaster. Cell Metab. 2010; 11:35-46.

431. Choi MJ, Kim BK, Park KY, Yokozawa T and Song YO and Cho EJ. Anti-aging effects of cyanidin under a stress-induced premature senescence cellular system. Biol Pharm Bull. 2010; 33:421-426.

432. Chondrogianni N, Kapeta S, Chinou I, Vassilatou K, Papassideri I and Gonos ES. Anti-ageing and rejuvenating effects of quercetin. Exp Gerontol. 2010; 45:763-771.

433. Lee KS, Lee BS, Semnani S, Avanesian A, Um CY, Jeon HJ, Seong KM, Yu K, Min KJ and Jafari M. Curcumin extends life span, improves health span, and modulates the expression of age-associated aging genes in Drosophila melanogaster. Rejuvenation Res. 2010; 13:561-570.

434. Onken B and Driscoll M. Metformin induces a dietary restriction-like state and the oxidative stress response to extend C. elegans healthspan via AMPK, LKB1, and SKN-1. PLoS One. 2010; 5: e8758.

435. Saul N, Pietsch K, Menzel R, Stürzenbaum SR and Steinberg CE. The longevity effect of tannic acid in Caenorhabditis elegans: Disposable Soma meets hormesis. J Gerontol A Biol Sci Med Sci. 2010; 65:626-635.

436. Cai WJ, Huang JH, Zhang SQ, Wu B, Kapahi P, Zhang XM and Shen ZY. Icariin and its derivative icariside II extend healthspan via insulin/IGF-1 pathway in C. elegans. PLoS One. 2011; 6: e28835.

437. Liao VH, Yu CW, Chu YJ, Li WH, Hsieh YC and Wang TT. Curcumin-mediated lifespan extension in Caenorhabditis elegans. Mech Ageing Dev. 2011; 132:480-487.

438. Lublin A, Isoda F, Patel H, Yen K, Nguyen L, Hajje D, Schwartz M and Mobbs C. FDA-

approved drugs that protect mammalian neurons from glucose toxicity slow aging dependent on cbp and protect against proteotoxicity. PLoS One. 2011; 6: e27762.

439. Powolny AA, Singh SV, Melov S, Hubbard A and Fisher AL. The garlic constituent diallyl trisulfide increases the lifespan of C. elegans via skn-1 activation. Exp Gerontol. 2011; 46:441-452.

440. Pietsch K, Saul N, Chakrabarti S, Stürzenbaum SR, Menzel R and Steinberg CE. Hormetins, antioxidants and prooxidants: defining quercetin-, caffeic acid- and rosmarinic acid-mediated life extension in C. elegans. Biogerontology. 2011; 12:329-347.

441. Sayed AA. Ferulsinaic acid attenuation of advanced glycation end products extends the lifespan of Caenorhabditis elegans. J Pharm Pharmacol. 2011; 63:423-428.

442. Saul N, Pietsch K, Stürzenbaum SR, Menzel R and Steinberg CE. Diversity of polyphenol action in Caenorhabditis elegans: between toxicity and longevity. J Nat Prod. 2011; 74:1713-1720.

443. Xue YL, Ahiko T, Miyakawa T, Amino H, Hu F, Furihata K, Kita K, Shirasawa T, Sawano Y and Tanokura M. Isolation and Caenorhabditis elegans lifespan assay of flavonoids from onion. J Agric Food Chem. 2011; 59:5927-5934.

444. Caesar I, Jonson M, Nilsson KP, Thor S and Hammarström P. Curcumin promotes A-beta fibrillation and reduces neurotoxicity in transgenic Drosophila. PLoS One. 2012; 7: e31424.

445. Cañuelo A, Gilbert-López B, Pacheco-Liñán P, Martínez-Lara E, Siles E and Miranda-Vizuete A. Tyrosol, a main phenol present in extra virgin olive oil, increases lifespan and stress resistance in Caenorhabditis elegans. Mech Ageing Dev. 2012; 133:563-574.

446 Grünz G, Haas K, Soukup S, Klingenspor M, Kulling SE, Daniel H and Spanier B. Structural features and bioavailability of four flavonoids and their implications for lifespan-extending and antioxidant actions in C. elegans. Mech Ageing Dev. 2012; 133:1-10.

447. Rascón B, Hubbard BP, Sinclair DA and Amdam GV. The lifespan extension effects of resveratrol are conserved in the honey bee and may be driven by a mechanism related to caloric restriction. Aging (Albany NY). 2012; 4:499-508.

448. Sutphin GL, Bishop E, Yanos ME, Moller RM and Kaeberlein M. Caffeine extends life span, improves healthspan, and delays age-associated pathology in Caenorhabditis elegans. Longev Healthspan. 2012; 1: 9.

449. Rallis C, Codlin S and Bähler J. TORC1 signaling inhibition by rapamycin and caffeine affect lifespan, global gene expression, and cell proliferation of fission yeast. Aging Cell. 2013; 12:563-573.

450. Si H, Fu Z, Babu PV, Zhen W, Leroith T, Meaney MP, Voelker KA, Jia Z, Grange RW and Liu D. Dietary epicatechin promotes survival of obese diabetic mice and Drosophila melanogaster. J Nutr. 2011; 141:1095-1100.

451. Shen LR, Xiao F, Yuan P, Chen Y, Gao QK, Parnell LD, Meydani M, Ordovas JM, Li D and Lai CQ. Curcumin-supplemented diets increase superoxide dismutase activity and mean lifespan in Drosophila. Age (Dordr). 2013; 35:1133-1142.

452. Blagosklonny MV. Aging and immortality: quasi-programmed senescence and its pharmacologic inhibition. Cell Cycle. 2006; 5:2087–2102.

453. Blagosklonny MV, Hall MN. Growth and aging: a common molecular mechanism. Aging (Albany NY). 2009; 1:357–362.

454. Goldberg AA, Beach A, Davies GF, Harkness TA, Leblanc A, Titorenko VI. Lithocholic bile acid selectively kills neuroblastoma cells, while sparing normal neuronal cells. Oncotarget. 2011; 2:761–782.

455. Hanahan D, Weinberg RA. Hallmarks of cancer: the next generation. Cell. 2011; 144:646–674.

456. Rodier F, Campisi J. Four faces of cellular senescence. J Cell Biol. 2011; 192:547–556.

457. Campisi J. Aging, cellular senescence, and cancer. Annu Rev Physiol. 2013; 75:685–705.

458. Goldberg AA, Titorenko VI, Beach A, Sanderson JT. Bile acids induce apoptosis selectively in androgen-dependent and -independent prostate cancer cells. PeerJ. 2013; 1: e122.

459. Partridge L. Intervening in ageing to prevent the diseases of ageing. Trends Endocrinol Metab. 2014; 25:555–557.

460. Piano A, Titorenko VI. The Intricate interplay between mechanisms underlying aging and cancer. Aging Dis. 2014; 6:56–75.

461. Lutchman V, Medkour Y, Samson E, Arlia-Ciommo A, Dakik P, Cortes B, Feldman R, Mohtashami S, McAuley M, Chancharoen M, Rukundo B, Simard E, and Titorenko VI. Discovery of plant extracts that greatly delay yeast chronological aging and have different effects on longevity-defining cellular processes. Oncotarget. 2016; 7: 16542-16566.

462. Demidenko ZN. Chronological lifespan in stationary culture: from yeast to human cells. Aging (Albany NY). 2011; 3:1041-1042.

463. Fabrizio P, and Wei M. Conserved role of medium acidification in chronological senescence of yeast and mammalian cells. Aging (Albany NY). 2011; 3:1127-1129.

464. Leontieva OV, and Blagosklonny MV. Yeast-like chronological senescence in mammalian cells: phenomenon, mechanism and pharmacological suppression. Aging (Albany NY). 2011; 3:1078-1091.

465. Blagosklonny MV. Cell cycle arrest is not yet senescence, which is not just cell cycle arrest: terminology for TOR-driven aging. Aging (Albany NY). 2012; 4:159-165.

466. McCubrey JA, Steelman LS, Chappell WH, Sun L, Davis NM, Abrams SL, Franklin RA, Cocco L, Evangelisti C, Chiarini F, Martelli AM, Libra M, Candido S, et al. Advances in targeting signal transduction pathways. Oncotarget. 2012; 3:1505-1521.

467. Leontieva OV, Demidenko ZN, and Blagosklonny MV. S6K in geroconversion. Cell Cycle. 2013; 12:3249-3252.

468. Blagosklonny MV. Geroconversion: irreversible step to cellular senescence. Cell Cycle. 2014; 13:3628-3635.

469. Colman RJ, Anderson RM, Johnson SC, Kastman EK, Kosmatka KJ, Beasley TM, Allison DB, Cruzen C, Simmons HA, Kemnitz JW, and Weindruch R. Caloric restriction delays disease onset and mortality in rhesus monkeys. Science. 2009; 325:201-204.

470. Colman RJ, Beasley TM, Kemnitz JW, Johnson SC, Weindruch R, and Anderson RM. Caloric restriction reduces age-related and all-cause mortality in rhesus monkeys. Nat Commun. 2014; 5: 3557.

471. Gems D. What is an anti-aging treatment? Exp Gerontol. 2014; 58:14-18.

472. Kennedy BK, and Pennypacker JK. Drugs that modulate aging: the promising yet difficult path ahead. Transl Res. 2014; 163:456-465.

473. Sinclair DA, and Guarente L. Small-molecule allosteric activators of sirtuins. Annu Rev Pharmacol Toxicol. 2014; 54:363-380.

474. Moskalev A, Chernyagina E, de Magalhães JP, Barardo D, Thoppil H, Shaposhnikov M, Budovsky A, Fraifeld VE, Garazha A, Tsvetkov V, Bronovitsky E, Bogomolov V, Scerbacov A,

Kuryan O, Gurinovich R, Jellen LC, Kennedy B, Mamoshina P, Dobrovolskaya E, Aliper A, Kaminsky D, Zhavoronkov A. Geroprotectors.org: a new, structured and curated database of current therapeutic interventions in aging and age-related disease. Aging (Albany NY). 2015; 7:616-628.

475. Pitt JN, and Kaeberlein M. Why is aging conserved and what can we do about it? PLoS Biol. 2015; 13: e1002131.

476. Health Canada. http://www.hc-sc.gc.ca/index-eng.php.

477. Lutchman V, Dakik P, McAuley M, Cortes B, Ferraye G, Gontmacher L, Graziano D, Moukhariq FZ, Simard É, Titorenko VI. Six plant extracts delay yeast chronological aging through different signaling pathways. Oncotarget. 2016; 7:50845-50863.

478. Lee D, Hwang W, Artan M, Jeong DE, Lee SJ. Effects of nutritional components on aging. Aging Cell. 2015; 14:8-16.

479. Madeo F, Eisenberg T, Pietrocola F, Kroemer G. Spermidine in health and disease. Science. 2018; 359: eaan2788.

480. Park SJ, Ahmad F, Philp A, Baar K, Williams T, Luo H, Ke H, Rehmann H, Taussig R, Brown AL, Kim MK, Beaven MA, Burgin AB, et al. Resveratrol ameliorates aging-related metabolic phenotypes by inhibiting cAMP phosphodiesterases. Cell. 2012; 148:421–433.

481. Sajish M, Schimmel P. A human tRNA synthetase is a potent PARP1-activating effector target for resveratrol. Nature. 2015; 519:370–373.

482. Berenbaum MC. What is synergy? Pharmacol Rev. 1989; 41:93–141.

483. Slinker BK. The statistics of synergism. J Mol Cell Cardiol. 1998; 30:723–731.

484. Nieuwenhuis S, Forstmann BU, Wagenmakers EJ. Erroneous analyses of interactions in neuroscience: a problem of significance. Nat Neurosci. 2011; 14:1105–1107.

485. Geary N. Understanding synergy. Am J Physiol Endocrinol Metab. 2013; 304: E237–E253.

486. Madeo F, Carmona-Gutierrez D, Kepp O, Kroemer G. Spermidine delays aging in humans. Aging (Albany NY). 2018; 10:2209-2211.

487. Strynatka KA, Gurrola-Gal MC, Berman JN, McMaster CR. How surrogate and chemical genetics in model organisms can suggest therapies for human genetic diseases. Genetics. 2018; 208:833-851.

488. Masoro EJ. Overview of caloric restriction and ageing. Mech Ageing Dev. 2005; 126:913-922.

489. Mair W, Dillin A. Aging and survival: the genetics of life span extension by dietary restriction. Annu Rev Biochem. 2008; 77:727-754.

490. Mattison JA, Colman RJ, Beasley TM, Allison DB, Kemnitz JW, Roth GS, Ingram DK, Weindruch R, de Cabo R, Anderson RM. Caloric restriction improves health and survival of rhesus monkeys. Nat Commun. 2017; 8: 14063.

491. Sinclair DA. Toward a unified theory of caloric restriction and longevity regulation. Mech Ageing Dev. 2005; 126:987-1002.

492. Ingram DK, Zhu M, Mamczarz J, Zou S, Lane MA, Roth GS, deCabo R. Calorie restriction mimetics: an emerging research field. Aging Cell. 2006; 5:97-108.

493. de Magalhães JP, Wuttke D, Wood SH, Plank M, Vora C. Genome-environment interactions that modulate aging: powerful targets for drug discovery. Pharmacol Rev. 2012; 64:88-101.

494. Lee SH, Min KJ. Caloric restriction and its mimetics. BMB Rep. 2013; 46:181-187.

495. Ingram DK, Roth GS. Calorie restriction mimetics: can you have your cake and eat it, too? Ageing Res Rev. 2015; 20:46-62.

496. Lee C, Longo V. Dietary restriction with and without caloric restriction for healthy aging. F1000Res. 2016; 5: F1000 Faculty Rev-117.

497. Kirkwood TB. Deciphering death: a commentary on Gompertz (1825) 'On the nature of the function expressive of the law of human mortality, and on a new mode of determining the value of life contingencies.' Philos Trans R Soc Lond B Biol Sci. 2015; 370: 20140379.

498. Creevy KE, Austad SN, Hoffman JM, O'Neill DG, Promislow DEL, 2016. The Companion Dog as a Model for the Longevity Dividend, pp. 107-120. In Olshansky SJ, Martin GM, Kirkland JL. (eds.), Aging: The Longevity Dividend. Cold Spring Harbor Laboratory Press, Cold Spring Harbor, NY.

499. Promislow DE, Tatar M, Khazaeli AA, Curtsinger JW. Age-specific patterns of genetic variance in Drosophila melanogaster. I. Mortality. Genetics. 1996; 143:839-848.

500. Burger O, Baudisch A, Vaupel JW. Human mortality improvement in evolutionary context. Proc Natl Acad Sci USA. 2012; 109:18210-18214.

501. Chen J, Senturk D, Wang JL, Müller HG, Carey JR, Caswell H, Caswell-Chen EP. A demographic analysis of the fitness cost of extended longevity in Caenorhabditis elegans. J Gerontol A Biol Sci Med Sci. 2007; 62:126-135.

502. Goldberg AA, Kyryakov P, Bourque SD, Titorenko VI. Xenohormetic, hormetic and cytostatic selective forces driving longevity at the ecosystemic level. Aging (Albany NY). 2010; 2:461-470.

503. Calabrese EJ, Mattson MP. Hormesis provides a generalized quantitative estimate of biological plasticity. J Cell Commun Signal. 2011; 5:25-38.

504. Sampaio-Marques B, Burhans WC, Ludovico P. Longevity pathways and maintenance of the proteome: the role of autophagy and mitophagy during yeast ageing. Microb Cell. 2014; 1:118-127.

505. Medkour Y, Dakik P, McAuley M, Mohammad K, Mitrofanova D, Titorenko VI. Mechanisms underlying the essential role of mitochondrial membrane lipids in yeast chronological aging. Oxid Med Cell Longev. 2017; 2017: 2916985.

506. Mitrofanova D, Dakik P, McAuley M, Medkour Y, Mohammad K, Titorenko VI. Lipid metabolism and transport define longevity of the yeast Saccharomyces cerevisiae. Front Biosci (Landmark Ed). 2018; 23:1166-1194.

507. Zorov DB, Juhaszova M, Sollott SJ. Mitochondrial reactive oxygen species (ROS) and ROS-induced ROS release. Physiol Rev. 2014; 94:909-950.

508. Yang W, Hekimi S. A mitochondrial superoxide signal triggers increased longevity in Caenorhabditis elegans. PLoS Biol. 2010; 8: e1000556.

509. Yee C, Yang W, Hekimi S. The intrinsic apoptosis pathway mediates the pro-longevity response to mitochondrial ROS in C. elegans. Cell. 2014; 157:897-909.

510. Hekimi S, Wang Y, Noë A. Mitochondrial ROS and the effectors of the intrinsic apoptotic pathway in aging cells: The discerning killers! Front Genet. 2016; 7: 161.

511. Rottenberg H, Hoek JB. The path from mitochondrial ROS to aging runs through the mitochondrial permeability transition pore. Aging Cell. 2017; 16:943-955.

512. Bárcena C, Mayoral P, Quirós PM. Mitohormesis, an antiaging paradigm. Int Rev Cell Mol Biol. 2018; 340:35-77.

513. Giorgi C, Marchi S, Simoes ICM, Ren Z, Morciano G, Perrone M, Patalas-Krawczyk P, Borchard S, Jędrak P, Pierzynowska K, Szymański J, Wang DQ, Portincasa P, Węgrzyn G, Zischka H, Dobrzyn P, Bonora M, Duszynski J, Rimessi A, Karkucinska-Wieckowska A, Dobrzyn A, Szabadkai G, Zavan B, Oliveira PJ, Sardao VA, Pinton P, Wieckowski MR. Mitochondria and reactive oxygen species in aging and age-related diseases. Int Rev Cell Mol Biol. 2018; 340:209-344.

514. Blasiak J, Glowacki S, Kauppinen A, Kaarniranta K. Mitochondrial and nuclear DNA damage and repair in age-related macular degeneration. Int J Mol Sci. 2013; 14:2996-3010.

515. Santos RX, Correia SC, Zhu X, Smith MA, Moreira PI, Castellani RJ, Nunomura A, Perry G. Mitochondrial DNA oxidative damage and repair in aging and Alzheimer's disease. Antioxid Redox Signal. 2013; 18:2444-2457.

516. Szczepanowska K, Trifunovic A. Different faces of mitochondrial DNA mutators. Biochim Biophys Acta. 2015; 1847:1362-1372.

517. Nissanka N, Moraes CT. Mitochondrial DNA damage and reactive oxygen species in neurodegenerative disease. FEBS Lett. 2018; 592:728-742.

518. Kaarniranta K, Pawlowska E, Szczepanska J, Jablkowska A, Blasiak J. Role of mitochondrial DNA damage in ROS-Mediated pathogenesis of age-related macular degeneration (AMD). Int J Mol Sci. 2019; 20: E2374.

519. Medkour Y, Mohammad K, Arlia-Ciommo A, Svistkova V, Dakik P, Mitrofanova D, Rodriguez MEL, Junio JAB, Taifour T, Escudero P, Goltsios FF, Soodbakhsh S, Maalaoui H, Simard É, Titorenko VI. Mechanisms by which PE21, an extract from the white willow Salix alba, delays chronological aging in budding yeast. Oncotarget. 2019; 10:5780-5816.

520. Dakik P, McAuley M, Chancharoen M, Mitrofanova D, Lozano Rodriguez ME, Baratang Junio JA, Lutchman V, Cortes B, Simard É, Titorenko VI. Pairwise combinations of chemical compounds that delay yeast chronological aging through different signaling pathways display synergistic effects on the extent of the aging delay. Oncotarget. 2019; 10:313-338.

521. Niccoli T, Partridge L. Ageing as a risk factor for disease. Curr Biol. 2012; 22: R741-R752.